DEVELOPMENT AND CONSTRUCTION OF LOW-CRACKING HIGH-PERFORMANCE CONCRETE (LC-HPC) BRIDGE DECKS: FREE SHRINKAGE TESTS, RESTRAINED RING TESTS, CONSTRUCTION EXPERIENCE, AND CRACK SURVEY RESULTS

BY

Jiqiu Yuan

Submitted to the graduate degree program in Civil Engineering
and the Graduate Faculty of the University of Kansas in partial fulfillment
of the requirements for the degree of Doctor of Philosophy.

_____
Chairperson

_____

_____

_____

_____
Committee Members

Date Defended:_____

The Dissertation Committee for Jiqiu Yuan
certifies that this is the approved version of the following dissertation:

DEVELOPMENT AND CONSTRUCTION OF LOW-CRACKING HIGH-PERFORMANCE CONCRETE (LC-HPC) BRIDGE DECKS: FREE SHRINKAGE TESTS, RESTRAINED RING TESTS, CONSTRUCTION EXPERIENCE, AND CRACK SURVEY RESULTS

_____
Chairperson

Date approved:_____

ABSTRACT

The development, construction, and evaluation of low-cracking high-performance concrete (LC-HPC) bridge decks are described based on laboratory test results and experiences gained during the construction of 13 LC-HPC bridge decks in Kansas, along with another deck bid under the LC-HPC specifications but for which the owner did not enforce the specification. This study is divided into four parts covering (1) an evaluation of the free shrinkage properties of LC-HPC candidate mixtures, (2) an investigation of the relationship between the evaporable water content in the cement paste and the free shrinkage of concrete, (3) a study of the restrained shrinkage performance of concrete using restrained ring tests, and (4) a description of the construction and preliminary evaluation of LC-HPC and control bridge decks constructed in Kansas.

The first portion of the study involves evaluating the effects of the duration of curing, fly ash, and a shrinkage reducing admixture (SRA) on the free-shrinkage characteristics of concrete mixtures. The results indicate that an increase of curing period reduces free shrinkage. With 7 days of curing, concretes containing fly ash as a partial replacement for cement exhibit higher free shrinkage than concretes with 100% portland cement. When the curing period is increased to 14, 28, and 56 days, the adverse effect of adding fly ash on free shrinkage is minimized and finally reversed. The addition of an SRA significantly reduces free shrinkage for both the 100% portland cement mixture and the mixture containing fly ash.

The second portion of the study investigates the relationship between the evaporable water content in the cement paste and the free shrinkage of concrete. A linear relationship between free shrinkage and evaporable water content in the cement paste is observed. For a given mixture, specimens cured for a longer period contain

less evaporable water and exhibit lower free shrinkage and less weight loss in the free shrinkage specimens than those cured for a shorter period.

The third portion of the study evaluates the cracking tendency of concrete mixtures using the restrained ring tests. Different concrete ring thicknesses and drying conditions have been tested. The results indicate that specimens with thinner concrete rings crack earlier than those with thicker concrete rings. Exposing specimens to severe drying conditions results in the earlier formation of cracks, although it does not result in increased crack width. Mixtures with a lower water-cement (*w/c*) ratio crack earlier than mixtures with a higher *w/c* ratio. Concretes with a higher paste content crack earlier than concretes with a lower paste content.

The final portion of the study details the development, construction, and preliminary performance (with most bridges at three years of age) of LC-HPC and control bridge decks in Kansas. The results indicate that the techniques embodied in the LC-HPC bridge deck specifications are easy to learn. Contractor personnel can be trained in a relatively short time. The techniques used for LC-HPC bridge decks are effective in reducing bridge deck cracking. The crack surveys indicate that LC-HPC bridge decks are performing much better than the control decks, with average crack densities reduced by about seventy five percent at three years of age. The factors that may affect bridge deck cracking are analyzed. The analyses indicate that an increase in paste content, slump, compressive strength, maximum daily air temperature, and daily air temperature range causes increased crack densities. Contractor techniques influence cracking.

Keywords: bridge construction, bridge deck, contractor, concrete mix design, compressive strength, cracking, curing, evaporable water, fly ash, free shrinkage, high-performance concrete, non-evaporable water, paste content, restrained shrinkage, restrained ring tests, shrinkage reducing admixture, slump

ACKNOWLEDGEMENTS

I would like to gratefully and sincerely thank Dr. David Darwin and Dr. JoAnn Browning for their guidance, understanding, patience, and support during my graduate studies at the University of Kansas. I would also like to thank my other committee members, Dr. Stan Rolfe, Dr. Adolfo Matamoros, and Dr. Donald Worster.

I am grateful for all my colleagues and friends at the University of Kansas. I very enjoyed the time of studying, researching, and relaxing with them. Thank you all for the friendship.

Finally, and most importantly, I would like to thank my dear wife, Jing Fu, for her support, encouragement, and unwavering love. I am grateful to have my lovely daughter, Kaylynn, during my graduate study. Kaylynn, you have made this period more precious in my life. I also want to thank my parents and parents-in-law for their endless support.

Funding for this research was provided by the Kansas Department of Transportation serving as the lead agency for the "Construction of Crack-Free Bridge Decks, Phase I" and "Construction of Crack-Free Bridge Decks, Phase II" Transportation Pooled Fund Study, Project Nos. TPF-5(051) and TPF-5(174). The Federal Highway Administration (FHWA) of the U.S. Department of Transportation (DOT), Colorado DOT, Delaware DOT, Idaho Transportation Department, Indiana DOT, Michigan DOT, Minnesota DOT, Mississippi DOT, Missouri DOT, Montana DOT, New Hampshire DOT, New York State DOT, North Dakota DOT, Ohio DOT, Oklahoma DOT, South Dakota DOT, Texas DOT, Wisconsin DOT, Wyoming DOT, Overland Park, KS, the University of Kansas Transportation Research Institute, BASF Construction Chemicals, and the Silica Fume Association provided funding to the pooled fund. Representatives from each sponsor served on a Technical Advisory Committee that provided advice and oversight to the project.

LRM Industries, BASF Construction Chemicals, Holcim US, Fordyce Concrete, Grace Construction Products, Ash Grove Cement, and Lafarge North America provided concrete materials.

TABLE OF CONTENTS

LIST OF TABLES

LIST OF FIGURES

CHAPTER 1 INTRODUCTION

1.1 GENERAL

In 2009, the American Society of Civil Engineers (ASCE) reported that 12.1 percent (72,868 out of 600,905) of U.S. bridges were structurally deficient. The American Association of State Highway and Transportation Officials (AASHTO) estimated that in 2008 it would cost about $48 billion to repair current structurally deficient bridges (ASCE 2009).

The High Performance Concrete Technology Delivery Team (HPC TDT), led by the Federal Highway Administration (FHWA), conducted a national survey among transportation agencies in 2004, and the top three bridge deficiencies noted by the states were cracking of concrete decks**,** corrosion of reinforcing steel, and cracking of girders and substructures (Triandafilou 2005).

Cracks provide easy access of water and deicing chemicals to reinforcing steel in concrete bridge decks, which consequently causes serious corrosion problems of reinforcing steel, and shortens the useful life of the bridges. Lindquist, Darwin, and Browning (2006) reported that at the level of the top reinforcing steel in bridge decks, the chloride concentration at cracks exceeded the corrosion threshold of conventional reinforcement within the first year. This level of chloride ingress was noted for all bridge types included in the survey, including those placed monolithically and those with silica fume and conventional high-density concrete overlays. The chloride content in uncracked concrete, however, remained below the critical chloride corrosion threshold through 12 years for most decks.

Over the past 40 years, researchers and transportation agencies have engaged in many studies to help solve the bridge deck cracking problem. This chapter reviews the significant aspects of previous work by describing the typical types of cracks observed in bridge decks, the cracking mechanisms, and the material and construction factors that affect bridge deck cracking. Restrained ring tests, as an experimental

method to evaluate the cracking tendency of concrete materials, have been used by many researchers. The restrained ring test procedures used by researchers are reviewed.

1.2 CRACK CLASSIFICATION

Cracks in bridge decks can be generally characterized by their orientation relative to the longitudinal axis of the bridge. The Portland Cement Association (Durability 1970) has classified cracks into six categories: transverse, longitudinal, diagonal, pattern (map), D-cracking, and random cracking. Transverse cracking (Figure 1.1a) is the most prevalent type and typically occurs perpendicular to the bridge centerline, directly above the reinforcing steel. Transverse cracking can be caused by subsidence, thermal contraction, drying shrinkage, and flexural cracking.

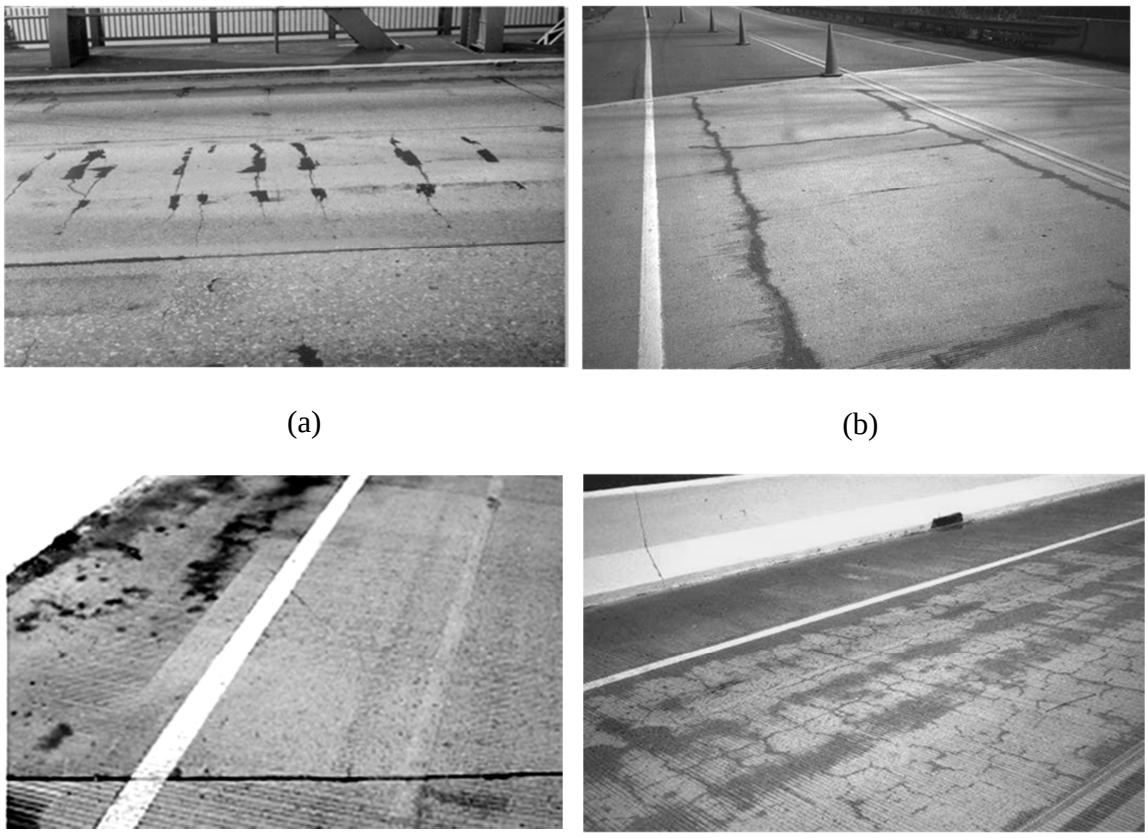

(a) (b)

(c) (d)

Figure 1.1 Examples of crack patterns (Russell 2004): (a) transverse cracking, (b) longitudinal cracking, (c) diagonal cracking, (d) map cracking.

Longitudinal cracking (Figure 1.1b), which is parallel to the bridge centerline, is primarily found in hollow and solid slab concrete bridges. Short longitudinal cracks also appear over the abutment, especially for deck slabs that are cast integrally with the abutment (Schmitt and Darwin 1995, Miller and Darwin 2000, Lindquist, Darwin and Browning 2005). Subsidence cracking over the top of the longitudinal reinforcing steel is believed to be the major cause for longitudinal cracking of the type shown in Figure 1.1b, while restraint provided by the abutment appears to be the major cause of longitudinal cracks over the abutment.

Diagonal cracking (Figure 1.1c) is primarily found at the ends of skewed bridges, integral abutments, and over single column piers. This cracking normally consists of parallel cracks having an angle other than 90 degrees with respect to the centerline of the roadway. Drying shrinkage and flexural cracking are the probable causes of diagonal cracking.

Pattern or map cracking (Figure 1.1d) includes the cracks that are interconnected. Plastic and drying shrinkage are believed to be the primary causes.

D-cracking refers to cracks that are roughly parallel to joints, edges, and structure members. Deterioration at the base of concrete slabs due to the destruction of aggregates by frost could cause the formation of D-cracking. D-cracking is far more prevalent for slabs on grade than on bridge decks.

Cracks that do not fit into any of the before mentioned types are called random cracks.

1.3 CRACKING MECHANISMS

Cracking in reinforced concrete bridge decks is affected by concrete material properties, construction practices, and, to a lesser extent, bridge design. This report will primarily focus on the effects of concrete material properties and construction practices.

Concrete is a brittle material that is strong in compression but weak in tension, typically with a tensile strength equal to about one-tenth of its compressive strength. When the tensile stresses developed in concrete exceed its tensile strength, cracking occurs.

Tensile stresses can be induced by many sources in bridge deck concrete. Shrinkage is a property of concrete, which can occur in fresh concrete as plastic shrinkage and in hardened concrete as drying shrinkage. Concrete shrinkage by itself will not cause cracking, but when it is restrained, such as by the girders in bridge decks, excessive tensile stress can develop. The magnitude of the resulting tensile stress depends on how much shrinkage the concrete experiences and the degree of restraint provided. Temperature differentials between the concrete and girders can also induce tensile stress in concrete when the concrete thermal contraction is restrained by the girders. Settlement of plastic concrete over reinforcing steel may cause tensile stress in an early age. Externally applied load, including dead and live load, can also induce tensile stress in concrete. The details of the causes of tensile stress in concrete bridge decks are discussed in this section.

1.3.1 Concrete Shrinkage

1.3.1.1 Plastic Shrinkage

Plastic shrinkage occurs in fresh concrete. When the rate of evaporation exceeds the rate of bleeding, the surface loses its sheen, and capillary tension develops. The approximate maximum capillary tension can be calculated using the following relationship (Powers 1960):

$$P_c = -\frac{\lambda\sigma\ \rho_f/\rho_c}{w/c} \tag{1.1}$$

where P_c is the capillary tension, λ is the surface tension of water in dynes/cm, σ is the specific surface area of cement in cm^2/cm^3, ρ_f and ρ_c are the densities of water

and cement in g/cm^3, respectively, and w/c is the water-cement ratio. The calculated maximum capillary tension based on this equation is from 0.5 atm (7.3 psi) upwards, depending on the surface area of the cement.

Capillary tension can exert a downward force on the particles at the top surface of plastic concrete. Compared with the downward force on those particles due to gravity only, which is about 0.001 atm (0.015 psi), capillary tension induces a greatly increased downward force. Therefore, when the evaporation rate exceeds the bleeding rate (rate at which bleed water moves upward in plastic concrete), the downward force that is applied to the surface particles is greatly increased. To offset the greatly increased force, the water surfaces retreat to the interior, and lateral consolidation begins. The lateral consolidation causes a reduction in the volume of the plastic concrete, which is called "plastic shrinkage."

Plastic shrinkage cracking can be a very serious problem, especially when the evaporation rate is not controlled and the bleeding rate is low. The evaporation rate can be controlled in multiple ways, including using evaporation retarders, windbreaks, water fogging systems, curing compounds, cooling the concrete or its constituents, early application of wet curing procedures, etc. (Lindquist, Darwin, and Browning 2008). The bleed water usually rises to the surface at a rate of about 0.2 lb/ft^2/h (1 kg/m^2/h) (Babaei and Fouladgar 1997), and the evaporation rate of conventional concrete is usually limited to a maximum 0.2 lb/ft^2/h (1 kg/m^2/h). The bleeding rate is influenced by a number of factors. An increased hydration rate, the use of entrained air, a reduced water content, and the presence of mineral admixtures will decrease the bleeding rate. In these cases, a lower limit of evaporation rate should be applied. Another aspect to consider is the fineness of cement, which has been steadily increasing over the past several decades (Mindess, Young, and Darwin 2003). As finer cement is used, plastic shrinkage can become more severe for several reasons: the bleeding rate is decreased as the rate of hydration is accelerated, the water

adsorbed on the surface of the particles is increased due to the increase in surface area provided by finer cement particles, and capillary tension is increased, also due to the higher surface area of the finer cement.

1.3.1.2 Drying Shrinkage

Drying shrinkage occurs in hardened concrete in bridge decks. When concrete is exposed to the air, it loses water to the environment and tends to shrink. When concrete drying shrinkage is restrained by girders, tensile stresses develop in the concrete and cause cracking. Drying shrinkage cracks usually form above the top transverse bars, initiating from weakened planes or cracks that form due to settlement cracking (discussed in Section 1.3.3), and can continue through the full depth of the slab. Analytical work by Babaei and Purvis (1996) and Babaei and Fouladgar (1997) indicate that about 400 microstrain of restrained shrinkage is needed to initiate cracking in bridge decks. Considering the superposition of thermal contraction and drying shrinkage, Babaei suggested limiting the 28-day free shrinkage (refer to ASTM C 157) to a maximum of 400 microstrain or 4-month free shrinkage to a maximum of 700 microstrain (Babaei and Purvis 1996, Babaei and Fouladgar 1997).

As water evaporates from concrete, three mechanisms are believed to contribute to drying shrinkage: capillary stress, disjoining pressure, and changes in surface free energy (Mindess et al. 2003).

Capillary stress: Hydrostatic tension develops inside capillary pores as concrete dries out. This hydrostatic tension draws the pore walls together and causes shrinkage. Mindess et al. (2003) state that the water in a small capillary pore can only be removed by evaporation through an air-water interface (meniscus), and hydrostatic tension develops when a meniscus forms in a capillary pore. The relationship between the hydrostatic tension, capillary pore radius, and relative humidity (*RH*) can be expressed as:

$$P_{cap} = \frac{2\gamma}{r} \quad (1.2\text{ a})$$

$$= \frac{\ln(RH)}{K} \quad (1.2\text{ b})$$

where P_{cap} is the hydrostatic tension, γ is the surface free energy of the water, r is the capillary pore radius, K is a constant, and RH is the relative humidity inside the concrete. Larger capillary pores can be emptied at a relative humidity down to 95% and very small capillary tension will develop. Thus, the shrinkage due to water loss in large capillary pores at high relative humidities is small. As the *RH* drops, water in smaller capillary pores can evaporate and the hydrostatic tension P_{cap} increases [based on Eq. (1.2 a) and (1.2 b)]. Thus, the shrinkage at lower *RH* is greater due to increased hydrostatic tension caused by water loss in smaller capillary pores. Capillary stresses cannot exist at relative humidities lower than 45% because the meniscus is no longer stable, and other mechanisms will provide the major force, as explained later in this section.

Powers (1960) presented a theory to explain how capillary water is lost from concrete during drying. In most cases, all the capillary spaces in cement paste are in the form of cavities isolated by cement gel. None of the water in the isolated cavities can evaporate before the water evaporates from the very small gel pores of the surrounding gel. In Powers' (1960) theory, when water evaporates from the outside surface of a body of cement gel enclosing one or more water-filled capillary spaces, hydrostatic tension develops and its magnitude is limited by the relative humidity of its surroundings. The increase in hydrostatic tension causes the water in the capillary pores, if initially saturated with air, to be supersaturated. When the degree of super-saturation is high enough, bubbles can develop in the capillary pores. At a given humidity and only when the size of capillary cavities is above certain values, the bubbles can develop and capillary

cavities can be emptied. The computed diameters of the capillary cavities that are capable of containing spherical bubbles at given humidities are given in Table 1.1.

Table 1.1 Computed diameters of capillary cavities able to contain spherical bubbles at given humidities (Powers 1960)

Relative humidity inside concrete, %	Hydrostatic tension, atm	Nucleation radius r*, $\times 10^{-10}$ m	Required radius of spherical cavity, r*+5, $\times 10^{-10}$ m
98	28	346	351
96	57	170	175
92	116	84	89
85	226	43	48
70	495	20	25
50	963	10	15
45	1100	[a]	
40	1200	[a]	

[a] Bubbles cannot exist at tensions above the fracture strength of water, which is between 1,100 and 1,200 atm.

From the calculated values in Table 1.1, as the relative humidity drops, the bubbles can develop at smaller capillary cavities, and correspondingly, the hydrostatic tension increases greatly. Hydrostatic tension is about 34 times higher at a relative humidity of 50% than it is at a relative humidity of 98%. Thus, at lower relative humidities, water can evaporate from smaller capillary pores, and the corresponding hydrostatic tension, which causes concrete to shrink, will be larger.

Disjoining pressure: Because the colloidal particles that compose the cement gel are exceedingly small, mutual attraction between particles, provided by van der Waals' force, is the major force holding adjacent particles together. When a dry paste is saturated with water, the mutual attraction between the water molecules and the gel particles causes water to spread over all of the surfaces of the gel particles that are

available to them. When the spread is obstructed by an adjacent particle, a disjoining pressure will develop. Once the disjoining pressure exceeds the van der Waals' force, the particles are forced apart and dilation or swelling occurs. By contrast, as a saturated material dries out, the van der Waals' forces between particles draw them closer together and shrinkage occurs. Because cement gel is formed in the dilated state during hydration, the disjoining pressure decreases on first drying at a lowered relative humidity (*RH*). The decreased disjoining pressure causes the particles to be drawn closer by van der Waals' forces, and shrinkage occurs. Disjoining pressure is *RH* dependent and is only a significant factor down to about 45% *RH* (Mindess et al. 2003).

Surface free energy: When the relative humidity is below 45%, the capillary stress and disjoining pressure are no longer the forces that cause shrinkage, and shrinkage is believed to be caused by the increase in the surface free energy of the solid. The increased surface free energy of the solid, caused by the removal of mostly strongly adsorbed water, causes increased compression in the solid, and shrinkage occurs (Mindess et al. 2003).

Autogenous shrinkage is a special case of drying shrinkage (Mindess et al. 2003). Autogenous shrinkage is the result of self desiccation. It is a phenomenon that occurs when no additional water is provided during curing and the concrete begins to dry internally due to water consumption during the hydration process. It normally occurs in concrete with low water cement ratios (< 0.40) or in dense concrete when external water cannot easily penetrate the dense concrete.

Carbonation is the process of hardened cement paste reacting with carbon dioxide. Carbonation causes the decomposition of hydrated silicate and aluminate phases, and the decalcification of C-S-H. Carbonation is usually accompanied with irreversible shrinkage, called **carbonation shrinkage**. Concrete at intermediate humidities is affected by exposure to carbon dioxide and the effect is maximized at a

relative humidity of 55%; concrete in a dry or saturated condition is not affected significantly by exposure to carbon dioxide (Powers 1959).

1.3.1.3 Evaporable Water Content Versus Drying Shrinkage

Moisture loss to the surroundings is the primary cause for drying shrinkage. The relationship between the moisture loss and drying shrinkage is of interest. Defining the relationship requires an understanding of how water molecules are held in cement paste.

Powers (1960) summarized the features of paste structure as follows: "cement gel is a substance that occupies about 2.2 times as much space as the cement from which it is derived." Because the total volume of the paste scarcely changes, the cement gel will occupy the spaces that are originally filled by water. The remaining spaces of the originally water-filled spaces that have not been filled with gel are called capillaries or capillary cavities. The cement gel itself also contains gel pores and has a porosity of about 28%. The average width of the gel pores is about 18×10^{-10} m, which is about 5 times the diameter of a water molecule. The width of capillary pores is considered to be much wider than gel pores, though the capillary pores tend to be narrower as the water-filled space is used up due to continued hydration (Taylor 1997). Capillary pores are isolated by cement gel and interconnected only by gel pores.

A typical shrinkage-weight loss curve for a cement paste is shown in Figure 1.2 (Mindess et al. 2003). There are five domains in the curve. Domain 1 represents the water lost from the large capillary pores at high relative humidities (down to about 95%). The corresponding shrinkage represents only a very little part of the total shrinkage. In domain 2, water is lost from both the finer capillary pores and the gel pores. In domains 3 and 4, water adsorbed on the particle surfaces and water at the interlayer of C-S-H (only in the domain 4) is removed. The shrinkage that occurs in domains 2, 3, and 4 represents the major part of the total shrinkage. All the water in

the first four domains can be removed at room temperature, or more quickly at 221° F (105° C). This part of water is also called evaporable water. In domain 5, further shrinkage can occur due to decomposition of C-S-H, while normally happens only at temperatures higher than 221° F (105° C).

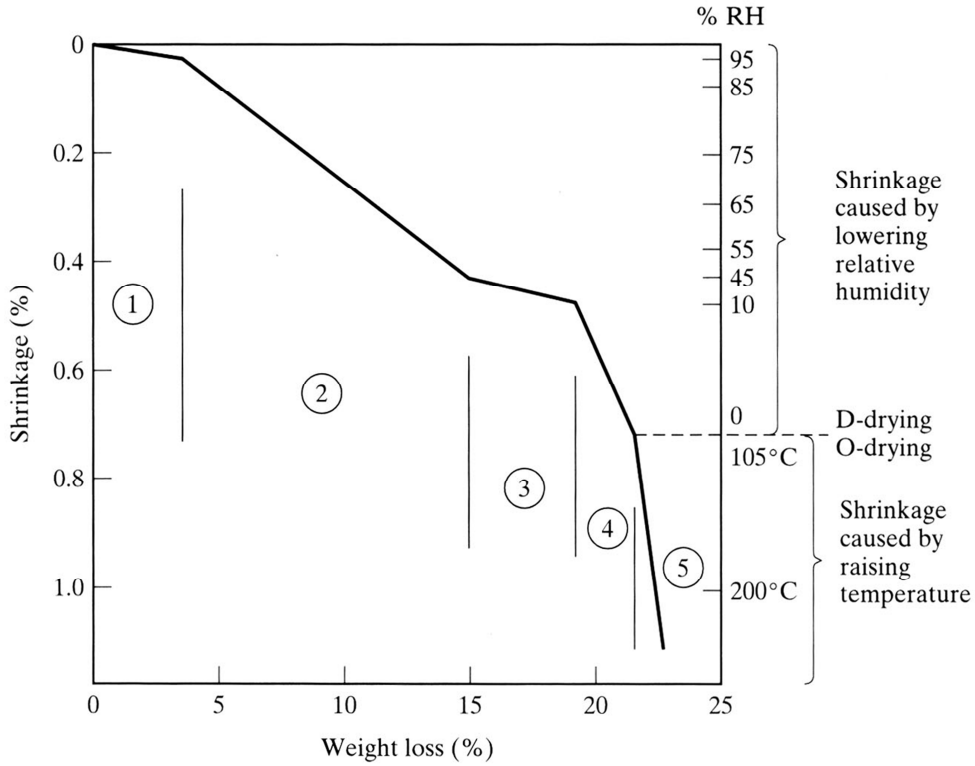

Figure 1.2 Schematic representation of shrinkage-water loss relationships for cement pastes during drying (Mindess et al. 2003)

Powers (1959) stated that the shrinkage caused by the loss of water depends on how much of the loss is capillary water and how much is adsorbed water. Shrinkage and swelling are believed to be mostly affected by the water molecules in direct contact with the solid surfaces of cement gel. When a dry paste takes up water in high humidities, water will enter the force field of the solid phase first and cause relatively large swelling per unit of water absorbed. As more water is absorbed by the paste, a point will be reached at which some water will enter large spaces where

mutual attraction between water and particles is weak. Capillary cavities are such large spaces that the water that enters the capillary cavities has little effect on the volume change. By contrast, when a saturated paste begins drying, water in the capillary cavities will be lost first, followed by adsorbed water within the force field of the solid phase. Due to the weak interaction between water and particles in the capillary cavities, smaller shrinkage per unit weight loss of water during early stages of drying would be expected than it is at later ages when the adsorbed water is removed.

Shrinkage is less correlated with capillary water and more affected by adsorbed water. To prove it, Powers (1959) presented the relationship between shrinkage and water loss (first published by Menzel at 1935) in Figure 1.3. The series of specimens represent mixtures that ranged from neat cement to a mixture composed of 25 percent cement and 75 percent pulverized silica. All specimens were cured for 7 days at 70° F (21° C), and the pulverized silica was believed to remain virtually inert under these conditions. The volume of the capillary cavities in the paste was lowest for the neat cement mixture and increased as the proportion of silica increased. As shown in the Figure 1.3, the shrinkage of the densest specimen (neat cement, 0% silica) was directly proportional to the water loss. The curved shape for the mixtures with silica illustrates the effect of an increase in capillary cavities. Because the water loss from the capillary cavities is less strongly correlated with shrinkage, as the volume of capillary cavities increases in the silica mixtures, the mixtures shrink less for the same water loss. It was also noted that towards the end of the drying period, the rate of shrinkage per unit weight of water loss was similar for all mixes because the loss involved adsorbed water.

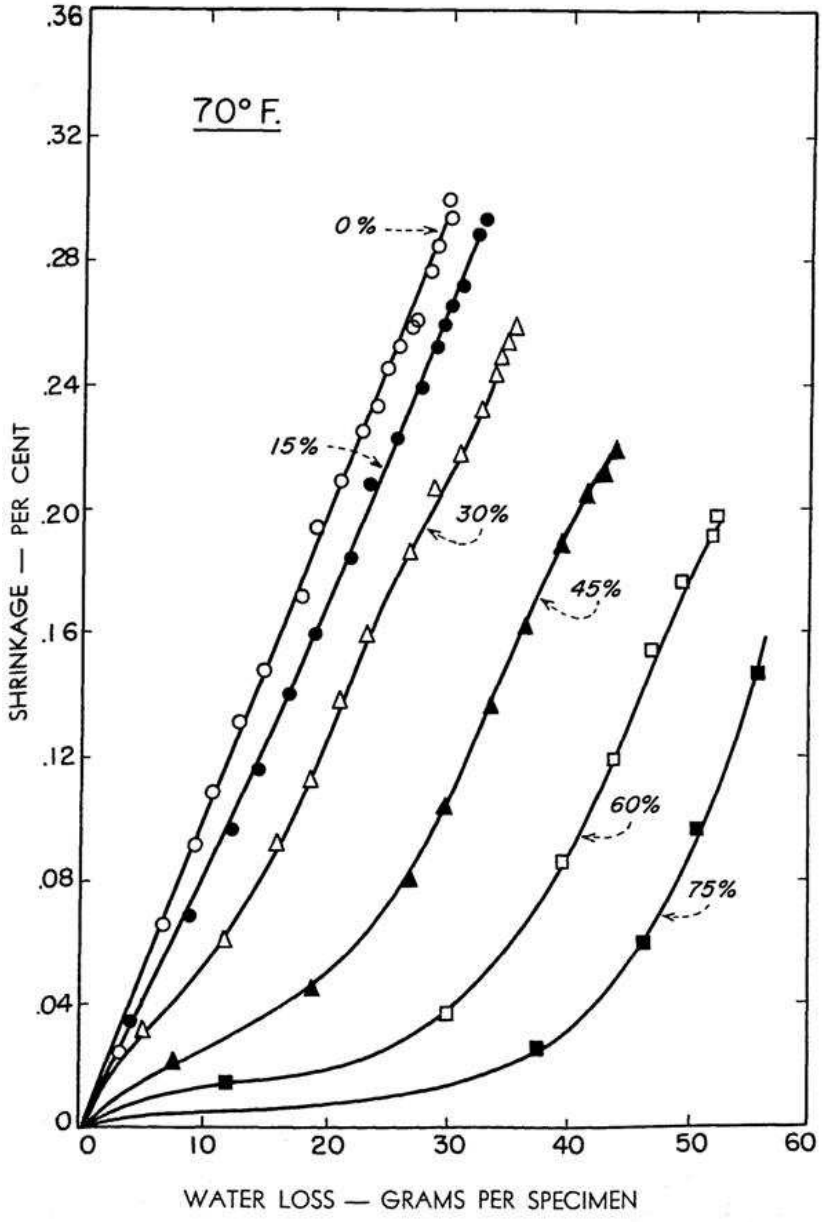

Figure 1.3 Relationships between shrinkage and water loss (Menzel 1935)
0%—100% cement and 0% silica, 15%—85% cement and 15% silica, 30%—70% cement and 30% silica, 45%—55% cement and 45% silica, 60%—40% cement and 60% silica, and 75%—25% cement and 75% silica

Cement particle size influences the size of capillary pores. The data shown in Figure 1.3 were published in 1935 when cement particles were much coarser than

they are today. The size of capillary pores would, thus, be larger than those obtained with modern cements. As discussed earlier, water loss from the larger capillary pores has relatively less effect on the volume change than water loss from smaller pores.

Lange et al. (2003) completed a series of tests to determine the relationship between free shrinkage and water loss. All concrete mixtures had a water-cementitious material ratio of 0.44 but contained different quantities of mineral admixtures. The mix proportions are listed in Table 1.2. Concrete prisms with dimensions of 3 × 3 × 11.25 in. (76 × 76 × 286 mm) were used to determine free shrinkage and water loss. All prisms were demolded 24 hours after casting and then moved to an environmental chamber maintained at 50% *RH* and 73° F (23° C). The specimens were kept in the chamber for a period of about 30 days. The relation between free shrinkage and water loss is shown in Figure 1.4. Since specimens IHPC1F and IHPC2F (shown in Figure 1.4) were prepared with materials from different sources, they are not compared in the following with the four mixes listed in Table 1.2.

Table 1.2 Concrete mixtures summary, based on yd^3 design (Lange et al. 2003)

Mix code	ISTD	IHPC1	IHPC2	IHPC4
Cement (type I), lb/yd^3	605	465	465	565
Fly ash, lb/yd^3	0	120	120	0
Silica fume, lb/yd^3	0	0	25	25
Metakaolin, lb/yd^3	0	27	0	0
Coarse Aggregate, lb/yd^3	1820	1820	1820	1820
Fine Aggregate, lb/yd^3	1130	1092	1095	1150
Water, lb/yd^3	266	269	268	260
Cementitious content, lb/yd^3	605	612	610	590
Paste content by volume, %	27.2%	28.1%	28.0%	26.8
Paste content by weight, %	22.8%	23.2%	23.1%	22.3
w/cm ratio	0.44	0.44	0.44	0.44

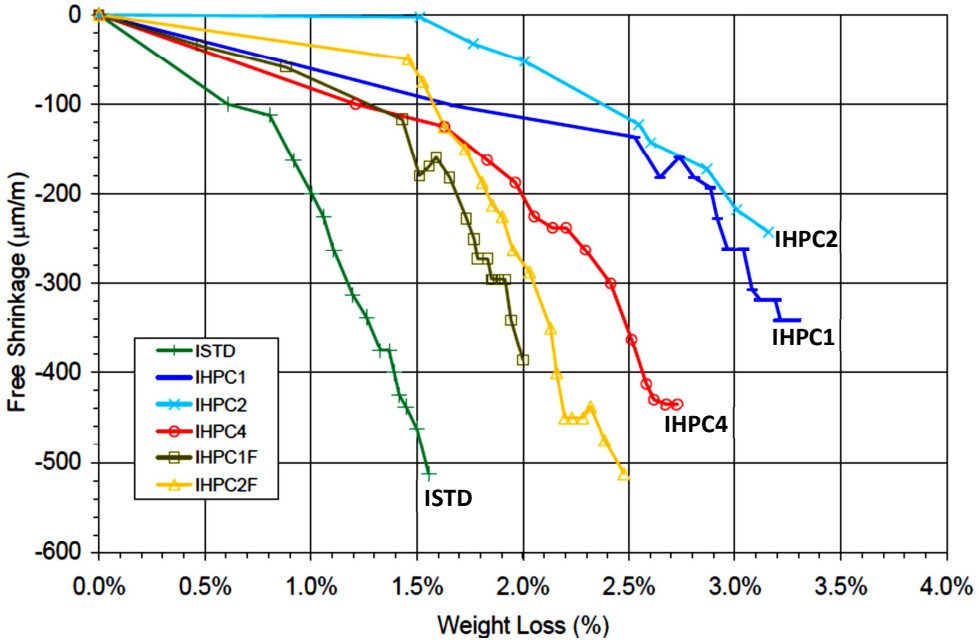

Figure 1.4 Free shrinkage vs. weight loss, *w/cm*=0.44 (Lange et al. 2003)

Although not summarized by Lange et al. (2003), the results in Figure 1.4 show similar trends as those observed in Figure 1.3 by Powers (1959). Because the concrete mixtures were only cured for 24 hours, the mineral admixtures would be virtually inert, and an increased mineral admixture content would be expected to increase the percentage of capillary pores. As shown in Figure 1.4, mix ISTD, without any mineral admixtures thus with the least capillary pores, has the highest shrinkage per unit weight loss. As the mineral admixture content increases, moving from mixture IHPC4 to mixtures IHPC1 and IHPC2, the shrinkage per unit weight loss decreases.

The shrinkage behavior of concrete mixtures can be related to the amount of evaporable water. Different categories of evaporable water, including capillary water and gel water, exist, and their effects on shrinkage will be different. No method involving drying has been devised to separate water into these categories, because capillary water and gel water evaporate simultaneously. It is of interest, however, to

investigate the relationship between shrinkage and the quantity of evaporable water. The way to determine the quantity of evaporable water is discussed in the following, and the relationship between shrinkage and the quantity of evaporable water is investigated in Chapter 4 of this report.

The amount of water that saturated cement paste is capable of holding in addition to the non-evaporable water is called evaporable water (Powers and Brownyard 1946), which can be expressed as

$$\frac{w_e}{c} = \frac{w_t}{c} - \frac{w_n}{c} \tag{1.3}$$

where $\frac{w_e}{c}$ = evaporable water, g per g of cement,

$\frac{w_t}{c}$ = total water at time of test, g per g of cement, and

$\frac{w_n}{c}$ = non-evaporable water, g per g of cement.

Powers and Brownyard (1946) defined non-evaporable water as "the water that is retained by a sample of cement paste after it has been dried at 73° F (23° C) to a constant weight in an evacuated desiccator over a system with Mg $(ClO_4)_2 \cdot 2H_2O$ + Mg $(ClO_4)_2 \cdot 4H_2O$ as a desiccant." The procedures of preparation of specimens (neat cement cylinders or mortar specimens) and drying of samples were given in detail by Powers and Brownyard (1946). After drying, the water left in the sample is the non-evaporable water and is determined by igniting one-gram portions of the dried samples at 1832° F (1000° C) for about 15 minutes. The amount of weight loss minus the weight loss of the original cement is called the non-evaporable water. Taylor (1997) described non-evaporable water as water retained in pastes that have been subjected to D-drying or equivalent procedures, where D-drying refers to a procedure in which a sample is "equilibrated with ice at –110° F (–79° C) by continuous evacuation with a rotary pump through a trap cooled in a mixture of solid CO_2 and ethanol, and the partial pressure of the water vapor is 5×10^{-4} torr."

Taylor (1997) stated that heating the sample to a constant mass at 221° F (105° C) in an atmosphere of uncontrolled humidity but free of CO_2 would yield approximately the same result as D-drying.

The total water-cement ratio of cement pastes will increase from the original value when maintained in a saturated condition. The moisture added is the water obtained from outside sources. The relationship between the original water-cement ratio and the total water-cement ratio is shown in Figure 1.5 and can be expressed as follows (Powers 1960):

$$\frac{w_t}{c} = \frac{w_o}{c} + 0.254m\ \frac{w_n^o}{c} \tag{1.4}$$

where

$\frac{w_t}{c}$ = total water-cement ratio, g per g of cement

$\frac{w_o}{c}$ = original water-cement ratio, g per g of cement

The term $0.254m\ \frac{w_n^o}{c}$ is the amount of water that the cement paste obtains from an external source when maintained in a saturated condition. This value correlates with the quantity of water that is chemically combined (Powers 1960).

w_n^o = non-evaporable water content of completely hydrated cement, g

$m = \frac{w_n}{w_n^o}$, where w_n =non-evaporable water content at the age of testing, g and m equals 1 for fully mature specimens and is less than 1 for incompletely hydrated specimens.

After the total and non-evaporable waters content are determined, the evaporable water content will be the difference of these two values.

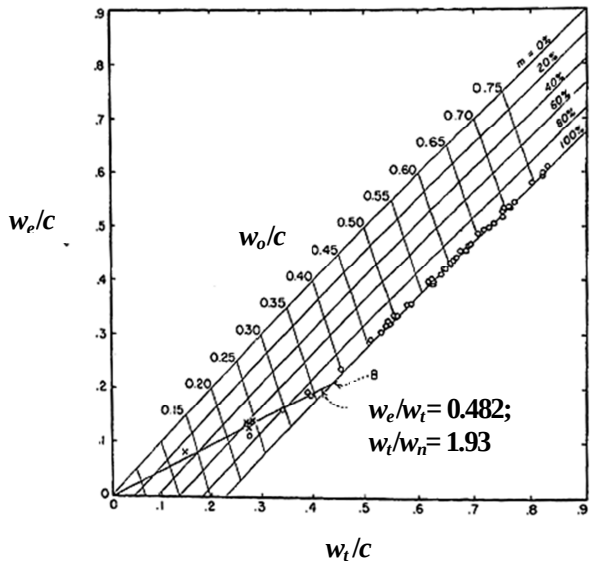

Figure 1.5 Relations between the initial (w_o/c), total (w_t/c), and evaporable (w_e/c) water-cement ratios for saturated pastes of a portland cement [m is defined follow in Eq. (1.4)] (Powers 1960)

1.3.2 Thermal Contraction

When thermally induced contraction is restrained by the girders, tensile stresses will develop in a concrete bridge deck. In the first few hours after casting, concrete temperature rises quickly due to the heat of hydration. The tendency to expand due to the initial temperature rise does not induce any measurable stresses in concrete due to its very low modulus of elasticity at this age. As hydration continues, concrete reaches its peak temperature and then begins to cool down to the ambient temperature. By the time the peak temperature is attained, the concrete has hardened and gained some strength. When the cooling-induced contraction is restrained by the girders, tensile stresses develop and cracks may form (Babaei and Fouladgar 1997).

To investigate thermally induced stresses in decks, an understanding of the temperature and stain changes of the deck and girders is needed. Krauss and Rogalla (1996) stated that the temperature changes in bridges can be represented by one of three temperature distributions or by combinations of these three. In the first temperature distribution, a large but nearly uniform temperature change in the

concrete deck occurs while the temperature change in girders remains small; this distribution will occur when there is sustained solar radiation on a bridge deck or shortly after casting when cement hydration continues generating heat. This can cause a large strain difference between the concrete deck and the girders. In the second temperature distribution, a linear temperature change occurs in the deck. It usually occurs in the morning when solar radiation raises the temperature of the upper portions of the deck more rapidly than the lower potions, and in the early evening or during rain when the upper portions of the deck cool much faster than the lower portions. As a result, a large strain difference occurs between the upper and lower portions of the deck, and the strain difference between the upper portions of the deck and the girders is even larger. In the third temperature distribution, applicable to steel girder bridges, both the concrete deck and the girders undergo similar temperature increases. Because they expand similarly [concrete has a coefficient of thermal expansion of 5.5 microstrain/° F (10 microstrain/° C) and steel has a coefficient of thermal expansion of 6.5 microstrain/° F (12 microstrain/° C)], the strain difference between the concrete deck and steel girders is small. The third distribution may occur in nearly uniform summer and winter temperature conditions.

Krauss and Rogalla (1996) monitored concrete temperatures in the Portland-Columbia Bridge between Pennsylvania and New Jersey for the first month after casting. They observed that the largest temperature changes occurred during the first 48 hours after placement. The initial concrete temperature was measured as 80° F (27° C). During the first 12 hours, the temperature in the new deck reached as high as 131° F (55° C) due to hydration-generated heat. By 48 hours, the temperature differential between the concrete and the steel girders had greatly reduced. Krauss and Rogalla (1996) also reported that the temperatures in the deck varied substantially along the length and across the width of the bridge.

Because a bridge deck is normally composite with its girders, strain differences between the bridge deck and the girders induce stresses at the interface between the deck and the girders. Therefore, for the three temperature distributions discussed by Krauss and Rogalla (1996), the first temperature distribution has a uniform temperature drop in the deck which Okcan cause large and nearly uniform tensile stress in the concrete; for the second temperature distribution, a linear temperature decrease in the deck can induce large tensile stresses at the upper face of the deck; for the third temperature distribution, a uniform temperature change in both the deck and the steel girders causes small deck stresses because of the small strain incompatibility between the concrete deck and the steel girders. Because girders restrain the deck at the soffit instead of the centroid, the eccentric restraint makes the stress distribution in a deck more complicated and stress reversals within a deck can occur.

Subramaniam and Agrawal (2009) measured temperature changes in the concrete decks and steel girders in two newly constructed bridges. Two thermocouples were placed in the concrete, one each near the top and bottom layers of the reinforcing steel. Two additional thermocouples were used to monitor the temperature changes in the top and bottom flanges of the steel girders. Figure 1.6 shows the temperature changes for one of the bridges, located in New York. The reinforcing steel was placed on August 3, 2005, and the concrete deck slab was cast on August 4, 2005. Time zero in the figure represents the casting start time of 7:45 a.m. The concrete slab had a thickness of 9.4 in. (240 mm) and rested on single-span, simply supported steel girders.

The authors did not identify the thermocouples from which the concrete temperatures, shown in Figure 1.6, were taken. It would seem obvious, however, that the light colored curve that reached peak temperature first was taken from the top thermocouple because solar radiation will heat the top surface first. Overall, the air

temperature-change curve and the concrete and steel girder temperature-change curves (48 hours after casting) have similar shapes with a peak and a valley in every 24 hours. During the first 48 hours, the concrete and steel girder temperatures appear to be influenced more by the hydration-generated heat of the concrete, and to a lesser extent, by the ambient air temperature. The concrete temperature reaches a peak about 12 hours after casting began. After 48 hours, the concrete and steel girder temperatures follow the air temperature with a lag of about 2 hours.

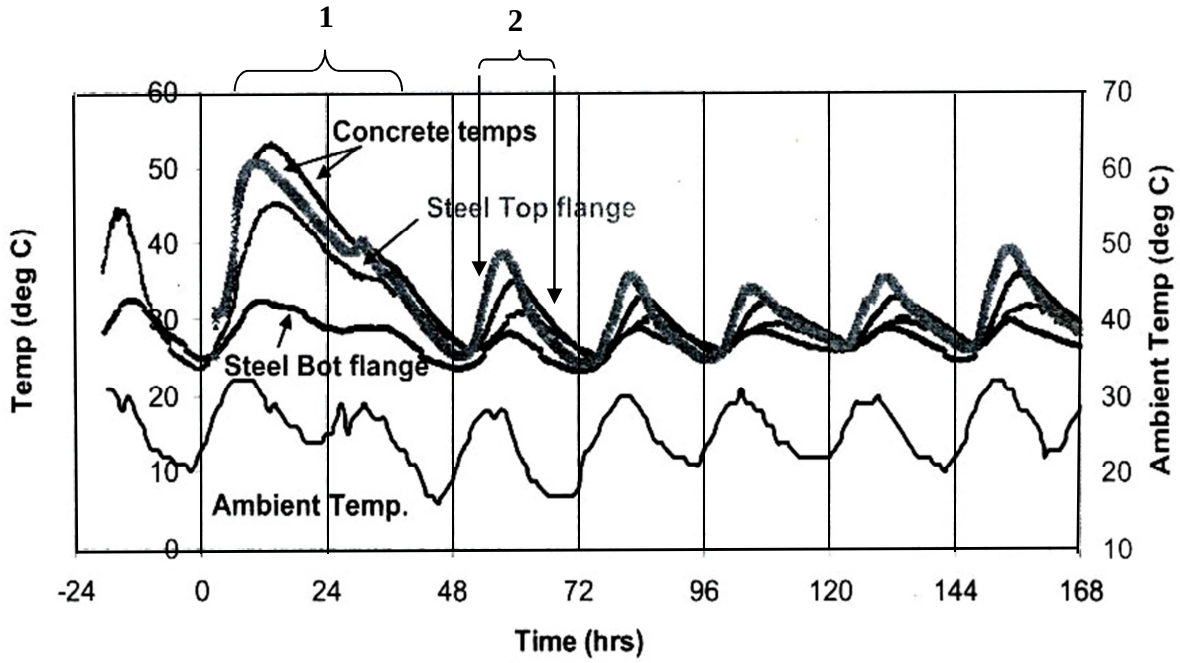

Figure 1.6 Temperature recorded from bridge deck and steel girders (Subramaniam and Agrawal 2009)

The three temperature distributions defined by Krauss and Rogalla (1996) can be identified in Figure 1.6. The concrete reaches its peak temperature about 12 hours after casting began. The peak temperature in the top flange of the steel girder is smaller than in the concrete, and the peak temperature in the bottom flange is even lower. After reaching the peak temperature, both the concrete and the steel girder begin cooling to the ambient air temperature. Because the temperature changes in the

deck are higher than those of the girder, thermal contraction in the concrete is restrained by the girders, inducing tensile stresses in the deck early in the life of the bridge. The temperature changes during the first 48 hours, identified as region 1 in Figure 1.6, result in temperature distribution 1, as defined by Krauss and Rogalla (1996). After 48 hours, when the temperature of the deck and the girder closely followed the ambient air temperature, faster temperature rises and decreases are noted in the top concrete than in the bottom concrete, as shown in region 2 in Figure 1.6. The difference in concrete temperature is most apparent in the morning, when the air temperature begins rising due to solar radiation, and at night, when the air temperature drops. The temperature changes in region 2 match those described as temperature distribution 2 by Krauss and Rogalla (1996).

Analytical work by Babaei and Fouladgar (1996) found that a restrained thermal contraction of 228 microstrain would initiate thermal cracking at an early age.

1.3.3 Settlement Cracking

Settlement cracking occurs as fresh concrete continues to settle after placement and initial consolidation. The concrete above fixed objects, which are steel reinforcing bars in most cases, is restrained from settling, while the rest of the fresh concrete subsides on either side of the object. The restraint of settlement causes local tensile stress around the reinforcing steel, and cracks or weakened planes directly above the reinforcing steel may form. Later, the effect of other factors, such as drying shrinkage and thermal contraction, may be superimposed on cracks or weakened planes caused by settlement, resulting in continuing crack propagation or initiation of new cracks where cracks were not originally visible. Settlement cracking increases with increasing slump, increasing bar size, or reduced concrete cover (Dakhil, Cady, and Carrier 1975). Because settlement cracks form directly above reinforcing bars, they provide a direct path for water and deicing chemicals to the bars.

1.3.4 External Load

Externally applied load, including self weight, dead load, and external live load, can induce tensile stresses in concrete bridge decks that may cause flexural cracking. The tensile stresses caused by traffic, however, are only a small percentage of the stresses caused by concrete shrinkage and thermal contraction (Krauss and Rogalla 1996).

1.4 MATERIAL FACTORS AFFECTING BRIDGE DECK CRACKING

1.4.1 General

Concrete properties affect bridge deck cracking more than any other factors in most bridges (Krauss and Rogalla 1996). Some concretes are more likely to crack than others. Concrete material factors, including cement content, water content, paste volume, cement type, aggregate type, mineral admixtures, chemical admixtures, plastic concrete slump, air content, and compressive strength of hardened concrete have been evaluated by many researchers, either in bridge construction or in laboratory tests. Some of the results are reviewed in this section.

1.4.2 Literature Review

Portland Cement Association (1970): The Portland Cement Association, Bureau of Public Roads, and 10 state highway departments studied concrete bridge deck durability starting in 1961 and produced a series of six reports. In the study, surveys of 1000 randomly selected bridges in eight states and detailed surveys of 70 bridges in four states were conducted. The types and extent of concrete bridge deck deterioration were determined. The types of deterioration included scaling, cracking, surface spalling, and other defects, such as joint spalling and popouts. The causes of scaling, cracking, and surface spalling were discussed in detail based on field and lab

observations. The study concluded that transverse cracking was the predominate type of cracking.

Recommendations were made with regard to concrete mix design: the largest practical maximum size aggregate (MSA) was recommended, in most cases 1-in. (25.4-mm) MSA was recommended to minimize the quantity of required mixing water. A maximum water-cement ratio of 0.44 and minimum cement contents ranging from 583 lb/yd^3 (346 kg/m^3) to 714 lb/yd^3 (424 kg/m^3) for different maximum coarse aggregate sizes, ranging from 1.5 in. to 0.5 in. (38.1 mm to 12.7 mm), were suggested to provide balance between sufficient workability and minimum paste content. By contrast, mixes with lower cement and water contents [cement content close to 540 lb/yd^3 (320 kg/m^3) and a water-cement ratio near 0.45] have been placed successfully in the construction of low-cracking high-performance concrete bridges in Kansas (Lindquist et al. 2008, McLeod et al. 2009). Excessive slump was believed to promote segregation and increase bleeding, drying shrinkage, and cracking tendency. A maximum slump within the range of 2 to 3 in. (50 to 76 mm) was suggested.

Krauss and Rogalla (1996): Krauss and Rogalla (1996) stated that concrete properties affect cracking more than any other factors. Restrained ring tests were used to measure the cracking tendency of different concrete mixtures. In the ring test, concrete is cast against an inner steel ring, which simulates the restraint provided by steel girders. When the concrete shrinkage is restrained, tensile stresses develop in the concrete and cracks are induced. The strain in the steel ring is measured using strain gages and the time-to-cracking of the concrete is determined as the time when an abrupt strain drop is noted. A detailed description of the ring tests procedure is provided in Section 1.6. Krauss and Rogalla concluded that cement content and type, concrete modulus of elasticity, creep, heat of hydration, and aggregate type affected concrete cracking the most.

The restrained ring tests used to determine the effect of water-cement ratio and cement content on cracking indicated that mixes with low cement content [470 lb/yd^3 (280 kg/m^3)], and low water-cement ratio (0.30 and 0.35) had the lowest crack potential; however, these two mixes were cast with no slump while others were cast with measurable slump; in contrast, mixes with high cement content [846 lb/yd^3 (500 kg/m^3)], low water-cement ratio (0.30 and 0.35), and a measurable slump cracked earliest. The study also pointed out that mixes with moderately-high cement content [658 lb/yd^3 (390 kg/m^3) cement] were not dramatically affected by water content or water-cement ratio for water-cement ratios ranging from 0.35 to 0.50. Excluding the two no-slump mixes, Krauss and Rogalla (1996) concluded that concrete with low water-cement ratios and high cement contents are more susceptible to cracking than concrete with high water-cement ratios and low cement contents.

The modulus of elasticity of the concrete greatly affected both thermal and free shrinkage stresses in the test specimens. Because the stresses are equal to product of the modulus of elasticity and the strain, at the same strain, a higher modulus of elasticity translates into higher tensile stresses and increased cracking potential. Four aggregate types were investigated, including lightweight expanded shale, crushed limestone, trap rock, and river gravel. Mixes with these four aggregates were cast with a cement content of 658 lb/yd^3 (390 kg/m^3) and a water-cement ratio of 0.44. The concrete containing the lightweight expanded shale had a modulus of elasticity of 2.1×10^6 psi (14.7 GPa), which is lower than that of the normalweight aggregate mixtures which ranged from 4.0 to 5.0×10^6 psi (27.6 to 34.5 GPa). The concrete containing the expanded shale cracked later (average of 60 days) than the concrete containing trap rock (32 days) or river gravel (20.5 days). The concrete containing limestone had a moderately-high modulus of elasticity, 4.9×10^6 psi (34.0 GPa); no through-thickness cracks were observed through 280 days, but surface cracks, about 1 in. (25 mm) deep, were noted. The behavior of the limestone

concrete indicated that, in addition to concrete modulus of elasticity, aggregate type or shape also plays a role in crack formation.

Krauss and Rogalla (1996) believed that cement properties have a large effect on bridge deck cracking, especially as cement has been ground with greater fineness starting in the 1970s. A survey of portland cement marketed in North America was conducted in 1994. The rates of strength gain of cement in the 1950s and 1990s are compared in Figure 1.7 (Concrete Technology Today 1996). The survey revealed that modern cements gain strength more rapidly than older cements during the first 7 days.

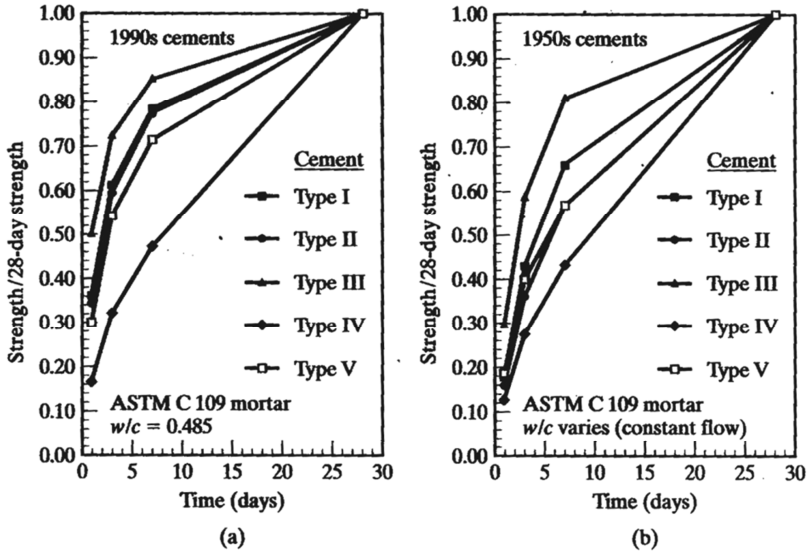

Figure 1.7 Average strength gain curves for portland cement manufactured in (a) the 1990s and (b) the 1950s (Concrete Technology Today 1996)

For Type I and Type II cement, which are usually used for bridge construction, the 1-day strength was about 35 percent of the 28-day strength for 1990s cement, compared to 16 percent for 1950s cement. The rapid strength gain is a direct function of the greater fineness of the newer cements. The early gain in strength, higher modulus of elasticity, and finer pore structure obtained with the finer cements increase the risk of cracking.

Creep has a positive effect on reducing bridge deck cracking as it reduces tensile stresses from restrained drying shrinkage and thermal contraction. Krauss and Rogalla (1996) suggested that concrete with high creep, particularly during the first month after casting, is desirable.

No relationship between cracking tendency and fresh concrete air content or slump was noted in the restrained ring tests.

The use of high compressive strength concrete was believed to result in increased cracking because increased cement content, high paste volume, higher early modulus of elasticity, higher hydration temperature, and much lower creep are normally associated with high strength concrete.

The effect of mineral admixtures, which have been used by many transportation agencies, was investigated. Concrete with a 28% replacement of cement by weight with Class F fly ash did not significantly affect the cracking time (about 4.3 days later than control specimens). For concrete containing 7.5% additional silica fume, the ring specimens cracked 5 to 6 days earlier than the control concrete without silica fume. Chemical admixtures including set accelerators and retarders caused the concrete to crack, on average, two days earlier than control specimens, although individual cracking times varied considerably.

Five different curing conditions were evaluated – no curing (forms were stripped immediately after the concrete reached final set), 6-hour delayed curing (no curing for the first 6 hours after the concrete was cast), 1-day curing (control specimens), 60-day wet curing, and thermally-insulated curing. No difference was observed between 6-hour delayed curing and 1-day curing, and a large scatter in the results was noted for thermally insulated curing. Specimens that were not cured cracked about two days earlier than control specimens. For high cracking tendency mixes [with 846 lb/yd^3 (501 kg/m^3) cement and a water-cement ratio of 0.35], 60-day wet curing delayed the cracking time about nine days compared with 1-day curing.

For mixes with a low cracking tendency [470 lb/yd^3 (278 kg/m^3) cement and a water-cement ratio of 0.50], however, mixed results were noted.

Babaei and Purvis (1996): In a three phase study for the Pennsylvania Department of Transportation, the causes and methods to minimize transverse cracking were investigated. In the first phase, 111 bridge decks in Pennsylvania that were less than 5 years old were visually surveyed for cracking. The surveys indicated that transverse cracking was the most prevalent type. Twelve bridges were surveyed in detail, which included mapping of cracks, measurement of crack width, determination of bar cover and depth, coring of concrete, petrographic examination, and gathering design and construction information. Concrete cores taken at crack locations showed that transverse cracks often intersected coarse aggregate, and it was concluded that cracks occurred in the hardened concrete as opposed to the plastic concrete. The causes of transverse cracking were thought to be shrinkage of hardened concrete instead of plastic shrinkage or settlement cracking.

The study also examined the effects of drying shrinkage and temperature change on cracking. As for parameters affecting drying shrinkage, the water content was not thought to be a primary factor for the 12 surveyed bridges, which had water contents varying from 267 to 292 lb/yd^3 (158 to 173 kg/m^3). Aggregate softness/hardness, as indicated by absorption values ranging from 0.34 percent to 1.17 percent for coarse aggregates and 0.43 percent to 1.97 percent for fine aggregates, was believed to affect shrinkage. Water content and aggregate hardness were analyzed based on the ACI 224R-80, which estimates that drying shrinkage will increase about 3 microstrain per 1-lb/yd^3 (0.59-kg/m^3) increase in water content, and increase from 320 microstrain to 1,160 microstrain (at one year) when the aggregate absorption is increased from 0.3 percent to 5.0 percent. It was determined that the threshold long-term shrinkage (drying shrinkage plus thermal contraction) to initiate cracks was about 400 microstrain, while a thermal contraction of 228 microstrain

would initiate cracking at an early age when enough concrete creep had not been developed to mitigate cracking. Babaei and Purvis also concluded that thermal contraction is primarily affected by the coefficient of thermal expansion of the aggregates. Typically, quartz, sandstone, and gravel have relatively high coefficients of thermal expansion, while limestone has a lower value.

In the Phase 2 of the study, eight newly constructed concrete bridges were evaluated. Thermal contraction was calculated based on recorded concrete temperatures during curing, and drying shrinkage was estimated based on laboratory tests of concrete samples taken from the site. The average spacing between transverse cracks was predicted using an analytical procedure; and the analysis was supported by field surveys of the eight bridges. Babei and Purvis (1996) recommended that to maintain a crack spacing greater than 30 ft (9 m), the 4-month drying shrinkage of unrestrained prism specimens [3 × 3 × 10 in. (76 × 76 × 254 mm)] should be less than 700 microstrain (equivalent to 400 microstrain shrinkage at 28 days), and the thermal contraction should be limited to 150 microstrain by controlling the maximum concrete/girder temperature difference to within 22° F (12° C).

The influence of the aggregate type, cement type, and cement source on drying shrinkage was investigated in the laboratory in the Phase 3 study. Soft aggregates (usually high in absorption and low in specific gravity) yielded high drying shrinkage, and different sources of cement performed quite differently with respect to drying shrinkage, though the study was too limited to suggest specific brands of cement in the report. Type II cement produced less drying shrinkage and less heat generation than Type I cement.

Schmitt and Darwin (1995), Miller and Darwin (2000), and Lindquist, Darwin, and Browning (2005): Three studies involving crack surveys of bridge decks in Kansas were completed and a total of 76 steel girder bridges were surveyed. Most of the bridges were located in northeast Kansas, and the surveys covered three

bridge deck types, those with monolithic, conventional overlay, and silica fume overlays. A standardized crack survey procedure was used in the three studies, which minimized deviations due to the use of different survey crews. Plans, information from construction diaries, mix designs, material test reports, and weather conditions were correlated with the survey results to investigate the factors that contribute to bridge deck cracking.

The investigations showed that a large percentage of cracks occur during the first three years in the life of bridges, but that cracking continues to increase over time. Crack density increases with increases in water content, cement content, and total paste volume. A paste content of less than 27 percent was recommended to limit bridge deck cracking. It was also noted that the least amount of cracking was observed for concrete with air contents greater than 6% in monolithic bridge decks and overlay subdecks, although no correlation between the crack density and the air content in the overlay concrete was observed. Increased compressive strength correlated with increases in bridge deck cracking. For monolithic bridge decks, average crack densities increased from 0.16 to 0.49 m/m^2 as the nominal compressive strength increased from 4500 to 7500 psi (31 to 52 MPa) (Lindquist, Darwin, and Browning 2005). Crack densities also increased as concrete slump increased in monolithic bridge decks, presumably due to the increase in settlement cracking associated with higher slump concrete.

When different bridge deck types were compared, the overall trend in crack performance was that monolithic bridge decks had the best performance, followed by conventional overlay and then silica fume overlay bridge decks. Because of the higher crack densities, Lindquist, Darwin, and Browning (2005) concluded that the application of high-density concrete overlays should be limited. The study by Lindquist et al. (2005) also showed that the chloride content in uncracked concrete

remained below the critical chloride corrosion threshold in most bridges for at least 12 years, regardless of deck type, versus 12 to 24 months at crack locations.

Subramaniam (2009): Five existing NYSDOT bridges built with high performance concrete were used to investigate the influence of in-place concrete properties on bridge cracking. The bridges were single span steel girder bridges (two of which had integral abutments, and the other three were simply supported on elastomeric bearings). All had similar traffic loads. Field surveys identified the approximate locations and patterns of cracks. Core samples from uncracked concrete, cracked concrete, and concrete immediately adjoining the cracks were taken. Image analysis was performed on cracked concrete cores to determine the nature of the cracking – crack width, crack depth from the surface, and crack path through or around the aggregates. Ultrasonic pulse velocity, split cylinder, and compression tests were performed on uncracked concrete cores. The main findings were that the concrete in all surveyed bridge decks had a relatively high tensile strength [greater than 660 psi (4.6 MPa)]; almost all cracks passed around the aggregate particles in the cracked concrete cores, while all load-induced cracks during the splitting tension test in mature concrete passed through the aggregate. It was concluded that the cracks likely formed at an early age. The ages of the bridges at the time of the surveys were not reported.

An analysis of crack paths indicated that for cores taken at longitudinal cracks in three of the five surveyed bridges, 94.7%, 100%, and 100% of the total crack length was around aggregate particles; for cores taken at transverse cracks in two of the five bridges, 61.6% and 74.0% of the total crack length was around aggregate particles. Cracks that pass around aggregate particles normally develop at an early age when the strength of paste is lower than the strength of the aggregates, and cracks that pass through aggregates usually form at a later age when the strength of the paste is higher than the strength of the aggregates. Although not noted by Subramaniam,

the analysis seems to indicate that most of the longitudinal cracks formed at an early age and did not develop much at a later age because almost all the crack lengths (94.7%, 100%, and 100%) were around aggregate particles, while transverse cracks formed at an early age and continued to grow as only part of the crack lengths (61.6% and 74%) were around aggregate particles and the rest were passed through the particles. Similar tests were completed in the study conducted by the Portland Cement Association (Durability 1970). In 46 of the 63 cores taken at transverse cracks, the cracks passed through aggregate particles. In 22 cores taken at longitudinal cracks, the cracks generally passed around aggregate particles in cores taken over longitudinal reinforcing bars and passed through aggregate particles or both around and through aggregate particles in cores taken over void tubes in hollow-slab bridges.

Kovler and Bentur (2009): Kovler and Bentur (2009) investigated the cracking performance of normal strength concrete (NSC) and high strength concrete (HSC). In NSC mixes, water-cement ratios (*w/c*) of 0.45 and 0.70 were used. For the mixes with a *w/c* of 0.70, concrete with cement contents of 490 lb/yd^3 (291 kg/m^3) and 386 lb/yd^3 (229 kg/m^3) were evaluated; for the mixes with a *w/c* of 0.45, concrete with cement contents of 757 lb/yd^3 (449 kg/m^3) and 625 lb/yd^3 (371 kg/m^3) were evaluated. In the HSC mixes, a *w/c* of 0.33 and a cement content of 853 lb/yd^3 (506 kg/m^3) were used. The effect of a shrinkage reducing admixture (SRA) and sealed curing were investigated for the HSC mixes. All specimens were demolded one day after casting and then dried in a controlled environment of 50 ± 4% relative humidity and 68.4 ± 3.6° F (20 ± 2° C). The HSC mixes (with and without SRA) were also cured in a sealed condition. Strength, free shrinkage, and restrained ring tests were performed.

Kovler and Bentur (2009) found that all NSC mixes had similar free shrinkage performance. If the mixes were ranked based on free shrinkage, the mix with a *w/c* of 0.45 and a cement content of 757 lb/yd^3 (449 kg/m^3) had the most free shrinkage,

followed by the mixes having 0.45 *w/c* ratio and 625 lb/yd^3 (371 kg/m^3) cement, 0.70 *w/c* ratio and 490 lb/yd^3 (291 kg/m^3) cement, and 0.70 *w/c* ratio and 386 lb/yd^3 (229 kg/m^3) cement in a 56-day testing period. Although not reported by Kovler and Bentur (2009), the paste contents can be calculated as 34.5%, 28.5%, 29.6%, and 23.3% (assuming the specific gravity of cement was 3.15) for the mixes in the order from highest to lowest free shrinkage. The time to cracking was reported to be between 14 and 21 days for all the NSC mixes, and the mixes with a *w/c* of 0.70 cracked earlier than the mixes with a *w/c* of 0.45. Data for time to cracking was not provided for each mix.

The HSC mixes contained both a lower *w/c* ratio and a higher cement content than the NSC mixes. The time to cracking was approximately 10, 20, 50 days, and no cracking was observed at 90 days for the HSC specimens without an SRA, the HSC specimens with an SRA, the sealed HSC specimens without an SRA, and the sealed HSC specimens with an SRA, respectively. The mixes with the highest to the lowest free shrinkage were, in order, HSC without an SRA, sealed HSC without an SRA, HSC with an SRA, and sealed HSC with an SRA.

1.4.3 Summary of Material Factors Affecting Bridge Deck Cracking

- In most cases, concrete material factors affect bridge deck cracking more than other factors;
- Transverse cracking is the most prevalent type of cracking in bridge decks;
- A large percent of cracks occur relatively early in the life of a bridge;
- Transverse cracks forming at an early age continue to grow at later ages;
- Crack path analysis in concrete cores indicates that longitudinal cracks appear to form at an early age and do not grow much at later ages;
- Cement types and sources affect bridge deck cracking;
- An increase in the concrete modulus of elasticity results in larger thermal and free shrinkage stresses in bridge decks;

- Increased compressive strength results in increased cracking in bridge decks;
- Crack density increases with an increase in water content, cement content, and total paste volume in concrete;
- The largest practical maximum size of coarse aggregate is recommended to provide a balance between sufficient workability and minimum paste content;
- Aggregate type influences both drying shrinkage and cracking potential;
- Increased slump results in increased cracking;

Limited work using the restrained ring tests indicates:

- Creep has positive effects on bridge deck cracking by reducing tensile stresses caused by restraining drying shrinkage and thermal contraction and, thus, reducing cracking potential;
- Concrete with low water-cement ratios and high cement contents are more susceptible to cracking than concrete with high water-cement ratios and low cement contents; concrete mixtures containing silica fume, set accelerators, or set retarders crack earlier, and concrete mixtures containing fly ash crack slightly later than the control mix with cement only;
- High strength concrete (HSC) cracks earlier than normal strength concrete (NSC). When a shrinkage reducing admixture (SRA) is used in HSC, the time to cracking increases as compared with a control HSC mix.

1.5 CONSTRUCTION-RELATED FACTORS THAT AFFECT BRIDGE DECK CRACKING

1.5.1 General

Construction practices affect bridge deck cracking. Based on the field surveys conducted in Kansas (Lindquist et al. 2005), it was noted that some contractors

consistently cast bridge decks with higher crack densities than other contractors, and the date of construction associated with different construction techniques and materials was found to have a measurable impact on bridge deck cracking. Bridge decks constructed in 1980s cracked less than those constructed in 1990s – the explanation is discussed later in the chapter. Cady et al. (1971) found that bridges built by two contractors had a much higher incidence of cracking than bridges built by nine other contractors in Pennsylvania. A list of construction factors that can affect bridge deck cracking were listed and ranked by Krauss and Rogalla (1996); ordered from major effect to minor, they were weather and time of casting, curing period and method, finishing procedures, vibration of fresh concrete, pour length and sequence, construction loads, traffic-induced vibration, and revolutions of the concrete truck. In this section, the influence of factors dealing with construction, including weather and time of casting, curing, placing, consolidation, and finishing on bridge deck cracking, are reviewed.

1.5.2 Weather and Time of Casting

Weather and time of casting were considered as the most critical construction factors affecting bridge deck cracking (Krauss and Rogalla 1996). High wind speed, high air temperature, and low humidity conditions increase the probability of plastic shrinkage cracking, as all these conditions increase the evaporation rate. Extreme high and low air temperatures can induce thermal stresses that make concrete more susceptible to cracking. The influence of weather conditions on crack performance was investigated by Lindquist et al. (2005), and it was found that crack density increased as the maximum air temperature and daily air temperature range on the day of placement increased. Subramaniam and Agrawal (2009) conducted research to evaluate the development of early-age tensile stresses in concrete decks by monitoring the temperature of concrete and steel girders and strain development in newly constructed bridges. Obvious thermal effects in the first 48 hours after casting

were noted due to a rapid concrete temperature rise (from heat of hydration) followed by a period of cooling when the concrete cools to ambient temperature. Concrete contraction during the cooling period after the initial temperature rise was restrained, and tensile stresses were induced in the concrete. After 48 hours, the measured temperatures in the steel girders and the concrete corresponded well with the ambient temperature, and the temperature variations between steel girders and concrete were small. Based on field surveys of 10 prestressed and 8 steel girder bridges, French et al. (1999) stated that bridges exhibited less cracking when the air temperature was between a high of 65° F to 70° F (18° C to 21° C) and a low of 45° F to 50° F (7° C to 10° C), and cracking increased when the range in air temperature on the day of construction was wide. A restrained thermal contraction of 228 microstrain can initiate early age thermal cracking, as reported by Babaei and Purvis (1996).

In hot weather, a concrete temperature above 80° F (27° C) may cause difficulties in placing and finishing, and extra mix water may be added by contractors to maintain the concrete slump. A high evaporation rate is expected during the placement of hot concrete. Crushed ice or other means to cool the concrete should be used in hot weather. Casting at night has also been recommended during hot weather. In cold weather (generally temperatures below 40° F or 4° C), in cases where the concrete is insulated by burlap or plastic during curing, the concrete temperature increases regardless of the low ambient air temperature. The net result is a higher temperature differential between the concrete and the girders, which consequently promotes thermal contraction cracking. To reduce the temperature differential, a method of heating the air underneath the deck to raise the steel girder temperature and/or controlling surface insulation should be used (Durability 1970, Babaei and Fouladgar 1997).

1.5.3 Curing

Proper curing is vital for quality concrete and especially important for bridge deck construction due to the large surface area of a bridge deck. Immediate initiation of curing after finishing is ideal. Early age curing and protection will minimize or prevent plastic shrinkage cracking. The Transportation Research Board (2006) recommended placing wet burlap or cotton mats as soon as possible but no more than 10 to 15 minutes after finishing. When Low-Cracking High-Performance Concrete (LC-HPC) bridge decks are constructed in Kansas, the first layer of presoaked burlap must be placed within 10 minutes after strike off, followed by a second layer within five minutes (Lindquist et al. 2008, McLeod et al. 2009). Wet curing during hot weather can also help cool the concrete and reduce the peak temperature (Krauss and Rogalla 1996).

Extended curing is another essential factor that helps minimize bridge deck cracking. Laboratory tests completed by West, Darwin, and Browning (2010), Deshpande, Darwin, and Browning (2007), and Lindquist, Darwin, and Browning (2008) showed that increased curing time can reduce free shrinkage. West et al. (2010) and Deshpande et al. (2007) found that for concrete (air entrained) cast with limestone coarse aggregate (with an absorption between 2.5 to 3.0%), the difference between shrinkage of concrete cured for 7 days, 14 days, and 28 days is significant, but the difference between 3-day and 7-day cured concrete is small in many cases. Lindquist et al. (2008) found that for concrete mixtures cast with limestone coarse aggregate (with an absorption between 2.5 to 3.0%) and Type I/II cement, increasing the curing period from 7 to 14 days or from 14 to 21 days was approximately equivalent to reducing the paste content by 2%. A reduction in free shrinkage for mixtures containing granite or quartzite coarse aggregate (with absorption less than 0.7%) was also noted when increasing the curing period from 7 to 14 days, although the reduction was not statistically significant. For the mixtures containing mineral

admixtures, such as silica fume, slag, and fly ash, and cast either with low-absorption aggregates (granite and quartzite) or high-absorption aggregate (limestone), longer curing resulted in a decrease in free shrinkage. When concrete containing silica fume (with a volume replacement of cement of 3 or 6%) or slag (with a volume replacement of cement of 30 or 60%) was cast with the low-absorption aggregates, the specimens cured for seven days exhibited more shrinkage than a control mixture with 100% Portland cement; however, specimens cured for 14 days shrank less than a control mixture with 100% Portland cement. A minimum 14-day curing period for all bridge deck placements was recommended.

An extended curing period has also been recommended for cold weather construction. An extra two days of curing was suggested when the average concrete temperature during curing dropped from 70° F to 50° F (Durability 1970).

Some curing methods were suggested in the Portland Cement Association Report (Durability 1970). The methods included covering the entire bridge surface with waterproof curing paper, plastic, damp burlap or other moisture-retaining fabric, and membrane curing with two perpendicular layers of a white-pigmented curing compound. Some of the methods are shown in Figure 1.8.

1.5.4 Placing, Consolidating, and Finishing

Concrete is usually placed with a crane and bucket, conveyor belt, or concrete pump. Considering efficiency, pumping is now the dominant method used to place concrete. To be successful, pumping usually requires concrete with a higher slump and higher paste content than concrete placed by other means. Unfortunately, higher slump increases the potential of settlement cracking and higher paste content leads to

(a) Burlap kept saturated with water is an effective medium for moist-curing

(b) Polyethylene sheets are effective, economical moisture barriers for moist-curing concrete

(c) Liquid membrane-forming compounds sprayed onto the surface are effective, economical moisture barriers for moist-curing concrete

(d) Straw or hay is still used to insulate fresh concrete in freezing weather

Figure 1.8 Curing methods (from http://www.cement.org/basics/concretebasics_curing.asp)

increased drying shrinkage and, subsequently, increased drying shrinkage cracking. In the construction of Low-Cracking High-Performance Concrete (LC-HPC) bridge decks led by the University of Kansas (Lindquist et al. 2008, McLeod et al. 2009), the placement method is not restricted as long as the contractor can demonstrate the ability to efficiently place the concrete prior to deck construction. A mix design with an optimized aggregate gradation plays an important role in producing pumpable concrete with a low slump and paste content. Concretes with a slump of less than 4 in. (100 mm) and cement contents between 540 and 535 lb/yd^3 (320 and 317 kg/m^3) have been pumped successfully on LC-HPC decks.

Adequate consolidation is necessary to minimize settlement cracking. After placement, consolidation helps remove the entrapped air and compact the fresh concrete into the corners of the forms and around the reinforcing steel. When concrete is consolidated by vibration, concrete flows as the coarse aggregate particles move away from the vibrator and the mortar begins to flow between the coarse aggregate particles. For proper vibration, cement paste begins to appear around the vibrator and then the vibrator is withdrawn slowly enough to allow the concrete to close the holes left by the vibrator. Undervibration leaves non-uniform concrete with excessive entrapped air, while overvibration brings excess paste to the surface and causes a loss of entrained air (Mindess et al. 2003). Excess paste on the surface makes the concrete susceptible to having cracking and scaling problems. To ensure adequate consolidation, the Kansas DOT requires the use of multiple vibrators spaced at 1-ft (0.3-m) intervals held in a mechanical system that is capable of uniformly consolidating concrete across the entire bridge deck.

Concrete finishing methods also affect bridge deck cracking. If finishing proceeds slowly, such as by hand, the concrete will be exposed to the environment longer and have more of a chance to develop plastic shrinkage cracking. Excessive finishing will bring more paste to the surface, which leads not only to increased

cracking, but also scaling problems. Lindquist et al. (2005) reported that roller screeds, which are used for virtually all current decks, bring more paste to the surface than vibrating screeds, which were primarily used in the early 1980s.

1.5.5 Summary of Construction-Related Factors that Affect Bridge Deck Cracking

- Construction techniques affect bridge deck cracking;
- Some contractors consistently construct bridges showing more cracks than others;
- As the maximum air temperature or daily air temperature range on the day of placement increases, crack density increases;
- Early application of wet curing and extended curing period are recommended;
- Crushed ice or other means to cool concrete should be used for hot weather concreting;
- Casting at night during hot weather placement is recommended;
- The girders should be heated, and/or the concrete temperature increase due to hydration should be controlled to minimize the temperature differential between deck and girders for cold weather concreting;
- An extended curing period is suggested during cold weather;
- Excessive finishing brings more paste to the surface and causes cracking and scaling problems;
- Optimized aggregate gradations play an important role in producing pumpable concrete with low slump and paste content.

1.6 REVIEW OF RESTRAINED RING TESTS METHODS

Various test methods have been developed to investigate concrete shrinkage and cracking properties, including free shrinkage tests, uniaxial restrained shrinkage tests, and restrained ring tests. Restrained ring tests have the advantages of simplicity and economy and have been used by many researchers. In the restrained ring test, a concrete ring is cast around a steel ring. When the concrete shrinks in a drying environment, the shrinkage is restrained by the inner steel ring and the strain accumulation in the steel ring and the time for cracking are used as indices of the cracking tendency of the concrete. Different geometries and boundary conditions of ring specimens have been used by researchers and are reviewed in this section.

ASTM C1581-04: This test method is designed to "determine the age at cracking and the induced tensile stress characteristics of mortar and concrete under restrained shrinkage." A steel ring with a wall thickness of 0.5 ± 0.05 in. (13 ± 0.12 mm), an outside diameter of 13 ± 0.12 in. (330 ± 3.3 mm), and a height of 6.0 ± 0.25 in. (152 ± 6 mm) is selected as the restraint component. A concrete ring with a wall thickness of 1.5 ± 0.12 in. (38 ± 3 mm) is cast around the steel ring. A minimum of two electrical resistance strain gages oriented in the circumferential direction are used to monitor the strain development in the steel ring.

The shrinkage mechanisms that this test investigates are drying shrinkage, autogenous shrinkage, and thermal stress due to the heat of hydration. The top and bottom surfaces of the concrete ring are sealed to prevent moisture loss while the outside circumferential surface is exposed in a dry environment [temperatures of 73.5 ± 3.5° F (23.0 ± 2.0° C) and relative humidities of 50 ± 4%]. The test results are used to provide a relative comparison of materials and for evaluating the effects of material variations on cracking potential and induced tensile stress, but cannot be used to determine the cracking age of materials in any specific structure, configuration, or exposure condition. A minimum of three test specimens is required for each material

and test condition. The nominal maximum size of coarse aggregate is limited to 0.5 in. (12.5 mm).

Strain in the steel ring is measured and the concrete is visually inspected for cracks during the test. Strain data are gathered at intervals not to exceed 30 minutes, and the specimen is visually inspected for cracks at intervals not greater than 3 days. The age at cracking is determined when a sudden decrease of the compressive strain in the steel ring is noted. The age at cracking can be used to compare the cracking potential of different mixes. If no crack is observed during the test period, the age when the test is terminated is reported.

AASHTO PP 34-99 (1998): This test method is useful "for determining the relative likelihood of early concrete cracking and for aiding in the selection of concrete mixtures that are less likely to crack." The steel ring used in this standard has a wall thickness of 1/2 ± 1/64 in. (12.7 ± 0.4 mm), an outside diameter of 12 in. (305 mm), and a height of 6 in. (152 mm). The steel ring is instrumented with strain gages that are connected to a data acquisition unit that records each strain gage independently. A 3-in. (76-mm) thick concrete ring is cast around the steel ring. A minimum of two specimens for each batch is required. Specimens are kept in a drying condition at a temperature of 73.4 ± 3° F (21.0 ± 1.7° C) and relative humidity of 50 ± 4%. The top and bottom surfaces of the concrete rings are sealed, and the exterior radial surface is exposed.

As in ASTM C1581, the strain in the steel ring is recorded every 30 minutes and the time-to-cracking is determined based on an abrupt decrease in the strain measured by one or more strain gages on the steel rings. Review of the strain measurements and a visual inspection of the concrete ring for cracks are performed every 2 to 3 days. The average results from the specimens cast for the same batch are reported. If the compressive strain in the steel ring decreases gradually after initial

increase and the concrete ring does not crack, the results are reported as “no cracking,” and the age when the test is terminated is reported.

Krauss and Rogalla (1996): Krauss and Rogalla (1996) used restrained ring tests to evaluate the cracking tendency of different concrete mixes. The strain in the steel ring and the time-to-cracking were used to evaluate cracking tendency. Concrete mixes that created less strain on the steel ring and took longer to crack were believed to have a lower cracking tendency. A concrete ring with a 3-in. (76-mm) radial thickness was cast around a steel ring with a 12-in. (305-mm) outside diameter, 3/4-in. (19-mm) radial thickness, and 6-in. (152-mm) height. Krauss and Rogalla (1996) pointed out that the diameter of the steel ring affected the shrinkage restraint provided by the ring and the larger the diameter, the more restraint would be provided. The 12-in. (305-mm) outside diameter of the steel ring was used to provide the approximate shrinkage restraint on a deck (such as those typically provided by large steel girders). For each mixture, two concrete rings, five 4 × 8 in. (100 × 200 mm) cylinders, and two 3 × 3 × 11 in. (75 × 75 × 280 mm) free-shrinkage specimens were cast. After the ring specimens were cast, they were moved to their final testing location (environmental chamber at 72° F (22° C) and 50% relative humidity) and connected to strain gage monitoring equipment. The specimens were removed from forms approximately 24 hrs after casting. The bottom form remained in place while the top surface of the concrete ring was covered with a double layer of polyethylene or rubber to prevent moisture loss. The strain accumulation in the steel rings was recorded automatically every 30 minutes. The concrete rings were carefully examined when a significant change of strain occurred. After a ring cracked, the crack width was measured with a visual crack comparator. The time-to-cracking was reported as the average value for the two specimens. If the compressive stain in the steel ring decreased gradually after the initial increase, the results were reported as “no cracking,” and the age when the test was terminated was reported.

The concrete mixes in the study had the cement contents ranging from 470 to 846 lb/yd^3 (278 to 501 kg/m^3) and water-cement ratios ranging from 0.30 to 0.50. The effects of aggregate type, mineral admixture (Class F fly ash and silica fume), chemical admixture (air entraining agent, set accelerator, and retarders), shrinkage compensating cement, and curing time on cracking tendency were investigated. Most specimens cracked with typical crack widths of 0.002 in. (0.05 mm) or wider.

The average time-to-cracking age was used to compare batches of concrete. For some batches, the cracking age of both specimens was reported. The difference in the time-to-cracking for the two specimens for one mixture ranged from 2 to 15 days, with the average time-to-cracking age ranging from 10 to 20 days.

Some batches had unusual crack paths and compressive strain development in the steel rings. One batch used to investigate the effect of aggregate type was cast with the crushed limestone coarse aggregate, a cement content of 658 lb/yd^3 (390 kg/m^3), and a water-cement ratio of 0.44. The ring specimens showed surface cracks of 1 in. (25 mm) deep that progressed into the central steel ring. No abrupt decrease in compressive strain was observed, but, instead, a gradual loss of strain was recorded. The test was continued for 280 days when the compressive strain became nearly constant. Another batch, containing lightweight expanded shale coarse aggregate, was also cast with a cement content of 658 lb/yd^3 (390 kg/m^3) cement and a water-cement ratio of 0.44. The ring specimens exhibited large external cracks but without a loss of compressive strain in the steel ring. A gradual change in the slope of the compressive strain-time curve was, however, noted. This behavior was explained based on the low modulus of elasticity of the lightweight aggregate, which resulted in low induced compressive stress in the steel rings. When the cracks developed, the low quantity of stored energy was only partially dissipated as the result of cracking and was absorbed through the interlocking aggregates across the crack.

Lange et al. (2003): Steel rings with a height of 6 in. (152 mm) and thicknesses of 3/8, 1/2, and 1 in. (9.5, 12.7, and 25.4 mm) were used in this study. An estimate of the stresses in concrete rings was used to estimate the performance of the concrete due to drying shrinkage.

A model was used to estimate the stresses in the concrete rings. Two stress distributions were superimposed in the model. The first represents the stresses caused by different drying and, therefore, shrinkage rates through the depth of the concrete. A drying gradient results, because the outer concrete (top and bottom surfaces on a bridge deck and circumferential surface on a concrete ring) dries faster than the inner concrete, causing, in turn, a shrinkage gradient through the depth of the concrete, with greater shrinkage in the outer concrete and less shrinkage in the inner concrete. The relatively larger shrinkage in the outer concrete is restrained by the inner concrete. As a result, the outer concrete is placed in tension while the inner concrete is placed in compression. The stress distribution is illustrated in Figure 1.9a for a deck slab drying from the top and bottom surfaces and Figure 1.9b for a ring specimen drying from the circumferential surface.

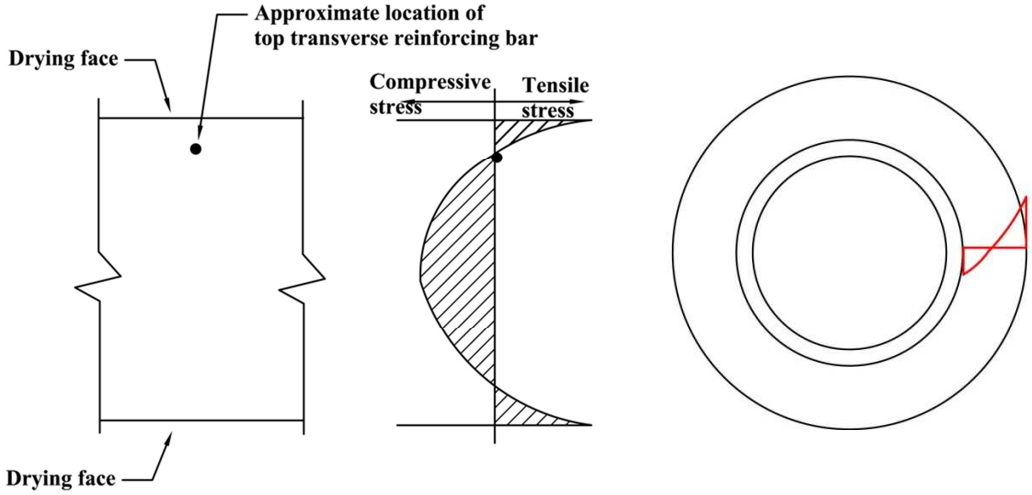

Figure 1.9 Stresses due to drying gradient: (a) stresses through the depth of a deck slab (Durability 1970); (b) stress distributions in a concrete ring (Lange et al. 2003)

The second stress distribution is the stress induced by the girder or the steel ring as they restrain the volume changes of the concrete. When concrete shrinkage is restrained by the girder or steel ring, tensile stresses develop in the concrete. This is illustrated in Figure 1.10a for a deck slab drying from the top and bottom surfaces and in Figure 1.10b for a ring specimen drying from the circumferential surface. For bridge decks, the tensile stresses are greatest at the bottom where concrete is in direct contact with the girders; for the restrained ring tests, the tensile stresses are the most at the inner face where concrete is contact with the steel ring, decreasing outwards, as shown in Figure 1.10b.

The superimposed effects of the two stress distributions represent the actual stresses in the concrete. In the restrained ring tests, Lange et al. (2003) stated that at the onset of drying, high tensile stresses develop at the outer surface of concrete, and

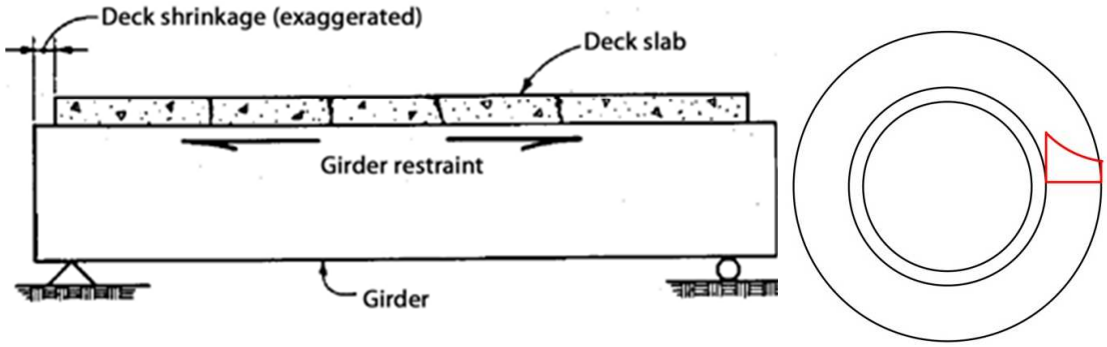

(a) (b)

Figure 1.10 Stresses due to restraint to volume change: (a) Girder restraint to volume change (Durability 1970); (b) Steel ring restraint to volume change (Lange et al. 2003)

the tensile stresses at the inner surface are relatively low. With time, the average total tensile stresses and the tensile stresses at the inner surface increase. Microcracking initiates at regions of highest tensile stress.

Lange et al. (2003) investigated the effects of pozzolanic admixtures on cracking tendency using restrained ring tests. Different combinations of cementitious materials were tested, including 515 lb/yd^3 (305 kg/m^3) of cement with 140 lb/yd^3 (83

kg/m^3) of fly ash, 465 lb/yd^3 (276 kg/m^3) of cement with 145 lb/yd^3 (86 kg/m^3) of fly ash and 25 lb/yd^3 (15 kg/m^3) of silica fume, 545 lb/yd^3 (323 kg/m^3) of cement with 25 lb/yd^3 (15 kg/m^3) of silica fume, and 445 lb/yd^3 (264 kg/m^3) of cement with 90 lb/yd^3 (53 kg/m^3) of fly ash and 25 lb/yd^3 (15 kg/m^3) of silica fume. Lange et al. (2003) could not determine the effect of pozzolans on cracking tendency and suggested that a broader range of the pozzolans content be used in future studies.

Tritsch, Darwin, and Browning (2005): Tritsch et al. (2005) evaluated concrete mixes using free shrinkage and restrained ring tests. The steel ring used in this study had a wall thickness of 0.5 in. (12.7 mm), an outside diameter of 12 ¾ in. (324 mm), and a height of 3 in. (76 mm). In a preliminary test, a concrete ring thickness of 3 in. (76 mm) was used, and the specimens were dried from the top and bottom surfaces; no cracks were observed. Specimens with 2¼-in. (57-mm) concrete ring thickness, dried from the circumferential surface, were used for the balance of the study. A total of 39 rings were cast, and the mixes evaluated included mortar and concrete with low and high paste content. Only one ring cracked – 101 days after casting. The cracked specimen was cast with a concrete mix containing a high cement content, 729 lb/yd^3 (423 kg/m^3), and a low water-cement ratio, 0.37. The free shrinkage and the strain in the gages attached to the steel ring were compared. The analysis indicated that the free shrinkage was a weak predictor of the actual restrained shrinkage. A steel ring thicker than 0.5 in. (12.7 mm) was recommended for future tests to increase the restraint and promote cracking.

Gong et al. (2006): Gong et al. (2006) investigated the cracking performance of high-performance concrete (HPC) mixtures using restrained ring tests. The tests were performed following the AASHTO PP 34-99 (1998) restrained ring test procedure. Two specimens were cast for each batch of concrete, and four strain gages were used to record the strain in the steel ring. All specimens were moved to an environmentally controlled chamber with an air temperature of 73° F (23° C) and a

relative humidity of 50% after they were demolded 24 hours after casting. Three different combinations of cementitious materials were evaluated, including cement with slag and silica fume, cement with fly ash and silica fume, and cement with metakaolin. The effects of water-cementitious material ratio (*w*/*cm*) and type of coarse aggregate were evaluated for each combination of cementitious material. Water-cementitious material ratios of 0.4, 0.35, and 0.3 were investigated, and paste contents of approximate 28%, 31%, and 33% were used for each *w/cm* ratio. Limestone from two sources and gravel from two sources were evaluated. Concrete slump was maintained in a range of 6.0 to 8.5 in. (152 to 216 mm) and the air content was kept between 6% and 8% for all mixes using water reducers and air entraining agents. Compressive strengths were consistently high, ranging from 6,630 to 12,470 psi (45.7 to 86.3 MPa). It was also reported that the concrete containing gravel coarse aggregate had a lower strength than the concrete containing limestone.

Thirty five of 36 specimens cracked. The time-to-cracking indicated that the mixtures with gravel generally cracked 2 to 8 days later than mixtures with limestone. This was believed to be due to the lower modulus of elasticity and higher creep of the mixtures containing gravel. It was also observed that mixes with lower *w/cm* ratios cracked earlier than those with higher *w/cm* ratios. The higher values of the paste content and modulus of elasticity of the low *w/cm* ratio mixes contributed to the higher cracking potential. The differences among the three combinations of cementitious materials were slight.

Hossain and Weiss (2006): Hossain and Weiss (2006) conducted experimental studies to evaluate the effects of specimen geometry and boundary conditions on the stress development and age at cracking in restrained ring tests. Mortars made with Type I cement, water-cement ratios of 0.30 and 0.50, and a fine aggregate volume of 50% were used. All mortar rings had an inner diameter of 12 in. (300 mm) and a height of 3 in. (75 mm). Three series of restrained ring test specimens

were prepared. The first series used steel wall thicknesses of 1/8, 3/8, and 3/4 in. (3.1, 9.5 mm, and 19 mm), and mortar with a constant wall thickness of 3 in. (75 mm) was cast outside the steel rings. The second series used a steel wall thickness of 3/8 in. (9.5 mm) and mortar thicknesses of 1.5, 3, 4.5, and 6 in. (37.5, 75, 112.5, and 150 mm). The third series was used to evaluate different boundary conditions by drying specimens from the circumference and from the top and bottom surfaces. The specimens were dried at 73° F (23° C) and 50% RH after demolding.

It was found that a thicker steel wall provided higher degrees of restraint and higher interfacial pressure (interfacial pressure is the idealized pressure that develops between mortar and steel ring, which pressurizes the inner surface of mortar ring and outer surface of steel ring). Cracking occurred at earlier ages for specimens with thicker steel walls. Restrained ring specimens with a thicker mortar wall cracked later than specimens with a thinner concrete wall. The surface subjected to drying was found to have a significant influence on the results of the restrained ring tests. Specimens that were dried from the top and bottom exhibited higher interfacial pressure than the specimens drying from the circumference due to the relatively higher concrete surface/volume ratio of specimens drying from the top and bottom. However, specimens allowed to dry from the circumferential surface cracked earlier, perhaps due to the added restraint due to shrinkage provided by the mortar itself.

Acoustic emission (AE) tests were used to follow the development and propagation of cracks in the specimens. In AE tests, crack formation is indicated by an increase in the acoustic energy release rate. Interfacial pressure and acoustic energy release rate were compared, and several relationships were observed: initially, as the interfacial pressure between concrete and steel ring increased, the acoustic energy release rate remained constant because no cracks developed; as the interfacial pressure kept increasing, the interfacial pressure began to level off, and an increase of acoustic energy release rate was observed, the latter believed to be the effect of

microcrack formation; when microcracks localized to form a critical length of a single crack, the interfacial pressure showed a sudden downward jump, while the acoustic energy release rate had a sudden increase, and visible cracks formed. Acoustic emission tests indicated that cracks initiated at the outer edge of the rings and propagated toward the inner face when drying from the circumference, and cracks developed in the opposite direction, which developed at inner face first and propagated outward, for drying from top and bottom surfaces.

Subramaniam and Agrawal (2009): Subramaniam and Agrawal (2009) used restrained ring tests to evaluate three high-performance concrete mixes for bridge decks. The concrete ring specimens had an outside radius of 9 in. (228.9 mm), inside radius of 6 in. (152.4 mm) and a height of 3 in. (76.2 mm). Steel rings with two different thicknesses, 1/2 in. (12.7 mm) and 3/4 in. (19.1 mm), were used in this study. Two specimens were cast for each test condition. Casting and finishing of the ring specimens were completed in an environmental chamber at 86° F (30° C) and 40% relative humidity. All specimens were demolded one day after casting and dried from the top and bottom surfaces in the chamber.

Three concrete mixes were evaluated. The first had a *w*/*cm* ratio of 0.40 and the cementitious materials consisted of 506 lb/yd^3 (300 kg/m^3) of cement, 137 lb/yd^3 (81 kg/m^3) of GGBFS (ground granulated blast-furnace slag), and 40 lb/yd^3 (24 kg/m^3) of silica fume. For the specimens with the 1/2-in. (12.7-mm) thickness steel ring, one specimen cracked at 15.9 days and the other did not crack during the 35 days of testing. The specimens with the 3/4-in. (19.1-mm) thick steel ring cracked at 25.8 and 17.9 days. The second mix was similar to the first, except that 42 lb/yd^3 (25 kg/m^3) of fly ash was used in place of the GGBFS and different aggregates were used. No cracks were observed up to 60 days using either the 1/2 or 3/4-in. (12.7 or 19.1-mm) thick steel ring. The third mix, containing 548 lb/yd^3 (325 kg/m^3) of blended cement (cement and silica fume), 135 lb/yd^3 (80 kg/m^3) of fly ash, and a *w*/*cm* ratio of 0.40,

was also tested. The specimens with the 1/2-in. (12.7-mm) thick steel ring cracked at 30.6 and 21.6 days, while the two specimens with the 3/4-in. (19.1-mm) thick steel ring cracked at 26.2 and 12.3 days.

1.7 OBJECTIVE AND SCOPE

Research during the past 40 years has addressed the causes of bridge deck cracking, but only a small number of these findings have been applied in practice. Starting in 2002, a pooled fund study on the construction of crack-free concrete bridge deck was initiated at the University of Kansas to implement this knowledge in bridge deck design and construction. Nineteen states, the Federal Highway Administration (FHWA), the University of Kansas Transportation Research Institute, BASF Construction Chemicals, and the Silica Fume Association have been involved in this research. Fourteen Low-Cracking High-Performance Concrete (LC-HPC) bridges (19 placements) have been built in Kansas. This report is part of that study and includes the following subjects:

1. **Laboratory investigation of concrete material properties**
    - *Free shrinkage tests* to evaluate the effects of curing period, water-cement ratio, mineral admixtures, and shrinkage reducing admixtures on free shrinkage properties;
    - *Evaporable water tests* to correlate the quantity of evaporable and non-evaporable water in hardened concrete with the free shrinkage performance of the concrete (concrete mixtures with 100% Portland cement, fly ash, slag, and a shrinkage reducing admixture are evaluated);
    - *Restrained ring test* to evaluate restrained ring test methods as a function of concrete ring thickness, and investigate the cracking potential of the concrete mixes as a function of water-cement ratio and mineral admixtures.

2. **Low-Cracking High-Performance Concrete (LC-HPC) bridge deck construction experience**
    - Fourteen LC-HPC bridges have been constructed in Kansas. The specifications and construction experience for the LC-HPC bridges are summarized.
3. **Crack Surveys**
    - Standardized crack survey procedures developed at the University of Kansas are described. Crack survey results, including crack maps and crack densities for all LC-HPC bridges and corresponding control bridges, are reported through 2010.
4. **Evaluating bridge performances**
    - The crack survey results are correlated with environmental and site conditions, construction techniques, and material properties.

CHAPTER 2 RESEARCH PROGRAM

2.1 GENERAL

Laboratory tests were performed to investigate the cracking potential of low-cracking high-performance concrete (LC-HPC) mixtures. The amount of evaporable and non-evaporable water in hardened concrete was determined and correlated to the free shrinkage performance of concrete mixtures. The procedures for free shrinkage tests, restrained ring tests, and evaporable and non-evaporable water content tests are described in this chapter. The materials information, including cement, mineral admixtures, coarse and fine aggregates, chemical admixtures, mixture proportions, fresh concrete properties, and compressive strength, are reported for each test.

Low-cracking high-performance (LC-HPC) concrete bridge decks were constructed in Kansas. The implementation of LC-HPC techniques during the bridge construction was recorded. The type of data that was collected during bridge construction is summarized in this chapter, and the results are reported in Chapter 6.

Field surveys were performed for both the LC-HPC bridge decks and corresponding control bridges. The crack survey procedures and the method to determine the crack density of a bridge deck are introduced.

2.2 MATERIALS

This section describes the materials used to develop the LC-HPC mixtures studied in the laboratory.

2.2.1 Cement

Type I/II portland cement meeting the requirements of the ASTM C150 for both Type I normal portland cement and Type II modified portland cement was used in this study. The Type I/II cement was obtained in eight samples over a period of

3½ years. The cement was analyzed by the Ash Grove Cement Company Technical Center in Overland Park, Kansas. The manufacturer, specific gravity, Blaine fineness, X-Ray Fluorescence (XRF) elemental analysis, and Bogue composition for each cement sample are listed in Table A.1 of Appendix A.

2.2.2 Mineral Admixtures

The manufacture, specific gravity, and chemical composition of the mineral admixtures used in this study are listed in Table A.2 of Appendix A.

Fly ash (Class F and Class C) and Grade 120 ground granulated blast-furnace slag (GGBFS) were used as partial replacements of portland cement. The fly ash was obtained in five samples (No. 1 – No. 5). Class F fly ash, samples No. 1 and No. 2, were obtained from Lafarge North America, Chicago, IL, and had a specific gravity of 2.40. Fly ash No. 3, trade name Durapoz® F, was provided by the Ash Grove, Louisville, NE. Durapoz® contains added gypsum ($CaSO_4 \cdot 2H_2O$) and had a specific gravity of 2.87. One batch (batch 680) was cast with fly ash No.4 (also a Durapoz® F), which was contaminated with about 30% cement. The batch was still used to provide information on evaluating the restrained ring test procedure in Chapter 5. The Class C fly ash in sample No. 5 had a specific gravity of 2.83 and was obtained from Ash Grove Resources, LLC, Topeka, KS.

Grade 120 ground granulated blast-furnace slag (GGBFS) was obtained from Lafarge in Chicago and had a specific gravity of 2.90.

2.2.3 Coarse Aggregates

Granite and limestone were used as coarse aggregates. Their properties are listed in Table A.3 of Appendix A. Both aggregates are Kansas Department of Transportation (KDOT) approved materials that were obtained from local concrete providers. A total of ten granite samples and two limestone samples were used in this study.

The sample numbers in Table A.3 are designated consecutively starting with samples used in two previous reports (Lindquist et al. 2008 and McLeod et al. 2009), but only the samples that are used in the current study are reported in Table A.3.

2.2.4 Fine Aggregates

Sand and pea gravel were used as fine aggregates in the mixes. KDOT approved Kansas River sand from the Victory Sand Gravel Company in Topeka, KS, was used. The pea gravel used in this study had the same maximum size as the Kansas River sand [4.75 mm (No.4)] but contained more coarse particles. The pea gravel was obtained from Midwest Concrete Materials in Manhattan, KS and is classified as UD-1 by KDOT.

The specific gravity and gradation for the sand and pea gravel are reported in Table A.4 of Appendix A. As for the coarse aggregates, sample numbers are designated consecutively starting with samples included in work reported by Lindquist et al. (2008) and McLeod et al. (2009).

2.2.5 Chemical Admixtures

Glenium® 3000NS, produced by BASF Construction Chemicals, was used to produce concrete with the desired slump. Glenium® 3000 NS is a high-range water-reducing admixture that meets the requirements of ASTM C-494 for Type A (water reducing) and Type F (high-range water-reducing) admixtures. The solids content ranges from 27 to 33%, and the specific gravity is 1.08.

Micro Air® from BASF Construction Chemicals was used to control the air content of fresh concrete. Micro Air® meets the requirements of ASTM C260, AASHTO M154, and CRS-C 13. It contains 13% solids and has a specific gravity of 1.01.

Tetraguard® AS20, a shrinkage reducing admixture, was selected for the study. Compatible with the air entraining admixture, Micro Air®, Tetraguard® AS20 reduces

drying shrinkage by reducing the capillary tension of the pore water, which is a primary cause of drying shrinkage.

2.3 MIX PROPORTIONING

Optimized aggregate gradations were used for all LC-HPC mixtures to provide improved workability at the low cement and paste contents used for these mixtures. The aggregate gradation was optimized by using a mix design program, KU Mix, which was developed at the University of Kansas. A complete discussion of aggregate optimization using the KU Mix method is discussed by Lindquist et al. (2008).

The KU Mix program can be downloaded from the website http://www.iri.ku.edu/projects/concrete/phase2.html.

2.4 CONCRETE MIXING PROCEDURES

Mixing procedures described in the *Silica Fume User's Manual* (Holland 2005), which were developed primarily for silica fume concrete, were adapted in the current study. The following steps were used:

1) Soak the coarse aggregates for at least 24 hours before mixing.
2) Prepare coarse aggregates in the saturated-surface-dry (SSD) condition in accordance with ASTM C127.
3) Determine the excess free surface moisture of fine aggregates in accordance with ASTM C70, and make corrections in the batch weights, based on the free surface moisture contents of the fine aggregates.
4) Dampen the interior surface of the mixer and add all of the coarse aggregates (SSD condition) and 80% of the mixing water.
5) Add silica fume, if any, to the revolving mixer, and mix for 1½ minutes.
6) Add cement and other mineral admixtures, if used, into the revolving mixer, and mix for 1½ minutes.

7) Add fine aggregates and mix for 2 minutes.
8) Continue mixing the concrete for another 5 minutes, and within the 5 minutes, add the water reducer with 10% of the mixing water in the first 1 minute, followed by the shrinkage reducing admixture, if used, in the next minute. Add the air-entraining admixture with the final 10% of the mixing water during the next minute. Use liquid nitrogen, if necessary, to cool the concrete to approximate 70° F (21° C).
9) Allow the concrete to rest for 5 minutes, and check the concrete temperature.
10) Mix for another 3 minutes, and add extra liquid nitrogen to control the concrete temperature if needed.
11) If a shrinkage reducing admixture is used, allow the mix to rest for 30 minutes followed by one minute of mixing to stabilize the air content.
12) Test and record the slump, air content, and temperature of the fresh concrete.

2.5 FREE SHRINKAGE TESTS

2.5.1 Test Procedures

Specimen Size:

Cold-rolled steel molds purchased from Humboldt Manufacturing Co. (Figure 2.1) were used to produce prisms with dimensions of 3 × 3 × 11¼ in. (76 × 76 × 286 mm). Gage studs were embedded at both ends, providing a gage length of 10 in. (254 mm) (Figure 2.2).

Casting:

Three specimens were cast for each test condition. The concrete was placed in the free shrinkage molds in two layers of approximately equal depth. After each layer of concrete was filled, the concrete was consolidated on a vibrating table with an amplitude of 0.006 in. (0.15 mm) and a frequency of 60 Hz for 20 to 35 seconds.

After the consolidation of the second layer, the extra concrete was struck off using a 2 × 5½ in. (50 ×135 mm) steel screed to get a smooth, flat surface.

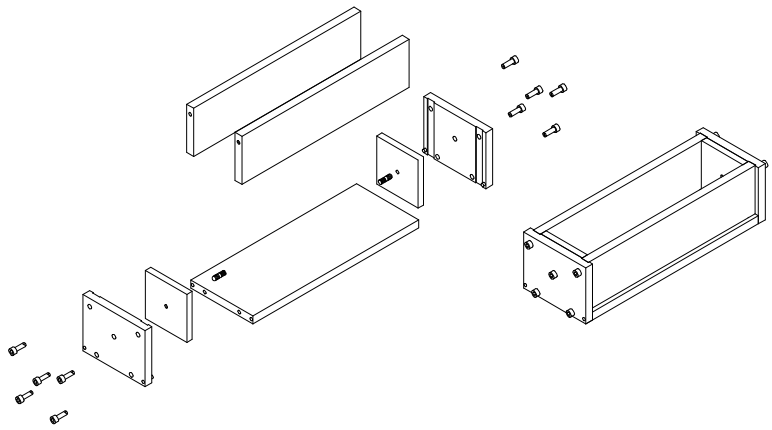

Figure 2.1 Free Shrinkage Molds [Tritsch et al. (2005)]

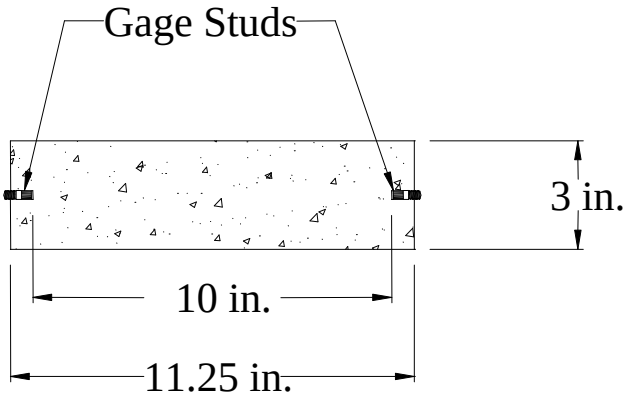

Figure 2.2 Free Shrinkage Specimens [Tritsch et al. (2005)]

Demolding and Curing:

After casting, the specimens were initially cured by covering the top surface with 6 mil (152 µm) Marlex® strips and wrapping the top and sides of each mold with 3.5 mil (89 µm) plastic sheets. The prisms were covered in a series of three using a ½-in. (12.7-mm) thick piece of Plexiglas®.

The specimens were demolded 23½ ± ½ hours after casting, and initial measurements were taken. The specimens were then cured in lime-saturated water prepared in accordance with ASTM C511.

Drying:

At the end of the curing period, the specimens were moved to an environmentally controlled chamber held at 73 ± 3° F (23 ± 2° C) and a relative humidity of 50 ± 4%. The specimens were maintained in this drying environment for a period of 365 days.

Data Collection:

Free shrinkage measurements were taken using a mechanical dial gage length comparator, as shown in Figure 2.3. The comparator has an accuracy of at least of 0.0001 in. (0.00254 mm) and a total range of 0.4 in. (10 mm).

Figure 2.3 Mechanical Dial Gage Length Comparator

Readings were taken when the specimens were demolded and when the specimens were first subjected to drying. Subsequent readings were taken every day for the first 30 days, every other day between 30 and 90 days, once a week between 90 and 180 days, and once a month between 180 and 365 days.

2.5.2 Test programs

Free shrinkage tests included three test programs. The effect of curing period, fly ash, and a shrinkage reducing admixture (SRA) on free shrinkage were evaluated. Three specimens for each test condition were cast.

Free shrinkage specimens along with strength cylinders [4 × 8 in. (100 × 200 mm)] were cast immediately after the slump and air content tests were completed for each batch of concrete. All specimens for the free shrinkage tests were cast with concrete having a slump of 3 ± 1 in. (75 ± 25 mm), an air content of 8.4 ± 0.5 %, and a concrete temperature of 70 ± 3° F (21.1 ± 1.7° C) to minimize the influence of these parameters on free shrinkage performance.

2.5.2.1 Program I (Curing Period)

The effect of curing period on free shrinkage was investigated in Program I. Specimens were cured for 7, 14, 28, and 56 days. Four sets of concrete mixtures were cast, including two control batches with a water-cement ratio of 0.45 and a cement content of 535 lb/yd^3 (317 kg/m^3) and two fly ash batches with a cement replacement of 40% by volume using Class F fly ash and Class C fly ash. The fly ash batches were designed to have the same water-cementitious materials (*w/cm*) ratio (0.45) and the same paste content (24.37% by volume) as the control batches. All batches were cast with granite as the coarse aggregate.

The mixtures are summarized in Table 2.1. The detailed mixture proportions and concrete properties are presented in Table A.5 of Appendix A.

Table 2.1 Free Shrinkage Tests: Program I Test Matrix[1]

Designation	***w/cm***	**Cement Content** lb/yd^3 (kg/m^3)	**Fly Ash Content** lb/yd^3 (kg/m^3)	**Paste Content** % by volume	**Batch Number**
Control 1	0.45	535 (317)	--	24.37	514
40%FA-F[2]	0.45	340 202 ()	173 (103)	24.37	530
40%FA-C[3]	0.45	340 (202)	173 (103)	24.37	557
Control 2	0.45	535 (317)	--	24.37	561

1. Cured for 7, 14, 28, or 56 days. 2. Class F fly ash. 3. Class C fly ash.

2.5.2.2 Program II (Fly Ash and SRA)

The combined effects of fly ash and shrinkage reducing admixture (SRA) on free shrinkage were investigated in Program II. All batches were cast with 0.64 gallon/yd^3 (3.2 L/m^3) of SRA. The control batch had a cement content of 535 lb/yd^3 (317 kg/m^3) and a *w/c* ratio of 0.42. The comparison batches had fly ash replacements of 20% and 40% of cement by volume while maintaining the same *w/cm* ratio and paste content as the control batch. The fly ash was Durapoz® Class F (0.97% gypsum by weight), and granite was used as the coarse aggregate. The specimens were cured for 7 or 14 days.

The mixtures are summarized in Table 2.2, and the detailed mixture proportions and concrete properties are presented in Table A.6 of Appendix A.

Table 2.2 Free Shrinkage Tests: Program II Test Matrix[1]

Designation	***w/cm***	**Cement Content** lb/yd^3 (kg/m^3)	**Fly Ash Content** lb/yd^3 (kg/m^3)	**Paste Content** % by volume	**Batch Number**
Control +SRA	0.42	535 (317)	--	23.42	480
20%FA[2]+SRA	0.42	433 (257)	97 (56)	23.42	482
40%FA[2]+SRA	0.42	329 (195)	197 (117)	23.42	484

1. Cured for 7 or 14 days. 2. Durapoz® Class F fly ash.

2.5.2.3 Program III (SRA)

Program III examined the effect of a shrinkage reducing admixture (SRA) on free shrinkage. Two SRA dosage rates, 0.32 gallon/yd^3 (1.6 L/m^3) and 0.64 gallon/yd^3 (3.2 L/m^3), were investigated with batches containing either 100% cement or 60% cement and 40% Class F fly ash by volume. The batches with 100% cement had a cement content of 540 lb/yd^3 (320 kg/m^3) and a *w/c* ratio of 0.44. SRA dosage rates of 0, 0.32, and 0.64 gallon/yd^3 (0, 1.6, and 3.2 L/m^3), equivalent respectively to 0, 0.5, and 1% by mass of cement, were used. The fly ash batches had the same *w/cm* ratio and paste content (24.12%) as the batches with 100% cement. Three batches

were repeated, as shown in Table 2.3, to check the repeatability of the test results. Granite was used as the coarse aggregate. The specimens were cured for 14 days.

The mixtures are summarized in Table 2.3, and the detailed mixture proportions and concrete properties are presented in Table A.7 of Appendix A.

Table 2.3 Free Shrinkage Tests: Program III Test Matrix[1]

Designation	***w/cm***	**Cement Content** lb/yd^3 (kg/m^3)	**Fly Ash Content** lb/yd^3 (kg/m^3)	**Paste Content** % by volume	**SRA** gallon/yd^3 (L/m^3)	**Batch Number**
Control	0.44	540 (320)	--	24.12	0 (0)	587
Control+0.32SRA	0.44	540 (320)	--	24.12	0.32 (1.6)	588
Control+0.64SRA	0.44	540 (320)	--	24.12	0.64 (3.2)	590
40%FA	0.44	341 (202)	173 (103)	24.12	0 (0)	601
40%FA+0.32SRA	0.44	341 (202)	173 (103)	24.12	0.32 (1.6)	605
40%FA+0.64SRA	0.44	341 (202)	173 (103)	24.12	0.64 (3.2)	594
Control+0.32SRA(R^2)	0.44	540 (320)	--	24.12	0.32 (1.6)	612(repeat 588)
40%FA+0.64SRA(R^2)	0.44	341 (202)	173 (103)	24.12	0.64 (3.2)	595(repeat 594)
40%FA+0.32SRA(R^2)	0.44	341 (202)	173 (103)	24.12	0.32 (1.6)	610(repeat 605)

1. Cured for 14 days. 2. Batches were repeated to check the repeatability of the test results.

2.6 EVAPORABLE AND NON-EVAPORABLE WATER CONTENT TESTS

Concrete shrinkage is related to water loss. A test procedure was developed in this study to evaluate the amount of evaporable and non-evaporable water in hardened concrete, and to investigate the relation between the amount of evaporable water and free-shrinkage performance of concrete.

2.6.1 Test Procedures

Free shrinkage specimens, 3 × 6 in. (75 × 150 mm) cylinders for evaporable and non-evaporable water content tests, and 4 × 8 in. (100 × 200 mm) strength cylinders were cast at the same time for all the batches.

The free shrinkage tests were performed using the procedures described in Section 2.4. In additional, weight loss due to evaporation was determined by weighing the free shrinkage specimens every time when free shrinkage readings were taken.

Strength tests were performed in accordance with ASTM C31 at 28 days.

The procedures developed in this study to evaluate the amount of evaporable and non-evaporable water were as follows.

Specimen Size:

Three 3 × 6 in. (75 × 150 mm) cylinders for each test condition were cast to investigate the amount of evaporable and non-evaporable water.

Casting:

The concrete was placed in 3 × 6 in. (75 × 150 mm) cylinders in two layers of approximately equal depth. Each layer was rodded with a rounded end, 3/8 in. (10 mm) diameter rod 25 times and then tapped 10 to 15 times with a mallet, as prescribed for strength specimens. The upper surface was struck off to obtain a smooth surface.

Demolding and Curing:

After casting, the specimens were initially cured by wrapping the top surface of the molds in two layers of 3.5 mil (89 μm) plastic.

The specimens were demolded 23½ ± ½ hours after casting. The cylinder surface was then placed in the saturated surface dry (SSD) condition by rinsing the cylinder to wet the surface, followed by drying with a dry towel. The weight of the SSD concrete specimens was recorded and designated as $w_{demold,cylinder,SSD}$. In the preliminary tests, cylinder weights at demolding were not taken.

The specimens were then cured in lime-saturated water in accordance with ASTM C511.

Crushing:

At the end of the curing period (designated curing period ± 1 hour), the cylinders were removed from the lime-saturated water. The cylinders were placed in the SSD condition in four steps: (1) the cylinder was rinsed to eliminate any lime that may have been deposited on the surface; (2) any water that may have been trapped in the air voids at the surface of the cylinder was dried using pressurized air; and (3) the cylinder surface was re-wet with a damp towel; and (4) the surface was dried with a dry towel to place it in a surface dry condition. In the preliminary tests, the surface was either prepared in an air-dry condition or with a wet surface that had extra water left in the air voids. The weight of the SSD concrete specimens at the end of curing was recorded and designated as $w_{cured,cylinder,SSD}$.

The concrete cylinders were then crushed to a particle size approximately equal to the original coarse aggregate size in two steps: first the cylinders were broken with a compression machine into large size pieces; these pieces were then crushed into smaller size particles with a sledge hammer. The two steps are shown in Figure 2.4. The weight of the crushed sample was recorded and designated as $w_{cured,crushed,SSD}$. The surface of the containers used in the test were rinsed and then dried before use. Crushing and weighing were completed within 10 minutes to minimize moisture loss.

The difference between $w_{cured,cylinder,SSD}$ and $w_{cured,crushed,SSD}$ was recorded as the weight loss during the crushing operation.

First Step

Second Step

Figure 2.4 Crushing cylinders in two steps

Oven Drying:

The crushed sample was placed in an oven at 221° F (105° C) for 24 ± 0.5 hours, and then removed from the oven and allowed to cool for about 15 minutes at room temperature. After this cooling period, the weight $w_{cured,crushed,OD}$ was recorded.

Ignition Loss:

The oven dry sample was then ignited at 1922° F (1050° C) in a furnace. When the oven dry sample could not be tested immediately, the sample was put in a zip-lock plastic bag with a minimum amount of air left in by pressing most air out, and then placed in a freezer at 0° F (-17.8° C).

A high temperature furnace produced by Thermolyne Thermo Scientific, shown in Figure 2.5, was used for the ignition test. The furnace was set to raise the temperature from 86° F (30° C) to 1922° F (1050° C) in 5 hours, remain at 1922° F (1050° C) for 2 hours, and then cool down to 86° F (30° C) in another 5 hours. The ignition test was run in a nitrogen atmosphere, free of CO_2. Extra-dry nitrogen with a minimum purity of 99.99% (LW 415 produced by Linweld, Inc.) was used.

The weight of the sample after ignition was recorded as $w_{crushed,furnace}$.

A summary of the test procedures is presented in Figure 2.6.

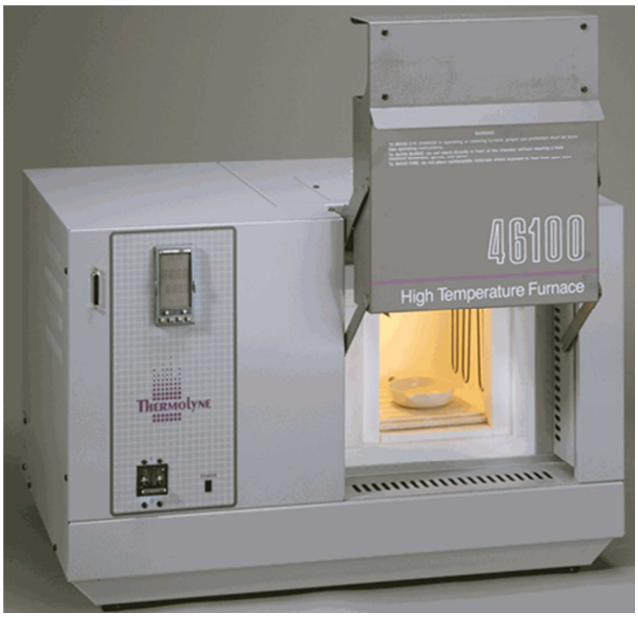

Figure 2.5 High Temperature Furnace

2.6.2 Calculation of Non-Evaporable Water Content

Each solid component (in oven dry condition) in the mixture, including the coarse and fine aggregates and cement, has a weight loss after ignition. The ignition loss rate of these components is determined first using samples of the component. Later when the amount of non-evaporable water is calculated as the total ignition loss of concrete samples, the ignition loss of each component is subtracted from the total loss. The ignition loss of each component, expressed as a fraction of oven dry and ignited weights, are respectively calculated as

$$I'_{fr,component} = \frac{w_{OD,component} - w_{furnace,component}}{w_{OD,component}} \quad (2.1)$$

$$I_{fr,component} = \frac{w_{OD,component} - w_{furnace,component}}{w_{furnace,component}} \quad (2.2)$$

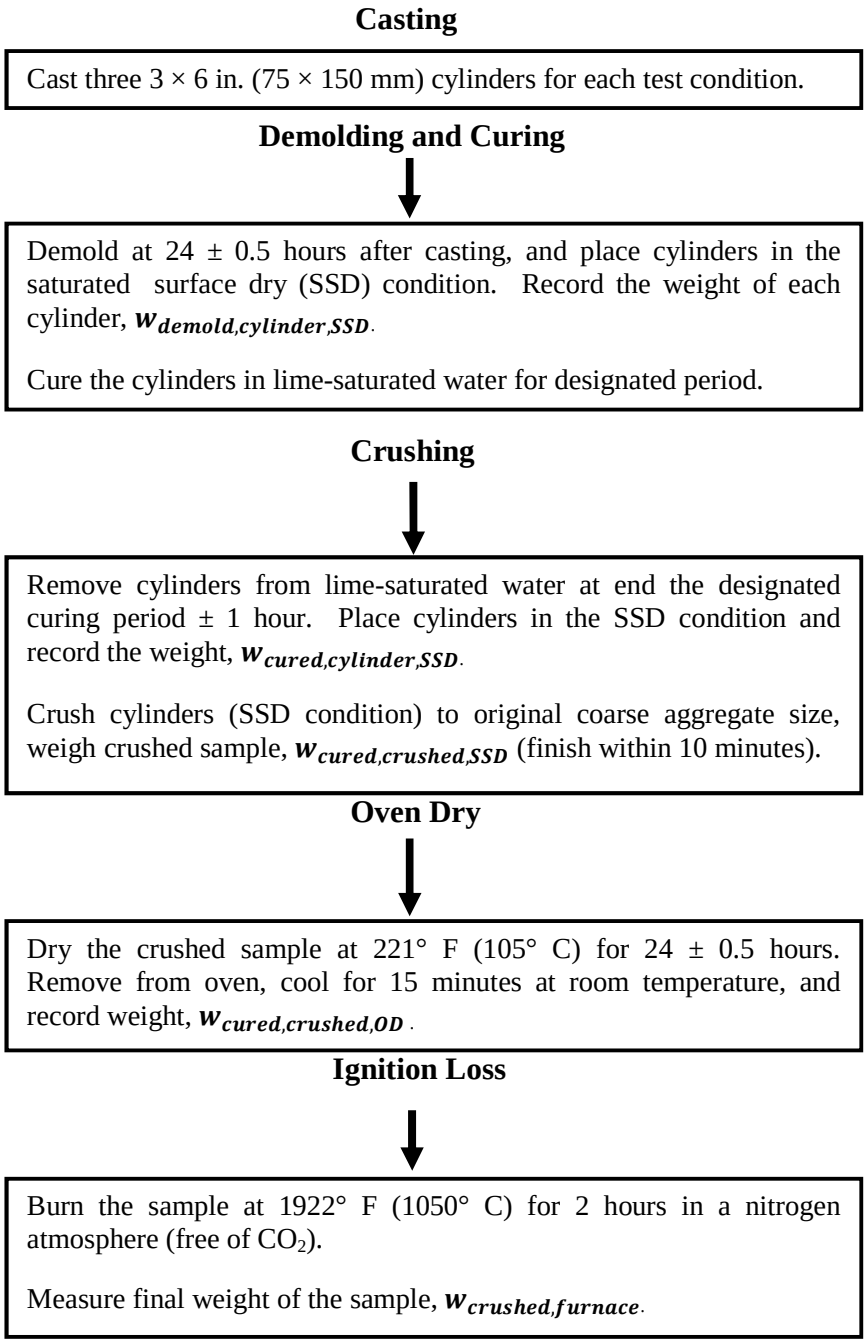

Figure 2.6 Summary of Evaporable and Non-Evaporable Water Content Test Procedures

where

$\boldsymbol{w_{OD,component}}$ = weight of a sample component after oven drying

$\boldsymbol{w_{furnace,component}}$ = weight of a sample component after ignition.

The quantity of evaporable water, expressed as a ratio to the cementitious material content, can be calculated as the difference between the amount of mix water and the amount of non-evaporable water normalized with respect to the weight of the cementitious material. The equivalent determination for non-evaporable water is presented first. Based on the data collected during the test, the non-evaporable water content normalized with respect to the cementitious material content is

$$\frac{\boldsymbol{w_n}}{\boldsymbol{cm}} = \frac{\boldsymbol{w_{cured,crushed,OD}} - \boldsymbol{w_{crushed,furnace}} - \sum \boldsymbol{w_{ignition\ loss,component}}}{(\boldsymbol{w_{crushed,furnace}} + \sum \boldsymbol{w_{ignition\ loss,component}}) \times \boldsymbol{M_{fr,cm,OD}}} \qquad (2.3)$$

where

$\frac{\boldsymbol{w_n}}{\boldsymbol{cm}}$ = non-evaporable water-cementitious material ratio

$\boldsymbol{w_{cured,crushed,OD}}$ = weight of the crushed sample that has finished curing and oven dried for 24 ± 0.5 hours at 221° F (105° C)

$\boldsymbol{w_{crushed,furnace}}$ = weight of the crushed sample after 2-hour ignition at 1922° F (1050° C)

$\boldsymbol{M_{fr,cm,OD}}$ = weight fraction of cementitious materials of all solid materials in the mixture in oven dry condition by weight, which is calculated as

$$\boldsymbol{M_{fr,cm,OD}} = \frac{\boldsymbol{w_{cm}}}{\sum \boldsymbol{w_{component,OD}}} \qquad (2.4)$$

$\boldsymbol{w_{cm}}$ = weight of cementitious materials in the mixture based on yd^3 or m^3

$\boldsymbol{w_{component,OD}}$ = oven dry weight of each solid component in the mixture based on yd^3 or m^3

$\boldsymbol{w_{ignition\ loss,component}}$ = ignition loss of each solid component in the crushed sample, which is calculated as

$$\boldsymbol{w_{ignition\ loss,component} = w_{crushed,furnace} \times M_{fr,component,ignited} \times I_{fr,component}} \quad (2.5)$$

$\boldsymbol{M_{fr,component,ignited}}$ = weight fraction of a component in the mixture, based on ignited weight, = $\frac{\boldsymbol{w_{component,furnace}}}{\sum \boldsymbol{w_{component,furnace}}}$

$\boldsymbol{w_{component,furnace}}$ = ignited weight of a component in the mixture based on yd^3 or m^3, = $\boldsymbol{w_{component,OD}} \times (\boldsymbol{1 - I'_{fr,component}})$.

2.6.3 Calculation of Evaporable Water Content

The quantity of evaporable water in the cement paste constituent of concrete can be calculated in two ways based on the test data. In the first, it is equal to the difference between the original mix water and the non-evaporable water in the cement paste and is designated as w_e; the calculation for w_e is presented in Section 2.6.3.1. In the second, it is equal to the difference in the weight of the concrete when the specimens are demolded 24 hours after casting and the weight after curing is complete and subsequently oven dried at 221° F (105° C), adjusted to account for the water lost from the initially saturated surface dry (SSD) aggregate, and is designated as w'_e; the calculation is presented in Section 2.6.3.2. Because the total water in cement paste increases over time when cement paste is maintained in a saturated condition, the quantity of evaporable water is also determined based on the total water in the cement paste after curing, designated as w_e^*; the calculation is presented in Section 2.6.3.3.

2.6.3.1 Evaporable Water Content as the Difference between the Amount of Original Mix Water and non-Evaporable Water, w_e

The evaporable water within the paste constituent of concrete, calculated as the difference between the original mix water (based on the original mixture proportions) and the non-evaporable water in the cement paste, is designated as w_e. The evaporable water-cementitious material ratio w_e/cm is calculated as

$$\frac{w_e}{cm} = \frac{w_o}{cm} - \frac{w_n}{cm} \tag{2.6}$$

where

$\frac{w_e}{cm}$ =evaporable water-cementitious material ratio based on the difference between the original mix water and the non-evaporable water in the cement paste

$\frac{w_o}{cm}$ = original water-cementitious material ratio based on mixture proportions

$\frac{w_n}{cm}$ = non-evaporable water-cementitious material ratio based on test [Eq. (2.3), Section 2.6.2].

2.6.3.2 Evaporable Water Content as the Quantity Lost During Oven Drying, not including Water Absorbed by the Cement Paste during Curing, w'_e

The evaporable water in the paste constituent of concrete, based on the quantity of water lost during oven drying, is designated as w'_e. It is equal to the difference in the weight of the concrete at demolding (i.e., after 24 hours of curing) and the weight after the curing period has been completed and the specimen has been oven dried, and adjusted to account for the water lost from the aggregate. Because it is based on the weight of concrete at demolding, rather than at the end of curing period, it does not include water absorbed by the cement paste during curing. The evaporable water-cementitious material ratio w'_e/cm is calculated as

$$\frac{w'_e}{cm} = \frac{w_{demold,cylinder,SSD} - w_{cured,cylinder,OD} - \sum w_{oven\ dry\ loss,aggregate}}{w_{demold,cylinder,SSD} \times M_{fr,cm,SSD}} \quad (2.7)$$

where

$\frac{w'_e}{cm}$ = evaporable water-cementitious material ratio based on the quantity of water lost during oven drying, not including water absorbed by the cement paste during curing

$w_{demold,cylinder,SSD}$= weight of concrete cylinder at initial removal from the cylinder mold in the saturated-surface-dry (SSD) condition

$w_{cured,cylinder,OD}$ = equivalent weight of cured concrete cylinder that has been oven dried for 24 ± 0.5 hours at 221° F (105° C). Due to loss of material during crushing and transferring of materials between different containers, there is always some weight difference between the original cylinder and crushed sample weights. The equivalent weight of the oven-dry cylinder, accounting for losses during the crushing operation, can be calculated based on the weight of oven-dry crushed samples as

$$w_{cured,cylinder,OD} = \frac{w_{cured,cylinder,SSD}}{w_{cured,crushed,SSD}} \times w_{cured,crushed,OD} \quad (2.8)$$

where

$w_{cured,cylinder,SSD}$ = weight of the cylinder after curing with the cylinder is placed in the SSD condition

$w_{cured,crushed,SSD}$ = weight of the crushed sample from the cured cylinder in SSD condition. Note that $w_{cured,crushed,SSD}$ is lower than the true value at the end of curing due to water lost during crushing and transferring to the oven. The water loss increases the calculated value of $w_{cured,cylinder,OD}$ in Eq. (2.8), which in turn causes a lower value of w'_e/cm in Eq. (2.7). More discussion is presented in Chapter 4.

$w_{cured,crushed,OD}$ = weight of the crushed sample after oven drying for 24 ± 0.5 hours at 221° F (105° C)

$\boldsymbol{w_{oven\ dry\ loss,aggregate}}$ = water lost from aggregate component from SSD condition during oven drying,

$= \boldsymbol{w_{demold,cylinder,SSD}} \times \boldsymbol{M_{fr,aggregate,SSD}} \times \mathbf{absorption}_{\boldsymbol{fr,aggregate,SSD}}$

where

$\boldsymbol{M_{fr,aggregate,SSD}}$ = aggregate component (SSD condition) as a weight fraction of all components = $\frac{\boldsymbol{w_{aggregate,SSD}}}{\sum \boldsymbol{w_{component,SSD}}}$

$\boldsymbol{w_{aggregate,SSD}}$ = weight of aggregate component in SSD condition in the mix based on yd^3 or m^3

$\boldsymbol{w_{component,SSD}}$ = weight of each component in the mix based on yd^3 or m^3, including cementitious materials, aggregates in SSD condition, and mixing water.

$\mathbf{absorption}_{\boldsymbol{fr,aggregate,SSD}}$ is computed as a fraction by subtracting the oven-dry weight from the saturated-surface-dry weight of the aggregate, and dividing by the saturated-surface-dry weight.

$\boldsymbol{M_{fr,cm,SSD}}$ = cementitious materials as a weight fraction of all components (cementitious materials, aggregates in SSD condition, and mixing water based on yd^3 or m^3).

$$\boldsymbol{M_{fr,cm,SSD}} = \frac{\boldsymbol{w_{cm}}}{\sum \boldsymbol{w_{component,SSD}}} \tag{2.9}$$

2.6.3.3 Evaporable Water Content as Quantity Lost during Oven Drying, based on Total Water Content at the End of Curing, w_e^*

When the quantity of evaporable water is calculated based on the total water in the cement paste in specimens after curing, the corresponding evaporable water is designated as w_e^*. The evaporable water-cementitious material ratio w_e^*/cm is calculated as follows.

$$\frac{\boldsymbol{w_e^*}}{\boldsymbol{cm}} = \frac{\boldsymbol{w_{cured,cylinder,SSD}} - \boldsymbol{w_{cured,cylinder,OD}} - \sum \boldsymbol{w_{oven\ dry\ loss,aggregate}}}{\boldsymbol{w_{demold,cylinder,SSD}} \times \boldsymbol{M_{f,cm,SSD}}} \tag{2.10}$$

where

$\frac{w_e^*}{cm}$ = evaporable water-cementitious material ratio, based on total water content of the cement paste after curing

The calculation of w_e^*/cm is identical to the calculation of w_e'/cm, except that the weight of concrete after curing, $w_{cured,cylinder,SSD}$, is used in Eq. (2.10) in place of the weight of concrete at demolding, $w_{demold,cylinder,SSD}$, in Eq. (2.7).

2.6.4 Total Water Content in the Cement Paste at the End of Curing

The total water content in the paste constituent of concrete at the end of curing is determined as the summation of the non-evaporable and evaporable water (including water absorbed by the paste during curing). Because the weight of the cylinders at demolding [needed for the calculations in Eq. (2.10)] was only measured for two concrete mixtures, an alternative method is needed to calculate the evaporable water content lost during oven drying based on the total water content at the end of curing. That alternative is based on the weight of the cured, crushed material.

$$\frac{w_e^{**}}{cm} = \frac{w_{cured,crushed,SSD} - w_{cured,crushed,OD} - \sum w'_{oven\ dry\ loss,aggregate}}{(w_{crushed,furnace} + \sum w_{ignition\ loss,component}) \times M_{fr,cm,OD}} \quad (2.11)$$

where

$w'_{oven\ dry\ loss,aggregate}$ = water lost from aggregate component from SSD condition during oven drying,

$=(w_{crushed,furnace} + \sum w_{ignition\ loss,component}) \times M_{fr,cm,OD} \times \mathbf{absorption}_{fr,aggregate,OD}$

$M_{fr,aggregate,OD}$ = aggregate component (oven dry condition) as a weight fraction of all solid components = $\frac{w_{aggregate,OD}}{\sum w_{component,OD}}$

$w_{aggregate,OD}$ = weight of aggregate component in oven dry condition in the mix based on yd^3 or m^3

$\mathbf{absorption}_{fr,aggregate,OD}$ is computed as a fraction by subtracting the oven-dry weight from the saturated-surface-dry weight of the aggregate, and dividing by the oven-dry weight.

The same denominator as in Eq. (2.3), which is the equation for w_n, is used in Eq. (2.11). The difference between w_e^*/cm and w_e^{**}/cm is within 0.002 (Chapter 4) .

The total water-cementitious material ratio w_t/cm is calculated as

$$\frac{\boldsymbol{w_t}}{\boldsymbol{cm}} = \frac{\boldsymbol{w_e^{**}}}{\boldsymbol{cm}} + \frac{\boldsymbol{w_n}}{\boldsymbol{cm}} \tag{2.12}$$

As mentioned in Section 2.6.3.2, $w_{cured,crushed,SSD}$ is lower than the actual value due to water lost during crushing and transferring to the oven. Therefore, w_e^{**}/cm [Eq. (2.11)] is lower than the actual value, which, in turn, causes lower value of w_t/cm [Eq. (2.12)]. The results of w_t/cm are presented in Chapter 4.

2.6.5 Test Programs

A total of nine batches were cast in the evaporable and non-evaporable water content test series. The concrete mixtures included those containing 100% cement, those with partial replacements of cement with fly ash or slag cement, and those containing a shrinkage reducing admixture (SRA).

Three 3 × 6 in. (75 × 150 mm) cylinders and three free shrinkage specimens were cast for each test condition immediately after the slump and air content tests were completed. All specimens were batched with concrete having a slump between 1.5 and 3 in. (40 and 75 mm), an air content of 8.4 ± 0.5 %, and a concrete temperature of 70 ± 3° F (21.1 ± 1.7° C), except for two batches cast with fly ash, batches 666 and 677, which had slumps of 6.25 in. (160 mm) and 6.5 in. (165 mm), respectively, without adding a water reducer. To keep all other factors the same as other mixtures, including the paste content, w/cm ratio, similar aggregate optimization, and air content range, the fly ash concrete had to be cast with high slump.

2.6.5.1 Preliminary Tests

The preparation of the cylinder surface influences the amount of water that evaporated during the oven drying process, but has no effect on the ignition loss of the oven-dry concrete samples. In the preliminary tests, the specimen surfaces were either air dry or wet, with water left in the air voids. In addition, the weights of the cylinders at demolding and the free shrinkage specimens were not recorded.

Four batches were cast in the preliminary tests, including two control batches (extra control batch was used to check repeatability), one batch with fly ash, and one batch with slag cement as s partial replacement for portland cement. The control batches had a *w/c* ratio of 0.44 and a cement content of 540 lb/yd^3 (320 kg/m^3), giving a paste content of 24.12%. The fly ash batch had a cement replacement of 40% by volume with Class F fly ash, with the same *w/cm* ratio and paste content as the control batches. The slag batch had a cement replacement of 60% with slag cement by volume, with the same *w/cm* ratio and paste content as the control batches. All batches were cast with granite as the coarse aggregate. Specimens were cured for 1, 3, 7, or 28 days.

The mixtures are summarized in Table 2.4, and the detailed mixture proportions and concrete properties are presented in Table A.8 of Appendix A.

Table 2.4 Evaporable and Non-Evaporable Water Content Tests: Preliminary Test Matrix[1]

Designation	***w/cm***	**Cement Content** lb/yd^3 (kg/m^3)	**Fly Ash Content** lb/yd^3 (kg/m^3)	**GGBFS** lb/yd^3 (kg/m^3)	**Paste Content** % by volume	**Batch Number**
Control 1	0.44	540 (320)	--	--	24.12	662
Control 2	0.44	540 (320)	--	--	24.12	664
FA 1	0.44	341 (202)	173 (103)	--	24.12	666
Slag 1	0.44	223 (132)	--	304 (180)	24.12	667

1. Cured for 1, 3, 7, or 28 days.

2.6.5.2 Evaporable and Non-Evaporable Water Content Tests

The methods for specimen preparation are described in Section 2.6.1.

Five batches were cast, including one control batch, one fly ash batch, two slag batches, and one SRA batch. The control, fly ash, and slag batches had the same mixture proportions as the batches in the preliminary tests (Section 2.5.4.1). The SRA batch had the same mixture proportions as the control batch, except that 0.64 gallon/yd^3 (3.2 L/m^3) of SRA (equivalent to 1% of cement by weight) was used. The specimens were cured for 3, 7, 14, or 28 days.

The mixtures are summarized in Table 2.5, and the detailed mixture proportions and concrete properties are presented in Table A.9 of Appendix A.

Table 2.5 Evaporable and Non-Evaporable Water Content Tests: Test Matrix[1]

Designation	***w/cm***	**Cement Content** lb/yd^3 (kg/m^3)	**Fly Ash Content** lb/yd^3 (kg/m^3)	**GGBFS** lb/yd^3 (kg/m^3)	**Paste Content** % by volume	**Batch Number**
Slag 2	0.44	223 (132)	--	304 (180)	24.12	676
FA 2	0.44	341 (202)	173 (103)	--	24.12	677
Control 3	0.44	540 (320)	--	--	24.12	678
Slag 3	0.44	223 (132)	--	304 (180)	24.12	681
SRA[2]	0.44	540 (320)	--	--	24.12	683

1. Cured for 3, 7, 14, or 28 days. 2. Shrinkage reducing admixture (SRA) dosage of 0.64 gallon/yd^3 (3.2 L/m^3) (equivalent to 1% by weight of cement).

The free shrinkage specimens for the Slag 3 batch and SRA batch (batches 681 and 683), and the 28-day cured free shrinkage specimens for the FA 2 batch and Control 3 batch (batches 677 and 678) were weighed each time the free shrinkage readings were taken. The free shrinkage readings were taken every day for the first 30 days, every other day between 30 and 90 days, once a week between 90 and 180 days, and once a month between 180 and 365 days.

2.7 RESTRAINED RING TESTS

In restrained ring tests, concrete is cast around a steel ring that resists the free shrinkage of the concrete. The compressive strain accumulation in the steel ring is monitored using strain gages that were attached to the inside surface of the ring. The

occurrence of a crack in the concrete is normally indicated by a sudden decrease of the measured compressive strain in the steel. The steel and concrete rings and the data acquisition system are described in this section. The test procedures including casting, curing, and drying practices are also introduced. Concrete mixtures were evaluated in six test programs that are summarized in this section.

2.7.1 Experimental Equipment

Steel Ring Dimensions

A steel ring with an outside diameter of 12.01 ± 0.01 in. (305.05 ± 0.25 mm), a thickness of 1.05 ± 0.05 in. (26.67 ± 1.27 mm), and a height of 6.25 ± 0.05 in. (158.75 ± 1.27 mm) was used.

Concrete Ring Thickness

The thickness of the concrete ring influences the time-to-cracking of a concrete mixture. Different concrete ring thicknesses were evaluated, including 2.5 in. (64 mm), 2 in. (50 mm), 1.5 in. (38 mm), and 1.125 in. (29 mm). The steel ring with the outside mold is shown in Figure 2.7.

Data Acquisition System

CEA-06-250 UW-120 strain gages from Vishay-Measurements Group, Inc. were used to instrument the steel rings. Four strain gages were attached on the inside surface of a ring. The strain gages were spaced at the mid-height of the ring and evenly spaced around the circumference (Figure 2.8). After the strain gages were attached, a layer of M-Coat A (Vishay-Measurements Group, Inc.) and then a layer of wax were used to protect the strain gages from moisture while the concrete was wet-cured. Another layer of Marin Goop (an adhesive sealant) was used on the outside of the wax to prevent mechanical damage to the wax.

Figure 2.7 Restrained Ring Tests Mold

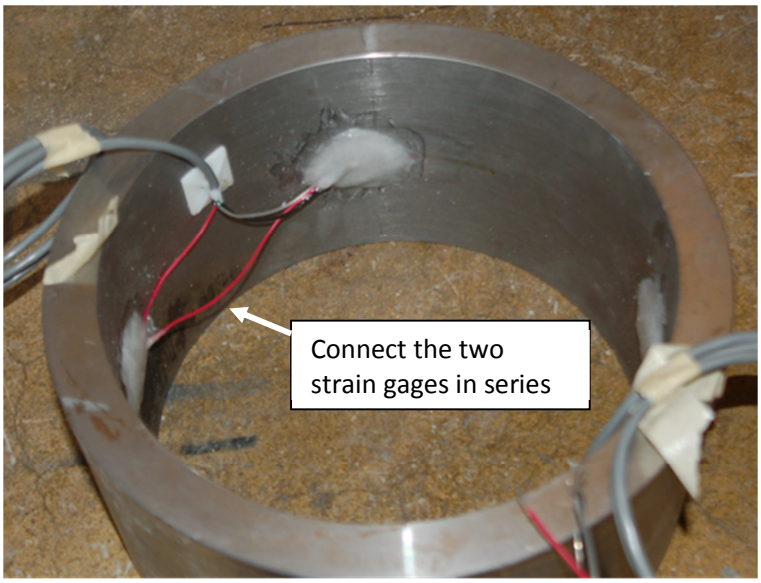

Figure 2.8 Strain Gage Alignments

A National Instrument Corp. data acquisition (DA) system was used. The system included a SCXI 1600 DAQ device, SCXI 1001 chassis, SCXI 1520 modules,

and SCXI 1314 terminal blocks. The DA system was programmed using Labview software to automatically record readings. The compressive strain was recorded once every 30 minutes in this study.

The DA system can be connected to Wheatstone bridge sensors in quarter, half, or full bridge configurations. Both half and quarter-bridge configurations were used at different times in the test. In the half-bridge configuration, two strain gages were connected in series to act as one sensor, as shown in Figure 2.8. The four stain gages on the steel ring acted as two equivalent active sensors and were monitored in a half-bridge configuration. As a result, only one strain reading was obtained from the four strain gages at a time. In the quarter-bridge configuration, the strain gages on the steel ring were monitored by four separate quarter bridges. Four strain readings were obtained at time.

While the half-bridge configuration lowers the number of Wheatstone bridges needed to monitor a ring specimen, it only provides an average result for the two pairs strain gages. If cracks in the concrete are wide and deep enough that the four strain gages note the same release of compressive stress around the steel ring, then the sudden change of compressive strain in the half-bridge configuration is the same as it would be using the quarter-bridge configuration. Otherwise, if only part of the compressive stress is released (as was the usual case), then the strain gage that is nearest to the crack senses the highest strain release, while the other strain gages sense less. In the case of a partial release in stress, the strain change upon crack formation in the half-bridge configuration is lower and less obvious than it is in the quarter-bridge configuration.

To compensate for the influences of temperature on the strain readings, reference rings, which were bare steel rings, were monitored at the same time and in the same environment as the ring with the test specimens. Strain results for concrete

ring specimens are reported as the difference between the strain readings of the test specimens and the average strain readings of the reference rings.

2.7.2 Test Procedures

Free shrinkage specimens, concrete ring specimens, and 4 × 8 in. (100 × 200 mm) strength cylinders were cast at the same time for the tests in Programs I, II, III, and IV, and Program V set 1 (see Section 2.7.3). Only concrete ring specimens and cylinders were cast for the mixtures in Program V sets 2 and 3 and Program VI (see Section 2.7.3).

The free shrinkage tests were performed using the procedures described in Section 2.4. Strength tests were performed in accordance with ASTM C31.

The procedures used for the restrained ring tests are presented in the following sections.

Casting

The concrete was placed in the ring molds in two layers of approximately equal depth, with each layer rodded 75 times using a rounded end rod [diameter 3/8 in. (10 mm)]. The concrete was then consolidated on a vibrating table with an amplitude of 0.006 in. (0.15 mm) and a frequency of 60 Hz for 30 to 40 seconds. Extra concrete was struck off to get a smooth surface.

Demolding and Curing

After casting, the specimens were initially cured by covering the top surface with one layer of 3.5 mil (89 µm) plastic sheets, followed by two layers of wet burlap and another layer of plastic outside. Due to the large area of the top surface of the specimen, the application of the wet burlap helps to prevent the top surface from drying.

The specimens were demolded at 23½ ± ½ hours after casting. During demolding, the specimen surface was kept wet by using a wet sponge.

The specimens were then cured either with wet burlap or in a moist room (complying with the requirements of ASTM C 511) for a designated period. For specimens cured with wet burlap, the specimens were wrapped with at least two layers of burlap and enclosed using a layer of plastic sheeting around. The burlap was checked daily and water was added, as necessary, to keep the burlap wet.

Drying

The concrete rings was allowed to dry from circumferential surface by covering the top and bottom surfaces with foil tape, as shown in Figure 2.9. This drying regime was varied in Program VI, when the specimens were allowed to dry from both the circumferential and top and bottom surfaces.

Different drying conditions were evaluated. Most specimens in this study were dried in an environmentally controlled chamber at 73 ± 3° F (23 ± 2° C) and a relative humidity of 50 ± 4%. For Program V set 3, the specimens were dried in an environmentally controlled chamber at 73 ± 3° F (23 ± 2° C) and a relative humidity of 40 ± 4%., and in program VI, the specimens were dried at 86 ± 3° F (30 ± 2° C) and a relative humidity of 14 ± 4%.

Figure 2.9 Ring Specimen under Drying

Visual check and crack map

The strain accumulation in the steel ring was checked daily. If a sudden strain release was observed, the concrete rings were inspected carefully for cracks. Routine visual checks for cracks were performed every 2 to 3 days. In the early tests (Programs I, II, and III), visual checks were completed with the naked eye, while a hand-held magnifier was used in Programs IV, V, and VI.

Once a crack was located, the date and crack width were recorded. A crack map (Figure 2.10), indicating crack width and crack path, was used to document the cracks. The results are presented in Chapter 5.

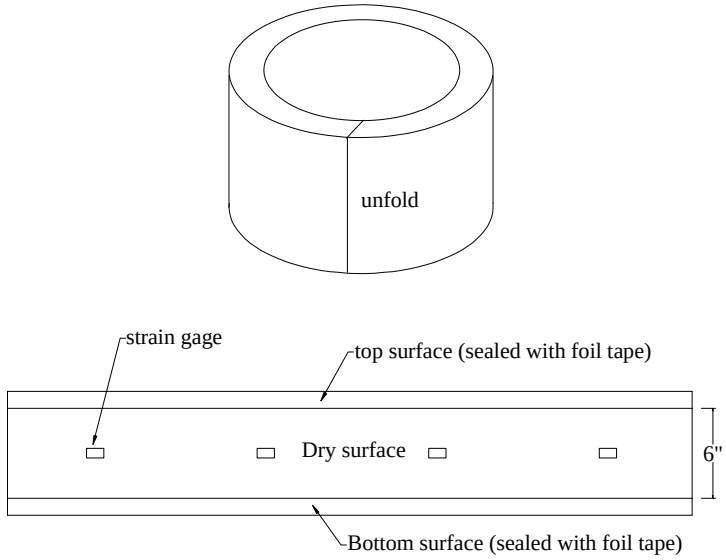

Figure 2.10 Ring Tests Crack Map (strain gages are on the inside surface of the steel ring)

2.7.3 Test Programs

A total 79 concrete ring specimens were cast in 25 batches, representing six programs in which different concrete ring thicknesses and drying conditions were evaluated.

A minimum of three ring specimens were cast for each test condition immediately after the slump and air content tests were conducted. All concrete mixtures in Programs I, II, III, and IV had a slump of 3 ± 1 in. (75 ± 25 mm) and an air content of

8.4 ± 0.5 %, with the exception of batch 566 in Program IV, which had a slump of 4.25 in. (110 mm), and batches 485 and 496, representing KDOT concrete, which had slumps of 6.0 in. (150 mm) and 7.0 in. (180 mm), respectively. Many mixtures in Programs V and VI had a higher paste content than those in Programs I, II, III, and IV, and the slumps of these mixtures were high without adding a water reducer. Mixtures with a wider range of slumps and air contents were used in Programs V and VI. Concrete temperatures at the time of casting were not controlled in Programs I and II and were influenced by the air temperature, while concrete temperatures were maintained at 70 ± 3° F (21.1 ± 1.7° C) in Programs III, IV, V, and VI, except for batches 651 and 652 in program V set 2, which had temperatures of 77° F (25° C) and 75° F (24° C), respectively. Fresh concrete properties are presented in Table A.10 through Table A.16 of Appendix A.

2.7.3.1 Program I [2.5 in. (64 mm) concrete ring]

The concrete in first series of restrained rings was 2.5 in. (64 mm) thick. The effect of *w/c* ratio on cracking tendency was evaluated using batches with *w/c* ratios of 0.45, 0.42, and 0.39. All three mixtures contained 535 lb/yd^3 (317 kg/m^3) of cement and used granite as the coarse aggregate. The reduction in the *w/c* was obtained by reducing the water content and replacing the water with an equal volume of aggregate. Specimens were cured for 7 or 14 days. A concrete typical of that used in the past for decks by Kansas Department of Transportation (KDOT) was cast using limestone coarse aggregate, a *w/c* ratio of 0.44, and 602 lb/yd^3 (357 kg/m^3) of cement. The KDOT specimens were cured for 7 days, matching the curing period used by KDOT prior to 2011.

The concrete mixtures are summarized in Table 2.6, and the detailed mixture proportions and concrete properties are presented in Table A.10 of Appendix A.

Table 2.6 Restrained Ring Tests: Program I Test Matrix

Designation	*w/c*	Cement Content lb/yd^3 (kg/m^3)	Paste Content % by volume	Batch Number
KDOT[1]	0.44	602 (357)	26.89	485
0.45*w/c*[2]	0.45	535 (317)	24.37	488
0.42*w/c*[2]	0.42	535 (317)	23.42	490
0.39*w/c*[2]	0.39	535 (317)	22.47	494

1. Limestone coarse aggregate. Cured for 7 days
2. Granite coarse aggregate. Cured for 7 or 14 days.

2.7.3.2 Program II [2.5 in. (64 mm) and 1.5 in. (38 mm) concrete rings]

The effect of concrete ring thickness on time to cracking was investigated in Program II. Rings with thicknesses of 2.5 in. (64 mm) and 1.5 in. (38 mm) were cast at the same batches. Two batches cast in Program I were repeated, including the batch with granite coarse aggregate, a *w/c* ratio of 0.45, and 317 kg/m^3 (535 lb/yd^3) of cement, and the KDOT batch with limestone coarse aggregate, a *w/c* ratio of 0.44, and 357 kg/m^3 (602 lb/yd^3) of cement.

The concrete mixtures are summarized in Table 2.7, and the detailed mixture proportions and concrete properties are presented in Table A.11 of Appendix A.

Table 2.7 Restrained Ring Tests: Program II Test Matrix

Designation	*w/c*	Cement Content kg/m^3 (lb/yd^3)	Paste Content % by volume	Batch Number
KDOT[1]	0.44	357 (602)	26.89	496
0.45*w/c*[2]	0.45	317 (535)	24.37	509

1. Limestone coarse aggregate. Cured for 7 days. 2. Granite coarse aggregate. Cured for 14 days.

2.7.3.3 Program III [1.5 in. (38 mm) concrete ring]

Rings with a thickness of 1.5 in. (38 mm) were used to evaluate the effect of water-cement ratio and fly ash on cracking tendency. The mixture proportions used in Program I for batches with *w/c* ratios of 0.45, 0.42, and 0.39 were used. The batch with a *w/c* ratio of 0.45 also served as a control batch for the mixture containing fly ash. The fly ash batch was cast with a 40% volume replacement of cement with Class

F fly ash, but at the same *w/cm* ratio and paste content as the control batch. All specimens were cured for 14 days.

The concrete mixtures are summarized in Table 2.8, and the detailed mixture proportions and concrete properties are presented in Table A.12 of Appendix A.

Table 2.8 Restrained Ring Tests: Program III Test Matrix

Designation	***w/cm***	**Cement Content** lb/yd^3 (kg/m^3)	**Fly Ash** lb/yd^3 (kg/m^3)	**Paste Content** % by volume	**Batch Number**
0.39*w/c*	0.39	535 (317)	--	22.47	532
0.45*w/c*	0.45	535 (317)	--	24.37	537
0.45*w/c*(R)	0.45	535 (317)	--	24.37	539(repeat 537)
0.42*w/c*	0.42	535 (317)	--	23.42	544
40%FA+0.45*w/c*	0.45	340 (202)	173 (103)	24.37	545

Note: Granite coarse aggregate. Cured for 14 days.

2.7.3.4 Program IV [1.125 in. (29 mm) concrete ring]

Three batches were cast to investigate the effects of *w/c* ratio and fly ash on cracking tendency. A ring thickness of 1.125 in. (29 mm) was used. The control batch with a *w/c* ratio of 0.45 was compared with one batch with a *w/c* ratio of 0.35 and another batch with a 40% replacement of cement with Class F fly ash. The two batches examining the effect of *w/c* ratio contained a cement content of 535 lb/yd^3 (317 kg/m^3) but different water contents. The fly ash batch had the same *w/cm* ratio and paste content as the control batch. All specimens were cured for 14 days.

The concrete mixtures are summarized in Table 2.9, and the detailed mixture proportions and concrete properties are presented in Table A.13 of Appendix A.

Table 2.9 Restrained Ring Tests: Program IV Test Matrix

Designation	***w/cm***	**Cement Content** lb/yd^3 (kg/m^3)	**Fly Ash** lb/yd^3 (kg/m^3)	**Paste Content** % by volume	**Batch Number**
0.45*w/c*	0.45	535 (317)	--	24.21	563
40%FA+0.45*w/c*	0.45	338 (200)	172 (102)	24.21	566
0.35*w/c*	0.35	535 (317)	--	21.04	568

Note: Granite coarse aggregate. Cured for 14 days.

2.7.3.5 Program V [2.0 in. (50 mm) concrete ring]

A ring thickness of 2.0 in. (50 mm) was used for Program V. While the half Wheatstone bridge configuration was used in the previous four Programs, a quarter Wheatstone bridge configuration was evaluated in Program V. Mixtures with high paste contents and the effect of different drying environments were evaluated.

Program V Set 1 (half vs. quarter bridges)

Two batches were cast to compare the half and quarter Wheatstone bridges. Four ring specimens were cast for each batch, with two specimens each in the half and quarter-bridge configurations. One batch was cast with a low paste content [24.21% by volume, a *w/c* ratio of 0.45, and 535 lb/yd^3 (317 kg/m^3) of cement] while the other batch was cast with a high paste content [32.99% by volume, a *w/c* of 0.45, and 729 lb/yd^3 (432 kg/m^3) of cement]. The low paste content batch contained a high-range water reducer and had a slump of 3.75 in. (95 mm) and an air content of 8.4%, while the high paste content batch did not contain a water reducer and had a slump of 8.0 in (205 mm) and an air content of 6.4%. Both batches were cast with granite coarse aggregate and cured for 14 days.

The concrete mixtures are summarized in Table 2.10, and the detailed mixture proportions and concrete properties are presented in Table A.14 of Appendix A.

Table 2.10 Restrained Ring Tests: Program V Set 1 Test Matrix

Designation	***w/c***	**Cement Content** lb/yd^3 (kg/m^3)	**Paste Content** % by volume	**Batch Number**
C535+0.45*w/c*	0.45	535 (317)	24.21	597
C729+0.45*w/c*	0.45	729 (432)	32.99	598

Note: Granite coarse aggregate. Cured for 14 days.

Program V Set 2 (high paste content mixes)

The concrete mixtures with high paste content were evaluated with 2-in. (50-mm) thick concrete rings. The first batch (batch 649) had a cement content of 700 lb/yd^3 (514 kg/m^3) and a *w/c* ratio of 0.35. The second batch (batch 650)

contained a 40% volume replacement of cement with Class F fly ash and had the same *w/cm* ratio and paste content as the first batch. The first two batches were air-entrained. The third batch (batch 651) contained the same cement content as the first batch but had a *w/c* ratio 0.44. The final batch (batch 652) had a 40% class F fly ash volume replacement of cement with the same *w/cm* ratio and paste content as the third batch. An air entraining agent was not used in the last two batches (batches 651 and 652).

The concrete mixtures are summarized in Table 2.11, and the detailed mixture proportions and concrete properties are presented in Table A.15 of Appendix A.

Table 2.11 Restrained Ring Tests: Program V Set 2 Test Matrix

Designation	***w/cm***	**Cement Content** lb/yd^3 (kg/m^3)	**Fly Ash** lb/yd^3 (kg/m^3)	**Paste Content** % by volume	**Batch Number**
0.35*w/c*	0.35	700 (415)	--	27.53	649
40%FA+0.35*w/c*	0.35	439 (260)	223 (132)	27.53	650
0.44*w/c*	0.44	700 (415)	--	31.26	651
40%FA+0.44*w/c*	0.44	442 (262)	224 (133)	31.26	652

Note: Granite coarse aggregate. Cured for 14 days.

Program V Set 3 (different drying environment)

The specimens in Program I through Program IV and Sets 1 and 2 of Program V were dried at 73 ± 3° F (23 ± 2° C) and a relative humidity of 50 ± 4%. In this set, three concrete mixtures were tested at 73 ± 3° F (23 ± 2° C) and a relative humidity of 40 ± 4%. One mixture had a cement content of 540 lb/yd^3 (320 kg/m^3) and a *w/c* ratio of 0.44, while the other two had a cement content of 535 lb/yd^3 (317 kg/m^3) with *w/c* ratios of 0.45 and 0.35.

The concrete mixtures are summarized in Table 2.12, and the detailed mixture proportions and concrete properties are presented in Table A.16 of Appendix A.

Table 2.12 Restrained Ring Tests: Program V Set 3 Test Matrix

Designation	*w/c*	Cement Content lb/yd^3 (kg/m^3)	Paste Content % by volume	Batch Number
C540+0.44*w/c*	0.44	540 (320)	24.12	635
C535+0.45*w/c*	0.45	535 (317)	24.21	636
C535+0.35*w/c*	0.35	535 (317)	21.04	637

Note: Granite coarse aggregate. Cured for 14 days.

2.7.3.6 Program VI [2.5-in. (64-mm) concrete ring and severe drying environment]

Two and a half inch (64 mm) thick concrete ring specimens were dried at 86 ± 3° F (30 ± 2° C) and a relative humidity of 14 ± 4%. The specimens were dried from the circumferential and top and bottom surfaces instead of only on the circumferential surface as in Program I through Program V.

Two concrete mixtures were evaluated. One was a control batch with a cement content of 540 lb/yd^3 (320 kg/m^3) and a *w/c* ratio of 0.44. The other contained a 40% volume replacement of cement with class F fly ash and had the same *w/cm* ratio and paste content as the control batch.

The concrete mixtures are summarized in Table 2.9, and the detailed mixture proportions and concrete properties are presented in Table A.17 of Appendix A.

Table 2.13 Restrained Ring Tests: Program VI Test Matrix

Designation	*w/cm*	Cement Content lb/yd^3 (kg/m^3)	Fly Ash lb/yd^3 (kg/m^3)	Paste Content % by volume	Batch Number
0.44*w/c*	0.44	535 (320)	--	24.12%	679
40%FA	0.44	340 (202)	173 (103)	24.12%	680

Note: Granite coarse aggregate. Cured for 14 days.

2.8 DATA COLLECTION DURING CONSTRUCTION OF LC-HPC BRIDGE DECKS

Specifications covering requirements for aggregates, concrete, and construction practices were written to guide the construction of LC-HPC bridge decks in Kansas. The specifications are presented in Chapter 6. The degree to which the

specifications were implemented during bridge construction was checked and recorded by the research team from the University of Kansas. The information is evaluated to examine the applicability of the LC-HPC specifications and determine what parameters affect bridge deck cracking.

2.8.1 Plastic Concrete Properties

During bridge deck construction, truck identification number, truck discharge time, and concrete volume in each truck were recorded and used later to check the concrete delivery rate and determine the approximate location on the deck where concrete from specific trucks was placed. Plastic concrete properties, tested either out of the truck or on the deck after delivery by pump or other methods, were recorded. The concrete slump, air content, unit weight, and temperature were tested at a frequency determined prior to the construction. A plan for sampling and testing of concrete during construction is included in the concrete specification for LC-HPC bridge decks. Compressive strength cylinders were cast by the KDOT inspection crew and the source (truck) of the concrete and number of cylinders were recorded. Air temperature was taken and recorded along with concrete temperature. Any observations or notes for interest, such as delays in concrete delivery or concrete that was suspected of being out specification when the concrete was not sampled, were also recorded.

The template for recording field date is presented in Table B.1 of Appendix B.

2.8.2 Time of Burlap Placement

The construction specification for LC-HPC bridge decks requires that the concrete be covered with the first layer of saturated burlap within 10 minutes of the strike off and with the second layer of saturated burlap within another 5 minutes. The times required to place the burlap were recorded using observation stations that were selected, in advance, by the recorder. Typically, the observation stations were spaced

evenly along the bridge, such as evenly 10 ft (3 m). The times of concrete placement, concrete strike-off, and placements of the first and second layers of saturated burlap were recorded. In some cases, both layers of burlap were placed at the same time. The time difference between the strike-off and the first layer of burlap placement was considered to be "the time used for burlap placement." Other items that were noted included burlap condition (saturated, dry, or partially wet), burlap placement delays and possible reasons for the delay, and areas that were not fully covered by burlap, and as well any other observations considered to be of interest.

The template for recording burlap placement is presented in Table B.2 of Appendix B.

2.8.3 Site Weather Conditions

The evaporation rate prior to casting the deck and at least one reading per hour during placement were recorded. The evaporation rate was determined using Figure C.1 in Appendix B (which is also included in the construction specifications for LC-HPC bridge decks) as a function of the air temperature, wind speed, relative humidity, and concrete temperature. Air temperature, wind speed, and relative humidity were recorded approximately 12 in. (0.3 m) above the surface of the deck.

The temperature of the steel girders during a bridge deck construction was occasionally checked using an infrared thermometer. The temperatures at the top flange, the middle of the web, and the bottom flange were recorded.

The template for recording site weather conditions is presented in Table B.3 of Appendix B.

2.8.4 Construction Notes and Data Collection after Construction

Construction notes, written by all attendees from the research group, cover all aspects of interest during construction, including an overall summary of concrete properties, placement methods, consolidation and finishing techniques, and curing

strategies, along with the efficiency of these methods was evaluated. Comments by concrete suppliers, contractors, bridge owners, and inspectors, and the lessons learned were also summarized.

Copies of concrete trip tickets, date of form removal, and cylinder strengths were obtained after bridge construction.

2.9 CRACK SURVEYS

On-site crack surveys were performed once per year to evaluate cracking for each low-cracking, high-performance concrete and control bridge deck. A standard procedure, described in previous reports (Schmitt and Darwin 1995, Miller and Darwin 2000, Lindquist, Darwin, and Browning 2005 and 2008, McLeod, Darwin, and Browning 2009) was used in this study and is summarized below.

Site Conditions: Surveys are only conducted on days that are at least mostly sunny with a temperature of no less than 60° F (16° C). The bridge deck must be completely dry before the survey can begin. At least one side (or one lane) of the bridge is closed to traffic when the crack survey is performed.

Crack Tracing: Three to five inspectors perform a crack survey. Using chalk or a lumber crayon, inspectors mark cracks that can be seen while bending at the waist, and once a crack is identified, the inspector continues to trace the crack to the end, even if parts of the crack are not initially visible while bending at the waist. At least two inspectors check each section of the deck.

Transferring Cracks to Paper: Cracks are transferred to a scaled plan drawing of the deck, using a scale of exactly 1 in. = 10 ft and using a 5 ft by 5 ft grid placed on the bridge deck surface prior to crack identification. The scaled drawing with cracks, or crack map, is used to determine the crack density.

Crack Density Determination: The crack density, expressed in linear meters of cracks per square meter of the bridge deck, is determined from the crack map. The crack map is digitally scanned at 100 dots per inch (dpi) so that the crack lines can be recognized as

adjacent pixels. In the digital picture, any lines that do not represent cracks are erased. Crack length is calculated using a program that tracks the number of adjacent pixels, and translates the number of pixels back to crack length. The crack density is determined by dividing the sum of all crack lengths (m) by the deck surface area (m^2). The crack density determination program is presented by Lindquist, Darwin, and Browning (2005).

A draft of the bridge deck survey specification is provided by Lindquist, Darwin, and Browning (2005) and updated by Gruman, Darwin, and Browning (2009). The updated bridge deck survey specification is present in Appendix C.

CHAPTER 3 FREE SHRINKAGE RESULTS AND EVALUATION

3.1 GENERAL

The primary goal of this chapter is to present the results of the investigation of the free shrinkage performance of concrete containing fly ash (as partial replacement of cement). Fly ash, a by-product of burning powdered coal to generate electricity, is widely used in the concrete industry. While fly ash is a low-cost substitute for cement, there are many other beneficial reasons to the use of fly ash in concrete, such as reducing the quantity of cement needed in concrete, decreasing concrete on permeability, and reducing the heat generated during hydration. On the negative side, however, fly ash has been observed to increase the free shrinkage of concrete mixtures cured for 7 and 14 days (Lindquist et al. 2008), which increases the potential for shrinkage cracking.

In the current study, free shrinkage is evaluated over a one-year period in accordance to ASTM C157. Special attention is given to shrinkage during the first 30 days, because a high percentage of free shrinkage occurs during this period. Early age shrinkage is especially important for bridge decks because little creep occurs during this period to reduce tensile stresses.

Unless noted, the free shrinkage results represent the average of three specimens that are cast and cured at the same time. Free shrinkage is calculated based on the initial length at demolding, 23½ ± ½ hours after casting and, plotted as a function of drying time. The Student's t-test is used to gage whether the difference between two samples is statistically significant. For the Student's t-test results, "Y" indicates that the difference between two values is statistically significant at a confidence level of $\alpha = 0.02$ (98% certainty that the difference does not arise by chance), while an "N" indicates that the difference between samples is not statistically significant at a confidence level of $\alpha = 0.2$ (80%). Statistically significant

differences at confidence levels of least $\alpha = 0.2$, $\alpha = 0.1$, $\alpha = 0.05$ are indicated by "80," "90," and "95," respectively.

Three programs were designed to investigate the free shrinkage performance of concrete containing fly ash: Program I investigated the effect of increasing the curing period, with specimens cured for 7, 14, 28, and 56 days; Programs II and III investigated the combined effect of fly ash and a shrinkage reducing admixture. The control mixtures in each program were prepared to match the specifications for Low-Cracking High-Performance Concrete (LC-HPC) bridges (more details are presented in Chapter 6). The mixtures containing fly ash were designed to have the same water-cementitious material ratio (*w*/*cm*) and paste content as the control mixtures. Comparisons are made between mixtures containing the same sample of cement to eliminate possible differences caused by different cement samples.

Unless noted, all mixtures were batched to have a slump between 2 and 4 in. (50 and 100 mm) and an air content between 7.9 and 8.9% by adjusting the dosage of water reducer and air entraining agent. The mixture proportions, plastic properties, and compressive strength for all mixtures in the three programs are presented in Tables A.5 through A.7 in Appendix A.

3.2 PROGRAM I (CURING PERIOD)

In Program I, two sets of concrete mixtures were used to examine the effect of curing period. In Set 1, a Class F fly ash was investigated while in Set 2 a Class C fly ash was evaluated. ASTM C618 divides fly ash into two classes (F and C) based on composition. Class F fly ash has a major acidic oxide ($SiO_2 + Al_2O_3 + Fe_2O_3$) content of over 70%, and Class C fly ash has a major acidic oxide ($SiO_2 + Al_2O_3 + Fe_2O_3$) content between 50 and 70% . Class C fly ash generally contains more than 20% CaO.

All mixtures in Program I had a water-cementitious material ratio (*w*/*cm*) of 0.45 and a paste content of 24.37% by volume [corresponding to the mixture with a cement content of 535 lb/yd^3 (317 kg/m^3) and a *w*/*c* ratio of 0.45]. Each set had its

own control mixture because different cement samples were used (all cements were Type I/II cement from Lafarge).

3.2.1 Program I Set 1

Program I Set 1 involved two mixtures—a control mixture with 100% cement and a fly ash (Class F) concrete mixture with a 40% volume replacement of cement by fly ash. The 28-day compressive strengths were 4240 and 3710 psi (29.2 and 25.6 MPa) for the control and fly ash concrete, respectively, a difference of 12.5%. The average shrinkage strains for drying periods of 0, 30, 60, 90, 180, and 365 days and curing periods of 7, 14, 28, and 56 days are summarized in Table 3.1. Average free shrinkage is plotted as a function of the drying period for the mixtures over 30 days in Figure 3.1.

Table 3.1 Average free shrinkage for the control mixture (100% cement) and the 40% FA mixture (a 40% volume replacement of cement by Class F fly ash) in Program I set 1.

Days of Drying	Control				40% FA - F†			
	7-d curing	14-d curing	28-d curing	56-d curing	7-d curing	14-d curing	28-d curing	56-d curing
0 d	-60	-80	-67	-77	-47	-40	-63	-80
30 d	343	347	310	286	376	347	289	230
60 d	410	390	377	347	430	400	337	267
90 d	437	437	413	367	450	427	347	303
180 d	473	473	443	407	490	470	383	317
365 d	492	482	466	408	499	467	390	356
FS_{30d}/FS_{365d} ††	69.8%	71.9%	66.6%	70.0%	75.3%	74.3%	74.1%	64.7%

† Class F fly ash. †† Free shrinkage (FS) at 30 days divided by free shrinkage (FS) at 365 days.

As shown in Table 3.1 and Figure 3.1, increasing the curing period consistently reduced shrinkage. Except when comparing the control mixture with 7 and 14-day curing, the differences in shrinkage for each mixture after 30 days of drying as a function of curing period are statistically significant (Table 3.2). Comparing the two mixtures, the fly ash concrete cured for 56 days had the lowest shrinkage (230 με) at 30 days, while the fly ash concrete cured for 7 days had the highest shrinkage (376 με) at 30 days. When cured for only 7 or 14 days, the fly ash concrete exhibited more free shrinkage than the

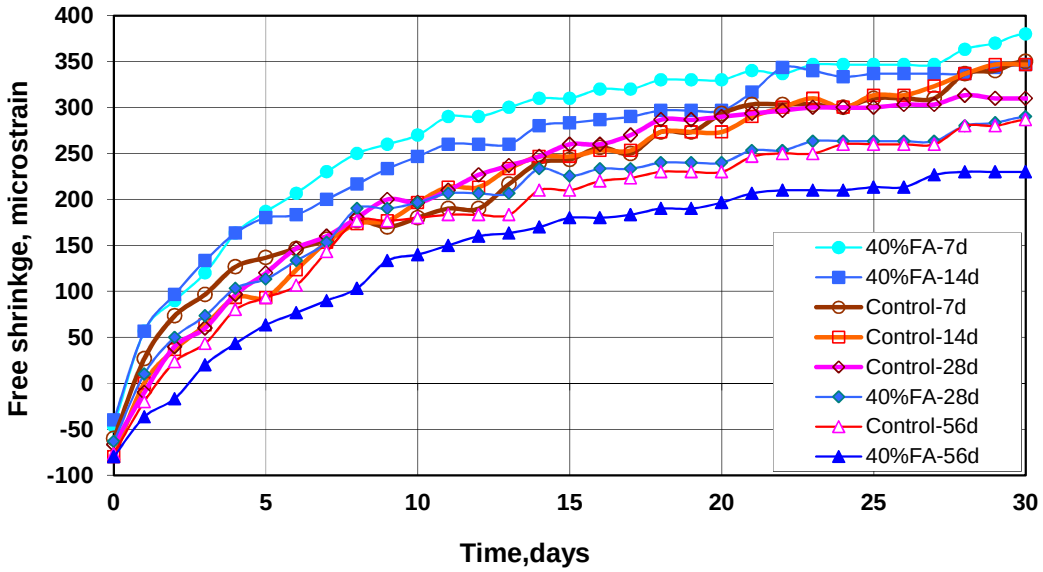

Figure 3.1 Average free shrinkage versus time through 30 days for control mixture (100% cement) and 40% FA mixture (with 40% volume replacement of cement by Class F fly ash) in Program I set 1.

Table 3.2 Student's t-test control mixture (100% cement) and 40% FA mixture (with 40% volume replacement of cement by Class F fly ash) in Program I set 1: 30-day free-shrinkage data.

Batch	Curing period	30-day free shrinkage	Control				40% FA			
			7-day	14-day	28-day	56-day	7-day	14-day	28-day	56-day
			343	347	310	286	376	347	289	230
Control	7-day	343		N	95%	Y	90%	N	Y	Y
	14-day	347			95%	Y	90%	N	Y	Y
	28-day	310				80%	Y	Y	80%	Y
	56-day	286					Y	Y	N	Y
40% FA	7-day	376						95%	Y	Y
	14-day	347							Y	Y
	28-day	289								Y
	56-day	230								

Note: For the results of the Student's t-test, "Y" indicates a statistical difference between the two samples at a confidence level of $\alpha = 0.02$ (98%). "N" indicates that the difference between samples is not statistically significant at a confidence level of $\alpha = 0.2$ (80%). Statistical difference at confidence levels at, but not exceeding $\alpha = 0.2$, 0.1, and 0.05 are indicated by "80," "90," and "95."

corresponding control mixture, an observation that agrees with the findings by Lindquist et al. (2008); when the curing period was increased to 28 and 56 days, the fly ash

concrete had less free shrinkage than the corresponding control mixture. The free shrinkage of fly ash concrete cured for 28 days is similar to that of the control mixture cured for 56 days; the difference between these two is, in fact, not statistically significant (Table 3.2). The fly ash concrete cured for 56 days had 56 με less free shrinkage than the control mixture cured for 56 days.

The average free-shrinkage curves over a one-year period are presented in Figure 3.2. The observation made at 30 days that increasing the curing period decreases the free shrinkage remains true at 365 days, and the differences in shrinkage as a function of curing period continue to be statistically significant (Table 3.3), except when comparing values for the control mixture for 7 and 14-day curing and for 14 and 28-day curing. The fly ash concrete cured for 7 days had the highest free shrinkage (499 με) at 365 days, although the difference with the shrinkage of the control mixture cured for 7 days (492 με) is not statistically significant (Table 3.3). The fly ash concrete

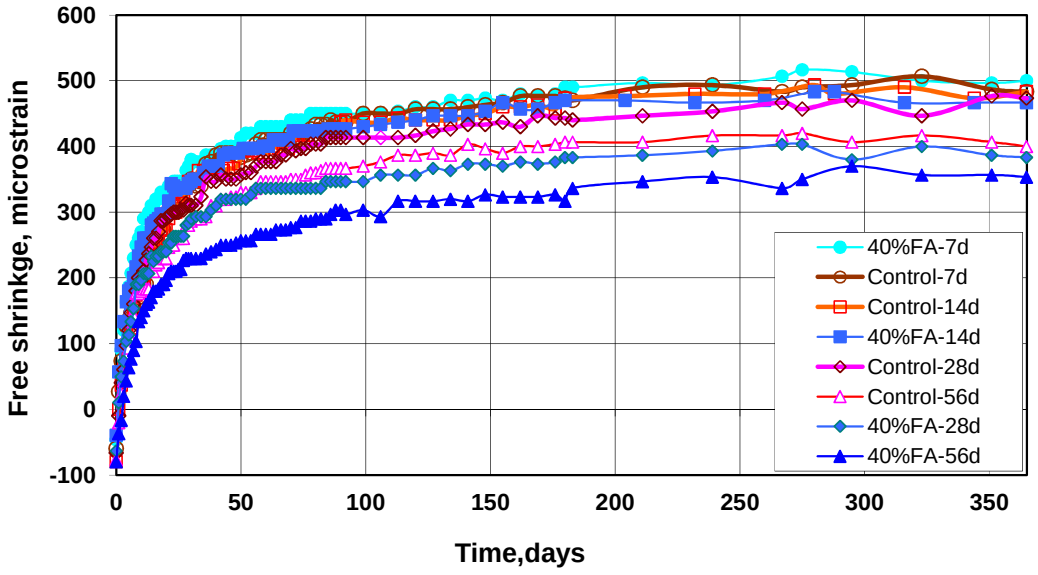

Figure 3.2 Average free shrinkage versus time through 365 days for control mixture (100% cement) and 40% FA mixture (with 40% volume replacement of cement by Class F fly ash) in Program I set 1.

Table 3.3 Student's t-test for control mixture (100% cement) and 40% FA mixture (with 40% volume replacement of cement by Class F fly ash) in Program I set 1: 365-day free-shrinkage data.

Batch	Curing period	365-day free shrinkage[†]	Control				40% FA			
			7-day	14-day	28-day	56-day	7-day	14-day	28-day	56-day
			492	482	466	408	499	467	390	356
Control	7-day	492		N	Y	Y	N	95%	Y	Y
	14-day	482			N	Y	N	N	Y	Y
	28-day	466				Y	Y	N	Y	Y
	56-day	408					Y	Y	N	95%
40% FA	7-day	499						95%	Y	Y
	14-day	467							Y	Y
	28-day	390								90%
	56-day	356								

Note: See the Table 3.2 note for an explanation of the terms "Y," "N," "80," "90," and "95."

cured for 56 days had the lowest shrinkage (356 με) at 365 days, 52 με less than the control mixture cured for the same period. Overall, the fly ash concrete cured for 7 and 14 days had similar performance to the corresponding control mixture at 365 days; the differences are not statistically significant (Table 3.3); the fly ash concrete cured for 28 and 56 days had lower free shrinkage than the corresponding control mixture at 365 days; the differences are statistically significant (Table 3.3).

Figure 3.2 shows that most free shrinkage occurs during the first month of drying, and after that the free shrinkage increases at a lower rate. As shown in Table 3.1, the free shrinkage at 30 days accounts for 69.8, 71.9, 66.6, and 70.0% of the free shrinkage at one year for the control mixture cured for 7, 14, 28, and 56 days, and 75.3, 74.3, 74.1, and 64.7% for the fly ash concrete. A higher percentage of the free shrinkage at one year of age occurs at 30 days for the fly ash concrete than for the control mixture, with the exception of specimens cured for 56 days.

As shown in Table 3.1, the specimens exhibit various amounts of swelling (negative values of shrinkage) at the end of the curing period, with values ranging from 40 to 80 με. Swelling is potentially beneficial to help reduce total shrinkage of concrete mixtures. To better understand the effect on free shrinkage of increasing the

curing period, free shrinkage is compared based on the length change both after demolding and after curing. The latter does not include swelling. The values of free shrinkage obtained for different curing periods for the control and fly ash mixtures are illustrated in Figures 3.3 and 3.4 for 30 and 365 days of drying, respectively. When the total length change after demolding is considered, it is apparent that extending the curing period reduced the free shrinkage at both 30 and 365 days for the two mixtures checked. It is also noted that the fly ash concrete cured for 7 days had 33 and 7 με more free shrinkage than the corresponding control mixture at 30 and 365 days, respectively. When the curing period was increased, the adverse effect of adding fly ash on free shrinkage was minimized and finally reversed. The fly ash concrete cured for 56 days had 56 and 52 με less free shrinkage than the corresponding control mixture at 30 and 365 days, respectively. When the shrinkage after curing is considered, it is still apparent that extending the curing period reduces the free shrinkage. In addition, after curing, the fly ash concrete cured for 7 days still had higher free shrinkage (19 με) at 30 days than the corresponding control mixture, but less free shrinkage (6 με) at 365 days. For curing periods of 14, 28, and 56 days, however, the fly ash concrete had less shrinkage after curing than the corresponding control mixture at both 30 and 365 days.

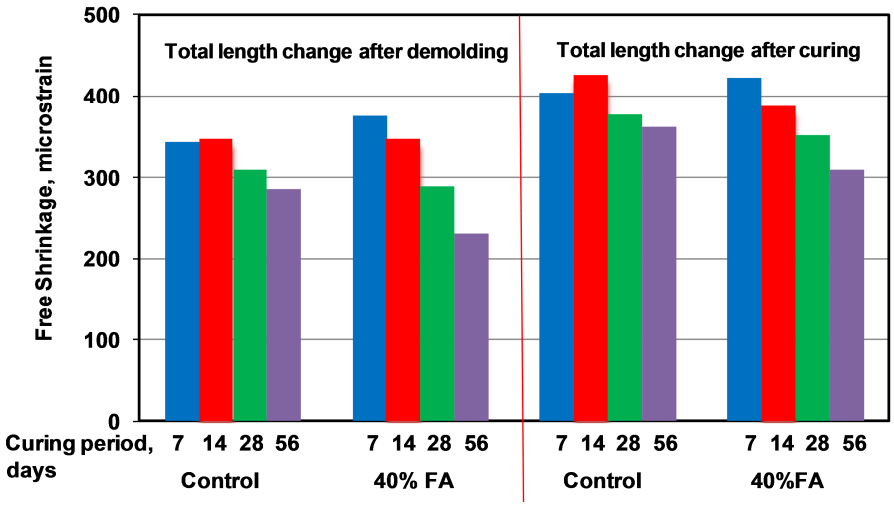

Figure 3.3 Free shrinkage at 30 days for control mixture (100% cement) and 40% FA mixture (with 40% volume replacement of cement by Class F fly ash) in Program I set 1.

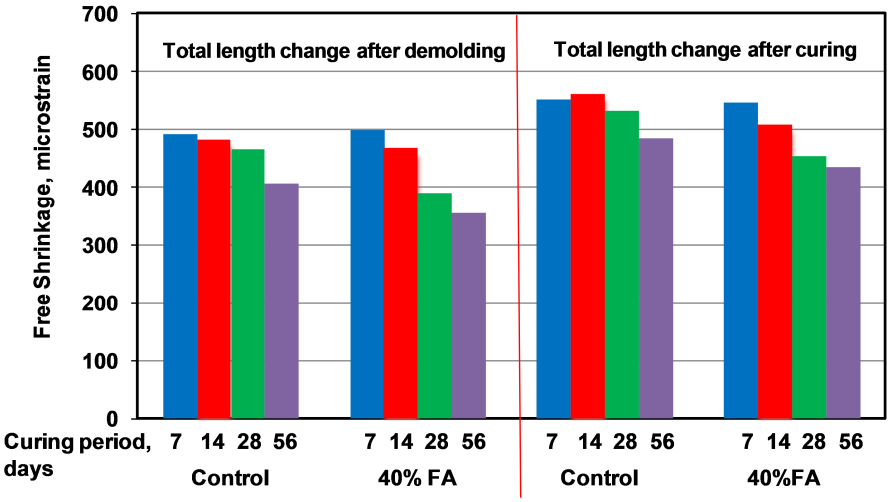

Figure 3.4 Free shrinkage at 365 days for control mixture (100% cement) and 40% FA mixture (with 40% volume replacement of cement by Class F fly ash) in Program I set 1.

Table 3.4 shows the reduction in free shrinkage (based on length change after demolding) resulting from curing longer than seven days. The table shows that the fly ash concrete benefits more from increased curing than does the control concrete. After 30 days of drying, the reductions for the control mixture are –1.0 (not a reduction), 9.7, and 16.8% for increasing the curing period to 14, 28, and 56 days, respectively; the corresponding reductions for the fly ash concrete are 7.7, 23.1, and 38.8%. Similar results are noted at 365 days.

Table 3.4 Reduction in free shrinkage (based on length change after demolding) resulting from curing longer than seven days for control mixture (100% cement) and 40% FA mixture (with 40% volume replacement of cement by Class F fly ash) in Program I set 1.

	Control				40% FA			
	7-d curing	14-d curing	28-d curing	56-d curing	7-d curing	14-d curing	28-d curing	56-d curing
Shrinkage at 30-d	343	347	310	286	376	347	289	230
Reduction	--	-1.0%	9.7%	16.8%	--	7.7%	23.1%	38.8%
Shrinkage at 365-d	492	482	466	408	499	467	390	356
Reduction	--	2.0%	5.4%	17.2%	--	6.5%	21.8%	28.7%

3.2.2 Program I Set 2

Class C fly ash is investigated in Program I Set 2. The set includes two mixtures: a control mixture with 100% cement and a fly ash (Class C) concrete with a 40% volume replacement of cement by fly ash. The 28-day compressive strengths are 4310 and 3430 psi (29.7 and 23.7 MPa) for the control and fly ash concrete, respectively, a difference of 20.4%. The average free shrinkage strains for drying periods of 0, 30, 60, 90, 180, and 365 days and curing periods of 7, 14, 28, and 56 days are summarized in Table 3.5. Average free shrinkage is plotted as a function of drying period for the mixtures over 30 days in Figure 3.5.

As shown in Table 3.5, the fly ash concrete cured for 56 days had the least free shrinkage at all ages (except at 30 days, the control mixture cured for 56 days had 5 με less free shrinkage), while the fly ash concrete cured for 7 days had the most free shrinkage at all ages. The fly ash concrete cured for 7 or 14 days had significantly more free shrinkage than the corresponding control mixture. For a curing period of 28 days, the fly ash concrete still had higher free shrinkage than the corresponding control concrete up through 90 days but about the same free shrinkage at 180 and 365 days. For a curing period of 56 days, the fly ash concrete had less free shrinkage than the corresponding control concrete.

Table 3.5 Average free shrinkage for control mixture (100% cement) and 40% FA mixture (with 40% volume replacement of cement by Class C fly ash) Program I Set 2.

Days of Drying	Control				40% FA-C†			
	7-d curing	14-d curing	28-d curing	56-d curing	7-d curing	14-d curing	28-d curing	56-d curing
0 d	-30	-40	-53	-50	-50	-57	-73	-93
30 d	326	293	281	258	435	413	329	263
60 d	407	380	347	320	490	480	360	307
90 d	423	420	367	340	515	500	383	333
180 d	483	460	400	373	560	540	407	360
365 d	479	467	423	390	553	523	406	369
$FS^{††}_{30d}/FS_{365d}$	68.0%	62.9%	66.9%	66.1%	78.6%	79.0%	81.1%	71.4%

† Class C fly ash. †† Free shrinkage (FS) at 30 days divided by free shrinkage at 365 days.

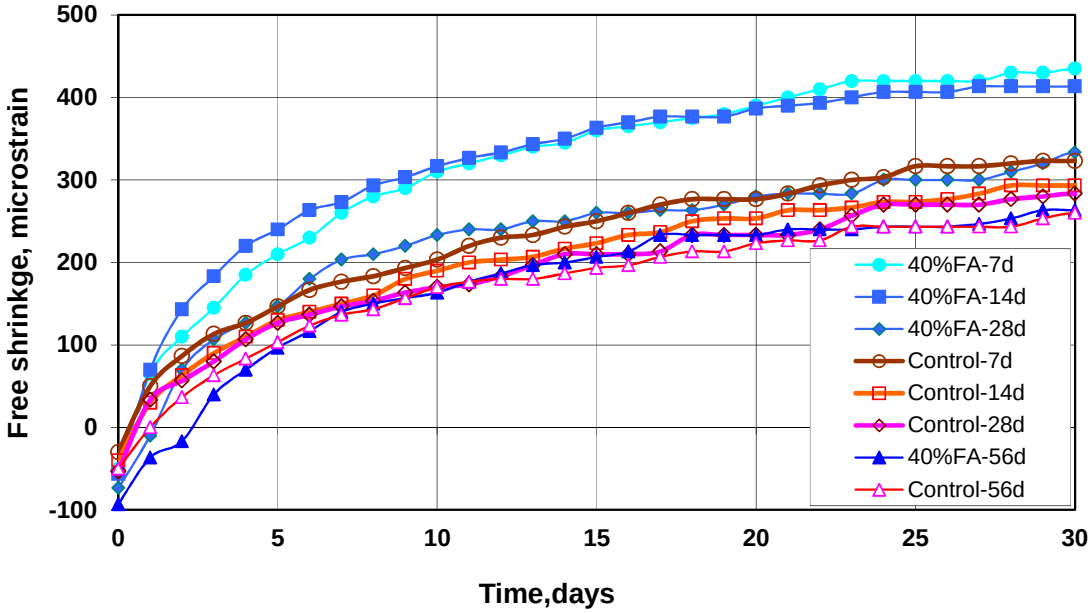

Figure 3.5 Average free shrinkage versus time through 30 days for control mixture (100% cement) and 40% FA mixture (with 40% volume replacement of cement by Class C fly ash) in Program I set 2.

Figure 3.5 shows the free shrinkage curves through 30 days for the two mixtures in Program I Set 2. The results, in the order from the highest to lowest free shrinkage, are fly ash concrete cured for 7 days, fly ash concrete cured for 14 days, fly ash concrete cured for 28 days, control mixture cured for 7 days, control mixture cured for 14 days, control mixture cured for 28 days, fly ash concrete cured for 56 days, and control mixture cured for 56 days. For specimens cured for 7, 14, and 28 days, the fly ash concrete had higher free shrinkage than the corresponding control concrete; the differences are statistically significant (Table 3.6). For specimens cured for 56 days, the fly ash concrete and control concrete exhibit very similar performance; the difference is not statistically significant (Table 3.6).

Table 3.6 Student's t-test for control mixture (100% cement) and 40% FA mixture (with 40% volume replacement of cement by Class C fly ash) in Program I set 2: 30-day free shrinkage data.

Batch	Curing period	30-day free shrinkage[†]	Control				40% FA			
			7-day	14-day	28-day	56-day	7-day	14-day	28-day	56-day
			326	293	281	258	435	413	329	263
Control	7-day	326		95%	Y	Y	Y	Y	N	Y
	14-day	293			N	80%	Y	Y	90%	95%
	28-day	281				N	Y	Y	95%	80%
	56-day	258					Y	Y	Y	N
40% FA	7-day	435						N	Y	Y
	14-day	413							Y	Y
	28-day	329								Y
	56-day	263								

Note: See the Table 3.2 note for an explanation of the terms "Y," "N," "80," "90," and "95."

The free shrinkage performance of the two mixtures through 365 days is shown in Figure 3.6 and Table 3.7. The effect of extending the curing period from 7 or 14 days to 28 or 56 days is apparent at 365 days. For the control mixture, the specimens cured for 14 days had slightly less free shrinkage (12 με less) than those cured for 7 days; the difference is not statistically significant (Table 3.7). The reduction for specimens cured for 28 and 56 days is more significant, with, respectively, 59 and 89 με less free shrinkage than the specimens cured for 7 days; the differences are statistically significant (Table 3.7). For the fly ash concrete, the reductions in free shrinkage for longer curing compared with the specimens cured for 7 days were 30, 148, and 184 με for specimens cured for 14, 28, and 56 days, respectively. The fly ash concrete cured for 7 and 14 days had more free shrinkage than the control concrete cured for 7 and 14 days (the differences are statistically significant); the fly ash concrete cured for 28 and 56 days had slightly less free shrinkage than the control concrete cured for 28 and 56 days, respectively; the differences are not statistically significant as shown in Table 3.7.

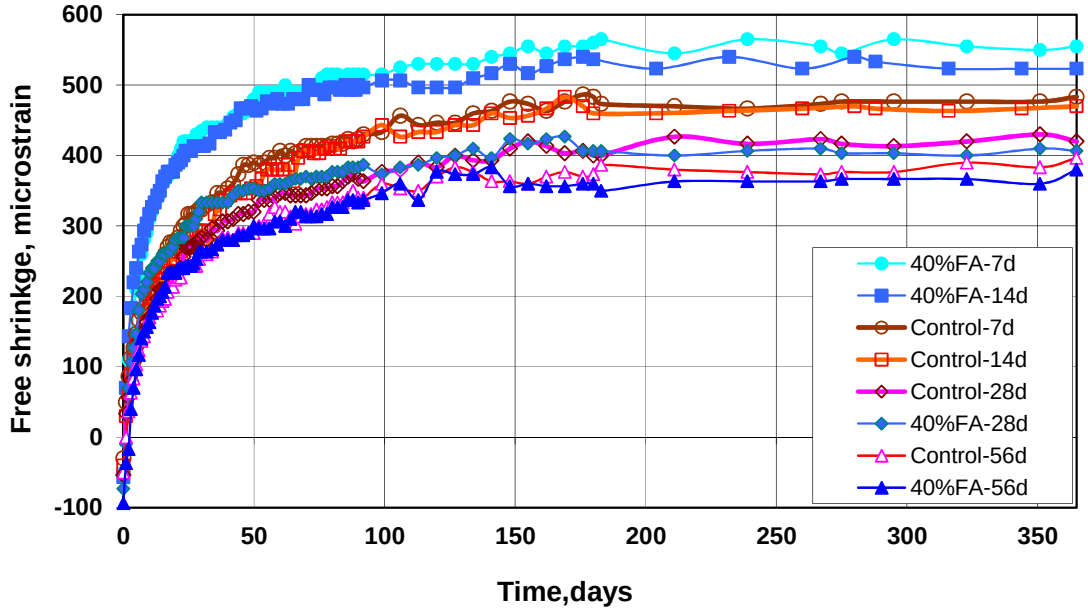

Figure 3.6 Average free shrinkage versus time through 365 days for control mixture (100% cement) and 40% FA mixture (with 40% volume replacement of cement by Class C fly ash) in Program I set 2.

Table 3.7 Student's t-test for control mixture (100% cement) and 40% FA mixture (with 40% volume replacement of cement by Class C fly ash) in Program I set: 365-day free shrinkage data.

Batch	Curing period	365-day free shrinkage	Control				40% FA			
			7-day	14-day	28-day	56-day	7-day	14-day	28-day	56-day
			479	467	423	390	553	523	406	369
Control	7-day	479		N	Y	Y	Y	95%	Y	Y
	14-day	467			95%	Y	Y	Y	Y	Y
	28-day	423				80%	Y	Y	N	95%
	56-day	390					Y	Y	N	N
40% FA	7-day	553						80%	Y	Y
	14-day	523							Y	Y
	28-day	406								90%
	56-day	369								

Note: See the Table 3.2 note for an explanation of the terms "Y," "N," "80," "90," and "95."

As shown in Figure 3.6 and as observed for the mixtures in Program I Set 1, most of the free shrinkage occurred during the first month of drying, and after that the free shrinkage increased at a low rate. The free shrinkage at 30 days accounted for

68.0, 62.9, 66.9, and 66.1% of the free shrinkage at one year of age for the control mixture cured for 7, 14, 28, and 56 days, and 78.6, 79.0, 81.1, and 71.4% for the fly ash concrete cured for 7, 14, 28, and 56 days (Table 3.5).

The values of free shrinkage calculated based on length change after demolding and after curing are compared for the two mixtures at 30 and 365 days in Figures 3.7 and 3.8. When the total length change after demolding is considered, extending the curing period reduced the free shrinkage for both the control and fly ash concrete mixtures; the reduction was greater for the fly ash concrete. For the specimens cured for 7 and 14 days, adding fly ash increased the free shrinkage by 109 and 120 με, respectively, at 30 days and by 74 and 56 με, respectively, at 365 days, when compared with the corresponding control mixture. For specimens cured for 28 and 56 days, adding fly ash increased the free shrinkage by 48 and 5 με, respectively, at 30 days but decreased the free shrinkage by 14 and 21 με, respectively, at 365 days, when compared with the corresponding control mixture. This is different from the mixture containing Class F fly ash, as discussed in Section 3.2.1. As shown in Figures 3.3 and 3.4 in Section 3.2.1, only the fly ash (Class F) concrete cured for seven days had higher free shrinkage than the corresponding control mixture at 30 and 365 days of drying; fly ash (Class F) concrete cured for 14, 28, and 56 days had the same or lower free shrinkage than the corresponding control mixture.

For length change after curing, the total free shrinkage was still reduced by increasing the curing period for both mixtures. The total free shrinkage after curing for the fly ash concrete was higher than it was for the corresponding control mixture at both 30 and 365 days, but the increase in the free shrinkage for the fly ash concrete compared to the control mixture decreased as the curing period increased. By way of comparison, as shown in Figures 3.3 and 3.4, the mixture containing Class F fly ash had less free shrinkage than the corresponding control concrete at 30 and 365 days,

except for the fly ash concrete cured for 7 days, which had slightly higher free shrinkage (19 με) than the corresponding control mixture at 30 days.

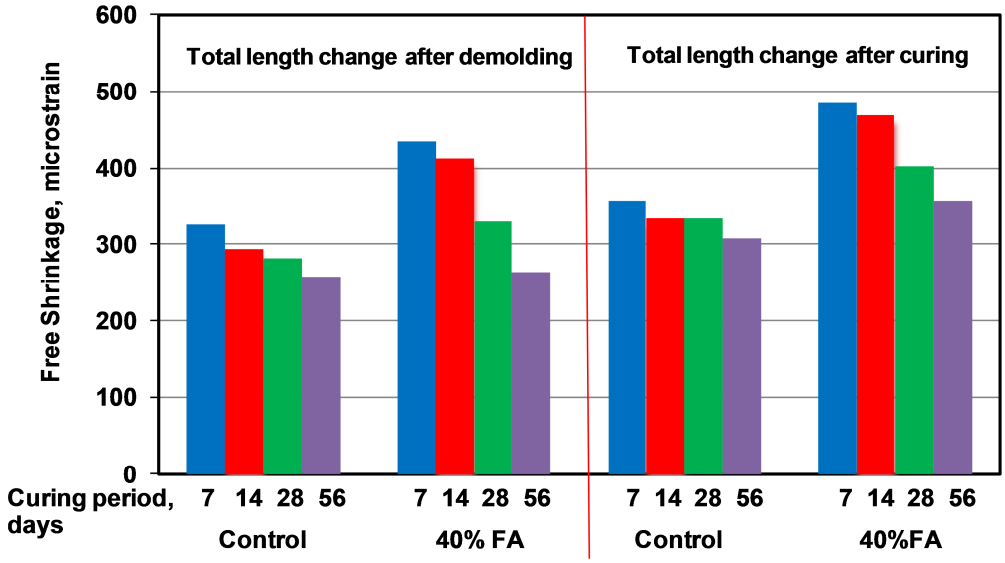

Figure 3.7 Free shrinkage at 30 days for control mixture (100% cement) and 40% FA mixture (with 40% volume replacement of cement by Class C fly ash) in Program I set 2.

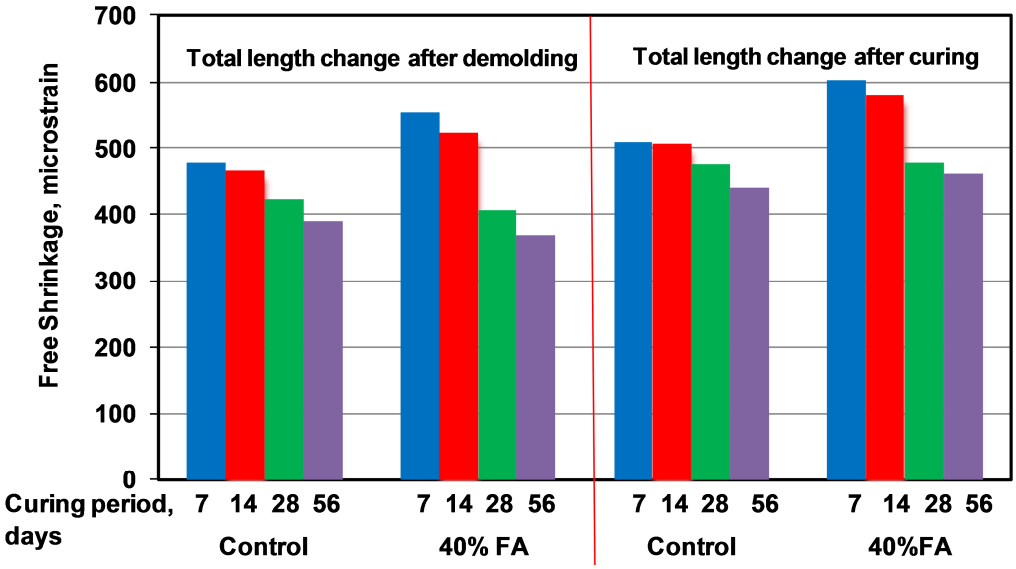

Figure 3.8 Free shrinkage at 365 days for control mixture (100% cement) and 40% FA mixture (with 40% volume replacement of cement by Class C fly ash) in Program I set 2.

Table 3.8 shows the reduction in free shrinkage resulting from curing longer than seven days. As observed for the mixtures in Program I Set I, the table shows that the fly ash concrete benefits more from increased curing than does the control concrete. After 30 days of drying, the reductions for the control mixture are 9.9, 13.7, and 20.8% for increased curing periods of 14, 28, and 56 days, respectively; the corresponding reductions for the fly ash concrete are 5.0, 24.4, and 39.5%. Similar results are noted at 365 days.

Table 3.8 Reduction in free shrinkage (based on length change after demolding) resulting from curing longer than seven days for control mixture (100% cement) and 40% FA mixture (with 40% volume replacement of cement by Class C fly ash) in Program I set 2.

	Control				40% FA			
	7-d curing	14-d curing	28-d curing	56-d curing	7-d curing	14-d curing	28-d curing	56-d curing
Shrinkage at 30-d	326	293	281	258	435	413	329	263
Reduction	--	9.9%	13.7%	20.8%	--	5.0%	24.4%	39.5%
Shrinkage at 365-d	479	467	420	390	553	523	406	369
Reduction	--	2.6%	12.3%	18.6%	--	5.4%	26.7%	33.3%

3.2.3 Summary of Program I

The effect of the curing period (7, 14, 28, and 56 days) is evaluated on the shrinkage for control mixtures containing 100% portland cement and concretes with a 40% volume replacement of cement with Class F and Class C fly ash and the same water-cementitious material ratio and paste content as the control mixture. The results of the comparisons indicate that

1. Using curing periods greater than 7 days decreases the free shrinkage for both the control and the fly ash concrete mixtures.
2. The reduction in the free shrinkage obtained by increasing the curing period is greater for concrete containing fly ash than for the control mixtures.

3. For the mixture containing Class F fly ash, specimens cured for 7 days had slightly higher free shrinkage (32 and 7 με at 30 and 365 days, respectively) than the corresponding control mixture; when cured for 14 days, the fly ash and control mixtures exhibited similar free shrinkage; when cured for 28 or 56 days, the fly ash concrete exhibited lower shrinkage than the corresponding control mixture by 21 and 56 με less at 30 days, and 76 and 52 με less at 365 days, respectively; and the fly ash concrete cured for 56 days had the least shrinkage.
4. For the mixture containing Class F fly ash, based on shrinkage after curing, the specimens cured for 7 days had slightly higher free shrinkage than the corresponding control specimens, while the specimens cured for 14, 28, and 56 days had less free shrinkage than the corresponding control specimens.
5. For the mixture containing Class C fly ash, all specimens exhibited greater free shrinkage (by 109, 120, 48, and 5 με more for curing periods of 7, 14, 28, and 56 days, respectively) than the corresponding control specimens at 30 days; at 365 days, the fly ash concrete specimens cured for 7 and 14 days still had 74 and 57 με more free shrinkage than the corresponding control specimens, but the fly ash concrete specimens cured for 28 and 56 days had 14 and 21 με less free shrinkage than the corresponding control specimens.
6. For the mixture containing Class C fly ash, based on shrinkage after curing, the specimens cured for 7, 14, 28, and 56 days had more free shrinkage than the corresponding control specimens at all ages.
7. Over two-thirds of the free shrinkage at one year occurred during the first 30 days, with averages of 70% and 66% for the two control mixtures, and 72% and 78% for the Class C and Class F fly ash concrete mixtures, respectively.

3.3 PROGRAM II (FLY ASH + SRA)

Lindquist et al. (2008) investigated the effect of incorporating a shrinkage reducing admixture (SRA) in concrete containing limestone coarse aggregate with a water-cement ratio of 0.42 and a cement content of 535 lb/yd^3 (317 kg/m^3). SRA dosages of 0, 1, and 2% by weight of cement were tested, and it was found that the addition of the SRA at dosage rates up to 2% by weight of cement resulted a significant reduction in both early-age and long-term drying shrinkage. Lindquist et al. (2008) also found that increasing the curing period from 7 to 14 days did not have a significant effect on the free shrinkage of mixtures containing an SRA. Because SRAs reduce free shrinkage by decreasing the surface tension of pore water, they can also make the air void system of concrete mixtures less stable. Lindquist et al. (2008) found that it was easier to maintain a stable air void system at an SRA dosage rate of 1% by weight of cement than at a dosage rate of 2%.

Considering the potential benefits of reducing free shrinkage using an SRA, mixtures containing both fly ash and an SRA were investigated in Program II, using three concrete mixtures: a mixture (0% FA) with a water-cement ratio of 0.42, a cement content of 535 lb/yd^3 (317 kg/m^3), and an SRA dosage of 1% by weight of cement [0.64 gallon/yd^3 (3.2 L/m^3)]; and two fly ash concrete mixtures, containing a 20% and 40% volume replacement of cement by fly ash and the same water-cementitious material (*w*/*cm*) ratio, paste content, and SRA dosage as the control mixture. Durapoz® Class F fly ash, which contains extra SO_3 (2.83% by weight), and granite coarse aggregate were used. The mixture proportions, plastic concrete properties, and compressive strength for all mixes in Program II are provided in Table A.6 in Appendix A.

The 28-day compressive strengths were 5260, 3970, 3880 psi (36.3, 27.4, and 26.8 MPa) for the 0% FA, 20% FA, and 40% FA concretes, respectively, representing a reduction in 28-day compressive strength of 24.5 and 26.2% with the use of 20 and 40% volume replacements of cement by fly ash, respectively.

The average free shrinkage strains for the drying periods of 0, 30, 60, 90, 180, and 365 days and curing periods of 7 and 14 days are summarized in Table 3.9. Average free shrinkage is plotted as a function of the drying period for the mixtures in Program II over 30 days in Figure 3.9.

Table 3.9 Average free shrinkage for control mixture (100% cement) and 20% and 40% FA mixtures (with 20% and 40% volume replacement of cement by Durapoz® Class F fly ash) in Program II. All mixtures contain an SRA dosage of 0.64 gallon/yd^3 (3.2 L/m^3).

Days of Drying	0% FA		20%FA†		40% FA†	
	7-d curing	14-d curing	7-d curing	14-d curing	7-d curing	14-d curing
0 d	13	-7	10	13	-7	-40
30 d	236	214	257	267	211	243
60 d	293	263	297	303	260	273
90 d	310	300	310	327	330	303
180 d	330	297	330	343	287	307
365 d	343	303	336	346	308	326
FS_{30d}/FS_{365d} ††	68.6%	70.7%	76.5%	77.2%	68.6%	74.7%

† Durapoz® Class F fly ash. †† Free shrinkage (FS) at 30 days divided by free shrinkage at 365 days.

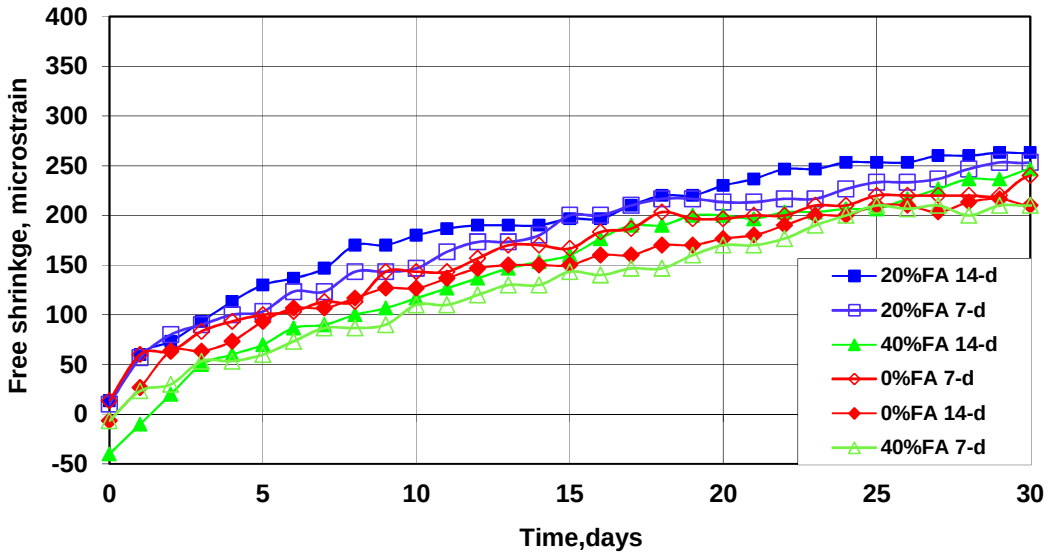

Figure 3.9 Average free shrinkage versus time through 30 days for control mixture (100% cement) and 20% and 40% FA mixtures (with 20% and 40% volume replacement of cement by Durapoz® Class F fly ash) in Program II. All mixtures contain an SRA dosage of 0.64 gallon/yd^3 (3.2 L/m^3).

As shown in Table 3.9 and Figure 3.9, extending the curing period from 7 to 14 days decreased the free shrinkage from 236 to 214 με at 30 days for the mixture without fly ash (0% FA), but increased the free shrinkage from 257 to 267 με and from 211 to 243 με for the 20% FA and 40% FA mixtures, respectively. All fly ash concrete specimens had higher free shrinkage than the 0% FA concrete specimens with the same curing period (except for the 40% FA concrete with 7-day curing); the differences are statistically significant (Table 3.10). The 20% FA concrete had greater free shrinkage than the 40% FA concrete.

Table 3.10 Student's t-test for control mixture (100% cement) and 20% and 40% FA mixtures (with 20% and 40% volume replacement of cement by Durapoz® Class F fly ash) in Program II. All mixtures contain an SRA dosage of 0.64 gallon/yd^3 (3.2 L/m^3). 30-day free shrinkage data.

Batch	Curing period	30-day free shrinkage	0% FA		20% FA		40% FA	
			7-day	14-day	7-day	14-day	7-day	14-day
			236	214	257	267	211	243
0% FA	7-day	236		90%	80%	Y	95%	N
	14-day	214			95%	Y	N	90%
20% FA	7-day	257				N	95%	N
	14-day	267					Y	90%
40% FA	7-day	211						95%
	14-day	243						

Note: See the Table 3.2 note for an explanation of the terms "Y," "N," "80," "90," and "95."

Average free shrinkage versus drying time through one year is shown in Figure 3.10. The 0% FA mixture with the 14-day curing period had the least free shrinkage and the 20% FA concrete with the 14-day curing period had the most free shrinkage at 365 days. Similar to the results at 30 days, increasing the curing period from 7 to 14 days decreased free shrinkage (by 40 με) for the 0% FA mixture, but increased the free shrinkage (by 10 and 18 με) for the 20% FA and 40% FA mixtures. The differences between the specimens cured for 7 and 14 days for both the 20% FA and 40% FA mixtures, however, are not statistically significant (Table 3.11).

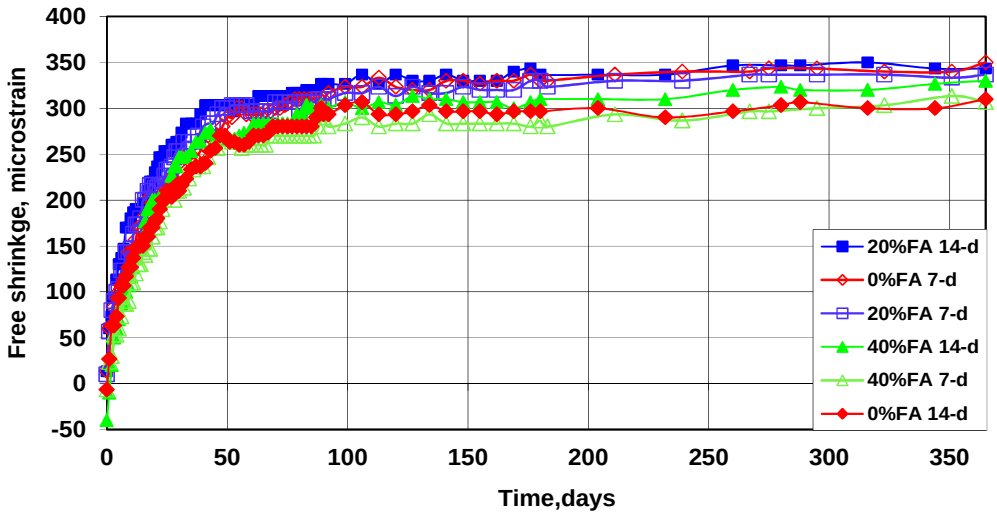

Figure 3.10 Average free shrinkage versus time through 365 days for control mixture (100% cement) and 20% and 40% FA mixtures (with 20% and 40% volume replacement of cement by Durapoz® Class F fly ash) in Program II. All mixtures contain an SRA dosage of 0.64 gallon/yd^3 (3.2 L/m^3).

Table 3.11 Student's t-test for control mixture (100% cement) and 20% and 40% FA mixtures (with 20% and 40% volume replacement of cement by Durapoz® Class F fly ash) in Program II. All mixtures contain an SRA dosage of 0.64 gallon/yd^3 (3.2 L/m^3). 365-day free shrinkage data.

Batch	**Curing period**	**365-day free shrinkage**	**0% FA**		**20% FA**		**40% FA**	
			7-day	14-day	7-day	14-day	7-day	14-day
			323	283	316	326	288	306
0% FA	7-day	323		Y	N	N	95%	90%
	14-day	283			80%	Y	N	90%
20% FA	7-day	316				N	N	N
	14-day	326					95%	90%
40% FA	7-day	288						N
	14-day	306						

Note: See the Table 3.2 note for an explanation of the terms "Y," "N," "80," "90," and "95."

Comparisons of the three mixtures at 30 and 365 days are presented in Figures 3.11 and 3.12 with the shrinkage calculated based on the length change after demolding and after curing, respectively. Based on shrinkage after demolding, as shown in Figures 3.11 (a) and 3.12 (a), for the specimens cured for 7 days, the fly ash concretes had lower free shrinkage than the 0% FA concrete at 365 days; the 40% FA

concrete also had lower shrinkage at 30 days. For the specimens cured for 14 days, the 0% FA concrete had the lowest free shrinkage followed by the 40% FA and the 20% FA mixtures. When the free shrinkage was calculated based on the length change after curing [Figures 3.11 (b) and 3.12 (b)], the same trend as observed based on the length change after demolding was observed, except that the 40% FA concrete cured for 14 days had greater free shrinkage than the 20% FA concrete cured for 14 days.

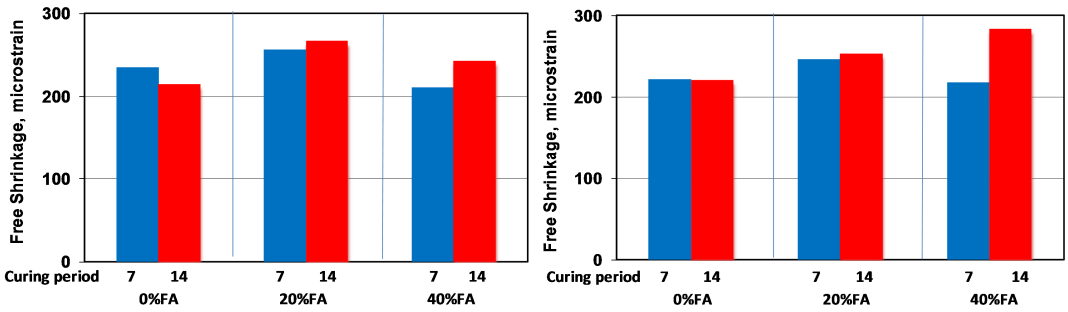

(a) (b)

Figure 3.11 Free shrinkage at 30 days for control mixture (100% cement) and 20% and 40% FA mixtures (with 20% and 40% volume replacement of cement by Durapoz® Class F fly ash) in Program II. All mixtures contain an SRA dosage of 0.64 gallon/yd^3 (3.2 L/m^3). (a) based on total length change after demolding; (b) based on total length change after curing.

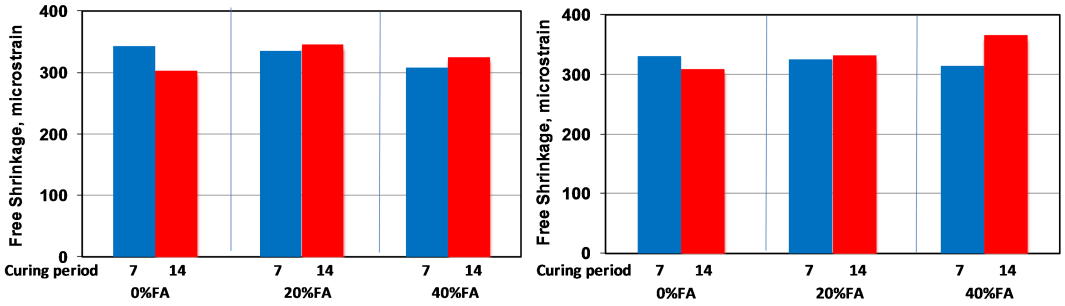

(a) (b)

Figure 3.12 Free shrinkage at 365 days for control mixture (100% cement) and 20% and 40% FA mixtures (with 20% and 40% volume replacement of cement by Durapoz® Class F fly ash) in Program II. All mixtures contain an SRA dosage of 0.64 gallon/yd^3 (3.2 L/m^3). (a) based on total length change after demolding; (b) based on total length change after curing.

3.3.1 Summary of Program II

Three mixtures containing 0, 20, and 40% volume replacements of cement by Class F fly ash and the same dosage rate [0.64 gallon/yd^3 (3.2 L/m^3)] of an SRA were tested in Program II. The free shrinkage results indicate that, for the 0% FA mixture, increasing the curing period from 7 to 14 days decreased the free shrinkage, although for the two fly ash concrete mixtures, increasing the curing period from 7 to 14 days also increased the free shrinkage (the differences at 365 days were not statistically significant). In general, increasing the curing period decreases free shrinkage, as shown in Program I and the research reported by Lindquist et al. (2008). In one case, Lindquist et al. (2008) also found that fly ash concrete cured for 14 days exhibited slightly higher free shrinkage than the same concrete cured for 7 days.

The 20% FA concrete exhibited higher free shrinkage than the 40% FA concrete when cured for 7 or 14 days. A similar phenomenon was also observed by Lindquist et al. (2008), although in general, Lindquist et al. (2008) observed that concrete containing a 40% volume replacement of cement by fly ash exhibited a greater free shrinkage than concrete containing a 20% volume replacement of cement by fly ash.

Overall, at the same dosage rate of SRA, for specimens cured for 14 days, the concrete containing fly ash had greater free shrinkage than the concrete without fly ash. For specimens cured for 7 days, the concrete containing fly ash had less free shrinkage than the concrete without fly ash. A more detailed comparison, including concretes with and without a shrinkage reducing admixture, is provided in Section 3.4.

3.4 PROGRAM III (SRA)

As discussed in Section 3.3, at the same dosage of a shrinkage reducing admixture (SRA), the concrete containing fly ash (with 14-day curing) exhibited higher free shrinkage than the concrete without fly ash. A more detailed comparison of concrete containing fly ash with concrete containing 100% portland cement at

different dosage rates of the SRA is provided by Program III. A total of six different mixtures were investigated: three non-fly ash mixtures [with a water-cement ratio of 0.44 and a cement content of 540 lb/yd^3 (320 kg/m^3)] with SRA dosages of 0, 0.32, and 0.64 gallon/yd^3 (0, 1.6, and 3.2 L/m^3), equal to 0, 0.5, and 1% of cement by weight; and concrete with a 40% volume replacement of cement by Class F fly ash and SRA dosages of 0, 0.32, and 0.64 gallon/yd^3 (0, 1.6, and 3.2 L/m^3). The fly ash concretes were designed with the same water-cementitious material ratio (*w*/*cm*) and paste content as the control mixes. The same Class F fly ash as used in Program I Set 1 was used in Program III. All specimens were cured for 14 days. The mixture proportions, plastic concrete properties, and compressive strengths for all mixtures in Program III are provided in Table A.7 of Appendix A.

Two batches were cast for three mixtures: the 0% FA concrete with 0.32 gallon/yd^3 (1.6 L/m^3) of SRA, the 40% FA concrete with 0.32 gallon/yd^3 (1.6 L/m^3) of SRA, and the 40% FA concrete with 0.64 gallon/yd^3 (3.2 L/m^3) of SRA. In each case, the results are averaged for comparison with other mixtures.

The 28-day compressive strengths for the mixtures in Program III are presented in Figure 3.13. The mixtures containing an SRA tended to have a lower compressive strength than those without an SRA, except for the 0% FA concrete with 0.32 gallon/yd^3 (1.6 L/m^3) of SRA, which was slightly stronger than the 0% FA concrete without an SRA. In all cases, at the same dosage of SRA, the fly ash concrete had a lower compressive strength than the 0% FA concrete. The fly ash concrete with 0.64 gallon/yd^3 (3.2 L/m^3) of SRA had the lowest 28-day compressive strength, 3120 psi (21.5 MPa).

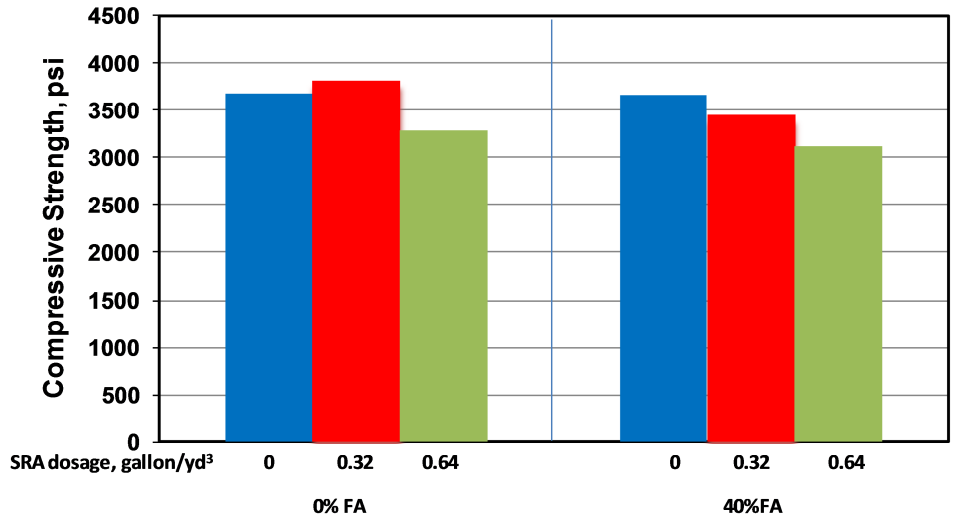

Figure 3.13 Compressive strength at 28 days for control mixture (100% cement) and 40% FA mixture (with 40% volume replacement of cement by Class F fly ash) at SRA dosages of 0, 0.32, and 0.64 gallon/yd^3 (0, 1.6, and 3.2 L/m^3) in Program III. 1 psi = 0.00689 MPa

The average free shrinkage strains for drying periods of 0, 30, 60, 90, 180, and 365 days are summarized in Table 3.12. The average free shrinkage versus drying time through 30 days is plotted in Figure 3.14.

As shown in Table 3.12 and Figure 3.14, the 40% FA concrete without the SRA had the highest free shrinkage at 30 days, 338 με, followed by the 0% FA concrete without the SRA, with a free shrinkage of 273 με; the mixtures with either 0.32 or 0.64 gallon/yd^3 (1.6 or 3.2 L/m^3) of SRA had a lower free shrinkage, ranging from 157 to 233 με. The differences between the mixtures with the SRA and the mixtures without the SRA are all statistically significant (Table 3.13). Free shrinkage decreased from 273 to 233 and 157 με as the SRA dosage increased from 0 to 0.32 and 0.64 gallon/yd^3 (0, to 1.6 and 3.2 L/m^3) for the 0% FA mixture; likewise, the free shrinkage decreased from 338 to 223 and 214 με as the SRA dosage increased from 0 to 0.32 and 0.64 gallon/yd^3 (0, to 1.6 and 3.2 L/m^3) for the 40% FA mixture. While the 40% FA concrete without the SRA had 65 με more shrinkage than the 0% FA concrete without the SRA, the 40% FA concrete with 0.32 gallon/yd^3 (1.6 L/m^3) of

SRA had virtually the same shrinkage as the 0% FA concrete with 0.32 gallon/yd^3 (1.6 L/m^3) of SRA. The 0% FA concrete with 0.64 gallon/yd^3 (3.2 L/m^3) of SRA had the best performance, with a shrinkage of 157 με at 30 days, equivalent to a 43% reduction compared to the 0% FA concrete without the SRA.

Table 3.12 Average free shrinkage for control mixture (100% cement) and 40% FA mixture (with 40% volume replacement of cement by Class F fly ash) at SRA dosages of 0, 0.32, and 0.64 gallon/yd^3 (0, 1.6, and 3.2 L/m^3) in Program III. All batches were cured for 14 days.

Days of Drying	0% FA			40% FA		
	0† SRA	0.32† SRA	0.64† SRA	0† SRA	0.32† SRA	0.64† SRA
0 d	-30	-17	-43	-33	-52	-57
30 d	273	233	157	338	223	214
60 d	323	297	190	407	293	277
90 d	357	347	250	427	330	320
180 d	393	372	280	470	358	333
365 d	400	396	292	490	383	353
FS_{30d}/FS_{365d}††	68.3%	58.8%	53.6%	68.9%	58.3%	60.6%

† SRA dosage, gallon/yd^3. †† Free shrinkage (FS) at 30 days divided by free shrinkage at 365 days.

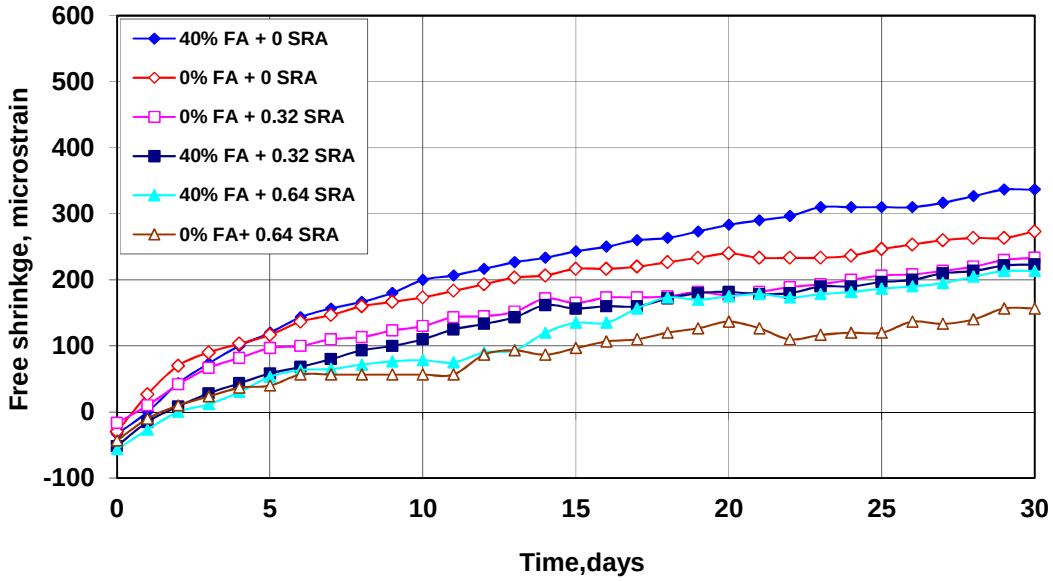

Figure 3.14 Average free shrinkage versus time through 30 days for control mixture (100% cement) and 40% FA mixture (with 40% volume replacement of cement by Class F fly ash) at SRA dosages of 0, 0.32, and 0.64 gallon/yd^3 (0, 1.6, and 3.2 L/m^3) in Program III. All batches were cured for 14 days.

Table 3.13 Student's t-test for control mixture (100% cement) and 40% FA mixture (with 40% volume replacement of cement by Class F fly ash) at SRA dosages of 0, 0.32, and 0.64 gallon/yd^3 (0, 1.6, and 3.2 L/m^3) in Program III. All batches were cured for 14 days. 30-day free shrinkage data.

Batch	SRA dosage, lb/yd^3	30-day free shrinkage	0% FA			40% FA		
			0 SRA	0.32 SRA	0.64 SRA	0 SRA	0.32 SRA	0.64 SRA
			273	233	157	338	223	214
0% FA	0	273		95%	Y	Y	95%	Y
	0.32	233			Y	Y	N	80%
	0.64	157				Y	Y	Y
40% FA	0	338					Y	Y
	0.32	223						N
	0.64	214						

Note: See the Table 3.2 note for an explanation of the terms "Y," "N," "80," "90", and "95."

The free shrinkage results through 365 days are presented in Figure 3.15 and Table 3.14. The trend observed at 30 days was again observed at 365 days. The 40% FA concrete without the SRA had the highest shrinkage, 90 με higher than the 0% FA concrete without the SRA. With 0.32 gallon/yd^3 (1.6 L/m^3) of SRA, the 40% FA concrete exhibited less shrinkage than the 40% FA and 0% FA concretes without the SRA and similar shrinkage to the 0% FA concrete with the same dosage of SRA. The 40% FA concrete with 0.64 gallon/yd^3 (3.2 L/m^3) of SRA performed slightly better than the 40% FA concrete with 0.32 gallon/yd^3 (1.6 L/m^3) of SRA, while the free shrinkage of the 0% FA concrete was significantly reduced as the SRA dosage increased from 0.32 to 0.64 gallon/yd^3 (1.6 to 3.2 L/m^3). The 0% FA concrete with 0.64 gallon/yd^3 (3.2 L/m^3) of SRA had the lowest free shrinkage at 365 days.

The free shrinkage at 30 days was about 70% of the free shrinkage at 365 days for concretes without the SRA. The ratio decreased to about 60% for the concretes with the SRA (Table 3.12).

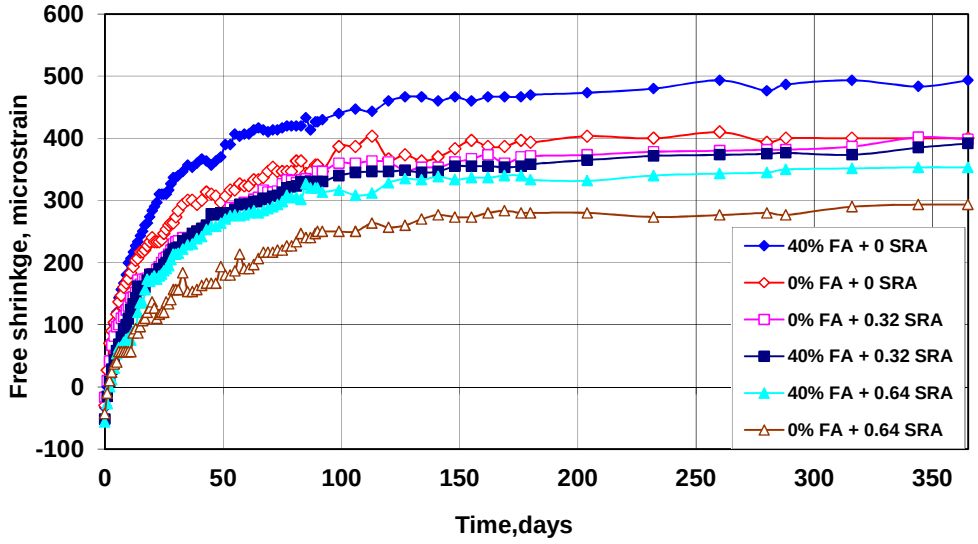

Figure 3.15 Average free shrinkage versus time through 365 days for control mixture (100% cement) and 40% FA mixture (with 40% volume replacement of cement by Class F fly ash) at SRA dosages of 0, 0.32, and 0.64 gallon/yd^3 (0, 1.6, and 3.2 L/m^3) in Program III. All batches were cured for 14 days.

Table 3.14 Student's t-test for control mixture (100% cement) and 40% FA mixture (with 40% volume replacement of cement by Class F fly ash) at SRA dosages of 0, 0.32, and 0.64 gallon/yd^3 (0, 1.6, and 3.2 L/m^3) in Program III. All batches were cured for 14 days. 365-day free shrinkage data.

Batch	**SRA dosage, lb/yd^3**	**365-day free shrinkage**	**0% FA**			**40% FA**		
			0 SRA	0.32 SRA	0.64 SRA	0 SRA	0.32 SRA	0.64 SRA
			400	396	292	490	383	353
0% FA	0	400		N	Y	Y	80%	Y
	0.32	396			Y	Y	N	Y
	0.64	292				Y	Y	95%
40% FA	0	490					Y	Y
	0.32	383						95%
	0.64	353						

Note: See the Table 3.2 note for an explanation of the terms "Y," "N," "80," "90," and "95."

The free shrinkage values calculated based on the length change after demolding and after curing are compared for the six mixtures at 30 and 365 days in Figures 3.16 and 3.17, respectively. As shown in Figures 3.16 (a) and 3.17 (a), for the fly ash concrete, the addition of the SRA reduced the free shrinkage significantly when compared to the mixture without the SRA; however, increasing the SRA dosage

from 0.32 to 0.64 gallon/yd^3 (1.6 to 3.2 L/m^3) had little of effect. For the 0% FA concrete, the free shrinkage decreased as the SRA dosage increased from 0 to 0.32 and 0.64 gallon/yd^3 (0 to 1.6 and 3.2 L/m^3). With 0.32 gallon/yd^3 (1.6 L/m^3) of SRA, the fly ash concrete performed slightly better than the concrete without fly ash. The concrete without fly ash and with 0.64 gallon/yd^3 (3.2 L/m^3) of SRA had the best performance. If the swelling during curing is not considered [Figures 3.16 (b) and 3.17 (b)], adding the SRA still significantly reduced free shrinkage for both mixtures. In every case, the fly ash concrete had greater free shrinkage than the corresponding 0% FA concrete at the same dosage of SRA.

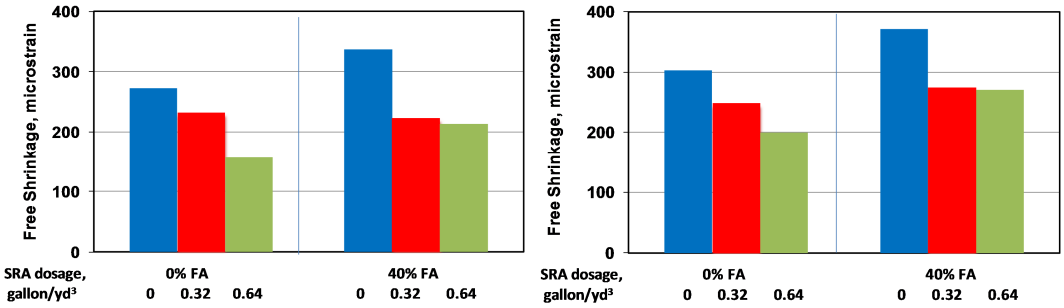

(a) (b)

Figure 3.16 Free shrinkage at 30 days for control mixture (100% cement) and 40% FA mixture (with 40% volume replacement of cement by Class F fly ash) at SRA dosages of 0, 0.32, and 0.64 gallon/yd^3 (0, 1.6, and 3.2 L/m^3) in Program III: (a) based on total length change after demolding; (b) based on total length change after curing.

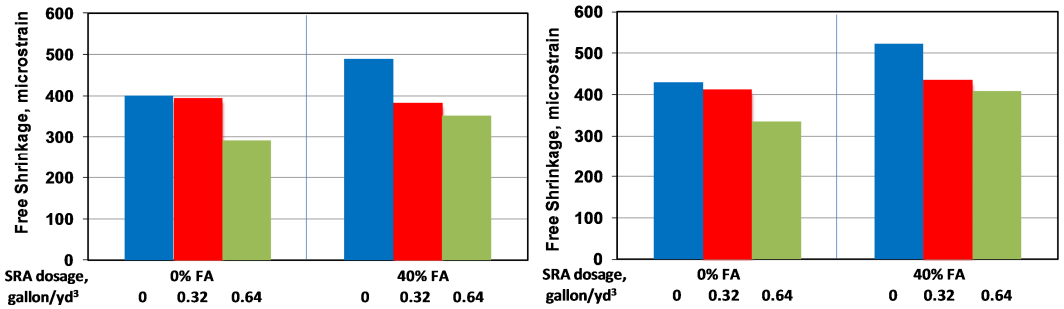

(a) (b)

Figure 3.17 Free shrinkage at 365 days for control mixture (100% cement) and 40% FA mixture (with 40% volume replacement of cement by Class F fly ash) at SRA dosages of 0, 0.32, and 0.64 gallon/yd^3 (0, 1.6, and 3.2 L/m^3) in Program III: (a) based on total length change after demolding; (b) based on total length change after curing.

Table 3.15 shows the free shrinkage reduction obtained with the addition of the SRA. For the 0% FA mixture, adding 0.32 and 0.64 gallon/yd^3 (1.6 and 3.2 L/m^3) of SRA reduced shrinkage by 14.8 and 42.7% at 30 days and 1.1 and 26.9% at 365 days compared to the similar mixture without the SRA. For the fly ash concrete, the reductions were 33.9 and 36.7% at 30 days and 21.8 and 28.7% at 365 days, corresponding to SRA dosages of 0.32 and 0.64 gallon/yd^3 (1.6 and 3.2 L/m^3).

Table 3.15 Free shrinkage reduction compared non-SRA specimens for control mixture (100% cement) and 40% FA mixture (with 40% volume replacement of cement by Class F fly ash) in Program III.

Days of Drying	0% FA			40% FA		
	0 SRA	0.32 SRA	0.64 SRA	0 SRA	0.32 SRA	0.64 SRA
Shrinkage at 30-d	273	233	157	338	223	214
Reduction	--	14.8%	42.7%	--	33.9%	36.7%
Shrinkage at 365-d	400	396	292	490	383	353
Reduction	--	1.1%	26.9%	--	21.8%	28.0%

The reduction in free shrinkage obtained by adding an SRA to concrete that is cured for 14 days can be compared with the reduction obtained by extending the curing period from 14 days to 28 or 56 days for concrete without an SRA. The concretes with the SRA are mixtures that are discussed in this section, and the concretes with the longer curing periods are those mixtures without an SRA in Program I Set 1, discussed in Section 3.2.1. The reductions in free shrinkage at 30 days, calculated as the difference with specimens cured for 14 days without an SRA, are presented in Figure 3.18. At 30 days, for the mixtures without fly ash, adding 0.64 gallon/yd^3 (3.2 L/m^3) of SRA resulted in the greatest reduction, 42.7%, followed by extending the curing period to 56 days, adding 0.32 gallon/yd^3 (1.6 L/m^3) of SRA, and extending the curing period to 28 days, with reductions of 17.6%, 14.8%, and 10.6%, respectively. For the mixtures with a 40% volume replacement of cement by fly ash, the mixtures with a curing period of 56 days and additions of 0.32 and 0.64 gallon/yd^3 (1.6 and 3.2 L/m^3) of SRA exhibited similar reductions, about 35%, and

the mixture with a curing period of 28 days had the lowest reduction in free shrinkage, 16.7%.

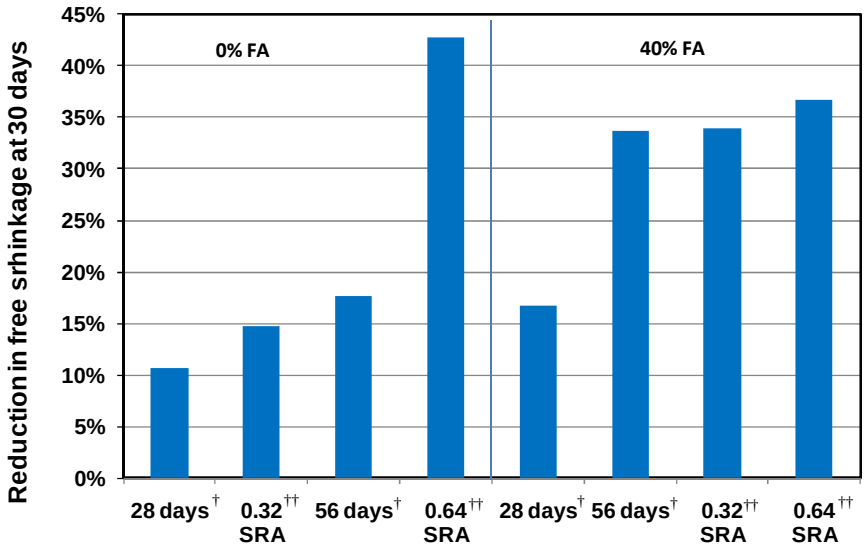

Figure 3.18 Reduction in free shrinkage at 30 days obtained by adding an SRA or extending curing period compared with specimens cured for 14 days without an SRA for control mixture (100% cement) and 40% FA mixture (with 40% volume replacement of cement by Class F fly ash). † Extending curing period to 28 or 56 days (Section 3.2.1); no SRA. †† Adding the SRA at the dosage of 0.32 or 0.64 gallon/yd^3 (1.6 or 3.2 L/m^3); cured for 14 days.

The reductions in free shrinkage at 365 days are presented in Figure 3.19. For the mixtures without fly ash, adding 0.32 gallon/yd^3 (1.6 L/m^3) of SRA or increasing the curing period to 28 days reduced free shrinkage by less than 15%, while increasing the curing period to 56 days or adding 0.64 gallon/yd^3 (3.2 L/m^3) of SRA, respectively, resulted in reductions of 15.4% and 26.9%, all with respect to concrete without an SRA cured for 14 days. For the mixtures with a 40% volume replacement of cement by fly ash, all the reductions were greater than 15%, and in the order from low to high, the shrinkage reduction increased by increasing curing period to 28 days, adding 0.32 gallon/yd^3 (1.6 L/m^3) of SRA, increasing curing period to 56 days and adding 0.64 gallon/yd^3 (3.2 L/m^3) of SRA.

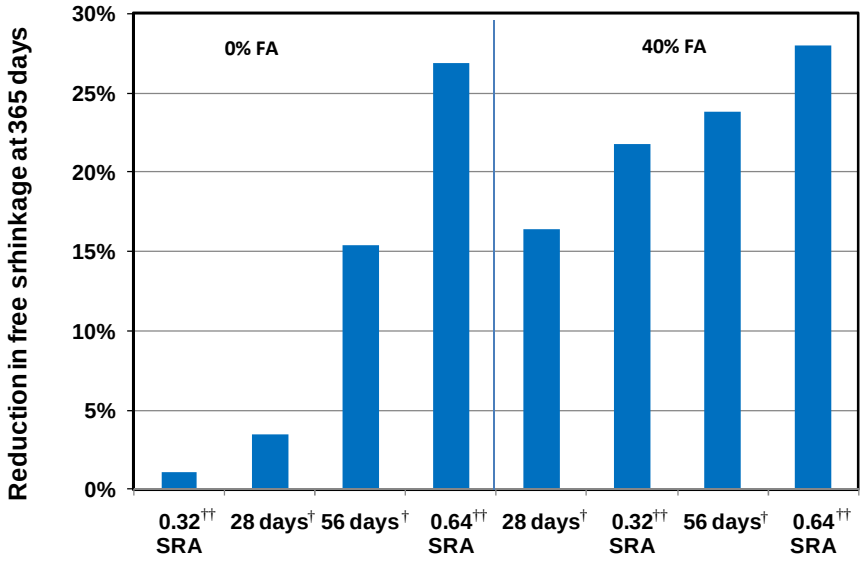

Figure 3.19 Reduction in free shrinkage at 365 days obtained by adding an SRA or extending curing period compared with specimens cured for 14 days without an SRA for control mixture (100% cement) and 40% FA mixture (with 40% volume replacement of cement by Class F fly ash). † Extending curing period to 28 or 56 days (Section 3.2.1); no SRA. †† Adding the SRA at the dosage of 0.32 or 0.64 gallon/yd^3 (1.6 or 3.2 L/m^3); cured for 14 days.

Lindquist et al. (2008) also investigated the effect of an SRA on shrinkage. They used dosage rates of 0, 0.64, and 1.28 gallon/yd^3 (0, 3.2 and 6.4 L/m^3) for concrete with a cement content of 535 lb/yd^3 (317 kg/m^3) and a *w/c* ratio of 0.42, giving a paste content of 23.3% by volume, and limestone coarse aggregate. The concrete was cured for 14 days. They observed reductions in shrinkage at 30 days of 36.4 and 60.1% for SRA dosage rates of 0.64 and 1.28 gallon/yd^3 (3.2 and 6.4 L/m^3), respectively, with reductions at 365 days of 22.4 and 39.4%.

3.4.1 Summary of Program III

Six different concrete mixtures were evaluated in Program III. They included 0% FA mixtures and 40% FA mixtures with a 40% volume replacement of cement by Class F fly ash. SRA dosages of 0, 0.32, and 0.64 gallon/yd^3 (0, 1.6, and 3.2 L/m^3) were used. All mixtures were cured for 14 days. The free shrinkage results indicate that

1. The addition of the SRA reduced free shrinkage significantly. With SRA dosages of 0.32 and 0.64 gallon/yd^3 (1.6 and 3.2 L/m^3), 30-day free shrinkage decreased by 14.8 and 42.7% for 0% FA concrete, and 33.9 and 36.7% for 40% FA concrete, and the 365-day free shrinkage decreased by 1.1 and 26.9% for 0% FA concrete, and 21.8 and 28% for 40% FA concrete, compared with similar mixtures without an SRA.
2. Without the SRA, the 40% FA concrete had higher free shrinkage than the 0% FA concrete at all ages.
3. With 0.32 gallon/yd^3 (1.6 L/m^3) of SRA, the concretes with and without fly ash exhibited similar shrinkage.
4. With 0.64 gallon/yd^3 (3.2 L/m^3) of SRA, the 40% FA concrete had slightly less free shrinkage than the 40% FA concrete containing 0.32 gallon/yd^3 (1.6 L/m^3) of SRA but more free shrinkage than the 0% FA concrete with 0.64 gallon/yd^3 (3.2 L/m^3) of SRA.
5. When the reductions in free shrinkage obtained by adding 0.32 or 0.64 gallon/yd^3 (1.6 and 3.2 L/m^3) of SRA (concrete cured for 14 days, Program III) and by extending the curing period from 14 to 28 or 56 days (Program I Set 1) were compared for mixtures with and without fly ash, it was noted that adding 0.64 gallon/yd^3 (3.2 L/m^3) of SRA resulted in the greatest reduction in shrinkage at 30 and 365 days for all mixtures; adding 0.32 gallon/yd^3 (1.6 L/m^3) of SRA resulted in more reduction than extending the curing period to 28 days (except for the concrete without fly ash at 365 days) and less reduction than extending the curing period to 56 days (except for the mixture with fly ash at 30 days).
6. The reductions in shrinkage at 365 days were, respectively, 1.1, 26.9, 21.8, 28.0% for the 0% FA mixtures with 0.32 and 0.64 gallon/yd^3 (1.6 and 3.2 L/m^3) of SRA and 40% FA mixtures with 0.32 and 0.64 gallon/yd^3 (1.6 and 3.2 L/m^3) of SRA, values that are consistently below the respective reductions at 30 days, 14.8, 42.7, 33.9, and 36.7%.

CHAPTER 4 EVAPORABLE WATER CONTENT AND FREE SHRINKAGE

4.1 GENERAL

The evaporable water in cement paste is defined as the water that can be removed at room temperature, or more quickly at 221° F (105° C) (Mindess et al. 2003). Concrete shrinkage is closely related to the water loss from the cement paste. In this chapter, the quantity of evaporable water in cement paste is correlated with the free shrinkage measured in companion specimens.

The quantity of evaporable water in the cement paste constituent of concrete, w_e (Section 2.6.3.1), equals the difference between the original mix water (based on the original mixture proportions and not including water in the aggregates) and the non-evaporable water in cement paste. The quantity of evaporable water can also be directly determined experimentally as the difference in the weight of the concrete when the specimens are demolded 24 hours after casting and the weight after curing is completed and subsequently oven drying at 221° F (105° C), adjusted to account for the water lost from the initially saturated surface dry (SSD) aggregate, w'_e (Section 2.6.3.2). Because the total water in cement paste increases over time when cement paste maintained in a saturated condition, the quantity of evaporable water is also determined based on the total water in the cement paste constituent of concrete after curing, designated as w_e^* (Section 2.6.3.3).

The free shrinkage specimens were prepared and tested in accordance with ASTM C157.

Two test series are described in this chapter. In the preliminary test series, the surfaces of the specimens were either air-dried or wet (water left in the surface air voids in both cases). The surface conditions did not affect the value of the non-evaporable water content or the evaporable water content of w_e, but did affect the measured

evaporable water contents w'_e and w_e^*. Thus, only w_e is valid for the preliminary tests. The specimens in the preliminary tests were cured for 1, 3, 7, or 28 days.

In the second test series, the specimens were prepared in the saturated surface dry (SSD) condition prior to initial weighing, allowing the values of w_e, w'_e and w_e^* to be determined. The specimens in the second series were cured for 3, 7, 14, or 28 days, with one batch cured for 35 days.

Four mixtures were evaluated, each with a water-cementitious material (*w/cm*) ratio of 0.44 and a paste content of 24.12%. The first, the control mixture, contained 100% cement as the binder. Three batches, designated as Control 1, 2, and 3, were cast in the two test series. The second mixture had a 40% volume replacement of cement by Class F fly ash and was cast twice (FA 1 and FA 2). The third mixture had a 60% volume replacement of cement by slag cement and was cast in three batches, designated as Slag 1, 2, and 3. The final mixture contained 100% cement and a shrinkage reducing admixture (SRA) added at a dosage rate of 0.5% by the weight of cement; one batch was cast. Control 1 and 2, FA 1, and Slag 1 were evaluated in the preliminary test series. Control 3, FA 2, Slag 2 and 3, and the SRA mixture were evaluated in the second test series.

With the exception of the mixtures containing fly ash, the concrete was batched to have a slump between 2 and 4 in. (50 and 100 mm) and an air content between 7.9 and 8.9% by adjusting the dosage of water reducer and air entraining agent. The mixtures containing fly ash had a slump over 6 in. (150 mm) even without the addition of a water reducer. This was done to keep all other factors the same as used in the other mixtures, including the paste content, *w/cm* ratio, aggregate gradation, and air content. The mixture proportions, plastic concrete properties, and compressive strengths are presented in Tables A. 8 and A. 9 in Appendix A.

Student's t-test is used to identify whether the differences between samples are statistically significant.

4.2 w_e VERSUS w'_e

In this section, the quantity of evaporable water in the cement paste constituent of the specimens, determined as the difference between the original mix water and the non-evaporable water w_e, is compared with the quantity of water lost from the cement paste constituent, based on the weight of the concrete at an age of 24 hours, during oven drying w'_e. The values of w_e and w'_e are calculated for specimens cured for 3, 7, 14, and 28 days in two batches, Slag 3 and the SRA mixture; the average value for three specimens is used for comparison. The results are shown in Figure 4.1. The horizontal axis shows the curing period, and the vertical axis shows the quantity of evaporable water of w_e and w'_e, expressed as a water-cementitious material ratio. The error bars parallel to the vertical axis show the minimum and maximum values for the three specimens in each batch.

As shown in Figure 4.1, for the concrete containing slag, w'_e/cm is consistently lower than w_e/cm (for all four curing periods), with differences ranging from 0.032 to 0.037. The same observation is noted for the SRA mixture, with differences ranging from 0.039 to 0.041. All of the differences between w_e and w'_e for the same mixture with the same curing period are statistically significant at a confidence level of $\alpha = 0.02$ (98% certainty that the difference does not arise by chance). The lower values of w'_e indicate a systematic difference in the two methods of measuring evaporable water, which may be due to water losses that occur during specimen handling (discussed in Section 2.6.3.2). The quantity of water lost during specimen handling is discussed more in Section 4.3. It should be noted that during the determination of w'_e, the original weight of the concrete is based on the weight of the specimens at an age of 24 hours, in which case part of the original mix water has been chemically combined during the hydration at the 24 hours. This will also cause lower values of w'_e than w_e. The error bars (three specimens for each batch) indicate that the w'_e values exhibit more scatter than the w_e values, except for the SRA

mixture cured for three days. In the remainder of this chapter, w_e is used to compare different mixtures.

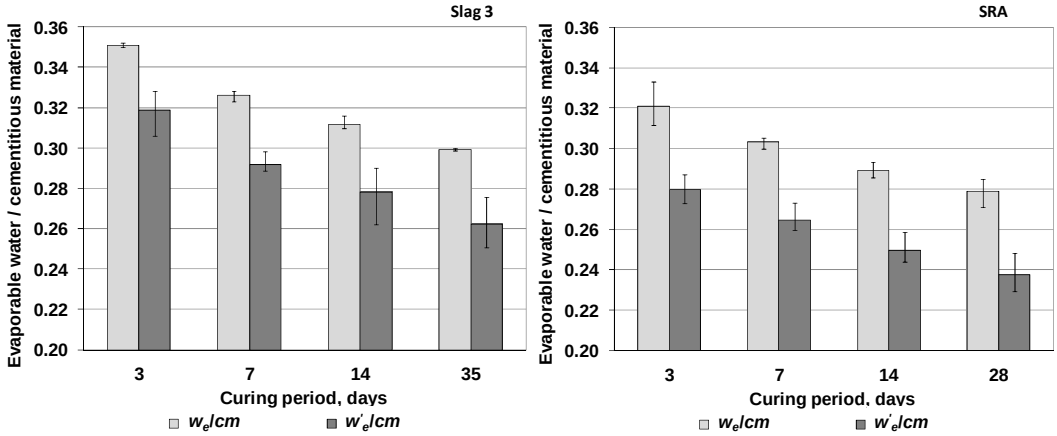

(a) (b)

Figure 4.1 Evaporable water content (expressed as water-cementitious material ratio, average value of three specimens) versus curing time: (a) Slag 3, (b) SRA (shrinkage reducing admixture) concrete. Note: w_e = original water content – non-evaporable water content. w'_e = total water lost– water lost of aggregate components during oven drying.

4.3 w'_e VERSUS w_e^*

As explained in Chapter 2, the concrete was cured in lime-saturated water. In this section, the quantity of evaporable water based on the weight of the specimens after wet curing w_e^* (Eq. 2.10) is compared with the quantity of evaporable water based on the weight of the specimens at demolding w'_e (Eq. 2.7) for the two mixtures presented in Section 4.2. It should be mentioned that the calculation of w_e^* is identical to the calculation of w'_e, except that the weight of concrete after curing is used for w_e^* while the weight of concrete at demolding is used for w'_e (see Section 2.6.3.3). The results are shown in Figure 4.2. The horizontal axis shows the curing period, and the vertical axis shows the quantities of evaporable water, w'_e and w_e^*, expressed as water-cementitious material ratios. The error bars parallel to the vertical axis show the minimum and maximum values for the three specimens in each batch. As shown

in Figure 4.2, the value of w_e^*/cm is consistently higher than w'_e/cm, with differences of 0.049, 0.055, 0.058 and 0.064 for the slag concrete cured for 3, 7, 14, and 35 days, and 0.028, 0.038, 0.047, and 0.055 for the SRA concrete cured for 3, 7, 14, and 28 days. The observation that w_e^* is higher than w'_e demonstrates that water was absorbed by the cement paste during the curing period. The value by which w_e^* exceeds w'_e increases with increased curing. Figure 4.2 also demonstrates that the difference between w_e^* and w'_e is greater for the concrete containing slag than for the SRA concrete.

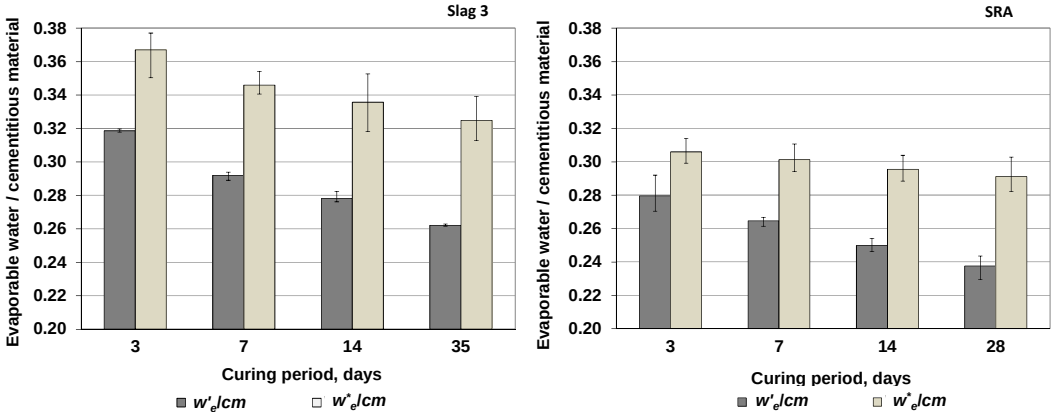

(a) (b)

Figure 4.2 w'_e/cm and w_e^*/cm versus curing period for concrete mixtures: (a) Slag 3, (b) SRA (shrinkage reducing admixture) concrete. Note: w'_e/cm is based on the weight of specimens when they are first removed from the molds, and w_e^*/cm is based on the weight of specimens after wet curing.

The comparisons of w'_e and w_e^* are only available for the concrete containing slag and the SRA concrete, where the weight of the specimens at demolding were measured. The ratios of the water content in the cement paste at the end of curing to the original water content at batching can also be used to compare the quantity of external water absorbed during curing for the control mixtures and the mixtures containing fly ash, slag, and SRA. The total water content in the cement paste at the end of curing w_t [Eq. (2.12)] equals to the summation of the non-evaporable water

w_n [Eq. (2.3)] and the evaporable water w_e^{**} [Eq. (2.11)]. The evaporable water w_e^{**} is determined in the same way as w_e^*, except that the weight of the cured, crushed material instead of the weight of cylinder at demolding is used to determine the weight of components in the sample. The difference between w_e^*/cm and w_e^{**}/cm is within 0.002.

The ratios of total to original water content in the cement paste for the four mixtures are plotted versus curing period in Figure 4.3. The higher the value of the ratio, the higher quantity of water absorbed. Figure 4.3 shows that for curing periods between 3 and 28 days (35 days for the slag concrete), the longer the concrete is cured under water, the greater the quantity of water absorbed for all mixtures. As shown in Figure 4.3, the ratios for the control concrete increased from 0.966 to 1.054, 1.066, and 1.114 as the curing period increased from 3 to 7, 14, and 28 days. The concrete containing fly ash has the lowest ratios for the mixtures studied, with values of 0.959, 0.993, 0.995, and 1.016 for specimens cured for 3, 7, 14, and 28 days. The ratios for the concrete containing slag remained fairly constant, increasing slightly from 1.037 to 1.046, 1.055, and 1.060 as the curing period increased from 3 to 7, 14, and 35 days. The ratios increase from 0.980, to 0.995, 1.014, and 1.028 for the concrete containing the SRA. The fact that some of the ratios are lower than 1.0, with the lowest value of 0.959 for the fly ash concrete cured for three days, is likely caused by water lost during specimen handling. As discussed in Section 2.6.3.2, water evaporates when the cylinders (originally in the SSD condition) are crushed and transferred to the oven.

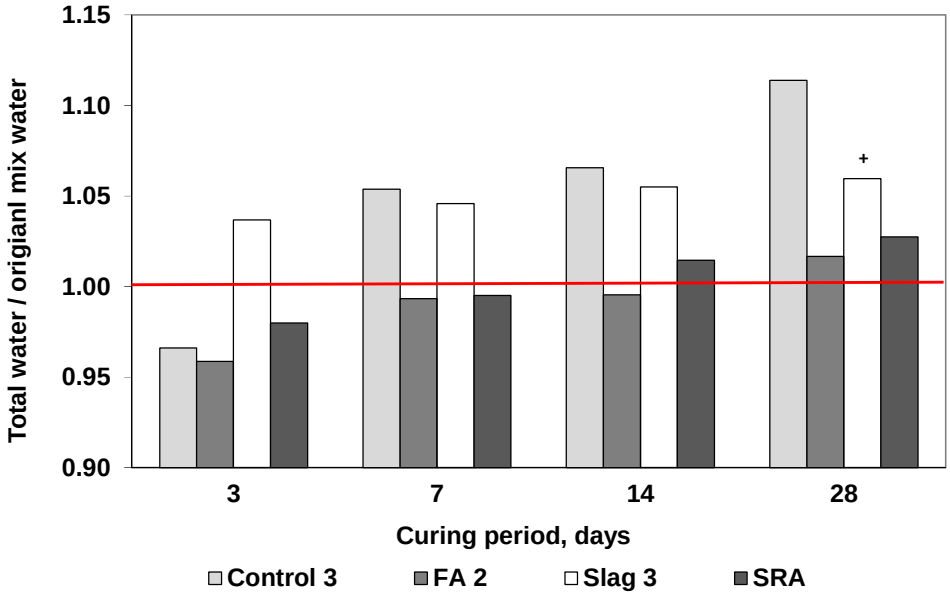

Figure 4.3 Ratio of total water content at end of curing to original water content at batching as a function of curing time and mixture type. + Specimens cured for 35 days.

The observation that water was absorbed during curing can be explained by the findings by Powers (1960), as discussed in Section 1.3.1.3. Powers (1960) stated that

$$\frac{w_t}{c} = \frac{w_o}{c} + 0.254m\ \frac{w_n^o}{c} \tag{4.1}$$

where

$\frac{w_t}{c}$ = total water-cement ratio

$\frac{w_o}{c}$ = original water-cement ratio

w_n^o = non-evaporable water content of completely hydrated cement

$m = \frac{w_n}{w_n^o}$, where w_n =non-evaporable water content at time of testing and m equals 1 for fully mature specimens and is less than 1 for incompletely hydrated specimens.

The term $0.254\,m\,\frac{w_n^o}{c}$ is the quantity of water, per unit weight of cement, that cement paste must obtain from an external source to remain in a saturated condition. This

value is related to the porosity of the hydrated cement paste and the quantity of water that is chemically combined at time of testing (Powers 1960).

According to Eq. (4.1), water is attracted to hydrated cement paste when specimens are cured under water, and the quantity $0.254\, m\, \frac{w_n^o}{c}$ is related to the degree of hydration. The higher ratio of the total water content to the original water content for the specimens that cure longer, as illustrated in Figure 4.3, can be explained by the higher degree of hydration and, thus, the higher quantity of water absorbed.

During the curing period, concrete normally expands as it absorbs water from an external source. The expansion, expressed as negative free shrinkage, is plotted versus curing period in Figure 4.4. As shown in the figure, the control concrete expanded 23, 50, 43, and 37 με for specimens cured for 3, 7, 14, and 28 days, respectively. The concrete containing fly ash exhibited similar amount expansion as the control concrete, with values of 33, 30, 40, and 33 με for specimens cured for 3, 7, 14, and 28 days, respectively. The slag concrete and the SRA mixture exhibited higher expansion than the control and fly ash concretes, with values of 85, 77, 147, and 103 με for specimens cured for 3, 7, 14, and 35 days for the slag concrete, and 103, 75, 50, and 100 με for specimens cured for 3, 7, 14, and 28 days for the SRA mixture. The specimens cured for longer periods contain more absorbed water than the specimens cured for shorter periods, as indicated in Figure 4.3, although they do not necessarily exhibit more expansion, as shown in Figure 4.4. Therefore, based on the four batches in this comparison, there is no direct correlation between the amount of expansion and the quantity of absorbed water. It is also noted that the control mixture absorbs more water during curing but exhibits less expansion than the other mixtures, except that it has slightly more expansion than the mixture containing fly ash cured for 7, 14, and 28 days.

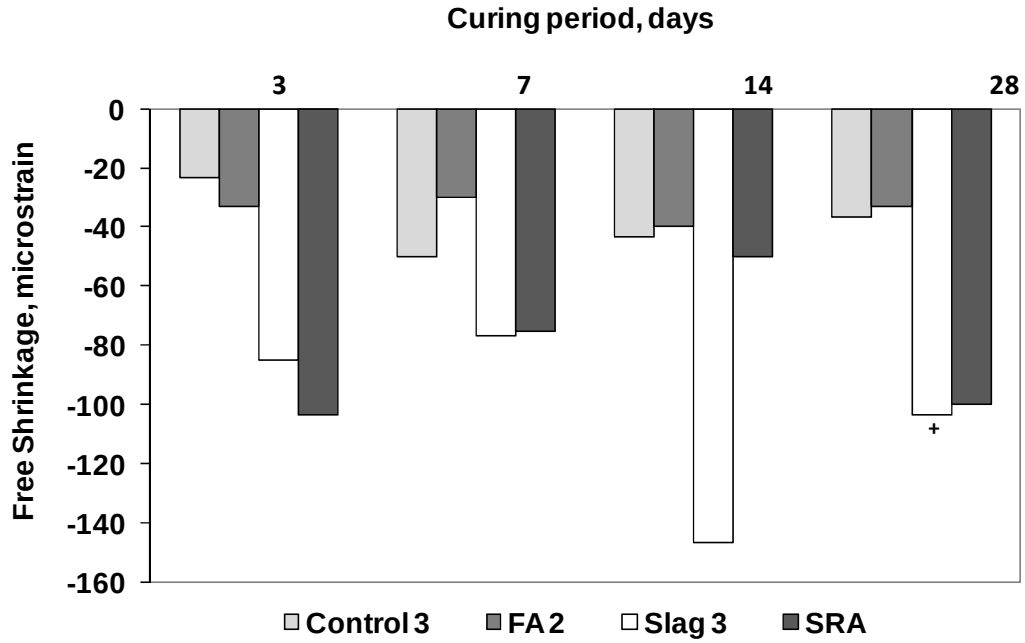

Figure 4.4 Expansion of free shrinkage specimens at the end of curing as a function of curing time and mixture type. Note: Negative values mean expansion. [+] Specimens cured for 35 days.

4.4 DEGREE OF HYDRATION REPRESENTED BY THE QUANTITY OF NON-EVAPORABLE WATER

The quantity of non-evaporable water serves as a measure of the degree of hydration. A high quantity of non-evaporable water means a high degree of hydration. The quantities of non-evaporable water (in the order of decreasing values) for the control mixture and mixtures containing SRA, slag, and fly ash with different curing periods are presented in Figure 4.5. The error bars parallel to the vertical axis show the minimum and maximum values for each batch.

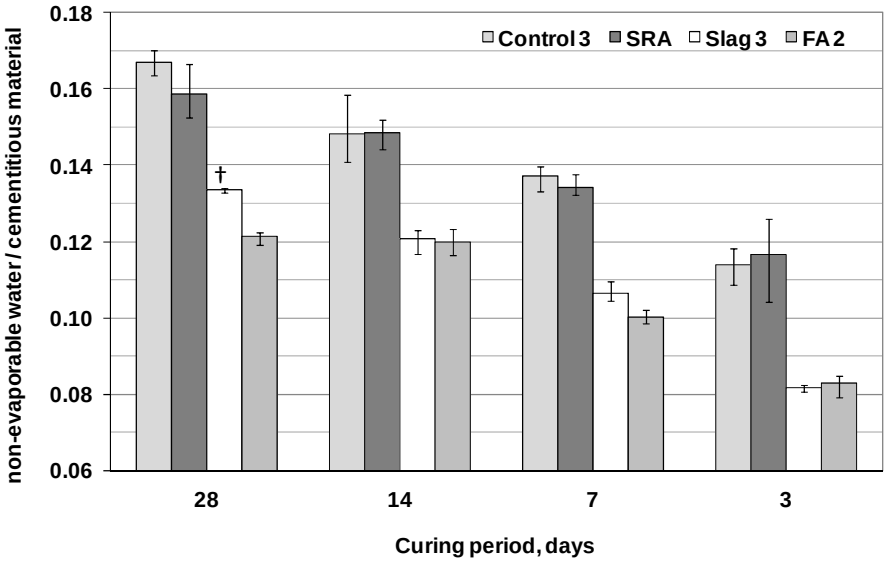

Figure 4.5 Non-evaporable water content for the control mixture and mixtures containing SRA, slag, and fly ash. Specimens cured for 28, 14, 7, and 3 days. † Specimens cured for 35 days.

As shown in Figure 4.5, for a given mixture, the specimens cured for longer periods contain more non-evaporable water because they have undergone a higher degree of hydration than the specimens cured for shorter periods. Of the four mixtures, the control mixture contains the highest quantity of non-evaporable water, with non-evaporable water-cementitious material (w_n/cm) ratios of 0.167, 0.148, 0.137, and 0.114 for specimens cured for 28, 14, 7, and 3 days; the mixture containing the SRA contains similar quantities of non-evaporable water, with corresponding w_n/cm ratios of 0.159, 0.148, 0.134, and 0.117. Based on this limited comparison, the addition of an SRA does not appear to influence the hydration rate. In contrast, Figure 4.5 shows that the mixtures containing slag and fly ash contain less non-evaporable water, with corresponding w_n/cm ratios of 0.133, 0.121, 0.106, and 0.082 for the slag concrete and 0.121, 0.120, 0.100 and 0.083 for the fly ash concrete, and have thus undergone less hydration than the control mixture. The lower degree of hydration of mixtures containing slag and fly ash compared to the control mixture can be explained as follows. Compared to cement, slag reacts slowly with water due

to an impervious coating that forms on the slag particles early in the hydration process (Mindess et al. 2003). For mixtures containing fly ash, the SiO_2 in the fly ash reacts with calcium hydroxide (CH) formed during the hydration of cement, a reaction that is also slow compared with cement hydration (Mindess et al. 2003).

4.5 EVAPORABLE WATER CONTENT VERSUS FREE SHRINKAGE

The free shrinkage values at 30 and 365 days are plotted versus the evaporable water content of the paste constituent (expressed as a water-cementitious material ratio) for the control concrete and mixtures containing fly ash, slag, and SRA in Figures 4.6 through 4.9. The best fit lines and corresponding equations are shown in the figures. Free shrinkage is based on the total length change after demolding. The quantity of evaporable water w_e equals the difference between the original mix water and the non-evaporable water measured when the specimens were removed from lime-saturated water at the end of curing, as shown in Eq. (2.6). The increasing quantities of evaporable water correlate with decreasing curing periods. As shown in Figures 4.6 through 4.9, a generally linear relationship between free shrinkage and evaporable water content is observed, especially for the control mixtures and the mixtures containing slag; the linear relationships for the mixtures containing fly ash and SRA are relatively weak. The figures demonstrate that mixtures containing less evaporable water also exhibit less free shrinkage. The trend is most apparent for the slag and control concretes, which have higher slopes than the fly ash and SRA concretes. It is also noted that the slopes of the curves for the 30-day free shrinkage results (Figures 4.6a through 4.9a) are higher than those for 365-day free shrinkage results (Figures 4.6b through 4.9b), except for the control mixture.

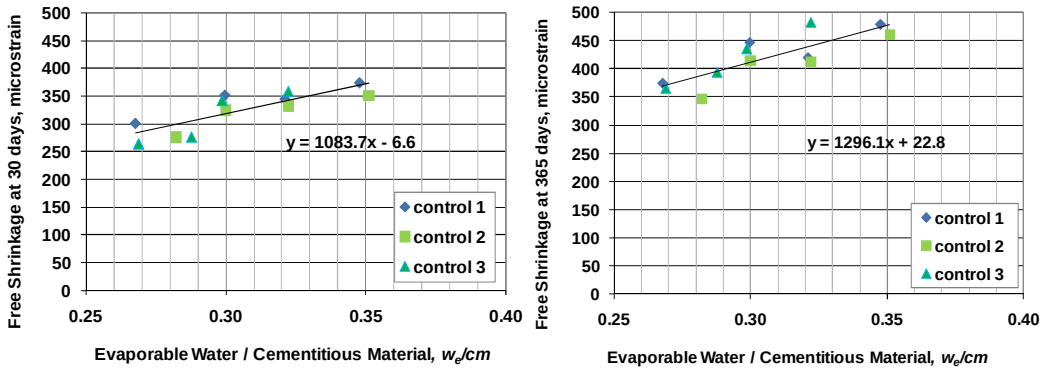

(a) (b)

Figure 4.6 Free shrinkage versus evaporable water content: control mixture, (a) 30-day free shrinkage, (b) 365-day free shrinkage.

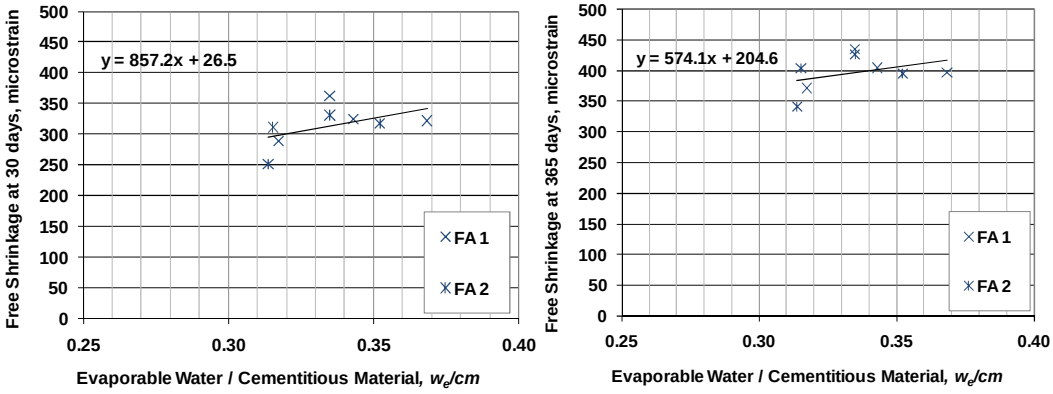

(a) (b)

Figure 4.7 Free shrinkage versus evaporable water content: fly ash mixture, (a) 30-day free shrinkage, (b) 365-day free shrinkage.

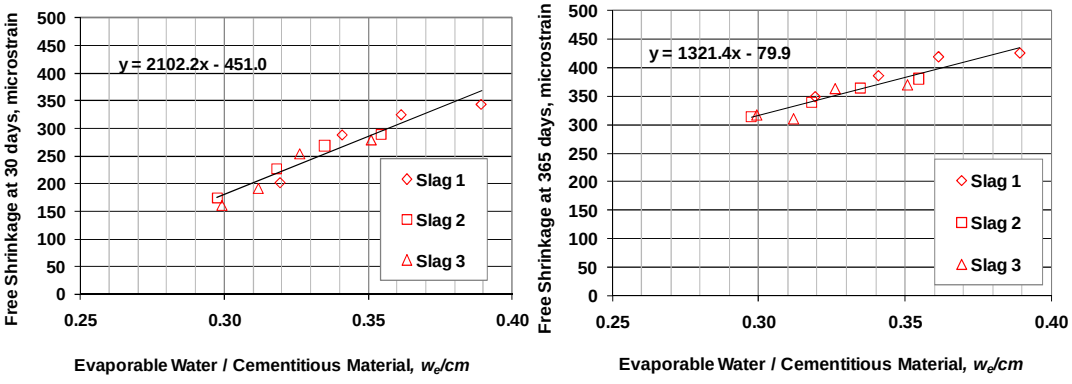

(a) (b)

Figure 4.8 Free shrinkage versus evaporable water content: slag mixture, (a) 30-day free shrinkage, (b) 365-day free shrinkage.

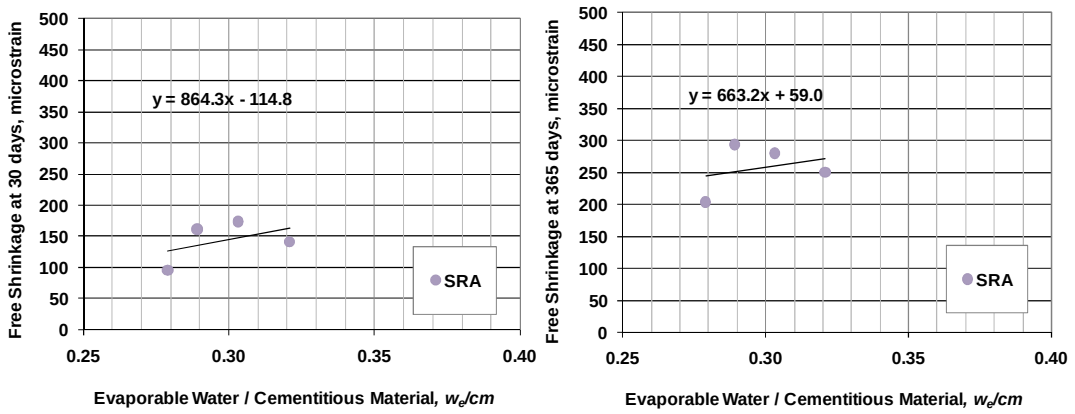

(a) (b)

Figure 4.9 Free shrinkage versus evaporable water content: SRA mixture, (a) 30-day free shrinkage, (b) 365-day free shrinkage.

Because of the correlation between the curing period and the value of evaporable water w_e and because mixtures containing less evaporable water exhibit less free shrinkage, it is appropriate to also investigate the relationship between free shrinkage and curing period. The free shrinkage, based on the total length change after demolding, at 30 and 365 days is plotted versus the curing period for the control concrete and mixtures containing fly ash, slag, and SRA in Figures 4.10 through 4.13. The best fit lines and corresponding equations are shown in the figures. As shown in the figures, a generally linear relationship between free shrinkage and curing period is observed. A negative slope indicates that the longer the concrete cured, the lower the free shrinkage, and for the four mixtures investigated in this study, all have negative slopes. For free shrinkage at 30 days, the slag concrete has the most negative slope, followed by the control, the SRA, and the fly ash concretes. Also, the slopes of the curves at 30 days for the slag and fly ash concretes (Figures 4.11a and 4.12a) are higher than those at 365 days (Figures 4.11b and 4.12b), indicating that the influence of curing period on free shrinkage is greater at early ages than at one year for these mixtures. For the control concrete, the slope at 365 days is higher than the slope at 30 days, while for the SRA concrete, the slope at 365 days is approximately the same as the slope at 30 days.

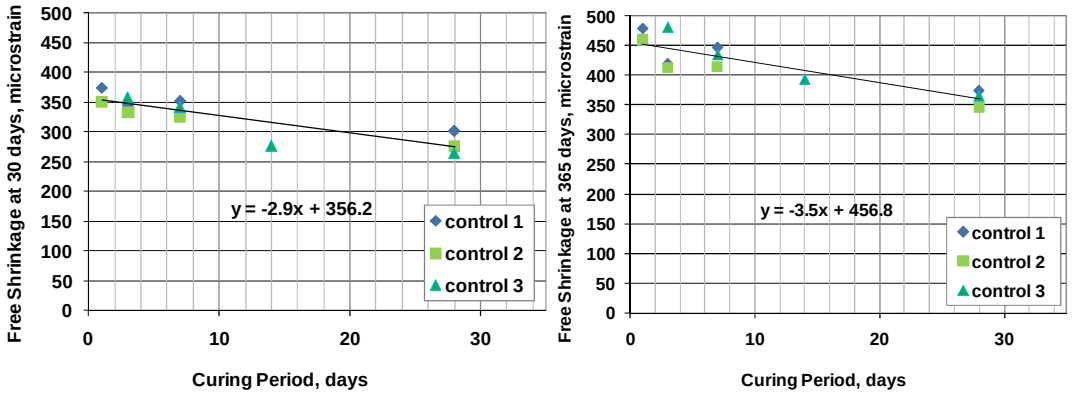

(a) (b)

Figure 4.10 Free shrinkage versus curing period: control mixture, (a) 30-day free shrinkage, (b) 365-day free shrinkage.

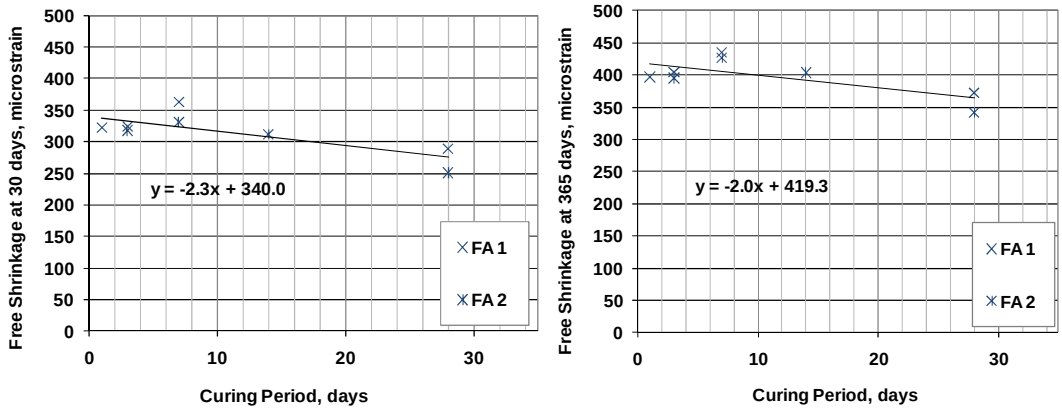

(a) (b)

Figure 4.11 Free shrinkage versus curing period: fly ash mixture, (a) 30-day free shrinkage, (b) 365-day free shrinkage.

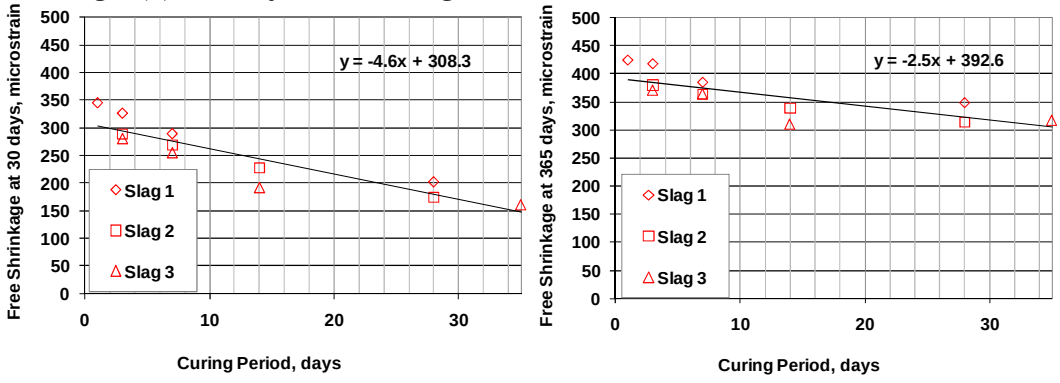

(a) (b)

Figure 4.12 Free shrinkage versus curing period: slag mixture, (a) 30-day free shrinkage, (b) 365-day free shrinkage.

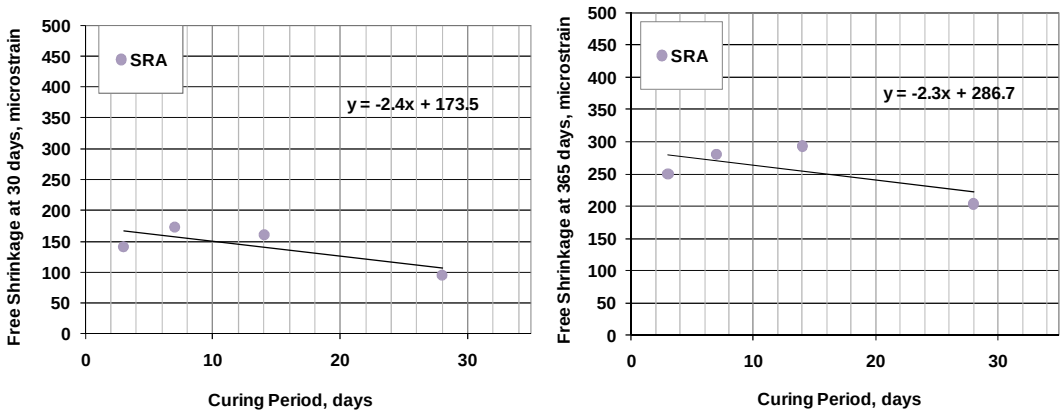

(a) (b)

Figure 4.13 Free shrinkage versus evaporable water content: SRA mixture, (a) 30-day free shrinkage, (b) 365-day free shrinkage.

4.6 FREE SHRINKAGE VERSUS WEIGHT LOSS DURING CURING

As discussed in reference to Figure 1.2 in Chapter 1, the shrinkage-weight loss curve for cement paste can be divided into five domains: in domain 1, water is lost from the large capillary pores; in domain 2, water is lost from both mesopores and micropores (i.e., finer capillary pores and the gel pores); in domains 3 and 4, adsorbed water on the particle surfaces and interlayer water of C-S-H (only in the domain 4) is removed; and in domain 5, decomposition of C-S-H is responsible for the additional shrinkage.

The weight loss of the free shrinkage specimens during drying can be used as a direct indicator of water loss, which can be correlated to the free shrinkage performance. It should be noted that the weight loss of free shrinkage specimens, by necessity, includes the water lost by the aggregates. It is not possible to separate the water loss of aggregates from the water loss of the concrete. Free shrinkage and weight loss are calculated relative the length and weight recorded at the start of drying. The weight loss is calculated as

$$weight\ loss_{x\ d} = \frac{weight_{at\ start\ of\ drying} - weight_{x\ d}}{weight_{\ 365d}} \tag{4.2}$$

where $weight_{at\ start\ of\ drying}$= weight of specimens at start of drying,

$weight_{x\ d}$ = weight of specimens on day *x* of drying, and

$weight_{365\ d}$ = weight of specimens on day 365 of drying.

For batches Control 3 and FA 2, only the specimens cured for 28 days were weighed when the free shrinkage readings were recorded. All specimens for the Slag 3 and SRA batches (batches 681 and 683) were measured for weight loss each time free shrinkage readings were recorded. The data represents the average of three specimens.

Free shrinkage versus weight loss for specimens cured for 3, 7, 14, and 28 days (35 days for the slag concrete) for mixtures containing slag and SRA are presented first in Sections 4.6.1 and 4.6.2. In Section 4.6.3, free shrinkage versus weight loss for different mixtures (control concrete and concretes containing fly ash, slag, and SRA) cured for 28 days is compared.

4.6.1 Slag Concrete (Slag 3)

Average free shrinkage is plotted versus average weight loss for the specimens in batch Slag 3 in Figure 4.14. The development of the curve can be analyzed in three phases (corresponding to domains 1 to 3 in Figure 1.2) based on its slope. The first phase includes the first few days of drying, where the slope is lower than slopes at later ages. The low slope can be correlated to water loss from the capillary pores (corresponding to domain 1 in Figure 1.2), as well as from the aggregates. Water lost from capillary pores causes less shrinkage than water lost from finer pores in later ages (Mindess et al. 2003); water lost from the aggregates does not influence free shrinkage.

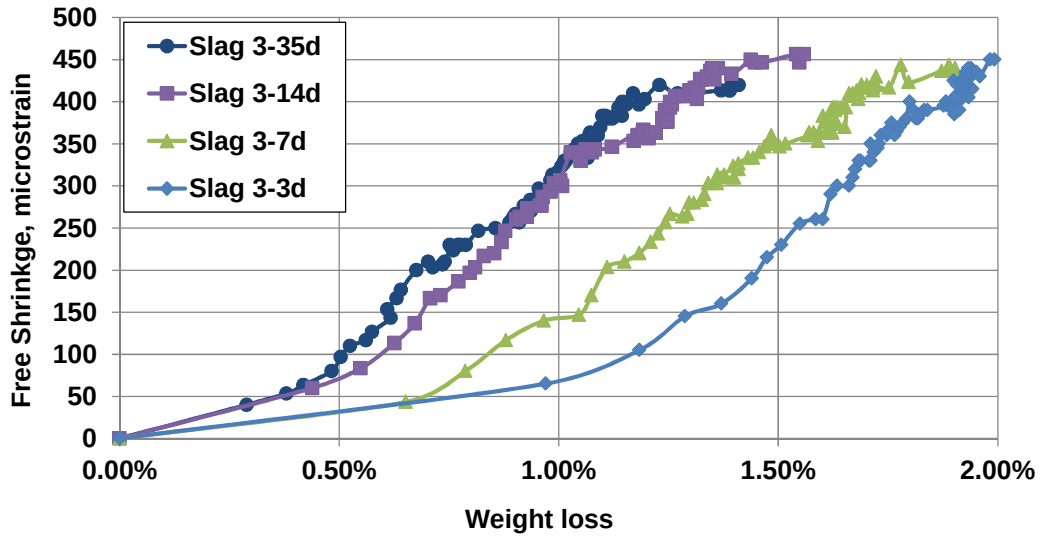

Figure 4.14 Average free shrinkage versus average weight loss for Slag concrete. Specimens cured for 3, 7, 14, or 35 days. Note: Measurements are taken every day for the first 30 days, every other day between 30 and 90 days, once a week between 90 and 180 days, and once a month between 180 and 365 days.

Figure 4.14 shows that on the first day of drying, specimens cured for shorter periods lose much more water than those cured for longer periods; for the first five days of drying, the slope of the curve for specimens cured for 35 days is highest, followed by those cured for 14, 7, and 3 days. The rate of water loss from the aggregates should be somewhat slower as the curing period increases because of the lower permeability of the paste. The relationship between curing period and rate of early water loss can be explained as follows. At early ages, capillary water will be lost through evaporation first. The free shrinkage (at an early age) per unit weight loss will be less for specimens that have more capillary cavities (Powers 1959). Because specimens that are cured for a shorter time have undergone less hydration, they have more capillary cavities (Powers 1959) and, thus, lower slopes at early ages. The degree of hydration can be demonstrated by the quantity of non-evaporable water in the concrete (Figure 4.5). The specimens cured for 35 days have the highest quantity of

non-evaporable water, and thus, the highest degree of hydration, followed in turn by those cured for 14, 7, and 3 days.

In the second phase (corresponding to domain 2 in Figure 1.2), the finer capillary pores and gel pores begin to lose water and the slope of the free shrinkage versus weight loss curve increases. In this phase, the slopes are nearly constant through about 250 days for the specimens cured for 3 and 7 days and through 230 days for specimens cured for 14 and 35 days. After that, the slopes decrease in the third phase (corresponding to domain 3 in Figure 1.2) as water adsorbed on solid surfaces is removed.

Weight loss versus time and free shrinkage versus time are plotted in Figures 4.15 and 4.16, respectively. It is noted that the weight loss curve and the free shrinkage curve have similar shapes, with most of the weight loss and free shrinkage occurring during the first 30 days of drying. After that, the rates of both weight loss and free shrinkage are much lower. In order from high to low weight loss, the specimens are those cured for 3, 7, 14, and 35 days. The specimens with less curing exhibit more weight loss. Figure 4.16 shows that at 30 days of drying, the specimens cured for 3 days exhibit the greatest free shrinkage, followed by the specimens cured for 7, 14, and 35 days. After 365 days of drying, the specimens cured for 3, 7, and 14 days exhibit similar values of free shrinkage, while the specimens cured for 35 days continue to exhibit the lowest value of free shrinkage. Figures 4.15 and 4.16 indicate that specimens cured for a longer period have less weight loss and less free shrinkage. For the concrete in batch Slag 3, the differences in free shrinkage tend to decrease over time.

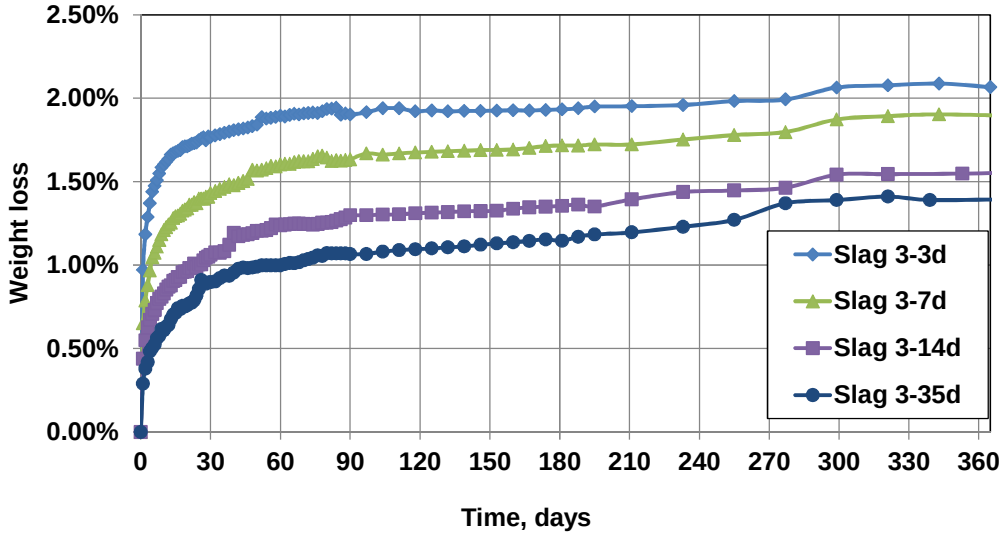

Figure 4.15 Average weight loss versus drying time for the slag concrete. Specimens cured for 3, 7, 14, or 35 days.

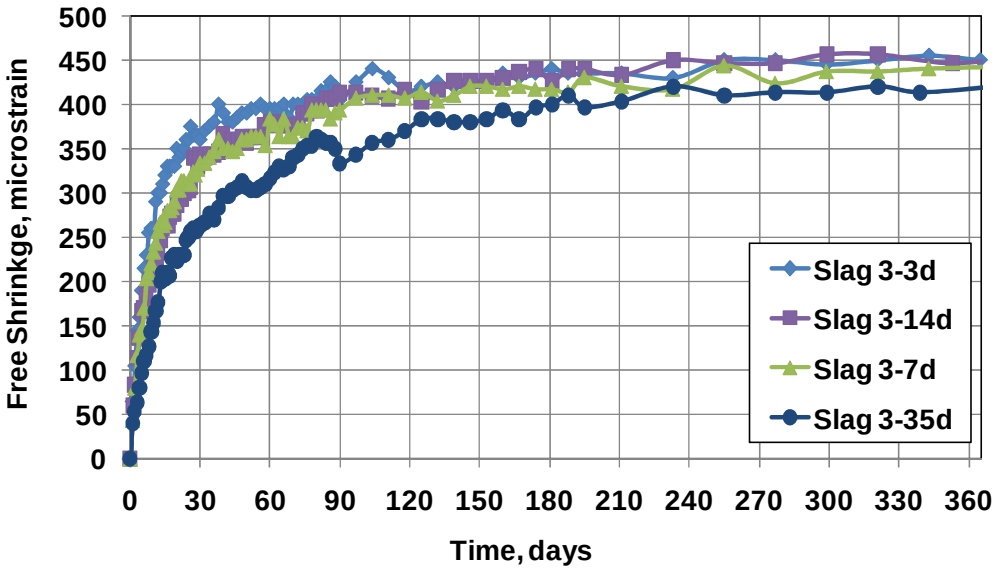

Figure 4.16 Average free shrinkage versus drying time for the slag concrete. Specimens cured for 3, 7, 14, or 35 days. Note: Free shrinkage based on the relative length change from the first day of drying.

4.6.2 Concrete with Shrinkage Reducing Admixture (SRA batch)

Average free shrinkage is plotted versus average weight loss for the SRA concrete with different curing periods in Figure 4.17. As shown in the figure and as noted for the slag concrete, the curves have a lower slope during the first few days due to the early loss of capillary water and water in aggregates. After that, the slopes increase and are nearly constant until for about 150 days, and then decrease. It is also noted that specimens with different curing times perform in a similar manner, which may be correlated with the mechanism by which SRAs work, reducing concrete shrinkage by reducing the surface tension of the pore water.

With the different curing periods, the specimens contain different quantities of evaporable water (Figure 4.1). Weight loss is plotted versus time for the SRA mixture in Figure 4.18. It is interesting to note that the specimens containing an SRA cured for different lengths of time exhibit very similar weight loss as a function of drying time.

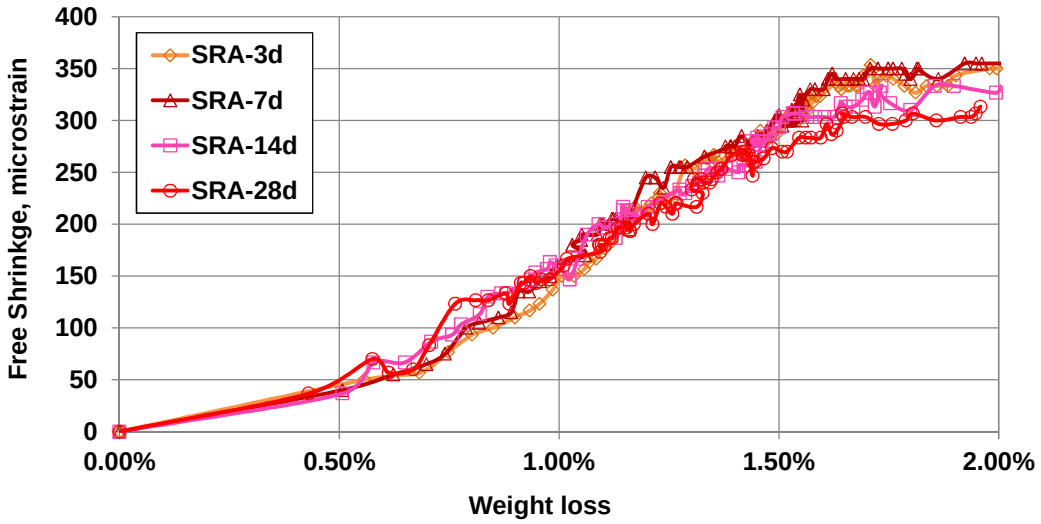

Figure 4.17 Average free shrinkage versus average weight loss for the SRA batch. Specimens cured for 3, 7, 14, and 28 days. Note: Measurements are taken every day for the first 30 days, every other day between 30 and 90 days, once a week between 90 and 180 days, and once a month between 180 and 365 days.

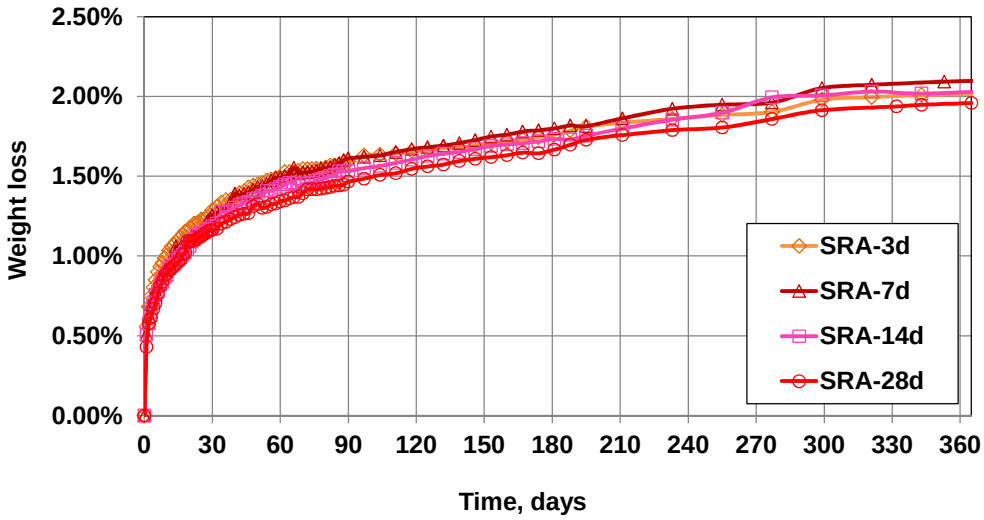

Figure 4.18 Average weight loss versus drying time for SRA concrete. Specimens cured for 3, 7, 14, or 28 days.

Free shrinkage is plotted versus time for the SRA mixtures cured for varying lengths of time in Figure 4.19. The specimens cured for 14 days exhibit slightly less free shrinkage than the specimens cured for 3 and 7 days. The specimens cured for 28 days exhibit the least free shrinkage. Thus, increasing the curing period reduces free shrinkage for this SRA mixture.

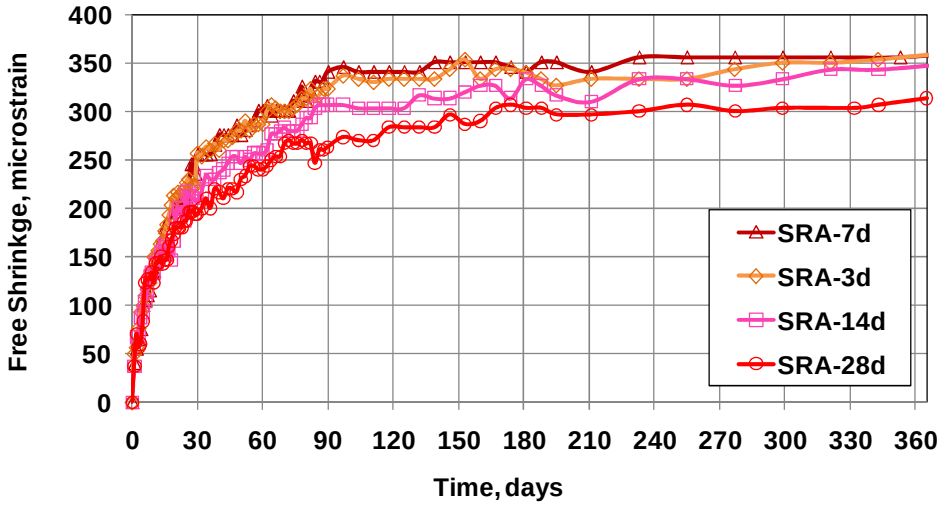

Figure 4.19 Average free shrinkage versus drying time for SRA concrete. Specimens cured for 3, 7, 14, or 28 days. Note: Free shrinkage based on the relative length change from the first day of drying.

4.6.3 Comparison of Control, Fly Ash (FA), Slag, and SRA Concrete Mixtures

For the control and fly ash concrete mixtures, only the specimens cured for 28 days were weighed when the free shrinkage readings were recorded. The results for specimens cured for 28 days for the control mixture and mixtures containing fly ash, slag, and SRA are compared in this section.

The four mixtures were designed to have the same paste content and water cementitious material ratio. With different cementitious materials, the quantities of mix water for different mixtures are different. The weight loss of the free shrinkage specimens involves both the mix water and the water in the aggregate particles, which are shown along with the total water content for the four mixtures in Table 4.1 (the mixture proportions are shown in Table A.9 in Appendix A). As shown in the table, the four mixtures have the same amount water in the aggregates but different quantities of mix water. The SRA mixture contains the most water, 255 lb/yd^3 (150 kg/m^3), followed by the control concrete [254 lb/yd^3 (150 kg/m^3)], the slag concrete [247 lb/yd^3 (146 kg/m^3)], and the fly ash concrete [243 lb/yd^3 (143 kg/m^3)].

Table 4.1 Total water (including actual mix water and water in aggregate particles) in concrete mixtures, based on yd^3 design.

Mixture	Control 3	FA 1	Slag 3	SRA
Mix water†, lb/yd^3	235	224	228	236
Water in aggregates, lb/yd^3	19	19	19	19
Total water, lb/yd^3	254	243	247	255

† Actual mix water after moisture correction of aggregates. Note: 1 lb/yd^3 = 0.59 kg/m^3

Free shrinkage is plotted versus weight loss in Figure 4.20 for specimens cured for 28 days. As described in Sections 4.6.1 and 4.6.2, the slope is low during the first few days for all mixtures, followed by an increase and then a decrease at the end of the test period. As described in Section 4.6.1, the slopes of the curves are based on three phases of drying.

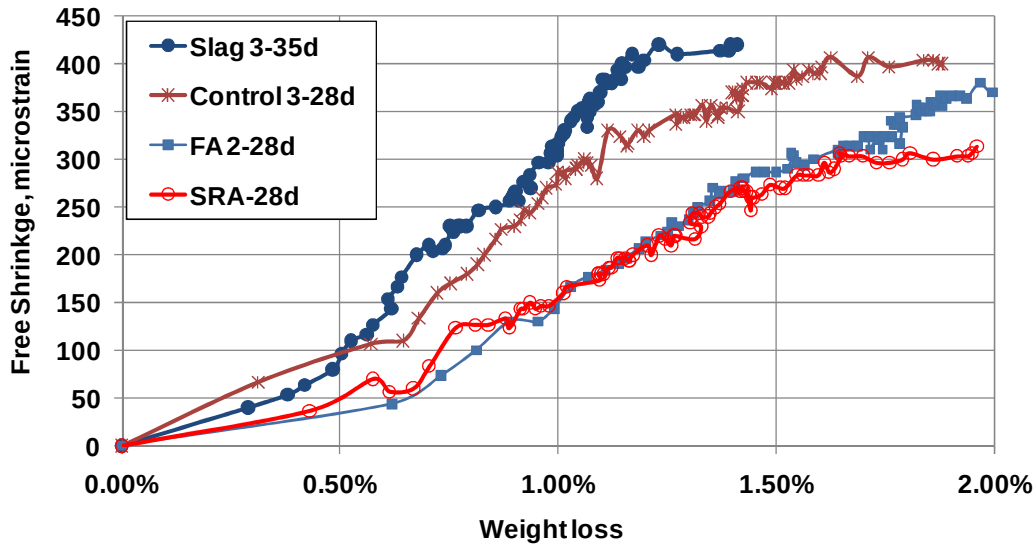

Figure 4.20 Average free shrinkage versus average weight loss for the control, fly ash (FA), slag, and SRA mixtures. Specimens cured for 28 days (35 days for slag concrete). Note: Measurements are taken every day for the first 30 days, every other day between 30 and 90 days, once a week between 90 and 180 days, and once a month between 180 and 365 days.

The first phase includes the first few days of drying, where water in large capillary pores and aggregates is lost. The slag and fly ash concretes have a lower slope than the control mixture at early ages. The lower slope means less free shrinkage for the same water loss. As discussed in Section 4.6.1, the lower slope of the slag and fly ash mixtures (due to rapid water loss) may be the result of their relatively low hydration (see Figure 4.5). It is noted that the quantity of non-evaporable water in the SRA mixture is similar to the quantity in the control mixture (Figure 4.5), although the slope of its free shrinkage versus weight loss curve is lower (Figure 4.20). With a similar degree of hydration as the control mixture, the mixture containing the SRA has less free shrinkage due to the reduced surface tension of the pore water, not due to any effect of hydration.

In the second phase, the slopes of the free shrinkage versus weight loss curves increase for all mixtures. The slopes remain nearly constant through 160, 190, 230, and 260 days of drying for mixture containing SRA, control mixture, and mixtures

containing slag and fly ash, respectively. The mixture containing slag has a slightly higher slope than the control mixture, while the mixture containing fly ash has a lower slope; they both contain less total water than the control mixture. The differences in performance between the mixtures contacting slag and fly ash may be related to different pore structures. Felman (1981) used mercury intrusion porosimetery to determine the pore-entry size distributions for pastes of portland and blended cements. The portland cement paste contained 100% Portland cement. Two blended cement pastes were evaluated, one with a 35% weight replacement of cement with fly ash and the other one with a 70% weight replacement of cement with slag. Felman (1981) found that at early ages (1 to 3 days), the distribution of pore entry sizes in fly ash and slag cement pastes were coarser than in comparable portland cement, and at later ages (cured for one year), the distribution of pore entry sizes was finer; the distribution of pore entry sizes for slag cement paste was finer than for fly ash paste at later ages. With 35 days of curing for the concrete containing slag in this study, it may have a finer distribution of pore sizes than the control concrete, and thus more free shrinkage at the same weight loss. With 28 days of curing, the concrete containing fly ash may still have a coarser distribution of pore sizes than the control concrete, and thus less free shrinkage at the same weight loss. As expected, the SRA mixture still has a lower slope due to the reduced surface tension of the pore water.

In the third phase, the slopes decrease as water adsorbed on the solid surfaces is removed.

Weight loss is plotted versus time in Figure 4.21. The concrete containing fly ash has the highest weight loss at all ages, even though it contains the lowest quantity of water (Table 4.1), which may be explained by a coarser distribution of pore sizes that allow easy water loss. The concrete containing slag has the lowest weight loss, which may be related to a finer distribution of pore sizes. With about the same water content in the specimens (Table 4.1), the concrete containing SRA has slightly higher

weight loss than the control mixture, which is caused by the reduced surface tension of pore water by SRA.

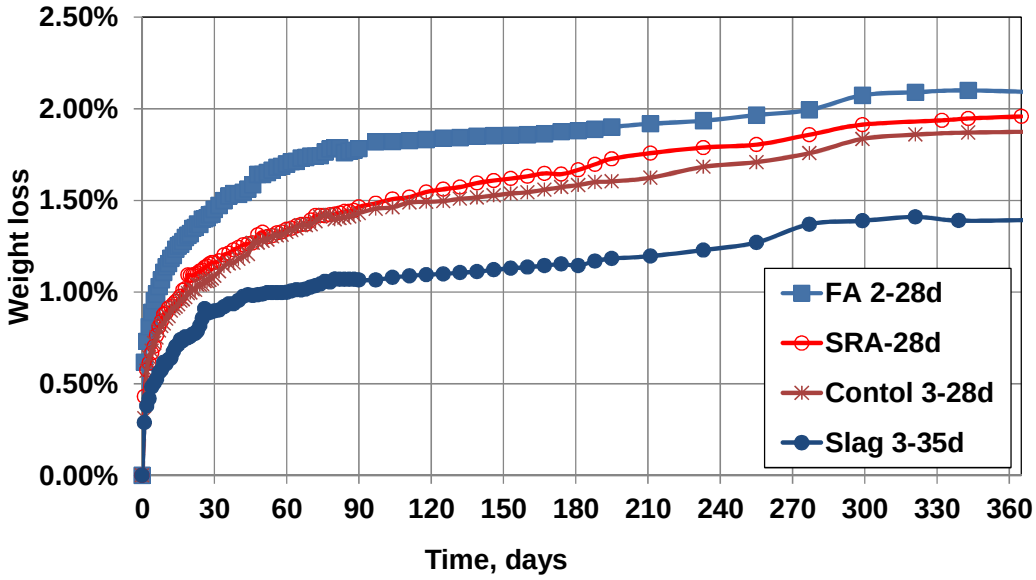

Figure 4.21 Average weight loss versus drying time for the 28-day cured specimens of the control, fly ash, slag and SRA mixtures.

Free shrinkage is plotted versus time in Figure 4.22 for the four mixtures. These curves are similar in shape to the weight loss versus time curves. During the first 60 days, the control concrete exhibits the most free shrinkage, followed by the concrete containing fly ash, slag, and SRA. At 365 days, the concrete containing slag exhibits the highest free shrinkage, followed by the control concrete and the concrete containing fly ash and SRA. The free shrinkage of the concrete containing slag surpasses the free shrinkage of the concrete containing slag at 60 days and the control concrete at 120 days. The concrete containing the SRA exhibits the least free shrinkage at all ages.

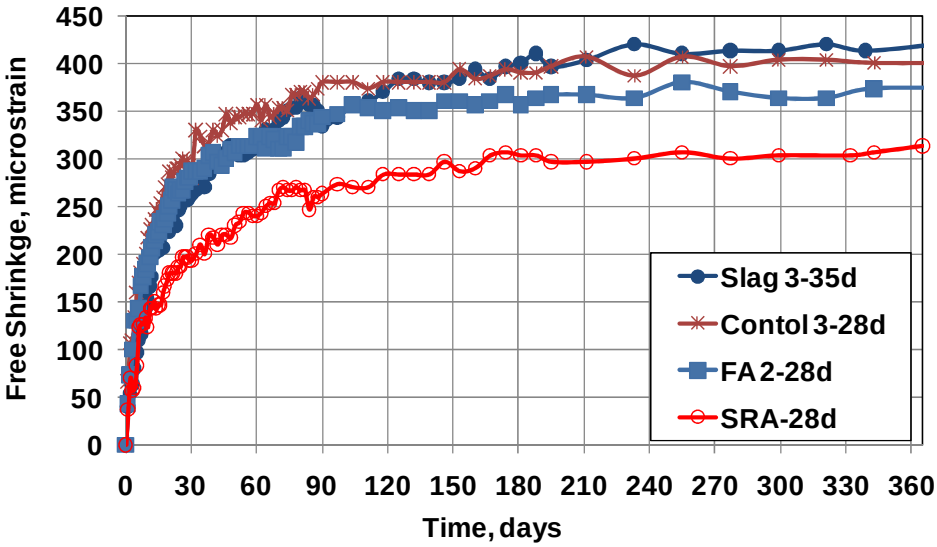

Figure 4.22 Average free shrinkage versus drying time for the control, fly ash, slag and SRA mixtures. Specimens cured for 28 days (35 days for slag concrete). Note: Free shrinkage is calculated starting from the first day of drying.

4.7 SUMMARY OF EVAPORABLE WATER CONTENT TESTS

Concrete shrinkage is closely related to water loss from the concrete. Methods to determine the quantity of evaporable water content in concrete are developed in this study. The results of the current study relating evaporable water content and free shrinkage of concrete indicate that

1. Cement paste absorbs water during curing in lime-saturated water. The longer the cement paste is cured under water, the greater the quantity of water it absorbs.
2. For the same curing period, the concrete containing fly ash absorbed the lowest quantity of water, followed by the concrete containing SRA and slag, and the control concrete (except that concrete containing slag and the SRA mixture cured for three days absorbed more water than the control concrete).
3. Concrete expands during curing. There was no direct correlation between the amount of expansion and the quantity of absorbed water in the current study.

4. For a given mixture, specimens cured for longer periods have a higher degree of hydration as measured by the quantity of non-evaporable water than those cured for shorter periods.
5. The addition of a shrinkage reducing admixture does not have much influence on hydration, while partial replacements of cement with fly ash or slag cement reduce the degree of hydration as represented by lower quantity of non-evaporable water held by the cement.
6. A linear relationship between free shrinkage and evaporable water content is observed, especially for concrete containing slag and the control concrete containing 100% portland cement.
7. For a given mixture, specimens cured for a longer period contain less evaporable water, less weight loss, and exhibit lower free shrinkage than specimens cured for a shorter period.
8. On the curves of free shrinkage versus weight loss for all mixtures, a lower slope during the first few days is noted, which indicates the early loss of capillary water and water in the aggregates. After that, the slope increases as water in mesopores and micropores begins to be lost, and then decreases as water adsorbed on the particle surfaces is removed.
9. Based on curves of free shrinkage versus weight loss and curves of weight loss versus time (all specimens cured for 28 days, except concrete containing slag cured for 35 days), the concrete containing slag may have finer distribution of pore sizes than the control mixture while the concrete containing fly ash may have coarser distribution than the control mixture.
10. Concrete containing SRA exhibits less shrinkage at the same water loss than the control mixture due to the reduced surface tension of pore water.

CHAPTER 5 RESTRAINED RING TESTS RESULTS

5.1 GENERAL

In the restrained ring tests, a concrete ring is cast around a steel ring. When the concrete shrinks in a drying environment, the shrinkage of the concrete is restrained by the inner steel ring, which induces tensile stresses in the concrete. If the shrinkage-induced tensile stresses are higher than the tensile strength of the concrete, cracks develop in the concrete. The time to cracking is used as an index of the cracking tendency of the concrete.

This chapter presents the restrained ring tests results. A steel ring with a fixed dimension was used in this study, which had an outside diameter of 12.01 ± 0.01 in. (305.05 ± 0.25 mm), a thickness of 1.05 ± 0.05 in. (26.67 ± 1.27 mm), and a height of 6.25 ± 0.05 in. (158.75 ± 1.27 mm). Different concrete ring thicknesses and drying conditions were evaluated in six test programs. The concrete ring thicknesses included 2.5, 2, 1.5, and 1.125 in. (64, 50, 38, and 29 mm). The drying conditions included the environment as specified by ASTM C1581-04 with a temperature of 73 ± 3º F (23 ± 2º C) and a relative humidity of 50 ± 4%, an environment with a temperature of 73 ± 3º F (23 ± 2º C) and a relative humidity of 40 ± 4%, and an environment with a temperature of 86 ± 3° F (30 ± 2° C) and a relative humidity of 14 ± 4%.

Unless noted, a minimum of three ring specimens were used for each test condition. Free shrinkage specimens were cast along with the ring specimens in Programs I, II, III, and IV and Program V Set 1. Only ring specimens were cast in Program V Sets 2 and 3 and Program VI. Mixtures that were used in each program were introduced in Chapter 2.

Only concrete mixtures that contain the same cement sample are compared to minimize to the possible influence of differences in the cement on the results.

5.2 DETERMINATION OF CRACKING TIME

The time to cracking of a ring specimen is used as a principal measure of the tendency of a mixture to crack. When cracks develop in the concrete, the shrinkage-induced tensile stress in the concrete dissipates, and correspondingly there is a sharp compressive strain drop in the steel ring. The time when the strain drop in the steel ring is noted indicates that a crack has formed in the concrete. Figure 5.1 shows examples of compressive strain in steel rings versus drying time. The notes in Figure 5.1 also indicate the time when visible cracks are first observed. It can be seen that the time when the cracks are visible is consistent with the time when the strain drop is noted.

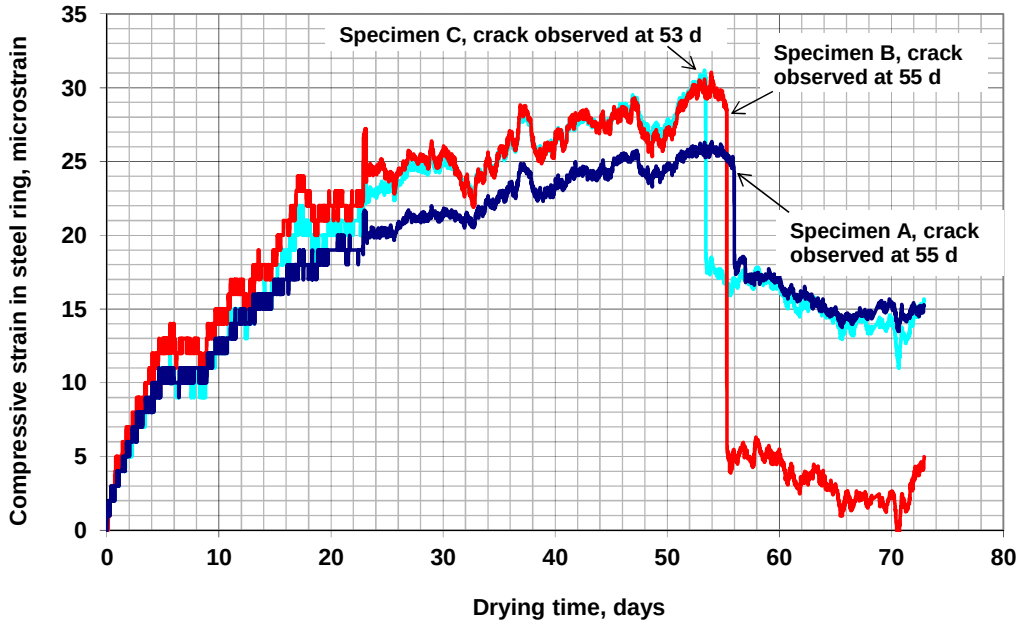

Figure 5.1 Compressive strain in steel ring versus drying time (from Section 5.3 Program I).

In contrast to Figure 5.1, however, compressive strain in the steel ring versus drying time plots often looked like the curves in Figure 5.2a, which indicate that the concrete underwent a gradual decrease in the restrained shrinkage. By way of comparison, the free shrinkage, as shown in Figure 5.2b, continues to increase,

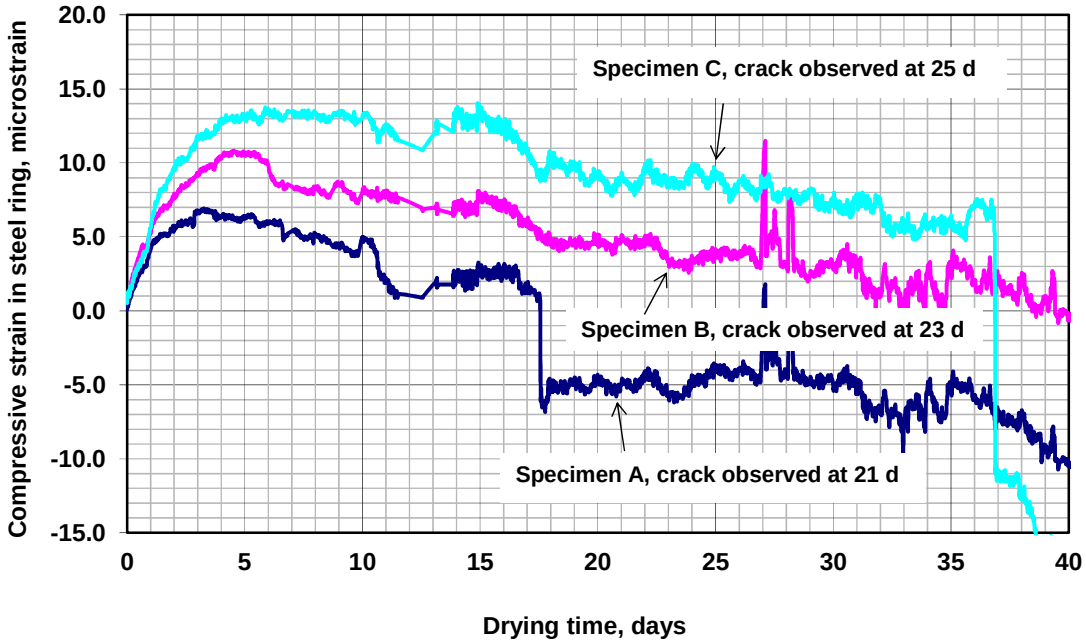

(a)

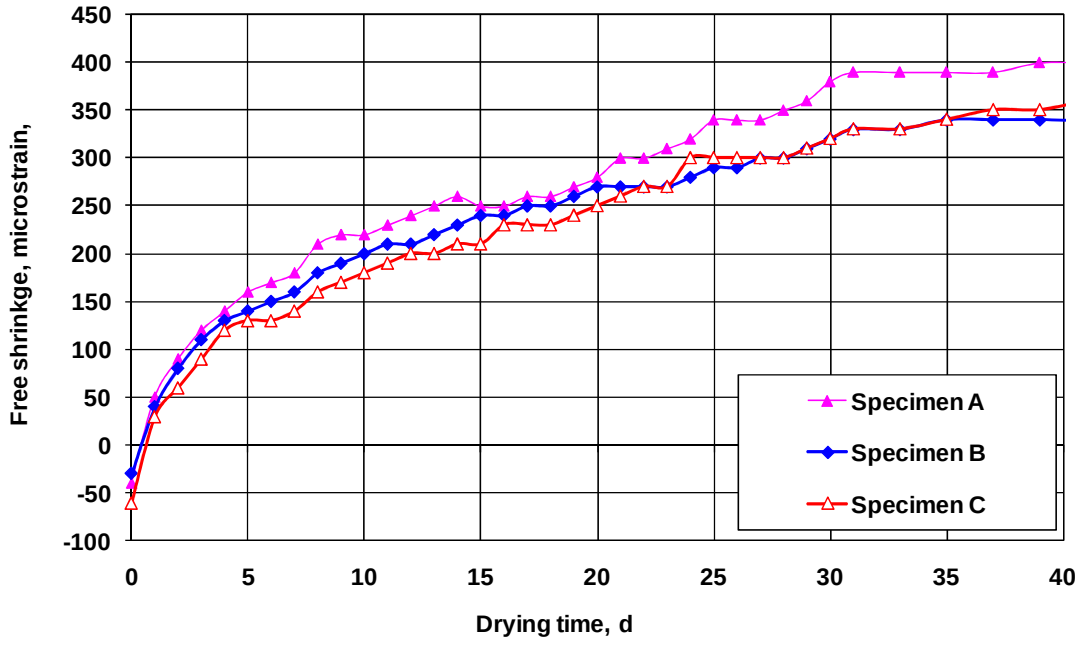

(b)

Figure 5.2 (a) Compressive strain in steel ring versus time, (b) free shrinkage versus time for the same mixture (From Section 5.6 Program IV).

even when the compressive strain in the steel ring begins to slowly decrease. The slow decrease in the compressive strain is explained as follows. When cracks form, the concrete may still be somewhat interconnected, especially when the cracks are microcracks. As a result, the tensile stresses in the concrete are only partially dissipated, and the compressive strain in the steel ring begins to decrease at a slow rate. Visible cracks are often found at a later time, as shown in Figure 5.2a.

In this study, the cracking time is determined in two ways – the time when the cracks are first visible and the time when the compressive strain in the steel ring first begins to decrease. For example, for the three specimens shown in Figure 5.2a, visible cracks are noted at 21, 23, and 25 days, while the compressive stain in steel ring begins to decrease slowly at 3, 5, and 6 days for Specimens A, B, and C, respectively. The slow decrease of the compressive strain in the steel ring indicates the formation of microcracks. The times to cracking for the concrete in Figure 5.2a are reported as 21, 23, and 25 days based on visual observation and 3, 5, and 6 days based on the compressive strain in the steel ring. It should be noted that specimens A and C in Figure 5.2a exhibit a rapid drop in compressive strain in the steel ring at 15 and 37 days, respectively, which may indicate that the microcracks have connected to form a bigger crack, which causes a relatively large and rapid strain drop in the steel ring.

5.3 PROGRAM I [2.5-in. (64-mm) CONCRETE RING]

In Program I, concrete rings with a radial thickness of 2.5 in. (64 mm) were tested along with matching free shrinkage specimens that were tested in accordance with ASTM C157. The effect of water-cement (*w*/*c*) ratio on both free and restrained shrinkage was investigated for three concrete mixtures with a cement content of 535 lb/yd^3 (317 kg/m^3) and *w*/*c* ratios of 0.45, 0.42, and 0.39. Granite was used as the coarse aggregate, and the specimens were cured for 7 or 14 days. A standard concrete mixture used by KDOT for bridge construction, which had a cement content of 602

lb/yd^3 (357 kg/m^3) and a *w/c* ratio of 0.44, was also evaluated in Program I. Limestone was used as the coarse aggregate, and the specimens were cured for 7 days. The mixture proportions, plastic concrete properties, and compressive strengths are presented in Table A.10 in Appendix A.

The times to cracking of the concrete mixtures based on visual observation and the compressive strain in the steel ring are summarized in Table 5.1. Out of 21 ring

Table 5.1 Restrained ring tests: summary of time to cracking. Program I.

2.5-in. (64-mm) ring		Time to cracking, days Based on compressive strain in steel ring		Time to cracking, days Based on visual observation		Crack width
Batch #	Description	Individual specimen	Average	Individual specimen	Average	in.
488-7d	Cement 535 + 0.45 *w/c*	175	108	NA†	NA†	--
		60		NA†		--
		90		NA†		--
488-14d	Cement 535 + 0.45 *w/c*	77	101	77	71	0.01
		65		65		0.01
		160		NA†		--
490-7d	Cement 535 + 0.42 *w/c*	55	55	55	55	0.013
		NA†††		NA†		--
		NA††		NA†		--
490-14d	Cement 535 + 0.42 *w/c*	NA††	55	NA†	NA†	--
		NA††		NA†		--
		55		NA†		--
494-7d	Cement 535 + 0.39 *w/c*	55	54	55	54	0.01
		55		55		0.013
		53		53		0.01
494-14d	Cement 535 + 0.39 *w/c*	99	65	99	74	0.01
		30		48		0.013
		NA††		NA†		--
485-7d	KDOT	50	50	NA†	NA†	--
		50		NA†		--
		NA†††		NA†		--

† No visible crack observed in 210 days. †† Compressive strain did not decrease. ††† Compressive strain data not available (the data acquisition system did not function properly). 1 in. = 25.4 mm.

specimens cast in Program I, visible cracks were found in only eight during the test period of 210 days. For the mixture with a *w*/*c* ratio of 0.45, no visible cracks were observed in the three specimens cured for 7 days; of the three specimens cured for 14 days, two had visible cracks at 77 and 65 days, respectively, and one did not have a visible crack during 210-day test. For the mixture with a *w*/*c* ratio of 0.42, of those cured for 7 days, only one had visible cracks at 55 days while the remaining two and all three specimens cured for 14 days had no visible cracks by 210 days. For the mixture with a *w*/*c* ratio of 0.39, visible cracks were found in all three specimens cured for 7 days, at 53, 55, and 55 days, respectively, while two of the three specimens cured for 14 days had visible cracks at 48 and 99 days, respectively. For the KDOT concrete, none of the specimens cured for 7 days had visible cracks by 210 days. Based on the cracking time determined from visual observation, the mixture with a *w*/*c* ratio of 0.39 and cured for 7 days had the highest cracking tendency. The differences in cracking tendency for the rest of the specimens is not clear, as most did not have visible cracks in 210 days.

For the eight cracked specimens, the crack widths ranged from 0.010 to 0.013 in. (0.254 to 0.330 mm). The compressive strain in the steel ring is plotted as a function of drying time, and the results are presented in Figures D.1 through D.4 in Appendix D. As shown in these figures, a sudden drop in compressive strain was noted when the crack was first visible.

The times to cracking, determined as when the compressive strain in the steel ring begins to decrease for the four mixtures in Program I, is shown in Table 5.1. The times to cracking of some specimens could not be determined because there was not a point at which the compressive strain began to decrease. In some cases, the data acquisition system did not function properly, and compressive strain data were not available. The average times to cracking for the mixtures based on the drop in compressive strain in the steel ring are presented in Figure 5.3. For the mixture with

a *w*/*c* ratio of 0.42, the time to cracking is based on only one specimen for each curing period. Figure 5.3 shows that the KDOT mixture (with a *w*/*c* ratio of 0.44), which had the highest paste content, cracked earliest, and the mixture with a *w*/*c* ratio of 0.45 had the longest time to cracking.

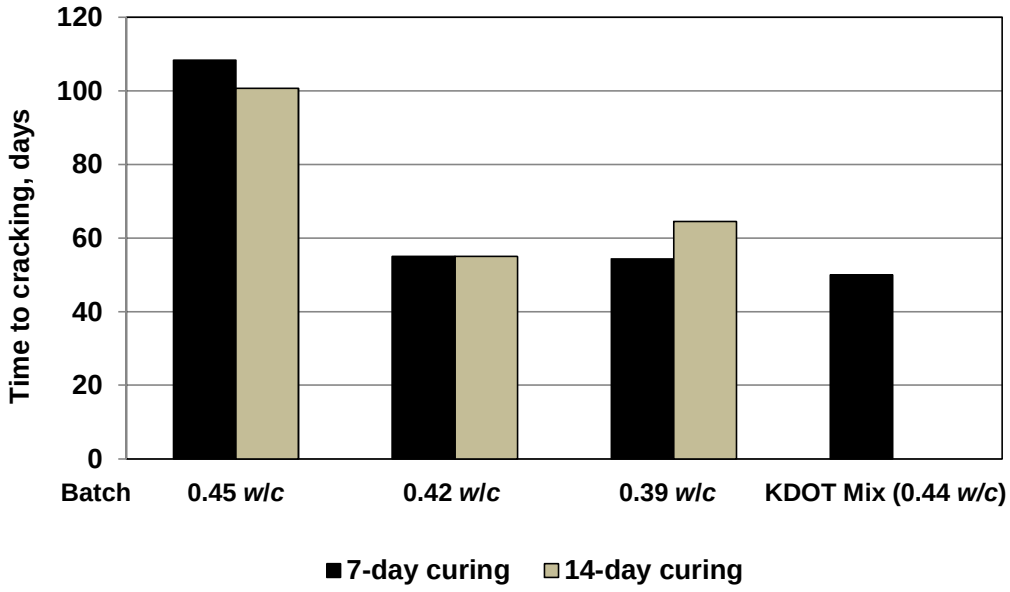

Figure 5.3 Time to cracking based on decrease in compressive strain in steel ring for mixtures in Program I.

The effect of curing time on cracking tendency is not clear in Program I. For the mixture with a *w/c* ratio of 0.45, the specimens cured for 14 days cracked earlier than those cured for 7 days; for the mixture with a *w/c* ratio of 0.42, the single specimens cured for 7 and 14 days cracked at the same age; for the mixture with a *w/c* ratio of 0.39, the specimens cured for 14 days cracked later than those cured for 7 days.

The values of free shrinkage and the compressive strain in the steel rings for the first 30 days of drying are shown in Figures 5.4 and 5.5, respectively. The values in Figures 5.4 and 5.5 represent the average of three specimens. As shown in Figure 5.4, the KDOT concrete, which had the highest paste content, had the highest free shrinkage at 30 days. The mixture with a *w*/*c* ratio of 0.39 (the mixture with the

lowest paste content) and cured for 14 days had the lowest free shrinkage; for the same mixture, the specimens cured for 7 days had more free shrinkage than all other specimens except the KDOT mixture and the mixture with a *w/c* ratio of 0.45. The trend continues to 365 days (the free shrinkage results through 365 days are presented in Figure D.5 in Appendix D). For the compressive strain in the steel ring, the KDOT concrete had the lowest compressive strain, which may be due to the low modulus of elasticity of the limestone coarse aggregate (all other specimens were cast with granite coarse aggregate). The mixtures with *w/c* ratios of 0.39, 0.42, and 0.45 exhibited similar restrained shrinkage performance for curing periods of both 7 and 14 days, except for the mixture with a *w/c* ratio of 0.45 cured for 14 days, which exhibited less compressive strain in the steel ring than the others.

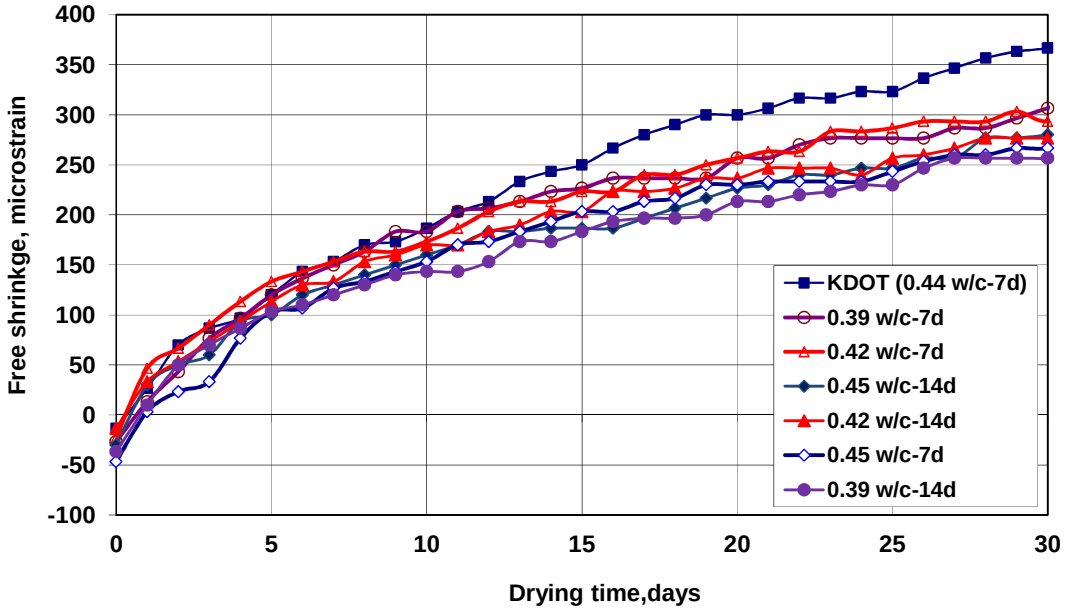

Figure 5.4 Average free shrinkage versus time during the first 30 days. Program I.

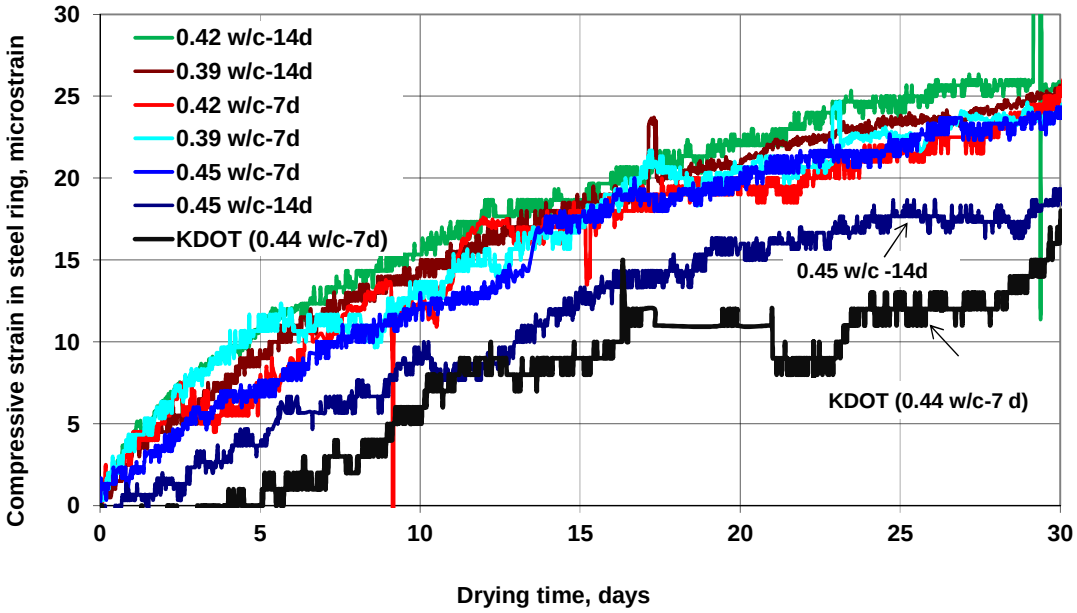

Figure 5.5 Average compressive strain in steel ring versus time during the first 30 days. Program I.

When the free shrinkage results are correlated with the cracking time shown in Figure 5.3, it is clear that the KDOT concrete has the highest free shrinkage and also the earliest cracking time, in spite of the relatively low strain induced in the steel ring; when comparing the mixtures with the same cement content but different *w/c* ratios, reducing the *w/c* ratio from 0.45 to 0.39 decreases the free shrinkage due to the reduction in paste content, but accelerates the rate of crack formation, presumably due to the increase in modulus of elasticity and the reduction of creep that accompanies the decrease in *w/c* ratio.

5.4 PROGRAM II [2.5 and 1.5-in. (64 and 38-mm) CONCRETE RINGS]

Because only eight of the 21 ring specimens in Program I [concrete ring thickness of 2.5 in. (64 mm)] had visible cracks in the test period of 210 days, a ring thickness of 1.5 in. (38 mm) was evaluated in Program II. Rings with thicknesses of 2.5 and 1.5 in. (64 and 38 mm) were cast at the same time to investigate the effect of reducing the concrete ring thickness on cracking time.

Two of the mixtures from Program I were used, one with a cement content of 535 lb/yd^3 (317 kg/m^3), a *w/c* ratio of 0.45, and granite coarse aggregate cured for 14 days. The other was the KDOT mixture with a cement content of 602 lb/yd^3 (357 kg/m^3), a *w/c* ratio of 0.44, and limestone coarse aggregate cured for 7 days. Free shrinkage specimens were cast along with the restrained ring specimens. The mixture proportions, plastic concrete properties, and compressive strengths are presented in Table A.11 in Appendix A. The mixtures were cast at low concrete temperatures, 53 and 56º F (11.7 to 13.3º C), respectively.

The times to cracking for each specimen based on visual observation and the compressive strain in the steel ring are summarized in Table 5.2. Visible cracks were observed in 11 of the 12 specimens.

Table 5.2 Restrained ring tests: summary of time to cracking. Program II.

2.5 and 1.5-in. (64 and 38-mm) concrete ring		Time to cracking, days Based on compressive strain in steel ring		Time to cracking, days Based on visual observation		Crack width
Batch #	Description	Individual specimen	Average	Individual specimen	Average	in.
496 (2.5-in.)	KDOT (0.44 *w/c*)	34	28	34	28	0.013
		22		22		0.013
		27		27		0.013
496 (1.5-in.)	KDOT (0.44 *w/c*)	6	6	6	9	0.03
		6		9		0.013
		7		12		0.013
509 (2.5-in.)	Cement 535 + 0.45 *w/c*	27	40	27	50	--**
		52		52		--**
		NA††		72		--**
509 (1.5-in.)	Cement 535 + 0.45 *w/c*	12	12	16	17	0.013
		12		17		--**
		12		NA†		--**

† No visible crack observed in 90 days. †† Compressive strain data not available (data acquisition system did not function properly). ** Crack width not measured. in. = 25.4 mm

Comparisons of the average times to cracking (based on visual observation) for the two mixtures are presented in Figure 5.6. As shown in Figure 5.6, the specimens with a concrete ring thickness of 1.5 in. (38 mm) cracked much earlier than those with a ring thickness of 2.5 in. (6.4 mm) – 19 days earlier for the KDOT concrete (*w*/*c* ratio of 0.44) and 33 days earlier for the mixture with a *w*/*c* ratio of 0.45. The KDOT concrete (paste content of 26.9%) cracked earlier than the 0.45 *w*/*c* mixture (paste content of 24.4%). For the 2.5-in. (64-mm) concrete rings, the KDOT concrete cracked at 28 days, 22 days earlier than the 0.45 *w*/*c* mixture; for the 1.5-in. (38-mm) concrete rings, the KDOT concrete cracked at nine days, eight days earlier than the 0.45 *w*/*c* mixture.

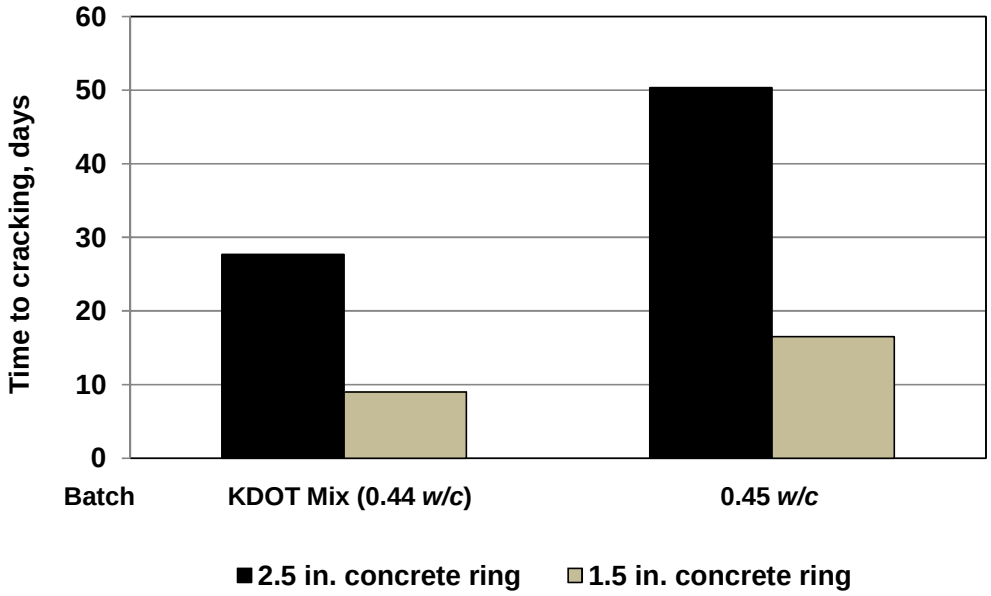

Figure 5.6 Cracking times based on appearance of visible cracks for mixtures in Program II.

The plots of compressive strain in the steel ring versus time for the mixtures in Program II are presented in Figures D.6 and D.7 of Appendix D. For the specimens with a ring thickness of 2.5 in. (6.4 mm), a rapid drop of compressive strain in the steel rings was noted when cracks first became visible, as shown in Figures D.6a and D.7a; for the specimens with a ring thickness of 1.5 in. (38 mm) (Figures D.6b and D.7b), however, the compressive strain began to decrease earlier than when the

cracks became visible. For example, a compressive strain drop was noted at about six days for KDOT concrete specimens A, B, and C (Figure D.6b), but only specimen B had a visible crack at 6 days, while cracks were not visible until 12 and 9 days for specimens A and C, respectively; for the mixture with a *w/c* ratio of 0.45, a slow strain release was noted starting at around 12 days for specimens A, B, and C (Figure D.7b), while cracks were first visible at 17 and 16 days for specimens A and B, and no visible cracks were noted for specimen C at 90 days.

The times to cracking for the two mixtures based on the initial decrease in compressive strain in the steel ring are compared in Figure 5.7. The trend is similar to that based on visual observation. The specimens with a ring thickness of 1.5 in. (38 mm) cracked earlier than those with a ring thickness of 2.5 in. (64 mm) (6 days versus 28 days for the KDOT concrete, and 12 days versus 40 days for the mixtures with a w/c ratio of 0.45), and the KDOT concrete cracked earlier than the mixture with a w/c ratio of 0.45 [6 and 12 days earlier for specimens with ring thicknesses of 1.5 and 2.5 in. (38 and 64 mm), respectively].

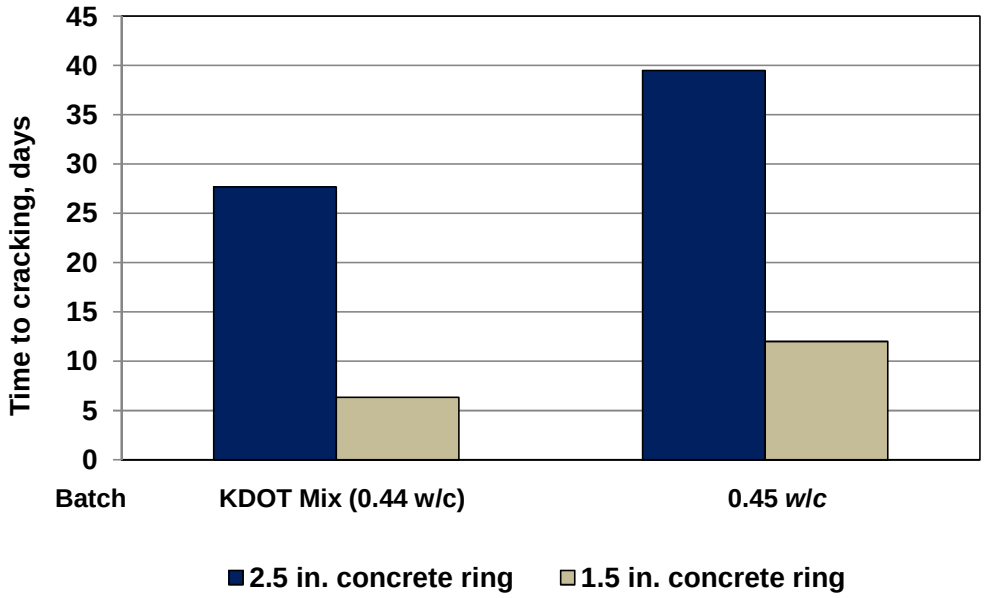

Figure 5.7 Time to cracking based on decrease in compressive strain in the steel ring for mixtures in Program II.

The average free shrinkage in concrete specimens and the average compressive strain in steel rings are plotted versus time for the first 30 days in Figures 5.8 and 5.9, respectively. As shown in Figure 5.8, the KDOT concrete had higher free shrinkage than the 0.45 *w/c* mixture (383 με versus 293 με at 30 days). In Figure 5.9, the KDOT concrete caused a higher compressive strain in the steel ring than the 0.45 *w/c* mixture during the first several days of drying and began to decrease at an earlier age. It is apparent that the KDOT concrete, with its higher cement content and strength, exhibited higher free shrinkage and earlier crack formation than the 0.45 *w/c* ratio mixture. It can also be noted that the specimens with a concrete thickness of 1.5 in. (38 mm) initially caused higher compressive strain in the steel ring than those with a thickness of 2.5 in. (64 mm), which may be explained by their higher drying surface/volume ratio, 0.72 in^{-1} (0.28 mm^{-1}), compared with 0.46 in^{-1} (0.18 mm^{-1}) for specimens with a concrete thickness of 2.5 in. (64 mm), which resulted in more rapid drying of the thinner concrete rings. The compressive strain in the steel rings for specimens with a concrete thickness of 1.5 in. (38 mm) began to drop at an earlier age than that of the thicker specimens.

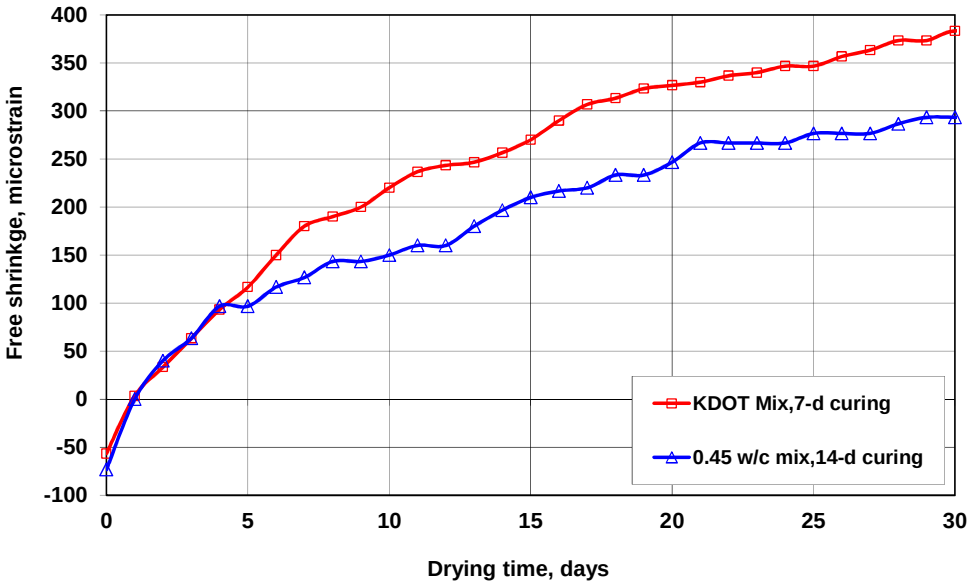

Figure 5.8 Average free shrinkage versus time during the first 30 days. Program II.

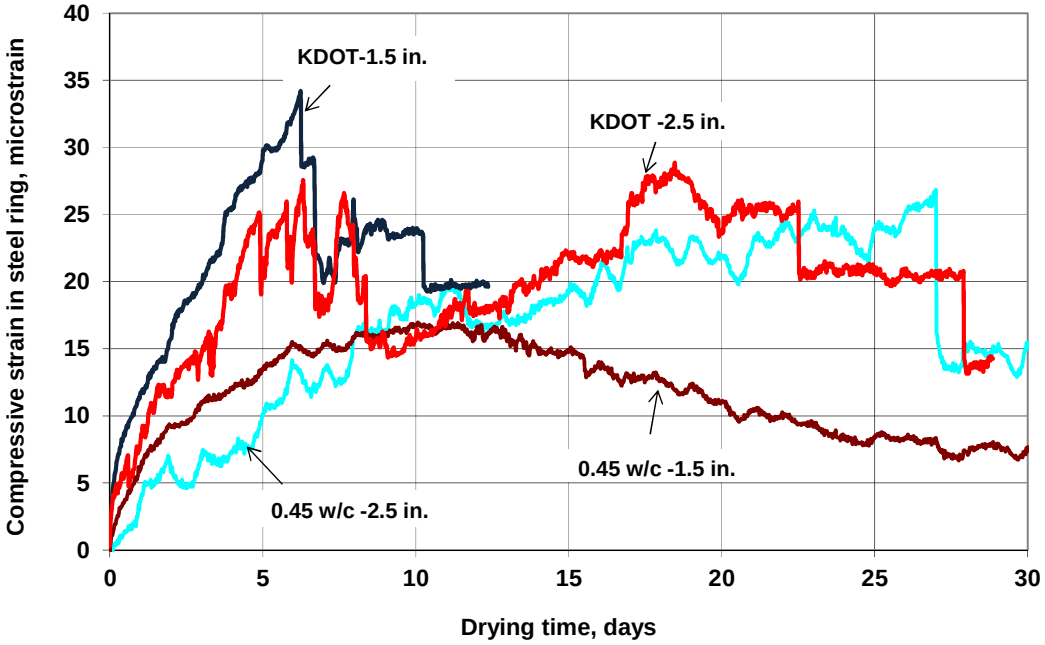

Figure 5.9 Average compressive strain in steel rings versus time during the first 30 days. Program II. 1.5 in. – a concrete ring thickness of 1.5 in. (38 mm), and 2.5 in. – a concrete ring thickness of 2.5 in. (64 mm).

5.5 PROGRAM III [1.5-in. (38-mm) CONCRETE RING]

Specimens with a ring thickness of 1.5 in. (38 mm) were cast in Program III. Four different mixtures were used – three mixtures with a cement content of 535 lb/yd^3 (317 kg/m^3) and *w/c* ratios of 0.39, 0.42, and 0.45, and a mixture with a 40% volume replacement of cement by fly ash and the same water-cementitious material (*w/cm*) ratio and paste content as the mixture containing a cement content of 535 lb/yd^3 (317 kg/m^3) and a *w/c* ratio of 0.45. The mixture with 100% cement and a *w/c* ratio of 0.45 was cast twice. Free shrinkage specimens meeting the requirements of ASTM C157 were cast at the same time. All specimens were cured for 14 days. The mixture proportions, plastic concrete properties, and compressive strengths are provided in Table A.12 in Appendix A.

The times to cracking of the mixtures in Program III based on visual observation and the compressive strain in the steel ring are presented in Table 5.3.

Visible cracks were observed in all 15 specimens, although, when the cracks were first visible, no strain drop was noted, as shown in Figures D.9 through D.13 in Appendix D. Crack width was not measured but it was recorded that the crack widths were narrower [less than 0.010 in. (0.254 mm)] than those in the specimens with the thicker concrete rings in Programs I and II.

Table 5.3 Restrained ring tests: summary of time to cracking. Program III.

1.5-in. (38-mm) ring		Time to cracking, days Based on compressive strain in steel ring		Time to cracking, days Based on visual observation	
Batch #	Description	Individual specimen	Average	Individual specimen	Average
532	Cement 535 + 0.39 *w/c*	10	10	27	25
		10		27	
		9		21	
537	Cement 535 + 0.45 *w/c*	26	14	28	28
		8		28	
		8		28	
539	Cement 535 + 0.45 *w/c*	NA[†]	13	25	26
		13		24	
		12		28	
544	Cement 535 + 0.42 *w/c*	17	14	31	28
		13		27	
		13		27	
545	40% FA+ 0.45 *w/cm*	9	9	26	26
		9		26	
		9		26	

[†] No point observed at which compressive strain began to decrease. 1 in. = 25.4 mm

The time to cracking based on visual observation ranged from 21 to 31 days, with most around 27 days. The Student's t-test results for comparisons of different times to cracking for the batches in Program III are presented in Table 5.4. When the average times to cracking for the batches are compared, the mixture with a *w/c* ratio of 0.39 (batch 532) cracked slightly earlier than the mixtures with *w/c* ratios of 0.45 and 0.42 (batches 537, 539, and 544), although the differences are not

statistically significant (Table 5.4); the 40% FA mixture (batch 545) cracked slightly earlier than one of the batches of the corresponding mixture containing 100% cement (batch 537) and at the same time as the other batch (batch 539); the difference in time to cracking between batches 537 and 545 is statistically significant (Table 5.4).

Table 5.4 Student's t-test. Average times to cracking based on visual observation.

Batch #	**Description**	**Batch #**	532	537	539	544	545
		Times to cracking, d	25	28	26	28	26
532	Cement 535 + 0.39 *w/c*	25		N	N	N	N
537	Cement 535 + 0.45 *w/c*	28			80%	N	Y
539	Cement 535 + 0.45 *w/c*	26				N	N
544	Cement 535 + 0.42 *w/c*	28					80%
545	40% FA+ 0.45 *w/cm*	26					

Note: See Table 3.2 note for an explanation of the terms "Y," "N," "80," "90," and "95."

The times to cracking based on the initial drop in the compressive strain in the steel ring are also shown in Table 5.3. The results of Student's t-test comparing the values for the different batches are presented in Table 5.5. The results show that the mixtures with *w/c* ratios of 0.45 (batches 537 and 539) and 0.42 (batch 544) have a similar average time to cracking, about 14 days, which is four days later than the mixture with a *w/c* ratio of 0.39 (batch 532); as shown in Table 5.5, all the differences with the 0.39 *w/c* batch are statistically significant, except for the difference between the 0.39 *w/c* batch and batch 537 (*w/c* = 0.45). The mixture with the 40% FA replacement of cement (batch 545) cracked earlier than the mixture containing 100% cement with the same paste content and *w/cm* ratio (batches 537 and 539); as shown in Table 5.5, the difference between batches 545 and 537 is not statistically significant while the difference between batches 545 and 539 is statistically

significant. The drop in compressive strain in the steel ring (Table 5.5) occurred about two weeks earlier than the cracks observed in the specimens (Table 5.4).

Table 5.5 Student's t-test. Average times to cracking based on compressive strain in steel rings.

Batch #	**Description**	**Batch #**	532	537	539	544	545
		Times to cracking, d	10	14	13	14	9
532	Cement 535 + 0.39 *w/c*	10		N	Y	95%	80%
537	Cement 535 + 0.45 *w/c*	14			N	N	N
539	Cement 535 + 0.45 *w/c*	13				N	Y
544	Cement 535 + 0.42 *w/c*	14					Y
545	40% FA+ 0.45 *w/cm*	9					

Note: See Table 3.2 note for an explanation of the terms "Y," "N," "80," "90," and "95."

The average free shrinkage in the concrete specimens and the average compressive strain in the steel rings are plotted versus time for the first 30 days in Figures 5.10 and 5.11, respectively. As shown in Figure 5.10, for the three mixtures with the same cement content but decreasing *w/c* ratios of 0.45, 0.42, and 0.39, the free shrinkage decreases slightly as the *w/c* ratio decreases. As observed in Program I, this is due to the decrease in paste content with the reduction in water content. The mixture with a 40% volume replacement of cement by fly ash has the highest free shrinkage.

As shown in Figure 5.11, the 40% FA mixture exhibits less average compressive strain in the steel ring, followed by the mixture with a *w/c* ratio of 0.45 and the mixtures with *w/c* ratios of 0.39 and 0.42. Because the compressive strain in the steel ring is a function of both free shrinkage and modulus of elasticity (a function of compressive strength) of the concrete, the low compressive strain of the 40% FA mixture can be explained by its lower compressive strength [28-day compressive strength of 3870 psi (26.7 MPa), Table 5.6], and the high restrained shrinkage of the

0.39 *w/c* mixture can be explained by it high compressive strength [28-day compressive strength of 5290 psi (36.5 MPa), Table 5.6].

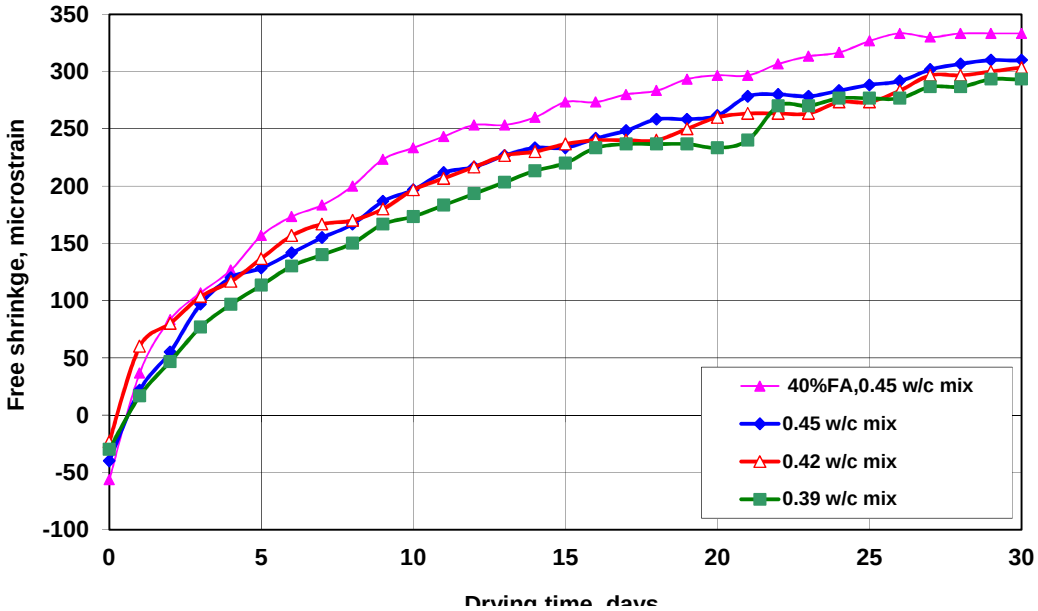

Figure 5.10 Average free shrinkage versus time during the first 30 days. Program III.

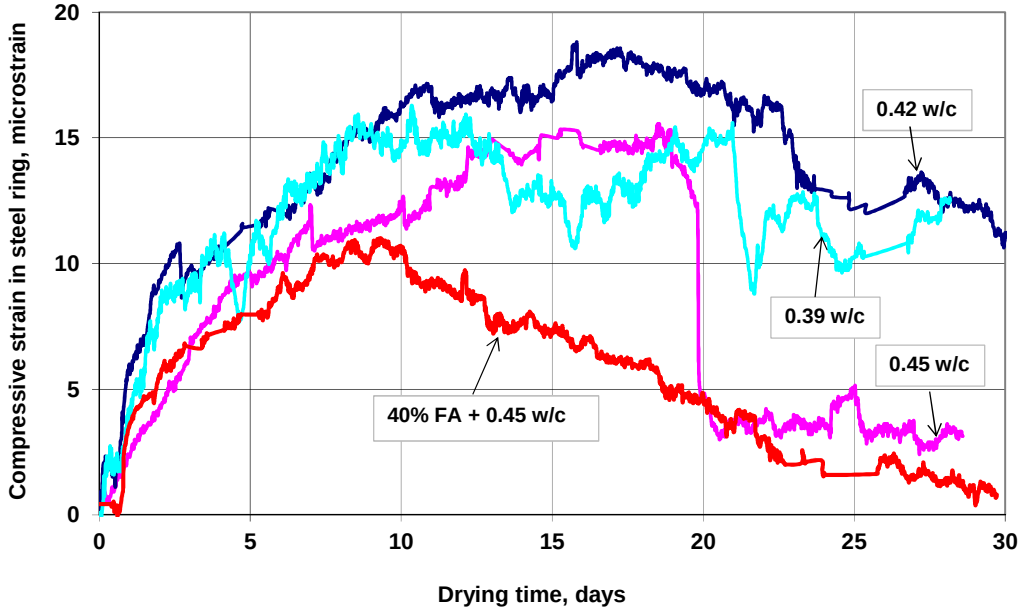

Figure 5.11 Average compressive strain versus time during the first 30 days. Program III.

Table 5.6 Seven and 28-day compressive strength: Program III.

Batch #	**532**	**537**	**539**	**544**	**545**
Description	Cement 535 + 0.39 *w/c*	Cement 535 + 0.45 *w/c*	Cement 535 + 0.45 *w/c*	Cement 535 + 0.42 *w/c*	40% FA +0.45 *w/cm*
w/c	0.39	0.45	0.45	0.42	0.45
Compressive Strength					
7-Day, psi (MPa)	4140 (28.6)	3590 (24.8)	3330 (23.0)	3470 (23.9)	2520 (17.4)
28-Day, psi (MPa)	5290 (36.5)	4370 (30.1)	4580 (31.6)	4280 (29.5)	3870 (26.7)

5.6 PROGRAM IV [1.125-in. (29-mm) CONCRETE RING]

The concrete ring thickness was further reduced to 1.125 in. (29 mm) in Program IV. Three concrete mixtures were used, a control mixture with a cement content of 535 lb/yd^3 (317 kg/m^3) and a water-cement ratio (*w/c*) of 0.45, a fly ash concrete mixture with a 40% volume replacement of cement by fly ash and the same paste content and water-cementitious material (*w/cm*) ratio as the control mixture, and a mixture with the same cement content as the control mixture but with a *w/c* ratio of 0.35. For the 0.35 *w/c* mixture, two rather than three specimens were cast. ASTM C157 free shrinkage specimens were cast at the same time as ring specimens. All specimens were cured for 14 days. The mixture proportions, plastic concrete properties, and compressive strengths are provided in Table A.13 in Appendix A.

The times to cracking for the three mixtures based on visual observation and the compressive strain in the steel ring are summarized in Table 5.7. Seven of the eight specimens had visible cracks during the 30-day test period. A sudden and rapid drop of the compressive strain in the steel ring at cracking, however, was not observed for any of the cracked specimens, as shown in Figures D.15 through D.17 in Appendix D; instead, the compressive strain began to decrease slowly at early ages. The crack widths were either 0.004 or 0.010 in. (0.102 or 0.254 mm). Based on visual observation, the mixture containing a 40% volume replacement of cement by

fly ash cracked at 14 days, nine days earlier than the control concrete. Because only one of the two specimens cracked for the mixture with a *w/c* ratio of 0.35, the cracking time observed for that specimen, 20 days, is not considered to be representative. Based on the compressive strain in the steel ring, the control concrete cracked at 5 days, one day later than the fly ash concrete and the concrete with a *w/c* ratio of 0.35; none of the differences in time to cracking are statistically significant. The cracking times based on the compressive strain in the steel ring were well below those based on visual observation.

Table 5.7 Restrained ring tests: summary of time to cracking. Program IV.

1.125-in. (29-mm) ring		Time to cracking, days Based on compressive strain in steel ring		Time to cracking, days Based on visual observation		Crack width
Batch #	Description	Individual specimen	Average	Individual specimen	Average	in.
563	Cement 535 + 0.45 *w/c*	6	5	21	23	0.010
		5		23		0.004
		3		25		0.004
566	40% FA + 0.45 *w/cm*	4	4	14	14	0.010
		3		14		0.004
		4		14		0.010
568	Cement 535 + 0.35 *w/c*	4	4	20	20	0.004
		4		NA[†]		--

[†] No visible crack observed. Note: Only two specimens were cast for batch 568. 1 in. = 25.4 mm

The average ASTM C157 free shrinkage and the average compressive strain in steel rings are plotted versus time for the first 30 days of drying in Figures 5.12 and 5.13, respectively. As shown in Figure 5.12, from most to least free shrinkage, the mixtures are in order the 40% FA (0.45 *w/cm*), 0.45 *w/c*, and 0.35 *w/c* mixtures. The free shrinkage results are consistent with the findings in Program III: adding fly ash increases free shrinkage and decreasing the *w/c* ratio (and therefore water content) while keeping the cement content constant reduces free shrinkage. For the compressive strain in steel ring, the order is reversed so that the 0.35 *w/c* mixture exhibits the highest compressive strain followed by the 0.45 *w/c* and 40% FA (0.45

w/cm) mixtures. Once again, this phenomenon can be explained by the fact that the compressive strain in the steel ring is a function of both the free shrinkage and modulus of elasticity of concrete (which is function of concrete compressive strength). At the same free shrinkage, the higher strength concrete places more pressure on the inner steel due to its higher modulus of elasticity. Among the three mixtures in Program IV, the 0.35 *w/c* mixture has the lowest free shrinkage but the highest compressive strength (see Table 5.8). Thus the 0.35 *w/c* mixture has the highest modulus of elasticity (and the least creep), which causes the highest compressive strain in the steel (Figure 5.13).

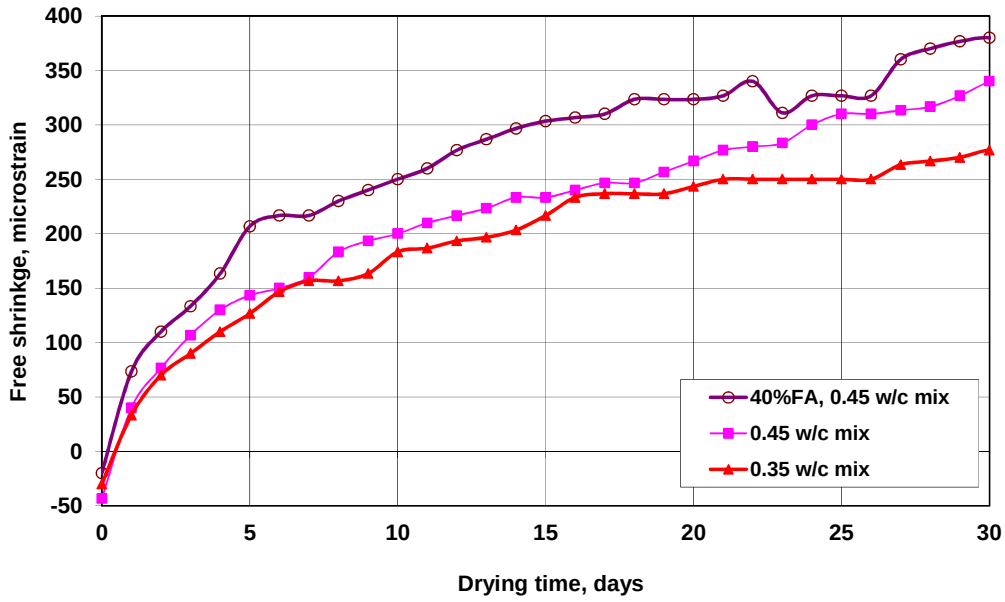

Figure 5.12 Average free shrinkage versus time during the first 30 days. Program IV.

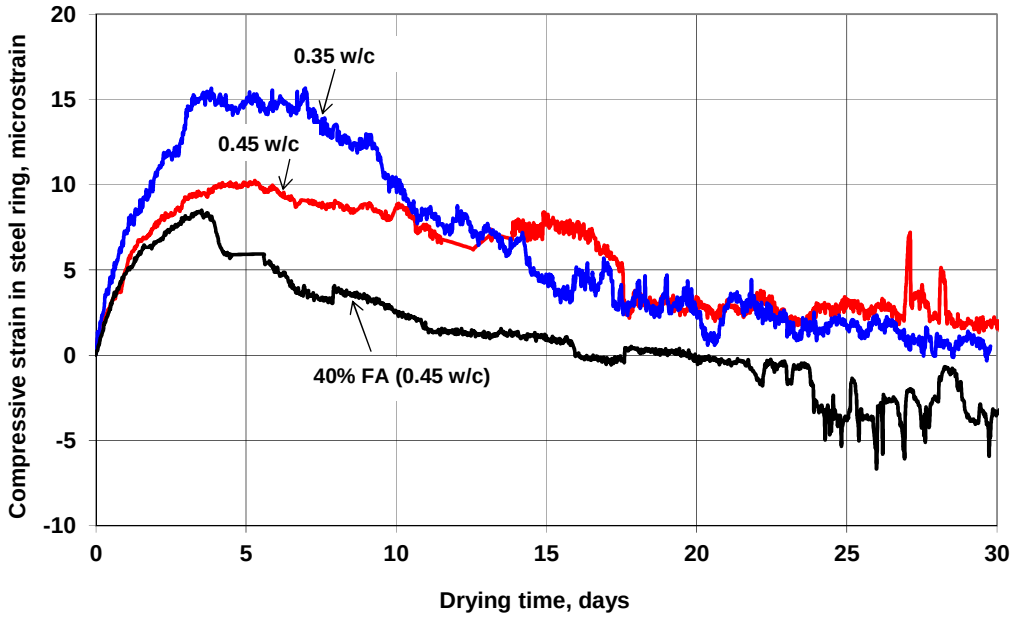

Figure 5.13 Average compressive strain versus time during the first 30 days. Program IV.

Table 5.8 Seven and 28-day compressive strength: Program IV. All rings 1.125 in. (29 mm) thick.

Batch #	**563**	**566**	**568**
Description	Cement 535 + 0.45 *w/c*	40% FA+ 0.45 *w/cm*	Cement 535 + 0.35 *w/c*
Compressive Strength			
7-Day, psi (MPa)	2830 (19.5)	2240 (15.4)	5460 (37.7)
28-Day, psi (MPa)	4100 (28.3)	3860 (26.6)	6080 (41.9)

5.7 PROGRAM V [2-in. (50-mm) CONCRETE RING]

In Programs III and IV, most specimens with concrete ring thicknesses of 1.5 or 1.125 in. (38 or 29 mm) exhibited visible cracks, although no sharp drop in the compressive strain in the steel ring was noted. Instead, the compressive strain in the steel ring began to decrease slowly before the cracks became visible. The concrete ring thickness was increased to 2 in. (50 mm) in Program V in an effort to establish a restrained ring test configuration that would produce a sharp strain drop that would

coincide with the formation of visible crack to allow the cracking time to be more precisely determined. To increase the sensitivity of the data acquisition system to catch strain drop at cracking, a quarter-Wheatstone bridge configuration was used instead of the half-Wheatstone bridge configuration that was used in the Programs I through IV. More details about the Wheatstone bridge configuration are provided in Chapter 2.

Starting with Program V, a crack map describing the crack path and crack width of the cracked ring specimens is reported.

5.7.1 Program V Set 1 (Half vs. Quarter Wheatstone bridges)

Two concrete mixtures were evaluated in Program V set 1. One mixture had a cement content of 535 lb/yd^3 (317 kg/m^3) and a *w/c* ratio of 0.45 (24.2% paste content). This mixture was tested in previous programs with different concrete ring thicknesses, so the results of the 2-in. (50-mm) thick concrete ring specimens can be compared with other test configurations. The other mixture had a cement content of 729 lb/yd^3 (432 kg/m^3) and a *w/c* ratio of 0.45 (33% paste content). The purpose of increasing the cement content was to determine if there would be a greater likelihood of observing a sharp drop in compressive strain in the steel rings at cracking for a high paste content mixture. Four specimens were cast for each mixture, and two were monitored with the half Wheatstone bridge setup while the other two were monitored with the quarter Wheatstone bridge setup. ASTM C157 free shrinkage specimens were cast at the same time. All specimens were cured for 14 days. The low cement content mixture was cast with a slump of 3.75 in. (95 mm) and an air content of 8.4%, and had a 28-day compressive strength of 4000 psi (27.6 MPa). The high cement content mixture was cast with a slump of 8 in. (205 mm) and an air content of 6.4%, and had a 28-day compressive strength of 4120 psi (28.4 MPa). The mixture proportions, plastic concrete properties, and compressive strengths are provided in Table A.14 in Appendix A.

The times to cracking for the two mixtures based on visual observation and the compressive strain in the steel ring are summarized in Table 5.9. Compressive strain data was collected for 90 days and the ring specimens were visually checked for 120 days. The compressive strain in the steel ring versus drying time, as well as the crack maps are presented in Figures D.19 through D.24 in Appendix D. Seven of the eight specimens had visible cracks. For specimens monitored with quarter Wheatstone bridges, shown in Figures D.19, D.20, D.22, and D.23, each curve represents the strain readings from one of the four strain gages on a steel ring, while for specimens monitored with half Wheatstone bridge, shown in Figures D.21 and D.24, each curve represents the average readings of the four strain gages on the steel ring.

Table 5.9 Restrained ring tests: summary of time to cracking. Program V Set 1.

2-in. (50-mm) ring		Time to cracking, days Based on compressive strain in steel ring		Time to cracking, days Based on visual observation		Crack width
Batch #	Description	Individual specimen	Average	Individual specimen	Average	in.
597	C 535 + 0.45 *w/c*	26[1]	28	34	54	<0.004
		24[1]		32		<0.004
		34[2]		36		<0.004
		NA[2 †]		115		--
598	C 729 + 0.45 *w/c*	15[1]	19	20	22	0.004
		17[1]		23		0.004
		22[2]		23		<0.004
		22[2]		22		0.004

[†] No point observed at which compressive strain began to decrease. [1]Quarter-Wheatstone bridge configuration. [2] Half-Wheatstone bridge configuration.

As shown in Figures D.19 through D.21, for the mixture with a cement content of 535 lb/yd^3 (317 kg/m^3) and a *w/c* ratio of 0.45, no sharp drop in the compressive strain in the steel ring was noted, except for specimen B (Figure D.20), which exhibited a sharp drop in strain in one gage at 37 days (the compressive strain began to decrease slowly at 24 days and a crack was first observed at 32 days). The

visible cracks were very narrow [less than 0.004 in. (0.100 mm) wide] and short [less than 2 in. (51 mm) long].

For the mixture with a cement content of 729 lb/yd^3 (432 kg/m^3) and a *w/c* ratio of 0.45 (Figures D.22 through D.24), a sharp drop in the compressive strain in the steel rings was noted at the same time that the crack became visible for all specimens, except for one specimen with the half-Wheatstone bridge configuration (Figure D.24, specimen D). The compressive strain in the steel rings, however, began to decrease slowly at earlier ages than the time that cracks became visible. Most cracks were about 0.004 in. (0.102 mm) wide, and almost all crossed full height of the specimen, as shown in Figures D.22 through D.24 in Appendix D.

In terms of the average times to cracking, the high cement content mixture cracked about 12 days earlier than the low cement content mixture based on visual observation and 9 days earlier based on compressive strain in the steel rings. With a 2-in. (50-mm) concrete ring, the cracks were visible from zero to nine days after the compressive strain in the steel ring began to decrease.

The average free shrinkage and the average compressive strain in the steel ring are plotted versus drying time during the first 30 days in Figures 5.14 and 5.15, respectively. The results in Figure 5.14 represent the average value of three specimens and the results in Figure 5.15 represent the average value of four specimens. As shown in Figure 5.14, the high cement content mixture exhibited higher free shrinkage than the low cement content mixture. As shown in Figure 5.15, the high cement content mixture also exhibited slightly higher compressive strain than the low cement content mixture during the first ten days and an earlier drop in compressive strain in the steel ring.

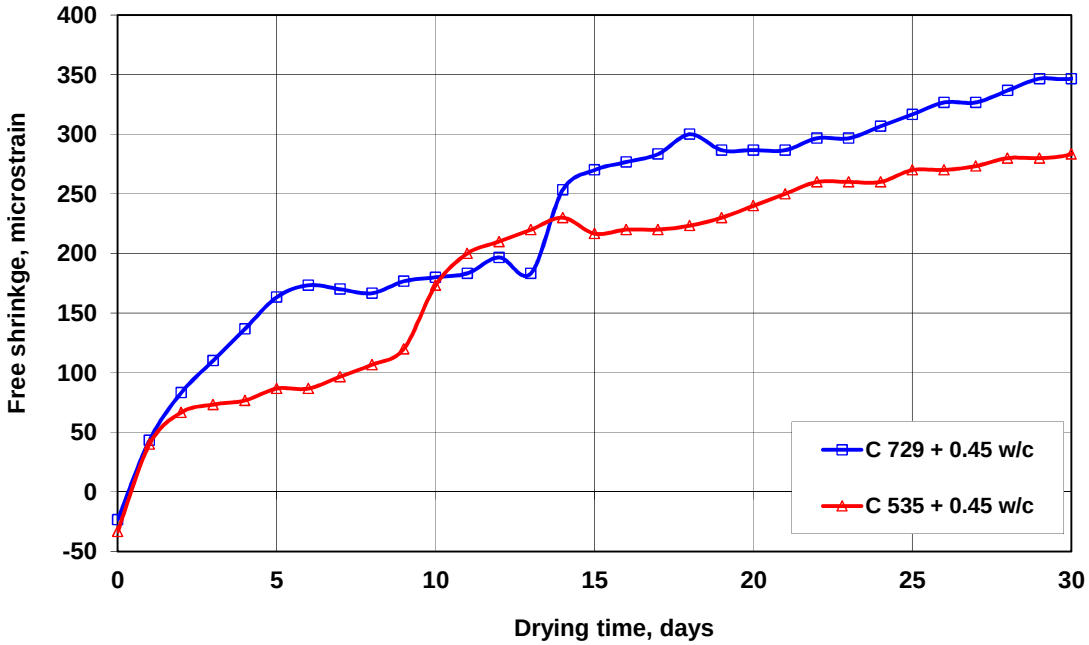

Figure 5.14 Average free shrinkage versus time during the first 30 days. Program V Set 1.

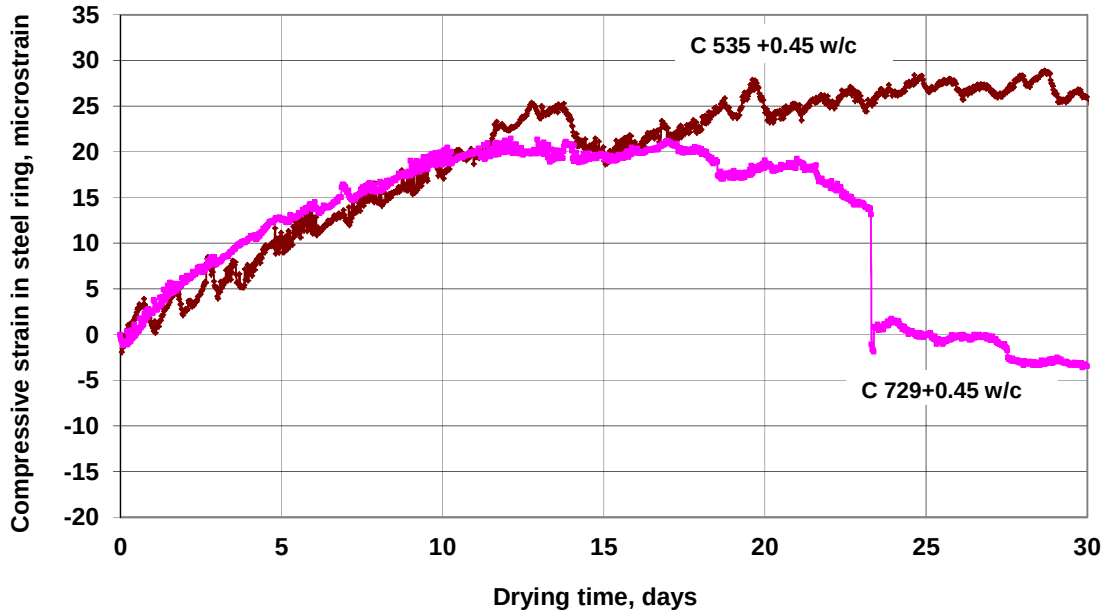

Figure 5.15 Average compressive strain versus time during the first 30 days. Program V Set 1.

5.7.2 Program V Set 2 (high paste content mixtures)

Because the mixture with high paste content in Program V Set 1 seemed to exhibit a rapid drop in compressive strain in the steel ring at cracking, additional high paste content mixtures were cast. The first two mixtures had a paste content of 27.5% and a water-cementitious material (*w/cm*) ratio of 0.35. One mixture contained 100% cement and a cement content of 700 lb/yd^3 (415 kg/m^3) and the other mixture had a 40% volume replacement of cement by fly ash. Because the air contents were high (above 10%), the 28-day compressive strengths of both mixtures were only about 4000 psi (28 MPa). Four ring specimens were cast for each mixture. Another two mixtures were cast with a paste content of 31.3% and a *w/cm* ratio of 0.44. One mixture contained 100% cement and a cement content of 700 lb/yd^3 (415 kg/m^3) and the other mixture had a 40% volume replacement of cement by fly ash. Both mixtures were non-air-entrained and the 28-day compressive strengths were above 5000 psi (34 MPa). Three ring specimens were cast for each mixture. No free shrinkage specimens were cast. The mixture proportions, plastic concrete properties, and compressive strengths are provided in Table A.15 in Appendix A.

Compressive strain data were collected for 60 days, and the ring specimens were visually checked for 90 days. The times to cracking for the four mixtures based on visual observation and compressive strain in the steel ring are summarized in Table 5.10. The compressive strain in the steel ring versus time and the crack maps are presented in Figures D.26 through D.39 in Appendix D. For the mixture with a cement content 700 lb/yd^3 (415 kg/m^3) and a *w/c* ratio of 0.35, only one specimen had a visible crack [about 2 in. (50 mm) long and 0.004 in. (0.102 mm) wide on the outside surface, extending through the full width of the top surface], which appeared at 41 days. A sharp drop in compressive strain in the steel rings coincided with the appearance of the crack, although the compressive strain began to decrease slowly at 10 days (Figure D.26 in Appendix D). For the other three specimens (Figures D.27

through D.29 in Appendix D), the compressive strain curves began to decrease at 7, 13, and 11 days, respectively, and no cracks were visible within 90-day test, except for a barely perceptible crack in Specimen B at 73 days (Figure D.27 in Appendix D). For the mixture with a 40% volume replacement of cement by fly ash and a *w/cm* ratio of 0.35, three of the four specimens exhibited visible cracks at 55, 36, and 55 days, respectively. A sharp drop in compressive strain in the steel rings was noted for only one of the specimens (Specimen B). As shown in Figure D.31 in Appendix D, Specimen B exhibited a sharp drop in compressive strain in the steel ring at cracking, with a crack crossing the whole section at 36 days, although the compressive strain began to drop slowly at an earlier age (at 12 days). Based on visual observation, the fly ash concrete cracked earlier than the concrete containing 100% cement; based on the compressive strain in the steel rings, the fly ash concrete had the same average time to cracking as the concrete containing 100% cement.

Table 5.10 Restrained ring tests: summary of time to cracking. Program V Set 2.

2-in. (50-mm) ring		Time to cracking, days Based on compressive strain in steel ring		Time to cracking, days Based on visual observation		Crack width
Batch #	Description	Individual specimen	Average	Individual specimen	Average	in.
649	Cement 700 + 0.35 *w/c*	10	10	41	57	0.004
		7		73		0.004
		13		NA†		--
		11		NA†		--
650	40% FA + 0.35 *w/cm*	10	10	55	49	<0.004
		12		36		0.004
		9		55		<0.004
		NA††		NA†		--
651	Cement 700 + 0.44 *w/c*	44	44	44	42	<0.004
		45		46		<0.004
		44		36		<0.004
652	40% FA + 0.44 *w/cm*	51	54	49	65	<0.004
		56		56		<0.004
		56		90		<0.004

† No visible crack observed in 90 days. †† Compressive strain did not decrease. 1 in. = 25.4 mm

For the non-air-entrained mixture with a cement content of 700 lb/yd^3 (415 kg/m^3) and a *w/c* ratio of 0.44, cracks were visible at 44, 46, and 36 days and the compressive strain in the steel rings began to decrease slowly at 44, 45, and 44 days. All cracks were short when they were first observed, as shown in Figures D.34 through D.36 in Appendix D. A small sharp drop in compressive strain in the steel ring coincided with the visual observation in two specimens (Specimens A and B in Figures D.34 and D.35). For the non-air-entrained mixture with a 40% volume replacement of cement by fly ash and *w/cm* ratio of 0.44, cracks were observed at 46, 56, and 90 days, and the compressive strain in the steel rings began to decrease slowly at 51, 56, and 56 days. All of the cracks were small, and a sharp drop in compressive in the steel ring did not occur (Figures D.37 through D.39 in Appendix D). For these two non-air-entrained mixtures, the fly ash concrete cracked at a later date than the mixture with 100% portland cement based on both visual observation and compressive strain in the steel rings.

5.7.3 Program V Set 3 (different drying environment)

The specimens in Programs I through IV and Program V, Sets 1 and 2 were dried at a temperature of 73 ± 3° F (23 ± 2° C) and a relative humidity of 50 ± 4%. In Set 3, concrete mixtures were dried at a temperature of 73 ± 3 °F (23 ± 2 °C) and a relative humidity of 40 ± 4%. Lowering the humidity was intended to lower the time to cracking by forcing the specimens to dry faster. Three mixtures were evaluated. One mixture had a cement content of 540 lb/yd^3 (320 kg/m^3) and a *w/c* ratio of 0.44 (24.1% paste content), while the other two had a cement content of 535 lb/yd^3 (317 kg/m^3) and *w/c* ratios of 0.45 and 0.35 (24.2 and 21.0% paste content, respectively). No free shrinkage specimens were cast. The mixture proportions, plastic concrete properties, and compressive strengths are provided in Table A.16 in Appendix A.

The times to cracking for the three mixtures based on visual observation and the compressive strain in the steel ring are summarized in Table 5.11. The compressive

strain versus time and the crack maps are presented in Figures D.40 through D.48 in Appendix D. For the mixture with a cement content of 540 lb/yd^3 (320 kg/m^3) and a *w/c* ratio of 0.44, only one of the three specimens had a visible crack at 37 days. The crack was about 2 in. (50 mm) long on the outside surface and extended about 1 in. (25 mm) on the top surface (Figure D.42 in Appendix D); no sharp drop in compressive strain in the steel rings was noted at the formation of this crack. For the other two specimens, sharp drops in compressive strain in the steel ring were noted at 41 and 35 days (Figures D.40 and D.41), respectively, although no cracks were visible.

Table 5.11 Restrained ring tests: summary of time to cracking. Program V Set 3.

2-in. (50-mm) ring (40% RH)		Time to cracking, days Based on compressive strain in steel ring		Time to cracking, days Based on visual check		Crack width
Batch #	Description	Individual specimen	Average	Individual specimen	Average	in.
635	Cement 540 + 0.44 *w/c*	41	38	NA†	--	--
		35		NA†		--
		NA††		37		<0.004
636	Cement 535 + 0.45 *w/c*	27	27	29	28	<0.004
		27		27		0.004
		NA††		28		0.004
637	Cement 535 + 0.35 *w/c*	28	19	29	28	<0.004
		15		27		0.004
		14		27		0.004

† No visible crack observed. †† No point observed at which compressive strain began to decrease. 1 in. = 25.4 mm.

For the mixture with a cement content of 535 lb/yd^3 (317 kg/m^3) and a *w/c* ratio of 0.45, the three specimens (A, B, and C) had visible cracks at 29, 27, and 28 days, respectively. Specimen A had a very narrow crack that was about 2 in. (50 mm) long and extended about 1 in. (25 mm) on the top surface; the compressive strain the steel ring began to decrease slowly at 27 days (Figure D.43 in Appendix D). Specimen B had a crack that crossed the full height of the outside surface and extended through the full width of top and bottom surfaces; a sharp drop in

compressive strain in the steel ring was noted at cracking (Figure D.44 in Appendix D). Specimen C had a crack that was similar to Specimen B but did not cross the top and bottom surfaces; no sharp drop in compressive strain in the steel ring was noted at cracking (Figure D.45 in Appendix D).

For the mixture with a cement content of 535 lb/yd^3 (317 kg/m^3) and a *w/c* ratio of 0.35, the three specimens (A, B, and C) had visible cracks at 29, 27, and 27 days, respectively. For specimen A, sharp drops in compressive strain in the steel ring were noted at 28 and 30 days, while cracks were first visible at 29 days (Figure D.46 in Appendix D). For specimens B and C (Figures D.47 and D.48), sharp drops in compressive strain in the steel ring were noted at 15 and 14 days, respectively, but the cracks were not visible until day 27.

When the three mixtures are compared, the mixture with a cement content of 540 lb/yd^3 (320 kg/m^3) and a *w/c* ratio of 0.44 cracked last (at 37 days based on visual observation and 38 days based on compressive strain curve). It also had the lowest 28-day compressive strength of 3510 psi (24.2 MPa). The other two mixtures exhibited visible cracks at an average of 28 days, although the 0.35 *w/c* and 0.45 *w/c* ratio mixtures cracked at 19 and 27 days, respectively, based on compressive strain in the steel rings. The 28-day compressive strengths for the 0.35 and 0.45 *w/c* ratio mixtures were 5670 and 4260 psi (39.1 and 29.4 MPa), respectively.

5.8 PROGRAM VI [2.5-in. (64-mm) CONCRETE RING AND SEVERE DRYING ENVIRONMENT]

The cracks that developed in the specimens with concrete ring thicknesses of 1.125, 1.5, and 2 in. (29, 38, and 50 mm) were so small that a sharp drop in compressive strain in the steel ring was rarely detected. The cracks that developed in the specimens with a concrete ring thickness of 2.5 in. (64 mm) (Program I) were relatively wide and could be detected at cracking, indicated by a compressive strain drop, but only eight of 21 specimens in that program had visible cracks. In Program

VI, specimens with a ring thickness of 2.5 in. (64 mm) were cast and placed in a severe drying environment at a temperature of 86 ± 3° F (30 ± 2° C) and a relative humidity of 14 ± 4%. The specimens were dried from the circumferential, top, and bottom surfaces rather than only the circumferential surface as in previous tests.

Two concrete mixtures were evaluated. One had a cement content of 540 lb/yd^3 (320 kg/m^3) and a *w/c* ratio of 0.44. The other had the same *w/cm* ratio and paste content (24.1%), but had a 40% volume replacement of cement by fly ash. The mixture proportions, plastic concrete properties, and compressive strengths are provided in Table A.16 in Appendix A. The mixture with 100% cement had a 28-day compressive strength of 3520 psi (24.3 MPa) (with an air content of 9.65%) and the fly ash concrete had a 28-day compressive strength of 5110 psi (35.2 MPa) (with an air content of 6.15%).

The times to cracking for the two mixtures based on visual observation and the compressive strain in the steel ring are summarized in Table 5.12. The plots of compressive strain in the steel ring versus time and the crack maps are presented in Figures D.49 through D.54 in Appendix D. As shown in Figures D.49 through D.54, all specimens exhibited a drop in the compressive strain in the steel ring, at six, five, and six days for the three specimens of the mixture containing 100% cement and all at four days for the three specimens of the mixture containing fly ash (Table 5.12). This drop, however, occurred much earlier than when the cracks were first visible at 15, 8, and 25 days for the three specimens of the mixture containing 100% cement and at 6, 13, and 6 days for the three specimens of the mixture containing fly ash (Table 5.12).

The fly ash concrete cracked earlier than the mixture with 100% cement, eight days earlier based on the visual observation and three days earlier based on the drop in compressive strain in the steel ring.

The results in Table 5.12 indicate that cracks were observed at much earlier ages – under 25 days – compared to about two months in Program I.

Table 5.12 Restrained ring tests: summary of time to cracking, Program VI.

2.5-in. (64-mm) ring		Time to cracking, days Based on compressive strain in steel ring		Time to cracking, days Based on visual observation		Crack width
Batch #	Description	Individual specimen	Average*	Individual specimen	Average*	in.
679	Cement 540 + 0.44 *w/c*	6	6	15	16	<0.004
		5		8		0.004
		6		25		<0.004
680	40% FA + 0.44 *w/c*	4	3	6	8	<0.004
		2		13		<0.004
		4		6		0.004

5.9 EFFECT OF CONCRETE RING THICKNESS ON CRACKING TIME

When the concrete ring thickness is reduced, the concrete will crack earlier. With a thinner concrete ring, the specimen has a higher drying-surface/volume ratio, and more restraint is provided by the steel ring since the thickness of the steel is fixed. Figures 5.16 through 5.18 compare times to cracking, based on visual observation and compressive strain in the steel ring, for specimens with different concrete ring thicknesses. In Figure 5.16, the time to cracking is shown for concrete rings with thicknesses of 2.5 and 1.5 in. (64 and 38 mm). The 2.5 and 1.5-in. (64 and 38-mm) thick concrete ring specimens were cast at the same time in Program II. Two mixtures were evaluated, one with a cement content of 602 lb/yd^3 (357 kg/m^3), a *w/c* ratio of 0.44, and limestone coarse aggregate (KDOT mix) and the other with a cement content of 535 lb/yd^3 (317 kg/m^3), a *w/c* ratio of 0.45, and granite coarse aggregate. The results indicate that the time to cracking for the 1.5-in. (38-mm) thick concrete ring specimens is less than that for the 2.5-in. (64-mm) thick concrete ring specimens.

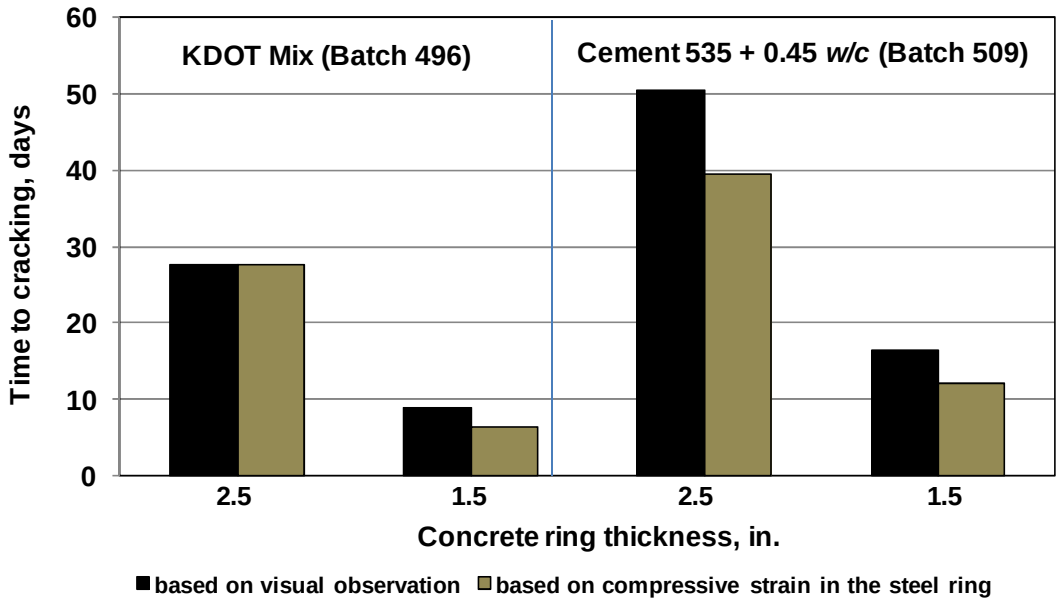

Figure 5.16 Time to cracking versus concrete ring thickness. KDOT mix with cement content of 602 lb/yd^3 (357 kg/m^3), *w/c* ratio of 0.44, and limestone coarse aggregate and mixture with cement content of 535 lb/yd^3 (317 kg/m^3), *w/c* ratio of 0.45, and granite coarse aggregate in Program II. Note: 1 in. = 25.4 mm.

In Figures 5.17 and 5.18, the time to cracking is also plotted versus concrete ring thickness. In this case, the specimens with different concrete ring thicknesses were cast with the same mixture proportions but at different times. In Figure 5.17, the mixture with a cement content of 535 lb/yd^3 (317 kg/m^3) and a *w/c* ratio of 0.45 was cast in Program I, V, III and IV with concrete ring thicknesses of 2.5, 2.0, 1.5, and 1.125 in. (64, 50, 38, and 29 mm), respectively. In Figure 5.18, the mixture with a 40% volume replacement of cement by fly ash and a *w/cm* ratio of 0.45 was cast in Program III and IV with concrete ring thicknesses of 1.5 and 1.125 in. (38 and 29 mm), respectively. The results shown in Figures 5.17 and 5.18 also demonstrate that the thinner the concrete ring, the earlier a crack will form.

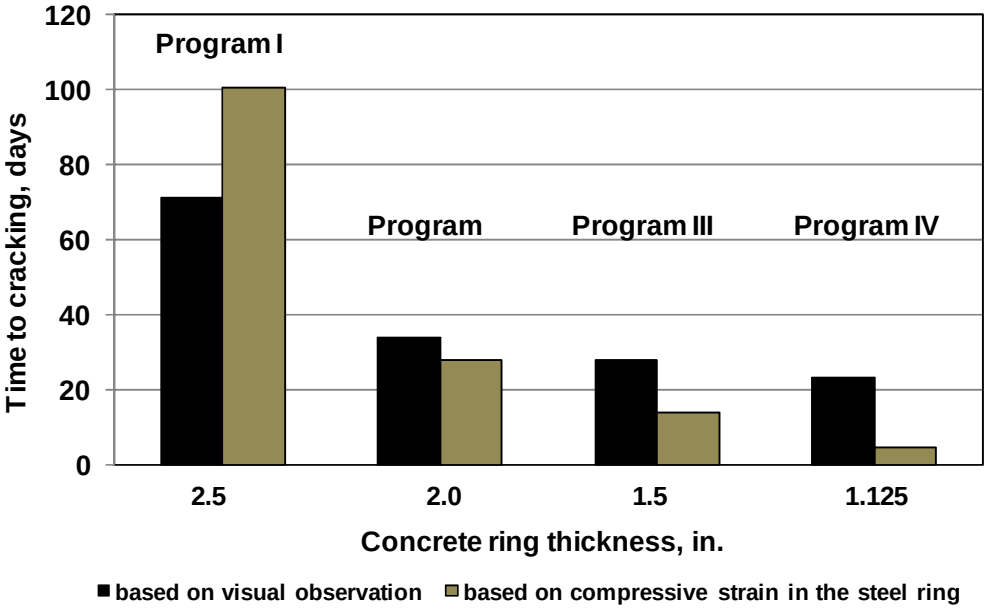

Figure 5.17 Time to cracking versus concrete ring thickness. Mixtures with cement content of 535 lb/yd^3 (317 kg/m^3) and *w/c* ratio of 0.45 in Programs I, V, III, and IV. Note: 1 in. = 25.4 mm.

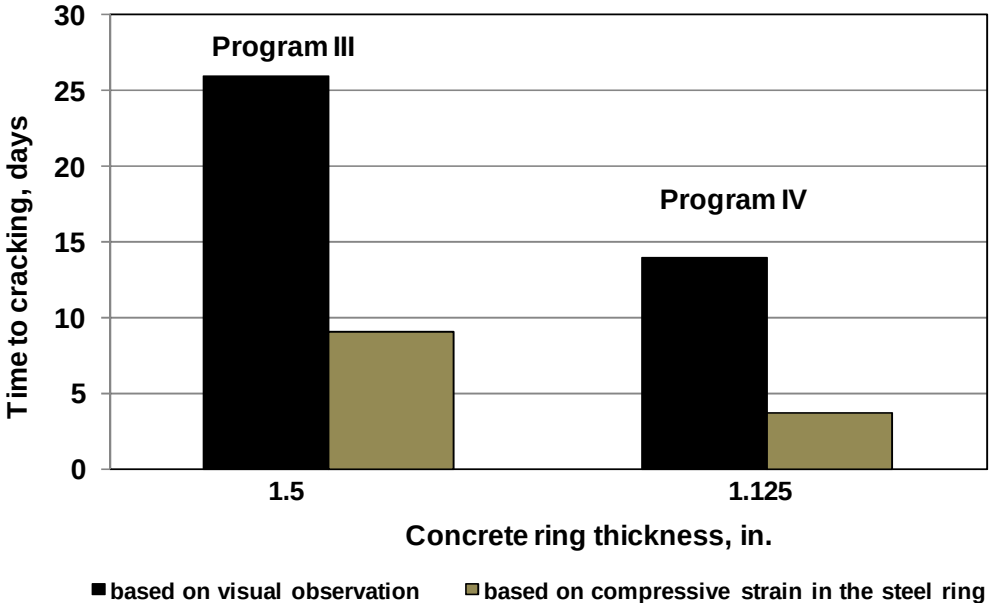

Figure 5.18 Cracking time versus concrete ring thickness. Mixtures with a 40% volume replacement of cement by fly ash and *w/cm* of 0.45 in Programs III and IV. Note: 1 in. = 25.4 mm.

5.10 SUMMARY OF RESTRAINED RING TESTS

The cracking tendency of concrete mixtures is evaluated using the restrained ring tests. A steel ring with a fixed dimension is used to provide the resistance to concrete shrinkage. Different concrete ring thicknesses were evaluated. The time to cracking is determined in two ways: when cracks first become visible and when the compressive strain in the steel ring first begins to decrease. The key observations from the tests were

1. Only eight of the 21 ring specimens with a concrete thickness of 2.5 in. (64 mm) in Program I had visible cracks when drying at a temperature of 73 ± 3º F (23 ± 2º C) and a relative humidity of 50 ± 4%; all six ring specimens with a concrete thickness of 2.5 in. (64 mm) in Program VI had visible cracks when drying at a temperature of 86 ± 3° F (30 ± 2° C) and a relative humidity of 14 ± 4%.
2. Most specimens with ring thicknesses of 2, 1.5, or 1.125 in. (50, 38, and 29 mm) had visible cracks.
3. For the mixtures investigated in this study, a sudden and rapid drop in compressive strain in the steel ring was not observed. Instead, a slow drop in strain was observed before the cracks became visible.
4. When the cracking tendency of different concrete mixtures are compared, the trend based on the time to cracking determined from visual observation of crack formation was similar to that based on the time to cracking determined from the initial drop of compressive strain in the steel ring.
5. Specimens with thinner concrete rings cracked earlier than those with thicker concrete rings.
6. Exposing specimens to severe drying conditions (Program V Set 2 and Program VI) resulted in the earlier formation of cracks, although it did not result in increased crack width.

7. The compressive strain in the steel ring is a function of both the shrinkage and modulus of elasticity of the concrete; in a number of cases, concrete with lower free shrinkage caused higher compressive strain in the steel due to its higher modulus of elasticity.
8. When the mixtures with a cement content of 535 lb/yd^3 (317 kg/m^3) but different water-cement (*w/c*) ratios, 0.45 and 0.35, were compared in Programs I, IV, and V Set 3, the mixtures with the lower *w/c* ratio cracked earlier.
9. When the mixture with a 40% volume replacement of cement by fly ash was compared with the mixture with 100% cement and the same paste content and *w/cm* ratio in Programs III, IV, V Set 2 and VI, the fly ash concrete cracked earlier than the mixture with 100% cement, except for the two non-air-entrained mixtures in Program V Set 2, where the non-air-entrained fly ash concrete cracked at a later age than the non-air-entrained mixture without fly ash.
10. The high paste content (33%) mixture cracked earlier than the low paste content (24.2%) mixture in Program V Set 1.

CHAPTER 6 LC-HPC AND CONTROL BRIDGE DECK CONSTRUCTION AND CRACKING RESULTS IN KANSAS

6.1 GENERAL

This chapter describes the construction of 13 low-cracking high-performance concrete (LC-HPC) bridge decks in Kansas, along with another deck bid under an LC-HPC specification but for which the owner did not enforce the specification. Following construction, the decks, along with corresponding control decks, are surveyed annually for cracks. The cracking performance of the bridge decks is evaluated, and the factors that influence bridge deck cracking are investigated.

LC-HPC bridge decks are constructed following LC-HPC specifications covering aggregates, concrete, and construction. As working documents, the LC-HPC specifications have been modified based on lessons learned during the construction of 14 LC-HPC bridge decks in Kansas, and to a lesser extent, based on laboratory findings. Seven versions of the concrete and construction specifications and six versions of the aggregate specification have been used. A complete discussion of the LC-HPC specifications is reported by McLeod et al. (2009) and Lindquist et al. (2008). The latest versions of each of the LC-HPC specifications are summarized in Section 6.2.

The construction experiences and lessons learned during the construction of the 14 LC-HPC bridge decks are summarized in Section 6.3. A description of the concrete materials and construction methods used is provided, and the data collected during the construction of each LC-HPC deck construction are reported.

Cracking is expressed as crack density, in units of m/m2. The most recent crack map (summer 2010), showing the crack distribution, crack density, bridge location, construction date, and dimensions, is presented for each deck.

The performance of the LC-HPC bridge decks is compared with that of the control decks, which are similar in design, traffic conditions, and date of construction to the LC-HPC decks, but are constructed based on the Kansas Department of Transportation (KDOT) standard bridge specifications.

The influences of deck age, material factors, and construction factors on crack density are analyzed in Section 6.4.

6.2 LOW-CRACKING HIGH-PERFORMANCE CONCRETE (LC-HPC) SPECIFICATIONS

The LC-HPC specifications consist of three individual documents covering the concrete, aggregate, and construction requirements. A brief description of the latest version of the specifications is presented in this section. The full specifications are presented in Appendix E.

6.2.1 Aggregates

To increase the workability of LC-HPC, a nominal maximum aggregate size of 1 in. (25.4 mm) is used and the combined aggregate gradation is optimized using a proven optimization method such as Shilstone (1990) Method or the KU Mix Method (Lindquist et al. 2008). The combined aggregate gradation limits for LC-HPC are shown in Table 6.1.

Table 6.1 Combined aggregate gradation limits for LC-HPC

Usage	Percent Retained on Individual Sieves – Square Mesh Sieves†									
	25.0 mm (1")	19.0 mm (3/4")	12.5 mm (1/2")	9.5 mm (3/8")	4.75 mm (No. 4)	2.39 mm (No. 8)	1.18 mm (No. 16)	600 µm (No. 30)	300 µm (No. 50)	150 µm (No. 100)
Optimized for LC-HPC Bridge Decks	2-6	5-18	8-18	8-18	8-18	8-18	8-18	8-15	5-15	0-10

†The maximum allowable percentage passing the 75 µm (No. 200) is 2.5%.

The maximum coarse aggregate absorption is limited to 0.7%. In addition to providing concrete with improved durability, the low absorption helps reduce slump loss over time and maintain workability if the concrete is pumped. In contrast, the standard KDOT aggregate specification allows up to 2% absorption for coarse aggregates.

6.2.2 Concrete

Mixtures for LC-HPC have a cement content between 500 and 540 lb/yd^3 (296 and 320 kg/m^3) and a water-cement ratio (*w/c*) between 0.44 and 0.45, which may be decreased to 0.43 on-site with approval of engineer. The 28-day compressive strength is specified to be in the range of 3500 to 5500 psi (24 and 38 MPa).

The slump, air content, and concrete temperature are carefully controlled. The designated slump ranges from 1½ to 3 in. (35 to 75 mm) at the point of placement with a maximum of 3½ in. (90 mm) at the truck discharge. The designated air content is specified to be 8.0 ± 1.0% with a maximum of 0.5% above or below these limits. The designated concrete temperature is between 55 and 70° F (13 and 21° C) but may exceed these limits by 5° F (3° C) with approval of engineer. The slump and air content can be modified by adjusting the dosage rate of water-reducing admixture and air entraining agent. All water must be added at the concrete plant and no extra water may be added after the initial mixing period.

A qualification batch is required to demonstrate the concrete supplier's ability to produce LC-HPC meeting the requirements for air content, slump, temperature, compressive strength, unit weight, and other tests as required by the Engineer. The qualification batch should be completed at least 35 days prior to placement of the bridge deck, and must be produced at the same ready-mix plant that will supply concrete for the bridge deck. Haul time from the ready-mix plant to the job site must be simulated during production of the qualification batch.

Prior to construction, the owner and inspectors must agree on a plan for how to handle concrete that arrives at the construction site with tested properties outside the limits allowed by the specifications. A concrete test schedule is included in the specification. The first truckload is tested by obtaining samples both at the truck discharge and at the discharge end of the conveyor, bucket, or pump. Subsequent concrete is tested at the discharge end of the conveyor, bucket, or pump. Slump, air content, unit weight, and concrete temperature are tested for each of the first three truckloads, then one of every three truckloads for slump and one of every six truckloads for slump, air content, and unit weight. Concrete temperature is checked at truck discharge for each truckload, and for each sample made for a slump test.

A minimum of one set of five cylinders for every 100 yd^3 (76.5 m^3) of concrete placed is required, and at least two sets of five cylinders are required per bridge deck placement.

The LC-HPC specifications provide guidance on cold and hot weather placements. In cold weather, a placement must be discontinued once the descending ambient air temperature reaches 40° F (4° C), and may not be initiated until an ascending ambient air temperature reaches 40° F (4° C). The ascending ambient air temperature increases to 45° F (7° C) if the maximum ambient air temperature is expected to be between 55 and 60° F (13 and 16° C) during or within 24 hours of the placement, and to 50° F (10° C) if the maximum ambient air temperature is expected to be greater than or equal to 60° F (16° C) during or within 24 hours of the placement. Concrete must not be placed if the air temperature will be more than 25° F (14° C) below the concrete temperature during the first 24 hours after placement unless insulation is provided for both the deck and the girders. Concrete must not be placed if the air temperature is less than 20° F (–7° C). In hot weather, when the ambient air temperature is above 90 °F (32 °C), the forms, reinforcing steel, steel beam flanges, and other contact surfaces must be cooled to below 90 °F (32 °C).

6.2.3 Construction

The LC-HPC construction specification covers placement, finishing, and curing requirements.

Placement

The concrete can be placed by conveyor belt, concrete bucket, or pump, in the latter case if the contractor demonstrates that the approved LC-HPC mix can be pumped prior to bridge construction – either during placement of the qualification slab (discussed later in this section) or during a pumping trial at least 15 days before deck construction.

The evaporation rate during concrete placement must be less than 0.2 lb/ft^2/hr (1.0 kg/m^2/hr). The evaporation rate is determined using a nomograph (see Appendix E) and is a function of air temperature, concrete temperature, wind speed, and relative humidity. It is measured prior to and at least once per hour during placement. When the evaporation rate is above the limit of 0.2 lb/ft^2/hr (1.0 kg/m^2/hr), actions (such as cooling concrete, installing windbreaks and sun screens, etc.) must be taken.

Fogging may be required during any unanticipated delays during placing, finishing, and curing operations, but water may not drip, flow or puddle on the concrete surface before it has reached its final set. Water landing on concrete surface (from fogging) cannot be used as a finishing aid and worked back into the concrete. Fogging is not considered in the estimation of the evaporation rate. To avoid problems with extra fogging water affecting concrete proportion, a better solution is to cover exposed concrete with wet burlap during unexpected delays.

Finishing

The concrete surface must be first struck off using a vibrating screed or a single-drum roller screed, then finished by a burlap drag and/or metal pan drag mounted to the finishing equipment. A bullfloat or other approved device can be used to remove any irregularities, as necessary. Water or other chemicals cannot be used as finishing aids.

Tining of the plastic concrete is prohibited. The final driving surface is achieved by grinding (if needed to remove irregulations) and grooving of the hardened concrete.

Curing

The curing period begins immediately after concrete placement. Plastic concrete must be covered with the first layer of wet burlap within ten minutes of strike-off, then with a second layer of wet burlap within another five minutes. The burlap should be pre-soaked for a minimum of 12 hours prior to placement and re-wetted if dry spots are noticed at any time during placement.

LC-HPC is wet cured for 14 days. The burlap and concrete surface must be kept wet continuously starting from burlap placement until the end of the curing period. Initially, when the concrete is still plastic, the burlap is kept wet using misting hoses or other approved devices; within 12 hours of placement, when the concrete has gained sufficient strength to allow foot traffic, soaker hoses are placed on top of the burlap, followed by white polyethylene film, which covers the hoses and the burlap. The deck must be inspected once every 6 hours during the curing period to ensure that it is kept wet.

The specifications include provisions for cold weather curing. If the ambient air temperature is expected to drop below 40° F (4° C) during the curing period, or if the ambient air temperature is expected to drop more than 25° F (14° C) below the LC-HPC temperature during the first 24 hours after placement, suitable measures are required to protect the deck and girders, such as straw, additional burlap, or other suitable blanketing materials, and/or housing and artificial heat to maintain the concrete and girder temperature between 40 and 75° F (4 and 25° C). Heating may be stopped after the first 72 hours if the curing period is extended at a minimum ambient air temperature of 50° F (10° C) for a period equal to any time that the ambient air temperature is below 40° F (4° C). At the end of the curing period, the

curing material and the protective measures must be removed so that the temperature of LC-HPC does not fall more than 25° F (14° C) in 24 hours.

At the end of the 14-day wet curing, two coats of an opaque curing membrane must be applied within 30 minutes of removing the polyethylene and wet burlap. The curing membrane, which slows drying of a bridge deck, must be protected for a minimum of 7 days. An extension of the wet curing period beyond 14 days, if permitted, does not reduce the membrane curing period of 7 days.

The concrete forms are removed upon the Engineer's approval, generally about two weeks after the end of curing period (removal of burlap). The maximum time allowed to remove the concrete forms is four weeks to minimize the moisture gradient that may develop between the bottom and top surfaces of the deck.

Qualification slab

A qualification slab must be constructed to demonstrate a contractor's ability to place, finish, and cure the LC-HPC bridge deck within the performance limits in the specifications. The qualification slab is constructed to comply with the LC-HPC construction specification using the same concrete approved in a qualification batch 15 to 45 days prior to bridge construction. The same personnel, placement method, and equipment (including the same concrete pump, if used) must be used in the qualification slab as for the bridge deck.

Approval of the qualification slab is based on the satisfactory execution of placement, consolidation, finishing, and curing operations. Consolidation is examined by checking four full-depth cores [4-in. (100-mm) diameter] that are cored a minimum of one day after the placement of the qualification slab.

6.3 LC-HPC AND CONTROL BRIDGE DECKS CONSTRUCTION EXPERIENCE IN KANSAS

Thirteen low-cracking high-performance concrete (LC-HPC) bridge decks were built in Kansas between 2005 and 2009, and a fourteenth bridge, designated OP,

was originally bid under the LC-HPC specifications, but the specifications were not fully enforced. A control deck for each LC-HPC deck was also constructed. The bridge number, project let date, bridge contractor, ready-mix supplier, and construction date for each LC-HPC and control bridge are listed in Table 6.2. LC-HPC bridge numbers were assigned in chronological order based on the project let date, and the control bridge numbers were assigned to match with the corresponding LC-HPC bridge.

This section describes the construction experiences and lessons learned during the construction of the LC-HPC bridge decks, in the order of construction date (bridges in the same contract are presented together). A qualification batch and a qualification slab were required for each LC-HPC bridge. Concrete material data and construction details are described for each qualification batch, qualification slab, and LC-HPC bridge deck. The concrete material data and crack survey results are presented for each control deck. Crack survey results are also discussed, and the most recent crack map is presented.

Crack performance is compared over time of each LC-HPC bridge and its corresponding control bridge deck pair.

Detailed descriptions of concrete materials (including mixture design, aggregate optimization, slump, air content, and concrete temperature control strategies) are also presented by Lindquist et al. (2008), and construction procedures (including concrete delivery, placement, finishing, and curing) are also presented by McLeod et al. (2009).

Table 6.2 Bridge number, project let date, bridge contractor, concrete supplier, and construction date for LC-HPC bridges and corresponding Control bridges in Kansas

Bridge number	Project let date	Contractor	Concrete supplier	Construction date
LC-HPC 1-p1	9/15/2004	Clarkson	Fordyce	10/14/2005
LC-HPC 1-p2	9/15/2004	Clarkson	Fordyce	11/2/2005
LC-HPC 2	9/15/2005	Clarkson	Fordyce	9/13/2006
Control 1-2-p1	9/15/2004	Clarkson	Fordyce	10/10/2008
Control 1-2-p2	9/15/2005	Clarkson	Fordyce	10/28/2005
LC-HPC 3	8/17/2005	Clarkson	Fordyce	11/13/2007
Control 3	8/17/2005	Clarkson	Fordyce	7/17/2007
LC-HPC 4-p1	8/17/2005	Clarkson	Fordyce	9/29/2007
LC-HPC 4-p2	8/17/2005	Clarkson	Fordyce	10/2/2007
Control 4	8/17/2005	Clarkson	Fordyce	11/16/2007
LC-HPC 5	8/17/2005	Clarkson	Fordyce	11/14/2007
Control 5	8/17/2005	Clarkson	Fordyce	11-25/2007
LC-HPC 6	8/17/2005	Clarkson	Fordyce	11/3/2007
Control 6	8/17/2005	Clarkson	Fordyce	10/20/2008
LC-HPC 7	10/19/2005	Capital	CST*	6/24/2006
Control 7-p1	8/17/2005	Clarkson	Fordyce	3/29/2006
Control 7-p2	8/17/2005	Clarkson	Fordyce	9/15/2006
LC-HPC 8	7/19/2006	AM Cohron	O'Brien	10/13/2007
Control 8-10	7/19/2006	AM Cohron	O'Brien	4/6/2007
LC-HPC 9	7/19/2006	United	O'Brien	4/15/2009
Control 9-p1	7/19/2006	United	O'Brien	5/21/2008
Control 9-p2	7/19/2006	United	O'Brien	5/29/2008
LC-HPC 10	7/19/2006	AM Cohron	O'Brien	5/17/2007
LC-HPC 11	8/16/2006	King	Mid-America	6/9/2007
Control 11	1/19/2005	AM Cohron	Builders Choice	3/28/2006
LC-HPC 12-p1	11/15/2006	AM Cohron	Builders Choice	4/4/2008
LC-HPC 12-p2	11/15/2006	AM Cohron	Builders Choice	3/18/2009
Control 12-p1	11/15/2006	AM Cohron	Builders Choice	4/1/2008
Control 12-p2	11/15/2006	AM Cohron	Builders Choice	4/14/2009
LC-HPC 13	1/17/2007	Beachner	O'Brien	4/29/2008
Control 13	1/17/2007	Beachner	O'Brien	7/25/2008
OP-p1	3/26/2007	Pyramid	Fordyce	12/19/2007
OP-p2	3/26/2007	Pyramid	Fordyce	5/2/2008
OP-p3	3/26/2007	Pyramid	Fordyce	5/21/2008

Note: For control bridges with separate subdeck and overlay placements, the construction date refers to the date of overlay placement. * Concrete Supply of Topeka

6.3.1 LC-HPC 1

The first LC-HPC bridge deck constructed was the eastbound bridge on Parallel Parkway over I-635 in Kansas City, KS (the westbound bridge serves as the

control bridge for both LC-HPC 1 and LC-HPC 2). LC-HPC 1 is a steel girder bridge with integral abutments and a skew of five degrees. It has two spans, each with a length of 77.6 ft (23.7 m). The bridge is 75.1 ft (22.9 m) wide and, due to its large width, LC-HPC 1 was constructed in two full-length partial-width placements, on October 14 and November 2, 2005, respectively.

6.3.1.1 Concrete

The concrete was designed to have a cement content of 540 lb/yd^3 (320 kg/m^3) and a water-cement ratio of 0.45, with a corresponding paste content of 24.6% [the LC-HPC specifications for LC-HPC 1 and 2 limited the cement content to values between 522 and 563 lb/yd^3 (310 and 334 kg/m^3) and the maximum *w/c* ratio to 0.45].

6.3.1.2 Qualification batch and slab

The qualification batch was produced on June 20, 2005 by the concrete supplier, Fordyce Concrete. The low-cracking high-performance concrete met the specifications for air content and slump, but not concrete temperature. The concrete temperature was 89° F (32° C), well above the maximum allowable for the specification for LC-HPC 1 and 2 of 75° F (24° C), and no attempts were taken to control the concrete temperature. The out-of-specification qualification batch was accepted because it was believed that the concrete temperature could be easily adjusted during the construction. The decision proved to be an error, as the first qualification slab failed due to high concrete temperature.

The first attempt to cast the qualification slab was made on July 12, 2005. Because the concrete supplier was unable to lower the concrete temperature below 78° F (26° C), the placement was cancelled. The experience demonstrated the importance of completing a qualification batch that meets all specifications prior to construction. This point was illustrated again in 2009 during a bridge constructed in Missouri. For the Missouri bridge, the contractor practiced with out-of-specification concrete (high

temperature) on a test slab and decided that they would continue with the scheduled deck placement and adjust the concrete temperature during the construction. On the day of construction, the concrete supplier tried over four hours but failed to achieve the specified concrete temperature. Bridge construction was cancelled at a considerable cost.

The second attempt to construct the qualification slab on September 8, 2005 was successful. Concrete was tested at the truck discharge and had an average slump of 3.0 in. (75 mm) and air content of 8.4%. Chilled water was used to control the concrete temperature, which ranged from 67 to 71° F (19 to 22° C). Due to the low cement content and low slump of the LC-HPC, there was concern about pumping the concrete, and the contractor used a conveyor belt to place the concrete. The concrete finished well with a single-drum roller screed followed by a metal pan drag. A bullfloat was used occasionally. A fogging system with spray nozzles mounted to a work bridge was used in the beginning but turned off later due to water dripping from the nozzles. Hand-held fogging was used. Procedures for burlap placement were practiced. As shown in Figure 6.1, burlap was placed by workers on two work bridges. The burlap placement was generally slow, with the time for placement ranging from 4 to 38 minutes.

Figure 6.1 Burlap placement on the trial slab for LC-HPC 1

After working with the concrete, however, the contractor felt that it could be pumped, and they successfully pumped 1 yd^3 (0.75 m^3) of LC-HPC in on September 30, 2005, about two weeks prior to bridge construction.

6.3.1.3 LC-HPC 1-p1 (placement 1)

The first placement (south side) occurred on October 14, 2005. The bridge was constructed between 6:30 and 9:30 a.m., starting from the east abutment.

The concrete was tested out of the pump, with the exception of the first truck, which was tested only at the truck discharge. The air content and slump losses through the pump were not established. Performing the test at the end of the pump resulted in one batch of out-of-specification concrete being placed in the deck [the concrete in truck No. 10 had an air content of 11.5% and a slump of 6.5 in. (165 mm), and was placed approximately 70 ft (21 m) from the east abutment].

A summary of concrete test results for LC-HPC 1-p1 is presented in Table 6.3. The slump ranged from 2.5 to 6.5 in. (65 to 165 mm) with an average of 3.75 in. (95 mm). Because increased slump increases cracking potential, the initial LC-HPC specification required a slump range of 1.5 to 3.0 in. (36 to 75 mm) with a maximum allowable slump of 4 in. (100 mm) to provide the flexibility to accept some concrete with a slump over 3.0 in. (75 mm) to continue construction. As it turned out, 88% of the recorded slumps were over 3.0 in. (75 mm), more than half (63%) of the slumps were greater than or equal to 3.5 in. (90 mm), and 13% of the slumps were greater than or equal to 4.0 in. (100 mm), demonstrating the tendency of the contractor to use the maximum allowable slump. The trend was also apparent on other bridge decks and will be discussed later. The air content met specifications except for one batch, and ranged from 6.0% to 11.5% with an average of 7.9%. The concrete temperature ranged from 61 to 72° F (16.0 to 22.0° C) with an average of 67° F (19.8° C) and also met the specification [75° F (23.9° C) for LC-HPC 1 and 2]. The 28-day compressive strength was 5210 psi (35.9 MPa).

Table 6.3 Summary table of concrete test results† for LC-HPC 1-p1

KU Bridge Number	Slump		Air Content	Unit Weight		Concrete Temperature		28-day compressive strength††	
LC-HPC 1, placement 1	in.	mm	%	lb/ft^3	kg/m^3	°F	°C	psi	MPa
Average	3.75	95	7.9	140.5	2251	67	19.8	5210	35.9
Minimum	2.50	65	6.0	136.6	2188	61	16.0		
Maximum	6.50	165	11.5	142.1	2276	72	22.0		

Slump Range			Air Content Range		
> 3.0 in.(75 mm)	≥ 3.5 in.(90 mm)	≥ 4.0 in (100 mm)	> 9%	≥9.5%	≥ 10%
88%	63%	13%	13%	13%	13%

† Test results are from samples at pump discharge

†† Average 28-day compressive strength for lab-cured specimens

The concrete in LC-HPC 1 was pumped, and it pumped well. The bridge surface was initially finished with a metal-pan finisher attached to the back of the single-drum roller screed. Because the metal pan tore the finished concrete surface at times, it was removed and the deck surface was finished with a bullfloat.

Fogging equipment was mounted on the finishing bridge, as shown in Figure 6.2; it placed a water mist into the air but also resulted in droplets falling on the

Figure 6.2 Fogging system mounted to the finishing bridge, followed by bullfloating operation

bridge surface. The extra water on the deck surface was worked back into the concrete by the bullfloat, and so fogging was eliminated.

The time for burlap placement after finishing ranged from 11 to 29 minutes with an average of 16 minutes. Burlap placement was slow, mostly due to the slow finishing operation. Initially, the problem with the metal pan drag caused delays in burlap placement. When the bullfloat was used, more than a single pass of the bullfloat was needed to get a smooth surface, and burlap placement was thus slowed.

Some of the burlap was not totally wet at the time of placement for the first quarter of the bridge length. Dry spots were noted, and the contractor was told to spray water with a hose on the dry burlap. Wet burlap was used for the rest of the deck. Soaker hoses were placed immediately following the burlap placement to keep the burlap wet, which caused some divots on the fresh deck surface. It was noted that the soaker hoses did not cover the entire deck and some areas were dry (predominantly at the west end of the deck). Leaking connections resulted in some excess water on certain points on the deck.

The evaporation rate was low during construction, ranging from 0.02 to 0.06 lb/ft^2/hr (0.10 to 0.29 kg/m^2/hr) with an average of 0.04 lb/ft^2/hr (0.20 kg/m^2/hr).

6.3.1.4 LC-HPC 1-p2 (placement 2)

The second placement (north side) of LC-HPC 1 was completed on November 2, 2005, about two weeks after the first placement. Construction was from 7:20 a.m. to 10:15 a.m. and from the east abutment to the west abutment.

The same concrete mixture as used for placement 1 was used for placement 2. The concrete was tested at the discharge end of the pump, and the test results are summarized in Table 6.4. The slump ranged from 2.5 to 4.25 in. (65 to 110 mm) with an average of 3.25 in. (85 mm). Similar to placement 1, the contractor tended to use the maximum allowable slump. Sixty percent of the recorded slump values were over 3.0 in. (75 mm), which, actually, were all greater than or equal to 3.5 in. (90 mm), and 20%

of the slumps were greater than or equal to 4.0 in. (100 mm). The air content ranged from 3.0 % to 9.5% with an average of 7.8%. The air content was well controlled with only one recorded air content (3.0%) that did not meet the specification. The concrete temperature ranged from 66° F to 70° F (19° C to 21° C), which was within the specified range. The 28-day compressive strength was 4980 psi (34.4 MPa).

Table 6.4 Summary table of concrete test results† for LC-HPC 1-p2

KU Bridge Number	Slump		Air Content	Unit Weight		Concrete Temperature		28-day compressive strength††	
LC-HPC-1, placement 2	in.	mm	%	lb/ft^3	kg/m^3	°F	°C	psi	MPa
Average	3.25	85	7.8	139.7	2238	68	20	4980	34.4
Minimum	2.50	65	3.0	136.9	2193	66	19		
Maximum	4.25	110	9.0	146.9	2354	70	21		

slump range			Air range		
> 3.0 in.(75 mm)	≥ 3.5 in.(90 mm)	≥ 4.0 in (100 mm)	> 9%	≥9.5%	≥ 10%
60%	60%	20%	0%	0%	0%

† Test results are from samples taken at pump discharge
†† Average 28-day compressive strength for lab-cured specimens

The experience gained in the first placement helped the contractor complete the second placement smoothly. The concrete was pumped without any problems. The consolidation and strike-off operations proceeded smoothly. The issue of water landing on the deck surface due to fogging remained. The extra water on the surface was used as a finishing aid by the contractor, and significant amount of paste was visible on the surface for about the first 15 ft (4.6 m). The fogging was turned off about 70 ft (21.3 m) from the east abutment, but turned back on by the contractor, at about 80 ft (24.4 m), to help finishing. Starting at approximately 95 ft (28.9 m), it was determined that the fogging would be off for the rest of the bridge. Rather than using the extra water from fogging as a finishing aid, the finishers were allowed to use the bullfloat until the surface was adequately smooth.

The burlap in this placement was placed faster than the first placement, 7 to 17 minutes with an average of 11 minutes after concrete strike-off. The improvement in the time of burlap placement indicates that the technique can be learned quickly. It took longer to place burlap in the very beginning and at the end of a placement. At the east end, where placement started, burlap placement was delayed because the concrete needed to consolidated using worker-operated spud vibrators, rather than using the gang vibrators mounted on the finishing machine, and hand finished; the roller screed was also set at this time. When it was close to the end (west end), finishing and burlap placement on the deck were delayed while waiting for the abutment to be filled and the finishing equipment to be removed.

As the soaker hoses, which were placed immediately after burlap placement, caused divots during the first placement, the contractor used a garden hose with a spray nozzle to keep the placed burlap wet, and it worked well. Soaker hoses were placed later when the concrete began to stiffen.

The evaporation rate during construction ranged from 0.04 to 0.09 $lb/ft^2/hr$ (0.20 to 0.44 $kg/m^2/hr$) with an average of 0.07 $lb/ft^2/hr$ (0.34 $kg/m^2/hr$).

The air temperature dropped below freezing on the 13th and 14th day of the curing period. No protection was provided.

6.3.1.5 Crack survey results for LC-HPC 1

LC-HPC 1 has been checked once every year since it was constructed, with five surveys completed to date. The bridge has been performing consistently well with low crack densities. The crack density has increased from 0.012 m/m^2 at 5.9 months to 0.032 m/m^2 at 55.6 months for placement 1 and from 0.003 m/m^2 at 5.3 months to 0.023 m/m^2 at 55.0 months for placement 2. The most recent crack map is shown in Figure 6.3. For placement 1 (south half), only a few cracks have developed; they are near the abutments and the negative moment region (over the pier). No transverse cracks that cross the full bridge width or long longitudinal

cracks have been observed. The restraint provided by the integral abutments makes the concrete more susceptible to cracking; the negative moment region over the piers is also an area where the concrete is under tension and more easily develops cracks. The location of the transverse cracks matches the location where the highest slump concrete [discussed in Section 6.3.1.3, with a slump of 6.5 in. (165 mm)] was cast. High-slump concrete is more susceptible to settlement cracking over the reinforcing steel.

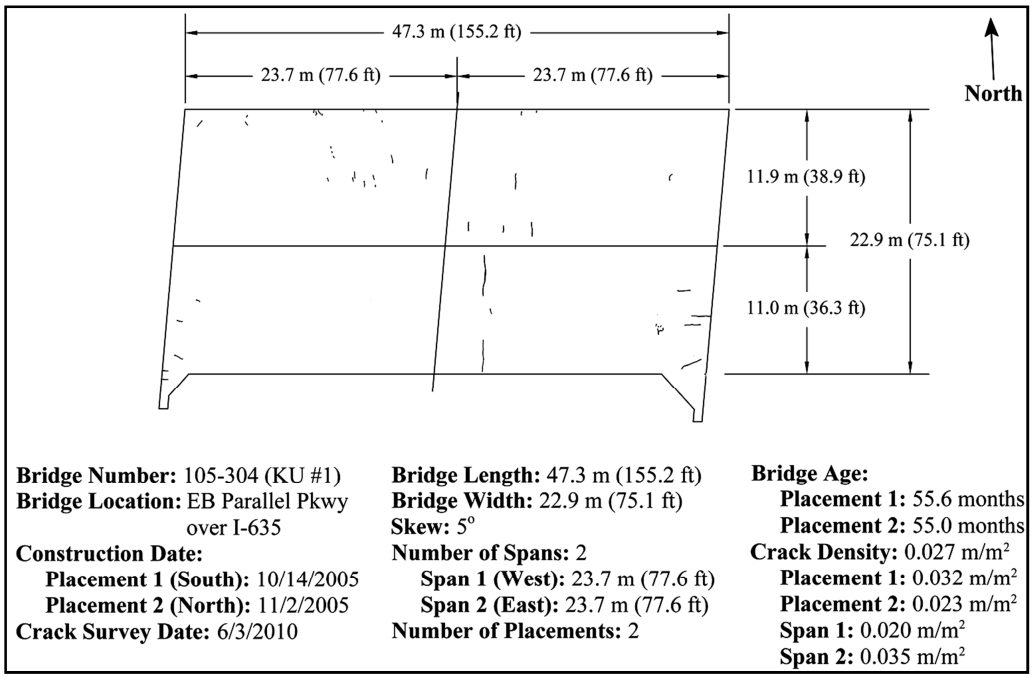

Figure 6.3 Crack map at about 55 months for LC-HPC 1

For placement 2, most cracks are very short transverse cracks. The extra water used as a finishing aid on the east half of the bridge and the extra finishing effort with bullfloating on the west half (discussed in Section 6.3.1.4) may have increased the paste content of the concrete surface, leading to an increased tendency to crack.

6.3.2 LC-HPC 2

LC-HPC 2 was let in the same contract as LC-HPC 1. It was constructed about 11 months after LC-HPC 1 and was the third LC-HPC deck constructed in Kansas.

LC-HPC 2 is the bridge on 34th Street over I-635 in Kansas City, KS. It is a two span steel girder bridge with integral abutments and no skew. The bridge is 175.1 ft (53.4 m) long, with two equal span lengths of 87.6 ft (26.7 m), and 40.0 ft (12.2 m) in width [30.2 ft (9.2 m) for the driving surface].

6.3.2.1 Concrete

The same concrete mixture as used for LC-HPC 1 was used for LC-HPC 2, with a cement content of 540 lb/yd^3 (320 kg/m^3) and a water-cement ratio of 0.45.

6.3.2.2 Qualification batch and slab

Because the same concrete supplier and the same concrete mixture design were used, the qualification batch prepared for LC-HPC 1 on September 20, 2005 also served as the qualification batch for LC-HPC 2.

The qualification slab for LC-HPC 2 was placed on May 24, 2006. As the air temperature was high and ranged from 70 to 91° F (21 to 33° C), the concrete temperature was controlled by replacing part of the mix water with chilled water and ice. The concrete temperature was maintained in the range of 66 to 72 °F (19 to 22 °C). The water content was not adjusted to account for the ice for the first ready-mix truck, and the first truck was rejected. The three remaining trucks had air contents that met the specifications but had slumps ranging from 4.0 to 5.5 in. (100 to 140 mm), which were greater than or equal to the maximum allowable slump of 4.0 in. (100 mm). The concrete was used to cast the qualification slab.

The concrete was pumped without any problems during placement of the qualification slab. The same crew as used for LC-HPC 1 constructed the qualification

slab. Concrete placement, consolidation, and finishing went smoothly. The concrete was finished using a single-drum roller screed and a bullfloat. Due to the high slump, the concrete finished easily.

Burlap was placed within 10 minutes of strike-off. Both the experienced crew and quick finishing operation contributed to the increased burlap placement rate. It was noted that the burlap placed over the guard rail reinforcing bars was not tucked in closely to the rail reinforcing, which left a space between the burlap and the concrete surface.

6.3.2.3 Deck construction

LC-HPC 2 was cast on September 13, 2006 between 6:00 a.m. and 9:30 a.m., starting at the east abutment.

The concrete was tested out of the pump. Seven out of 22 truckloads were tested. The test results are summarized in Table 6.5. All tested concrete met the specifications for slump, air content, and concrete temperature, although improper slump test procedures (tilting cone on lift and jerking cone prior to lift) were noted. In addition, two trucks with suspiciously high slump [approximately 6.0 in. (150 mm) by visual inspection] were cast in the deck at about the half-way point. Close to the end of the placement, three trucks had to be remixed with extra water-reducer because the concrete had zero slump and could not be discharged from the truck; the concrete was placed in the deck without re-testing. The measured slump ranged from 1.5 to 4.0 in. (35 to 100 mm) with an average of 3.0 in. (75 mm). The majority (71%) of the slump values were greater than 3.0 in. (75 mm), 29% were greater than or equal to 3.5 in. (90 mm), and 14% were equal to 4.0 in. (100 mm). Air content ranged from 7.0 to 8.5% with an average of 7.7%. The concrete temperature ranged from 61° F to 69° F (16.1° C to 20.6° C) with an average of 67° F (19.2° C). The 28-day compressive strength was 4600 psi (31.7 MPa).

Table 6.5 Summary table of concrete test results† for LC-HPC 2

KU Bridge Number	Slump		Air Content	Unit Weight		Concrete Temperature		28-day compressive strength††	
LC-HPC 2	in.	mm	%	lb/ft^3	lb/yd^3	°F	°C		
Average	3.0	75	7.7	--	--	67	19.2	4600	31.7
Minimum	1.5	35	7.0	--	--	61	16.1		
Maximum	4.00	100	8.5	--	--	69	20.6		

slump range			Air range		
> 3.0 in.(75 mm)	≥ 3.5 in.(90 mm)	≥ 4.0 in (100 mm)	> 9%	≥9.5%	≥ 10%
71%	29%	14%	0%	0%	0%

† The concrete was tested at pump discharge

†† Average 28-day compressive strength for lab-cured specimens

The concrete was pumped without any problems during the construction, including one truckload with a slump of 1.5 in. (35 mm).

The deck was finished using a single-drum roller screed and a bullfloat. This worked well. Approximately two-thirds through the deck, it was noted that the concrete was getting stiffer, and the contractor had to float the surface more often to get a smooth surface. With about 15 ft (4.6 m) to go, the contractor began spraying water on the surface to help the finishing operation. This was stopped right away. Fogging was not used during construction

Burlap placement was slow and the time ranged from 10 to 28 minutes with an average of 16 minutes. Delays occurred because finishing operations were halted several times to wait for concrete trucks to arrive. Delays also occurred when the only concrete pump at the site was re-positioned and when the west abutment was filled. All burlap was not fully saturated; dry spots were noted when it was laid out on a work bridge, and a spray hose was used to rewet it.

The evaporation rate was low, ranging from 0.01 to 0.02 lb/ft^2/hr (0.05 to 0.10 kg/m^2/hr) with an average of 0.02 lb/ft^2/hr (0.10 kg/m^2/hr).

6.3.2.4 Crack survey results for LC-HPC 2

Four surveys have been performed, at 7.2, 21.2, 32.5, and 44.5 months. As with LC-HPC 1, the crack density has been consistently low, increasing from 0.013 m/m^2 at 7.2 months to 0.059 m/m^2 at 44.5 months. The crack map at 44.5 months is shown in Figure 6.4. As shown in Figure 6.4, some short transverse cracks have formed, primarily in the negative moment region. No transverse cracks that cross the full bridge width or long longitudinal cracks have been observed.

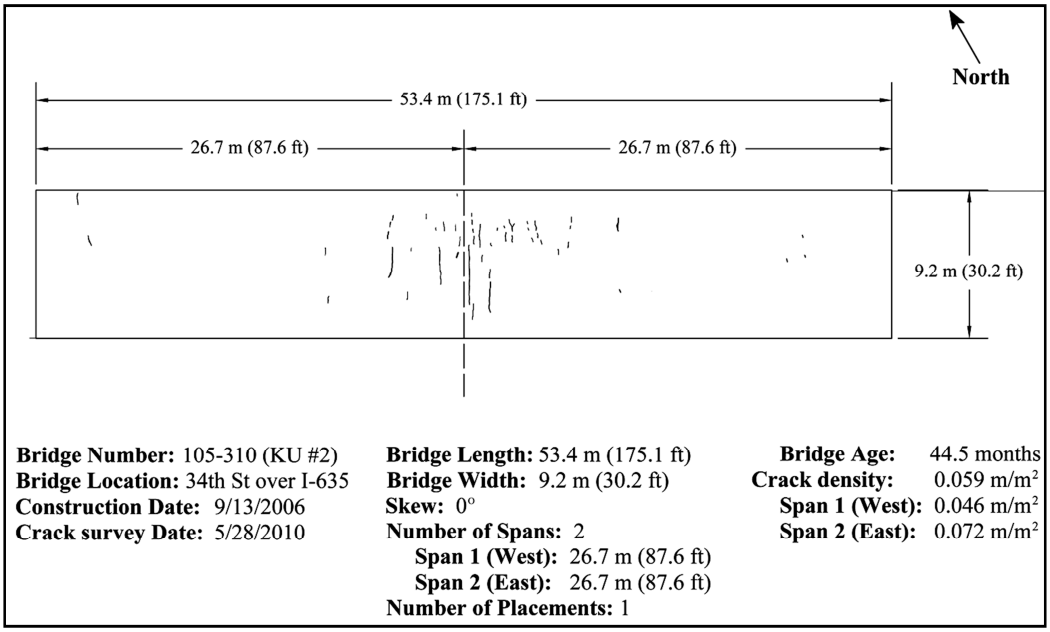

Figure 6.4 Crack map at 44.5 months for LC-HPC 2

6.3.3 Control 1-2

Control 1-2 is the control deck for both LC-HPC 1 (p1 and p2) and LC-HPC 2. It is the westbound bridge on Parallel Parkway over I-635 in Kansas City, KS. Control 1-2 was constructed under the same contract as LC-HPC 1 and 2 by the same contractor and concrete supplier, but following the Kansas Department of Transportation (KDOT) standard bridge specifications.

Control 1-2 is a steel girder bridge with internal abutments and a skew of five degrees. It has two spans with lengths of 77.6 ft (23.7 m) and a total width of 66.8 ft (20.4 m).

Control 1-2 was constructed in four placements, two placements for the subdeck and two placements for the silica fume overlay (SFO). The concrete mixtures and construction dates for the subdeck and the SFO are presented in **Error! Reference source not found.**. Compared with the low-cracking high-performance concrete used in LC-HPC 1 and 2, the subdeck concrete had a higher cement content, 602 lb/yd^3 (357 kg/m^3) for the north subdeck and 605 lb/yd^3 (359 kg/m^3) for the south subdeck, and a lower *w/c* ratio, 0.40, than the cement content of 540 lb/yd^3 (320 kg/m^3) and *w/c* ratio of 0.45. Limestone was used as the coarse aggregate for the subdeck concrete, while granite was used as the coarse aggregate for LC-HPC.

The SFO cementitious material consisted of 583 lb/yd^3 (346 kg/m^3) cement and 44 lb/yd^3 (26 kg/m^3) silica fume. A water-cementitious material ratio of 0.37 was used.

The average concrete properties for Control 1-2 are presented in **Error! Reference source not found.**. For the subdeck concrete, the average slumps for the two placements were 4.25 and 3.25 in. (110 and 80 mm), the average air contents were 5.3 and 6.5%, and the average compressive strengths were 5670 and 5090 psi (39.1 and 35.1 MPa), respectively. The SFO concrete for the two placements had slumps of 5.0 and 4.5 in. (125 and 115 mm), air contents of 5.5 and 7.0%, and compressive strengths of 5810 and 8060 psi (40.1 and 55.6 MPa), respectively. Generally, the concrete for the control bridges, especially the silica fume overlay concrete, has higher slump, lower air content, and higher compressive strength than LC-HPC.

Table 6.6 Mix design information for Control 1-2

Bridge Number	Portion Placed	Date of Placement	*w/cm*	Cement Content		Water Content		Silica Fume Content		Design Air Content	Design Volume of Paste	Coarse Aggregate Type
				(lb/yd^3)	(kg/m^3)	(lb/yd^3)	(kg/m^3)	(lb/yd^3)	(kg/m^3)	%	(%)	
Control 1 / 2	North 1-2 - Subdeck	09/30/05	0.40	602	357	241	143	0	0	6.5	25.6%	Limestone
	North 1-2 - Overlay	10/10/05	0.37	583	346	233	138	44	26	6.5	26.0%	Granite
	South 1-2 - Subdeck	10/18/05	0.40	605	359	241	143	0	0	6.5	25.7%	Limestone
	South 1-2 - Overlay	10/28/05	0.37	583	346	233	138	44	26	6.5	26.0%	Granite

Table 6.7 Average concrete properties for Control 1-2

Bridge Number	Portion Placed	Date of Placement	Average Air Content	Average Slump		Average Concrete Temperature		Average Unit Weight		Average Compressive Strength	
				(in.)	(mm)	(°F)	(°C)	(lb/yd^3)	(kg/m^3)	(psi)	(MPa)
Control 1 / 2	North 1-2 - Subdeck	09/30/05	5.3	4.25	110	66	19.0	144.7	2318	5670	39.1
	North 1-2 - Overlay	10/10/05	5.5	5.00	125	64	18.0	142.4	2281	5810	40.1
	South 1-2 - Subdeck	10/18/05	6.5	3.25	80	76	24.7	142.4	2274	5090	35.1
	South 1-2 - Overlay	10/28/05	7.0	4.50	115	68	20.0	140.7	2254	8060	55.6

6.3.3.1 Crack survey results for Control 1-2

Five crack surveys have been performed on Control 1-2, at 5.8, 18.3, 31.9, 43.9, and 55.5 months (average age of two placements). The crack density increased from 0 m/m^2 at 6.1 months to 0.132 m/m^2 at 55.8 months for placement 1, and from 0 m/m^2 at 5.5 months to 0.106 m/m^2 at 55.2 months for placement 2. Overall, Control 1-2 has performed well, and it is, in fact, the best performing control bridge in this study. The crack map at 55.5 months is shown in Figure 6.5. Transverse cracks have developed in the negative moment region and longitudinal cracks have formed at the abutments. Longitudinal cracks adjacent to the cold joint between the two placements have also been noted.

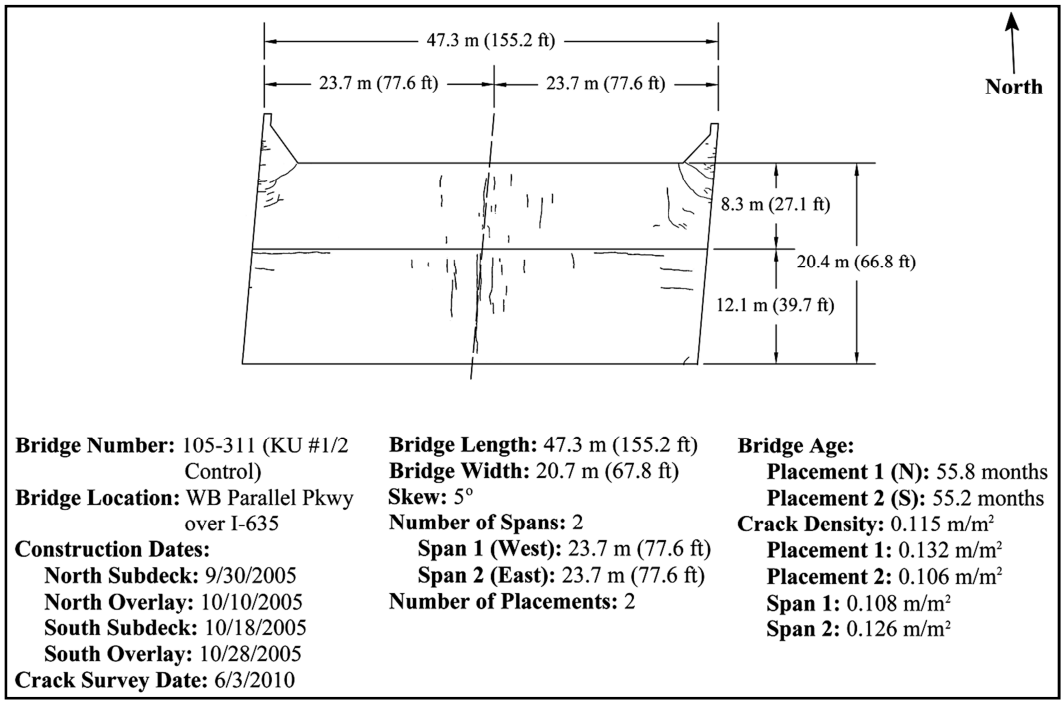

Figure 6.5 Crack map at 55.5 months for Control 1-2

6.3.3.2 The crack density versus age for LC-HPC 1 and 2 and Control 1-2

Crack density is plotted versus age for LC-HPC 1 (p1 and p2) and 2 and Control 1-2 (p1 and p2) in Figure 6.6. The LC-HPC bridges (three placements) have

performed consistently better than the control bridge (two placements) over a period of about 55 months. The most recent results, at about 55 months, indicate that the crack densities of the LC-HPC bridges are about one third of the crack densities of the control bridge.

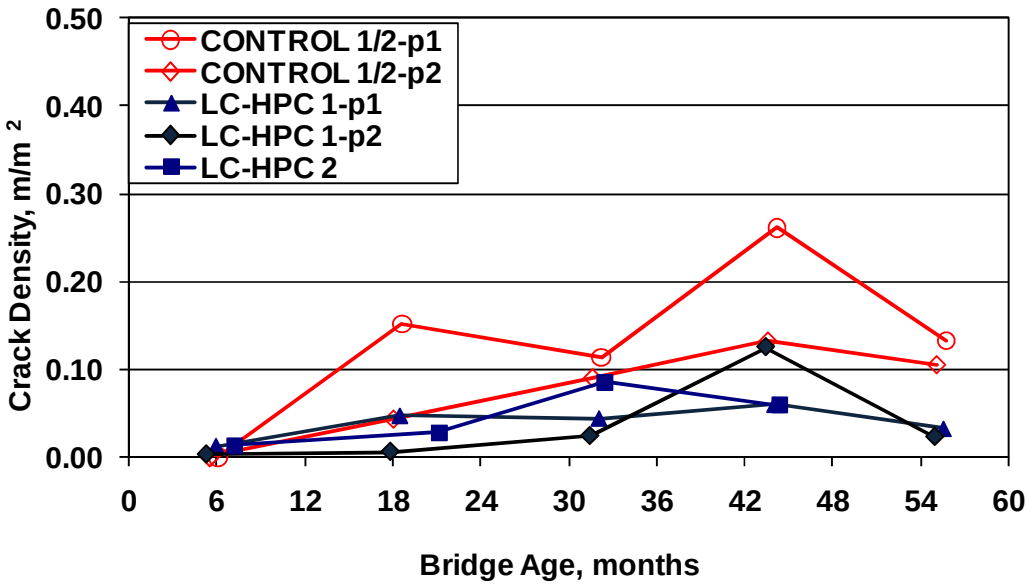

Figure 6.6 Crack density versus age for LC-HPC 1, 2 and Control 1-2

Overall, crack densities for both LC-HPC and Control bridges have increased over time, although some decreases have been noted in Figure 6.6, with a maximum decrease of 0.129 m/m^2 for Control 1-2-p1. As different crews have completed the surveys (most of the time with the same lead graduate student but different undergraduate workers), the decrease may have been caused by human error. The nature of the short cracks developed on these bridges in particular maximizes the possibility that they may be missed by different crews each year. The air temperature on the day of the survey may also affect the visibility of the cracks, as higher air temperature causes the bridge girders to expand more, which, in turn, makes the cracks more visible. The average air temperature on the survey taken at about 44

months was about 7° F (3.9° C) higher than it was on survey at about 55 months when the largest decrease in crack densities occurred.

6.3.4 LC-HPC 7

LC-HPC 7 was the seventh LC-HPC bridge let in Kansas but the second constructed. It is located on County Road 150 over US-75, north of Topeka, KS. The bridge is a two span steel plate girder bridge with integral abutments and no skew. It is 278.9 ft (85.0 m) long with two equal span lengths of 139.5 ft (42.5 m), and a width of 52.2 ft (15.9 m).

6.3.4.1 Concrete

The concrete mixture had a cement content of 540 lb/yd^3 (320 kg/m^3) and a *w/c* ratio of 0.45. No water reducer or superplasticizer was needed to obtain adequate slump.

6.3.4.2 Qualification batch and qualification slab

The qualification batch, which was called trial batch in the LC-HPC specifications for this bridge, was produced on May 31, 2006 at the plant of the Concrete Supply of Topeka (CST) in Topeka, KS.

Unlike the qualification batch for LC-HPC 1, where Fordyce Concrete practiced batching LC-HPC prior to the qualification batch and then demonstrated their ability (to the contractor and bridge owner) that they could produce LC-HPC during the qualification batch, CST made "trial batches" on the day of the qualification batch. Three consecutive trial batches were made. The third batch met the specifications with a slump of 3.75 in. (95 mm), an air content of 6.5%, and a concrete temperature of 73° F (23° C).

The qualification slab, which was called a trial slab in the LC-HPC specifications for this bridge, was placed on June 8, 2006. Overall, in-specification concrete was delivered but at a slow rate. The specification allowed water [up to 2

gallons/yd^3 (10 L/m^3)] to be withheld from the mixture at the batching site, and if needed, added back at the work site to adjust the slump. During the qualification slab, the concrete supplier withheld as much as 2.6 gal/yd^3 (13 L/m^3) of water, which resulted in a reduction of *w/c* ratio from 0.45 to 0.41. Ice was used to control the concrete temperature.

The concrete was consolidated using a gang-vibrator system (required by the specifications) with six vibrators. It was suggested that the contractor add several more vibrators to the system to minimize the number of insertion points for across the bridge.

Finishing was performed using a double-drum roller screed with one drum removed, followed by a metal pan drag. Due to delays caused by a slow concrete delivery, the contractor had some difficulties finishing the slab surface.

Burlap was placed with only one work bridge, which slowed placement. It was suggested that the contractor use two work bridges to place burlap for the deck placement.

The fogging nozzles were originally attached at the bottom of the finishing bridge, right next to the finishing drum, and, as a result, spayed water on the unfinished concrete surface. The water was then worked back into the concrete by the drum roller. The contractor was notified that this was not the desired fogging system and that no extra water should be worked back into concrete; then the contractor mounted the fogging system after a pan drag, which was mounted on the roller screed.

The concrete supplier and contractor learned a great deal from the qualification batch and qualification slab. A KDOT inspector commented at the end the qualification slab that “it proved the value of the trial slab. We were able to see how much the contractor learned (materials, fogging, finishing) from the beginning to the end of the trial slab.”

As the result of the less than detailed preparation by the concrete supplier and contractor, the terms “trial batch” and “trial slab” have been replaced by “qualification batch” and “qualification slab” with the purpose of emphasizing the importance of completing both in accordance with the specifications.

6.3.4.3 Deck construction

The bridge deck was cast about two weeks after the qualification slab, on June 24, 2006. The concrete was placed starting at approximately 1:00 a.m. and ending at approximately 9:30 a.m. and was completed moving from east to west.

The concrete test results are summarized in Table 6.8. The slump ranged from 2.25 to 6.0 in. (55 to 150 mm) with an average of 3.75 in. (95 mm). Sixty one percent of the recorded slump values were higher than 3.0 in. (75 mm) [actually greater than or equal to 3.5 in. (90 mm)], and 52% of the slump values were greater than or equal to the maximum slump of 4.0 in. (100 mm). This, again, demonstrated the tendency for contractors to use the maximum allowable slump. The air content was well controlled and ranged from 6.5 % to 10.5% with an average of 8.0%. Only one of the 14 samples had an out-of-specification air content (10.5%). The concrete temperature

Table 6.8 Summary table of concrete test results† for LC-HPC 7

KU Bridge Number	Slump		Air Content	Unit Weight		Concrete Temperature		31-day Compressive Strength	
LC-HPC-7	in.	mm	%	lb/ft^3	kg/m^3	°F	°C	psi	MPa
Average	3.75	95	8.0	138.6	2221	71	21.9	3790	26.1
Minimum	2.25	55	6.5	134.1	2148	68	20.0		
Maximum	6.00	150	10.5	143.1	2292	75	23.9		

slump range			Air range		
> 3.0 in.(75 mm)	≥ 3.5 in.(90 mm)	≥ 4.0 in (100 mm)	> 9%	≥9.5%	≥ 10%
61%	61%	52%	7%	7%	7%

† The concrete was tested at pump discharge. †† Average compressive strength for lab-cured specimens

was adjusted by replacing part of the mix water with ice and ranged from 68 to 75° F (20.0 to 23.9° C) with an average of 71° F (21.9° C). The concrete was tested at 31 days and had a compressive strength of 3190 psi (26.1 MPa), the lowest of any decks in the study.

The concrete pumped well. It was finished with a double-drum roller screed with one drum removed, followed by a pan drag and burlap drag attached to the trailing edge of the roller screed. A bullfloat was also used to smooth the surface. The finishing operation is shown in Figure 6.7. The fogging equipment leaked and had to be turned off.

Figure 6.7 Finishing operation for LC-HPC 7

Only three stations along the bridge were timed for burlap placement, at approximately the beginning of the construction, midpoint, and about 30 ft (9.1 m) past the midpoint, with times of 13, 11, and 7 minutes, respectively. Other burlap placement, however, was slow. The crew placing the burlap was not the same crew

as used for the trial slab. The process was inefficient and physically cumbersome. The burlap was rolled and carried by workers along the side of the deck. It was hard to unroll it on the narrow work bridges. The rolled burlap was often found twisted when it was unrolled. Because the burlap was presoaked, the wet burlap was heavy and difficult for the workers to handle. Only four workers were assigned to burlap placement (unroll, re-wet, untwist, and then place the burlap), and the process was labor-intensive and slow. If the burlap had been pre-folded like an accordion, delivered by a crane, and placed by experienced workers, the process would have been much faster.

After the burlap was placed, it was kept wet using garden hoses and lawn sprinklers. The garden hoses worked well, but the sprinklers placed too much water on the deck. Water runoff from the bridge was noted, as shown in Figure 6.8.

Figure 6.8 Water runoff the bridge when wetting the burlap on deck surface

The evaporation rate was low during construction, ranging from 0.02 to 0.05 lb/ft^2/hr (0.10 to 0.24 kg/m^2/hr with an average of 0.04 lb/ft^2/hr (0.20 kg/m^2/hr).

Finishing and curing were delayed for the last 40 ft (12.2 m) of the deck due to the placement of the west abutment. It was estimated that the concrete in the last 15 to 20 ft (4.6 to 6.1 m) of deck remained exposed for about 90 minutes.

6.3.4.4 Crack survey results

Four surveys have been completed, at 11.4, 24.2, 34.8 and 46.8 months with the crack densities of 0.003, 0.019, 0.012, and 0.005 m/m^2, respectively. The bridge has been performing very well. The crack map at 46.8 months is shown in Figure 6.9. Only a few very short longitudinal cracks have developed at the west abutment, where the concrete remained exposed for about 90 minutes without any protection. In fact, the crack map for the first survey at 11.4 months is very similar to the crack map at 46.8 months. When the second and third surveys were conducted, some very short cracks that were observed in the middle of the deck. None of these were found at the fourth survey at 46.8 months.

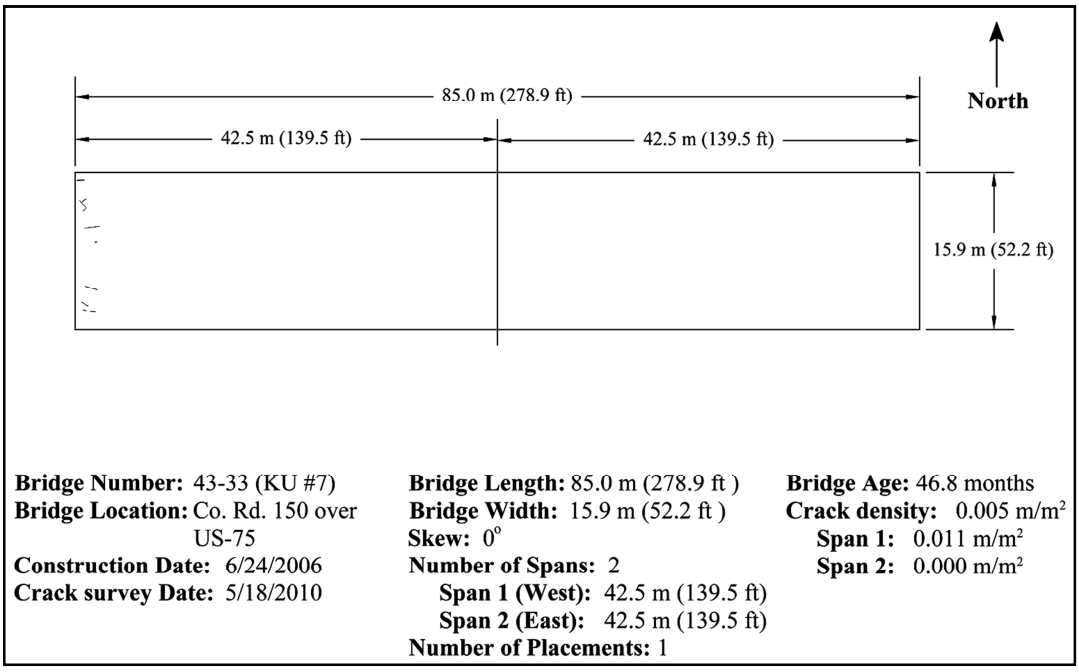

Figure 6.9 Crack map at 46.8 months for LC-HPC 7

6.3.5 Control 7

Control 7 is the northbound bridge on Antioch Rd over I-435 in Kansas City, KS. It is a steel girder bridge with integral abutments and has a skew of three degrees. The bridge is 192.9 ft (58.8 m) long and 51.2 ft (15.6 m) wide. It has two spans with span lengths of 89.9 and 103.0 ft (27.4 and 31.4 m).

The deck was constructed in four placements. The east 2/3 of the bridge was finished first, followed by the west 1/3, both with two parallel placements, one for the subdeck and one for the silica fume overlay (SFO). The construction dates and concrete mixture information for each placement are listed in **Error! Reference source not found.** Fly ash was used in the subdeck as a partial replacement (20% by weight) of cement. The cementitious material consisted of 536 lb/yd^3 (318 kg/m^3) cement and 133 lb/yd^3 (79 kg/m^3) fly ash; the concrete had a water-cementitious material (*w*/*cm*) ratio of 0.40. Granite was used as the coarse aggregate.

The SFO concrete had a 7% (by weight) replacement of cement with silica fume, which consisted of a combination of 583 lb/yd^3 (346 kg/m^3) of cement and 44 lb/yd^3 (26 kg/m^3) of silica fume. A *w*/*cm* ratio of 0.37 was used.

The average concrete properties are listed in Table 6.10. The concrete had high slumps, all over 7.0 in. (180 mm); the average air content ranged from 5.9 to 7.4% for the four placements. The compressive strength was about 5500 psi (38 MPa) for both subdecks and 7370 psi (50.8 MPa) for the SFO on the west 1/3 of the bridge. The compressive strength of the SFO on the east 2/3 of the bridge was not recorded.

6.3.5.1 Crack survey results for Control 7

The deck has been surveyed annually since it was constructed and four surveys have been completed. The crack density for the east 2/3 of the bridge was high at an early age and has increased significantly over the intervening period, from 0.293 m/m^2 at 16.9 months to 1.037 m/m^2 at 51.1 months; for the west 1/3 of the bridge, it has increased from 0.030 m/m^2 at 10.8 months to 0.359 m/m^2 at 45.5 months.

Table 6.9 Mix design information for Control 7

Bridge Number	Portion Placed	Date of Placement	*w/cm*	Cement Content		Water Content		Silica Fume Content		Class F Fly Ash Content		Design Air Content	Design Volume of Paste	Coarse Aggregate Type
				lb/yd^3	kg/m^3	lb/yd^3	kg/m^3	lb/yd^3	kg/m^3	lb/yd^3	kg/m^3	%	(%)	
Control 7	East - Subdeck	03/15/06	0.40	536	318	268	159	0	0	133	79	6.5	29.0%	Granite
	East - Overlay	03/29/06	0.37	583	346	233	138	44	26	0	0	6.5	26.0%	Granite
	West - Subdeck	08/16/06	0.40	536	318	268	159	0	0	133	79	6.5	29.0%	Granite
	West - Overlay	09/15/06	0.37	583	346	233	138	44	26	0	0	6.5	26.0%	Granite

Table 6.10 Average concrete properties for Control 7

Bridge Number	Portion Placed	Date of Placement	Average Air Content	Average Slump		Average Concrete Temperature		Average Unit Weight		Average Compressive Strength†	
				(in.)	(mm)	(°F)	(°C)	(lb/yd^3)	(kg/m^3)	(psi)	(MPa)
Control 7	East - Subdeck	03/15/06	5.9	9.25	235	80	26.5	139.8	2239	5540	38.2
	East - Overlay	03/29/06	7.4	7.50	190	73	23.0	139.8	2239	NA	NA
	West - Subdeck	08/16/06	7.3	7.75	195	70	21.3	139.0	2226	5500	37.9
	West - Overlay	09/15/06	6.4	7.00	175	64	18.0	140.6	2252	7370	50.8

The most recent crack map is shown in Figure 6.10. As shown in Figure 6.10, the east 2/3 of the bridge has cracked badly. Most cracks are transverse and some of them have crossed the full bridge width. Some longitudinal cracks have also formed at the abutments and in the middle of the bridge. Some of the longitudinal cracks are interconnected with transverse cracks. The west 1/3 of the bridge has performed better than the east 2/3. Most cracks are transverse. Longitudinal cracks are close to the cold joint and have almost crossed the full length of the bridge.

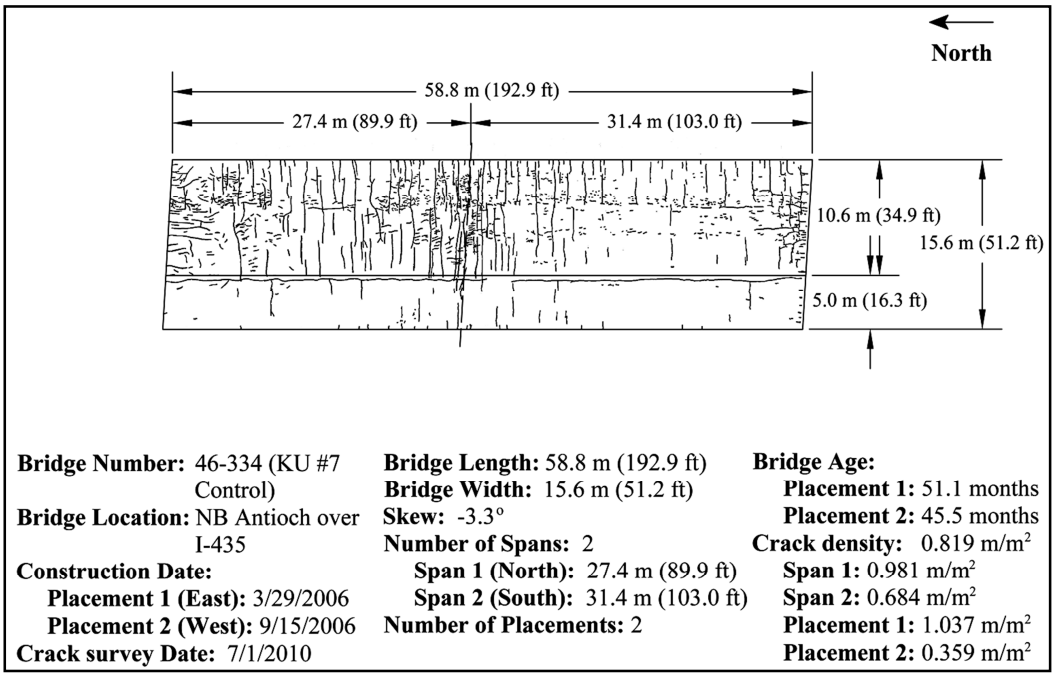

Figure 6.10 Crack map at 51.1 months for Control 7

6.3.5.2 Crack density versus age for LC-HPC 7 and Control 7

The crack density versus age for LC-HPC 7 and Control 7 (p1 and p2) is plotted in Figure 6.11. Over the four-year period, LC-HPC 7 has been performing much better than Control 7. Control 7 has higher crack densities than LC-HPC 7 at all ages, and the crack density has continued to increase.

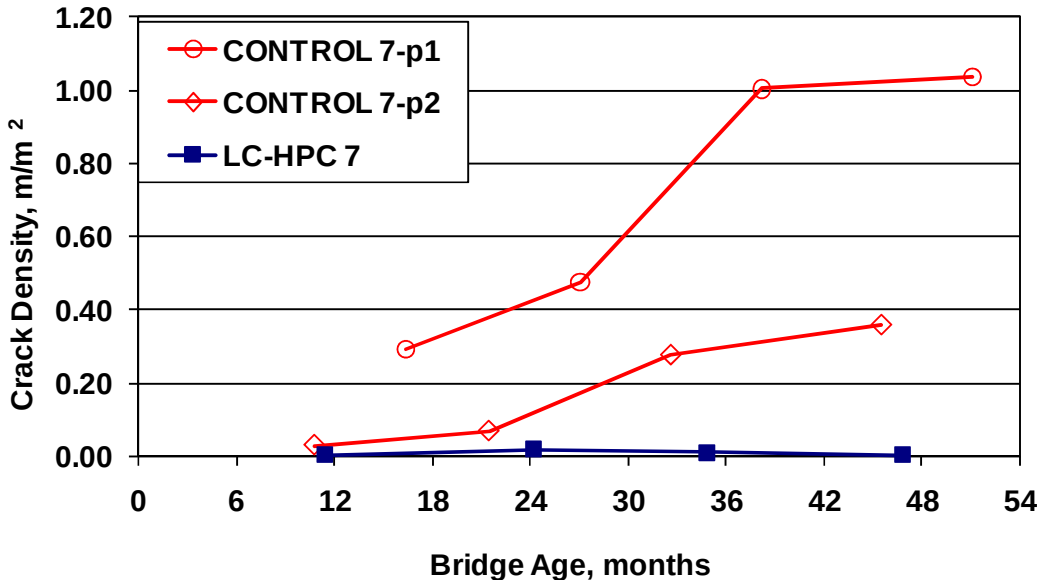

Figure 6.11 Crack density versus age for LC-HPC 7 and Control 7

6.3.6 LC-HPC 10

LC-HPC 10 and LC-HPC 8 are the only prestressed concrete girder bridges constructed with low-cracking high-performance concrete in Kansas. The construction of LC-HPC 10 will be discussed first as it was constructed first.

LC-HPC 10 is the bridge on E 1800 Rd over US-69 in Linn County, KS. It is a prestressed concrete girder bridge with integral abutments and a skew of 21 degrees. The bridge is 335.0 ft (102.1 m) long and 36.1 ft (11.0 m) wide. It has four spans with lengths of 75.5, 97.8, 97.8, and 63.9 ft (23.0, 29.8, 29.8, and 19.5 m).

6.3.6.1 Concrete

The concrete mixture used for this bridge had a cement content of 535 lb/yd^3 (317 kg/m^3) and a water-cement ratio of 0.42. The mixture contained less paste (23.3% by volume) than the mixtures used for LC-HPC 1, 2, and 7 (paste content 24.6% by volume), which had a cement content of 540 lb/yd^3 (320 kg/m^3) and a water-cement ratio of 0.45. The purpose of lower paste content is to reduce concrete shrinkage.

6.3.6.2 Qualification batch and qualification slab

The qualification batch was conducted on April 11, 2007, and it met the specification with a slump of 1.75 in. (45 mm), an air content of 8.6%, and a concrete temperature of 59° F (15° C). The concrete supplier planned to withhold a portion of the mix water to have the flexibility of adjusting slump during construction.

The qualification slab was placed on April 26, 2007 as part of a driveway at a farm. Four truckloads of concrete were placed. Water was withheld at the plant and added back on site to adjust the slump. The concrete met the requirements for the slump, air content, and temperature. The concrete delivery was very slow because the concrete supplier tested each truck at the plant, and a new truckload was batched only after the previous truck was accepted on site. The inspector suggested that the concrete supplier only check the first truck at the plant and then send on the others to be checked on site during bridge construction.

The concrete pumped adequately. For the third truck, additional water reducer was added on site because the pump operator thought the concrete would not pump, although the concrete in the other three trucks [slumps of 2.5, 3.25, and 3.25 in. (65, and 85, and 85 mm)] pumped without any problems. This increased the slump from original 2.75 in. (70 mm) to 5.0 in. (130 mm).

The slow concrete delivery slowed the consolidation, finishing, and curing of the entire slab.

While waiting for concrete, the contractor left the roller screed on. As a result, it made at least six passes on some sections of the slab. It was pointed out that the additional passes were not “doing anything” and the surface was not completely “sealed” until a bullfloat was used. The importance of keeping the operation moving and not overfinishing the surface was emphasized. The individual pieces of burlap were rolled, and they were difficult to handle. It was suggested that the contractor fold the burlap in accordion style and deliver the burlap with a crane during the

bridge placement. The fogging equipment produced a fine mist in the air, but it dripped when it was turned off. The contractor was notified of the need to fix the dripping problem.

Overall, the contractor was pleased with the concrete.

6.3.6.3 Deck construction

LC-HPC 10 was constructed on May 17, 2007. The bridge was constructed in about nine hours from 3:30 a.m. to 12:30 p.m. starting at the east abutment.

The concrete was tested out of the pump and the test results are summarized in Table 6.11. The slump ranged from 1.75 to 5.0 in. (45 to 125 mm) with an average of 3.25 in. (80 mm). Sixty percent of the recorded slump values were higher than 3.0 in. (75 mm), 33% were greater than or equal to 3.5 in. (90 mm), and 13% were greater than or equal to the maximum allowable slump of 4.0 in. (100 mm). The air content ranged from 5.1 % to 9.2% with an average of 7.3%. The concrete supplier had trouble getting the correct air content for the first three trucks, low on the first two trucks at about 5% and high on the third truck at 11% (the third truck waited onsite

Table 6.11 Summary table of concrete test results† for LC-HPC 10

KU Bridge Number	Slump		Air Content	Unit Weight		Concrete Temperature		28-day compressive strength††	
LC-HPC 10, placement	in.	mm	%	lb/ft^3	kg/m^3	°F	°C	psi	MPa
Average	3.25	80	7.3	138.1	2212	66	18.6	4580	31.6
Minimum	1.75	45	5.1	134.2	2149	60	15.6		
Maximum	5.0	125	9.2	142.1	2276	72	22.2		

Slump Range			Air Content Range		
> 3.0 in.(75 mm)	≥ 3.5 in.(90 mm)	≥ 4.0 in (100 mm)	> 9%	≥9.5%	≥ 10%
60%	33%	13%	5%	0%	0%

†: Test results were from samples taken after concrete being pumped

††: Average 28-day compressive strength for lab cured specimens

for 20 minutes and the air content dropped to 7.7%). The admixture dosage was adjusted, and the majority of the remaining trucks had the proper air content. The concrete temperature ranged from 60 to 72° F (15.6 to 22.2° C) with an average of 66° F (19.6° C). The 28-day compressive strength was 4580 psi (31.6 MPa).

Because water was withheld at the ready-mix plant, the *w/c* ratio ranged from 0.40 to 0.42 with an average of 0.41.

The concrete was pumped. Only one pump was available during construction, and the contractor had to re-locate the pump once so that it could reach the rest of the deck. The relocation of the pump delayed concrete placement, finishing, and curing. The pump clogged once when placing the west pier cap (about 3/4 of the bridge had been cast) and some water was added to the pump hopper to clear the jam. It was not possible to know how much water was added. The concrete went into the pier cap instead of the deck. For all follow-on LC-HPC bridge decks, two pumps (or other placement equipment, as appropriate) have been required so that construction does not have to be interrupted to re-locate the pump and to provide a backup in case one piece of equipment has problems.

The concrete was finished using a single-drum roller screed followed by a metal pan drag. The screed advanced so slowly that it caused delays in burlap placement. For most of the deck, a bullfloat was not needed to finish the concrete.

Burlap placement was slow, and the time for placement ranged from 6 to 41 minutes with an average of 17 minutes. Several reasons caused the slow burlap placement. First, the finishing bridge advanced so slowly that it took a long time to leave enough space between the finishing bridge and burlap placing bridge to begin placing the burlap. Second, there were not enough workers assigned to burlap placement, and some of the burlap workers also had to help with finishing and fogging. The inconsistent concrete supply and relocating the concrete pump also caused delays.

It was noted that the burlap was not presoaked. During construction, the burlap was briefly submerged in a water tank for about 2 minutes, then moved to the work bridge with a crane. In many cases, the burlap dripped water on the deck surface. The briefly soaked burlap dried fast and needed to be rewetted less than 20 minutes after placement. The contractor was told to wet the burlap, though it was difficult to communicate the goal of this "wetting" process while constructing the bridge. Several attempts were made, but in the end there was still a single worker who wetted down a small area of the burlap for 10 minutes or so and let the rest dry.

The main fogging system attached to the finishing bridge leaked and was turned off. Hand fogging, shown in Figure 6.12, was used intermittently during delays. In one instance, the water from the supplemental hand fogger was used to aid the finishing operation near the third pier cap (from the east), and so it was stopped.

Figure 6.12 Hand-held fogging in LC-HPC 10

The evaporation rate during construction ranged from 0.04 to 0.07 lb/ft^2/hr (0.20 to 0.32 kg/m^2/hr).

6.3.6.4 Crack survey results for LC-HPC 10

Three crack surveys have been completed, at 3.9, 25.4, and 36.2 months. When LC-HPC 10 was first surveyed at 3.9 months, the bridge had not been grooved. Because all of the other bridges surveyed in the study have a grooved deck surface, to have a fair comparison with other bridges, the second survey for LC-HPC 10 was not performed until it had been grooved (about two years later). The crack density has decreased over the three surveys, from 0.248 to 0.076 and then to 0.029 m/m^2. Possible reasons for the decrease will be discussed in Section 6.3.8.2. The crack map at 36.2 months is shown in Figure 6.13. As shown in the figure, only a few cracks appear at 36.2 months. Most cracks are transverse. One short longitudinal crack is apparent at the west abutment.

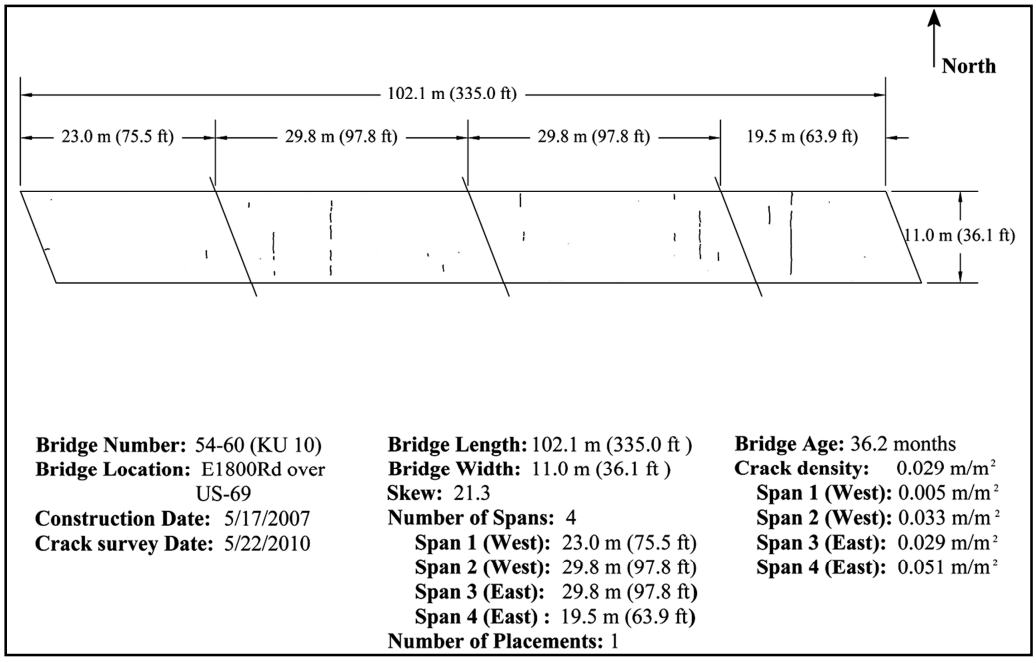

Figure 6.13 Crack map at 36.2 months for LC-HPC 10

6.3.7 LC-HPC 8

LC-HPC 8 is located on E 1350 Rd over US-69 in Linn County, KS. It was constructed under the same contract by the same contractor and concrete supplier as LC-HPC 10.

LC-HPC 8 was the second prestressed concrete girder bridge constructed with LC-HPC in Kansas. It has integral abutments and no skew. The bridge is 303.0 ft (92.4 m) long and 36.1 ft (11.0 m) wide. There are four spans, with lengths of 60.3, 91.2, 91.2, and 60.3 ft (18.4, 27.8, 27.8, and 18.4 m).

6.3.7.1 Concrete

The concrete mixture used for LC-HPC 10 was used on LC-HPC 8, with a cement content of 535 lb/yd^3 (317 kg/m^3) and a *w*/*c* ratio of 0.42. The slump was adjusted by withholding part of the mix water at the concrete plant and then adding it back at the jobsite, if needed.

6.3.7.2 Qualification batch and qualification slab

Since it was the same concrete mix design and concrete supplier, the qualification batch conducted on April 11, 2007 for LC-HPC 10 was used as the qualification batch for LC-HPC 8.

Due to the difficulties that occurred during the placement of LC-HPC 10, the qualification slab was not waived and was constructed on September 26, 2007. Several issues were observed and resolved during the qualification slab construction. It was noted that the burlap was dry and needed to be wetted on a work bridge with a spray hose. The contractor was required to pre-soak the burlap for a minimum of 12 hours in preparation for deck placement. Burlap workers did not seem to know what to do and had to be reminded to get up on the work bridges to place the burlap. Fogging, which used a 400 psi (2.8 MPa) pressure, sprayed a layer of water on the deck surface. The contractor was required to use a higher pressure [determined to be 1000 psi (6.9 MPa) during a teleconference after the qualification slab). It was decided to have two pumps for deck construction and that the diaphragms would be pre-placed to avoid delays in deck placement.

6.3.7.3 Deck construction

The deck was cast on October 3, 2007, one week after the qualification slab. Construction started about at 7:30 a.m. and finished around 2:30 p.m., moving from the west abutment to the east abutment.

The concrete was tested out of the pump, and the test results are summarized in Table 6.12. Slump, air content, and concrete temperature were well controlled during the construction. The slump ranged from 1.0 to 3.0 in. (25 to 75 mm) with an average of 2.0 in. (50 mm). The slump was controlled by withholding part of the mix water. As a result, the *w/c* ratio varied between 0.39 and 0.41 with an average of 0.40, below the specified value of 0.42. The air content ranged from 5.7 % to 10.2% with an average of 7.9%. Of the 23 trucks (a total of 56 truckloads of concrete were cast) that were checked for air content, three had air contents that were out of specification, with values of 5.7, 10.2, and 9.7%. Ice was used to control the concrete temperature, which ranged from 59 to 73 °F (15.0 to 22.8 °C) with an average of 67 °F (19.5 °C). The 28-day compressive strength was 4590 psi (31.7 MPa), a relatively low value considering the low *w/c* ratio.

Table 6.12 Summary table of concrete test results† for LC-HPC 8

KU Bridge Number	Slump		Air Content	Unit Weight		Concrete Temperature		28-day compressive strength††	
LC-HPC 8, placement	in.	mm	%	lb/ft^3	kg/m^3	°F	°C	psi	MPa
Average	2.0	50	7.9	141.3	2264	67	19.5	4590	31.7
Minimum	1.0	25	5.7	137.0	2194	59	15.0		
Maximum	3.0	75	10.2	144.9	2321	73	22.8		

Slump Range			Air Content Range		
> 3.0 in.(75 mm)	≥ 3.5 in.(90 mm)	≥ 4.0 in (100 mm)	> 9%	≥9.5%	≥ 10%
0%	0%	0%	9%	9%	4%

† Test results were from samples taken at pump discharge.
†† Average 28-day compressive strength for lab-cured specimens

The concrete was placed with two pumps, one at the west end and one at the east end. The diaphragms and the final abutment were filled in three layers by filling the first layer about 20 ft (6 m) ahead of the most recently placed concrete, the second layer about 10 ft (3 m) ahead, and the third layer when the concrete in the deck reached the diaphragm or abutment. This method worked well and reduced delays.

The concrete finished well with a single-drum roller screed followed by a metal pan drag. Bullfloating was occasionally used.

Burlap was placed smoothly, and the time for burlap placement ranged from 4 to 27 minutes with an average of 12 minutes. The burlap was kept wet using a hand-held spray hose, which worked well. A crew of five workers plus one supervisor was assigned to burlap placement. This deck demonstrated the importance of having a person with authority assigned to monitor the burlap placement and wetting operations.

Fogging was used only on the very last section [about 8 ft (2.4 m) from east end] while waiting for the final load of concrete. Fogging produced a fine water mist and little water accumulated on the finished deck surface, even when fogging continued on the same portion for 15 minutes.

6.3.7.4 Crack survey results for LC-HPC 8

Two crack surveys have been performed, at 20.9 and 31.8 months, giving crack densities of 0.298 and 0.348 m/m^2, respectively. At 20.9 months, the bridge was still not open to traffic due to the ongoing construction in that area. An earlier crack survey had been attempted when the bridge was about one year old and was canceled because the bridge surface was covered with mud (from construction trucks). The crack map at 31.8 months is shown in Figure 6.14. As shown in Figure 6.14, many cracks have developed. Most are transverse and approximately evenly distributed along the bridge. LC-HPC 8 has the highest crack density among all similar-age LC-HPC bridges constructed in Kansas.

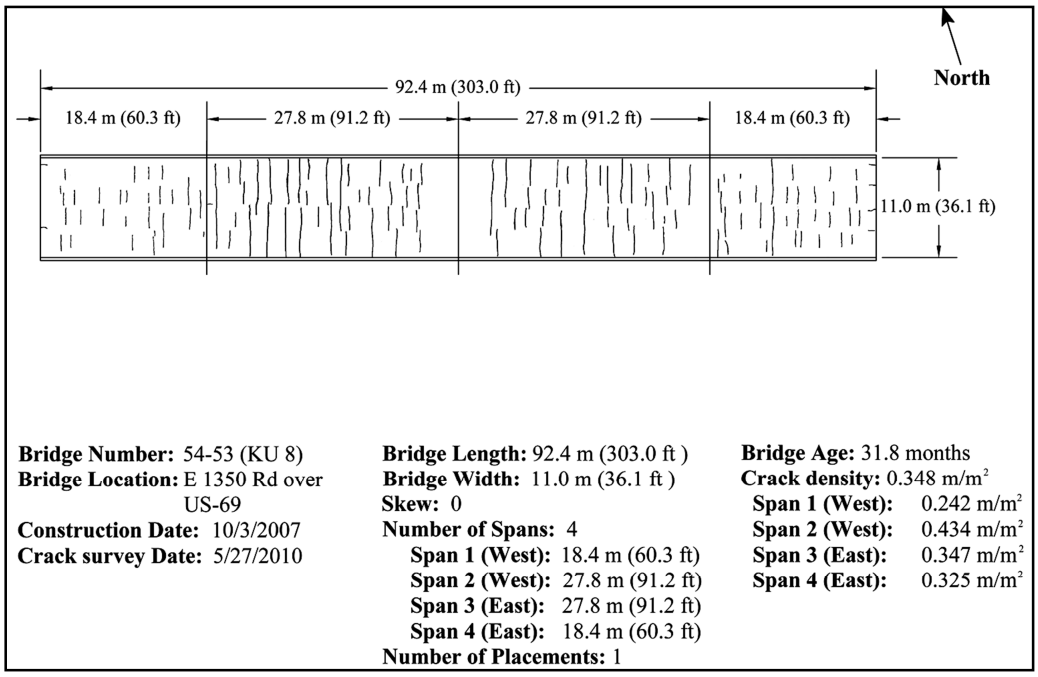

Figure 6.14 Crack map at 31.8 months for LC-HPC 8

6.3.8 Control 8-10

Control 8-10 is located on K-52 over US-69 in Linn County, KS. It is a prestressed concrete girder bridge that is similar in size to LC-HPC 8 and 10. It has integral abutments and no skew. The bridge is 317.7 ft (96.8 m) long and 40.0 ft (12.2 m) wide. It has four spans with lengths of 73.4, 91.2, 91.2, and 62.0 ft (22.4, 27.8, 27.8, and 18.9 m).

The bridge was constructed in a single phase on April 16, 2007. Information on the concrete mixture is presented in Table 6.13. The concrete had a cement content of 612 lb/yd^3 (363 kg/m^3) and a *w/c* ratio of 0.40.

Table 6.13 Mix design information for Control 8-10

w/c	Cement Content		Water Content		Design Air Content	Design Volume of Paste	Coarse Aggregate Type	Types of Admixtures
	lb/yd^3	kg/m^3	lb/yd^3	kg/m^3	%	%		
0.40	612	363	244	145	6.5	26.0%	Limestone	AEA, Type A-D WR

The concrete test results are listed in Table 6.14. The plastic concrete had an average slump of 5.25 in. (135 mm), an air content of 7.4 %, and a temperature of 70° F (21.2° C). The average 28-day compressive strength was 4830 psi (33.3 MPa).

Table 6.14 Average concrete properties for Control 8-10

Average Air Content	Average Slump		Average Concrete Temperature		Average Unit Weight		Average 28-day Compressive Strength	
	(in.)	(mm)	(°F)	(°C)	(lb/yd^3)	(kg/m^3)	(psi)	(MPa)
7.4	5.25	135	70	21.2	139.4	2234	4830	33.3

6.3.8.1 Crack survey results for Control 8-10

Three crack surveys have been completed on Control 8-10, at 14.3, 25.5, and 37.3 months, giving crack densities of 0.177, 0.127, and 0.137 m/m^2, respectively. The crack density decreased between the first and the second surveys. Possible reasons for the decrease are discussed in Section 6.3.8.2. The crack map at 37.3 months is shown in Figure 6.15. Most cracks are transverse and located at span 2. Some longitudinal cracks have developed at the west abutment and one longitudinal crack has developed at the east abutment.

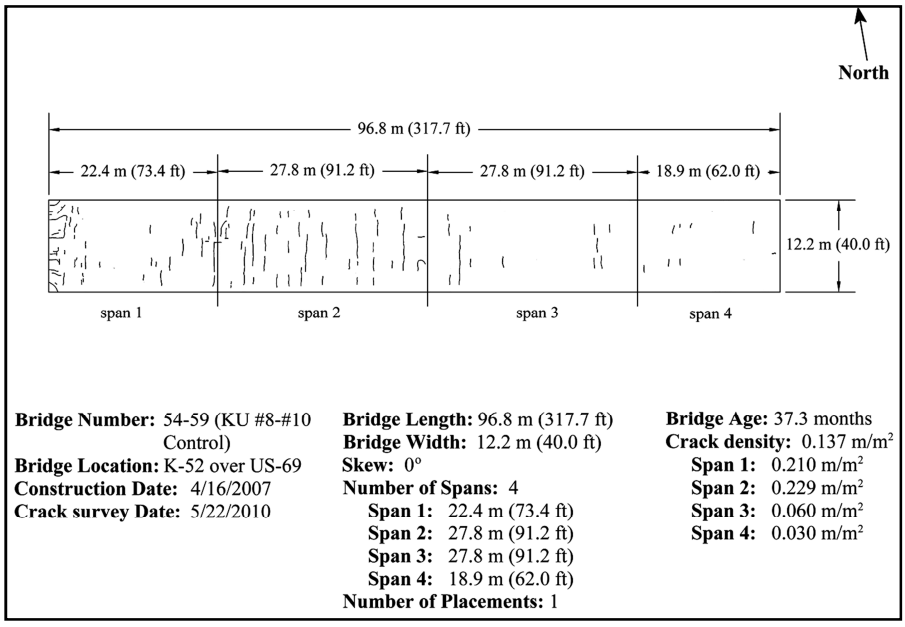

Figure 6.15 Crack map at 37.4 months for Control 8-10

6.3.8.2 Crack density versus age for LC-HPC 8 and 10 and Control 8-10

Crack density is plotted versus age for LC-HPC 8, LC-HPC 10, and Control 8-10 in Figure 6.16. Overall, LC-HPC 10 has performed better than the control bridge, while LC-HPC 8 has, to date, exhibited more than twice the crack density of Control 8-10.

As shown in Figure 6.16, the crack density of LC-HPC 10 has decreased over time. LC-HPC 10 had its highest crack density, 0.248 m/m^2, at 3.9 months. The non-grooved surface may have made the cracks more visible and contributed to the high crack density at 3.9 months. The crack density for LC-HPC 10 decreased to 0.076 m/m^2 at 25.4 months and decreased again to 0.029 m/m^2 at 36.2 months. A similar phenomenon was also noted for the prestressed control bridge (Control 8-10), which had the crack density of 0.177 m/m^2 at 14.4 months and 0.127 m/m^2 at 25.5 months. A prime reason for this decrease in crack density may be a decrease in camber and shortening of the girder, which are influenced by creep, shrinkage, and relaxation losses in the prestress force. More surveys of prestressed concrete girder bridges will be needed to determine of this effect is universally beneficial to prestressed girder bridges.

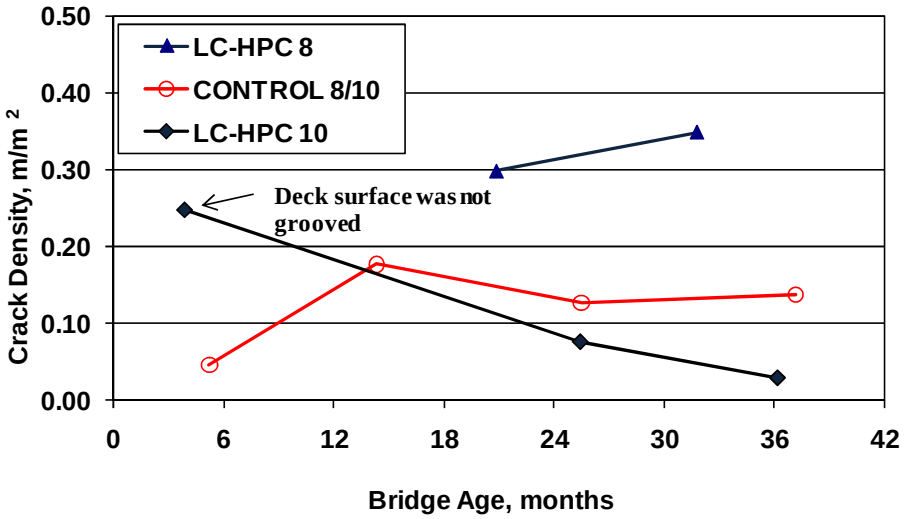

Figure 6.16 Crack density versus age for LC-HPC 8, 10 and Control 8-10

6.3.9 LC-HPC 11

LC-HPC 11 is the eastbound bridge on US-50 over the K&O railroad in Hutchinson, KS. It is a three-span steel girder bridge with integral abutments and has a very slight skew of 0.7 degree. The bridge is 117.8 ft (35.9 m) long and 40.0 ft (12.2 m) wide. The span lengths are 35.9, 45.9, and 35.9 ft (11.0, 45.9, and 11.0 m).

6.3.9.1 Concrete

The LC-HPC used for this bridge had a cement content of 535 lb/yd^3 (317 kg/m^3) and a *w/c* ratio of 0.42. Unlike any other LC-HPC bridges in this study, KDOT representatives took charge of the LC-HPC mixture design due to the inexperience of the ready-mix supplier in working with optimized aggregate gradations. The process worked well.

6.3.9.2 Qualification batch and qualification slab

Four trial batches were made. The first one was conducted on May 22, 2007. The concrete temperature was well controlled by partial replacement of mix water with ice, but the slump and air content were out-of-specifications. The second trial batch was made on May 23, 2007. The slump and air content were maintained in the specified range, but no measures were taken to control the concrete temperature. It was decided to proceed to the qualification slab despite the first two unsuccessful qualification batches. Difficulties in consistently supplying in-specification concrete were encountered during placement of the qualification slab, and two more qualification batches were made after the qualification slab, which are discussed later in this section.

The qualification slab was cast on May 25, 2007, two days after the second trial batch. Concrete supply turned out to be the weakest link in the process, and it further reinforced the importance of completing a qualification batch that meets all of the specifications. A total of six truckloads of concrete were batched for the

qualification slab. The first truck was rejected due to high slump [7.5 in. (190 mm)] and air content (11%). No concrete met the specification, being either high on slump or low on air content.

The concrete supply was slow and delayed. The qualification slab was supposed to start around 9:00 a.m., but the first concrete truck did not arrive until about 11:00 a.m. The long wait time between truckloads (56, 12, 12, 23, and 30 minutes) made the process so slow that it took over four hours to place the qualification slab.

The concrete was pumped, although the pump became clogged with concrete from truck #4. Coarse aggregate particles that were very long [about 5 in. (130 mm)] and angular were found (a picture of a coarse aggregate particle taken during deck construction is shown in Figure 6.17); this was probably the reason that the pump clogged. It was decided to use a conveyor belt for deck placement to avoid possible problems with the pump.

Figure 6.17 An aggregate particle found during placement of LC-HPC 11

A single-drum roller screed was used for strike-off. During the long delays, the contractor kept the roller screed moving back and forth across the deck when it was not advancing. It was suggested to idle the roller if there were delays to avoid over finishing. A bullfloat was used extensively after the roller screed. It was emphasized that the bullfloat should be used carefully and its use minimized, especially when water accumulated on the deck surface due to fogging. A metal pan and/or burlap drag was suggested as a replacement for the bullfloat.

The contractor practiced the burlap placement procedure while working on the qualification slab.

Due to the problems with the concrete during construction of the qualification slab, extra qualification batches were required. It took the concrete supplier two extra trials to get the concrete in specification.

6.3.9.3 Deck construction

LC-HPC 11 was cast on June 9, 2007. The placement started from the west abutment at about 6:00 a.m. and finished at around 11:00 a.m.

The concrete test results are summarized in Table 6.15. Concrete was tested out of the truck, except for one truck for which the concrete was tested at both the truck and at the end of the conveyor. The slump ranged from 2.25 to 4.0 in. (55 to 100 mm) with an average of 3.0 in. (75 mm). All recorded slump values were within the specified range. Forty six percent of the slump values were greater than 3.0 in. (75 mm), 38% of the slump values were greater than or equal to 3.5 in. (90 mm), and 31% of the slump values were equal to 4.0 in. (100 mm). The air content ranged from 6.0 % to 9.2% with an average of 7.8%. For the concrete batch that was tested at both the truck chute and the end of conveyor, the air loss was 2.4%. The relatively high air loss was probably caused by the high free fall, 12 to 15 ft (3.7 to 4.6 m), at the end of the conveyor. In addition, approximately 20 minutes elapsed between the time the sample was taken at the truck and the time it was sampled at the end of the conveyor belt.

Table 6.15 Summary table of concrete test results† for LC-HPC 11

KU Bridge Number	Slump		Air Content	Unit Weight		Concrete Temperature		28-day compressive strength††	
LC-HPC 11, placement	in.	mm	%	lb/ft^3	kg/m^3	°F	°C	psi	MPa
Average	3.0	75	7.8	142.2	2278	60	15.8	4680	32.3
Minimum	2.25	55	6.0	139.5	2235	59	14.7		
Maximum	4.0	100	9.2	144.6	2317	64	18.0		

Slump Range			Air Content Range		
> 3.0 in.(75 mm)	≥ 3.5 in.(90 mm)	= 4.0 in (100 mm)	> 9%	≥9.5%	≥ 10%
46%	38%	31%	8%	0%	0%

† Test results were from samples taken directly from the ready-mix truck

†† The lab-cured specimens were tested at 27 days

The air content would also be expected to drop during this 20 minutes period. Ice was used to control the concrete temperature, which ranged from 59 to 64° F (14.7 to 18.0° C), with an average of 60° F (15.8° C), meeting the specifications. The average compressive strength was 4680 psi (32.3 MPa) at 27 days.

Extra water was added to trucks #3, 4, and 5. For trucks #3 and 4, 0.5 gal/yd^3 (2.48 L/m^3) [4.2 lb/yd^3 (2.48 L/m^3)] water were added, resulting in an increase in the *w/c* ratio from 0.42 to 0.43. Truck #4 was rejected due to low air content (5.4%). For truck #5, 1 gal/yd^3 (4.96 L/m^3) [8.4 lb/yd^3 (4.96 L/m^3)] water was added, giving a *w/c* ratio of 0.44. No water was added to any of the other trucks.

The concrete was placed using the conveyor belt without any problems.

A single-drum roller screed with a metal pan drag was used for finishing. Bullfloating was not used until the last 3 ft (0.9 m) of the deck when the finishing bridges were removed. A hand float was used at the north and south edges of the deck.

The burlap was pre-soaked and hung over the formwork railing to avoid dripping water to deck surface, and it worked well. The time for burlap placement ranged from 4 to 19 minutes, with an average of 14 minutes.

The fogging system was mounted on the finishing bridge (on top of the metal pan drag), as shown in Figure 6.18. It worked well and produced a fine mist.

Figure 6.18 Fogging system mounted on the finishing bridge for LC-HPC 11

A hand-held fogger was used to keep the placed burlap wet, operated from the south side of the bridge only. Ponded water was noticed under the barrier steel on the south side over about the last 16 ft (5 m) of the deck.

The evaporation rate during construction ranged from 0.02 to 0.07 lb/ft^2/hr (0.10 to 0.34 kg/m^2/hr).

6.3.9.4 Crack survey results for LC-HPC 11

Two surveys have been completed, at 23.4 and 36.2 months, for LC-HPC 11, with crack densities of 0.059 and 0.241 m/m^2, respectively. The crack map at 36.2 months is shown in Figure 6.19. As shown in Figure 6.19, transverse cracks have developed in each of the three spans, and none of them have crossed the full width of the bridge. Many longitudinal cracks have formed at the west abutment with relatively fewer cracks being noted at the east abutment. The ponded water on the

south side of the last 16 ft (5 m) of the bridge (ending at the east abutment) does not seem to have increased cracking.

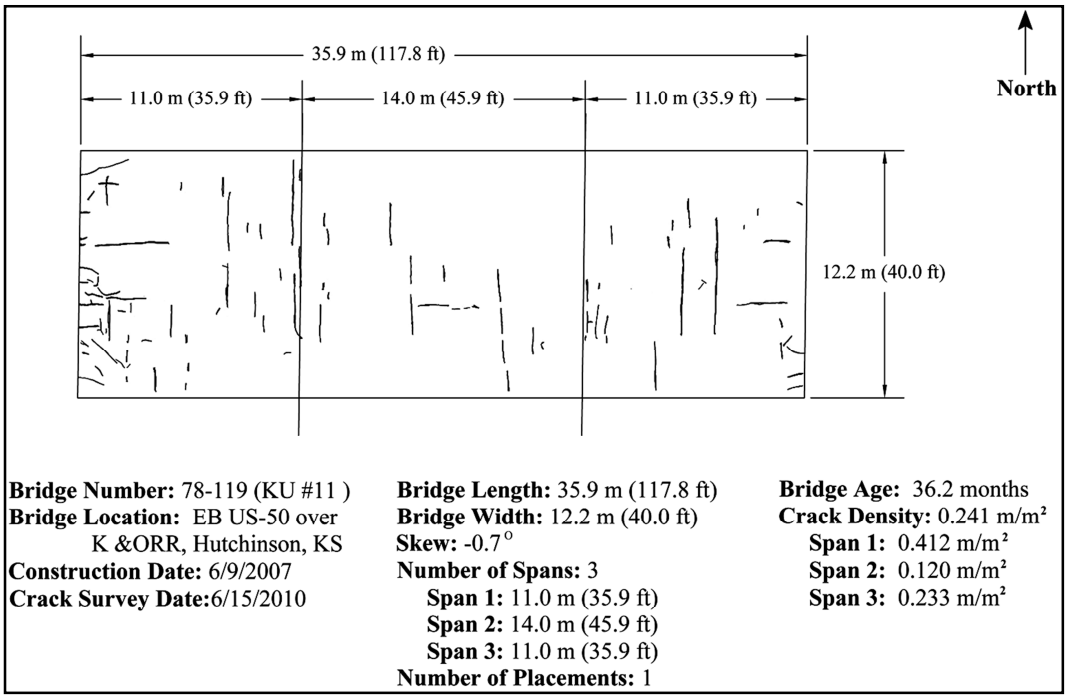

Figure 6.19 Crack map at 36.2 months for LC-HPC 11

6.3.10 Control 11

Control 11 is the bridge on US-50 over BNSF Railroad in Emporia, KS. It is a three-span, steel plate girder bridge. It has integral abutments and a skew of 24.3 degrees. The bridge is 284.9 ft (86.8 m) long and 52.5 ft (16.0 m) wide (not including the barrier width). The three spans have lengths of 83.4, 118.1, and 83.4 ft (25.4, 36.0, and 25.4 m).

The bridge was constructed in three placements, with two placements for the subdeck and one placement for the silica fume overlay (SFO). The construction date and concrete mixture information for each placement are listed in Table 6.16. The subdeck concrete had a cement content of 602 lb/yd^3 (357 kg/m^3), a *w/c* ratio of 0.40, and contained limestone coarse aggregate. The SFO contained 583 lb/yd^3 (346 kg/m^3)

of cement, 44 lb/yd^3 (26 kg/m^3) of silica fume (7% replacement of cement by weight), and a *w/cm* ratio of 0.37. Quartzite was used as the coarse aggregate.

The average concrete properties are listed in Table 6.17. The north subdeck concrete had an average slump of 3.5 in. (90 mm) and an air content of 6.8%, while the south subdeck concrete had an average slump of 5.25 in. (135 mm) and an air content of 7.0%. The compressive strengths were 5890 and 5440 psi (40.6 and 37.5 MPa) for north and south subdecks concrete, respectively. The SFO concrete had an average slump of 3.0 in. (75 mm), an air content of 6.0%, and a compressive strength of 7640 psi (52.7 MPa).

6.3.10.1 Crack survey results for Control 11

Four surveys have been completed at ages of 16.5, 27.1, 37.8, and 50.2 months. Many cracks developed at an early age; the crack density was 0.351 m/m^2 at 16.5 months. A significant increase of crack density was noted between the first and second survey, at 27.1 months, when the crack density was determined to be 0.665 m/m^2. In the following survey, at 37.8 months, there was a slight decrease in crack density to 0.599 m/m^2 because some of the cracks were obscured by scaling of the deck surface. The crack density was 0.636 m/m^2 at 50.2 months. As shown in the crack map (Figure 6.20), most of the cracks are transverse spaced at about 1 ft (0.3 m) intervals. A longitudinal crack traversing the full length of the bridge and some longitudinal cracks at the abutments have also developed. Severe scaling on the north and south gutter areas and some scaling in the middle of the bridge have been observed.

Table 6.16 Concrete mix design for Control 11

Bridge Number	Portion Placed	Date of Placement	*w/cm*	Cement Content		Water Content		Silica Fume Content		Design Air Content	Design Volume of Paste	Coarse Aggregate Type
				lb/yd^3	kg/m^3	lb/yd^3	kg/m^3	lb/yd^3	kg/m^3	%	(%)	
Control 11	North 1-2 - Subdeck	02/03/06	0.40	602	357	241	143	0	0	6.5	25.6%	Limestone
	South 1-2 - Subdeck	02/14/06	0.40	602	357	241	143	0	0	6.5	25.6%	Limestone
	Overlay	03/28/06	0.37	583	346	233	138	44	26	6.5	26.0%	Quartzite

Table 6.17 Average concrete properties for Control 11

Bridge Number	Portion Placed	Date of Placement	Average Air Content	Average Slump		Average Concrete Temperature		Average Unit Weight		Average Compressive Strength†	
				(in.)	(mm)	(°F)	(°C)	(lb/yd^3)	(kg/m^3)	(psi)	(MPa)
Control 11	North 1-2 - Subdeck	02/03/06	6.8	3.50	90	72	22.0	141.3	2263	5890	40.6
	South 1-2 - Subdeck	02/14/06	7.0	5.25	135	73	23.0	140.6	2252	5440	37.5
	Overlay	03/28/06	6.0	3.00	75	60	15.5	142.1	2277	7640	52.7

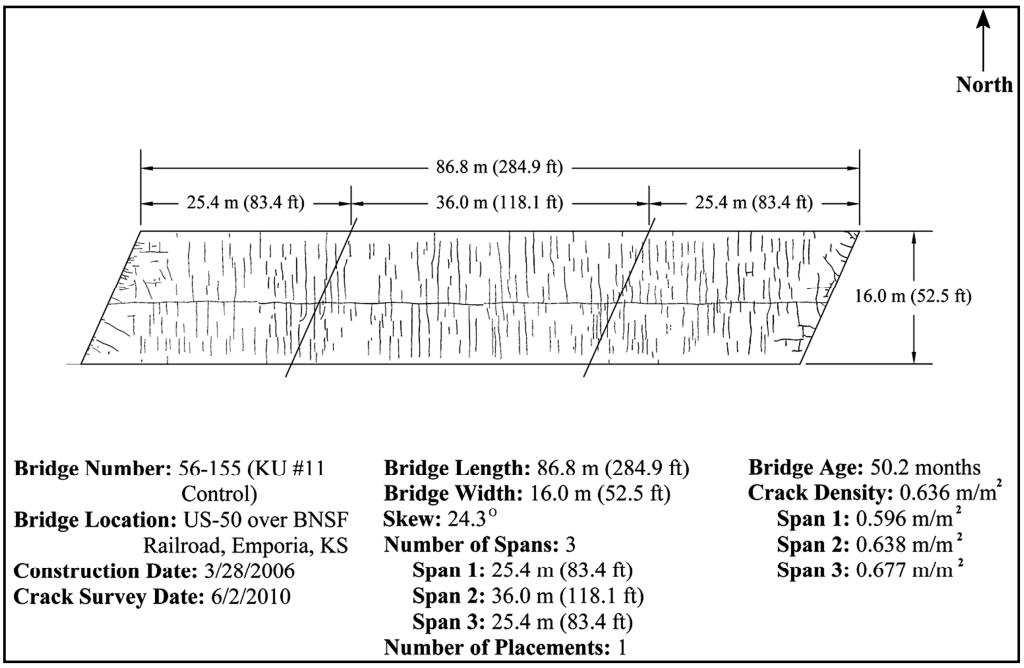

Figure 6.20 Crack map at 50.2 months for Control 11

6.3.10.2 Crack density versus age for LC-HPC 11 and Control 11

Crack density is plotted versus age for LC-HPC 11 and Control 11 in Figure 6.21. The crack density of LC-HPC 11 is much lower than Control 11 at similar ages. The increase of crack density, from 23.4 to 36.2 months, for LC-HPC 11 is greater than has occurred for any of the other LC-HPC bridges at similar ages (the crack density increase rate for both LC-HPC and Control bridges will be discussed in Section 6.4). As described in Section 6.3.10.1 for Control 11, the crack density increased significantly, from 16.5 to 27.1 months; during the third survey at 37.8 months, the density dropped because some cracks were obscured by the scaling that developed on the bridge deck surface; the crack density increased slightly in the fourth survey to 50.2 months.

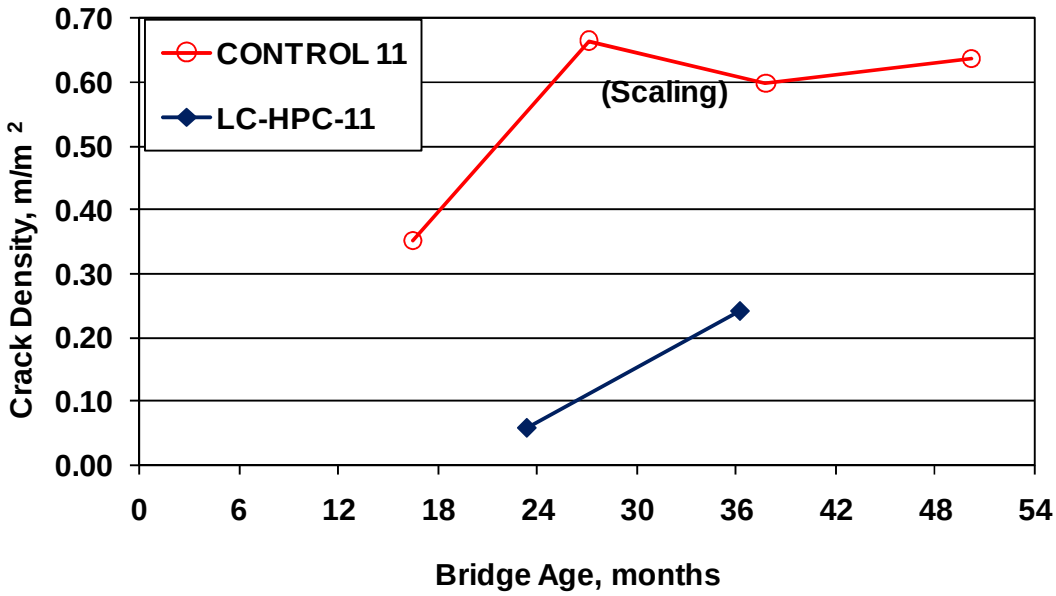

Figure 6.21 Crack density versus age for LC-HPC 11 and Control 11

6.3.11 LC-HPC 4

LC-HPC 3, 4, 5, and 6 and Control 3, 4, 5 and 6 were let in a single contract. The same contractor (Clarkson Construction) and concrete supplier (Fordyce Concrete) worked on these eight bridges. Clarkson Construction and Fordyce Concrete had successfully completed LC-HPC 1 and 2 in 2005 and 2006, respectively. At the contractor's request, only one qualification batch and one qualification slab were completed for the four LC-HPC bridges. The four LC-HPC bridges were constructed in about one and half months. The construction dates for the qualification batch, qualification slab, and LC-HPC decks are listed in Table 6.18. In the order of construction date, LC-HPC 4 will be discussed first, followed by LC-HPC 6, 3, and 5. The construction of the four control bridges will be presented together.

Table 6.18 Construction dates for LC-HPC 3 through 6

Batch or Placement	Date Completed
Qualification Batch	6/7/2007
Qualification Slab	9/14/07
LC-HPC 4-p 1(placement 1)	9/29/2007
LC-HPC 4-p 2(placement 2)	10/2/2007
LC-HPC 6	11/3/2007
LC-HPC 3	11/13/2007
LC-HPC 5	11/14/2007

6.3.11.1 Concrete mixture

Fordyce Concrete successfully provided concrete for LC-HPC 1 and 2 with a cement content of 540 lb/yd^3 (320 kg/m^3) and a *w/c* ratio of 0.45. Although the concrete specifications for LC-HPC 3 to 6 were unchanged from those used for LC-HPC 1 and 2, the contractor agreed to use concrete containing a cement content of 535 lb/yd^3 (317 kg/m^3) and a *w/c* ratio of 0.42, which had a lower paste content of 23.4% (compared with 24.6% for the previous mix) to match the latest LC-HPC specifications in use at that time. Lower paste content mixtures had been used for LC-HPC 8, 10, and 11.

The aggregate gradation was optimized by blending two granite coarse aggregates, a coarse manufactured sand, and a natural river sand. Two mix designs (with different aggregate blends but the same cement content and *w/c* ratio) were prepared. The first mixture was designed using KU Mix and 33.1% of the total aggregates (by weight) consisted of manufactured sand; the second mixture, an alternate mix modified by the concrete supplier, incorporated only 13.0% manufactured sand because of concerns that the manufactured sand might result in difficulties in pumping and finishing due its angular nature. The two mixes are

discussed in greater detail by Lindquist et al. (2008). Both mixtures met the LC-HPC specifications and were evaluated in qualification batches and in the qualification slab.

6.3.11.2 Qualification batch

The qualification batches were tested on June 7, 2007. The mixture with 33.1% manufactured sand was batched first. The concrete was tested after a simulated haul time of 27 minutes and had a slump of 4.0 in. (100 mm), an air content of 9.6%, and a temperature of 71° F (21.7° C). The concrete supplier and transportation officials were satisfied with the mixture.

The concrete supplier also batched the alternate mix (with 13.0% manufactured sand) in an attempt to compare the workability of the two mixes. It was batched with the same dosage of water reducer and air entraining agent as the previous mixture. Again, after 27 minutes simulated haul time, the concrete had a slump of 5.0 in. (125 mm), an air content of 9.5%, and a temperature of 72° F (22.2° C). It was decided to use both mixes at the qualification slab.

6.3.11.3 Qualification slab

The qualification slab was cast on September 14, 2007. Four truckloads of concrete were used, with the first two truckloads using the alternate mix (with 13.0% manufactured sand) and the other two truckloads using the mixture with 33.1% manufactured sand. The concrete from the first two trucks had slumps of 2.75 and 2.25 in. (70 and 55 mm), air contents of 7.0 and 7.0%, and concrete temperatures of 65 and 63° F (18.5 and 17.0° C), respectively; the last two trucks had slumps of 1.5 and 1.25 in. (40 and 35 mm), air contents of 6.9 and 5.6%, and concrete temperatures of 63 and 62° F (17.0 and 16.5° C), respectively.

Both mixtures were pumped without difficulty. A single-drum roller screed followed by a bullfloat was used for finishing. No problems were apparent

The contractor practiced the burlap placement. At times, the burlap was too wet and quite a bit of water dripped onto the slab surface. The contactor was notified of the need to correct this.

The fogging system was mounted to the finishing bridge, and it produced a fine mist, although the nozzles were pointed about 15 degrees downward and sprayed water on the slab surface. This was corrected, and the nozzles were pointed up.

Because both mixtures pumped and finished well, and it was decided to use the mixture containing 33.1% manufactured sand for deck construction.

6.3.11.4 LC-HPC 4-p1 (placement 1)

LC-HPC 4 is the southbound bridge on US-69 connecting to the I-435 ramp in Overland Park, KS. It is a steel plate girder bridge with non-integral abutments and no skew. The bridge is 377 ft (115.0 m) long and 38.1 ft (11.6 m) wide (not including the rail width). There are four spans with lengths of 82.0, 105.0, 105.0, and 85.3 ft (25.0, 32.0, 32.0, 26.0 m).

The original plan was to construct the deck in a single placement on September 29, 2007, but construction was halted due to an electrical outage at the ready mix plant. About a quarter of the bridge was cast in the first placement with the remainder constructed on October 2, 2007.

The concrete supplier had difficulties in consistently supplying in-specification concrete during the first placement. The first truck was tested both before and after pumping. It had a slump of 1.25 in. (30 mm) and an air content of 7.8% out of truck, and a slump of 1.25 in. (30 mm) and an air content of 7.0% after pumping (the pump had a bladder valve to limit air loss). The rest of the concrete was tested out of the truck. The second truck arrived with a slump of just 0.75 in. (20 mm) and an air content of 6.8%. The concrete in the first two trucks was difficult to pump and finish. The admixture dosage was adjusted at the ready mix plant for the third truck, and it arrived with a 4 in. (100 mm) slump and 10.4% air content. As the

air content was above the maximum allowable of 9.5%, the third truck was rejected. The concrete supplier struggled throughout the placement. Increasing the water reducer dosage to increase the slump resulted in an increased air content, often above the maximum. During the placement, the decision was made to switch to the alternate mix with 13.0% manufactured sand. The electrical outage at the ready mix plant, however, ended the placement operation and no concrete with the alternate mix design was batched. At the end of the placement, two truckloads of concrete with 4.25 in. (105 mm) slump and 11.6% air content and 3.5 in. (90 mm) slump and 10.6% air content, respectively, were cast into the deck to reach a header placed in the negative moment area.

The concrete test results are summarized in Table 6.19. The slump ranged from 0.75 to 4.25 in. (20 to 105 mm) with an average of 2.0 in. (50 mm). Actually, all recorded slump values were below or equal to 2.25 in. (55 mm), except for the last two trucks. The average slump would have been 1.25 in. (30 mm) without the last two trucks. The air content ranged from 6.8% to 11.6% with an average of 8.7%. Concrete temperature was not recorded, and no cylinders were made to determine compressive strength.

Table 6.19 Summary table of concrete properties† for LC-HPC 4-p1

KU Bridge Number	Slump		Air Content	Unit Weight		Concrete Temperature		28-day compressive strength	
LC-HPC 4-p1, placement 1	in.	mm	%	lb/ft^3	kg/m^3	°F	°C	psi	MPa
Average	2.0	50	8.7	137.4	2202	--	--	--	--
Minimum	0.75	20	6.8	132.4	2116	--	--		
Maximum	4.25	105	11.6	140.8	2255	--	--		

Slump Range			Air Content Range		
> 3.0 in.(75 mm)	≥ 3.5 in.(90 mm)	≥ 4.0 in (100 mm)	> 9%	≥9.5%	≥ 10%
22%	22%	0%	29%	29%	29%

† Test results were from samples taken from the ready-mix truck.

The difficulties of producing in-specification concrete were likely complicated due to an overestimation of the free-surface moisture of the manufacture sand. The ready-mix supplier stockpiled the manufactured sand next to lightweight aggregate, which was kept continuously saturated. A free surface moisture content of 7.1% was used for the first truck, and reduced to 6.5% for the rest of the trucks. By comparison, a free surface moisture content of 4.0% was used for the second placement three days later. If 4.0% was the correct value for first placement, the actual *w/c* ratio would have been only 0.37, instead of the design value of 0.42.

The concrete did not pump well. A number of factors contributed to the pumping difficulties. First, the concrete had very low slump, with an average of 1.25 in. (30 mm) not counting the last two trucks. Second, a much larger pump was used for the deck than the pump used for the qualification slab. Because larger pumps operate at a lower pressure with longer stroke lengths, the lower pressure may have caused problems in pumping the low paste content, low slump LC-HPC. The pump used for the placement also may have had some potential mechanical issues. It was found to be not operating properly (a part needed to be replaced) after the placement, although it is not clear if the part broke prior to or during the placement.

The deck was finished using a single-drum roller screed followed by two bullfloats, as shown in Figure 6.22. The workers walked back and forth on a work bridge and bullfloated the surface from opposite sides of the work bridge. The finishers had to work the surface four to five times to get a good seal. At times a wooden float was used.

Due to the concrete problems and pumping difficulties, the placement was inconsistent and delayed. Some burlap was placed well after the concrete was placed. Most of the concrete was refinished with a bullfloat following the delays prior to burlap placement. The time between bullfloating and burlap placement was recorded (instead of time between strike-off and burlap placement for most other bridges) and ranged from 7 to 13 minutes with an average of 9 minutes.

Figure 6.22 Bullfloating with two workers for LC-HPC 4-p1

Fogging was used extensively.

The contractor wetted the placed burlap with a spray nozzle and this worked well.

6.3.11.5 LC-HPC 4-p2 (placement 2)

The second placement was completed on October 2, 2007, three days after the first placement.

Due to the difficulties with pumping the concrete during the first placement, the alternate mix with 13.0% manufactured sand was used this time. One day before construction, on October 1, 2007, 4 yd^3 (3.1 m^3) of concrete was trial pumped with the same pump that was going to be used to complete the second placement. It pumped successfully.

The concrete test results for placement 2 are summarized in Table 6.20. The concrete was tested out of the ready-mix truck prior to the pump, except that the air content of the first truck was tested both before and after pumping. An air content loss of 2% was recorded as no measures were taken to restrict the concrete flow in the pump line. This contrasts with the 0.8% air content loss recorded in the first placement where

a bladder valve was used on the pump line. The slump ranged from 1.5 to 4.0 in. (35 to 100 mm) with an average of 3.0 in. (75 mm). All slump values were in the specified range. Sixty three percent of the recorded slump values were higher than 3.0 in. (75 mm), 58% were greater than or equal to 3.5 in. (90 mm), and 26 were equal to 4.0 in. (100 mm). The air content ranged from 7.2 to 10.4% with an average of 8.8%. The concrete with an air content higher than 9.5% was accepted because it was assumed that the concrete would lose 2% air through the pump. No attention was given to the low air content values that were close to the minimum allowable air content. The concrete temperature ranged from 59 to 71° F (15.0 to 21.7° C) with an average of 64° F (17.5° C). The 28-day compressive strength was 4790 psi (33.1 MPa).

Table 6.20 Summary table of concrete properties[††] for LC-HPC 4-p2

KU Bridge Number	Slump		Air Content	Unit Weight		Concrete Temperature		28-day compressive strength[††]	
LC-HPC 4-p2, placement 2	in.	mm	%	lb/ft^3	kg/m^3	°F	°C	psi	MPa
Average	3.0	75	8.8	137.9	2210	64	17.5	4790	33.1
Minimum	1.5	35	7.2	135.1	2164	59	15.0		
Maximum	4.0	100	10.4	141.1	2260	71	21.7		

Slump Range			Air Content Range		
> 3.0 in.(75 mm)	≥ 3.5 in.(90 mm)	= 4.0 in (100 mm)	> 9%	≥9.5%	≥ 10%
63%	58%	26%	45%	36%	9%

[†] Test results were from samples taken directly from the ready-mix truck prior to pump
[††] Average 28-day compressive strength for lab-cured specimens

The concrete pumped, consolidated, and finished well. The deck was finished with a single-drum roller screed followed by a bullfloat. Two workers were assigned for bullfloating, as shown previously in Figure 6.22, and the surface was bullfloated extensively. This contractor put more effort into bullfloating than other contractors, and the same bullfloating techniques were used on the subsequent LC-HPC bridges in this contract, LC-HPC 3, 5, and 6.

Burlap placement was often slow, with the time for burlap placement ranging from 7 to 43 minutes with an average of 16 minutes. Placement was consistently 10 to 15 minutes after strike-off for the middle portion of the deck. Burlap placement on the last 25 ft (7.6 m) was delayed significantly due to delays in concrete delivery and removal of the equipment from the end of the bridge. The concrete was exposed for about 40 minutes without any protection (the contractor was reluctant to turn on the fogger, which was otherwise not needed on this deck).

Fogging was not used for the placement. Fogging was not a concern as the evaporation rate was very low during the construction. It was checked once during construction and it was 0.008 lb/ft^2/hr (0.039 kg/m^2/hr).

6.3.11.6 Crack survey results

Three surveys have been completed, at 9.5, 21.3, and 32.8 months. Many cracks have developed in placement 1; the crack density increased from 0.017 to 0.113, and then to 0.261 m/m^2 during the three surveys. Fewer cracks have formed in placement 2, with crack densities of 0.004, 0.079, and 0.094 m/m^2 for the three surveys. The crack map at 32.8 months is shown in Figure 6.23. Most cracks are transverse and short in length.

6.3.12 LC-HPC 6

LC-HPC 6 along LC-HPC 5 is the flyover bridge connecting southbound US-69 to westbound I-435 in Overland Park, Kansas. LC-HPC 6 is the portion of the bridge closest to US-69, while LC-HPC 5 is the portion closest to I-435.

LC-HPC 6 is a steel plate-girder bridge with non-integral end conditions and no skew. The bridge is 593.8 ft (181.0 m) long and 25.9 ft (7.9 m) wide (not including the rail width). It has four spans that are 128.0, 167.3, 167.3, and 131.2 ft (39.0, 51.0, 51.0, and 40.0 m) in length. The bridge is superelevated; the southeast side of the deck is raised.

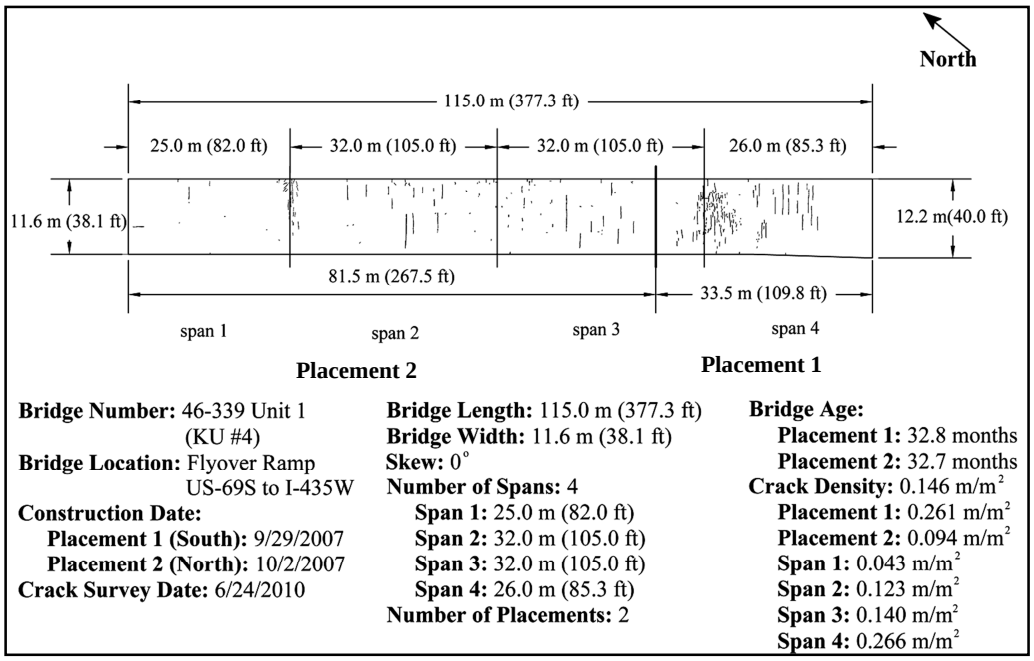

Figure 6.23 Crack maps at 32.8 months for LC-HPC 4

6.3.12.1 Concrete

Due to the difficulties of pumping the concrete during the construction of LC-HPC 4-p1, the concrete mixture design was modified. The *w*/*c* ratio was increased from 0.42 to 0.45, and a Type A/F high-range water reducer was used instead of the mid-range water reducer used for LC-HPC 4. The cement content remained at 535 lb/yd^3 (317 kg/m^3). The alternate mix (described in Section 6.3.11) with 13.0% manufactured sand was used.

6.3.12.2 Qualification batch

No qualification batch was made, even though this mixture had not been used before.

6.3.12.3 Deck construction

LC-HPC 6 was constructed on November 3, 2007. Construction began at 5:30 a.m. and was completed by 12:30 p.m. Concrete was placed from the southwest to the northeast.

The concrete test results are summarized in Table 6.21. The concrete was tested out of truck. The slump ranged from 2.25 to 6.0 in. (60 to 150 mm) with an average of 4.0 in. (100 mm). Overall, slump was high. Eighty five percent of the slump values exceeded 3.0 in. (75 mm), 70% were greater than or equal to 3.5 in. (90 mm), and 52% were greater than or equal to 4.0 in. (100 mm). The air content ranged from 7.5 to 11.5% with an average of 9.5%. Overall the air content was also high, with 69% of the air content values higher than 9%, 54% of the air content values greater than or equal to 9.5% (the maximum allowable), and 38% of the air content values greater than or equal to 10%. The concrete temperature ranged from 52 to 64° F (11.1 to 17.8° C) with an average of 60° F (15.3° C). The 28-day compressive strength was 5840 psi (40.3 MPa).

Table 6.21 Summary table of concrete test results† for LC-HPC 6

KU Bridge Number	Slump		Air Content	Unit Weight		Concrete Temperature		28-day compressive strength††	
LC-HPC 6	in.	mm	%	lb/ft^3	kg/m^3	°F	°C	psi	MPa
Average	4.0	100	9.5	--	--	60	15.3	5840	40.3
Minimum	2.25	60	7.5	--	--	52	11.1		
Maximum	6.0	150	11.5	--	--	64	17.8		

Slump Range			Air Content Range		
> 3.0 in.(75 mm)	≥ 3.5 in.(90 mm)	≥ 4.0 in (100 mm)	> 9%	≥9.5%	≥ 10%
85%	70%	52%	69%	54%	38%

† Test results were from samples taken directly from the ready-mix truck prior to pump

†† Average 28-day compressive strength for lab-cured specimens

The concrete pumped well. Two pumps were available during the construction. The first pump was used for the first three of four spans; it did not have a bladder valve. The second pump delivered concrete for the last span and had a bladder valve. Air content and slump losses through the pump were checked. Concrete from the first truck was tested both out of the truck and after pumping to the

ground, in which case the pump boom was positioned straight up and down. No air cuff was used. An air content loss of 2.9% and a slump loss of 2.0 in. (50 mm) through the pump were recorded. KDOT personnel assumed the same air content and slump losses on the deck without considering the changing elevation of the deck. The first two trucks that arrived with out-specification concrete [slumps of 4.25 and 4.75 in. (105 and 120 mm), air contents of 9.9% and 11.5%] were accepted based on the measured air content and slump losses on the earlier trucks. As it turns out, the elevation of the pump discharge on the deck has a significant effect. Another two trucks were tested both out of the truck and out of the pump (using the first pump without an air cuff) ,and air content losses of 1.4 and 1%, respectively, were noted. No slump tests were taken on the deck because there was only one set of slump test equipment available during construction. When the second pump, which had an air cuff, was used, the air content loss was only 0.6% for the truck checked.

The concrete was finished with a single-drum roller screed followed by two bullfloats. Again, two workers were assigned for bullfloating, as shown in Figure 6.22. The bullfloats were used extensively, although the surface was not finished as well as on other bridges, and there were some visible voids in the surface in spite of the high slump of the concrete.

The time between bullfloating and burlap placement recorded instead of the time between strike-off and burlap placement, ranged from 2 to 20 minutes with an average of 7 minutes. The contractor kept the in-place burlap wet with a spray hose.

The bridge is superelevated as shown in Figure 6.24. Because the soaker hoses were placed in the middle of bridge during the curing period, the southeast (upper) edge may not have received enough curing water. The crack surveys (discussed later in Section 6.3.12.4) reveal that many cracks along the southeast edge.

Because the air temperature dropped below freezing on the third and fourth days of the curing period, the girders and decks were wrapped and heated, as shown in Figure 6.25, to meet the requirements for cold weather curing.

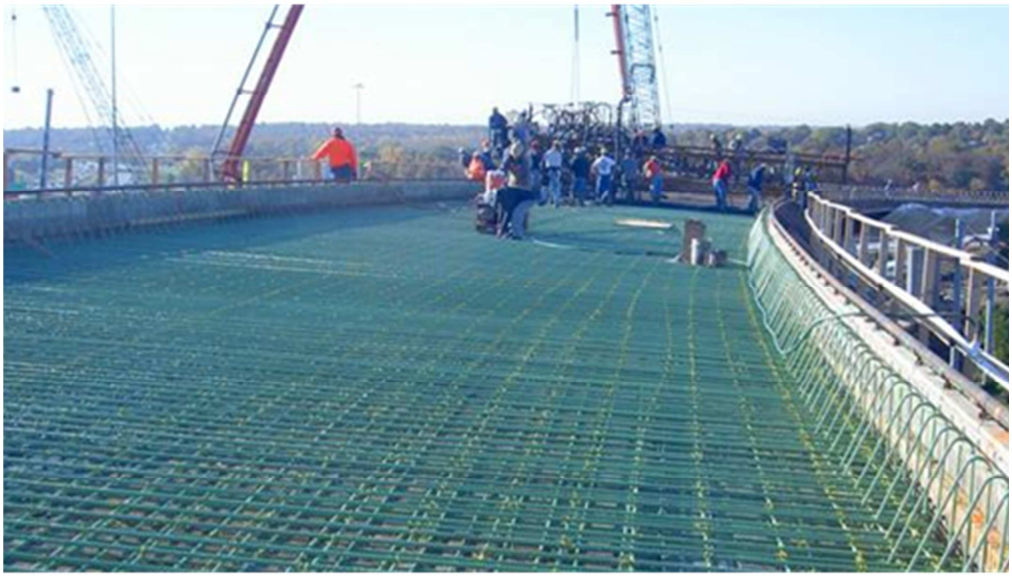

Figure 6.24 Superelevation of the southeast side of LC-HPC 6

Figure 6.25 Deck and girders protection during curing in cold weather for LC-HPC 6

6.3.12.4 Crack surveys for LC-HPC 6

Three crack surveys have been completed, at 6.6, 19.7, and 31.4 months, with respective crack densities of 0.063, 0.238, and 0.231 m/m^2. Only a few cracks were apparent at 6.6 months, but a significant increase in crack density was recorded at 19.7 months, which changed little by 31.4 months. The most recent crack map, at 31.4 months, is presented in Figure 6.26. As shown in Figure 6.26, a majority of the cracks are transverse with many initiating from the superelevated southeast edge. Some very short transverse cracks adjacent to the northwest edge are also noted.

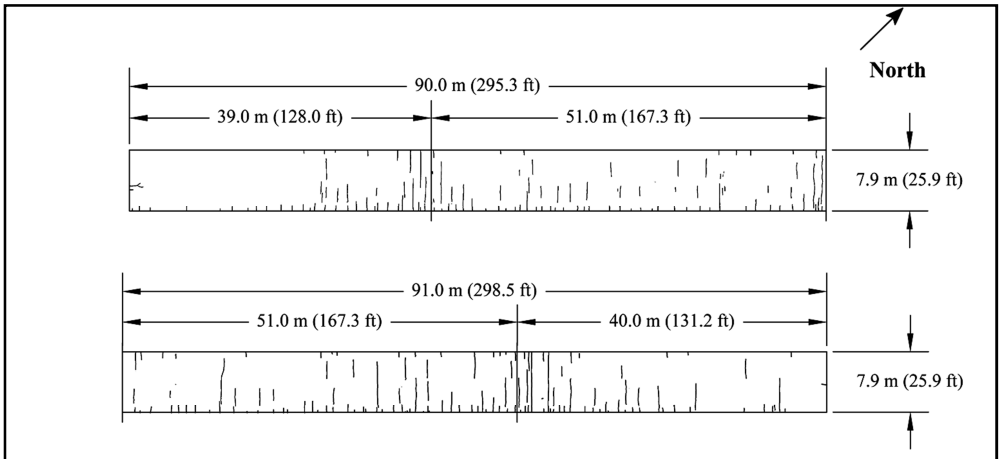

Figure 6.26 Crack map at 31.4 months for LC-HPC 6

6.3.13 LC-HPC 3

LC-HPC 3 is the westbound bridge on 103rd Street over US-69 in Overland Park, KS. It is a steel plate-girder bridge with non-integral end conditions and has a skew of six degrees. The bridge is 380.2 ft (115.9 m) long and 49.9 ft (15.2 m) wide. It has four spans with lengths of 74.3, 115.8, 115.8, and 74.3 ft (22.6, 35.3, 35.3, and 22.6 m).

6.3.13.1 Concrete

The concrete mixture used for LC-HPC 3 was the same as used for LC-HPC 6, with a cement content of 535 lb/yd^3 (317 kg/m^3) and a *w*/*c* ratio of 0.45.

6.3.13.2 Qualification batch and qualification slab

LC-HPC 3 was constructed ten days after LC-HPC 6. A qualification batch and slab were not required.

6.3.13.3 Deck construction

LC-HPC 6 was constructed on November 13, 2007. The construction began at about 2:30 a.m. and was concluded by 9:30 a.m. Concrete placement proceeded from the east to the west abutment.

The concrete test results are summarized in Table 6.22. The concrete was tested out of the truck. The slump ranged from 1.75 to 4.0 in. (45 to 100 mm) with an average of 3.25 in. (85 mm), and all slump values met the specification. Sixty five percent of the slump values were greater than 3.0 in. (75 mm), 50% were greater

Table 6.22 Summary table of concrete test results† for LC-HPC 3

KU Bridge Number	Slump		Air Content	Unit Weight		Concrete Temperature		28-day compressive strength††	
LC-HPC 3,	in.	mm	%	lb/ft^3	kg/m^3	°F	°C	psi	MPa
Average	3.25	85	8.7	--	--	58	14.4	5990	41.3
Minimum	1.75	45	6.5	--	--	52	11.1		
Maximum	4.0	100	10.5	--	--	62	16.7		

Slump Range			Air Content Range		
> 3.0 in.(75 mm)	≥ 3.5 in.(90 mm)	= 4.0 in (100 mm)	> 9%	≥9.5%	≥ 10%
65%	50%	26%	50%	29%	14%

† Test results were from samples taken directly from the ready-mix truck prior to pump

†† Average 28-day compressive strength for lab-cured specimens

than or equal to 3.5 in. (90 mm), and 26% equaled 4 in. (100 mm). The air content ranged from 6.5 to 10.5% with an average of 8.7%. As planned prior to the construction, concrete with in-specification slump but air contents higher than 9.5% was retested on the deck (after pumping). Two truckloads of concrete were rechecked on the deck. One truck arrived with an air content of 9.5% and dropped to 8.4% after pumping, and the other truck dropped from 10.5% to 9.0%. Concrete temperature ranged from 52 to 62° F (11.1 and 16.7° C) with an average of 58° F (14.4° C). The 28-day compressive strength was 5990 psi (41.3 MPa).

Two pumps were available during the construction with one at each end of the bridge. The concrete pumped adequately.

The concrete was finished with a single-drum roller screed followed by two bullfloats. The contractor complained that the deck was not "sealing" well and wanted to use water as a finishing aid. The KDOT inspector instructed the contractor to finish the deck to the best of their ability, working it as much as needed but without using water. The finish appeared to be about the same as other LC-HPC decks. The contractor used water as a finishing aid for about the first 50 ft (15.2 m) of the sidewalk.

A new crew (different from qualification slab and previous construction of LC-HPC 4 and 6) was assigned to burlap placement. The time between strike-off and burlap placement ranged from 9 to 25 minutes with an average of 15 minutes. The contractor did a good job keeping the placed burlap wet.

Fogging was not used during the construction. The evaporation rate during construction was low, ranging from 0.03 to 0.07 lb/m^2/hr (0.15 to 0.32 kg/m^2/hr) with an average of 0.04 lb/m^2/hr (0.20 kg/m^2/hr).

A new issue encountered during LC-HPC 3 construction was how to place, finish, and cure the sidewalk at the same time as the roadway. Because there was a barrier with reinforcing steel between the roadway and sidewalk, the sidewalk could

not be struck-off and finished at the same time as the roadway. After discussions with the contractor and KDOT personnel, it was determined that the sidewalk would be hand vibrated and screeded with 2 × 4 in. (50 × 100 mm) lumber, then bullfloated, hand troweled, and finally broom finished. To protect the broom finish, the burlap placement was postponed until the concrete had set enough so that the burlap would not mar the surface. During this period, the sidewalk surface was sprayed with water mist every 10 minutes to keep it wet. No curing compound was used during this period. The procedure worked well. It was noted that the contractor placed the first burlap about two hours after finishing. After that, the burlap placement on the sidewalk was much faster, approximately 20 to 30 minutes behind the finishing operation. A KDOT inspector later indicated that the final surface finish on the sidewalk was fine.

The air temperature dropped below freezing during the 14-day curing period. The girders were wrapped and heated as required by the specifications for cold weather curing.

6.3.13.4 Crack survey results for LC-HPC 3

Three crack surveys have been completed, at 6.5, 19.2, and 31.5 months. As with LC-HPC 6, only a few cracks had developed by 6.5 months, at which time the crack density was 0.028 m/m^2. The crack density increased to 0.110 m/m^2 by 19.2 months. When the survey was conducted at 31.5 months, a strip of about 18 ft (5.5 m) wide (close to the sidewalk) crossing the full length of the bridge was dirty and covered with dust. The bridge was still surveyed, giving a crack density of 0.108 m/m^2. The crack maps at both 19.2 and 31.5 months are presented in Figure 6.27. As shown in Figure 6.27, most cracks observed at 19.2 months are still apparent at 31.5 months. The majority of the cracks are transverse, and most are short, except for some relatively long cracks in the negative moment regions over the two outer piers.

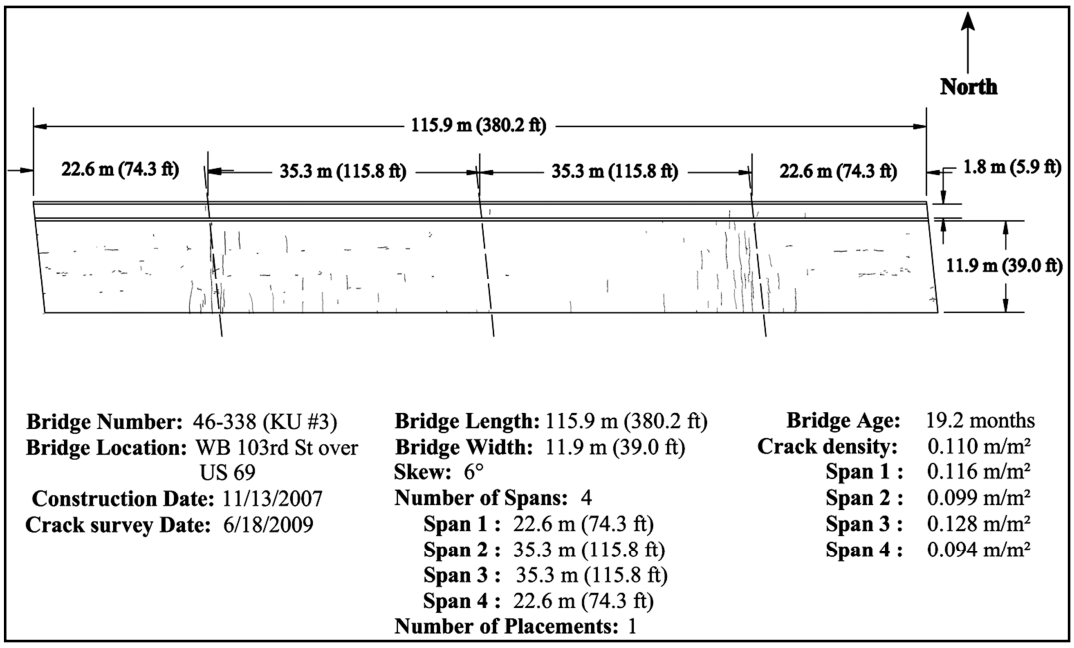

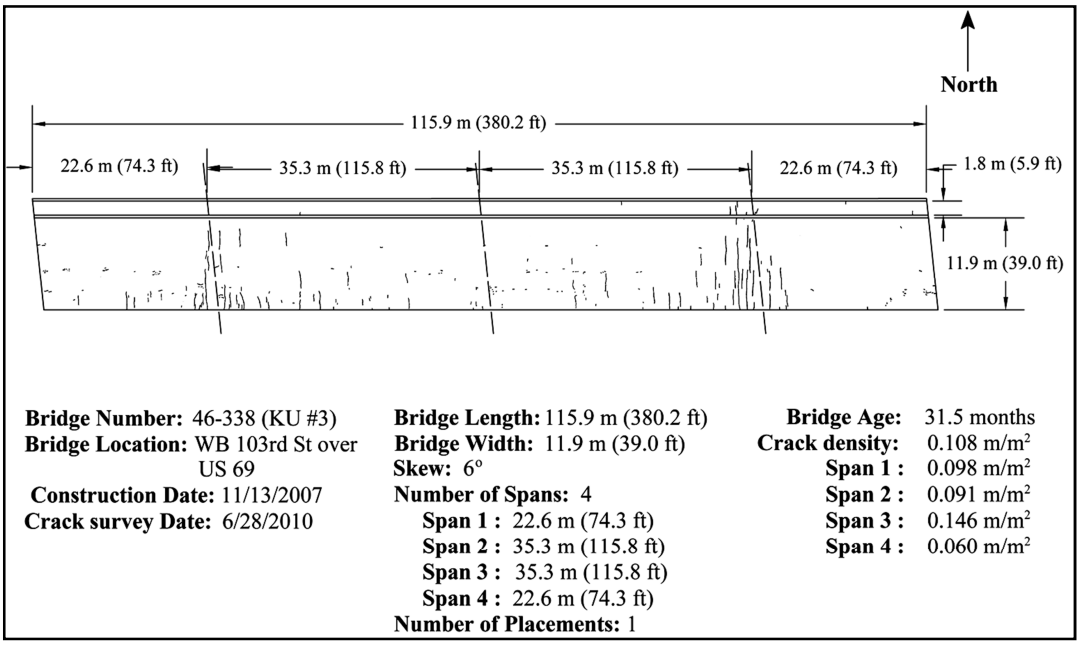

Figure 6.27 Crack maps at 19.2 and 31.5 months for LC-HPC 3

6.3.14 LC-HPC 5

As mentioned in Section 6.3.12, LC-HPC 5 together with LC-HPC 6 is the flyover bridge connecting southbound US-69 to westbound I-435 in Overland Park, Kansas. LC-HPC 5 is the portion closest to I-435.

LC-HPC 5 is a steel plate-girder bridge with non-integral end conditions and no skew. The bridge is 555.7 ft (169.4 m) long and 25.9 ft (7.9 m) wide (not including the rail width). It has four spans that are 96.4, 164, 164, and 131.2 ft (29.4, 50.0, 50.0, and 40.0 m) in length.

6.3.14.1 Concrete

As stated previously, LC-HPC 3, 4, 5, and 6 were in the same contract, although different mix designs, with different *w*/*c* ratios but the same cement content, were used. A *w*/*c* ratio of 0.42 was used for the qualification slab and LC-HPC 4, then the *w*/*c* ratio was increased to 0.45 to produce more workable concrete for LC-HPC 3 and 6. When LC-HPC 5 was constructed, it was decided to try a *w/c* ratio of 0.42 again to take advantage of the lower shrinkage of the lower *w/c* ratio mixture*. The *w*/*c* ratio, however, was increased to 0.43 and finally to 0.45 during construction to help resolve pumping difficulties.

6.3.14.2 Qualification batch and qualification slab

LC-HPC 5 was constructed one day after LC-HPC 3. A qualification batch and slab were not required.

6.3.14.3 Deck construction

LC-HPC 5 was constructed on November 14, 2007. The construction started at about 2:00 a.m. and finished at 10:00 a.m. Concrete placement proceeded from west to east.

* It has since been established that a lower *w/c* ratio at a fixed cement content does not translate into reduced cracking, even though it does result in reduced shrinkage.

The concrete test results are summarized in Table 6.23. The concrete was tested out of the truck. A total of 26 trucks (48 truckloads of concrete were placed) were tested for slump. The first truck was tested both out of the truck and at the discharge end of the pump. A bladder valve was used on the pump and a slump loss of 0.5 in. (12.5 mm) and an air content loss of 0.6% were noted. The slump ranged from 2.0 to 4.0 in. (50 to 140 mm) with an average of 3.0 in. (75 mm). About half (46%) of the slump values were greater than 3.0 in. (75 mm), 27% were greater than or equal to 3.5 in. (90 mm), and 12% equaled 4.0 in. (100 mm). The air content ranged from 6.8 to 10.3% with an average of 8.7%. The concrete temperature ranged from 57 to 64° F (13.9 and 17.8° C) with an average of 61° F (15.9° C). The 28-day compressive strength for concrete with a *w/c* ratio of 0.42 was 6380 psi (44.0 MPa).

Table 6.23 Summary table of concrete test results[†] for LC-HPC 5

KU Bridge Number	Slump		Air Content	Unit Weight		Concrete Temperature		28-day compressive strength	
LC-HPC 5,	in.	mm	%	lb/ft^3	kg/m^3	°F	°C	psi	MPa
Average	3.0	75	8.7	139.6	2236	61	15.9	6380[††]	44.0
Minimum	2.0	50	6.8	136.1	2181	57	13.9		
Maximum	4.0	100	10.3	143.2	2294	64	17.8		

Slump Range			Air Content Range		
> 3.0 in.(75 mm)	≥ 3.5 in.(90 mm)	= 4.0 in (100 mm)	> 9%	≥9.5%	≥ 10%
46%	27%	12%	23%	23%	15%

[†] Test results are from samples taken directly from the ready-mix truck prior to pump

[††] Average 28-day compressive strength for lab-cured specimens, *w/c* = 0.42

There were problems pumping the concrete. The pump seized three times when pumping the first seven truckloads of concrete, which had a *w/c* ratio of 0.42. The concrete supplier began to add water to the next seven trucks on site at a rate of 0.5 gal/yd^3 (2.5 kg/m^3) to improve the pumpability, which caused an increase in the

w/*c* ratio from 0.42 to 0.43. It was decided to increase the *w*/*c* ratio at the plant from 0.42 to 0.43 shortly thereafter, and nine additional trucks were batched with a *w*/*c* ratio of 0.43. The concrete with a *w*/*c* ratio of 0.43, however, did not appear to pump any easier. The *w*/*c* ratio was finally increased to 0.45 at the plant, and the concrete was pumpable and construction proceeded. In summary, with a total of 48 truckloads concrete placed, the first seven trucks had a *w/c* ratio of 0.42, then the next 16 trucks had a *w/c* ratio of 0.43, and the final 25 trucks had a *w/c* ratio of 0.45.

The concrete was finished using a single-drum roller screed followed by two bullfloats. The finish looked fairly good for most of the placement.

Burlap was placed differently from previous placements, where contractors usually used two pieces of burlap (overlap in the middle) to cover the full width of the deck. For LC-HPC 5, each piece of burlap was 1 to 3 ft (0.3 to 0.9 m) short of covering the full width of the deck. The contractor decided to cover the bridge transversely with one piece of burlap first, which left a 1 to 3 ft (0.3 to 0.9 m) strip on the south edge exposed; after placing four or five pieces of burlap transversely, workers then covered the exposed strip longitudinally with one piece of burlap. This burlap placement procedure left the concrete on the south edge [about 1 to 3 ft (0.3 to 0.9 m) strip] unprotected for extended periods of time – the time it took to place four or five transverse pieces of burlap. The time for transverse burlap placement ranged from 5 to 22 minutes with an average of 12 minutes.

The superelevation on the south side was similar to that of LC-HPC 6 (Figure 6.24). Because the soaker hoses were again placed in the middle of deck during the curing period, the south side may not have received enough curing water.

The evaporation rate during construction was not recorded. McLeod et al. (2009) estimated the evaporation rate to range from 0.10 to 0.19 lb/ft^2/hr (0.49 to 0.93 kg/m^2/hr).

The deck and girders were wrapped (as shown in Figure 6.25) and periodically heated during the 14-day curing period to meet the cold weather curing specifications.

6.3.14.4 Crack survey results

Three crack surveys have been completed, at 8.0, 19.4 and 31.1 months, giving crack densities of 0.059, 0.123, and 0.128 m/m^2, respectively. As noted for LC-HPC 3 and 6, LC-HPC 5 also had few cracks at the first survey, then exhibited an increase at about two years of age, with little change after another year. The crack map at 31.1 months is shown in Figure 6.28. As shown in the figure, all cracks are transverse. A majority of the cracks appear to initiate at the south edge of the deck, which may be the result of extended exposure period due to slow burlap placement and inadequate curing due to placement of the soaker hoses on the superelevated bridge (discussed in Section 6.3.14.2).

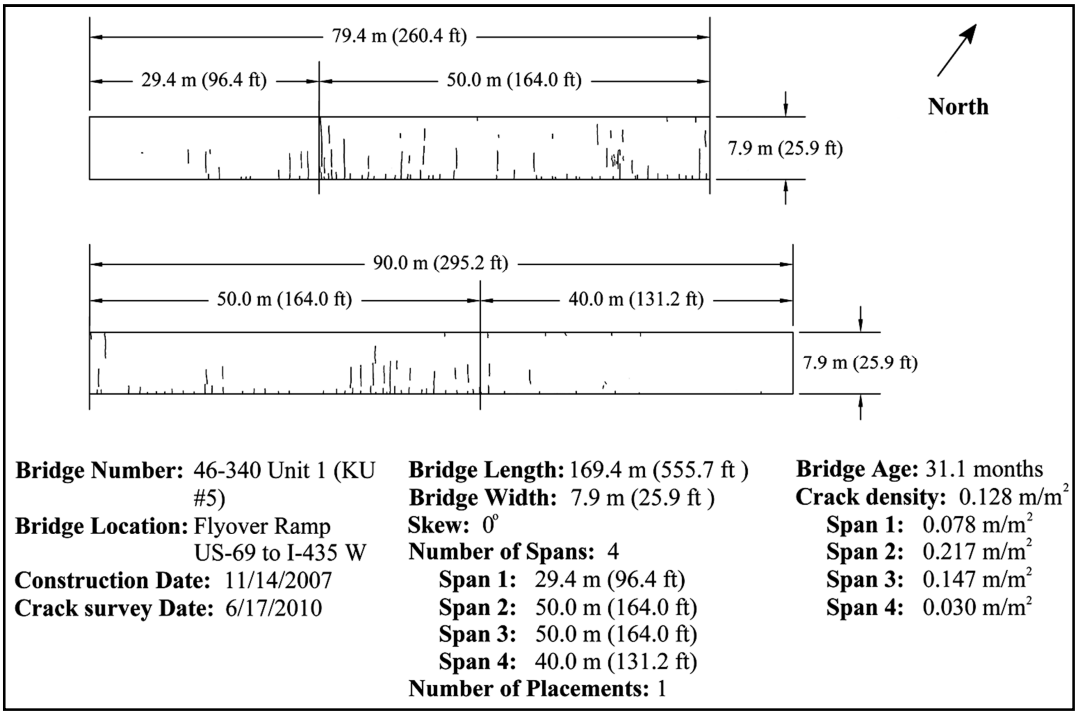

Figure 6.28 Crack map at 31.1 months for LC-HPC 5

6.3.15 Control 3, 4, 5 and 6

Control 3, 4, 5, and 6 were constructed under the same contract as LC-HPC 3, 4, 5, and 6. They will be presented together in this section.

The construction date and concrete mixture information for the four control bridges are listed in Table 6.24. There were two phases of construction for the control bridges, one for the subdeck and one for the silica fume overlay (SFO). Some phases required more than one placement. The same concrete mixture was used for all subdeck construction. The subdeck concrete contained 536 lb/yd^3 (318 kg/m^3) of cement and 133 lb/yd^3 (79 kg/m^3) of fly ash with a water-cementitious material ratio (*w*/*cm*) of 0.40, which provided a paste content of 29.0% by volume. Granite was used as the coarse aggregate. The SFO concrete contained 583 lb/yd^3 (346 kg/m^3) of cement and 44 lb/yd^3 (26 kg/m^3) of silica fume with a *w*/*cm* ratio of 0.37. Granite was used as the coarse aggregate.

The average concrete properties are listed in Table 6.25. In general, the concretes for the control bridges had much higher slumps and compressive strengths than LC-HPC. For the four control bridges listed in Table 6.25, the average slump ranged from 5.75 to 9.25 in. (145 to 230 mm) with most values over 7.0 in. (175 mm); the compressive strength was over 7700 psi (53 MPa) for the SFO concrete and ranged from 4950 to 6340 psi (34.1 to 43.7 MPa) for the subdeck concrete.

Table 6.24 Concrete mix design for Control 3, 4, 5, and 6

Bridge Number	Portion Placed	Date of Placement	*w/cm*	Cement Content		Water Content		Silica Fume Content		Class F Fly Ash Content		Design Air Content	Design Volume of Paste	Coarse Aggregate Type
				lb/yd^3	kg/m^3	lb/yd^3	kg/m^3	lb/yd^3	kg/m^3	lb/yd^3	kg/m^3	%	(%)	
Control 3	Subdeck	07/06/07	0.40	536	318	268	159	0	0	133	79	6.5	29.0%	Granite
	Overlay	07/17/07	0.37	583	346	233	138	44	26	0	0	6.5	26.0%	Granite
Control 4	Subdeck	10/20/07	0.40	536	318	268	159	0	0	133	79	6.5	29.0%	Granite
	Overlay	11/16/07	0.37	583	346	233	138	44	26	0	0	6.5	26.0%	Granite
Control 5	Subdeck-Seq.1 & 2	11/08/08	0.40	536	318	268	159	0	0	133	79	6.5	29.0%	Granite
	Subdeck-Seq.3,5, & 6	11/13/08	0.40	536	318	268	159	0	0	133	79	6.5	29.0%	Granite
	Subdeck-Seq.4 & 7	11/17/08	0.40	536	318	268	159	0	0	133	79	6.5	29.0%	Granite
	Overlay- West Half	11/22/08	0.37	583	346	233	138	44	26	0	0	6.5	26.0%	Granite
	Overlay - East Half	11/25/08	0.37	583	346	233	138	44	26	0	0	6.5	26.0%	Granite
Control 6	Subdeck-Seq.1 & 2	09/16/08	0.40	536	318	268	159	0	0	133	79	6.5	29.0%	Granite
	Subdeck Seq. 3	09/18/08	0.40	536	318	268	159	0	0	133	79	6.5	29.0%	Granite
	Subdeck-Seq.5 & 6	09/23/05	0.40	536	318	268	159	0	0	133	79	6.5	29.0%	Granite
	Subdeck Seq. 4	09/26/08	0.40	536	318	268	159	0	0	133	79	6.5	29.0%	Granite
	Subdeck - Seq. 7	09/30/08	0.40	536	318	268	159	0	0	133	79	6.5	29.0%	Granite
	Overlay - West 2/3	10/16/08	0.37	583	346	233	138	44	26	0	0	6.5	26.0%	Granite
	Overlay - East 1/3	10/20/08	0.37	583	346	233	138	44	26	0	0	6.5	26.0%	Granite

Table 6.25 Average concrete properties for Control 3, 4, 5, and 6

Bridge Number	Portion Placed	Date of Placement	Average Air Content	Average Slump		Average Concrete Temperature		Average Unit Weight		Average Compressive Strength†	
				(in.)	(mm)	(°F)	(°C)	(lb/yd^3)	(kg/m^3)	(psi)	(MPa)
Control 3	Subdeck	07/06/07	5.8	6.75	170	81	27.1	140.5	2251	5690	39.2
	Overlay	07/17/07	7.3	7.25	185	86	29.9	140.4	2249	8350	57.6
Control 4	Subdeck	10/20/07	7.3	7.75	195	73	22.8	139.9	2240	6340	43.7
	Overlay	11/16/07	6.9	5.75	145	68	20.0	140.0	2239	7700	53
Control 5	Subdeck - Seq. 1 & 2	11/08/08	5.6	7.75	200	66	19.0	142.2	2278	--	--
	Subdeck Seq. 3, 5, & 6	11/13/08	6.8	9.25	230	68	20.0	140.1	2245	--	--
	Subdeck - Seq. 4 & 7	11/17/08	5.5	8.00	205	63	17.0	142.0	2275	--	--
	Overlay - West Half	11/22/08	7.6	6.00	150	64	18.0	140.5	2250	8510	58.7
	Overlay - East Half	11/25/08	6.6	9.00	230	63	17.0	141.2	2262	--	--
Control 6	Subdeck - Seq. 1 & 2	09/16/08	7.4	8.00	205	75	24.0	139.7	2238	4950	34.1
	Subdeck Seq. 3	09/18/08	7.3	7.00	180	70	21.0	140.2	2246	--	--
	Subdeck - Seq. 5 & 6	09/23/05	6.4	6.75	175	88	31.0	141.1	2261	--	--
	Subdeck Seq. 4	09/26/08	6.6	6.25	160	86	30.0	140.7	2254	--	--
	Subdeck - Seq. 7	09/30/08	5.5	8.75	225	79	26.0	141.6	2269	--	--
	Overlay - West 2/3	10/16/08	7.7	7.00	175	72	22.0	141.0	2258	--	--
	Overlay - East 1/3	10/20/08	8.1	8.25	210	72	22.0	139.3	2231	7700	53.1

6.3.15.1 Crack survey results for Control 3 to 6

Control 3 is the eastbound bridge (LC-HPC 3 is the westbound bridge) on 103rd Street over US 69. It is a steel plate-girder bridge with non-integral end conditions. Three surveys have been completed, giving the crack densities of 0.037, 0.216, and 0.232 m/m^2 at 10.4, 22.6, and 35.4 months, respectively. The crack map at 35.4 months is shown in Figure 6.29. Almost all cracks are transverse; they are distributed over most of the bridge.

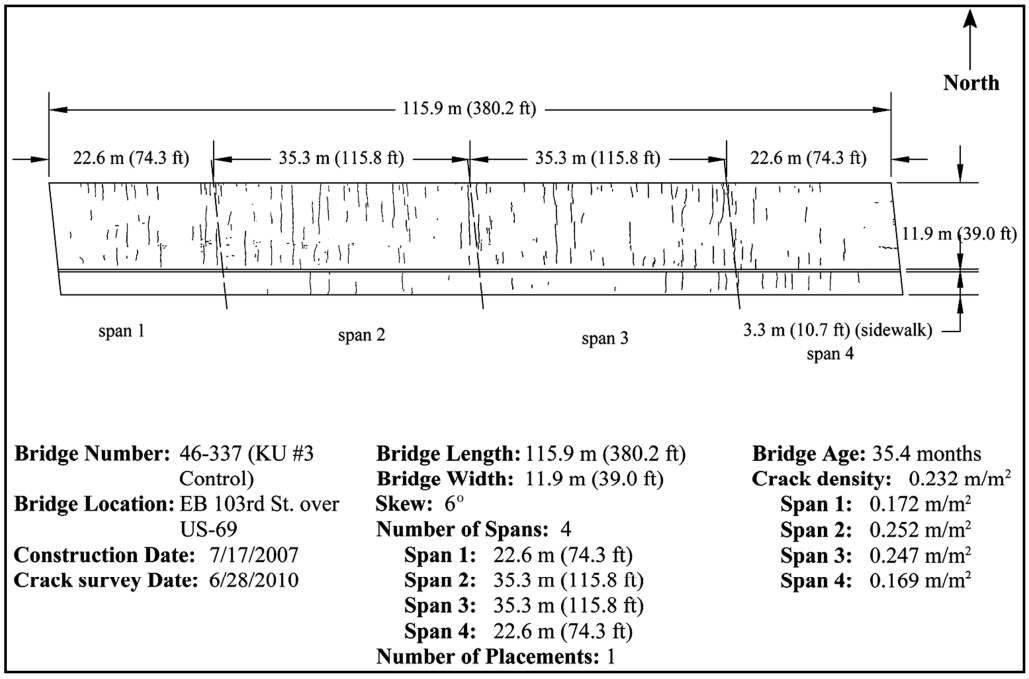

Figure 6.29 Crack map at 35.4 months for Control 3

Control 4 is the ramp from Antioch Road to westbound I-435 in Kansas City, Kansas. It is a steel plate-girder bridge with non-integral end conditions. Three surveys have been completed, giving the crack densities of 0.050, 0.366, and 0.473 m/m^2 at 6.8, 19.7, and 31.6 months, respectively. The crack map at 31.6 months is shown in Figure 6.30. Most cracks are transverse; some longitudinal cracks have developed at the north edge of the bridge and at abutments. Many cracks are located

in the negative moment regions over the piers. Diagonal cracks over the second pier (from the west) are also noted.

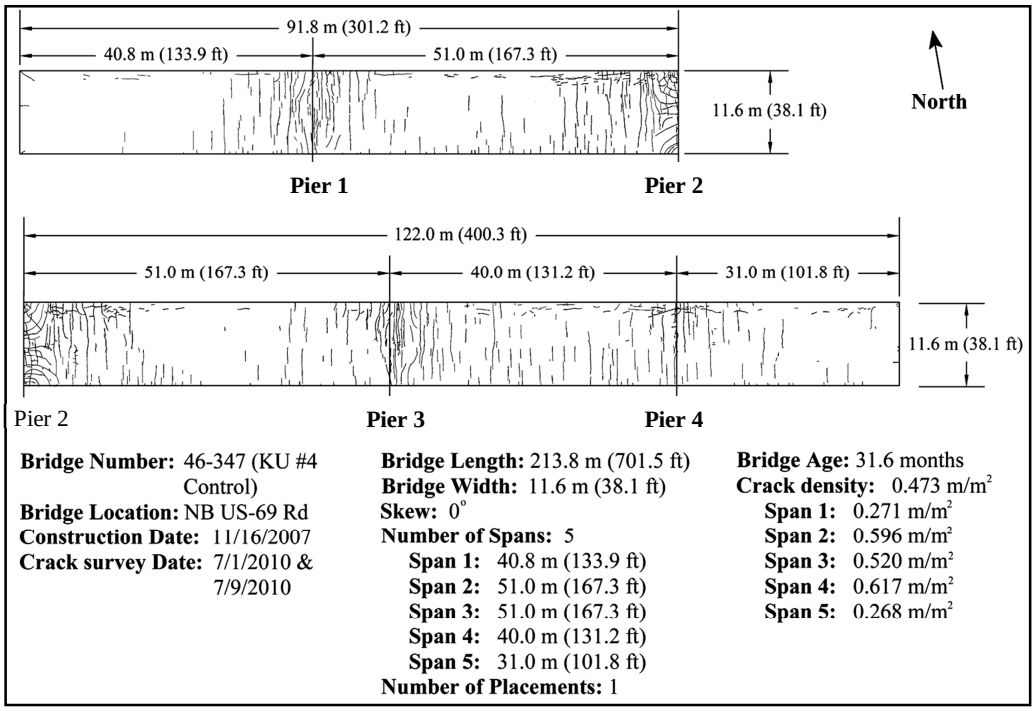

Figure 6.30 Crack map at 31.6 months for Control 4

Control 5 and 6 together make up the flyover bridge connecting southbound US-69 to eastbound I-435 in Overland Park, KS. It is a steel plate-girder bridge. Control 5 (on the west) has non-integral end conditions and Control 6 (on the east) has an integral abutment at the east end and a non-integral end condition at the west end. Two crack surveys have been completed for each bridge. Control 5 exhibits significant cracking and had a crack density of 0.670 m/m^2 at 7.4 months, which increased to 0.857 m/m^2 at 18.9 months. The crack map for Control 5 at 18.9 months is shown in Figure 6.31. Transverse cracking dominates. Many of the transverse cracks cross the full width of the bridge. Longitudinal cracks are also apparent, some of which interconnect with transverse cracks.

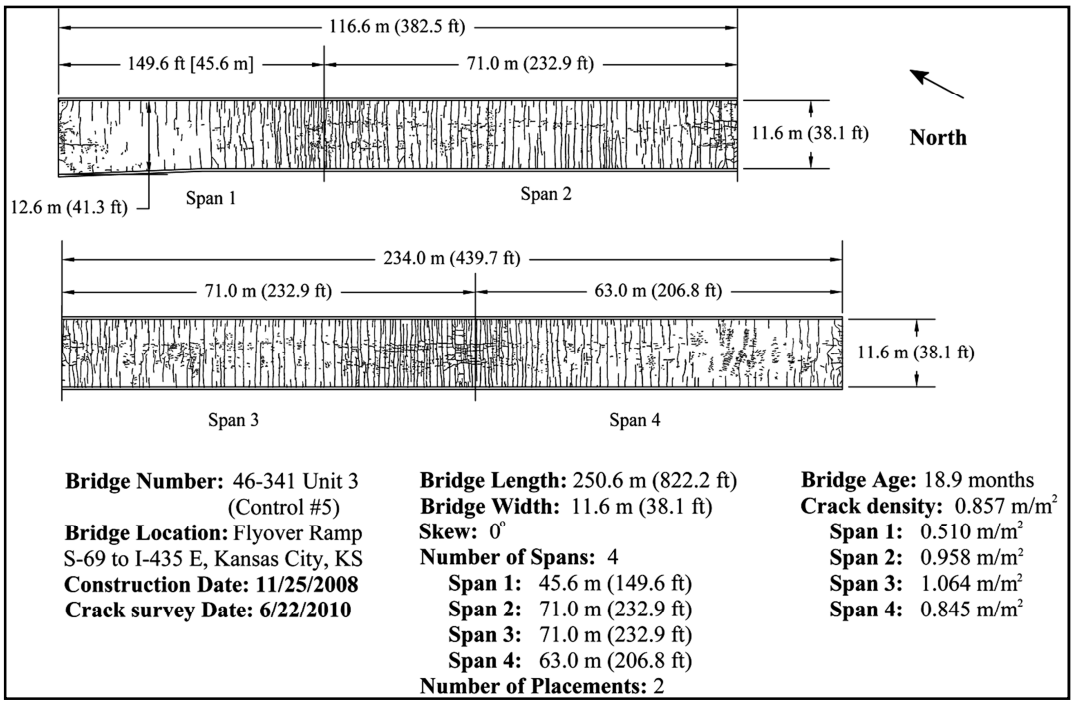

Figure 6.31 Crack map at 18.9 months for Control 5

Control 6 had crack densities of 0.142 and 0.282 m/m^2 at 8.6 and 20.0 months, respectively. The crack map at 20.0 months is presented in Figure 6.32. As shown in Figure 6.32, transverse cracks dominate. It appears that the negative moment regions have more cracks than other locations along the bridge and many of the cracks cross the full width of the bridge. Longitudinal cracks are found at the abutments.

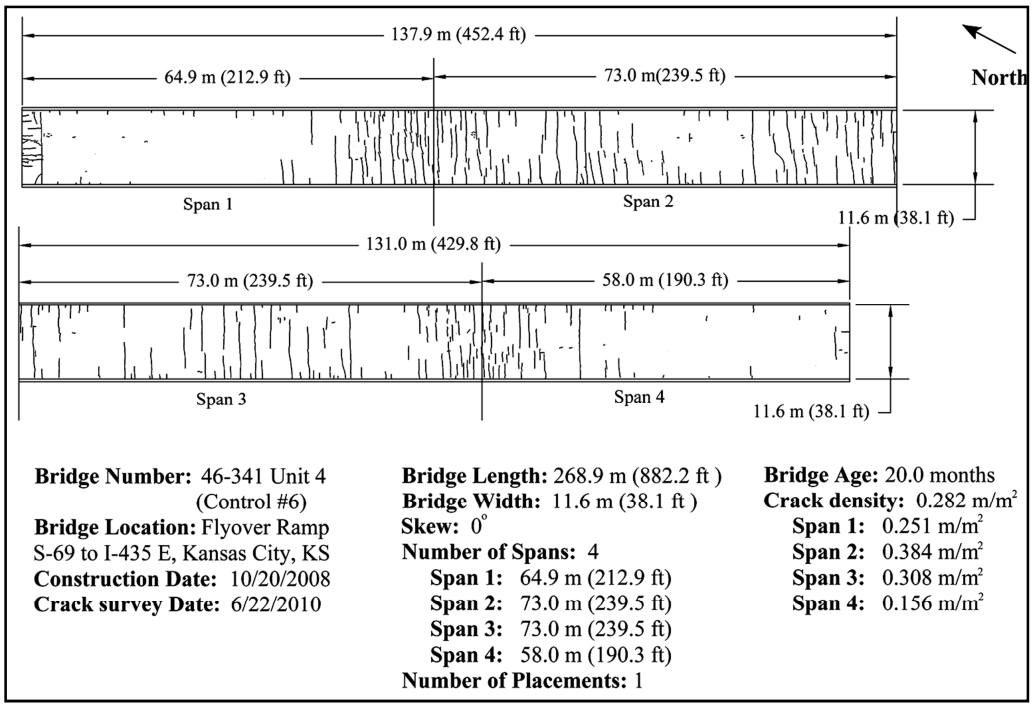

Figure 6.32 Crack map at 20.0 months for Control 6

6.3.15.2 Crack density versus age for LC-HPC and Control 3, 4, 5, and 6

Plots of crack density versus age for LC-HPC and Control 3, 4, 5, and 6 are presented in Figure 6.33. The LC-HPC bridges performed better than the corresponding Control bridges. The most recent crack surveys indicate that the crack density remains around 0.10 m/m^2 for the LC-HPC bridges, except for LC-HPC 4-p1 and LC-HPC 6, which have crack densities of about 0.250 m/m^2. As discussed previously, LC-HPC 4-p1 could possibly have had a *w*/*c* ratio of 0.37 and there were many difficulties involved with placing and finishing the concrete. LC-HPC 6 was constructed with relatively high slump concrete [with an average of 4.0 in. (100 mm)] compared to the other three LC-HPC bridges in this contract, which increased its potential for settlement cracking. The effect of slump on cracking is discussed in Section 6.4.

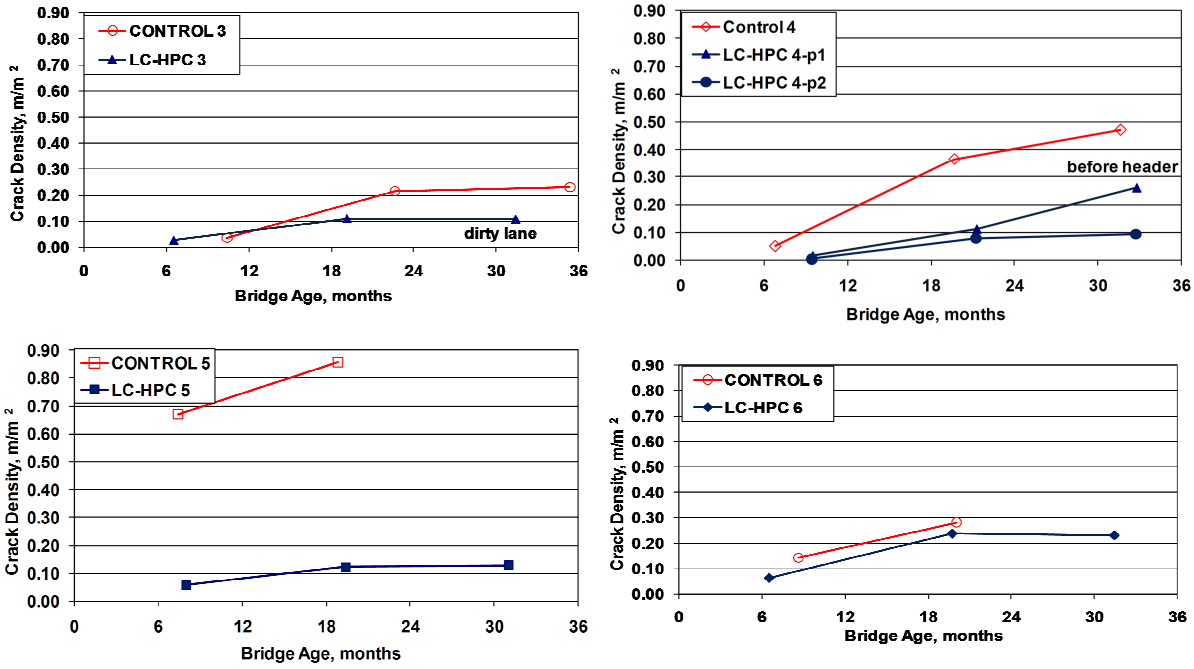

Figure 6.33 Crack density versus age for LC-HPC and Control 3, 4, 5 and 6

The crack densities increased between the first two surveys for both the LC-HPC and Control bridges; the first surveys were performed when the decks were less than one year old and the second surveys were completed about 12 months after the first. For the four LC-HPC bridges (except for LC-HPC 4-p1), the rate of crack density increase dropped significantly after the bridges were more than two years old. Only two of the four control bridges were surveyed after they were more than two years old, and one (Control 3) had a small increase and the other (Control 4) had a more significant increase in crack density between the second and third surveys. The crack density increase rate for both LC-HPC and Control bridges is discussed in Section 6.4.

6.3.16 LC-HPC 12

LC-HPC 12 and Control 12 are parts of the same bridge, which runs north-south on K-130 over the Neosho River near Hartford, KS. Control 12 includes the south three spans, while LC-HPC 12 includes the north three spans. Both units were constructed in two phases, with Phase 1 as the east half and Phase 2 as the west half of the bridge.

The steel plate-girder bridge has integral abutments. LC-HPC 12 is 416.5 ft (127.0 m) long and 36.0 ft (11.0 m) wide, with span lengths of 142.5, 142.5, and 131.5 ft (43.4, 43.4, and 40.1 m).

6.3.16.1 LC-HPC 12-p1

6.3.16.1.1 Concrete

The specifications for LC-HPC 12 required a maximum cement content of 535 lb/yd^3 (317 kg/m^3) and a *w*/*c* ratio of 0.42. Because of the difficulties in pumping and finishing the concrete for LC-HPC 4 and 5 (Section 6.3.11 and 6.3.14) and OP-p1 (discussed in Section 6.3.19) and concerns with producing concrete with higher strength, it was decided to increase the cement content to 540 lb/yd^3 (320 kg/m^3) and the *w*/*c* ratio to 0.44.

6.3.16.1.2 Qualification batch and qualification slab

The qualification batch was tested on March 25, 2008, and in-specification concrete was produced successfully.

The qualification slab was cast on March 28, 2008. The air temperature during the placement was low, close to 40° F (4.4° C). The concrete temperatures, as a result, were also low in the mid-50° F's (10° C). The concrete had a slump between 3.5 and 6.0 in. (90 and 150 mm). Letting the truck sit for an additional 15 to 30 minutes decreased the slump values no more than 0.5 in. (12.7 mm). Trucks #2 and #3 were rejected due to high slump, but as the placement could not be delayed for an

extended period of time, truck #2 was brought back and placed anyway. The air content met the specifications.

At one point, the ready-mix supplier asked if they could withhold water to adjust the slump. It was pointed out that all water should be added at plant to maintain a *w*/*c* ratio of 0.44. Withholding water would result in a lower *w*/*c* ratio, and consequently, a higher compressive strength, which increases the cracking potential. Adjusting the dosage of mid-range water reducer (MRWR) was recommended to control the slump.

The concrete was placed with buckets, rather than a pump or conveyor belt, because flooding under the bridge made it impossible to set up a truck mounted pump or belt at the job site. Two buckets with capacities of 0.75 and 1 yd^3 (0.57 and 0.76 m^3), respectively, were used. The placement rates with the buckets were fine, and it was estimated that the average placement rate on the deck would be between 30 to 40 yd^3/hr (23 to 31 m^3/hr).

The concrete finished well with a single drum-roller screed followed by a burlap drag. No bullfloat was used.

Burlap placement was practiced. It was verified that a hose was in place to re-wet the burlap if needed. The fogging system was checked and found to be adequate.

6.3.16.1.3 Deck construction

The first placement for LC-HPC 12 was completed on April 4, 2008. Construction started at about 9:00 a.m. at the north abutment and was completed at 2:40 p.m. at the south end.

The first truck arrived with a *w*/*c* ratio of 0.42 because some water had been withheld. The concrete supplier was required to add all of the water on site to bring the *w*/*c* ratio up to 0.44. No water was withheld for the rest of the trucks, and the slump was controlled by adjusting the dosage of the mid-range water reducer (MRWR).

The concrete supplier did a good job of supplying quality concrete. The concrete was tested on the deck after being placed with buckets, and the test results are listed in Table 6.26. The slump ranged from 1.75 to 3.5 in. (45 to 90 mm) with an average of 2.75 in. (70 mm). A total of 16 slump tests (28 truckloads concrete were placed) were conducted, with five slump values (31%) over 3.0 in. (75 mm), one slump value equaling 3.5 in. (90 mm), and none exceeding 3.5 in.(95 mm). The air content ranged from 6.2 to 8.1% with an average of 7.4%, and the concrete temperature ranged from 53 to 67° F (11.9 to 19.6° C) with an average of 58° F (14.5° C). The 28-day compressive strength was 4570 psi (31.5 MPa).

Table 6.26 Summary table of concrete test results† for LC-HPC 12 p-1

KU Bridge Number	Slump		Air Content	Unit Weight		Concrete Temperature		28-day compressive strength††	
LC-HPC 5,	in.	mm	%	lb/ft^3	kg/m^3	°F	°C	psi	MPa
Average	2.75	70	7.4	141.0	2259	58	14.5	4570	31.5
Minimum	1.75	45	6.2	139.5	2235	53	11.9		
Maximum	3.5	90	8.1	143.5	2299	67	19.6		

Slump Range			Air Content Range		
> 3.0 in.(75 mm)	≥ 3.5 in.(90 mm)	≥ 4.0 in (100 mm)	> 9%	≥9.5%	≥ 10%
31%	6%	0%	0%	0%	0%

† Concrete was tested on deck at the discharge end of buckets

†† Average 28-day compressive strength for lab-cured specimens, *w/c* = 0.44

The concrete was placed using crane buckets. Two buckets, with capacities of 0.75 and 1 yd^3 (0.57 and 0.76 m^3) were used. The crane operated from the west half of the existing bridge and moved forward as the construction continued, as shown in Figure 6.34. One bucket was swung by the crane, while the other one was filled. The system worked well and gave a placement rate of about 39 yd^3/hr (30 m^3/hr).

Figure 6.34 Placement with buckets for LC-HPC 12

The deck surface was finished using a single-drum roller screed followed by a pan drag. Bullfloating was used only at the beginning and at the end of the placement when the screed and pan drag could not reach the area. The concrete finished well.

Burlap was placed very quickly for this placement [17 ft (5.2 m) wide], with times raining from 4 to 12 minutes and an average of 7 minutes. A worker was assigned to re-wet the burlap after it was placed, as shown in Figure 6.35. Because the worker only sprayed water from the east side of the bridge and the bridge is superelevated on west side, ponded water was noted on the east side surface. The west side was kept wet but no ponded water was noted. To date (through 26.8 months), there has been no apparent influence of the ponded water on cracking (crack map shown in Figure 6.38).

Fogging was not used at all during construction. The evaporation rate was low, ranging from 0.01 to 0.04 lb/ft^2/hr (0.05 to 0.20 kg/m^2/hr).

Figure 6.35 Burlap re-wetting for LC-HPC 12-p1

Because the temperature dropped below 40° F (4° C) during the 14-day curing period, cold weather curing procedures were required. Although the LC-HPC specifications for LC-HPC 12 required wrapping the deck and heating the girders to maintain the temperature between 40 and 75° F (4 and 24° C), alternative procedures for cold weather curing in the newest version of the specifications were followed. The alternative procedures allow heating of the girder to be stopped after the first 72 hours if the time for curing is extended: for any period that the ambient air temperature is below 40° F (4° C), an equal period with a minimum ambient air temperature of 50° F (10° C) is added.

The curing for LC-HPC 12-p1 was extended from 14 days to 17 days, although no records of how the extended curing period was established were made at the time. The air temperature during the curing period was obtained from a weather station in Emporia, KS, shown in Table 6.27, and it indicated that there were 11 days during the 14-day curing period that the air temperature dropped below 40° F (4° C). The extension of the extra 3-day curing, with two days (15-d and 16-d) having minimum air temperate below 50° F (10° C), did not meet the new specification.

McLeod et al. (2009) determined that there were 81 hours during which the air temperature was below 40° F (4° C) during the 14-day curing period and that the extra 3-day curing provided about 47 hours during which the temperature was above 50° F (10° C). Thus, the additional curing period was insufficient. In addition, curing during the first 72 hours, the specification was not met because the air temperature dropped below 40° F (4° C) on days 1 and 3, but no measures were taken to maintain the temperature of the concrete and girders.

Table 6.27 Air temperature records† during the 14-day curing period for LC-HPC 12-p1

Curing timeline	Bridge pour	1-d	2-d	3-d	4-d	5-d	6-d	7-d	8-d
Daily High,℉	60	64	72	57	50	51	62	46	53
Daily Low,℉	36	37	46	33	39	28	42	37	33
Average,℉	48	50	60	44	44	39	53	41	44

Curing timeline	9-d	10-d	11-d	12-d	13-d	14-d	15-d††	16-d††	17-d††
Daily High,℉	52	57	72	73	66	55	72	80	80
Daily Low,℉	30	28	39	55	46	39	37	48	61
Average,℉	40	42	56	64	56	47	54	64	70

† Temperature data were obtained from www.weatherunderground .com for Emporia, KS
†† Extra 3-day curing for LC-HPC 12 p1

6.3.16.2 LC-HPC 12-p2

6.3.16.2.1 Concrete

The second phase of LC-HPC 12 was completed about one year after the first placement. A different concrete mix design, containing a cement content of 535 lb/yd^3 (317 kg/m^3) and a *w*/*c* ratio of 0.45 was used in place of the mixture used for Phase 1 [a cement content of 540 lb/yd^3 (317 kg/m^3) and a *w*/*c* ratio of 0.44].

6.3.16.2.2 Qualification batch and qualification slab

A qualification batch was tested on March 12, 2009. The batch had a slump of 3.75 in. (95 mm), an air content of 7.0%, and a temperature of 61° F (16° C). The qualification batch was accepted.

The qualification slab was waived considering the contractor's experience on LC-HPC 8 and 10 and on Phase 1 of this deck.

6.3.16.2.3 Deck construction

Deck construction was completed on March 18, 2009, with concrete placement staring from the south end at 10:30 a.m. and finishing at the north abutment at 8:00 p.m.

Overall the concrete supply was inconsistent. The concrete supplier had to switch the *w*/*c* ratio back and forth between 0.45 and 0.44 to adjust the slump and help control the concrete temperature. For the first six (of 28) trucks, the qualified mix with a cement content of 535 lb/yd^3 (317 kg/m^3) and a *w*/*c* ratio of 0.45 was used. As all of the water was added at the plant and no water reducer was needed for the mix, the concrete supplier attempted to adjust the slump by using heated water. The slump for the first six trucks ranged from 3.5 to 5.75 in. (90 to 145 mm) with an average of 4.5 in. (115 mm). Due to the high slumps of the first six trucks, the concrete supplier was told to reduce the *w*/*c* ratio to 0.44. Four truckloads of concrete with 0.44 *w*/*c* ratio were delivered and two trucks were checked having a slump of 4.0 and 3.5 in. (100 and 95 mm). After that, the *w*/*c* ratio was switched back to 0.45 from truck #11 to truck #20 per the contractor's requirements (most likely to ease finishing, as KU was not involved in this decision). Four of the ten trucks were tested and the slump values were 4.75, 3.5, 3.5, and 5 in. (120, 90, 90, and 125 mm), respectively. Then, at one point, a lower concrete temperature was required to control the evaporation rate. To avoid even higher slumps with lower concrete temperature, the *w*/*c* ratio was again reduced from 0.45 to 0.44.

The concrete test results are summarized in Table 6.28. The slump ranged from 3.5 to 6.25 in. (90 to 160 mm) with an average of 4.25 in. (110 mm). All recorded slump values were greater than or equal to 3.5 in. (90 mm), and half of the slump values were greater than or equal to 4.0 in. (100 mm). The air content ranged

from 6.3 to 9.0% with an average of 7.8%. The concrete temperature ranged from 61 to 72° F (16.3 to 22.2° C) with an average of 67° F (19.5° C). Two sets of cylinders were made, one with concrete having a *w*/*c* ratio of 0.44 and the other one with concrete having a *w*/*c* ratio of 0.45. The 28-day compressive strengths were 4180 psi (28.8 MPa) and 4580 psi (31.6 MPa) for the 0.45 and 0.44 *w*/*c* ratio mixes, respectively.

Table 6.28 Summary table of concrete test results† for LC-HPC 12 p-2

KU Bridge Number	Slump		Air Content	Unit Weight		Concrete Temperature		28-day compressive strength	
LC-HPC 5,	in.	mm	%	lb/ft^3	kg/m^3	°F	°C	psi	MPa
Average	4.25	110	7.8	140.1	2258	67	19.5	4180[1]	28.8
Minimum	3.5	90	6.3	138.0	2210	61	16.3	4580[2]	31.6
Maximum	6.25	160	9.0	143.2	2294	72	22.2		

Slump Range			Air Content Range		
> 3.0 in.(75 mm)	≥ 3.5 in.(90 mm)	≥ 4.0 in (100 mm)	> 9%	≥9.5%	≥ 10%
100%	100%	50%	0%	0%	0%

† About half samples were tested out of truck, and half were tested on deck after placed with buckets

[1] Average 28-day compressive strength for lab cured specimens, *w*/*c* = 0.45

[2] Average 28-day compressive strength for lab cured specimens, *w*/*c* = 0.44

The concrete was placed with buckets, and this worked well.

The concrete was somewhat over-vibrated. The vibration time for LC-HPC 12-p2 ranged from 8 to 10 seconds in the beginning of the construction. The contractor was then notified to reduce the time to 5 to 6 seconds.

The deck was finished using a single-drum roller screed followed by a pan drag. Bullfloating was used at each end of the bridge. The concrete finished and sealed well.

The burlap was placed fairly quickly, with placement times ranging from 1 to 24 minutes with an average of 6 minutes. At the end of construction, there was a long delay (about 50 minutes) as the contractor had to back-order concrete. The contractor was required to cover all of the placed concrete, including the portions that were not consolidated and finished, with wet burlap while waiting for the back-ordered concrete.

Fogging was not used during construction. The evaporation rate during placement ranged from 0.06 to 0.22 lb/ft^2/hr (0.29 to 1.07 kg/m^2/hr). At one point, about 1/3 of the deck from the north end, the evaporation rate exceeded the maximum allowable value of 0.2 lb/ft^2/hr (1.0 kg/m^2/hr). The contractor reduced the evaporation rate by lowering the concrete temperature.

The plastic concrete temperature, air temperature, and the top surface temperature of steel girders were monitored during the construction. The concrete temperature was checked according to ASTM C1064, the air temperature was monitored with a weather meter (Kestrel® 3000), and the top surface temperature of steel girders was checked with an infrared thermometer (Fluke® 561). The results are presented in Figure 6.36. As shown in Figure 6.36, the top surface of the steel girders was cooler than the ambient air before 10:00 a.m. and after 5:30 p.m., and during this time period, the concrete temperature was higher than both the air temperature and the top surface temperature of the steel girders. During most of the day between 10:00 a.m. and 5:30 p.m., the top surface of the steel girders had a higher

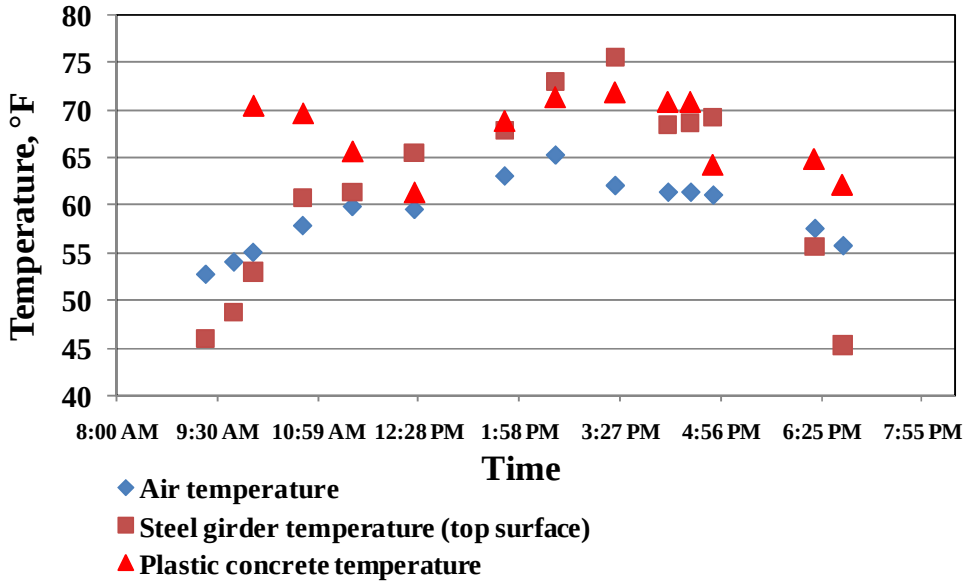

Figure 6.36 The concrete, air, and steel girder top surface temperatures during the construction of LC-HPC 12 –p2

temperature than the ambient air, with a maximum gap of 14° F (4.3° C) at around 3:30 p.m.; the concrete temperature was higher than the air temperature but a little lower than the top surface temperature of the steel girders. The effects of temperature differences on cracking will be discussed in Section 6.4.

Cold weather curing procedures were applied. Again, like Phase 1, the new alternative provision of extended curing period was used. An extra 15 days of curing were required after the initial 14-day curing period. As summarized by McLeod et al. (2009), there were 112 hours with air temperature below 40° F (4° C) during the 14-day curing period that were balanced by an extra 15 days of curing, which provided about 128 hours with air temperature above 50° F (10° C). This met the requirements.

6.3.16.2.4 Unusually heavy loads during the construction

There were unusually heavy loads on the east half bridge (LC-HPC 12-p1) when the west half (LC-HPC 12-p2) was constructed. As shown in Figure 6.37, the crane, buckets, and concrete trucks placed heavy loads on the east half of the bridge. When the

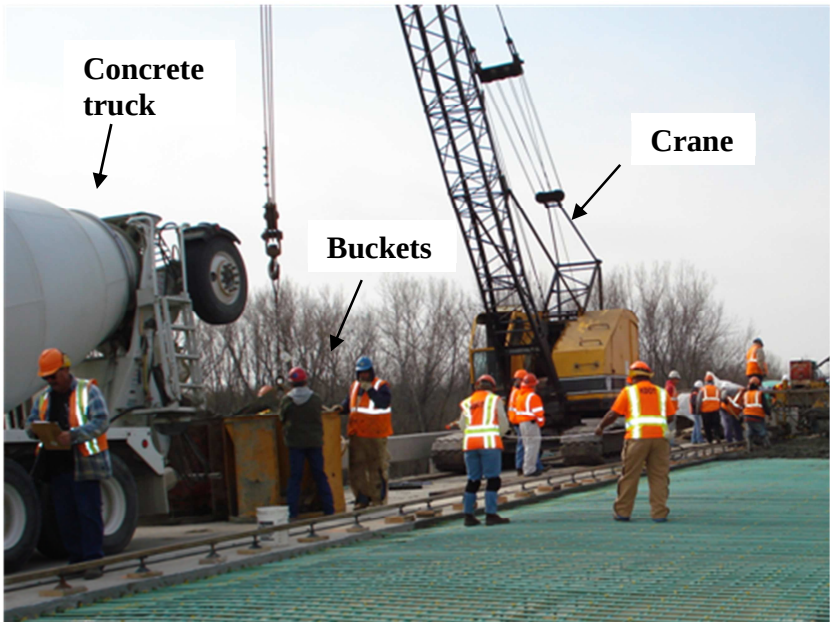

Figure 6.37 Heavy load during construction for LC-HPC 12-p2

crane was between the piers and swinging a bucket full of concrete, the vertical movement of the deck was quite noticeable [estimated to be up to 1.5 in. (38 mm)]. The heavy loads were expected to have caused more cracks on LC-HPC 12-p1 that, in turn, have the potential to initiate cracks on LC-HPC 12-p2.

6.3.16.3 Crack survey results for LC-HPC 12

Two crack surveys have been completed for LC-HPC 12. The crack densities were 0.271 and 0.256 m/m^2 at 16.3 and 26.8 months, respectively, for LC-HPC 12-p1 and 0.254 and 0.244 m/m^2 at 4.9 and 15.4 months, respectively, for LC-HPC 12-p2. The slight decrease of the crack density for the second survey (for both placements) is likely due to different readings produced by two different survey crews. The crack maps for both LC-HPC 12-p1 and p2 at 26.8 and 15.4 months, respectively, are shown in Figure 6.38. Most cracks are transverse. Some, over the middle of the bridge, cross the full width of the deck.

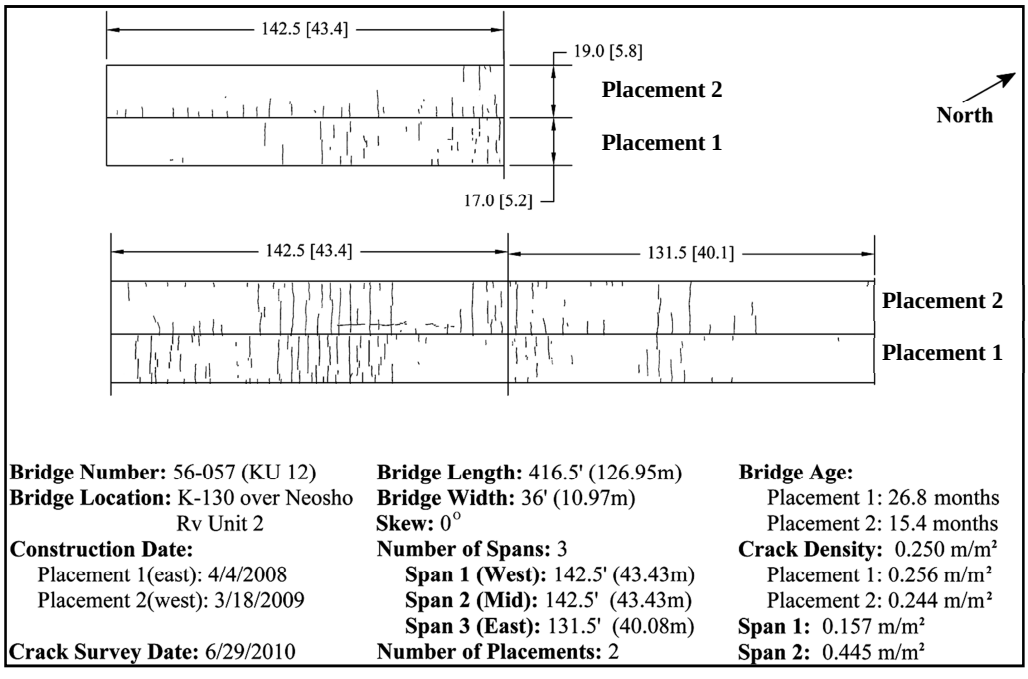

Figure 6.38 Crack map at 26.8 and 15.4 months for LC-HPC 12 p-1 and p-2, respectively

6.3.17 Control 12

Control 12 consists of the south three spans of the bridge on K-130 over the Neosho River near Hartford, KS.

Like LC-HPC 12, Control 12 was constructed in two phases. The east half of the bridge was constructed first. There were two placements in each phase of construction, one for the subdeck and one for the silica fume overlay.

The construction date and concrete mixture information for each subdeck and SFO are presented in Table 6.29. The subdeck concrete had a cement content of 602 lb/yd^3 (357 kg/m^3) and a *w*/*c* ratio of 0.44. Limestone was used as the coarse aggregate. The SFO concrete had a 7% silica fume weight replacement of cement and contained 581 lb/yd^3 (345 kg/m^3) of cement and 44 lb/yd^3 (26 kg/m^3) of silica fume, with a *w*/*cm* ratio of 0.37. Quartzite was used as the coarse aggregate.

The average concrete properties for each placement of Control 12 are listed in Table 6.30. The average slump values, for both the subdeck concrete or for the SFO concrete, were less than or equal to 4.5 in. (120 mm). The average slump values for Control 12 were lower than most of the other Control bridges, which normally have an average slump greater than 5.0 in. (125 mm). The average air content was about 7%. The construction diaries indicate that there were many problems with air content for the silica fume overlay concrete for the Phase 1 construction. Some concrete was placed with an air content of just 2.5% and some with an air content of 9.9%. Difficulties in achieving the proper deck depth were encountered during construction of the west half of the bridge due to the heavy construction loads, and a number of significantly shallow locations were noted.

Table 6.29 Concrete mix design for Control 12-p1 and p2

Bridge Number	Portion Placed	Date of Placement	*w/cm*	Cement Content		Water Content		Silica Fume Content		Design Air Content	Design Volume of Paste	Coarse Aggregate Type
				lb/yd^3	kg/m^3	lb/yd^3	kg/m^3	lb/yd^3	kg/m^3	%	(%)	
Control 12 Phase 1	Subdeck	3/11/2008	0.44	602	357	265	157	0	0	6.5	27.1%	Limestone
	Overlay	4/1/2008	0.37	581	345	231	137	44	26	6.5	25.8%	Quartzite
Control 12 Phase 2	Subdeck	3/13/2009	0.44	602	357	265	157	0	0	6.5	27.1%	Limestone
	Overlay	4/14/2009	0.37	581	345	231	137	44	26	6.5	25.8%	Quartzite

Table 6.30 Average concrete properties for Control 12-p1 and p2

Bridge Number	Portion Placed	Date of Placement	Average Air Content	Average Slump		Average Concrete Temperature		Average Unit Weight		Average Compressive Strength†	
				(in.)	(mm)	(°F)	(°C)	(lb/yd^3)	(kg/m^3)	(psi)	(MPa)
Control 12 Phase 1	**Subdeck**	**3/11/2008**	**6.9**	**4.25**	**110**	**72**	**21.9**	**140.5**	**2250**	**5270**	**36.4**
	Overlay	**4/1/2008**	**6.8**	**3.75**	**95**	**59**	**14.8**	**140.7**	**2254**	**6240**	**43.0**
Control 12 Phase 2	**Subdeck**	**3/13/2009**	**7.2**	**4.5**	**120**	**72**	**22.2**	**--**	**--**	**5010**	**34.5**
	Overlay	**4/14/2009**	**7.7**	**2.25**	**55**	**62**	**16.7**	**--**	**--**	**7710**	**53.1**

6.3.17.1 Crack survey results for Control 12

The east half of the bridge (placement 1) has been surveyed twice, with crack densities of 0.606 and 0.669 m/m^2 at 16.4 and 26.9 months, respectively; the west half of the bridge (placement 2) has been surveyed once, at 14.5 months, and the crack density was 0.442 m/m^2. The crack maps at 26.9 months for placement 1 and at 14.5 months for placement 2 are presented in Figure 6.38. For both placements, almost all cracks are transverse and distributed most of the deck. The first and last 50 ft (15.2 m) of the deck, however, appear to have fewer cracks than other locations.

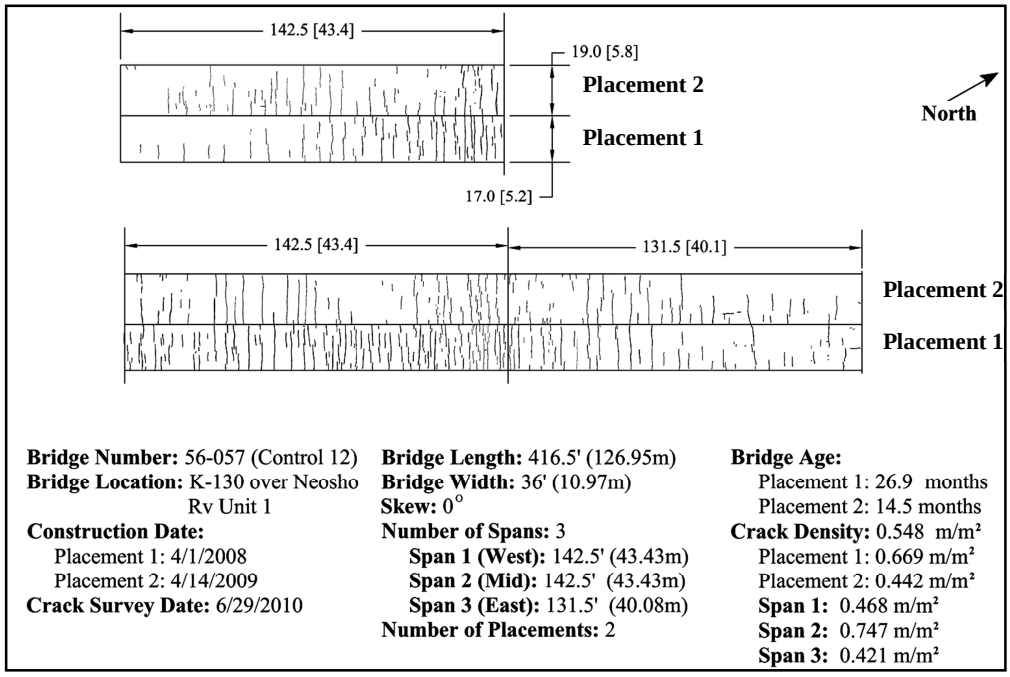

Figure 6.39 Crack map at 26.9 months for placement 1 and 14.5 months for placement 2 for Control 12

6.3.17.2 Crack density versus age for LC-HPC 12 and Control 12

Crack density versus age for LC-HPC 12 (p1 and p2) and Control 12 (p1 and p2) is presented in Figure 6.40. It is obvious that LC-HPC 12-p1 and p2 are performing much better than Control 12-p1 and p2. It can also be noted that the

crack density has remained about the same for the two surveys for each placement of LC-HPC 12. For Control 12, crack density has increased from 0.606 to 0.669 m/m^2 for placement 1 between the two surveys; only one survey has been completed for placement 2.

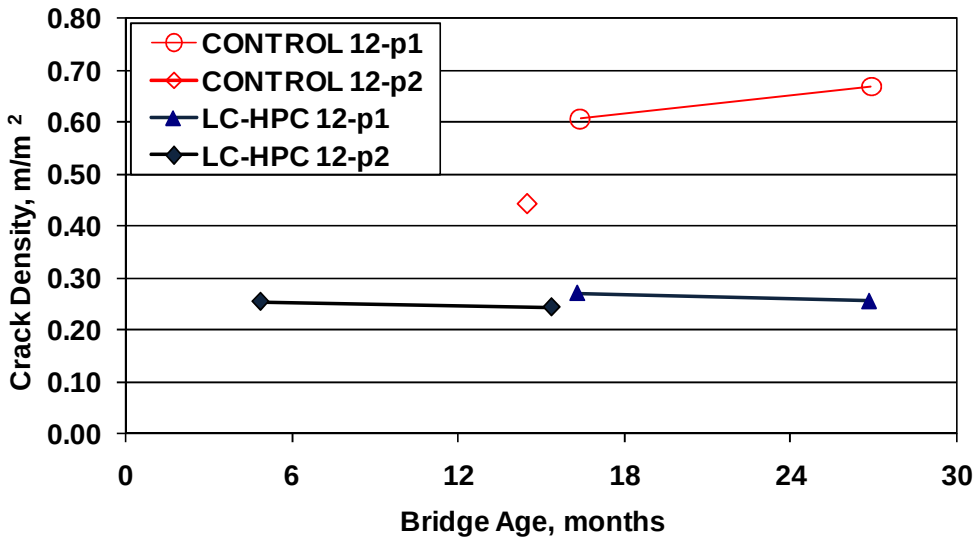

Figure 6.40 Crack density versus age for LC-HPC 12 (p1 and p2) and Control 12 (p1 and p2)

6.3.18 LC-HPC 13

LC-HPC 13 is the northbound bridge on US-69 over BNSF railroad in Linn County, Kansas. The bridge is a three span, steel rolled-beam bridge. It has integral abutments and a skew of 34.8 degrees. LC-HPC 13 is 295.6 ft (90.1 m) long and 40 ft (12.2 m) wide (not including the barrier width). There are three spans with span lengths of 90.4, 114.8, and 90.4 ft (27.5, 35.0, and 27.5 m).

6.3.18.1 Concrete

Similar to LC-HPC 12, the specifications for LC-HPC 13 required a maximum cement content of 535 lb/yd^3 (317 kg/m^3) and a *w*/*c* ratio of 0.42. At the time that LC-HPC 13 was constructed, the mixture design was prepared based on the LC-HPC 12-p1 mixture, which was placed about two weeks prior to the qualification

batch and slab for LC-HPC 13. The mixture had a cement content of 540 lb/yd^3 (320 kg/m^3) and a *w*/*c* ratio of 0.44, which provided better pumpability and workability. The cement content was later reduced to 535 lb/yd^3 (317 kg/m^3) after the qualification slab to help control the concrete slump.

6.3.18.2 Qualification batch and qualification slab

O'Brien Ready Mix was the concrete supplier for the bridge. Considering O'Brien Ready Mix's experience in previous LC-HPC bridges construction (LC-HPC 8 and 10), the qualification batch was waived.

The contractor, Beachner Construction, was new to constructing low-cracking high-performance concrete (LC-HPC) bridges. The qualification slab, which was constructed on a private property and served as part of a backyard slab for a farmer, was placed on April 16, 2008.

Some difficulties were encountered with the concrete. The first two trucks arrived with in-specification slump but the air content was low (5.7 and 6.0%), and the concrete temperatures were at the high end [73.6 and 75.3° F (23.1 and 24.1° C)]. It was noted that approximately 1.5 gallon/yd^3 (7.5 L/m^3) of water had been withheld from the first two trucks and that a mid-range water-reducer had been added. The concrete supplier was told that all water should be added at the plant to avoid a low *w*/*c* ratio. For the next two trucks, no water was withheld and no water reducer was needed. Slump values were greater than 4.0 in. (100 mm) with an average of 4.25 in. (110 mm) when tested out of the truck, and the air content increased slightly with an average of 6.1%. To limit the slump, it was suggested that the cement content be reduced from 540 to 535 lb/yd^3 (317 kg/m^3) while keeping the same *w*/*c* ratio. The concrete supplier was also required to be ready to cool the concrete during the deck construction.

The concrete was finished using a double-drum roller screed with one drum removed, followed by a metal pan drag. Bullfloating was used to help finish the surface. This worked well.

The contractor practiced on burlap placement. During the qualification slab, two layers of burlap were placed at the same time. It was suggested that the burlap layers be separately to shorten the exposure time of the concrete.

6.3.18.3 Deck construction

LC-HPC 13 was constructed on April 29, 2008. Construction started at approximately 11:15 a.m. and ended at about 6:30 p.m., starting at the south abutment.

The concrete had a cement content of 535 lb/yd3, a w/c ratio of 0.44, and no water reducer. The concrete test results are summarized in Table 6.31. The slump ranged from 1.75 to 5.0 in. (45 to 125 mm) with an average of 3.0 in. (75 mm). Twenty nine percent of the recorded slump values exceeded 3.0 in. (75 mm), 26% were greater than or equal to 3.5 in. (90 mm), and 19% of the slump values were greater than or equal to 4.0 in. (100 mm). The air content ranged from 6.8 to 9.5%

Table 6.31 Summary table of concrete test results† for LC-HPC 13

KU Bridge Number	Slump		Air Content	Unit Weight		Concrete Temperature		28-day compressive strength††	
LC-HPC 5,	in.	mm	%	lb/ft^3	kg/m^3	°F	°C	psi	MPa
Average	3.0	75	8.1	141.5	2266	69	20.4	4280	29.5
Minimum	1.75	45	6.8	137.0	2195	61	16.1		
Maximum	5.0	125	9.5	144.6	2317	72	22.2		

Slump Range			Air Content Range		
> 3.0 in.(75 mm)	≥ 3.5 in.(90 mm)	≥ 4.0 in (100 mm)	> 9%	≥9.5%	≥ 10%
29%	26%	19%	24%	6%	0%

† Concrete was tested at the discharge end of pump

†† Average 28-day compressive strength for lab-cured specimens

with an average of 8.1%. All recorded air contents were within the specifications. The concrete temperature ranged from 61 to 72° F (16.1 to 22.2° C) with an average of 69° F (20.4° C). The 28-day compressive strength was 4280 psi (29.5 MPa) for lab cured specimens.

A half-gallon of water per cubic yard of concrete was withheld for the last five truckloads to account for extra water believed to be in the aggregate, which was taken from the bottom of a stockpile at the ready-mix plant.

Two pumps were used during construction. The first pump was set up at the south end of the bridge and the other one at the north end. While the second pump was still operating on the deck [about 40 ft (12 m) from the end of the bridge], the first pump was relocated and used to fill the end abutment. Unfortunately, this did not prevent delays at the end of the placement because the contractor had not ordered enough concrete.

The surfaces were finished with a double-drum roller screed with one drum removed, followed by a pan drag. Bullfloating was used for the first half of the bridge but not for the second half. For the second half, water dripped from the fogging system after it was turned off; as a result, only hand finishing was allowed, as needed, to avoid working the dripped water back into the concrete.

The time for burlap placement ranged from 2 to 24 minutes with an average of 12 minutes. Burlap placement was slow at the beginning but accelerated when there was a consistent supply of concrete. At the beginning, it took about 15 minutes to place burlap after strike-off; later, the time used for burlap placement was less than 10 minutes when the concrete supply was consistent. There were long delays on the last 6 to 10 ft (1.8 to 3.0 m) of the bridge. The contractor had to back-order concrete, and the crew had to wait about 20 minutes on two occasions at the end of the placement for the last concrete to be delivered. The time to burlap placement ranged from 14 to 18 minutes for the last 20 ft (6.1 m) of the bridge.

After the burlap was placed, the contractor began spraying water on it to keep it wet. Ponding water on the east side of the bridge was noted, but the influence on cracking (see Figure 6.41) has not been apparent through 24.8 months.

The evaporation rate during construction ranged from 0.03 to 0.09 lb/ft^2/hr (0.15 to 0.44 kg/m^2/hr) with an average of 0.05 lb/ft^2/hr (0.24 kg/m^2/hr).

6.3.18.4 Crack survey results for LC-HPC 13

Two surveys have been completed, at 13.8 and 24.8 months, with crack densities of 0.050 and 0.129 m/m^2, respectively. Only a few cracks had developed at 13.8 months, but the crack density had increased by 24.8 months. The crack map at 24.8 months is presented in Figure 6.41. Except for two short longitudinal cracks at the south abutment, all cracks are transverse and short in length. The south half of the

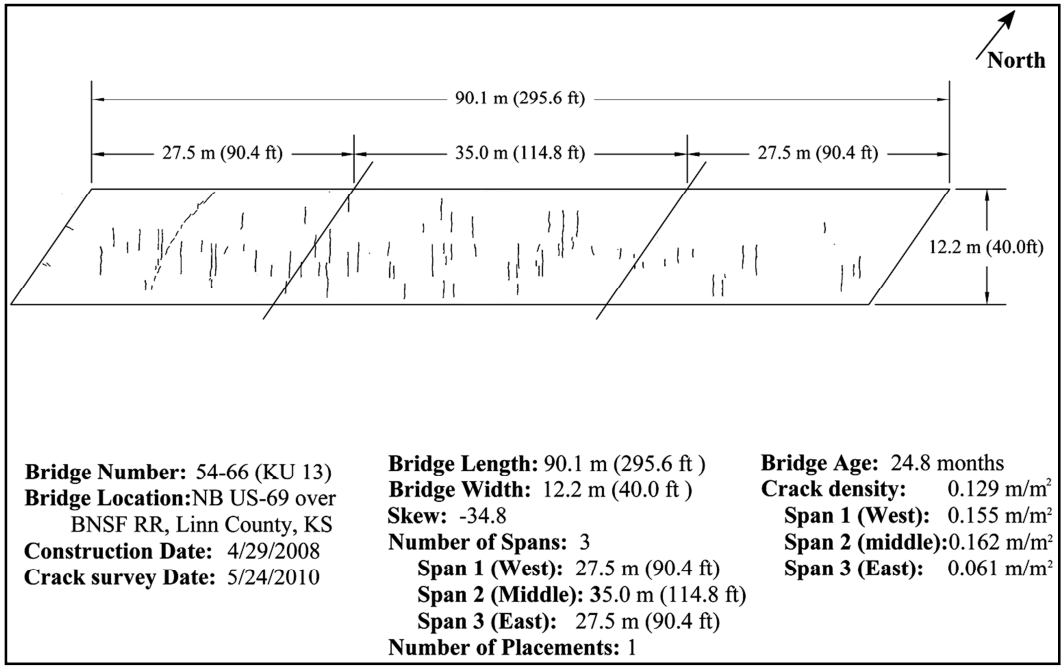

Figure 6.41 Crack map at 24.8 months for LC-HPC 13

bridge appears to have more cracks than the north half, which may be due to use of the bullfloat operation, which was not used on the north half. A bullfloat brings more paste to the deck surface, and consequently, may cause the surface concrete to be more prone to shrinkage cracking.

6.3.19 Control 13

Control 13 is the southbound bridge (LC-HPC 13 is the northbound bridge) on US-69 over the BNSF railroad in Linn County, Kansas. It was constructed by the same contractor and concrete supplier as LC-HPC 13, but followed the KDOT standard deck construction specifications.

Control 13 is a three span, steel rolled-beam bridge that is structurally identical to LC-HPC 13. It has integral abutments and a skew of 34.8 degrees. The bridge is 295.6 ft (90.1 m) long and 40 ft (12.2 m) wide (not including the barrier width). There are three spans with span lengths of 90.4, 114.8, and 90.4 ft (27.5, 35.0, and 27.5 m).

The deck was constructed in two placements, one for the subdeck and one for the silica fume overlay (SFO). The construction date and concrete mixture information for each placement are listed in Table 6.32. The subdeck concrete had a cement content of 612 lb/yd^3 (363 kg/m^3) and a *w/c* ratio of 0.40. Limestone was used as the coarse aggregate. The SFO concrete contained 590 lb/yd^3 (350 kg/m^3) of cement and 44 lb/yd^3 (26 kg/m^3) of silica fume (7% replacement of cement by weight) and had a *w/c* ratio of 0.37. Quartzite was used as the coarse aggregate.

The average concrete properties are listed in Table 6.33. The subdeck concrete had an average slump of 3.5 in. (90 mm), an air content of 5.8%, and a concrete temperature of 89° F (31.7° C). The compressive strength of the subdeck concrete was not recorded. The SFO concrete had an average slump of 5.25 in. (135 mm), an air content of 6.3%, and a concrete temperature of 91° F (33.0° C). The compressive strength was 8280 psi (57.1 MPa).

Table 6.32 Concrete mix design for Control 13

Bridge Number	Portion Placed	Date of Placement	*w/cm*	Cement Content		Water Content		Silica Fume Content		Design Air Content	Design Volume of Paste	Coarse Aggregate Type
				lb/yd^3	kg/m^3	lb/yd^3	kg/m^3	lb/yd^3	kg/m^3	%	(%)	
Control 13	Subdeck	07/11/08	0.40	612	363	244	145	0	0	6.5	26.0%	Limestone
	Overlay	07/25/08	0.37	590	350	234	139	44	26	6.5	26.2%	Quartzite

Table 6.33 Average concrete properties for Control 13

Bridge Number	Portion Placed	Date of Placement	Average Air Content	Average Slump		Average Concrete Temperature		Average Unit Weight		Average Compressive Strength†	
				(in.)	(mm)	(°F)	(°C)	(lb/yd^3)	(kg/m^3)	(psi)	(MPa)
Control 11	Subdeck	07/11/08	5.8	3.50	90	89	31.7	141.7	2271	--	--
	Overlay	07/25/08	6.3	5.25	135	91	33.0	141.6	2269	8280	57.1

6.3.19.1 Crack survey results for Control 13

Two surveys have been completed for Control 13, at 11.0 and 21.9 months, with crack densities of 0.028 and 0.154 m/m^2, respectively. The crack map at 21.9 months is shown in Figure 6.42. Most cracks are transverse and short, with somewhat higher crack densities in the negative moment regions and the area close to the north abutment.

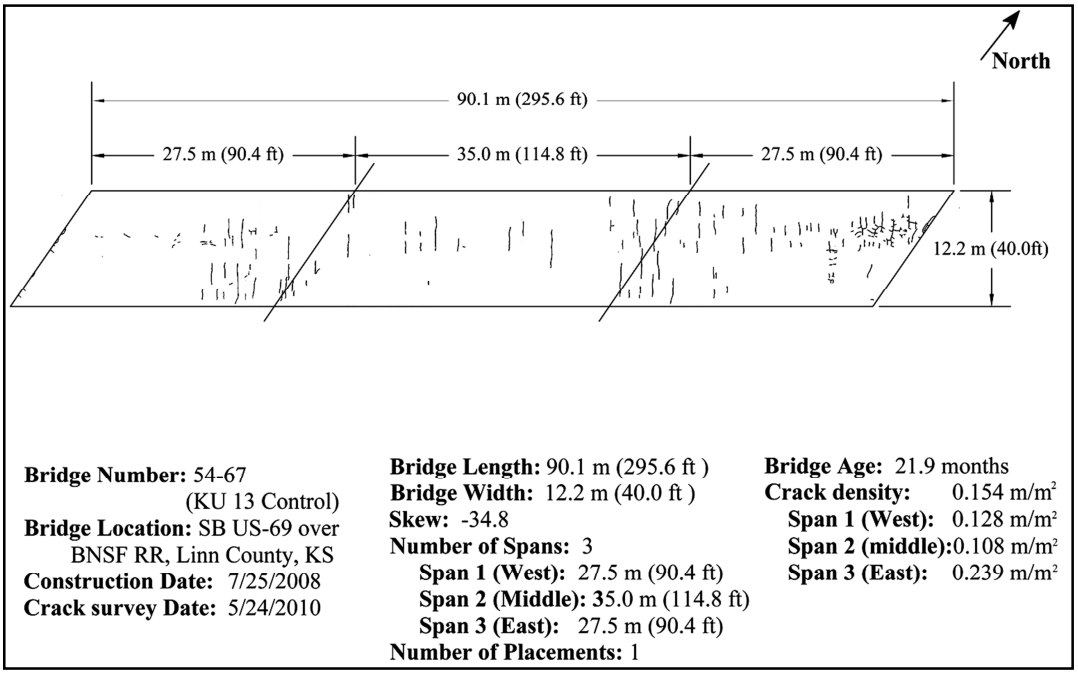

Figure 6.42 Crack map at 21.9 months for Control 13

6.3.19.2 Crack density versus age for LC-HPC 13 and Control 13

Crack density versus age for LC-HPC 13 and Control 13 are presented in Figure 6.43. To date, LC-HPC 13 has performed slightly better than Control 13. When the first survey was completed at about 12 months for both the LC-HPC and the control decks, few cracks had formed; one year later, the crack density had increased significantly for both.

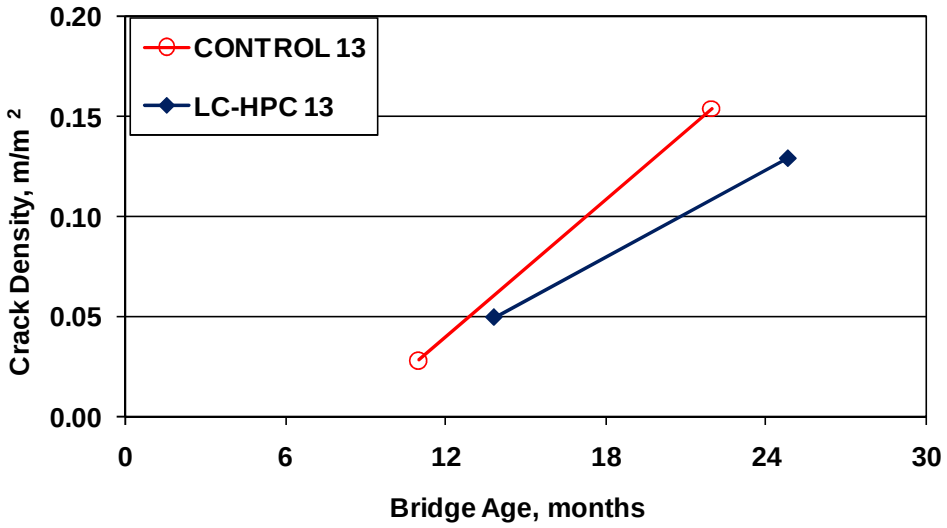

Figure 6.43 Crack density versus age for LC-HPC 13 and Control 13

6.3.20 LC-HPC 9

LC-HPC 9 is the northbound bridge on US-69 over the Marais Des Cygnes River in Linn County, Kansas. It is a three span, steel plate-girder bridge with non-integral abutments and a skew of 27.7 degrees. The bridge is 431.9 ft (131.7 m) long and 40.0 ft (12.2) wide. There are three spans, with lengths of 134.0, 164.0, and 133.9 ft (40.8, 50.0, and 40.8 m).

6.3.20.1 Concrete

The concrete had a cement content of 535 lb/yd^3 (317 kg/m^3) and a *w*/*c* ratio of 0.44.

6.3.20.2 Qualification batch and qualification slab

Per the contractor's request, the first truckload of concrete during the qualification slab (second attempt) served as the qualification batch. Detailed concrete information will be discussed in the qualification slab description.

Three attempts were made to cast the qualification slab due to the difficulties experienced when pumping the concrete. The first attempt was made on March 23,

2009. The concrete arrived with a slump of 1.75 in. (45 mm) and an air content of 7.4%. Even with the low slump, the concrete appeared to be workable and it was decided to pump the concrete. The concrete pump clogged, however, and placement was cancelled. The low slump was thought to be the primary reason for the pump clogging, and it was decided to try to pump again on another day with a higher slump concrete.

The second attempt was made on March 25, 2009. Per the contractor's request, the first truckload of concrete served as the qualification batch for LC-HPC 9. The concrete arrived with a slump of 3.5 in. (90 mm) and an air content of 9.2%. The same pump as used on March 23, 2009 was used. The pump was lubricated with a mortar mix first, although it was still not able to pump the concrete. The concrete and the pump were checked closely. It was noted that the coarse aggregate included 1.5 and 2.0 in. (38.1 or 50.8 mm) particles. Because the pump diameter was only about 4.5 in. (114.3 mm), it is likely that the larger pieces of aggregate became lodged in the pump and stopped the concrete flow.

The third attempt to cast the qualification slab, on April 1, 2009, was successful. The contractor used a conveyor belt instead of a pump. The first truckload of concrete was tested both out of the truck and after the conveyor belt. It had a slump of 4.0 in. (100 mm), an air content of 9.7%, and a concrete temperature of 55° F (13° C) out of the truck; when retested at the discharge end of the conveyor belt, it had a slump of 3.0 in. (75 mm), an air content of 7.6%, and a concrete temperature of 58° F (14° C). The second truckload of concrete was tested at the discharge end of the conveyor belt, and it did not meet the specification because of both high slump [4.75 in. (115 mm)] and air content (9.9%). The third truck was tested for air content only and had an air content of 9%. The out-specification concrete was cast in the qualification slab, but the contractor and concrete supplier were notified that it would not be accepted during deck construction.

Placement and finishing went very smoothly, in part because the concrete had a high slump. The contractor practiced burlap placement.

6.3.20.3 Deck construction

LC-HPC 9 was constructed on April 15, 2009. Construction started at about 9:30 a.m. at the north end and finished at approximately 6:00 p.m.

The first truckload of concrete was tested three times. Initially, the concrete has a lower air content. Additional air entraining agent was first added and then the water withheld (during batching) was added. During the third trial, the concrete had a slump of 4.0 in. (100 mm) and an air content of 6.5%. The concrete supplier was told that no water should be withheld for the rest of the trucks. The three tests on the first truck prompted the inspector to complain about the high number of tests. The result, however, was to bring the concrete into specification in terms of air content. Several of the early trucks contained concrete with slumps in excess of 4.0 in. (100 mm) that were cast in the deck. By the sixth truck, the slump had dropped below 4.0 in. (100 mm) and stayed there for most of the day.

The concrete test results are listed in Table 6.34. The concrete was tested at the discharge end of the conveyor belt. Out of a total of 49 truckloads, 19 truckloads of concrete were tested for slump. The slump ranged from 2.25 to 5.25 in. (55 to 135 mm) with an average of 3.5 in. (90 mm). Fifty eight percent of the slump values were greater than 3.0 in. (75 mm), 47% were greater than or equal to 3.5 in. (90 mm), and 32% were greater than or equal to 4.0 in. (100 mm). Fifteen trucks were tested for air content. The air content ranged from 5.7 to 7.6% with an average of 6.7%. Four truckloads of concrete had air contents below the minimum required air content of 6.5% with values of 5.9, 5.7, 6.1, and 6.1%; they were placed in the deck. The concrete temperature ranged from 60 to 69° F (15.6 to 20.6° C) with an average of 64° F (17.9° C). The compressive strength cylinders were tested at 30 days and had an average strength of 4190 psi (28.9 MPa).

Table 6.34 Summary table of concrete test results† for LC-HPC 9

KU Bridge Number	Slump		Air Content	Unit Weight		Concrete Temperature		28-day compressive strength††	
LC-HPC 5,	in.	mm	%	lb/ft^3	kg/m^3	°F	°C	psi	MPa
Average	3.5	90	6.7	141.3	2264	64	17.9	4190	28.9
Minimum	2.25	55	5.7	139.6	2237	60	15.6		
Maximum	5.25	135	7.6	143.0	2291	69	20.6		

Slump Range			Air Content Range		
> 3.0 in.(75 mm)	≥ 3.5 in.(90 mm)	≥ 4.0 in (100 mm)	> 9%	≥9.5%	≥ 10%
58%	47%	32%	0%	0%	0%

† Concrete was tested at the discharge end of the conveyor belt

†† Average 30-day compressive strength for lab-cured specimens

The concrete was placed with two conveyor belts. Using two conveyor belts minimized delays caused by relocating the belts during construction.

A double-drum roller screed with one roller removed, followed by two metal pans, did a good job finishing the concrete at all slumps. No hand finishing of the middle portion of the slab was required, although hand floating was required near the rails.

Burlap placement was fairly quick. The time to burlap placement ranged from 3 to 18 minutes with an average of 10 minutes. The burlap was presoaked and prepositioned along the bridge. Later during the construction, the burlap began to get dry. Workers, initially, chose to place the dry burlap and then spray water on it after it was placed. This procedure was stopped, and they were told to rewet the burlap before placing it. Because the burlap was rolled up tight, spraying the surface still left the inside still dry. The contractor had to be reminded on a regular basis to spray water on the burlap before it was place.

As concrete placement proceeded, an hour or so after placement of the burlap, the contractor placed soaker hoses on the upper edge (west side) of the super elevated slab. The hoses were set for a very slow flow rate but water covered most of the slab surface. As water ponded on the lower east side, the contractor was asked to drill

holes through the side of the form to allow the water to drain. Many cracks initiating from the lower side of the bridge were noted during the crack survey conducted at 13.6 months (Figure 6.46).

The contractor had to backorder concrete, which delayed slab completion. The contractor was required to place wet burlap on the unfinished final portions of the deck to protect the placed concrete while waiting for the final concrete.

The plastic concrete temperature, air temperature, and top surface temperature of steel girders were monitored during construction. The concrete temperature was checked according to ASTM C1064, the air temperature was monitored using a weather meter (Kestrel® 3000), and the top surface temperature of steel girders was checked with an infrared thermometer (Fluke® 561). The results are shown in Figure 6.44 and are generally similar to the results found during the construction of LC-HPC 12-p2. The top surface of the steel girders was cooler than the ambient air before 10:30 a.m., and then warmer than the air temperate during the rest of the construction through 5:00 p.m. The temperature gap between the top surface of the steel girders and air was

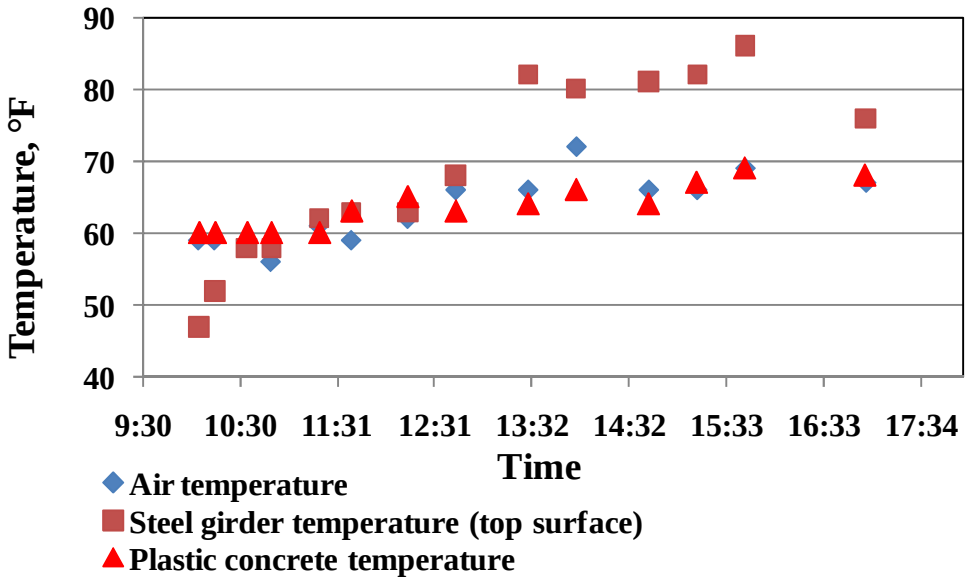

Figure 6.44 The concrete, air, and steel girder top surface temperatures during the construction of LC-HPC 9

most apparent from 1:30 to 3:30 p.m. with a value of about 16° F (9° C). The concrete temperature closely matched the air temperature, which started at around 60° F (15.6° C) then increased slowly to around 70° F (21° C).

Temperature distributions on the steel girders were recorded (using an infrared thermometer Fluke® 561) during the construction. Four locations were checked between 4:00 and 4:30 p.m. when the air temperature was about 70° F (21.1° C). First, locations where concrete had not been cast on the top of the girders were checked. The girders on both the east and west sides were checked and the results are shown in Figure 6.45 (a) and (b). The temperature distributions on the east and west side of the girders were very similar, and the top flanges had the highest temperatures

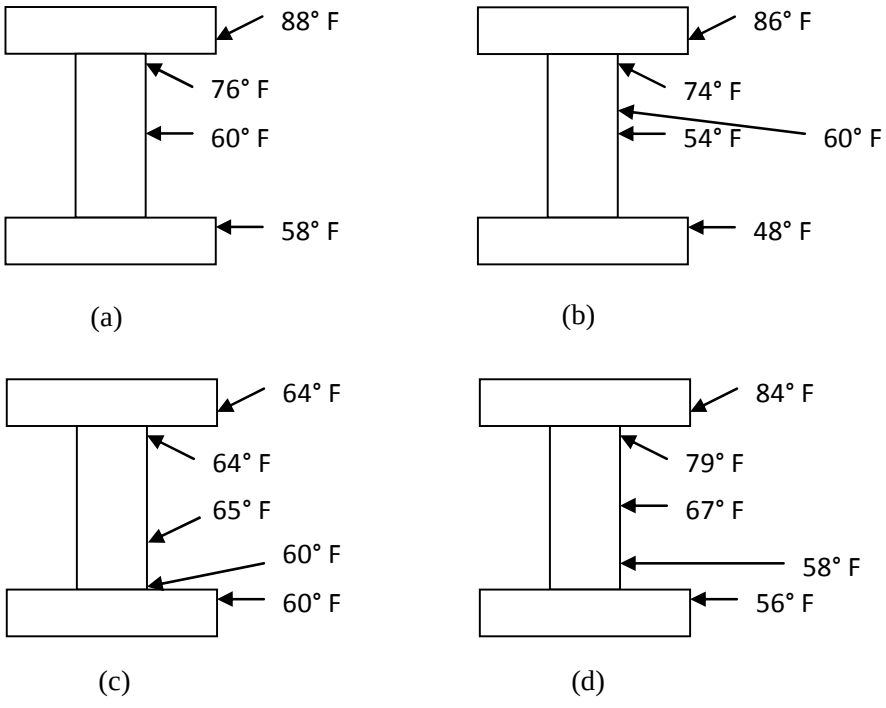

Figure 6.45 Steel girder temperatures during construction of LC-HPC 9
(a) Girder on east side, without concrete cast on top; (b) Girder on west side, without concrete cast on top; (c) Girder on east side, about five hours after concrete cast on top; (d) Girder on east side, without concrete cast on top, half hour after the girder temperature in (a) was checked.

of 88 and 86° F (30.0 and 31.1° C), respectively; a significant temperature gradient from the top flange to the bottom flange was noted, with maximum temperature differences of 30 and 38° F (15.6 and 22.2° C) for the east and west girders, respectively. The east side girder located on the north end of the bridge, where the concrete had been cast for about five hours, (17.8° C) for the top flange and most of the web, and 60° F (15.6° C) for the bottom flange. About half hour after the girder temperature in Figure 6.45 (a) was checked, the temperature of a girder on the east side and without concrete on the top was checked again [Figure 6.45 (d)] to see if the results obtained in Figure 6.45 (a) were representative, and a similar temperature distribution was noted.

6.3.20.4 Crack survey results for LC-HPC 9

To date, only one survey has been completed, at 13.6 months, giving a crack density of 0.130 m/m2. The crack map is presented in Figure 6.46. Most cracks are transverse and short, but several long cracks are apparent on top of the south pier.

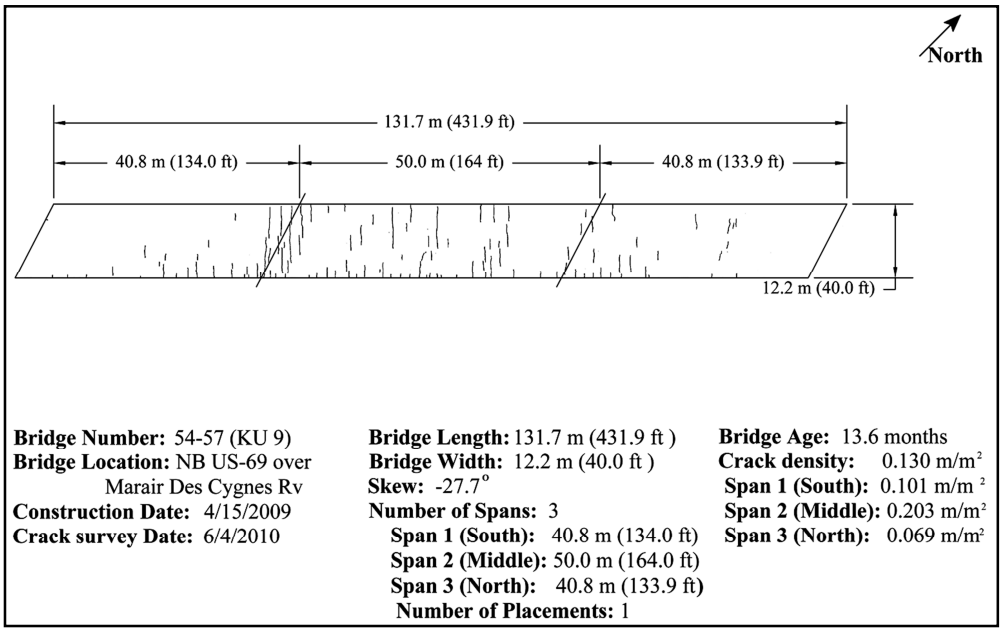

Figure 6.46 Crack map at 13.6 months for LC-HPC 9

Most cracks are located in the middle of the bridge, and not many cracks have developed in the first and last 100 ft (30.4 m). A larger number of cracks have initiated from the east edge than on the west edge of the bridge.

6.3.21 Control 9

Control 9 is the southbound bridge (LC-HPC 9 is the northbound) on US-69 over the Marais Des Cygnes River in Linn County, Kansas. It was constructed by the same contractor and concrete supplier as the LC-HPC 9.

Control 9 is a three-span, steel-plate girder bridge with non-integral abutments and a skew of 23.9 degrees. The bridge is 431.8 ft (131.6 m) long and 40.0 ft (12.2 m) wide (not including the barrier width). There are three spans, with lengths of 134.0, 164.0, and 133.8 ft (40.8, 50.0, and 40.8 m).

The deck was constructed in three placements – one placement for the subdeck and two placements for the silica fume overlay (SFO). The construction dates and concrete mixture design information are listed in Table 6.35. The subdeck concrete had a cement content of 612 lb/yd^3 (363 kg/m^3) and a *w/c* ratio of 0.40. Limestone was used as the coarse aggregate. For the SFO concrete, the mix contained 590 lb/yd^3 (350 kg/m^3) cement and 44 lb/yd^3 (26 kg/m^3) silica fume (7% replacement of cement by weight) and had a *w/cm* ratio of 0.37. Quartzite was used as the coarse aggregate.

The average concrete properties are listed in Table 6.36. The subdeck concrete had an average slump of 2.75 in. (60 mm), an average air content of 6.2%, and an average concrete temperature of 66° F (19.0° C). The 28-day compressive strength of the subdeck concrete was 4850 psi (33.5 MPa). The SFO concrete for the west half of the bridge overlay had an average slump of 3.5 in. (90 mm), an air content of 5.6%, and a concrete temperature of 77° F (24.7° C). The 28-day compressive strength was 6380 psi (44.0 MPa). The SFO concrete for the east half of the deck overlay had an average slump of 5.0 in. (130 mm), an average air content of 6.2%, and an average concrete temperature of 71° F (21.7° C). The 28-day compressive strength was 6170 psi (42.6 MPa).

Table 6.35 Concrete mix design for Control 9

Bridge Number	Portion Placed	Date of Placement	*w/cm*	Cement Content		Water Content		Silica Fume Content		Design Air Content	Design Volume of Paste	Coarse Aggregate Type
				lb/yd^3	kg/m^3	lb/yd^3	kg/m^3	lb/yd^3	kg/m^3	%	(%)	
Control 9	Subdeck	11/3/07	0.40	612	363	244	145	0	0	6.5	26.0%	Limestone
	West-Overlay	5/21/08	0.37	590	350	234	139	44	26	6.5	26.2%	Quartzite
	East-Overlay	5/28/08	0.37	590	350	234	139	44	26	6.5	26.2	Quartzite

Table 6.36 Average concrete properties for Control 9

Bridge Number	Portion Placed	Date of Placement	Average Air Content	Average Slump		Average Concrete Temperature		Average Unit Weight		Average Compressive Strength†	
				(in.)	(mm)	(°F)	(°C)	(lb/yd^3)	(kg/m^3)	(psi)	(MPa)
Control 9	Subdeck	11/3/07	6.2	2.75	65	66	19.0	142.7	2286	4850	33.5
	West-Overlay	5/21/08	5.6	3.5	90	77	24.7	142.4	2282	6380	44.0
	East-Overlay	5/28/08	6.2	5.0	130	71	21.7	141.2	2262	6170	42.6

6.3.21.1 Crack survey results for Control 9

Only one survey has been conducted and this occurred when the silica fume overlay of Control 9 was about 24 months old. The crack density was 0.395 m/m^2 for overlay placement 1 at 24.2 months and 0.368 m/m^2 for overlay placement 2 at 24.0 months. The crack map at 24 months is shown in Figure 6.47. Cracks are primarily transverse and are distributed over the length of the bridge, with the exception that the first and last 50 ft (15.7 m) of the bridge seem to have a lower crack density. As shown in Figure 6.47, longitudinal cracks have also developed along the bridge, primarily in placement 1.

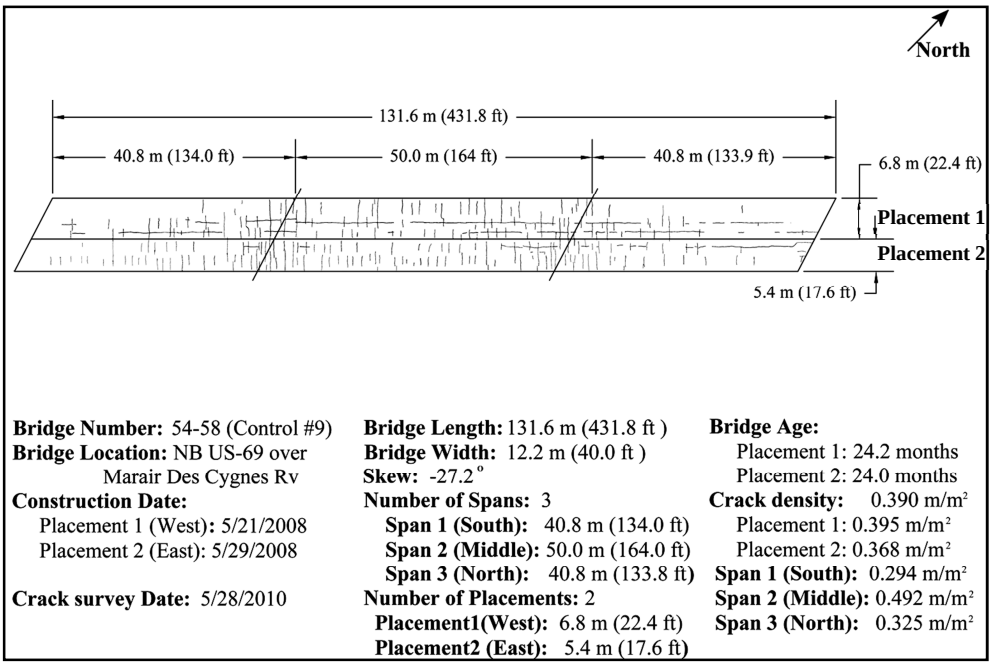

Figure 6.47 Crack map at 24 months for Control 9

6.3.21.2 Crack density versus age for LC-HPC 9 and Control 9

Crack density is plotted versus age for LC-HPC 9 and Control 9 in Figure 6.48. Additional surveys will be needed to compare the performance of the decks at equal ages.

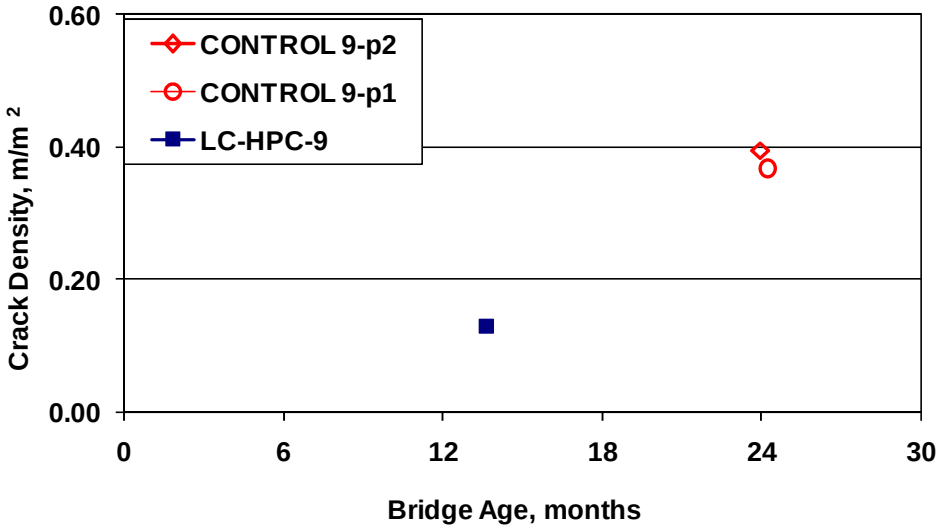

Figure 6.48 Crack Density versus age for LC-HPC 9 and Control 9

6.3.22 OP Bridge ("LC-HPC 14")

The fourteenth LC-HPC bridge let in Kansas is the bridge on Metcalf Avenue over Indian Creek in Overland Park, Kansas. During construction, the contractor, Pyramid Construction, Inc., did not follow and was not required by the owner (City of Overland Park) to follow many aspects of the LC-HPC specifications. Thus the bridge is designated as "OP" instead of "LC-HPC 14".

The bridge is a three-span, rolled steel-girder bridge with integral abutments and a skew of 18 degrees. It is 217.6 ft (66.3 m) long and 140 ft (42.7 m) wide. Due to its great width, the bridge was constructed in three placements, with the center portion [60 ft (18.2 m) wide] constructed first, followed in turn by the west portion [47.5 ft (14.4 m) wide] and the east portion [32.5 ft (9.9 m) wide]. The three placements are discussed separately in this section.

6.3.22.1 Concrete

The LC-HPC specifications for this bridge specified a mixture with a cement content of 535 lb/yd^3 and a *w*/*c* ratio of 0.42. However, due to difficulties met during the construction, which will be discussed later, the *w*/*c* ratio was increased to 0.45.

6.3.22.2 Qualification batch and qualification slab

Because the concrete supplier, Fordyce Concrete, was concurrently supplying concrete for LC-HPC 3 through 6 on a separate project, the qualification batch was waived.

The qualification slab was completed on November 13, 2007. Concrete with a cement content of 535 lb/yd^3 and a *w*/*c* ratio of 0.42 was planned for LC-HPC 14. However, concrete with a *w*/*c* ratio of 0.45 (with the same cement content) was initially delivered and placed in the slab without the knowledge of the contractor or owner. It was pumped and finished well. The city officials and the contractor decided to order one more truck with a *w*/*c* ratio of 0.42. The new concrete arrived with a slump of 3.0 in. (75 mm) and an air content of 7.4% and it was pumped and finished well with no significant difference from the 0.45 *w*/*c* mixture. It was decided to use the mixture with a *w*/*c* ratio of 0.42 for deck construction. Because of concerns with pumping concrete with a *w*/*c* ratio of 0.42, an extra concrete pump test was performed on November 16, 2007. The concrete arrived with a slump of 1.5 in. (38 mm) and an air content of 8.5%. The concrete pumped well as long as pumping was continuous. It took a little bit of effort to get the pump restarted when a stoppage occurred in that concrete supply. The contractor and city officials were satisfied, but stated the importance of having a higher slump.

As this bridge was the contractor's first experience with LC-HPC, many issues were discussed and solved during the qualification slab. The contractor asked if they should use a bullfloat; it was suggested to use a pan drag and/or burlap drag so that the concrete could be covered with burlap as soon as possible; a bullfloat could be used if necessary. It was emphasized that no water should be used as a finishing aid. The contractor asked if the concrete should be vibrated longer; as the contractor's originally demonstrated procedures did not provide adequate consolidation, further clarification was made to vibrate 2 to 3 seconds or until the

coarse aggregate dropped below the concrete surface. The contractor asked if they could place two layers of burlap at the same time; they were told that they could place two layers simultaneously as long as the burlap was placed within 10 minutes after strike-off and overlapped well. The contractor was reminded that the same crew for the qualification slab should be used for the deck construction. Because the bridge was going to be constructed in cold weather (in the middle of November), the contractor planned to wrap and heat the deck to meet the cold weather construction specification. The contractor asked if they could turn off the heater during the curing period as they were concerned that the girders might overheat; they were told that the heater could be turned off to keep the temperature within the specified limits.

6.3.22.3 OP-p1(Placement 1):

Placement 1 is the central portion of the bridge and it was constructed in two attempts.

Attempt 1 (11/19/2007): The first attempt was made on November 19, 2007, and it was a failure. A number of problems occurred, including placement of concrete that did not meet the specifications, a pump that clogged, and a job layout that prevented the movement of a backup pump to replace the initial one.

The first several trucks arrived at the job site with air contents and slumps exceeding the maximum allowed values. These trucks were held out to let the slump and air content drop. As a result, a large number of the waiting trucks were used early in the placement. By the time the concrete in the waiting trucks was placed, the slump was very low and the contractor had difficulty placing it. The concrete started to become unpumpable. The narrow job site, which only allowed one truck to discharge at a time, caused many stops and restarts of the pump, which in turn caused more difficulties pumping the concrete. At one point, the pump blew a gasket. By the time it was fixed, the pump was clogged. The job layout prevented the movement of a backup pump into position. Construction was stopped by the contractor.

A meeting was held on November 20, 2007, with representatives from the concrete supplier, the contractor, the City of Overland Park, the structural designer, the pumping company, and KU. The contractor stated that they were going to tear out the concrete. It was decided that conveyor belts would be used to place the concrete. There was a great deal of discussion on how to start deck in terms of accepting concrete, but no final decision was made.

Attempt 2 (12/19/2007): The bridge deck was placed on December 19, 2007. The concrete from Attempt 1 placed in the south abutment had been retained and did not have to be replaced. The north abutment was placed first, and then the deck was cast starting at the south end at about 10:30 a.m. and ending at the north end at approximately 3:30 p.m.

The concrete mix design was changed by increasing the *w*/*c* ratio from 0.42 to 0.45. The concrete was tested out of the truck, and the test results are listed in Table 6.37. The slump ranged from 1.75 to 5.25 in. (45 to 135 mm) with an average of 3.75 in. (95 mm). Three-quarters of the recorded slump values were greater than or equal to 3.5 in. (90 mm), and 50% of the slump values were greater than or equal to 4.0 in. (100 mm). The air content ranged from 7.8 to 9.7% with an average of 8.7%.

Table 6.37 Summary table of concrete test results† for OP-p1

KU Bridge Number	Slump		Air Content	Unit Weight		Concrete Temperature		28-day compressive strength††	
LC-HPC 14-p1	in.	mm	%	lb/ft^3	kg/m^3	°F	°C	psi	MPa
Average	3.75	95	8.7	139.7	2237	65	18.1	4440	30.6
Minimum	1.75	45	7.8	136.6	2188	60	15.6		
Maximum	5.25	135	9.7	142.0	2274	69	20.6		

Slump Range			Air Content Range		
> 3.0 in.(75 mm)	≥ 3.5 in.(90 mm)	≥ 4.0 in (100 mm)	> 9%	≥9.5%	≥ 10%
75%	75%	50%	30%	10%	0%

† Concrete was tested out of truck

†† Average 28-day compressive strength for lab-cured specimens

The concrete temperature ranged from 60 to 69° F (15.6 to 20.6° C) with an average of 65° F (18.1° C). The 28-day compressive strength was 4440 psi (30.6 MPa) for lab-cured specimens. Construction notes indicated that due to the long travelling time and a few delays at the deck, some of the concrete loads were close to being rejected based on the time since batching.

The consolidation for OP-p1 was inadequate and inappropriate. During the qualification slab, the contractor was instructed to leave the vibrator in the concrete for 2 to 3 seconds or until the coarse aggregate dropped below the concrete surface. The contractor did not follow the instructions and did not obtain adequate consolidation. Coarse aggregate remained visible at the concrete surface after the vibrators were removed. The workers lifted the vibrator too fast so that holes were left in the concrete, as shown in Figure 6.49.

Figure 6.49 Inappropriate consolidation during construction of OP-p1

The bridge was finished with a double-drum roller screed with one roller removed followed by a metal pan drag. Early during the placement, the screed left some regions with coarse aggregate showing. The contractor worked hard to finish those regions by adding additional concrete and using a bullfloat. The contractor said

that the flexibility in the finishing bridge, as affected by the location of the gang vibrator, affected the ability of the single drum to finish the concrete. Two of the contractor's personnel stated that the double-drum roller screed would have been able to finish the concrete without additional work. Bullfloating was used extensively and was performed in longitudinal direction, as shown in Figure 6.50. The bullfloating caused several issues. First, it slowed the burlap placement rate because the bullfloating operation required extra space in longitudinal direction, leaving areas exposed for an extended period. Also, as water accumulated on the deck surface due to fogging, bullfloating worked that water back into the concrete. Overall, the contractor put more effort into finishing than any of other LC-HPC bridge placements. The extra finishing likely led to plastic shrinkage cracking and worked more paste to the surface of the deck, increasing the potential for drying shrinkage cracking. The crack survey at 30.0 months, as shown in Figure 6.51, did show that there were a high number of short cracks of the type expected from plastic shrinkage cracking or local cracking due to a layer of paste at the deck surface.

Figure 6.50 Bullfloating in longitudinal direction for OP-p1 (fogging was on)

Burlap placement was very slow. The time to place the burlap ranged from 20 to 40 minutes with an average of 28 minutes. One of the key reasons was the extra distance needed for the bullfloat between the finishing bridge and the two work bridges for burlap placement made it impossible to place the burlap right after strike-off. The large width of the bridge, which required three pieces of burlap to cover the full width, also slowed burlap placement.

The bridge was enclosed underneath and eight heaters (four at each end of the deck) were used to heat the air under the deck. Installation of all of the heaters was not completed by 9:30 a.m., the time that concrete placement started at the north abutment. The air temperature at the bottom of the girders, measured near the north abutment, was checked a few times during the day. The temperature was 42° F (5.6° C) at 9:00 a.m., increased to 65° F (18.3° C) at about 10:00 a.m., and 80° F (26.7° C) later in the day. It was reported (by city officials) that the temperature rose to 85° F (29.4° C) on the evening of the placement, but was within the range of 55 to 70° F (12.8 to 21.1° C) during the balance of the 14-day curing period.

The evaporation rate was low during construction, ranging from 0.06 to 0.08 $lb/ft^2/hr$ (0.29 to 0.39 $kg/m^2/hr$) with an average of 0.07 $lb/ft^2/hr$ (0.34 $kg/m^2/hr$).

6.3.22.4 Crack survey results for OP-p1

Two surveys have been completed, at 18.3 and 30.0 months. The crack density has been high, with values of 0.341 m/m^2 at 18.3 months and 0.502 m/m^2 at 30.0 months. The crack map at 30.0 months is shown in Figure 6.51. Most cracks are transverse with some longitudinal cracks at both abutments. A significant number cracks are short, as discussed in Section 6.3.22.3.

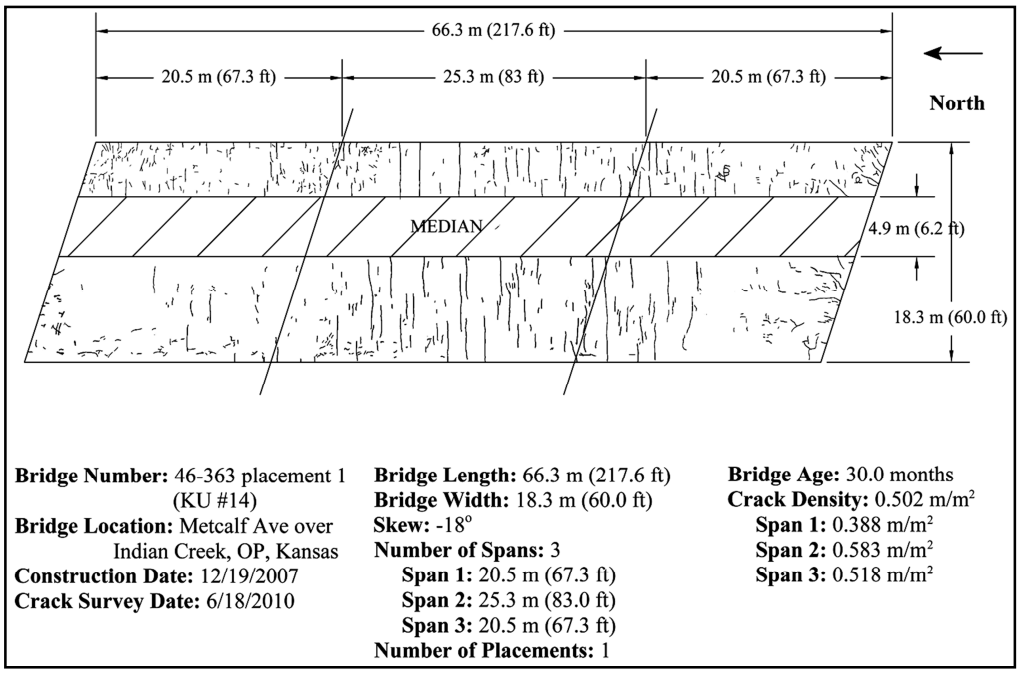

Figure 6.51 Crack map at 30 months for OP-p1

6.3.22.5 OP-p2 (Placement 2)

Placement 2, the west portion of the bridge, was constructed on May 2, 2008. The deck was placed from south to north, with the placement starting about 9:15 a.m. and ending at approximately 4:00 p.m., using the same concrete mixture as placement 1 with a cement content of 535 lb/yd^3 and a *w*/*c* ratio of 0.45.

Concrete was tested out of the truck. Two trucks were tested before and after the conveyor belt. The air content losses were 1.4 and 2.4%, and the slump losses were 0.75 and 0.5 in. (19.1 and 12.7 mm), respectively. These values were consistently used as an excuse for not rejecting concrete with a high slump and/or high air content. The Overland Park city officials, unfortunately, were also influenced by the contractor to accept out-of-specification concrete.

The concrete test results are shown in Table 6.38. The slump ranged from 2.5 to 6.0 in. (65 to 150 mm) with an average of 4.25 in. (110 mm). Ten of the 11 (91%) slump values were greater than or equal to 3.5 in. (90 mm), and eight of the 11 slump

values (73%) were greater than or equal to 4.0 in. (100 mm). The air content ranged from 7.0 to 11.0% with an average of 9.8%. Only three of the 12 (25%) air content values met the specification with air contents lower than 9.5%. Nine of the 12 (75%) air content values were equal or greater than 10%. The concrete temperature ranged from 63 to 65° F (17.2 to 18.3° C) with an average of 64° F (17.9° C). The 28-day compressive strength was 3710 psi (25.6 MPa).

Table 6.38 Summary table of concrete test results† for OP-p2

KU Bridge Number	Slump		Air Content	Unit Weight		Concrete Temperature		28-day compressive strength††	
LC-HPC 14-p2	in.	mm	%	lb/ft^3	kg/m^3	°F	°C	psi	MPa
Average	4.25	110	9.8	138.1	2213	64	17.9	3710	25.6
Minimum	2.5	65	7.0	134.7	2157	63	17.2		
Maximum	6.0	150	11.0	142.6	2284	65	18.3		

Slump Range			Air Content Range		
> 3.0 in.(75 mm)	≥ 3.5 in.(90 mm)	≥ 4.0 in (100 mm)	> 9%	≥9.5%	≥ 10%
91%	91%	73%	75%	75%	75%

† Concrete was tested out of truck

†† Average 28-day compressive strength for lab-cured specimens

The concrete was placed using a conveyor belt without any problems.

The roadway and sidewalk portion were finished separately. For the roadway, finishing was performed using a double-drum roller screed followed by a pan drag and a burlap drag. The burlap drag was mounted on an extra work bridge, as shown in Figure 6.52. The extra work bridge between the strike-off and burlap work bridges made it impossible to place burlap right behind the finishing equipment. It was estimated that the burlap drag added 3 to 5 minutes to the burlap placement. Bullfloating was used on a limited basis. For the last 30 ft (9.1 m) of the deck, there were delays because concrete had to be backordered. During this period, some concrete that had been placed in the wing wall was transferred to the deck in an attempt

to complete the placement. Bullfloating and hand floating were used extensively. A finishing aid was also used because the concrete was difficult to finish. Overall, the concrete finished well, but as for OP-P1, the contractor put more effort into finishing compared with other contractors.

Figure 6.52 Burlap drag during construction of OP-p2

The sidewalk portion of the deck was leveled with a piece of 2 × 4 in. (50 × 100 mm) lumber and then finished by hand. Bullfloating was also used.

Burlap placement was slow. The time of burlap placement on the roadway portion ranged from 12 to 74 minutes with an average of 21 minutes. The 74-minute burlap placement time occurred due to significant concrete delays close to the end portion of the deck. Burlap placement on the sidewalk was even slower. The burlap on the sidewalk was placed longitudinally so that for approximately every four pieces of burlap placed transversely on the roadway, one piece of burlap was placed with its longest dimension along the length of the sidewalk. The time of burlap placement on the sidewalk ranged from 20 to 50 minutes.

Fogging was performed only once, at the north end of the deck, using a hand fogger while waiting for back-ordered concrete. Hand fogging resulted in some water ponding on the deck, primarily on the east side of the placement. Some of this water was worked back into the concrete.

The evaporation rate during the placement was not recorded and estimated to be about 0.06 lb/ft2/hr (0.29 kg/m2/hr).

6.3.22.6 Crack survey results for OP-p2

Two crack surveys have been completed on placement 2, at 13.7 and 25.5 months. This portion of the deck had a high crack density, 0.640 m/m^2, even at an early age of 13.7 months; the crack density increased to 0.727 m/m^2 at 25.5 months. The crack map at 25.5 months is shown in Figure 6.53. Most cracks are transverse, with some short longitudinal cracks found mainly near the abutment. The high crack density, in all likelihood, is caused by increased settlement cracking due to the high slump concrete. The significant number of short cracks are probably caused by extra paste worked to the surface due to the combined effects of increased slump and the extra finishing effort on the deck.

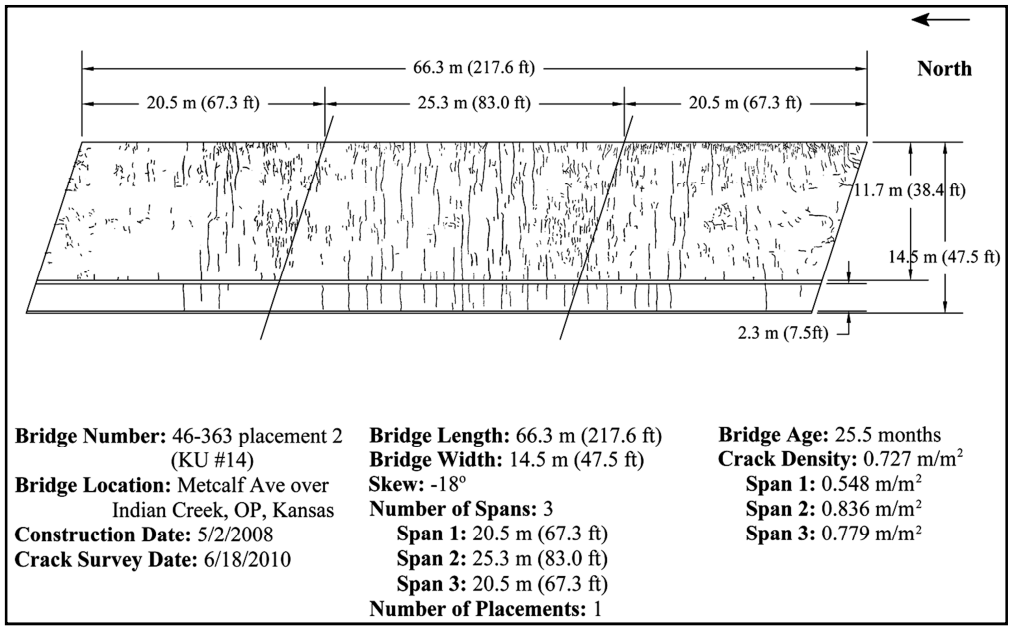

Figure 6.53 Crack map at 25.5 months for OP-p2

6.3.22.7 OP-p3 (Placement 3)

Placement 3, the east portion of the bridge, was constructed on May 21, 2008. Concrete placement started at the south abutment at about 6:00 p.m. and ended at the north abutment at approximately 9:30 p.m. The north abutment had been preplaced on May 16, 2011.

Placement 3 was conducted 19 days after placement 2 using the same construction methods. This discussion will focus on the concrete used in placement 3.

The concrete test results are shown in Table 6.39 and the concrete was tested out of the truck. The slump ranged from 4.25 to 6.5 in. (110 to 165 mm) with an average of 5.25 in. (130 mm). All the slump values were greater than the maximum allowable slump of 4.0 in. (100 mm). The air content ranged from 9.5 to 10.5% with an average of 9.9%. Two truckloads of concrete were tested both out of the truck and at the discharge end of the conveyor belt to establish the air loss, producing values of 0.5 and 1.2%. The concrete temperature ranged from 62 to 67° F (16.7 to 19.4° C) with an average of 65° F (18.3° C). The 28-day compressive strength was 3830 psi (26.4 MPa).

Table 6.39 Summary table of concrete test results† for OP-p3

KU Bridge Number	Slump		Air Content	Unit Weight		Concrete Temperature		28-day compressive strength††	
LC-HPC 14-p3	in.	mm	%	lb/ft^3	kg/m^3	°F	°C	psi	MPa
Average	5.25	130	9.9	137.1	2195	65	18.3	3830	26.4
Minimum	4.25	110	9.5	135.1	2165	62	16.7		
Maximum	6.5	165	10.5	138.3	2215	67	19.4		

Slump Range			Air Content Range		
> 3.0 in.(75 mm)	≥ 3.5 in.(90 mm)	≥ 4.0 in (100 mm)	> 9%	≥9.5%	≥ 10%
100%	100%	100%	100%	100%	29%

† Concrete was tested out of truck

†† Average 28-day compressive strength for lab-cured specimens

As stated previously, the engineers and inspectors were influenced by the contractor to use high slump concrete. The average slump was 3.75 in. (95 mm) for placement 1, increased to 4.25 in. (110 mm) for placement 2, and increased again to 5.25 in. (130 mm) for the placement 3. The air content also increased during the three placements, with respective values of 8.7, 9.8, and 9.9%.

The burlap was placed a little faster in placement 3 than in placements 1 and 2. Placement times ranged from 9 to 21 minutes with an average of 15 minutes.

The evaporation rate during the placement was not recorded but estimated to be about 0.03 lb/ft^2/hr (0.15 kg/m^2/hr).

6.3.22.8 Crack survey results for OP-p3

Two surveys have been completed on placement 3, at 13.3 and 24.9 months, giving crack densities of 0.421 and 0.871 m/m^2, respectively. The crack map at 24.9 months is shown in Figure 6.54. Similar to placements 1 and 2, both long and short transverse cracks have developed. The high-slump concrete and extra finishing effort are probably the main reasons for the high crack density. All three placements have a significant number of short cracks.

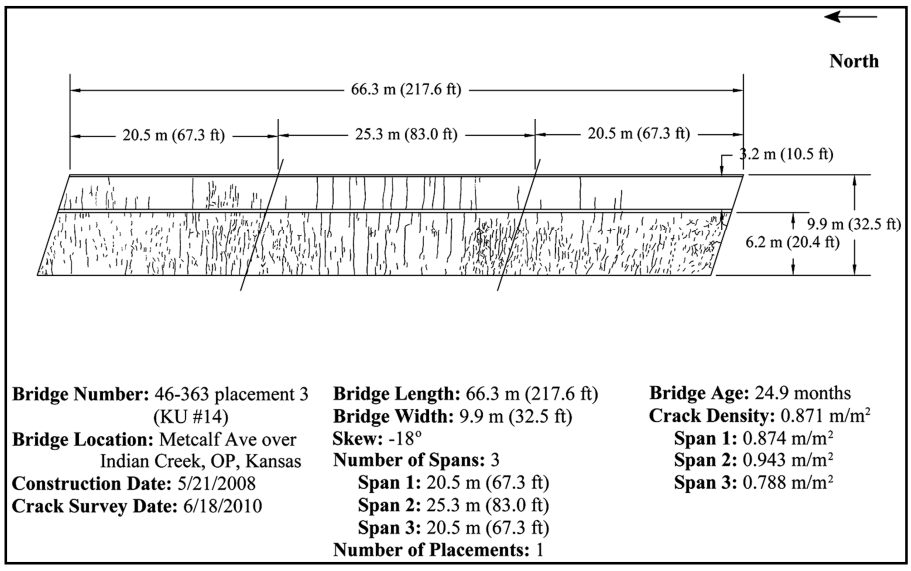

Figure 6.54 Crack map at 24.9 months for OP-p3

6.3.22.9 Crack density versus age for the OP and other LC-HPC decks

A plot of the crack density versus age for OP-p1, p2, and p3 is presented in Figure 6.55, along with the crack density of the LC-HPC decks described in this report. All three placements on the OP bridge had a high crack density at an early age (12 to 18 months old), which increased to a much higher value when the surveys were conducted a year later. The high crack density results from a number of causes, including out-of-specification concrete, with high slump and air content; inadequate and improper consolidation; over-finishing; and slow burlap placement. When the OP deck is compared with the LC-HPC decks in this study, the OP deck (three placements) has much higher crack densities at similar ages. The crack density increase rate for the OP deck is much higher than it is for the LC-HPC decks.

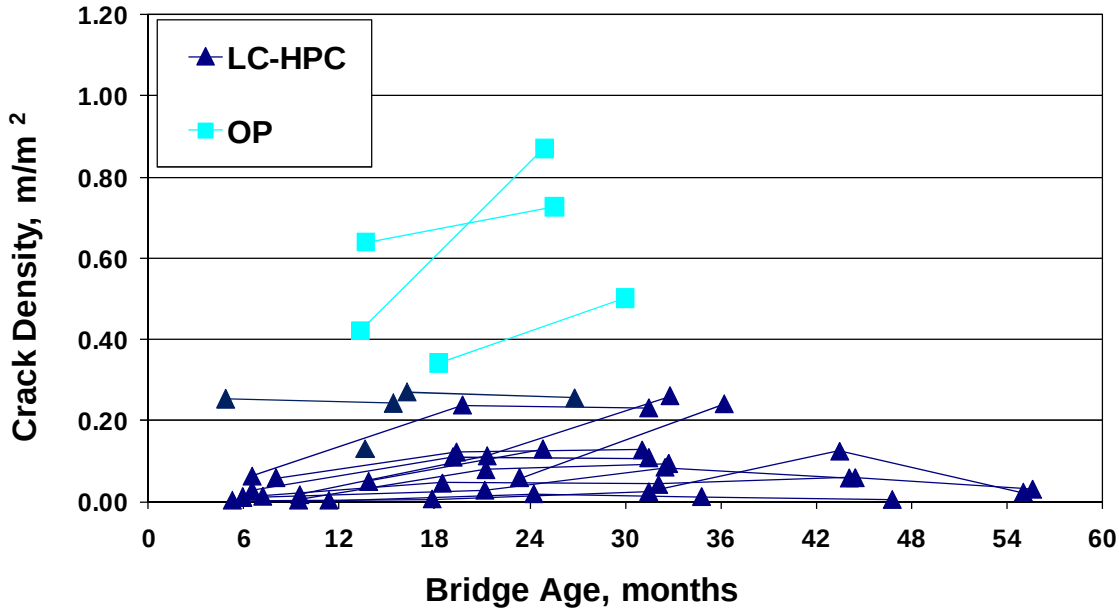

Figure 6.55 Crack density versus age of Overland Park (OP) and LC-HPC decks

6.3.23 Summary of Construction of LC-HPC Bridges

The techniques embodied in the low-cracking high-performance concrete bridge deck specifications are easy to learn. The contractors can be trained in a

relatively short time. Thirteen LC-HPC bridge decks have been successfully constructed in Kansas. A fourteenth deck was constructed that does not qualify as an LC-HPC deck because key aspects of the specifications were not followed by the contractor. The LC-HPC bridge decks and their corresponding control bridges have been surveyed annually for crack performance. The survey results indicate that LC-HPC bridge decks are performing much better than the control decks. The techniques used for LC-HPC bridge decks are effective in reducing bridge deck cracking.

During the construction of the thirteen LC-HPC and OP decks, many lessons have been learned. These lessons are summarized next.

6.3.23.1 Concrete mixture design

One of the key aspects of constructing LC-HPC bridge deck successfully is a constant supply of workable, placeable concrete. The concrete mixture proportions have been modified several times during the course of the project. For the first three LC-HPC decks that were constructed (LC-HPC 1, 2, and 7), the concrete mixture had a cement content of 540 lb/yd^3 (320 kg/m^3) and a *w*/*c* ratio of 0.45. The concrete was pumped, consolidated, and finished without any problems. In an effort to further reduce the free shrinkage and thus reduce the cracking potential of the concrete, the cement and water contents in the mixture were reduced. A concrete mixture having a cement content of 535 lb/yd^3 (317 kg/m^3) and a *w*/*c* ratio of 0.42 was used in the next three bridges (LC-HPC 8, 10, and 11), and the concrete was cast successfully. However, it has since been established that while reducing the *w/c* ratio for a given cement content will reduce drying shrinkage, it will not reduce cracking in bridge decks because it also results in higher tensile stresses in the deck due to an increased modulus of elasticity and decreased creep. In addition, when concrete with this cement content and *w/*c ratio, but different aggregate, was tried for LC-HPC 4, 5, and OP (three placements for the latter), many obstacles were encountered in achieving a

workable and placeable concrete. The difficulties are believed to have been caused by the use of a manufactured sand, which is more angular than natural sand. To minimize the sensitivity of the mixture to aggregate shape and produce workable concrete, the cement content and/or *w*/*c* ratio was increased. In the next bridges that were constructed, three different concrete mixtures were used, with a cement content of 535 lb/yd^3 (317 kg/m^3) and a *w*/*c* ratio of 0.45, a cement content of 535 lb/yd^3 (317 kg/m^3) and a *w*/*c* ratio of 0.44, or a cement content of 540 lb/yd^3 (320 kg/m^3) and a *w*/*c* ratio of 0.44.

The most recent LC-HPC specification requires a cement content between 500 and 540 lb/yd^3 (296 and 320 kg/m^3) and a water-cement (*w/c*) ratio of 0.44 or 0.45.

6.3.23.2 Concrete slump control

To minimize settlement cracking caused by high slump concrete, the LC-HPC specifications require a designated slump range of 1½ to 3.0 in. (40 to 75 mm). For the 14 bridge decks described in this study, a maximum slump of 4 in. (100 mm) was permitted to allow the flexibility during construction, with the expectation that the mix would be modified to meet the designated range. As it turns out, however, the slump of 4.0 in. (100 mm) was interpreted as the maximum allowable slump. Thus, in many cases, concrete with an average slump over 3.0 in. (75 mm) was used, and in fact preferred, by contractors. The percentage of slump tests with values greater than 3.0 in. (75 mm) for each LC-HPC placement is shown in Figure 6.56. The first placement for LC-HPC 4 is not included due to the suspected low water content and low w/c ratio of the concrete, which resulted from an incorrect moisture correction. As shown in Figure 6.56, 13 of the 18 LC-HPC placements had more than half of the recorded slump values greater than 3.0 in. (75 mm). On average for all 18 placements, 63% of the concrete that was tested had slumps greater than 3.0 in. (75 mm), 52% had slumps greater than or equal to 3.5 in. (90 mm), and 32% had slumps greater than or equal to 4.0 in. (100 mm).

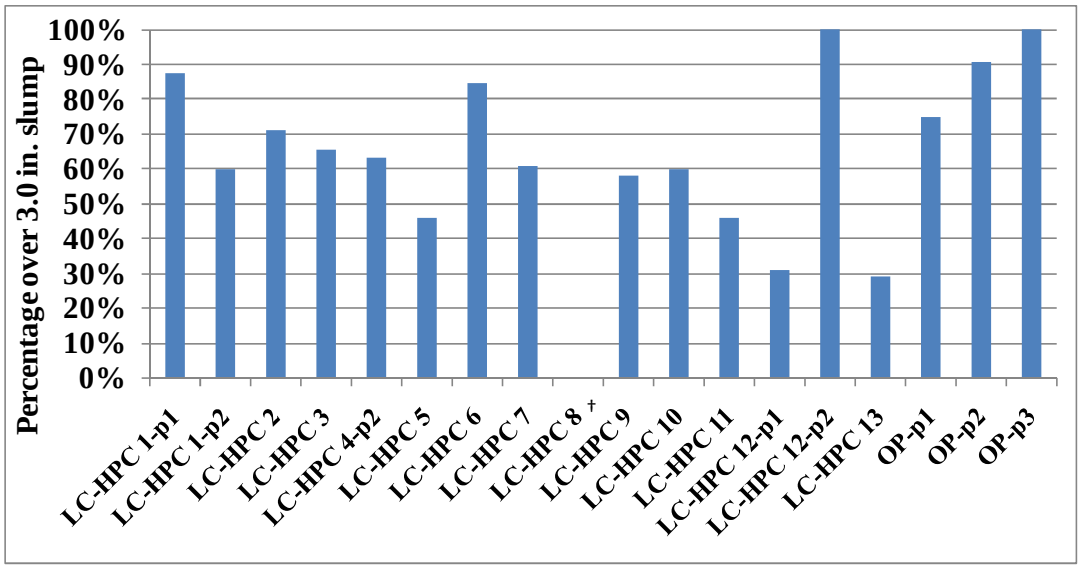

Figure 6.56 Percentage of slump tests with values greater than 3.0 in. (75 mm).
† All slump tests for LC-HPC 8 had values less than or equal to 3.0 in. (75 mm).

The slump tests results clearly demonstrate the tendency of contractors to use the maximum allowable slump. For this reason, the most recent specification has reduced the maximum slump at the truck to 3½ in. (90 mm) and limited the maximum slump on the deck to 3 in. (75 mm).

6.3.23.3 Concrete temperature control

In hot weather, the concrete temperature was controlled by replacing part of the mix water with chilled water, ice, or both, which worked well. However, the need for advanced planning can be underestimated by concrete suppliers. In several cases, the concrete supplier produced the qualification batch without considering the concrete temperature with the belief that this could be easily adjusted during construction. As a result, some placements were cancelled when the supplier could not produce in-specification concrete.

Concrete temperature during cold weather construction was not an issue in this study.

6.3.23.4 Concrete testing and acceptance

It is important to have a clear schedule and plan for how to handle out-of-specification concrete. Experience in this study indicates that a good method is to test the first few trucks for all requirements, including slump, air content, temperature, and unit weight, and not allow any out-of-specification concrete to be cast in the deck. The careful check of the first few trucks sets the tone for testing for the contractor and the concrete supplier. Later in the placement, when testing is performed at a lower frequency, if one truckload concrete is found to be out-of-specification, the following trucks should be checked until the specifications are met. An experienced inspector should be assigned to visually check all of the concrete out of the truck, and any suspected out-of-specification concrete should be checked.

For out-of-specification concrete, some adjustment on site has been allowed, including re-dosing with chemical admixtures and letting the truck sit for a period of time to allow a high slump and/or air content to drop. Under the latest LC-HPC specifications, all mix water must be added at the concrete plant.

6.3.23.5 Concrete compressive strength

The average 28-day compressive strength for the LC-HPC bridges ranged from 3710 to 6380 psi (25.6 to 44.0 MPa). The concrete mixtures for the 14 bridges had cement contents of 535 or 540 lb/yd^3 (317 or 320 kg/m^3) and water-cement (*w*/*c*) ratios ranging from 0.42 to 0.45. The type of water reducer was found to have a great influence on the compressive strength.

In Figure 6.57 the bridges are grouped into three categories based on *w/c* ratio. Three LC-HPC bridges [with the designation KU (in place of LC-HPC) 3, 5, and 6] with a Type A-F high-range water reducer (polycarboxylate-based) had the highest compressive strengths, around 6000 psi (41.4 MPa) regardless of the *w*/*c* ratio. The influence of Type A or Type A-F mid-range water reducers (lignosulfonate-based) on compressive strength is less apparent in this study.

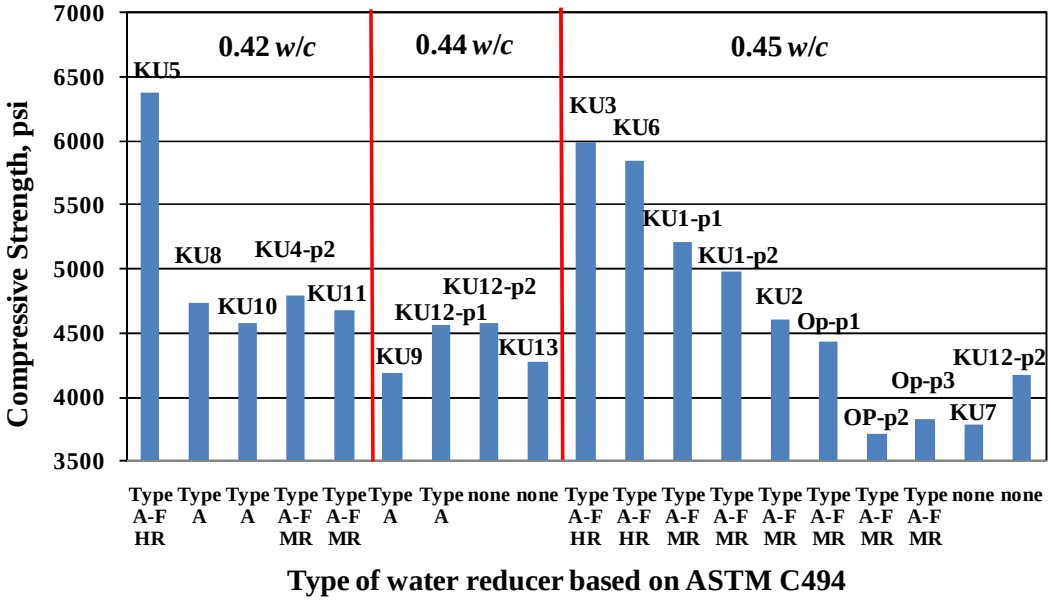

Figure 6.57 Compressive strength versus water-cement ratio and type of water-reducer (Type A-F HR: Type A-F high range water reducer (polycarboxylate-based), Type A: Type A water reducer (lignosulfonate-based), Type A-F MR: Type A-F middle range reducer (lignosulfonate-based), none: water reducer was not used for mix). Note: The actual *w/c* ratio for KU 8 and 10 was a little lower than designed because some water was withheld during construction; 1000 psi = 6.895 MPa

Because an increase in concrete strength normally results in an increase in cracking, high-strength concrete should be avoided in bridge decks. The most recent LC-HPC specifications limit compressive strength to values between 3500 and 5500 psi (24.1 and 37.9 MPa).

6.3.23.6 Qualification batch and qualification slab

The importance of the qualification batch and slab has been proven for the LC-HPC decks constructed in Kansas. Experience demonstrates that completing a qualification batch that meets all specifications is vital for successful placement of the qualification slab and the deck.

The importance of the qualification slab has also been demonstrated. Most importantly, contractor personnel gain experience working with LC-HPC, which has a low slump and paste content. The placing procedures, by pump, conveyor belt, or

bucket, can be evaluated and modified, if needed. For example, in two placements, the concrete was originally planned to be pumped, but due to pumping difficulties during the qualification slab caused by larger-sized aggregate particles, conveyor belts were used. The methods of consolidating, finishing, and curing are examined and modified, if needed. Burlap placement, which must be complete within 10 minutes of strike-off and is totally new to most contractors, can be practiced. One KDOT inspector remarked that one could see how much the contractor learned from the beginning to the end of the qualification slab.

6.3.23.7 Concrete placement method

Of the 18 placements described in this report, 11 used a pump, five used a conveyor belt, and two used a bucket. The estimated placement rate for each type of construction is presented in Figure 6.58; the placement rates for LC-HPC 4-p1, 7, and OP-p1 are not included because the total number of truckloads was not recorded. As expected, buckets provided the slowest placement rate, while a concrete pump provided the fastest. Overall, average placement rates of 35 yd^3/hr (26.7 m^3/hr), 52 yd^3/hr (39.6 m^3/hr), and 63 yd^3/hr (48.4 m^3/hr) were obtained using buckets, conveyor

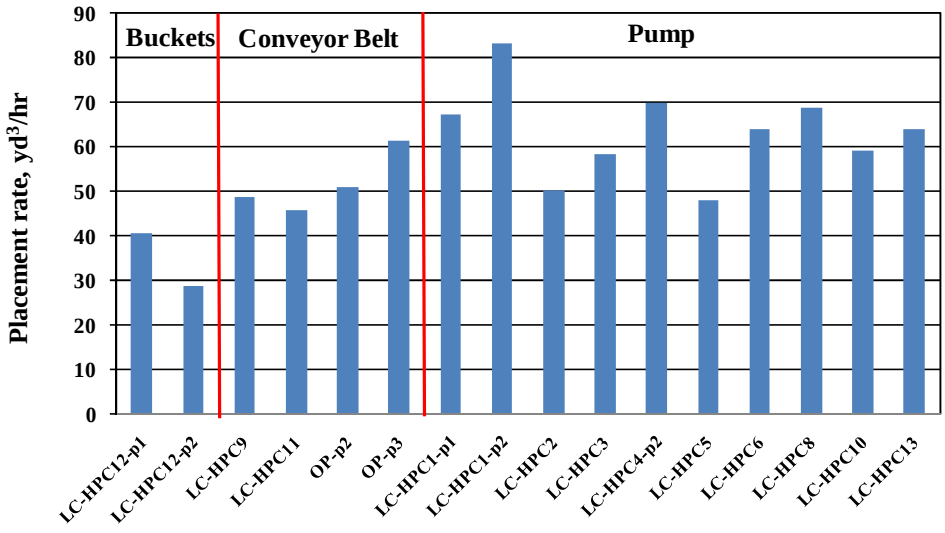

Figure 6.58 Estimated placement rate for different placement methods. Note: 1 yd^3/hr = 0.765 m^3/hr

belts, and pumps, respectively. The relative rates for conveyor belts and pumps, however, likely reflect the rate of concrete delivery, as much as they do the speed of placement. In addition, long delays occurred at the end of construction, in many cases due to the contractor's need to back-order concrete.

Air content losses through a pump and off a conveyor belt were recorded for 18 trucks across nine placements. The air content loss for each truck is listed in Figure 6.59. For concrete delivered by a pump with a bladder valve that was operated to limit the rate of drop of the concrete or with an S-hook, the air loss was just 0.5 to 0.8%, with an average of 0.65%. For concrete delivered by pump for which no measures were taken to restrict the concrete flow, the air loss increased to be between 1.1 and 2%, with an average of 1.5%. For concrete delivered by a conveyor belt, the air loss ranged from 0.5 and 2.4%, with an average of 1.6%.

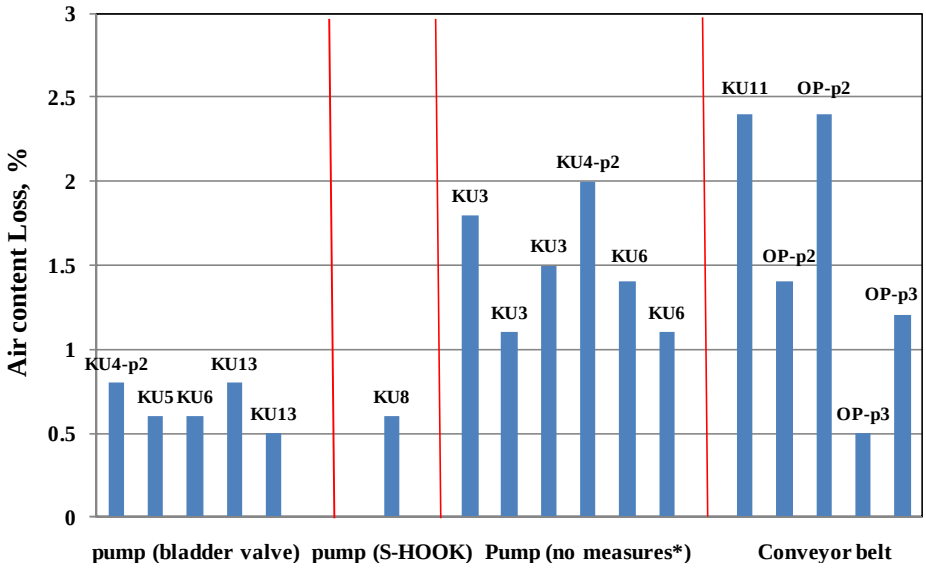

Figure 6.59 Air content loss through a pump or conveyor belt. * No measure taken to limit air loss.

The latest LC-HPC specifications now require that the maximum drop from the end of a conveyor belt, pump, or a concrete bucket is 5 ft (1.5 m). For pumps, an air cuff/bladder valve must be used to limit air loss.

Two pumps or two conveyor belts are required on the job site to minimize delays caused by relocating the equipment and to ensure that the contractor is prepared in case one pump or conveyor belt does not function properly.

6.3.23.8 Consolidation and finishing

Different contractors performed differently in terms of consolidation and finishing operations. Some contractors tended to put more effort into finishing than others. The general rule with regard to finishing is "less is more."

6.3.23.9 Crack survey results

Crack surveys for both LC-HPC and Control bridge decks are performed annually. The most recent surveys have been completed with the LC-HPC decks at an age of about three years, with the youngest deck at 13.6 months and the oldest at 55.6 months. The survey results indicate that all LC-HPC decks (except LC-HPC 8, one of two decks constructed on prestressed concrete girders) have performed better than the corresponding control decks at similar ages. An apparent increase in crack density from year one to year two has been noted for many decks; after two years, the crack density increase rate slows for most LC-HPC decks, while the same is not true for control decks.

Crack maps for both LC-HPC and control bridges consistently indicate that transverse cracks are the dominant type observed on bridge decks. Longitudinal cracks are found primarily near the abutment. Most cracks on LC-HPC decks are short, with few cracks crossing the full width of the bridge. Both short and long cracks are noted on control decks with many crossing the full width.

For the OP deck (with many aspects not meeting the LC-HPC specifications, including out-of-specification concrete with high slump and air content; inadequate and improper consolidation; over-finishing; and slow burlap placements), cracking has been similar to that observed on control decks.

Additional discussion of cracking performance is presented in Section 6.4.

6.4 FACTORS AFFECTING BRIDGE DECK CRACKING

In this section, the factors influencing bridge deck cracking, including material factors and site conditions, are investigated. The cracking performance of LC-HPC decks is compared with control decks, as well as with decks surveyed in the three previous studies at the University of Kansas (Schmitt and Darwin 1995, Miller and Darwin 2000, Lindquist et al. 2005).

6.4.1 Cracking Rate of LC-HPC and Control Decks

Crack density is plotted versus age for the LC-HPC and control decks in Figures 6.60 and 6.61, respectively. Data points connected by lines indicate the same bridge has been surveyed multiple times. Several LC-HPC placements are excluded here: LC-HPC 4-p1 is excluded due to its unknown, but, low water-cement ratio and construction difficulties (discussed in Section 6.3.11.4). LC-HPC 12-p1 is excluded due to the unusually heavy load caused during construction of LC-HPC 12-p2 (discussed in Section 6.3.16.2). Because the three placements of the OP deck were completed with many aspects not meeting the LC-HPC specifications (discussed in Section 6.3.22), they are not included in the LC-HPC deck analysis. LC-HPC 8 and 10 are the only two decks constructed on the prestressed concrete girders, while all other LC-HPC and control decks are constructed on steel girders; they are not included in the analysis either.

Over the life of the decks, the crack density of LC-HPC decks has ranged from 0.003 to 0.254 m/m^2 with the majority under 0.15 m/m^2, while the crack density for the control decks has ranged widely, from 0 to 1.040 m/m^2. As shown in Figure 6.60, many LC-HPC decks have very low crack densities between 6 and 12 months, and then the crack densities increase slightly in later ages; for LC-HPC decks demonstrating high crack densities during the first survey, normally at one year of age, no apparent increase is noted in the following surveys. Control decks exhibit more cracking and a higher rate of cracking over time than LC-HPC decks, as shown in

Figure 6.61. Some control decks also have relatively low crack densities at early ages but values above that for the matching LC-HPC decks and much higher crack densities than LC-HPC decks at later ages.

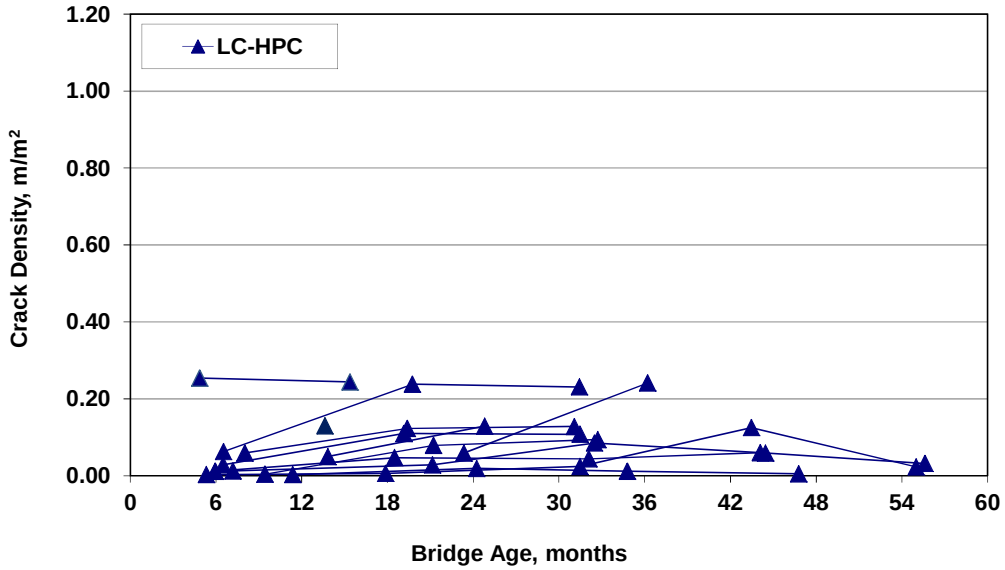

Figure 6.60 Crack density versus age for LC-HPC decks. Data points connected by lines represent the same deck.

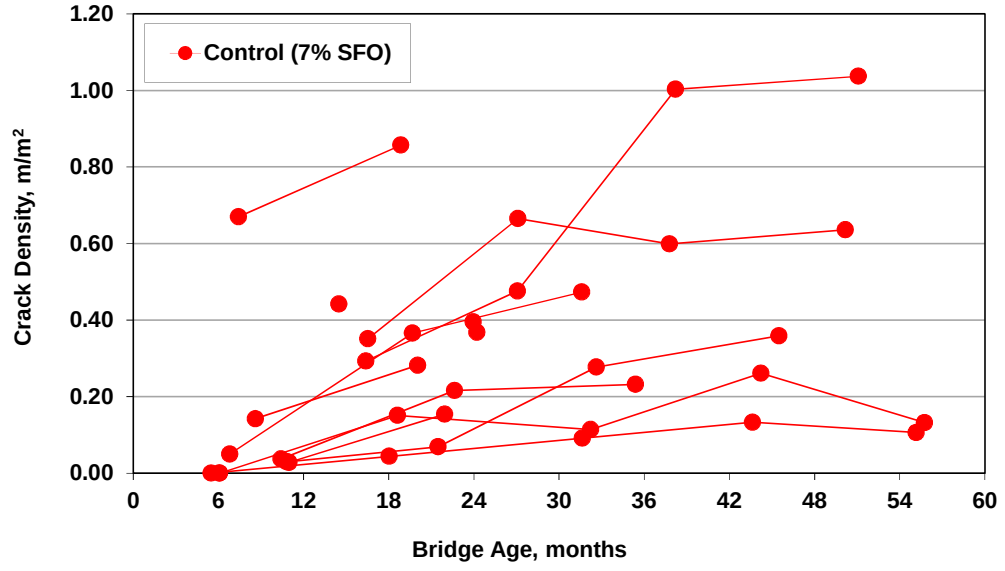

Figure 6.61 Crack density versus age for control decks. Data points connected by lines represent the same deck.

The cracking rate for both LC-HPC and control decks can be determined periodically using the results of two successive surveys; the results are presented in Figure 6.62. For the purpose of the plots, decks with a drop in crack densities from one survey to next are treated as having no increase between the two surveys.

Because the decks were built and surveyed at different times, the time range of two successive surveys between the LC-HPC and control bridges may differ to some extent. As shown in Figure 6.62, the average cracking rate for LC-HPC decks is 0.0044 m/m^2/month (Figure 6.62a) between 8 and 18 months; by way of comparison, the average cracking rate for control decks is 0.0138 m/m^2/month (Figure 6.62b) between 11 and 22 months, or about three times the rate for LC-HPC decks. The cracking rate for the LC-HPC decks decreases to 0.0025 m/m^2/month between 21 and 33 months (Figure 6.62c), while the cracking rate for the control decks decreases to 0.0114 m/m^2/month between 22 and 34 months (Figure 6.62d). Only a few surveys have been completed after three years of age and the cracking rate is zero for LC-HPC decks (Figure 6.62e) and 0.0027 m/m^2/month for control decks (Figure 6.62f). More surveys will be done in the future.

To summarize, control decks have a much higher (three times or more) cracking rate than LC-HPC decks at all ages. Both LC-HPC and control decks have a high cracking rate during the first two years; the cracking rate for LC-HPC decks between two and three years decreases quickly to about half of the rate during the first two years and, to date, has decreased to zero after three years of age; the cracking rate for control decks decreases at a much lower rate. The higher rate for control decks can be correlated to their higher paste contents, which range from 25.6 to 29%, compared with 23.4 to 24.6% for LC-HPC decks.

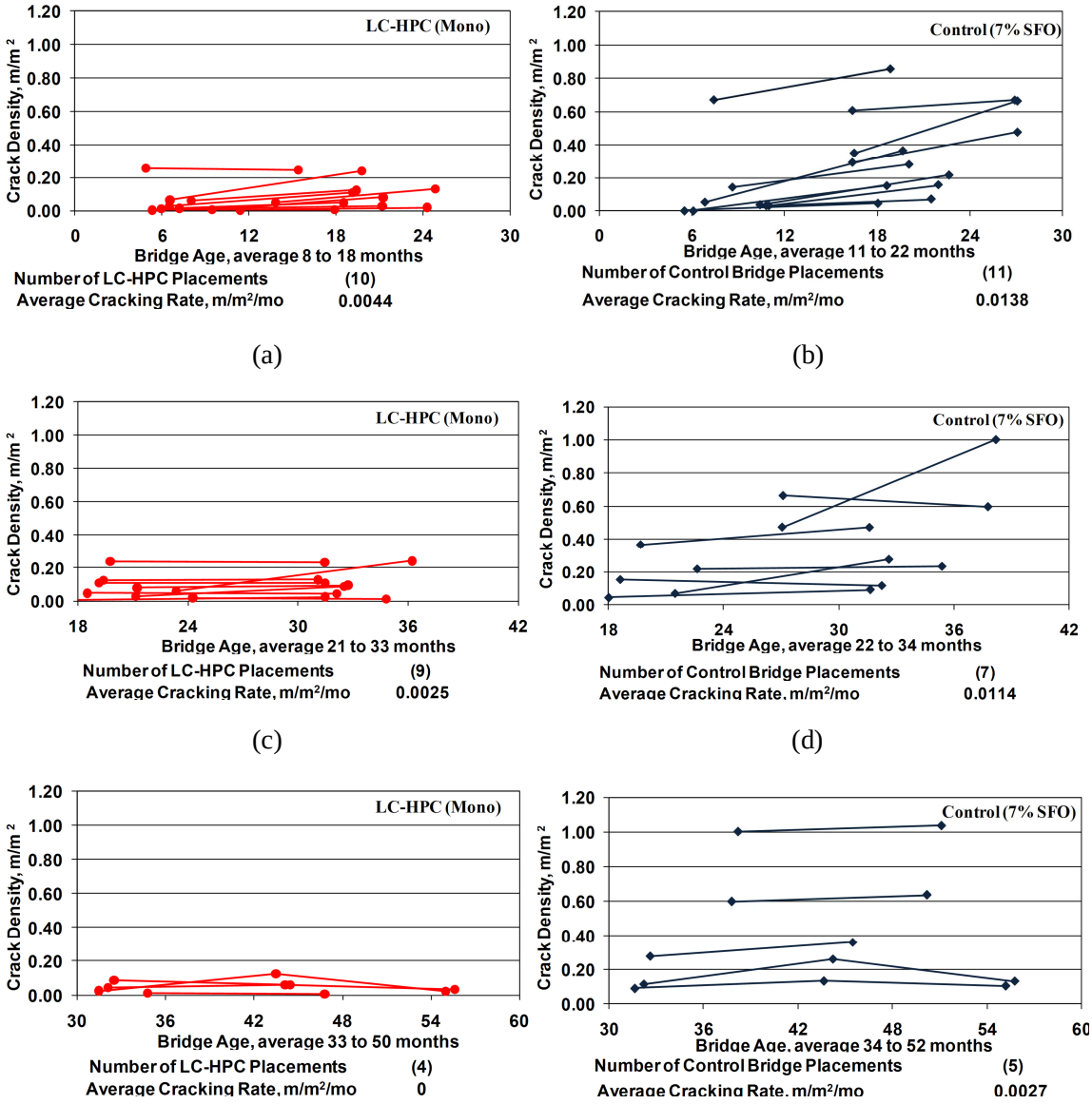

Figure 6.62 Cracking density versus age for different time periods for LC-HPC and Control decks. (a) cracking between 8 and 18 months for LC-HPC decks; (b) cracking between 11 and 22 months for Control decks; (c) cracking between 21 and 33 months for LC-HPC decks; (d) cracking between 22 and 34 months for Control decks; (e) cracking between 33 and 50 months for LC-HPC decks; (f) cracking between 34 and 52 months for Control decks.

6.4.2 Cracking Rate of Bridge Decks Surveyed in Previous Studies

Prior to this study, three bridge deck cracking studies (Schmitt and Darwin 1995, Miller and Darwin 2000, Lindquist et al. 2005) were completed by the University of Kansas. The studies evaluated four bridge deck types: 5% and 7% silica fume overlays (SFO), conventional high-density overlays, and conventional monolithic placements. A total of 139 surveys involving 76 bridges (160 individual concrete placements) had been completed. The average cracking rate at different age ranges (depending on available data) for these conventional monolithic and overlay bridges are determined in this section and compared with LC-HPC (monolithic) and control bridges (7% SFO).

The cracking rates of conventional monolithic decks in the three previous studies (Schmitt and Darwin 1995, Miller and Darwin 2000, Lindquist et al. 2005) are compared with the rates for LC-HPC decks in Figure 6.63. The age of the LC-HPC decks ranges from 5 to 56 months, with many surveys having been completed during the first three years. For the conventional monolithic bridge decks in previous studies,

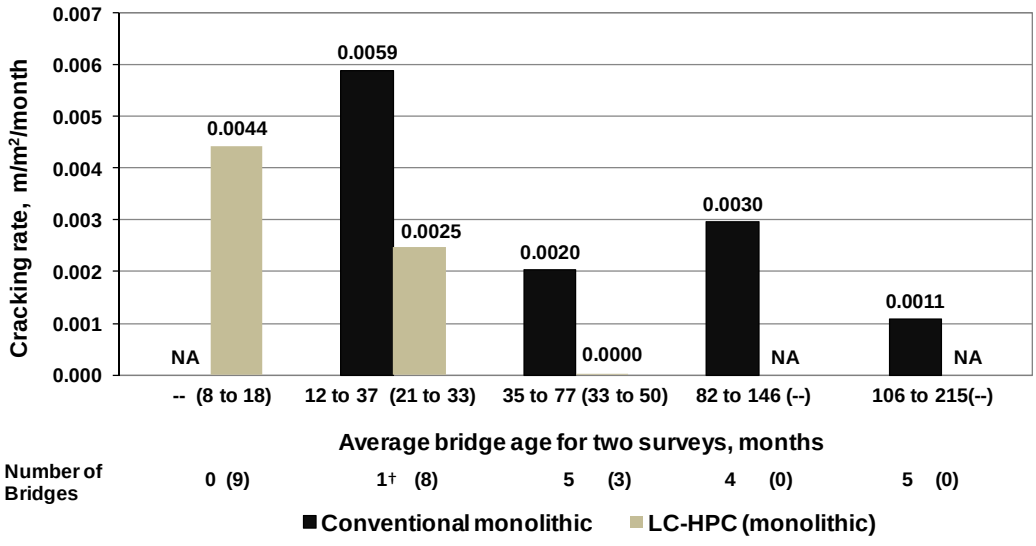

Figure 6.63 Cracking rate for different time periods, including conventional monolithic decks in previous studies (Schmitt and Darwin 1995, Miller and Darwin 2000, Lindquist et al. 2005) and LC-HPC decks in this study. † This deck was surveyed in this study.

most have been first surveyed at three years of age or later. One conventional monolithic bridge was surveyed twice within three years of construction in this study and has a cracking rate of 0.0059 m/m^2/month between 12 and 37 months. The conventional monolithic decks have an average cracking rate of 0.0020 m/m^2/month between 35 and 77 months, 0.0030 m/m^2/month between 82 and 146 months, and 0.0011 m/m^2/month between 106 and 215 months. The cracking rate is lowest between 106 and 215 months. The LC-HPC decks have an average cracking rate of 0.0044 m/m^2/month between 8 and 18 months, 0.0025 m/m^2/month between 21 and 33 months, and, to date, zero after 33 months.

The control decks in this study have 7% silica fume overlays (SFO) and an average cracking rate of 0.0138 m/m^2/month between 11 and 22 months, 0.0114 m/m^2/month between 22 and 34 months, and 0.0027 m/m^2/month between 34 and 52 months, as shown in Figure 6.64a. The 7% SFO decks in previous studies (Schmitt and Darwin 1995, Miller and Darwin 2000, Lindquist et al. 2005) were only surveyed once. Lindquist et al. (2005) found that the 7% and 5% silica fume overlay decks had nearly the same mean crack densities and, thus, considered the two silica fume overlays as a single deck type. As shown in Figure 6.64b, the cracking rates of the 5% silica fume overlays are 0.0043, 0.0038 and 0.0041 m/m^2/month between 12 and 68 months, 26 and 76 months, and 35 and 88 months, respectively. It should mention that different SFO decks were surveyed for the three age categories.

When LC-HPC, conventional monolithic, and 5% and 7% (control) SFO decks are considered together, it can be concluded that at similar ages the LC-HPC decks have the lowest cracking rate, followed by conventional monolithic decks, and then SFO decks.

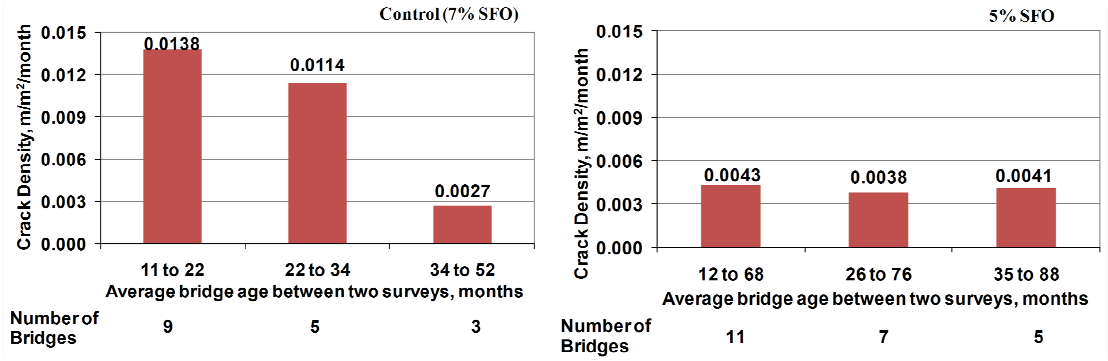

(a) (b)

Figure 6.64 Cracking rate at different time periods: (a) Control decks with 7% silica fume overlay, (b) 5% silica fume overlay decks in previous studies (Schmitt and Darwin 1992, Miller and Darwin 2000, Lindquist et al. 2005).

6.4.3 Crack Densities at 36 Months

As discussed in Sections 6.4.1 and 6.4.2, crack density increases over time for all bridge deck types. To eliminate bridge age as a variable and allow bridges to be compared on an equal-age basis, the crack density at 36 months is determined as follows. For LC-HPC (monolithic) and Control (7% SFO) decks which are surveyed annually after they are constructed, if the deck is surveyed at before and after 36 months, the crack density at 36 months is interpolated between the two crack densities; if the latest survey is between 30 and 36 months, the latest crack density is used as the crack density at 36 months; if the latest survey is at ages younger than 30 months, the deck is not included in the current analysis. It should be mentioned that the crack density for Control 11 deck decreased from 0.665 m/m^2 at 27.1 months to 0.599 m/m^2 at 37.8 months because some cracks were obscured by scaling of the deck surface. The crack density at 27.1 months (0.665 m/m^2) is, therefore, used as the value for 36 months. For decks in the previous three studies (Schmitt and Darwin 1992, Miller and Darwin 2000, Lindquist et al. 2005), if crack densities are available both before and after 36 months, the crack density at 36 months is interpolated between the two. In many cases, however, the first survey is conducted after 36 months, and the crack density is then extrapolated back to 36 months based on the

two consecutive surveys after 36 months. In those cases, it is assumed that the crack density for conventional monolithic and overlay decks increases at a constant rate after 36 months. In some cases, the crack density has decreased over time, and the crack density between 36 and 48 months, if available, is used; otherwise, the deck is not included in the analysis. Because the bridge decks with a 7% SFO in previous studies (Miller and Darwin 2000, Lindquist et al. 2005) were only surveyed once, they are excluded from the analysis. The crack densities at the time of survey and the interpolated crack densities at 36 months for each placement are presented in Tables F.1 to F.5 in Appendix F.

The average crack densities at 36 months for each bridge deck type are presented in Figure 6.65. LC-HPC decks have the lowest crack density at 36 months, 0.104 m/m^2. When control decks (7% SFO), with similar design, traffic conditions, and date of construction as the LC-HPC decks but constructed based on the Kansas Department of Transportation (KDOT) standard bridge specifications, are analyzed, the average crack density at 36 months is 0.399 m/m^2, which is about four times the value for LC-HPC decks. Only one placement of the OP deck is old enough (surveyed at 30 months) and has a crack density of 0.502 m/m^2. For the decks surveyed in previous studies, the crack densities at 36 months for conventional monolithic, conventional overlay, and 5% SFO are 0.319, 0.582, and 0.410 m/m^2, respectively. LC-HPC decks have the best performance among all bridge decks surveyed in Kansas.

In the comparisons that follow, the crack densities at 36 months are used to evaluate the influence of material and site conditions on cracking.

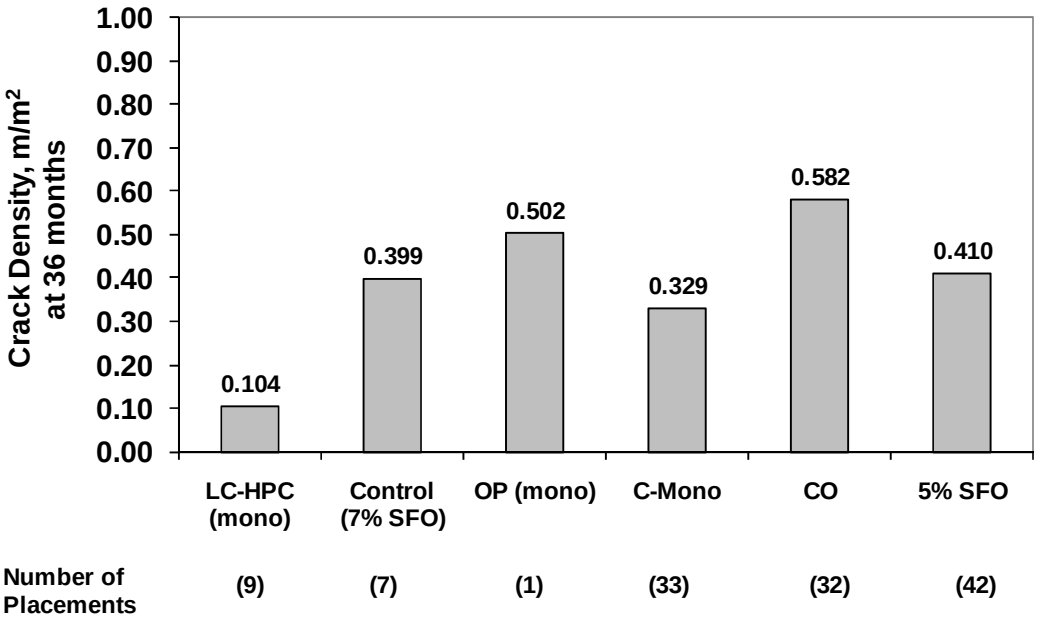

Figure 6.65 Crack density at 36 months for each deck type: LC-HPC (monolithic), Control (7% silica fume overlay), OP deck, Conventional Monolithic bridge decks (C-Mono), Conventional Overlay (CO), and Silica Fume Overlay (5% SFO).

6.4.4 Factors Affecting Cracking of Monolithic Bridge Decks – Dummy Variable Analysis

As discussed in Section 6.4.3, the crack densities at 36 months are determined, which make it possible to compare decks on an equal-age basis and determine the factors affecting cracking. The LC-HPC bridge decks in this study were placed monolithically on steel girders, with the exception of LC-HPC 8 and 10, which were placed on prestressed concrete girders. In addition the LC-HPC decks, the crack density at 36 months of the OP deck (first placement) and 15 monolithic bridge decks (including 33 placements) in previous studies (Schmitt and Darwin 1995, Miller and Darwin 2000, Lindquist et al. 2005) are also determined. Among the 33 placements surveyed in previous studies (Schmitt and Darwin 1995, Miller and Darwin 2000, Lindquist et al. 2005), the construction data of three placements are not available and not included in the analysis. In total, the data pool consists of 21 monolithic decks and 40 individual placements involving nine different contractors. For each

placement, the crack density at 36 months, material data including concrete mixture proportions, slump, air content, and compressive strength, and weather conditions are available. For that data pool, the factors that affect cracking for monolithic bridge decks are discussed as follows.

Based on the available data for each placement, five factors, paste content, slump, compressive strength, maximum air temperature and air temperature range on the day of construction, are used to evaluate their effects on cracking. The concrete behaviors that influence cracking, associated for each factor, are listed in Table 6.40. A higher paste content usually corresponds to more drying shrinkage of a concrete mixture and a higher heat of hydration at a constant *w/c* ratio, and thus, an increased potential for shrinkage cracking and thermal contraction; increased slump increases settlement cracking; increased compressive strength may result in increased cracking in bridge decks because less creep occurs at early ages; a high maximum air temperature results in an increased potential for both plastic shrinkage and thermal cracking; and an increase of the range of air temperature on the day of construction increases the potential for thermal contraction.

Table 6.40 Investigated factors that may affect bridge deck cracking

Factor	**Higher paste content**	**Higher slump**	**Higher compressive strength**	**Maximum daily air temperature**	**Higher daily air temperature range**
Concrete behavior that influences cracking	Drying Shrinkage, thermal contraction (heat of hydration)	Settlement cracking	Creep	Plastic shrinkage, thermal contraction	Thermal contraction

To determine the contribution of each factor to cracking, it is assumed that the crack densities are a function of the independent factors listed in Table 6.40. The coefficient corresponding to each independent factor is determined using least square regression analysis. Because the construction techniques applied by a contractor have

influence on bridge deck cracking (Cady et al. 1971, Lindquist et al. 2005), the dummy variable technique (Draper and Smith 1981) is used, where a dummy variable is assigned for each contractor. The analysis is based on the assumption that the independent factors have a similar effect on the dependent variable, in this case the crack density for all contractors, although there may be systematic differences between contractors, which are represented using the dummy variables. The calculation is illustrated in Eq. (6.1).

$$Y = \alpha_1 X_1 + \alpha_2 X_2 \ldots + \alpha_n X_i + \beta_1 Z_1 + \beta_2 Z_2 \ldots . + \beta_{n-1} Z_{n-1} \quad (6.1)$$

where Y = dependent, age-corrected crack densities

$X_1, X_2, \ldots X_i$ = independent factors that may affect bridge deck cracking, which are paste content, slump, compressive strength, maximum daily air temperature, and daily air temperature range, respectively, in this analysis

$\alpha_1, \alpha_2, \ldots \alpha_n$ = coefficients corresponding to each X-value

$Z_1, Z_2, \ldots Z_{n-1}$ = dummy variables assigned to each contractor

= 0 for one contractor and 1.0 for all others

$\beta_1, \beta_2, \ldots \beta_{n-1}$ = coefficients corresponding to each Z-value

The range in the values of the independent factors for the 21 monolithic decks (40 individual placements) is shown in Table 6.41. The coefficient corresponding to each independent factor is shown in Table 6.42. The analysis demonstrates that paste content affects bridge deck cracking, with a confidence level of 85%, and an increase of 1% paste content increases crack density by 0.066 m/m^2. The slump ranges from 1.5 to 4 in. (40 to 100 mm) in the data pool, and an increase of 1 in. (25 mm) slump increases crack density by 0.054 m/m^2, with a confidence level of less than 80%. The influence of slump on cracking would likely be clearer if the percentage of slump values over 3.5 in. (90 mm) for each placement were used in the analysis (see Section

6.4.5.2), but those data are not available for the decks in previous studies (Schmitt and Darwin 1995, Miller and Darwin 2000, Lindquist et al. 2005). The compressive strength has the greatest influence, and an increase of 1000 psi (6.89 MPa) in compressive strength increases crack density by 0.140 m/m^2, with a confidence level of 95%. The maximum air temperature and daily air temperature range also influence bridge deck cracking with coefficients of 0.006 and 0.003 and confidence levels of 90% and less than 80%, respectively. An increase of 10° F (5.6° C) in the maximum daily air temperature increases crack density by 0.06 m/m^2, and an increase of 10° F (5.6° C) of the daily air temperature range increases crack density by 0.03 m/m^2. It should be noted that curing methods for LC-HPC decks have reduced impact of temperature on cracking.

Table 6.41 Value range of each independent factor for the 40 monolithic deck placements

Factors	Paste content %	Average slump in.	Compressive strength, psi	Maximum daily air temperature, °F	Daily air temperature range, °F
Minimum	23.3	1.5	3790	43	4
Maximum	28.7	4.0	7430	97	40
Average	26.4	2.5	5560	68	24

Note: 1 in.. = 25.4 mm, temperature in °F = temperature in °C × 5/9 + 32. 1 psi = 0.0069 MPa

Table 6.42 Relationship between crack densities (at 36 months) and individual factors

Factors	Paste content %	Average slump in.	Compressive strength, ksi	Maximum daily air temperature °F	Daily air temperature range, ° F
Coefficient α	0.066	0.054	0.140	0.006	0.003
T-Test, Confidence Level	90%	<80%	95%	90%	<80%
R^2	0.839				
F-Test	0.00001%				

T-Test, confidence level: the confidence level that each coefficient is useful in estimating the crack densities.
R^2: the coefficient of determination
F-Test: the probability that the observed relationship between the dependent and independent variables occurs by chance

The coefficients corresponding to the contractors are shown in Table 6.43. The contractor Z9 serves as the reference contractor. A positive coefficient for a contractor indicates that more cracking is expected for decks constructed by that contractor than expected for contractor Z9, while a negative coefficient indicates less cracking is expected, in all cases independent of the variables in Tables 6.40 through 6.42. The coefficients range from –0.591 to 0.685. The variation in coefficients within the group of contractors suggests that contractor techniques can influence cracking.

Table 6.43 Coefficient for each dummy variable assigned for each contractor

Contractor	Z1	Z2	Z3	Z4	Z5	Z6	Z7	Z8	Z9
Coefficient β	0.084	-0.591	0.051	-0.032	0.182	-0.004	0.685	0.455	-
T-Test, Confidence Level	<80%	95%	<80%	<80%	<80%	<80%	99%	95%	-

When the values in Tables 6.42 and 6.43 are used in Eq. (6.1), the crack density for each placement can be calculated based on the actual paste content, slump, compressive strength, maximum daily air temperature, daily air temperature range, and dummy variables assigned to the corresponding contractor. The calculated crack densities based on the coefficients determined in the dummy variable analyses are compared with the interpolated crack densities at 36 months in Figure 6.66. As shown in the figure, the crack density for conventional monolithic decks ranges widely, from 0 to over 1 m/m^2, while the crack density for LC-HPC decks remains in a small range, all below 0.3 m/m^2. Overall, the crack densities of the LC-HPC decks are much lower than the crack densities of the conventional monolithic decks. Using the coefficients shown in Tables 6.42 and 6.43 can provide a fair predication of the crack density at 36 months.

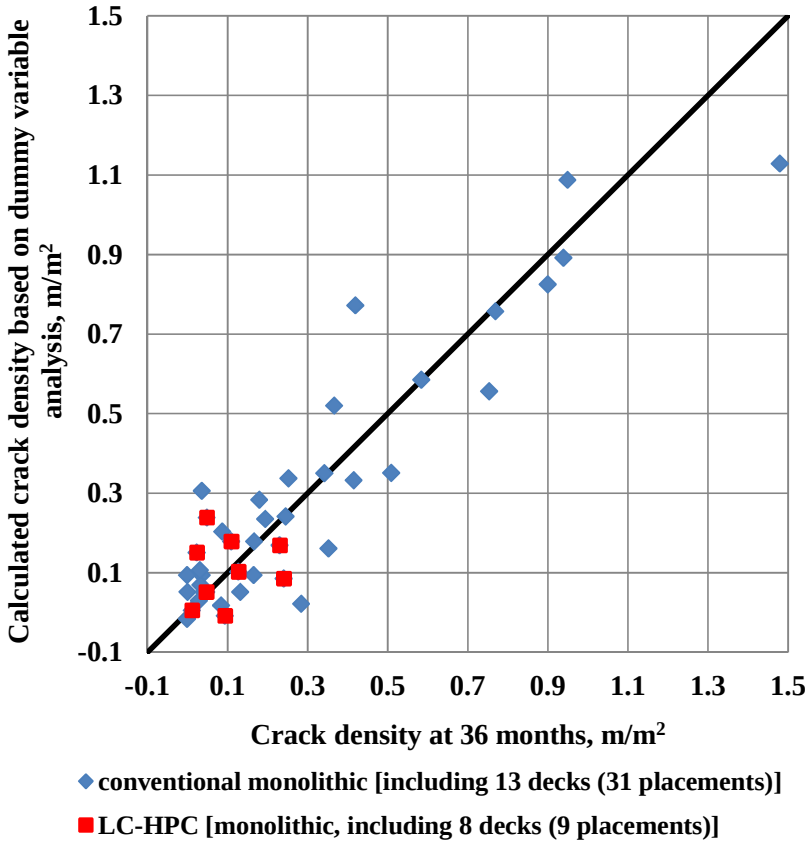

Figure 6.66 Calculated crack density based on dummy variable analysis versus interpolated crack density at 36 months.

6.4.5 Material Factors Affecting LC-HPC Bridge Deck Cracking

Detailed material information was gathered during LC-HPC deck construction. The material factors, including paste content, slump, compressive strength, and air content, are investigated for their influence on bridge deck cracking based on crack density at 36 months.

6.4.5.1 Paste Content

Previous research (Lindquist et al. 2005) found that the level of cracking was significantly reduced by using paste content less than 27%. For paste contents below 27%, little change in crack density was noted. The paste content for the LC-HPC decks ranges from 23.4 to 24.6%, and the change in paste content primarily

corresponds to changes in water-cement (*w/c*) ratio between 0.42 and 0.45, as shown in Figure 6.67, when crack density at 36 months is plotted versus paste content and w/c ratio (LC-HPC is designated as KU to avoid over-crowding the figure). The influence of lower paste content on reducing crack densities is not apparent in Figure 6.67 within the narrow range of the paste contents considered, suggesting that other factors play more important roles once the paste content is sufficiently low.

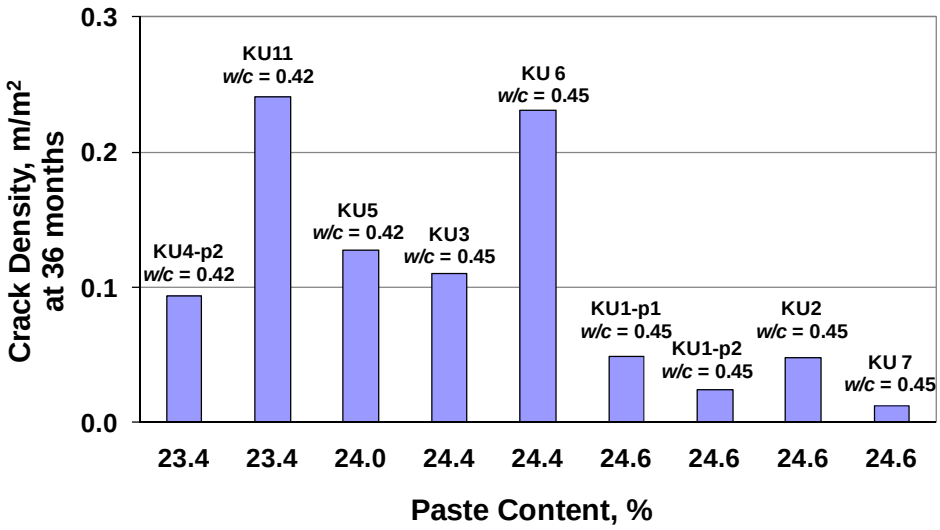

Figure 6.67 Crack density at 36 months versus paste content and water-cement (*w/c*) ratio for LC-HPC bridges

6.4.5.2 Slump

Crack density at 36 months is plotted versus slump for LC-HPC decks (designated as KU) in Figure 6.68. The three placements for the OP deck are included in this comparison. It should be noted that the crack densities for KU12-p2, OP-p2, and OP-p3 are at 15.4, 25.5, and 24.9 months, respectively, while all others are at 36 months. The relationship between high slump and high crack density is quite obvious in that the five decks with the highest crack densities (OP-p1, KU 6, KU 12-p2, OP-p2, and OP-p3) also have the highest slump values, four of them with an average slump of greater than or equal to 4.0 in. (100 mm) and other having an average slump of 3.75 in. (95 mm).

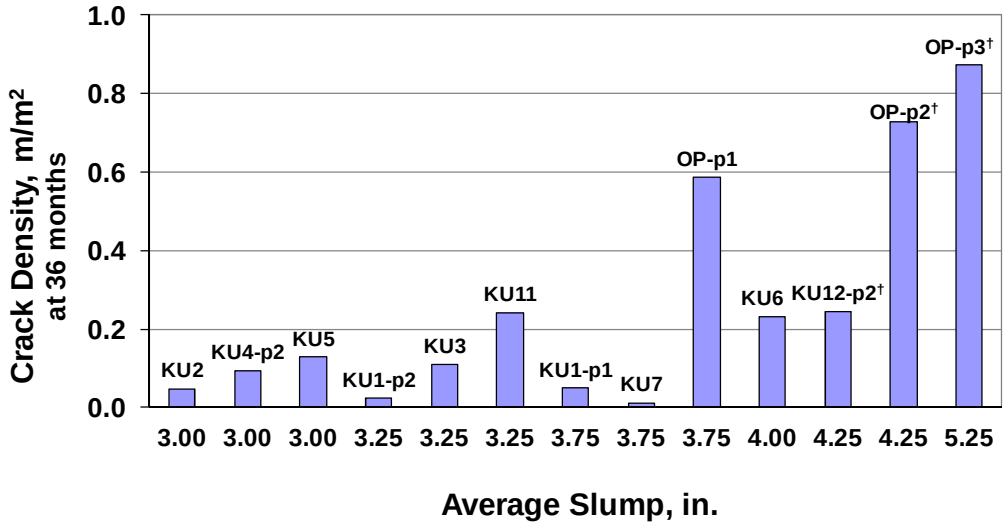

Figure 6.68 Crack density at 36 months versus average slump. 1 in. = 25.4 mm.
† Crack densities for KU12-p2, OP-p2, and OP-p3 are at 15.4, 25.5, and 24.9 months, respectively.

Crack density at 36 months (except for KU12-p2, OP-p2 and OP-p3) is plotted versus the percentage of slump tests with values greater than or equal to 3.5 in. (90 mm) in Figure 6.69. Crack density increases significantly for decks with 70% or more of the slump tests having values greater than or equal to 3.5 in. (90 mm).

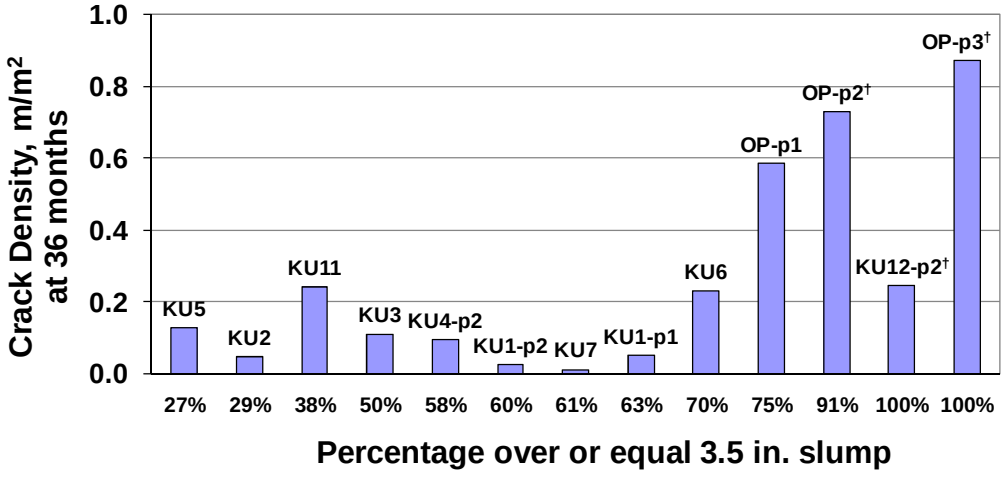

Figure 6.69 Crack density at 36 months versus percentage of slump tests with values greater than or equal to 3.5 in. (90 mm). † Crack densities for KU12-p2, OP-p2, and OP-p3 are at 15.4, 25.5, and 24.9 months, respectively.

The trend of increasing crack density with higher slump concrete agrees with the findings by Lindquist et al. (2005). Lindquist et al. (2005) examined 31 monolithic placements and found that crack density increased by 0.11 m/m^2 as slump increased from 1.5 to 3 in. (40 to 75 mm).

Lindquist et al. (2005) observed that there has been a consistent increase in cracking in bridge decks since the mid 1980s. There has also been a general increase in the slump of concrete used in bridge decks over the same period. Average slumps for Kansas bridges between 1984 and 2009 are plotted in Figure 6.70, which shows values for conventional monolithic and LC-HPC decks and subdecks for conventional, 5%, and 7% silica fume overlay (SFO) decks. As shown in Figure 6.70, concretes with slumps between 1½ and 2 in. (38 and 50 mm) were used in 1980s. Slump increased somewhat, to 2 and 3 in. (50 and 75 mm), in 1990s. After 2000, slump increased

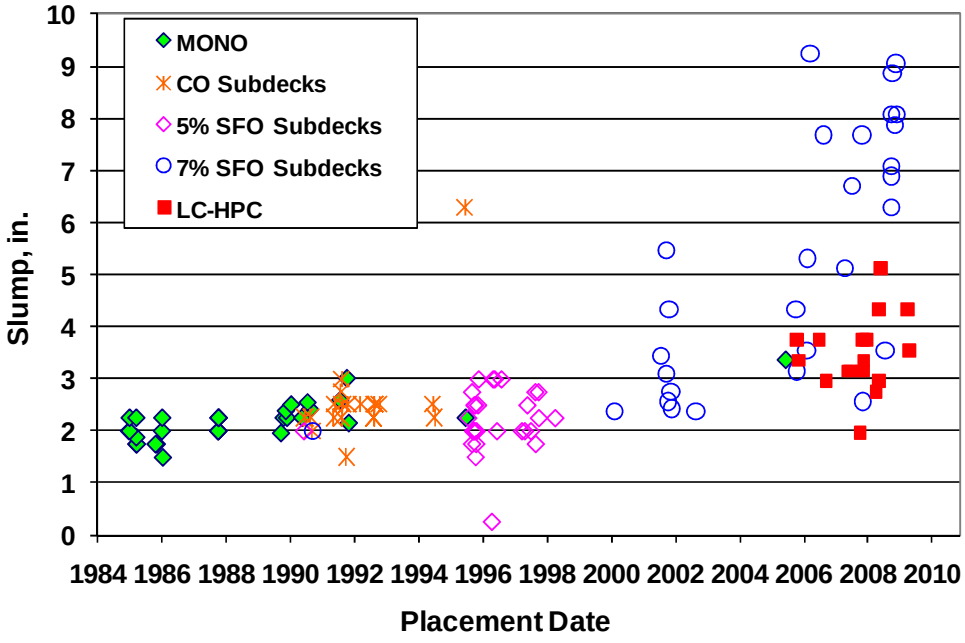

Figure 6.70 Slump versus date of placement for bridge decks in Kansas (for LC-HPC placements, LC-HPC 4-p1, 8, 10, 12-p1 and OP decks are included). NOTE: 1 in. = 25.4 mm.

quickly, with most values well over 3 in. (75 mm). Most slump values were over 4.0 in. (100 mm) and as high as 9.25 in. (235 mm) after 2005. The introduction of superplasticizers and concrete pumps (which generally require high paste contents and high slumps) likely have played a major role in contributing to the increase in slump used in bridge decks.

Even with a designated slump range of 1.5 to 3 in. (38 to 75 mm) and a maximum allowable slump of 4 in. (100 mm), the concrete slump on LC-HPC bridge decks has continued to follow the trend established over the years. While the average slumps on LC-HPC decks are not as high as on the Control decks, most have been over 3 in. (75 mm) and several have been over 4 in. (100 mm). The slump values used on LC-HPC bridge decks in Figure 6.70 are not surprising because, as discussed in Section 6.3, contractors prefer to use higher slump concrete.

Crack density at 36 months is plotted versus slump for both LC-HPC (designated as KU) and control decks (designated as C) in Figure 6.71. For the LC-HPC decks, the average slump ranges from 3.0 to 4.0 in. (75 to 110 mm) and the crack density ranges from 0.024 to 0.241 m/m^2; for the control decks, the slump of the concrete used in the subdeck ranges from 3.25 to 9.75 in. (85 to 250 mm) and the crack density ranges from 0.106 to 0.898 m/m^2.

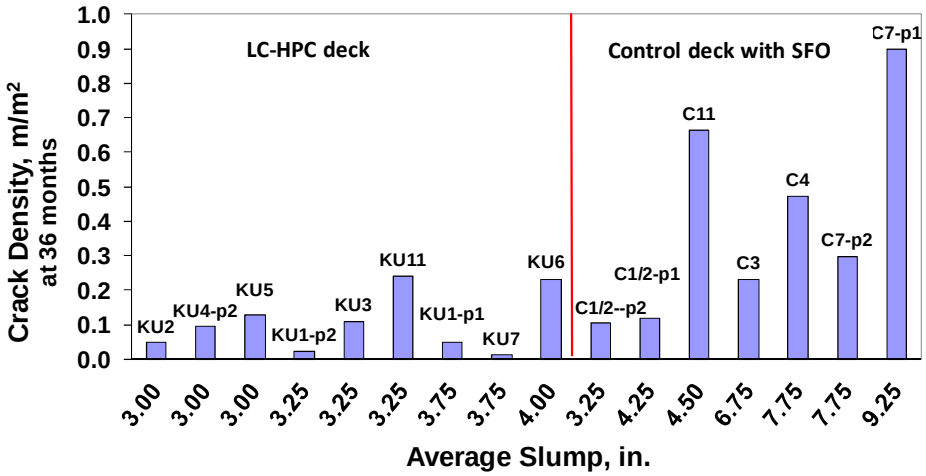

Figure 6.71 Crack density at 36 months versus slump for LC-HPC and Control decks.

6.4.5.3 Compressive Strength

The compressive strength for LC-HPC placements ranges from 3790 to 6380 psi (26.1 to 44.0 MPa). These placements are grouped into two categories based on compressive strength, between 3500 and 5500 psi (24.1 and 37.9 MPa, specified in the most recent LC-HPC specifications) and over 5500 psi (37.9 MPa), and are plotted versus crack density in Figure 6.72. An increase in compressive strength from between 3500 to 5500 psi (24.1 and 37.9 MPa) to over 5500 psi (37.9 MPa) results in a doubling in average crack density from 0.08 to 0.16 m/m^2.

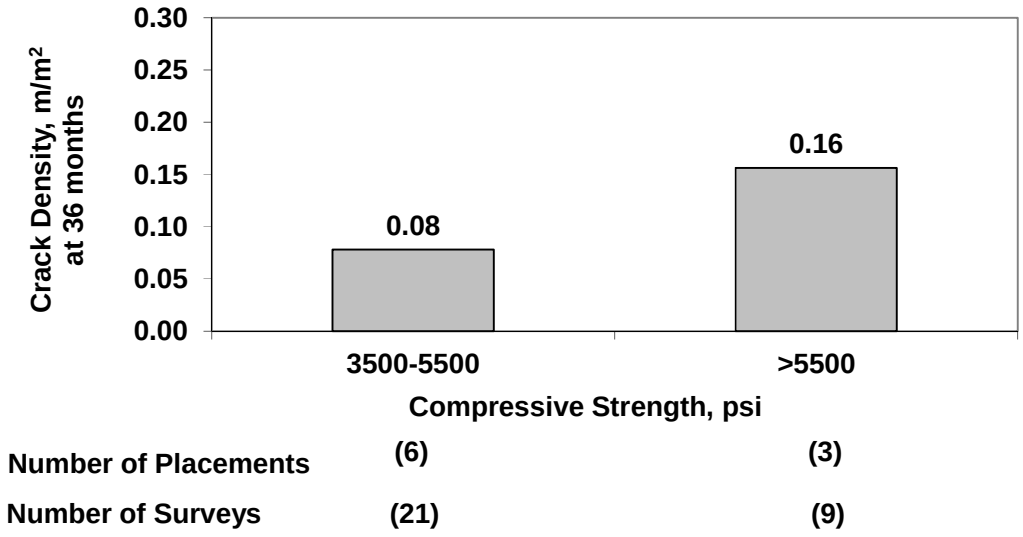

Figure 6.72 Crack density at 36 months versus compressive strength for LC-HPC bridges. 1 psi = 0.0069 MPa.

The relationship between compressive strength and cracking noted for LC-HPC decks is also true for the conventional monolithic decks analyzed by Lindquist et al. (2005). The crack density on the earlier decks increased from 0.16 to 0.49 m/m^2 as the compressive strength increased from 4500 to 6500 psi (31 to 45 MPa).

Crack density at 36 months is plotted versus compressive strength for LC-HPC (designated as KU) and control decks (designated as C) in Figure 6.73. For the LC-HPC decks, the compressive strength ranges from 3790 to 6380 psi (26.1 to 44.0 MPa)

and the crack density at 36 months ranges from 0.012 to 0.241 m/m^2; for control decks, the compressive strength of the silica fume overlay ranges from 5090 to 6340 psi (35.1 to 43.7 MPa) and the crack density ranges from 0.106 to 0.898 m/m^2.

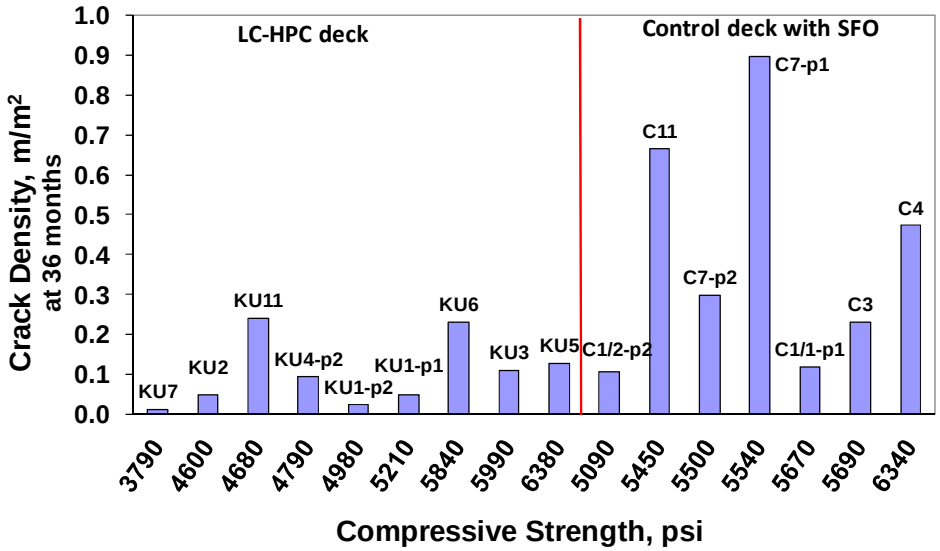

Figure 6.73 Age-corrected crack density versus compressive strength for both LC-HPC and control bridges. 1 psi = 0.0069 MPa.

6.4.5.4 Air Content

Lindquist et al. (2005) found that for monolithic bridge placements, the crack density of placements with air content less than 5.5% was about three times the crack density of placements with air content of 6.5%. Similarly, Schmitt and Darwin (1995) and Miller and Darwin (2000) found that monolithic placements with air contents below 6% had increased levels of cracking.

The LC-HPC specifications establish minimum and maximum air contents of 6.5% and 9.5%, respectively. The average air contents for LC-HPC placements in this study range from 7.7% to 9.5%; the crack density at 36 months is plotted versus air content in Figure 6.74. For these decks, all with air contents is excess of 6.5%, and no trend between the crack density and air content is apparent.

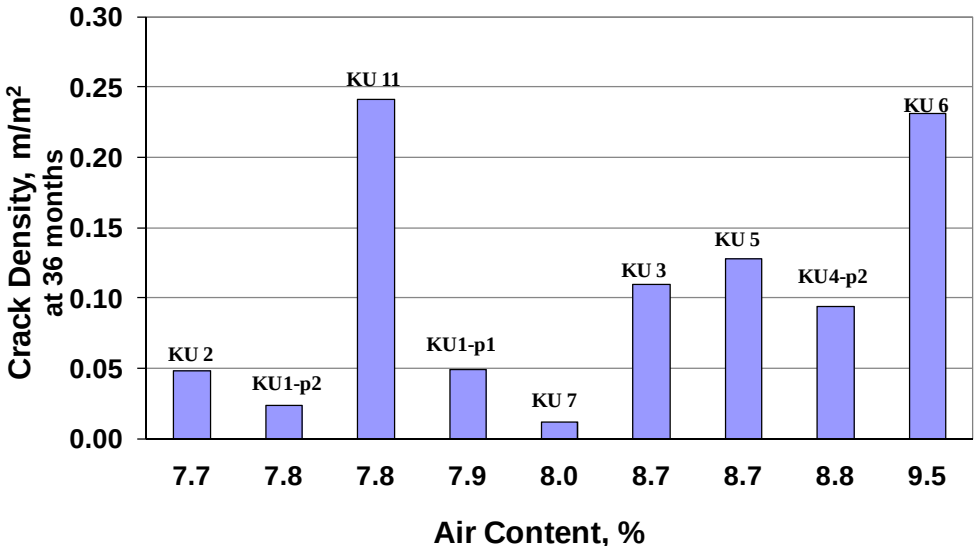

Figure 6.74 Crack density at 36 months versus air content for LC-HPC placements.

CHAPTER 7 SUMMARY AND CONCLUSIONS

7.1 SUMMARY

Cracks in concrete bridge decks provide easy access for water and deicing chemicals that can cause corrosion of reinforcing steel and shorten the useful life of the decks. Research during the past 40 years has addressed the causes of bridge deck cracking, but only a small number of these findings have been applied in practice. This study implements this knowledge through the development and construction of low-cracking high-performance concrete (LC-HPC) bridge decks.

The first portion of the study (Chapter 3) involves evaluating the effects of the duration of curing, fly ash, and a shrinkage reducing admixture (SRA) on the free-shrinkage characteristics of concrete mixtures. The free shrinkage work includes a total of 16 individual concrete batches, divided into three test programs. Program I evaluates the effect of extending the curing period from 7 to 14, 28, and 56 days. Mixtures with 100% portland cement and mixtures with a 40% volume replacement of cement with Class C or Class F fly ash are investigated. In Program II, at an SRA dosage rate of 0.64 gallon/yd^3 (3.2 L/m^3), 100% cement mixtures and mixtures with 20 and 40% volume replacements of cement with Durapoz® Class F fly ash are compared. In Program III, a 100% cement mixture and mixtures with a 40% volume replacement of cement with Class F fly ash are compared at SRA dosage rates of 0, 0.32, and 0.64 gallon/yd^3 (0, 1.6, and 3.2 L/m^3).

The relationship between the evaporable water content in the cement paste constituent of concrete and the free shrinkage of concrete is investigated in Chapter 4. Methods to determine the quantity of non-evaporable water and evaporable water in the cement paste are developed in this study. One hundred percent portland cement mixtures, mixtures with a 40% volume replacement of cement with Class F fly ash, mixtures with a 60% volume replacement of cement with slag, and mixtures with an SRA are evaluated.

Chapter 5 describes the restrained ring tests that are used to evaluate the cracking tendency of concrete. Ring specimens with fixed steel ring dimensions and different concrete ring thicknesses, 2.5, 2, 1.5, and 1.125 in. (64, 50, 38, and 29 mm), are evaluated. The effect of drying conditions on the time to cracking of ring specimens is also investigated. The times to cracking, based on both visual observations and the initial drop of the compressive strain in the steel ring, are used to compare mixtures with different water-cement ratios (at the same cement content), mixtures with 100% cement and a 40% volume replacement of cement with Class F fly ash, and mixtures with high and low paste contents.

Chapter 6 details the development, construction, and preliminary performance (with most bridges at three years of age) of LC-HPC and control bridge decks in Kansas. The LC-HPC specifications, including specifications for aggregates, concrete, and construction, are described first. The experiences and lessons learned during construction of the LC-HPC decks and the construction data for each control deck are then presented. Crack maps for each LC-HPC and control deck are shown, and the factors that affect bridge deck cracking are discussed.

7.2 CONCLUSIONS

The following observations and conclusions are based on the results and analyses presented in this report.

7.2.1 Free Shrinkage Tests

1. Using curing periods of 14 days or more decreases the free shrinkage of mixtures containing 100% portland cement and mixtures with a 40% volume replacement of cement with Class C of Class F fly ash.

2. The reduction in free shrinkage obtained by increasing the curing period is greater for concrete containing fly ash than for the mixtures with 100% portland cement.
3. With 7 days of curing, concretes containing fly ash exhibit greater free shrinkage than concretes with 100% portland cement. When the curing period is increased to 14, 28, and 56 days, the adverse effect of adding fly ash on free shrinkage is minimized and finally reversed.
4. For all mixtures tested, over sixty percent of the free shrinkage at one year occurred during the first 30 days.
5. The addition of an SRA significantly reduces free shrinkage. With an SRA dosage of 0.64 gallon/yd^3 (3.2 L/m^3), 30-day free shrinkage decreased by more than 35% for all mixtures tested in this study. The reductions at 365 days were relatively lower than those at 30 days, but exceeded 25% for all mixtures. Lower reductions in free shrinkage were observed for mixtures with an SRA dosage of 0.32 gallon/yd^3 (1.6 L/m^3).
6. When the reductions in free shrinkage obtained by adding 0.32 or 0.64 gallon/yd^3 (1.6 and 3.2 L/m^3) of SRA (concrete cured for 14 days,) and by extending the curing period from 14 to 28 or 56 days are compared for mixtures with and without fly ash, adding 0.64 gallon/yd^3 (3.2 L/m^3) of SRA provides the greatest reduction in shrinkage at 30 and 365 days for all mixtures; adding 0.32 gallon/yd^3 (1.6 L/m^3) of SRA provides a greater reduction than extending the curing period from 14 to 28 days (except for the concrete without fly ash at 365 days) and a lower reduction than extending the curing period to 56 days (except for the mixture with fly ash at 30 days).

7.2.2 Evaporable Water Content, Non-Evaporable Water Content, and Free Shrinkage

1. Cement paste absorbs water during curing in lime-saturated water. For curing periods up to 35 days, the longer the cement paste is cured under water, the greater the quantity of water it absorbs.
2. For curing periods of 3, 7, 14 or 28 days, the concrete containing fly ash absorbed the lowest quantity of water, followed by the concretes containing SRA and slag, and the 100% cement mixture (except that concrete containing slag cured for three days and the SRA mixture cured for three days absorbed more water than the 100% cement mixture).
3. Concrete expands during curing. There was no direct correlation between the amount of expansion and the quantity of absorbed water in the current study.
4. For a given mixture, specimens cured for longer periods have a higher degree of hydration than those cured for shorter periods as measured by the quantity of non-evaporable water.
5. The addition of a shrinkage reducing admixture has little, if any, influence on the degree of hydration, while partial replacements of cement with fly ash or slag cement reduce the degree of hydration, as represented by a lower quantity of non-evaporable water.
6. A linear relationship between free shrinkage and evaporable water content is observed. For a given mixture, specimens cured for a longer period contain less evaporable water and exhibit lower free shrinkage and less weight loss in the free shrinkage specimens than those cured for a shorter period.
7. For curves relating free shrinkage to weight loss during drying, a lower slope (lower shrinkage for a given weight loss) is noted during the first

few days, which may be due to the early loss of capillary water and water in the aggregates. After that, the slope increases, in all likelihood as water in the mesopores and micropores begins to evaporate, and finally decreases, likely the result of the loss of adsorbed water from particle surface.

8. Based on curves of free shrinkage versus weight loss and curves of weight loss versus time (all specimens cured for 28 days, except concrete containing slag, which was cured for 35 days), the results suggest that concrete containing slag may have a finer pore size distribution than the 100% cement mixture, while the concrete containing fly ash may have a coarser distribution.
9. Concrete containing SRA exhibits less shrinkage at the same water loss than mixtures without an SRA.

7.2.3 Restrained Ring Tests

1. For mixtures that investigated in this study, when drying ring specimens at a temperature of 73 ± 3º F (23 ± 2º C) and a relative humidity of 50 ± 4%, visible cracks did not develop in a large portion of the rings specimens with a concrete thickness of 2.5 in. (64 mm), while visible cracks developed in most specimens with concrete thicknesses of 2, 1.5, or 1.125 in. (50, 38, and 29 mm).
2. When drying ring specimens at a temperature of 86 ± 3° F (30 ± 2° C) and a relative humidity of 14 ± 4%, visible cracks developed in the ring specimens with a concrete thickness of 2.5 in. (64 mm).
3. For the mixtures investigated in this study, the compressive strain in the steel ring did not exhibit a sudden and rapid drop. Instead, the compressive strain dropped slowly before the cracks become visible.
4. When the cracking tendency of different concrete mixtures are compared, the *trends* observed in this study based on the times to cracking determined

from visual observations agree with the trends based on the times to cracking determined from the initial drop of compressive strain in the steel ring.

5. Specimens with thinner concrete rings crack earlier than those with thicker concrete rings.
6. Exposing specimens to severe drying conditions results in the earlier formation of cracks, although it does not result in increased crack width.
7. The compressive strain in a steel ring is a function of both the shrinkage and modulus of elasticity of the concrete; concrete with lower free shrinkage can cause higher compressive strain in the steel if it has a higher modulus of elasticity.
8. Mixtures with a lower *w/c* ratio (0.35 in the current study) crack earlier than mixtures with a higher *w/c* ratio (0.45).
9. At the same *w/c* ratio, concrete with a higher paste content (33%) cracks earlier than concrete with a lower paste content (24%).

7.2.4 Construction Experiences and Bridge Deck Cracking

7.2.4.1 LC-HPC Construction Experience

1. The techniques embodied in the low-cracking high-performance concrete bridge deck specifications are easy to learn. Contractor personnel can be trained in a relatively short time.
2. During the construction of the LC-HPC decks, concrete with *w/c* ratios of 0.44 and 0.45 and cement contents of 535 or 540 lb/yd^3 (317 or 320 kg/m^3) have consistently pumped and finished well; for concrete with a *w/c* ratio of 0.42 and a cement content of 535 lb/yd^3 (317 kg/m^3), when angular manufactured sand was used, obstacles were encountered in achieving a workable and placeable concrete.

3. The slump test results clearly demonstrate the tendency of contractors to use the maximum allowable slump. Give a slump range of 1.5 to 3 in. (40 to 75 mm) as specified in the LC-HPC specifications and a maximum slump of 4 in. (100 mm), on average (for all 18 LC-HPC placements), 63% of the slump readings were greater than 3 in. (75 mm), 52% were greater than or equal to 3.5 in. (90 mm), and 32% were greater than or equal to 4 in. (100 mm).
4. In hot weather, using chilled water, ice, or both as a replacement for mix water work well to control the concrete temperature. However, the need for advanced planning is often underestimated by concrete suppliers.
5. It is important to have a clear schedule and plan for how to handle out-of-specification concrete.
6. Concretes cast with high-range water reducers tend to exhibit increased compressive strength compared to concrete cast with mid-range water reducers or without a water reducer.
7. The importance of the qualification batch and slab has been proven for the LC-HPC decks constructed in Kansas. Experience demonstrates that completing a qualification batch that meets all specifications is vital for successful placement of the qualification slab and the deck.
8. Using a concrete pump with (1) a bladder valve that is operated to limit the rate of drop of the concrete or (2) an S-hook limits the air content loss to 0.5 to 0.8%, compared with values of 1.1 to 2% when no measures are taken. Using a conveyor belt with a free drop of 12 to 15 ft (3.7 to 4.6 m) can result in air content losses as high as 2.4%.
9. Contractors exhibit different levels of expertise in consolidating and finishing decks.

7.2.4.2 Bridge Deck Cracking

1. The techniques used for LC-HPC bridge decks are effective in reducing bridge deck cracking. Crack surveys indicate that LC-HPC bridge decks perform better than the control decks, with average crack density reduced by about 75% at three years of age.
2. At an age of about three years, the crack density of LC-HPC decks ranges from 0.012 to 0.241 m/m^2 with the majority under 0.15 m/m^2, while the crack density for the control decks has ranges from 0.106 to 0.898 m/m^2.
3. The cracking rate of the control decks is three times or more of that of the LC-HPC decks at ages up to four years.
4. LC-HPC decks perform at a level approximately equal to or exceeding the best performing conventional monolithic decks in previous studies (Schmitt and Darwin 1995, Miller and Darwin 2000, Lindquist et al. 2005).
5. The analyses of 21 monolithic decks (including 40 individual placements) indicate that an increase in paste content, slump, compressive strength, maximum daily air temperature, and daily air temperature range causes increased crack densities. Contractor techniques influence cracking.
6. For decks constructed under the LC-HPC specifications, but with concrete slump exceeding values in the designated range of 1 to 3 in. (25 to 75 mm), crack density increases significantly for decks with 70% or more of the slump tests with values greater than or equal to 3.5 in. (90 mm).
7. For decks constructed under the LC-HPC specifications, an increase in compressive strength from between 3500 to 5500 psi (24.1 and 37.9 MPa) to values over 5500 psi (37.9 MPa) results in a doubling in average crack density from 0.08 to 0.16 m/m^2.

7.3 RECOMMENDATIONS

1. Durability tests of the concrete containing shrinkage reducing admixtures (SRAs) should be conducted before they are recommended for bridge deck concrete.
2. Research that combines fly ash as a partial replacement for cement and lightweight aggregate as a partial replacement for normalweight aggregate is recommended. The recommendation is based on the observation that with extended curing periods of 28 and 56 days, concretes containing fly ash have less free shrinkage than those with 100% cement.
3. Concrete with a cement content between 500 and 540 lb/yd^3 (296 and 320 kg/m^3) and a water-cement (*w/c*) ratio of 0.44 or 0.45 is recommended for bridge deck construction.
4. The maximum allowable slump for future LC-HPC bridge placements should be limited to 3½ in. (90 mm) at the truck and 3 in. (75 mm) on the deck.
5. The compressive strength for concrete in bridge decks should be limited to between 3500 and 5500 psi (24.1 and 37.9 MPa).
6. When a pump is used for placement, an air cuff/bladder valve should be used to limit air loss. The maximum drop from the end of a conveyor belt, pump, or a concrete bucket should be limited to 5 ft (1.5 m).
7. Two pumps or two conveyor belts should be required on the job site to minimize delays caused by relocating the equipment and to ensure that the contractor is prepared in case one pump or conveyor belt does not function properly.
8. A person with authority should be assigned to monitor the burlap placement and wetting operations.
9. Finishing should be minimized for bridge decks.
10. Thermal effects on bridge deck cracking should be investigated further.

REFERENCES

AASHTO PP 34-99 (1998). *"Standard Practice for Estimating the Crack Tendency of Concrete,"* AASHTO Provisional Standards, 5 pp.

ACI Committee 224 (1972). "Control of Cracking in Concrete Structures," *ACI Journal,* December, pp. 712-753.

American Society of Civil Engineering (ASCE) (2009). "Report Card for America's Infrastructures." *http://www.infrastructurereportcard.org/fact-sheet/bridges*

ASTM C157-04 (2004). *"Standard Test Method for Length Change of Hardened Hydraulic-Cement Mortar and Concrete,"* ASTM International, West Conshohocken, PA., 7 pp.

ASTM C511-09 (2009). *"Standard Specification for Mixing Rooms, Moist Cabinets, Moist Rooms, and Water Storage Tanks Used in the Testing of Hydraulic Cements and Concretes,"* ASTM International, West Conshohocken, PA., 3 pp.

ASTM C1581-04 (2004). *"Standard Test Method for Determining Age at Cracking and Induced Tensile Stress Characteristics of Mortar and Concrete under Restrained Shrinkage,"* ASTM International, West Conshohocken, PA., 6 pp.

Babaei, K. and Purvis, R. L. (1996). "Minimizing Premature Cracking in Concrete Bridge Decks," *Proceedings, 13th Annual International Bridge Conference*, Pittsburgh, PA., pp. 411-420

Babaei, K. and Fouladgar, A. M. (1997). "Solutions to Concrete Bridge Deck Cracking," *Concrete International*, Vol. 19, Issue 7, July, pp. 34-37.

Cady, P. D., Carrier, R. E, Bakr, T., and Theisen, J. (1971). *"Final Report on the Durability of Bridge Decks –Part 1: Effect of Construction Practices on Durability,"* Department of Civil Engineering, Pennsylvania State University.

Concrete Technology Today (1996). Portland Cement Association, Vol. 17, No. 2, Skokie, IL, July, 7 pp.

Dakhil, F. H., Cady, P. D., and Carrier, R. E. (1975). "Cracking of Fresh Concrete as Related to Reinforcement," *ACI Journal, Proceedings*, Vol. 72, No. 8, Aug., pp. 421-428.

Deshpande, S., Darwin, D., and Browning, J. (2007). "Evaluating Free Shrinkage of Concrete for Control of Cracking in Bridge Decks," *SM Report No. 89*, University of Kansas Center for Research, Inc., Lawrence, KS, 290 pp.

Durability of Concrete Bridge Decks – A Cooperative Study, Final Report (1970). The state highway departments of California, Illinois, Kansas, Michigan, Minnesota, Missouri, New Jersey, Ohio, Texas, and Virginia; the Bureau of Public Roads; and Portland Cement Association, 35 pp.

French, C., Eppers L., Le, Q., and Hajjar, J. F. (1999). "Transverse Cracking in Concrete Bridge Decks," *Transportation Research Record 1688*, Paper No. 99-0888, pp. 21-29.

Gong, Z., Barth, K. E., Davalos, J. F., Liu, X., Mukdadi S., and Ray, I. (2006). *"Cracking Studies of High-Performance Concrete for Bridge Deck,"* Department of Civil and Environmental Engineering, West Virginia University, Morgantown, West Virginia, 224 pp.

Hossain, A. B. and Weiss, J. (2006). "The Role of Specimen Geometry and Boundary Conditions on Stress Development and Cracking in the Restrained Ring Test," *Cement and Concrete Research*, Vol. 36, No.1, Portland Cement Association, Skokie, IL, pp. 189-199.

Hogan, F. J., and Meusel, J. W. (1981). "Evaluation for Durability and Strength Development of a Ground Granulated Blast-Furnace Slag," *Cement, Concrete, and Aggregates*, Vol. 3, No. 1, pp. 40-52.

Kovler, K. and Bentur, A. (2009). "Cracking Sensitivity of Normal- and High-Strength Concrete," *ACI Materials Journal*, Vol. 106, No. 6, Nov.-Dec., pp. 537-542.

Krauss, P. D., and Rogalla, E. A. (1996). "Transverse Cracking in Newly Constructed Bridge Decks," *National Cooperative Highway Research Program Report 380*, Transportation Research Board, Washington, D.C., 126 pp.

Lange, D. A., Roesler, J. R., D'Ambrosia, M. D., Cowen, D. R., and Lee, C. J. (2003). "High Performance Concrete for Transportation Structures," *Civil Engineering Studies, Transportation Engineering Series No. 126, Illinois Cooperative Highway and Transportation Series No. 287*, University of Illinois at Urbana-Champaign, IL., 306 pp.

Lindquist, W. D., Darwin, D., and Browning, J. (2005). "Cracking and Chloride Contents in Reinforced Concrete Bridge Decks," *SM Report No. 78*, University of Kansas Center for Research, Inc., Lawrence, KS, 482 pp.

Lindquist, W. D., Darwin, D., Browning, J., and Miller, G. G. (2006). "Effect of Cracking on Chloride Content in Concrete Bridge decks," *ACI Materials Journal*, Vol. 103, No. 6, Nov.-Dec., pp. 467-473.

Lindquist, W. D., Darwin, D., and Browning, J. (2008). "Development and Construction of Low-Cracking High-Performance Concrete (LC-HPC) Bridge Decks: Free Shrinkage, Mixture Optimization, and Concrete Production," *SM Report No. 92*, University of Kansas Center for Research, Inc., Lawrence, KS, 540 pp.

McLeod, H., Darwin, D., and Browning, J. (2009). "Development and Construction of Low-Cracking High-Performance Concrete Bridge Decks: Construction Methods, Temperature Effects, and Resistance to Chloride Ion Penetration," SM Report 94, University of Kansas Center for Research, Inc., Lawrence, KS, 848 pp.

Miller, G. G. and Darwin, D. (2000). "Performance and Constructability of Silica Fume Bridge Deck Overlays," *SM Report No. 57*, University of Kansas Center for Research, Inc., Lawrence, KS, 423 pp.

Menzel, C. A. (1935). "Strength and Volume Change of Steam Cured Portland Cement Mortar and Concrete," *Proceedings, American Concrete Institute*, pp. 125-148.

Mindess, S., Young, F., and Darwin, D. (2003). *Concrete*, second edition, Prentice-Hall, Inc., Englewood Cliffs, NJ, 644 pp.

Powers, T. C., and Brownyard, T. L. (1946). "Studies of the physical properties of hardened Portland cement paste – part 2 studies of water fixation," Journal of the American Concrete Institute, *Proceedings* Vol. 18, No. 3, Nov., pp. 249-335.

Powers, T. C. (1959). "Causes and Control of Volume Change," *Journal of PCA Research and Development Laboratories*, Vol. 1, No. 1, pp. 29-39.

Powers, T. C. (1960). "Session V. Properties of Cement Paste and Concrete—Paper V-1 Physical Properties of Cement Paste," *Fourth International Symposium on the Chemistry of Cement*, Proceedings, Washington, D.C., pp. 577-609.

Russell, H. G. (2004). "Concrete Bridge Deck Performance," *National Cooperative Highway Research Program (NCHRP) Synthesis 333*, Transportation Research Board, Washington, D.C., pp. 32.

Schmitt, T. R. and Darwin, D. (1995). "Cracking in Concrete Bridge Decks," *SM Report No. 39*, University of Kansas Center for Research, Inc., Lawrence, KS, 151 pp.

Schmitt, T. R., and Darwin, D. (1999). "Effect of Material Properties on Cracking in Bridge Decks," *Journal of Bridge Engineering*, ASCE, Feb., Vol. 4, No. 1, pp. 8-13.

Shilstone, J. M., Sr. (1990). "Concrete Mixture Optimization," *Concrete International*, Vol. 12, No. 6, Jun., pp. 33-39.

Subramaniam, K. and Agrawal, A. K. (2009). "Concrete Deck Material Properties," *SPR Project C-02-03*, New York State Department of Transportation, 115 pp.

Taylor, H. F. W. (1997). *Cement Chemistry*, second edition, Thomas Telford Services Ltd., 459 pp.

Triandafilou, L. N. (2005). "Implementation of High-Performance Materials – When Will They Become Standard," *6th International Bridge Engineering Conference Reliability, Security, and Sustainability in Bridge Engineering*, July, pp. 36.

Tritsch, N., Darwin, D., and Browning, J. (2005). "Evaluating Shrinkage and Cracking Behavior of Concrete Using Restrained Ring and Free Shrinkage Test," *SM Report No. 77*, University of Kansas Center for Research, Inc., Lawrence, KS, 178 pp.

West, M., Darwin, D., and Browning, J. (2010). "Effect of Materials and Curing Period on Shrinkage of Concrete," *SM Report No. 98*, University of Kansas Center for Research, Inc., Lawrence, KS, 269 pp.

APPENDIX A: CONCRETE MIXTURE PROPORTIONS

Table A.1– Cement Chemical Composition

Oxides	**Percentages by Weight**			
	Portland Cement Type I/II			
Sample No.	C1	C2[†]	C3	C4
Manufacture	Ash Grove	Lafarge	Lafarge	Lafarge
Specific Gravity	3.20	3.15	3.15	3.15
Blaine Fineness, cm^3/g	3730	--	3660	3810
Bogue Analysis				
C_3S	47	--	59	58
C_2S	24	--	15	15
C_3A	7	--	7	7
C_4AF	10	--	9	9
XRF:				
SiO_2	20.88	--	20.53	20.58
Al_2O_3	4.85	--	4.70	4.69
Fe_2O_3	3.42	--	3.01	3.10
CaO	62.91	--	63.70	63.45
MgO	1.92	--	1.76	2.06
SO_3	2.79	--	3.06	2.69
Na_2O	0.21	--	0.28	0.25
K_2O	0.52	--	0.43	0.50
TiO_2	0.30	--	0.32	0.29
P_2O_5	0.10	--	0.13	0.10
Mn_2O_3	0.11	--	0.10	0.11
SrO	0.20	--	0.12	0.23
BaO	--	--	--	--
LOI	1.99	--	2.36	2.31
Total	100.20	--	100.48	100.34

[†]: Sample was not obtained.

Table A.1 (con't) – Cement Chemical Composition

Oxides	**Percentages by Weight**			
	Portland Cement Type I/II			
Sample No.	C5	C6	C7	C8
Manufacture	Lafarge	Ash Grove	Ash Grove	Ash Grove
Specific Gravity	3.15	3.20	3.20	3.20
Blaine Fineness, cm^3/g	3790	3820	3890	3600
Bogue Analysis				
C_3S	55	60	58	53
C_2S	18	13	15	19
C_3A	7	7	7	7
C_4AF	10	9	10	11
XRF:				
SiO_3	20.83	20.26	20.28	20.50
Al_2O_3	4.70	4.47	4.55	4.97
Fe_2O_3	3.20	3.12	3.13	3.57
CaO	63.13	62.90	62.60	62.46
MgO	2.22	2.11	1.96	2.06
SO_3	2.69	2.66	2.78	2.49
Na_2O	0.32	0.25	0.24	0.35
K_2O	0.51	0.48	0.46	0.49
TiO_2	0.29	0.27	0.27	0.29
P_2O_5	0.08	0.11	0.10	0.11
Mn_2O_3	0.11	0.11	0.10	0.11
SrO	0.24	0.24	0.22	0.26
BaO	--	--	--	--
LOI	1.88	3.0	3.01	2.60
Total	100.17	99.95	99.70	100.25

Table A.2 –Mineral admixtures chemical composition

Oxides	**Percentages by Weight**						
	Class F Fly ash					Class C Fly Ash	GGBFS
Sample No.	FA1 a	FA1 b	FA2	FA3 (Durapoz®)	FA4† (Durapoz®)	FA5	GGBFS 1
Manufacture	Lafarge		Lafarge	Ashgrove	Ashgrove	Ashgrove	Lafarge
Specific Gravity	2.40		2.40	2.87		2.83	2.90
XRF:							
SiO_3	64.97	64.36	50.56	57.17	--	26.70	34.86
Al_2O_3	17.47	17.47	15.10	18.65	--	15.57	10.83
Fe_2O_3	3.10	3.08	6.46	3.08	--	6.19	0.74
CaO	8.55	8.95	14.36	11.61	--	32.01	39.61
MgO	2.06	1.97	4.61	2.21	--	7.30	10.30
SO_3	0.23	0.29	0.97	2.83	--	4.17	2.57
Na_2O	0.63	0.61	3.62	0.63	--	2.35	0.24
K_2O	0.85	0.84	2.20	0.81	--	0.31	0.36
TiO_2	1.06	0.97	0.59	1.03	--	--	0.46
P_2O_5	0.11	0.12	0.11	0.18	--	--	0.01
Mn_2O_3	0.04	0.04	0.07	0.04	--	--	0.41
SrO	0.16	0.16	0.30	0.17	--	--	0.05
BaO	0.18	--	0.50	--	--	--	--
LOI	0.40	0.73	0.14	1.26	--	--	0.00
Total	99.81	99.59	99.59	99.67	--	96.60	100.44

†: Contaminated with about 30% cement.

Table A.3 – Coarse Aggregate Gradations

Sieve Size	**Percent Retained on Each Sieve**															
	Granite															
Sample Number	7	7(a)	7(b)	7(c)	8	8(a)	8(b)	8(c)	9	9(a)	9(b)	9(c)	11	11(a)	11(b)	11(c)
Specific Gravity	2.60				2.60				2.60				2.59			
Absorption	--				--				--				--			
37.5-mm (1½-in.)	0 0		0	0	0	0	0	0	0	0	0	0	0	0	0	0
25-mm (1-in.)	0	0	0	0	0	0	0	0	0	0	0	0	0	0	0	0
19-mm (¾-in.)	0	0	0.1	0	0	0	0	0	0.4	0	0	0	0	0	0	0
12.5-mm (½-in.)	13.9	98.1	0	0	10.2	95.6	0	0	36.1	99.0	0	0	20.6	97.4	0	0
9.5-mm (⅜-in.)	30.8	0	98.0	0	24.2	0	95.2	0	32.6	0	99.0	0	34.6	0	97.4	0
4.75-mm (No. 4)	48.9	0	0	90	47.1	0	0	73.8	29.4	0	0	97.4	40.2	0	0	92.6
2.36-mm (No. 8)	4.4	0	0	8.0	13.3	0	0	20.8	0.5	0	0	1.6	2.0	0	0	4.6
1.18-mm (No. 16)	0	0	0	0	0	0	0	0	0	0	0	0	0	0	0	0
0.60-mm (No. 30)	0	0	0	0	0	0	0	0	0	0	0	0	0	0	0	0
0.30-mm (No. 50)	0	0	0	0	0	0	0	0	0	0	0	0	0	0	0	0
0.15-mm (No. 100)	0	0	0	0	0	0	0	0	0	0	0	0	0	0	0	0
0.075-mm (No. 200)	0	0	0	0	0	0	0	0	0	0	0	0	0	0	0	0
Pan	2.0	1.9	2.0	2.0	5.2	4.4	4.8	5.4	1.0	1.0	1.0	1.0	2.6	2.6	2.6	2.8

Table A.3 (Con't) –Coarse Aggregate Gradations

Sieve Size	**Percent Retained on Each Sieve**																
	Granite																
Sample Number	12	12(a)	12(b)	13	13(a)	13(b)	14	14(a)	14(b)	15	15(a)	15(b)	17	18	20	20(a)	20(b)
Specific Gravity		2.60			2.59			2.60			2.60		2.60	2.61		2.60	
Absorption, %		--			0.70			0.76			--		0.71	0.71		0.71	
37.5-mm (1½-in.)	0	0	0	0	0	0	0	0	0	0	0	0	0	0	0	0	
25-mm (1-in.)	0	0	0	0	0	0	0	0	0	0	0	0	5.8	3.5	0	0	0
19-mm (¾-in.)	0	0	0.1	0	0	0	0	0	0.4	0	0	0	11.4	8.6	0	0	0
12.5-mm (½-in.)	15.7	35.0	0	24.2	38.8	0	8.8	21.5	0	17.3	32.5	0	29.6	23.4	18.8	37.0	0
9.5-mm (⅜-in.)	27.9	61.6	0	37.0	59.5	0	31.2	76.1	0	35.1	65.9	0	22.7	25.8	30.1	59.3	0
4.75-mm (No. 4)	46.5	0	96.3	35.7	0	94.5	53.6	0	90.7	43.2	0	92.5	26.9	33.2	42.1	0	85.5
2.36-mm (No. 8)	3.9	0	7.0	0.8	0	2.2	3.8	0	6.5	2.5	0	5.4	2.1	3.3	5.2	0	10.5
1.18-mm (No. 16)	0	0	0	0	0	0	0	0	0	0	0	0	0	0	0	0	0
0.60-mm (No. 30)	0	0	0	0	0	0	0	0	0	0	0	0	0	0	0	0	0
0.30-mm (No. 50)	0	0	0	0	0	0	0	0	0	0	0	0	0	0	0	0	0
0.15-mm (No. 100)	0	0	0	0	0	0	0	0	0	0	0	0	0	0	0	0	0
0.075-mm (No. 200)	0	0	0	0	0	0	0	0	0	0	0	0	0	0	0	0	0
Pan	6.0	3.4	6.7	2.3	1.7	3.3	2.6	2.4	2.8	1.9	1.6	2.1	1.5	2.2	3.8	3.7	4.0

Table A.3 (Con't) –Coarse Aggregate Gradations

Sieve Size	**Percent Retained on Each Sieve**								
	Granite							Limestone	
Sample Number	22	24	24(a)	24(b)	25	25(a)	25(b)	LS(6)	LS(7)
Specific Gravity	2.60	2.61			2.60			2.57	2.57
Absorption, %	0.61	0.60			--			2.55	2.51
37.5-mm (1½-in.)	0	0	0	0	0	0	0	0	0
25-mm (1-in.)	0	0	0	0	0	0	0	0	0
19-mm (¾-in.)	4.5	1.0	2.2	0	3.2	5.4	0	0.4	0
12.5-mm (½-in.)	33.1	23.5	52.9	0	26.0	44.2	0	30.7	6.9
9.5-mm (⅜-in.)	25.1	18.6	41.7	0	28.8	48.9	0	28.9	28.5
4.75-mm (No. 4)	33.1	50.2	0	90.4	38.2	0	92.7	30.4	60.9
2.36-mm (No. 8)	1.9	3.6	0	6.4	1.8	0	4.3	4.8	2.2
1.18-mm (No. 16)	0	0	0	0	0	0	0	0	0
0.60-mm (No. 30)	0	0	0	0	0	0	0	0	0
0.30-mm (No. 50)	0	0	0	0	0	0	0	0	0
0.15-mm (No. 100)	0	0	0	0	0	0	0	0	0
0.075-mm (No. 200)	0	0	0	0	0	0	0	0	0
Pan	2.3	3.1	3.2	3.2	2.0	1.5	3.0	4.8	1.5

Table A.4 – Fine Aggregate Gradations

Sieve Size	**Percent Retained on Each Sieve**								
	Pea Gravel								
Sample Number	PG(8)	PG(9)	PG(10)	PG(11)	PG(12)	PG(13)	PG(14)	PG(15)	PG(16)
Specific Gravity	2.61	2.62	2.62	2.62	2.61	2.62	2.61	2.60	2.60
Absorption, %	--	--	--	--	--	--	--	0.92	0.62
37.5-mm (1½-in.)	0	0	0	0	0	0	0	0	0
25-mm (1-in.)	0	0	0	0	0	0	0	0	0
19-mm (¾-in.)	0	0	0	0	0	0	0	0	0
12.5-mm (½-in.)	0	0	0	0	0	0	0	0	0
9.5-mm (⅜-in.)	0	0	0	0	0	0	0	0	0
4.75-mm (No. 4)	11.9	12.1	20.5	9.7	16.0	8.2	11.3	8.1	11.3
2.36-mm (No. 8)	49.4	48.9	50.2	48.1	57.6	45.1	57.4	45.0	46.1
1.18-mm (No. 16)	31.6	30.6	23.7	31.1	24.2	39.4	29.3	32.7	32.1
0.60-mm (No. 30)	5.4	5.9	3.7	6.8	1.8	5.9	1.5	8.9	6.2
0.30-mm (No. 50)	1.2	1.8	1.1	3.0	0.1	0.9	0.3	3.7	2.7
0.15-mm (No. 100)	0.2	0.3	0.3	0.9	0.1	0.3	0.1	1.1	1.1
0.075-mm (No. 200)	0.1	0.1	0.1	0.2	0	0.1	0	0.4	0.3
Pan	0.3	0.3	0.4	0.3	0.2	0.3	0.1	0.2	0.3

Table A.4 (Con't) – Fine Aggregate Gradations

Sieve Size	**Percent Retained on Each Sieve**											
	Sand											
Sample Number	S(7)	S(8)	S(9)	S(10)	S(11)	S(12)	S(13)	S(14)	S(15)	S(16)	S(17)	S(18)
Specific Gravity	2.63	2.63	2.63	2.63	2.63	2.63	2.62	2.61	2.62	2.62	2.62	2.63
Absorption, %	--	--	--	--	--	--	0.33	--	--	--	0.28	0.56
37.5-mm (1½-in.)	0	0	0	0	0	0	0	0	0	0	0	0
25-mm (1-in.)	0	0	0	0	0	0	0	0	0	0	0	0
19-mm (¾-in.)	0	0	0	0	0	0	0	0	0	0	0	0
12.5-mm (½-in.)	0	0	0	0	0	0	0	0	0	0	0	0
9.5-mm (⅜-in.)	0	0	0	0	0	0	0	0	0	0	0	0
4.75-mm (No. 4)	1.1	1.3	1.1	1.7	1.2	1.4	0.9	0.6	1.5	1.2	1.2	1.4
2.36-mm (No. 8)	13.8	11.6	8.5	10.9	9.8	10.4	10.1	8.1	12.6	7.0	8.4	9.8
1.18-mm (No. 16)	24.8	19.7	15.9	20.1	18.3	19.3	20.7	17.8	23.9	16.1	20.4	22.6
0.60-mm (No. 30)	279	26.6	45.9	26.5	26.5	26.3	29.1	24.2	28.1	24.8	24.8	25.4
0.30-mm (No. 50)	23.4	31.1	13.4	29.4	29.5	29.3	29.9	32.6	28.1	37.7	33.2	32.1
0.15-mm (No. 100)	8.3	8.4	13.4	9.9	12.0	11.0	8.1	14.4	5.5	12.0	10.8	8.3
0.075-mm (No. 200)	0.6	0.8	1.2	0.6	2.0	1.1	0.6	1.5	0.2	0.7	0.9	0.4
Pan	0	0.4	0.5	0.8	0.6	1.1	0.6	0.8	0.1	0.5	0.3	0.1

Table A.5 Free Shrinkage Test: Program I Curing Period Series

Mixture Proportions and Concrete Properties

Batch	**514**	**530**	**557**	**561**
Batch Designation	Control 1	40%FA-F	40%FA-C	Control 2
w/c	0.45	0.45	0.45	0.45
Paste Content, %	24.37	24.37	24.37	24.37
Cementitious Material, lb/yd^3 (kg/m^3)				
C-4	535 (317)	340 (202)	--	--
C-5	--	--	340 (202)	535 (317)
FA-2 (Class F)	--	173 (103)	--	--
FA-5 (Class C)	--	--	173 (103)	--
Water content, lb/yd^3 (kg/m^3)	241 (143)	231 (137)	231 (137)	241 (143)
Coarse Aggregate, lb/yd^3 (kg/m^3)				
G-11 (a)	290 (172)	--	--	--
G-11 (b)	524 (311)	--	--	--
G-11 (c)	355 (211)	--	--	--
G-12 (a)	--	830 (492)	--	--
G-12 (b)	--	507 (301)	--	--
G-14 (a)	--	--	703 (417)	703 (417)
G-14 (b)	--	--	426 (253)	426 (253)
Pea Gravel, lb/yd^3 (kg/m^3)				
PG-10	598 (355)	--	--	--
PG-11	--	864 (512)	--	--
PG-12	--	--	685 (406)	685 (406)
Fine Aggregate, lb/yd^3 (kg/m^3)				
S-10	989 (586)	--	--	--
S-11	--	775 (460)	--	--
S-12	--	--	1164 (690)	--
S-13	--	--	--	1164 (690)
Admixtures oz/yd^3 (mL/m^3),				
Type A-F HRWR	11.1 (429)	7.2 (280)	18. 1 (700)	10.9 (420)
Air-entraining agent	1.9 (75)	3.5 (135.4)	5.1 (197)	1.8 (70)
Batch Size, yd^3 (m^3)	0.056 (0.043)			
Slump, in. (mm)	4.0 (100)	3.75 (95)	2.0 (50)	2.0 (50)
Air Content, %	8.15	8.9	8.15	7.9
Temperature, °F (°C)	70° (21°)	71° (21°)	72° (22°)	70° (21°)
Compressive Strength, psi (MPa)				
7-Day Strengths	3490 (24.1)	2300 (15.9)	2280 (15.7)	3090 (21.3)
28-Day Strengths	4240 (29.2)	3710 (25.6)	3430 (23.7)	4310 (29.7)

Table A.6 Free Shrinkage Test: Program II Fly Ash and SRA Series

Mixture Proportions and Concrete Properties

Batch	**480**	**482**	**484**
Batch Designation	Control+SRA	20%FA+SRA	40%FA+SRA
w/c	0.42	0.42	0.42
Paste Content, %	23.42	23.42	23.42
Cement Content, lb/yd^3 (kg/m^3) C-2 FA-3 (Durapoz®)	 535 (317) --	 433 (257) 97 (56)	 329 (195) 197 (117)
Water content, lb/yd^3 (kg/m^3)	225 (133)	223 (132)	221 (131)
Coarse Aggregate, lb/yd^3 (kg/m^3) G-7 (a) G-7 (b) G-7 (c)	 298 (177) 541 (321) 501 (297)	 296 (176) 541 (321) 501 ()297	 299 (177) 538 (319) 502 (298)
Pea Gravel, lb/yd^3 (kg/m^3) PG-8	 661 (392)	 668 (396)	 668 (396)
Fine Aggregate, lb/yd^3 (kg/m^3) S-17	 1020 (605)	 1016 (602)	 1015 (602)
Admixtures, oz/yd^3 (mL/m^3) Type A-F HRWR Air-entraining agent SRA	 31.2 (1206) 2.7 (104) 82. 1 (3173)	 24.5 (947) 2.9 (111) 82. 1 (3173)	 19.4 (751) 3.0 (114) 82. 1 (3173)
Batch Size, yd^3 (m^3)	0.040 (0.031)		
Slump, in. (mm)	2.75 (70)	3.5 (90)	3.0 (75)
Air Content, %	7.9	8.4	8.4
Temperature, °F (°C)	73° (23°)	68° (20°)	68° (20°)
Compressive Strength, psi (MPa) 7-Day Strengths 28-Day Strengths	 4190 (28.9) 5260 (36.3)	 3250 (22.4) 3970 (27.4)	 2610 (18.0) 3880 (26.8)

Table A.7 Free Shrinkage Test: Program III SRA Series

Mixture Proportions and Concrete Properties

Batch	**587**	**588**	**590**
Batch Designation	Control	Control+0.32SRA	Control+0.64SRA
w/c	0.44	0.44	0.44
Paste Content, %	24.12	24.12	24.12
Cement Content, lb/yd^3 (kg/m^3) C6	540 (320)	540 (320)	540 (320)
Water content, lb/yd^3 (kg/m^3)	238 (141)	238 (141)	238 (141)
Coarse Aggregate lb/yd^3 (kg/m^3) G-17	1564 (927)	1564 (927)	1564 (927)
Pea Gravel, lb/yd^3 (kg/m^3) PG-13	544 (323)	544 (323)	544 (323)
Fine Aggregate, lb/yd^3 (kg/m^3) S-14	874 (518)	874 (518)	874 (518)
Admixtures, oz/yd^3 (mL/m^3) Type A-F HRWR Air-entraining agent SRA	9.7 (373) 2.6 (100) --	3.3 (128) 2.8 (109) 41.5 (1606)	1.7 (64) 3.8 (146) 83. 1 (3212)
Batch Size, yd^3 (m^3)	0.063 (0.048)		
Slump, in. (mm)	3.5 (90)	3.0 (75)	2.5 (65)
Air Content, %	8.4	8.4	8.9
Temperature, °F (°C)	71° (22°)	71° (22°)	71° (22°)
Compressive Strength, psi (MPa) 7-Day Strengths 28-Day Strengths	-- 3680 (25.4)	-- 3790 (26.1)	-- 3290 (22.7)

Table A.7 (Con't) Free Shrinkage Test: Program III SRA Series

Mixture Proportions and Concrete Properties

Batch	**594**	**595 (repeat 594)**	**601**
Batch Designation	40%FA+0.64SRA	40%FA+0.64SRA (R)	40%FA
w/c	0.44	0.44	0.44
Paste Content, %	24.12	24.12	24.12
Cementtitious Material, lb/yd^3 (kg/m^3) C-6 FA-2 (Class F)	 341 (202) 173 (103)	 341 (202) 173 (103)	 341 (202) 173 (103)
Water content, lb/yd^3 (kg/m^3)	226 (134)	226 (134)	226 (134)
Coarse Aggregate, lb/yd^3 (kg/m^3) G-17 G-18	 1579 (936) --	 1579 (936) --	 -- 1584 (939)
Pea Gravel, lb/yd^3 (kg/m^3) PG-13	 510 (302)	 510 (302)	 512 (303)
Fine Aggregate, lb/yd^3 (kg/m^3) S-13	 898 (532)	 898 (532)	 898 (532)
Admixtures, oz/yd^3 (mL/m^3) Type A-F HRWR Air-entraining agent SRA	 -- 1.7 (65) 83.1 (3212)	 -- 2.1 (80) 83.1 (3212)	 -- 3.6 (140) --
Batch Size, yd^3 (m^3)	0.026 (0.020)		
Slump, in. (mm)	5.75 (145)	5.5 (140)	5.5 (140)
Air Content, %	7.9	8.9	8.15
Temperature, °F (°C)	68° (20°)	71° (22°)	69° (21°)
Compressive Strength, psi (MPa) 7-Day Strengths 28-Day Strengths	 -- 3360 (23.2)	 -- 2880 (19.9)	 -- 3670 (25.3)

Table A.7 (Con't) Free Shrinkage Test: Program III SRA Series

Mixture Proportions and Concrete Properties

Batch	**605**	**610 (repeat 605)**	**612 (repeat 588)**
Batch Designation	40%FA+0.32SRA	40%FA+ 0.32SRA(R)	Control+ 0.32SRA(R)
w/c	0.44	0.44	0.44
Paste Content, %	24.12	24.12	24.12
Cementitious material, lb/yd^3 (kg/m^3) C-6 FA-2 (Class F)	 341 (202) 173 (103)	 341 (202) 173 (103)	 540 (320) --
Water content, lb/yd^3 (kg/m^3)	226 (134)	226 (134)	238 (141)
Coarse Aggregate, lb/yd^3 (kg/m^3) G-17 G-18	 -- 1585 (940)	 -- 1585 (940)	 -- 1582 (938)
Pea Gravel, lb/yd^3 (kg/m^3) PG-13	 512 (304)	 512 (304)	 511 (303)
Fine Aggregate, lb/yd^3 (kg/m^3) S-13	 899 (533)	 899 (533)	 897 (532)
Admixtures, oz/yd^3 (mL/m^3) Type A-F HRWR Air-entraining agent SRA	 -- 1.0 (40) 41.5 (1606)	 -- 0.9 35 () 41.5 (1606)	 3.5 (134) 2.1 (80) 41.5 (1606)
Batch Size, yd^3 (m^3)	0.026 (0.020)		
Slump, in. (mm)	5.75 (145)	5.25 (130)	2.75 (70)
Air Content, %	8.4	8.4	8.65
Temperature, °F (°C)	68° (20°)	67° (19°)	67° (19°)
Compressive Strength, psi (MPa) 7-Day Strengths 28-Day Strengths	 -- 3250 (22.4)	 -- 3650 (25.2)	 -- 3860 (26.6)

Table A.8 Evaporable and Non-Evaporable Water Series: Preliminary Tests

Mixture Proportions and Concrete Properties

Batch	**662**	**664**	**666**	**667**
Batch Designation	Control 1	Control 2	FA 1	GGBFS 1
w/c	0.44	0.44	0.44	0.44
Paste Content, %	24.12	24.12	24.12	24.12
Cementitious Material, lb/yd^3 (kg/m^3) C-8 FA-2 (Class F) GGBFS-1	 540 (320) -- --	 540 (320)-- --	 341 (202) 173 (103) --	 223 (132) -- 304 (180)
Water content, lb/yd^3 (kg/m^3)	238 (141)	238 (141)	226 (134)	232 (138)
Coarse Aggregate, lb/yd^3 (kg/m^3) G-22 G-24 (a) G-24 (b) G-25 (a) G-25 (b)	 1442 (855) -- -- -- --	 1442 (855) -- -- -- --	 1454 (862) -- -- -- --	 1448 (859) -- -- -- --
Pea Gravel, lb/yd^3 (kg/m^3) PG-15 PG-16	 707 (419) --	 707 (419) --	 723 (429) --	 716 (425) --
Fine Aggregate, lb/yd^3 (kg/m^3) S-16 S-17	 831 (493) --	 -- 831 (493)	 -- 806 (478)	 -- 815 (483)
Admixtures, oz/yd^3 (mL/m^3) Type A-F HRWR Air-entraining agent	 9.7 (375) 2.6 (100)	 9.7 (375) 2.6 (100)	 0 (0) 2.6 (100)	 13.2 (510) 6.6 (256)
Batch Size, yd^3 (m^3)	0.056 (0.043)			
Slump, in. (mm)	2.75 (70)	2.5 (65)	6.25 (160)	2.5 (65)
Air Content, %	8.9	8.4	8.65	8.65
Temperature, °F (°C)	69° (21°)	72° (22°)	70° (21°)	72° (22°)
Compressive Strength, psi (MPa) 7-Day Strengths 28-Day Strengths	 -- 3720 (25.7)	 -- 4220 (29.1)	 -- 3160 (21.8)	 -- --

Table A.9 Evaporable and Non-Evaporable Water Series

Mixture Proportions and Concrete Properties

Batch	**676**	**677**	**678**	**681**	**683**
Batch Designation	GGBFS 2	FA 2	Control 3	GGBFS 3	SRA
w/c	0.44	0.44	0.44	0.44	0.44
Paste Content, %	24.12	24.12	24.12	24.12	24.12
Cementitious Material, lb/yd^3 (kg/m^3) C-8 FA-2 (Class F) GGBFS-1	 223 (132) -- 304 (180)	 341 (202) 173 (103) --	 540 (320) -- --	 223 (132) -- 304 (180)	 540 (320) -- --
Water content, lb/yd^3 (kg/m^3)	232 (138)	226 (134)	238 (141)	232 (138)	238 (141)
Coarse Aggregate, lb/yd^3 (kg/m^3) G-22 G-24 (a) G-24 (b) G-25 (a) G-25 (b)	 1448 (859) -- -- -- --	 1455 (863) -- -- -- --	 1454 (862) -- -- -- --	 -- 934 (554) 438 (260) -- --	 -- -- -- 915 (543) 423 (251)
Pea Gravel, lb/yd^3 (kg/m^3) PG-15 PG-16	 683 (405) --	 691 (410) --	 723 (429) --	 -- 779 (462)	 -- 798 (473)
Fine Aggregate, lb/yd^3 (kg/m^3) S-18	 850 (504)	 840 (498)	 806 (478)	 837 (496)	 848 (503)
Admixtures, oz/yd^3 (mL/m^3) Type A-F HRWR Air-entraining agent SRA	 14.5 (560) 5.9 (229) --	 9.7 (375) 2.5 (96) --	 0 (0) 2.6 (100) --	 9.7 (375) 2.5 (96) --	 2.1 (82) 3.0 (117) 82.9 (3204)
Batch Size, yd^3 (m^3)	0.056 (0.043)				
Slump, in. (mm)	2.0 (50)	6.5 (165)	2.5 (65)	1.5 (40)	1.5 (40)
Air Content, %	8.65	7.9	8.15	8.4	8.15
Temperature, °F (°C)	71° (22°)	67° (19°)	67° (19°)	70° (21°)	68° (20°)
Compressive Strength, psi (MPa) 7-Day Strengths 28-Day Strengths	 -- 4620 (31.9)	 -- 4250 (29.3)	 -- 4760 (32.8)	 -- 4820 (33.2)	 -- 4260 (29.4)

Table A.10 Ring Tests Series Program I:
Mixture Proportions and Concrete Properties

Batch	**485**	**488**	**490**	**494**
Concrete Ring Thickness	**2.5 in.**			
Batch Designation	KDOT	0.45w/c	0.42w/c	0.39w/c
w/c	0.44	0.45	0.42	0.39
Paste Content, %	26.89	24.37	23.42	22.47
Cement Content, lb/yd^3 (kg/m^3)				
C-1	602 (357)	--	--	--
C-3	--	535 (317)	535 (317)	535 (317)
Water content, lb/yd^3 (kg/m^3)	264 (157)	241 (143)	241 (143)	241 (143)
Coarse Aggregate, lb/yd^3 (kg/m^3)				
LS-6	1448 (859)	--	--	--
G-8 (a)	--	305 (181)	281 (167)	--
G-8 (b)	--	532 (315)	568 (337)	--
G-8 (c)	--	619 (367)	598 (355)	--
G-9 (a)	--	--	--	291 (173)
G-9 (b)	--	--	--	533 (316)
G-9 (c)	--	--	--	429 (254)
Pea Gravel, lb/yd^3 (kg/m^3)				
PG-8	--	502 (298)	--	--
PG-9	--	--	629 (373)	873 (518)
Fine Aggregate, lb/yd^3 (kg/m^3)				
S-7	1448 (859)	1019 (604)	--	--
S-8	--	--	946 (561)	--
S-9	--	--	--	938 (556)
Admixtures, oz/yd^3 (mL/m^3)				
Type A-F HRWR	23.6 (911)	11.9 (462)	25.2 (975)	42.8 (1654)
Air-entraining agent	0.51 (19.7)	2.1 (80)	1.6 (60)	1.8 (71)
Batch Size, yd^3 (m^3)	0.150 (0.115)			
Slump, in. (mm)	6.0 (150)	3.5 (90)	3.0 (75)	3.75 (95)
Air Content, %	6.15	7.9	8.4	8.4
Temperature, °F (°C)	77° (25°)	72° (22°)	66° (79°)	60° (16°)
Compressive Strength, psi (MPa)				
7-Day Strengths	3820 (26.3)	2980 (20.6)	3550 (24.5)	4200 (29.0)
28-Day Strengths	4350 (30.0)	3900 (26.9)	4450 (30.7)	5310 (36.6)

Table A.11 Ring Tests Series Program II:

Mixture Proportions and Concrete Properties

Batch	**496**	**509**
Concrete Ring Thickness	**2.5 in. and 1.5 in.**	
Batch Designation	KDOT	0.45w/c
w/c	0.44	0.45
Paste Content, %	27.06	24.37
Cement Content, lb/yd^3 (kg/m^3) C-4	602 (357)	535 (317)
Water content, lb/yd^3 (kg/m^3)	264 (157)	241 (143)
Coarse Aggregate, lb/yd^3 (kg/m^3) LS-7 G-11 (a) G-11 (b) G-11 (c)	 1422 (843) -- -- --	 -- 290 (172) 524 (311) 355 (211)
Pea Gravel, lb/yd^3 (kg/m^3) PG-10	 --	 817 (485)
Fine Aggregate, lb/yd^3 (kg/m^3) S-9 S-10	 1422 (843) --	 -- 989 (586)
Admixtures, oz/yd^3 (mL/m^3) Type A-F HRWR Air-entraining agent	 18.7 (724) 0.51 (19.7)	 9.9 (381) 2.3 (87)
Batch Size, yd^3 (m^3)	0.120 (0.092)	
Slump, in. (mm)	7.0 (180)	3.75 (95)
Air Content, %	5.9	7.9
Temperature, °F (°C)	53° (12°)	56° (13°)
Compressive Strength, psi (MPa) 7-Day Strengths 28-Day Strengths	 3540 (24.4) 4460 (30.8)	 2950 (20.3) 4230 (29.2)

Table A.12 Ring Tests Series Program III:

Mixture Proportions and Concrete Properties

Batch	**532**	**537**	**539 (repeat 537)**	**544**	**545**
Concrete Ring Thickness	**1.5 in.**				
Batch Designation	0.39w/c	0.45w/c	0.45w/c (R)	0.42w/c	0.45w/c+FA
w/c	0.39	0.45	0.45	0.42	0.45
Paste Content, %	22.47	24.37	24.37	23.42	24.37
Cementitious Material, lb/yd^3 (kg/m^3) C-5 FA-2	 535 (317) --	 535 (317) --	 535 (317) --	 535 (317) --	 340 (202) 173 (103)
Water content, lb/yd^3 (kg/m^3)	209 (124)	241 (143)	241 (143)	225 (133)	231 (137)
Coarse Aggregate, lb/yd^3 (kg/m^3) G-12 (a) G-12 (b) G-13 (a) G-13 (b)	 848 (503) 527 (313) -- --	 825 (489) 512 (303) -- --	 825 (489) 513 (304) -- --	 -- -- 849 (503) 401 (238)	 -- -- 842 (499) 399 (237)
Pea Gravel, lb/yd^3 (kg/m^3) PG-11 PG-12	 851 (505) --	 828 (491) --	 828 (491) --	 -- 717 (425)	 -- 717 (425)
Fine Aggregate, lb/yd^3 (kg/m^3) S-11 S-12	 836 (496) --	 813 (482) --	 813 (482) --	 -- 1050 (623)	 -- 1012 (600)
Admixtures, oz/yd^3 (mL/m^3) Type A-F HRWR Air-entraining agent	 36.6 (1415) 1.9 (72)	 13.0 (501) 1.6 (61)	 18.0 (697) 1.4 (52)	 28.7 (1110) 1.5 (59)	 7.3 (283) 3.4 (131)
Batch Size, yd^3 (m^3)	0.046 (0.060)				
Slump, in. (mm)	2.75 (70)	3.5 (90)	3.0 (75)	2.25 (60)	3.5 (90)
Air Content, %	8.4	7.9	8.4	8.15	7.9
Temperature, °F (°C)	71° (22°)	71° (22°)	69° (21°)	70° (21°)	72° (22°)
Compressive Strength, psi (MPa) 7-Day Strengths 28-Day Strengths	 4140 (28.6) 5290 (36.5)	 3590 (24.8) 4370 (30.1)	 3330 (23.0) 4580 (31.6)	 3470 (23.9) 4280 (29.5)	 2520 (17.4) 3870 (26.7)

Table A.13 Ring Tests Series Program IV:

Mixture Proportions and Concrete Properties

Batch	**563**	**566**	**568**
Concrete Ring Thickness	**1.125 in.**		
Batch Designation	0.45w/c	40%FA+ 0.45w/c	0.35w/c
w/c	0.45	0.45	0.35
Paste Content, %	24.21	24.21	21.04
Cementitious material, lb/yd^3 (kg/m^3) C-6 FA-2 (Class F)	 535 (317) --	 338 (200) 172 (102)	 535 (317) --
Water content, lb/yd^3 (kg/m^3)	241 (143)	230 (136)	184 (109)
Coarse Aggregate, lb/yd^3 (kg/m^3) G-14 (a) G-14 (b) G-15 (a) G-15 (b)	 704 (417) 427 (253) -- --	 705 (418) 427 (253) -- --	 -- -- 822 (487) 449 (266)
Pea Gravel, lb/yd^3 (kg/m^3) PG-12	 687 (407)	 687 (407)	 755 (448)
Fine Aggregate, lb/yd^3 (kg/m^3) S-13	 1167 (692)	 1168 (693)	 1098 (651)
Admixtures, oz/yd^3 (mL/m^3) Type A-F HRWR Air-entraining agent	 14.0 (542) 2.2 (86)	 -- 3.6 (140)	 66.0 (2549) 1.4 (54)
Batch Size, yd^3 (m^3)	0.053 (0.041)		
Slump, in. (mm)	2.75 (70)	4.25 (110)	3.75 (95)
Air Content, %	8.4	7.9	8.65
Temperature, °F (°C)	72° (22°)	70° (21°)	71° (22°)
Compressive Strength, psi (MPa) 7-Day Strengths 28-Day Strengths	 2830 (19.5) 4100 (28.3)	 2240 (15.4) 3860 (26.6)	 5460 (37.7) 6080 (41.9)

Table A.14 Ring Tests Series Program V Set 1:

Mixture Proportions and Concrete Properties

Batch	**597**	**598**
Concrete Ring Thickness	**2.0 in.**	
Batch Designation	C535+0.45w/c	C729+0.45w/c
w/c	0.45	0.45
Paste Content, %	24.21	32.99
Cementitious material, lb/yd^3 (kg/m^3)		
C-6	535 (317)	729 (432)
C-8	--	--
FA-2 (Class F)	--	--
Water content lb/yd^3 (kg/m^3)	241 (143)	328 (195)
Coarse Aggregate, lb/yd^3 (kg/m^3)		
G-15	--	1323 (785)
G-15 (a)	1075 (637)	--
G-15 (b)	444 (263)	--
G-20 (a)	--	--
G-20 (b)	--	--
Pea Gravel, lb/yd^3 (kg/m^3)		
PG-13	578 (343)	503 (298)
PG-14	--	--
Fine Aggregate, lb/yd^3 (kg/m^3)		
S-13	888 (468)	768 (455)
S-16	--	--
Admixtures, oz/yd^3 (mL/m^3)		
Type A-F HRWR	9.2 (356)	--
Air-entraining agent	1.7 (67)	2.6 (100)
Batch Size, yd^3 (m^3)	0.068 (0.052)	
Slump, in. (mm)	3.75 (95)	8.0 (205)
Air Content, %	8.4	6.4
Temperature, °F (°C)	71° (22°)	70° (21°)
Compressive Strength, psi (MPa)		
7-Day Strengths	--	--
28-Day Strengths	4000 (27.6)	4120 (28.4)

Table A.15 Ring Tests Series Program V Set 2:

Mixture Proportions and Concrete Properties

Batch	**649**	**650**	**651**	**652**
Concrete Ring Thickness	**2 in.**			
Batch Designation	C700+ 0.35w/c	40%FA+ 0.35w/c	C700+ 0.44w/c	40%FA+ 0.44w/c
w/c	0.35	0.35	0.44	0.44
Paste Content, %	27.53	27.53	31.26	31.26
Cementitious material, lb/yd^3 (kg/m^3) C-8 FA-2 (Class F)	 5 700 ()41 --	 439 (260) 223 (132)	 700 (415) --	 442 (262) 224 (133)
Water content, lb/yd^3 (kg/m^3)	245 (145)	232 (138)	308 (183)	293 (174)
Coarse Aggregate, lb/yd^3 (kg/m^3) G-20 G-20 (a) G-20 (b)	 -- 728 (432) 518 (307)	 -- 735 (436) 512 (303)	 1330 (789) -- --	 1333 (790) -- --
Pea Gravel, lb/yd^3 (kg/m^3) PG-14	 797 (473)	 830 (492)	 517 (307)	 544 (323)
Fine Aggregate, lb/yd^3 (kg/m^3) S-16	 788 (467)	 760 (451)	 821 (487)	 797 (473)
Admixtures, oz/yd^3 (mL/m^3) Type A-F HRWR Air-entraining agent	 33.8 (1306) 3.5 (135)	 25.4 (980) 3.8 (146)	 -- --	 -- --
Batch Size, yd^3 (m^3)	0.060 (0.046)			
Slump, in. (mm)	2.0 (50)	4.25 (110)	8.5 (215)	9.0 (230)
Air Content, %	10.65	10.15	1.15	0.65
Temperature, °F (°C)	71° (22°)	73° (23°)	77° (25°)	75° (24°)
Compressive Strength, psi (MPa) 7-Day Strengths 28-Day Strengths	 -- 4120 (28.4)	 -- 3960 (27.3)	 -- 5380 (37.1)	 -- 5120 (35.3)

Table A.16 Ring Tests Series Program V Set 3:
Mixture Proportions and Concrete Properties

Batch	**635**	**636**	**637**
Concrete Ring Thickness	**2 in.**		
Batch Designation	C540+0.44w/c	C535+0.45w/c	C535+0.35w/c
w/c	0.44	0.45	0.35
Paste Content, %	24.12	24.21	21.04
Cementitious material, lb/yd^3 (kg/m^3)			
C-8	540 (320)	535 (317)	535 (317)
Water content, lb/yd^3 (kg/m^3)	238 (141)	241 (142)	187 (111)
Coarse Aggregate, lb/yd^3 (kg/m^3)			
G-18	1525 (904)	--	--
G-20 (a)	--	741 (439)	775 (460)
G-20 (b)	--	494 (293)	518 (307)
Pea Gravel, lb/yd^3 (kg/m^3)			
PG-14	419 (248)	809 (480)	847 (502)
Fine Aggregate, lb/yd^3 (kg/m^3)			
S-15	1046 (620)	935 (554)	978 (580)
Admixtures, oz/yd^3 (mL/m^3)			
Type A-F HRWR	9.6 (373)	9.3 (358)	65.9 (2547)
Air-entraining agent	2.6 (100)	1.8 (68)	1.4 (55)
Batch Size, yd^3 (m^3)	0.055 (0.042)		
Slump, in. (mm)	3.75 (95)	4.0 (100)	9.0 (230)
Air Content, %	9.15	8.65	12.15
Temperature, °F (°C)	72° (22°)	69° (21°)	72° (22°)
Compressive Strength, psi (MPa)			
7-Day Strengths	--	--	--
28-Day Strengths	3510 (24.2)	4260 (29.4)	5670 (39.1)

Table A.17 Ring Tests Series Program VI:

Mixture Proportions and Concrete Properties

Batch	**679**	**680**
Concrete Ring Thickness	**2.5 in.**	
Batch Designation	C540+0.44w/c	40%FA
w/c	0.44	0.44
Paste Content, %	24.12	24.12
Cementitious material, lb/yd^3 (kg/m^3) C-8 FA-4 (Class F)	 540 (320) --	 340 (202) 173 (103)
Water content, lb/yd^3 (kg/m^3)	238 (141)	226 (134)
Coarse Aggregate, lb/yd^3 (kg/m^3) G-25 (a) G-25 (b)	 915 (543) 423 (251)	 922 (547) 428 (254)
Pea Gravel, lb/yd^3 (kg/m^3) PG-16	 798 (473)	 812 (482)
Fine Aggregate, lb/yd^3 (kg/m^3) S-18	 848 (503)	 824 (489)
Admixtures, oz/yd^3 (mL/m^3) Type A-F HRWR Air-entraining agent	 10.0 (388) 2.5 (96)	 -- 2.6 (98)
Batch Size, yd^3 (m^3)	0.064 (0.049)	
Slump, in. (mm)	2.75 (70)	6.15 (155)
Air Content, %	9.65	6.15
Temperature, °F (°C)	71° (22°)	72° (22°)
Compressive Strength, psi (MPa) 7-Day Strengths 28-Day Strengths	 -- 3520 (24.3)	 -- 5110 (35.2)

APPENDIX B: DATA COLLECTION TABLES FOR LC-HPC BRIDGE CONSTRUCTION

Table B.1—Plastic Concrete Properties

Project No. :		**Date/Time:**	
Bridge Location:		**Recorded by:**	

Truck Identification No.[1]	**Discharge Time**	**Truck Load**[1], yd^3	**Concrete Temp,** °F	**Slump,** in.	**Air Content,**%	**Unit Weight,** lb/yd^3	**Air Temp,** °F	**Cylinders**[2]	**Test Station**[3]	**Note**[4]

Note: 1. The truck identification No. and truck load in yd^3 can be obtained from the trip tickets on the site.
2. The truck from which the concrete was sampled and number of cylinders made should be recorded.
3. Note of the test station is at the truck discharge or on the deck.
4. Delays in concrete delivery, suspected of out specification concrete, or any observations of interest should be recorded.

Table B.2—Time for Burlap Placement

Project No. :		Date/Time:	
Bridge Location:		Recorded by:	

Observation Stations[1]	Concrete placement time	Strike off time	1st layer of burlap time	2nd layer of burlap time	Time used[2], minutes	Notes:

Note: 1. Observation stations should be pre-selected by the recorder before the construction begins.
2. Time used for burlap placement is the difference between the strike off time and placement of the 1st layer of burlap placing time.

Table B.3—Site Weather Conditions

Project No. :		**Date/Time:**	
Bridge Location:		**Recorded by:**	

Time	Air Temp[1], °F	Relative Humidity[1], %	Concrete Temp, °F	Wind Velocity[1], mph	Evaporation Rate, lb/sq ft/hr	Girder Temperature-Bottom flange[2], °F	Girder Temperature-Mid web[2], °F	Girder Temperature-Top flange[2], °F	Note

Note: 1. Should be taken approximately 12 in. above the deck surface.
2. An infrared thermometer can be used to check the girder temperature.

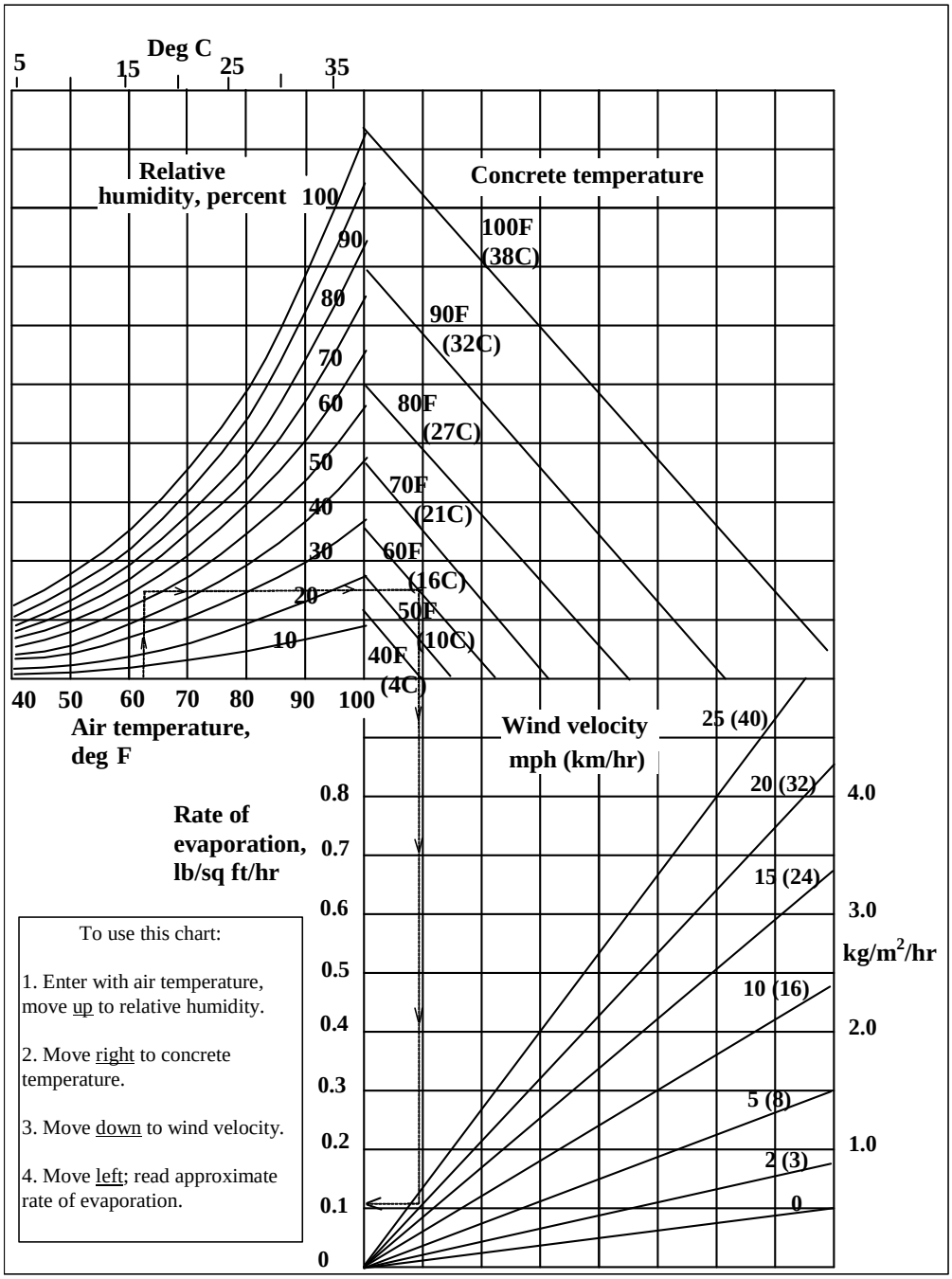

Effect of concrete and air temperatures, relative humidity, and wind velocity on the rate of evaporation of surface moisture from concrete. This chart provides a graphic method of estimating the loss of surface moisture for various weather conditions. To use the chart, follow the four steps outlined above. When the evaporation rate exceeds 0.2 lb/ft^2/hr (1.0 kg/ m^2/hr), measures shall be taken to prevent excessive moisture loss from the surface of unhardened concrete; when the rate is less than 0.2 lb/ft^2/hr (1.0 kg/m^2/hr) such measures may be needed. When excessive moisture loss is not prevented, plastic cracking is likely to occur.

Figure B.2 Standard Practice for Curing Concrete

APPENDIX C BRIDGE DECK SURVEY SPECIFICATION

1.0 DESCRIPTION.

This specification covers the procedures and requirements to perform surveys of reinforced concrete bridge decks.

2.0 SURVEY REQUIREMENTS.

a. Pre-Survey Preparation.

(1) Prior to performing the crack survey, related construction documents need to be gathered to produce a scaled drawing of the bridge deck. The scale must be exactly 1 in. = 10 ft (for use with the scanning software), and the drawing only needs to include the boundaries of the deck surface

NOTE 1 – In the event that it is not possible to produce a scaled drawing prior to arriving at the bridge deck, a hand-drawn crack map (1 in. = 10 ft) created on engineering paper using measurements taken in the field is acceptable.

(2) The scaled drawing should also include compass and traffic directions in addition to deck stationing. A scaled 5 ft by 5 ft grid is also required to aid in transferring the cracks observed on the bridge deck to the scaled drawing. The grid shall be drawn separately and attached to the underside of the crack map such that the grid can easily be seen through the crack map.

NOTE 2 – Maps created in the field on engineering paper need not include an additional grid.

(3) For curved bridges, the scaled drawing need not be curved, i.e., the curve may be approximated using straight lines.

(4) Coordinate with traffic control so that at least one side (or one lane) of the bridge can be closed during the time that the crack survey is being performed.

b. Preparation of Surface.

(1) After the deck has been closed to traffic, station the bridge in the longitudinal direction at ten feet intervals. The stationing shall be done as close to the centerline as possible. For curved bridges, the stationing shall follow the curve.

(2) Prior to beginning the crack survey, mark a 5 ft by 5 ft grid using lumber crayons on the portion of the bridge closed to traffic corresponding to the grid on the scaled drawing. Measure and document any drains, repaired areas, unusual cracking, or any other items of interest.

(3) Starting with one end of the closed portion of the deck, using a lumber crayon, begin tracing cracks that can be seen while bending at the waist. After beginning to trace cracks, continue to the end of the crack, even if this includes portions of the crack that were not initially seen while bending at the waist. Areas covered by sand or other debris need not be surveyed. Trace the cracks using a different color crayon than was used to mark the grid and stationing.

(4) At least one person shall check over the marked portion of the deck for any additional cracks. The goal is not to mark every crack on the deck, only those cracks that can initially be seen while bending at the waist.

NOTE 3 – An adequate supply of lumber crayons should be on hand for the survey. Crayon colors should be selected to be readily visible when used to mark the concrete.

c. Weather Limitations.

(1) Surveys are limited to days when the expected temperature during the survey will not be below 60° F.

(2) Surveys are further limited to days that are forecasted to be at least mostly sunny for a majority of the day.

(3) Regardless of the weather conditions, the bridge deck must be completely dry before the survey can begin.

3.0 BRIDGE SURVEY.

a. Crack Surveys.

Using the grid as a guide, transfer the cracks from the deck to the scaled drawing. Areas that are not surveyed should be marked on the scaled drawing. Spalls, regions of scaling, and other areas of special interest need not be included on the scale drawings but should be noted.

b. Delamination Survey.

During or after the crack survey, bridge decks shall be checked for delamination. Any areas of delamination shall be noted and drawn on a separate drawing of the bridge. This second drawing need not be to scale.

c. Under Deck Survey.

Following the crack and delamination survey, the underside of the deck shall be examined and any unusual or excessive cracking noted.

APPENDIX D RESTRAINED RING TESTS

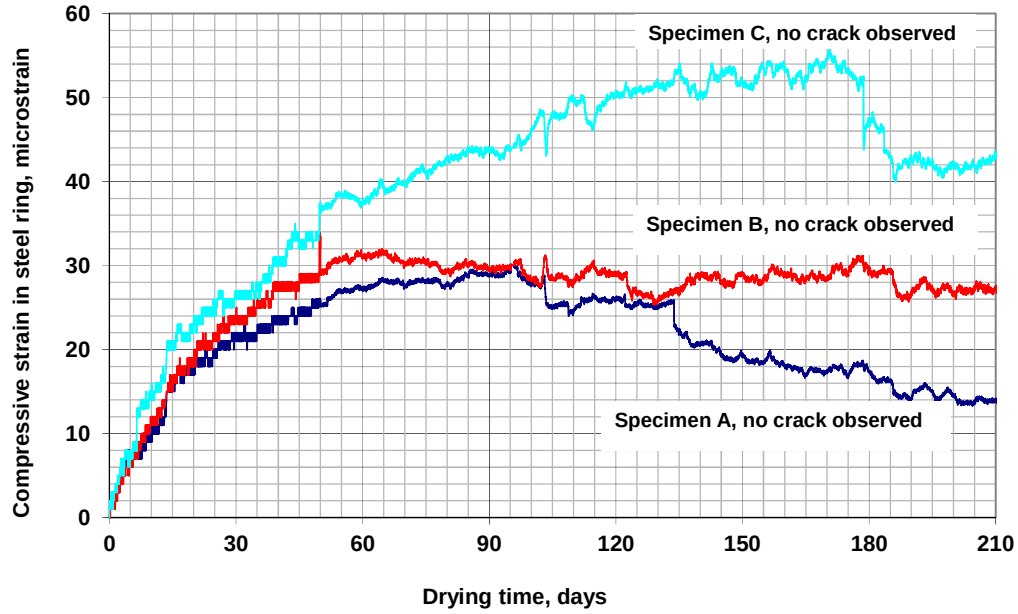

(a)

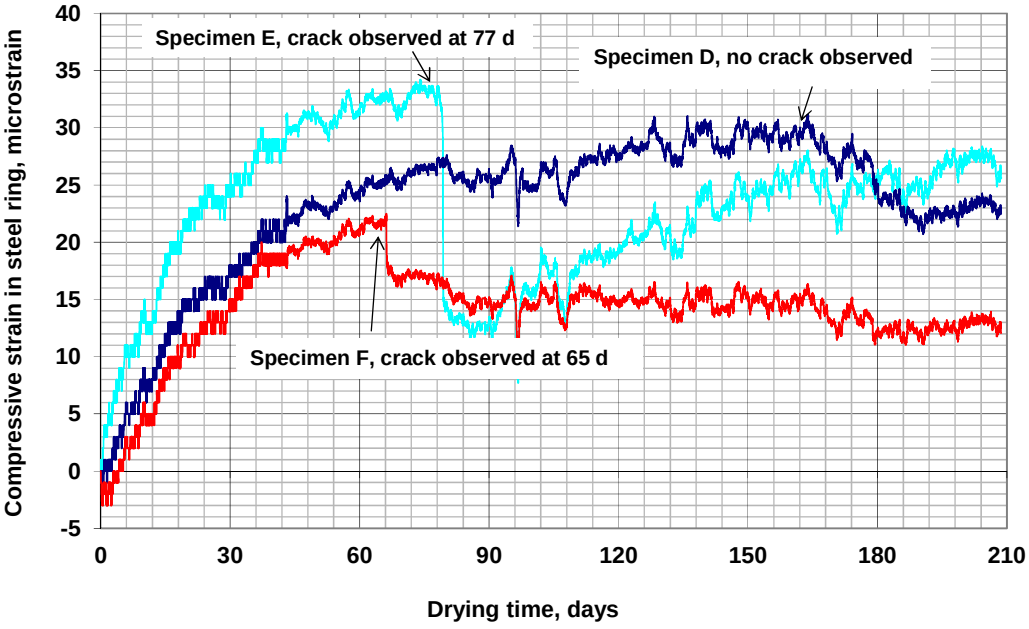

(b)

Figure D.1 Compressive strain in steel ring versus drying time: (a) Program I-0.45 *w/c* (batch 488) with 7-day curing. (b) Program I-0.45 *w/c* (batch 488) with 14-day curing. 2.5-in. (64-mm) concrete ring thickness.

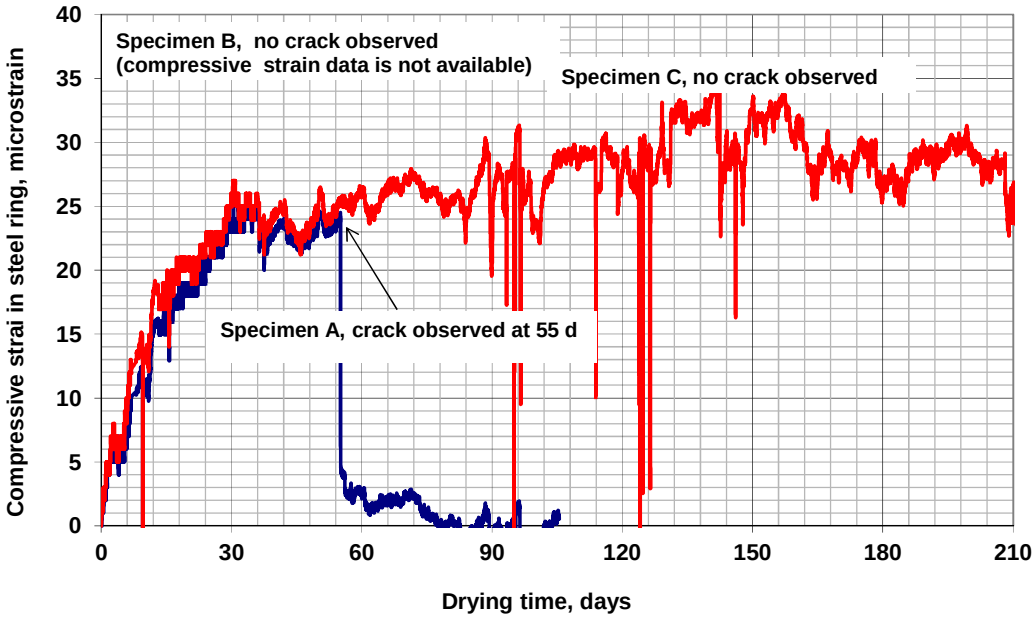

(a)

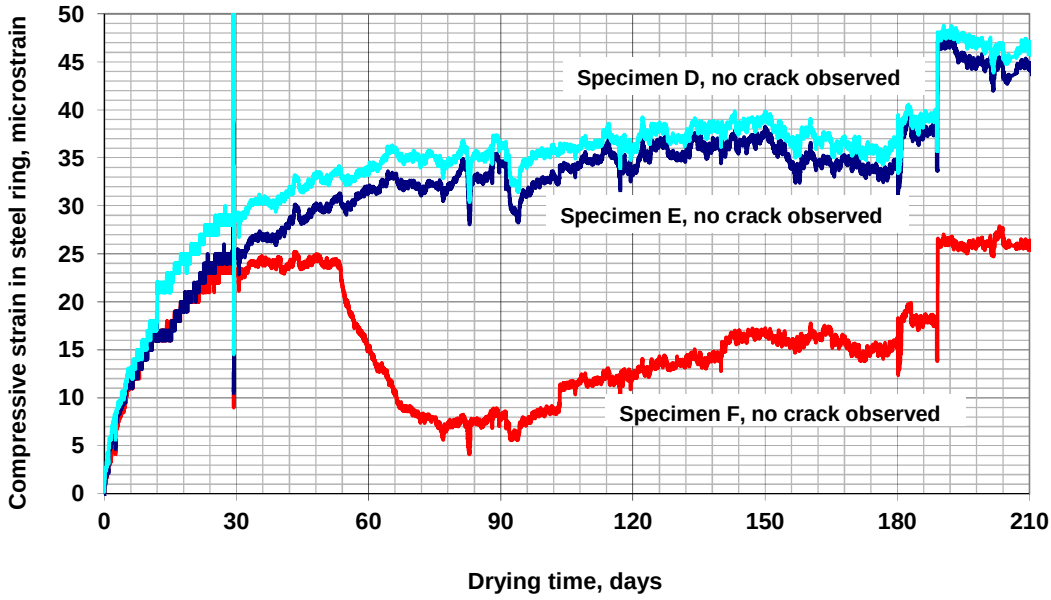

(b)

Figure D.2 Compressive strain in steel ring versus drying time: (a) Program I-0.42 *w/c* (batch 490) with 7-day curing, (b) Program I-0.42 *w/c* (batch 490) with 14-day curing. 2.5-in. (64-mm) concrete ring thickness.

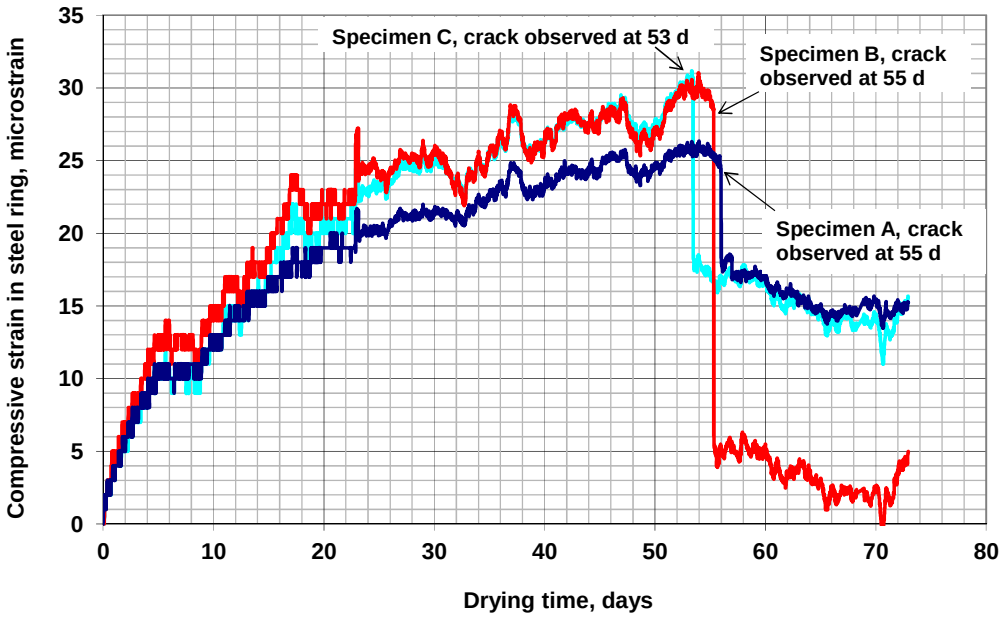

(a)

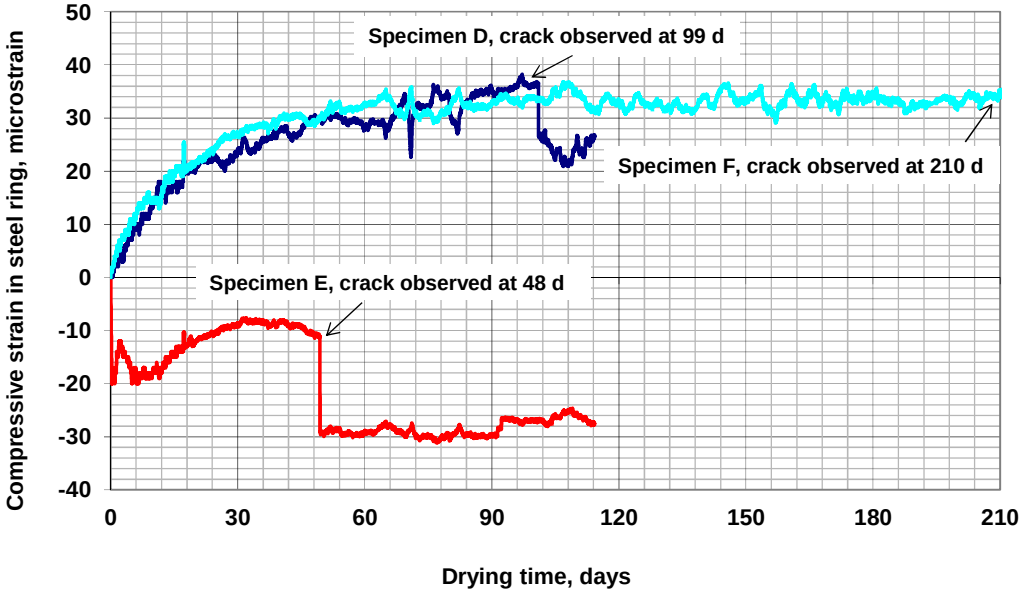

(b)

Figure D.3 Compressive strain in steel ring versus drying time: (a) Program I-0.39 w/c (batch 494) with 7-day curing (b) Program I-0.39 w/c (batch 494) with 14-day curing. 2.5-in. (64-mm) concrete ring thickness.

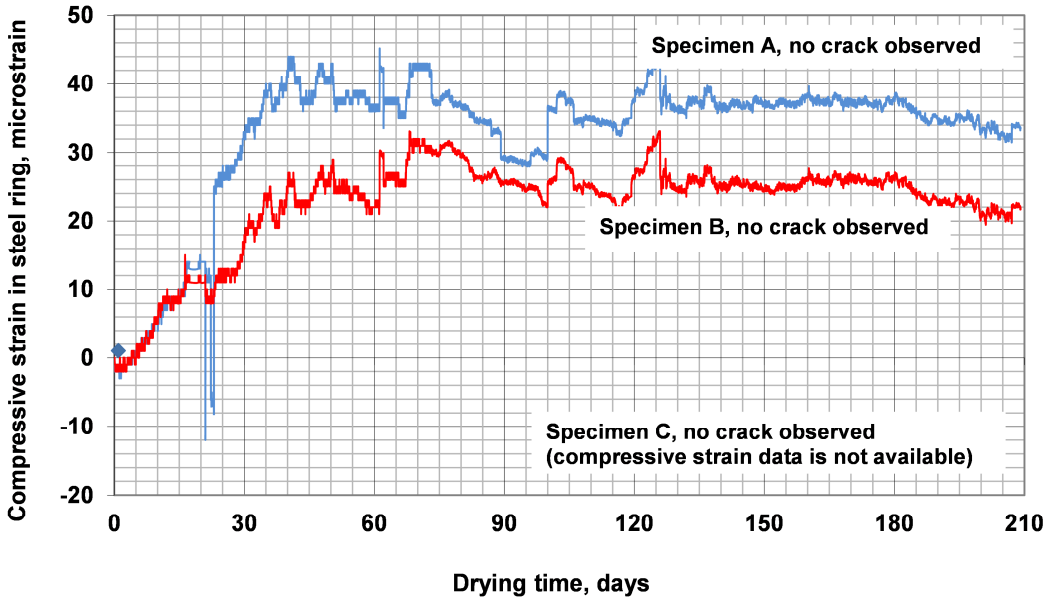

Figure D.4 Compressive strain in steel ring versus drying time: Program I-KDOT mix (batch 485) with 7-day curing. Note: the channel of the data acquisition system for specimen C did not function properly. 2.5-in. (64-mm) concrete ring thickness.

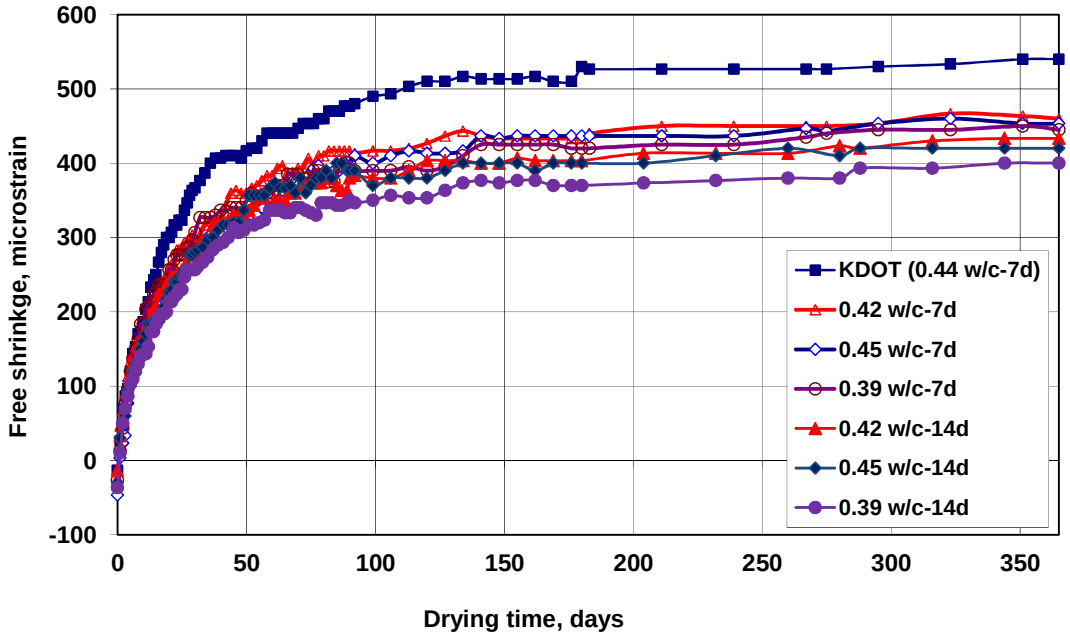

Figure D.5 Free shrinkage versus time through 365 days. Program I.

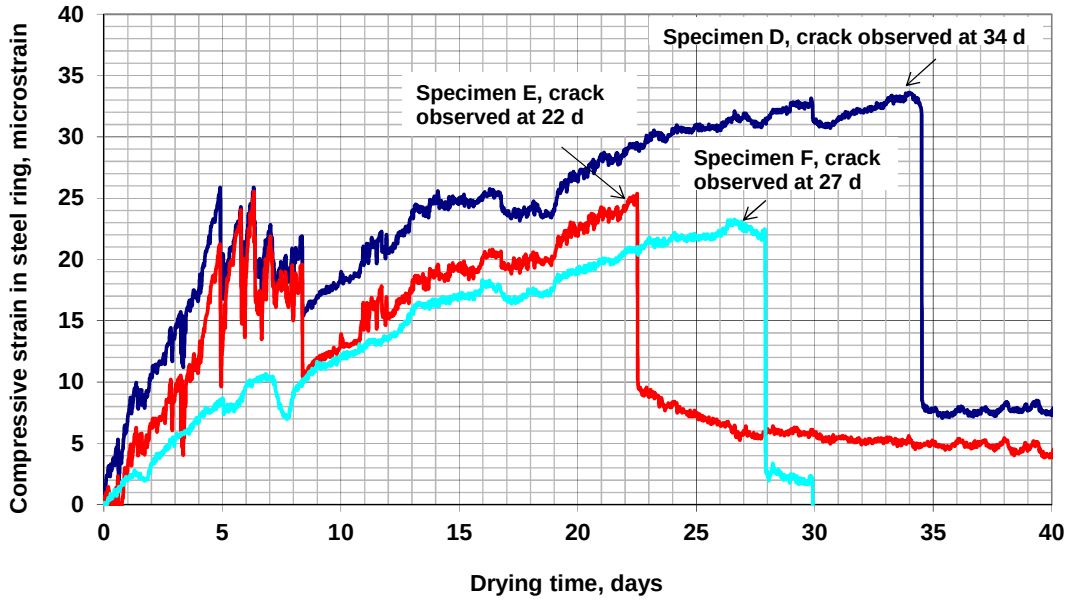

(a)

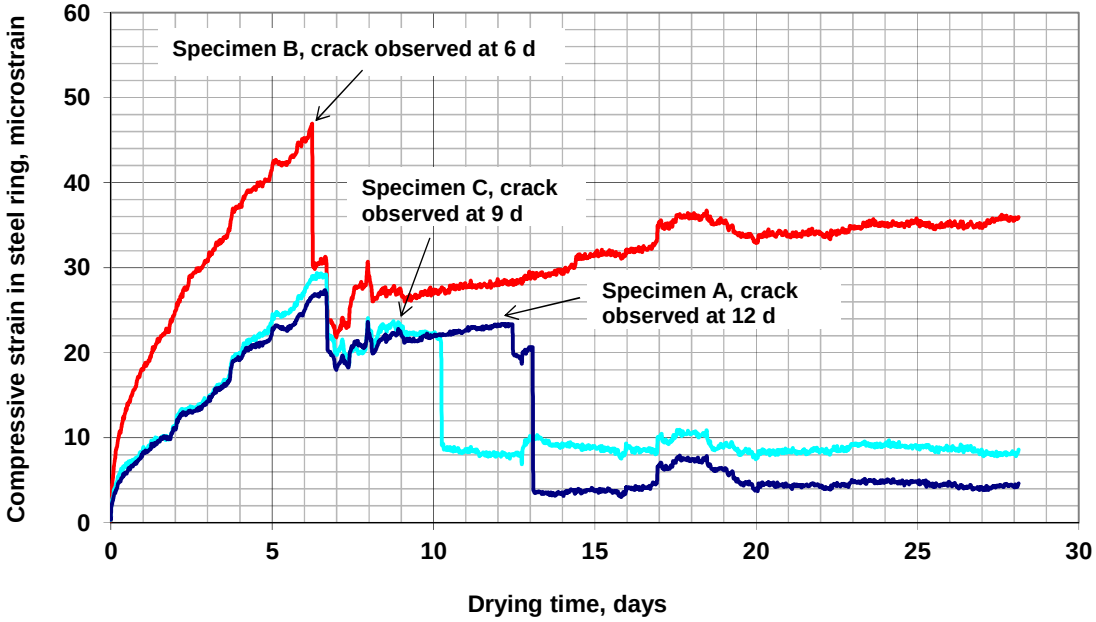

(b)

Figure D.6 Compressive strain in steel ring versus drying time: (a) Program II-KDOT mix (batch 496) with 7-day curing, 2.5-in. (64-mm) concrete ring thickness (b) Program II-KDOT mix (batch 496) with 7-day curing, 1.5-in. (38-mm) concrete ring thickness.

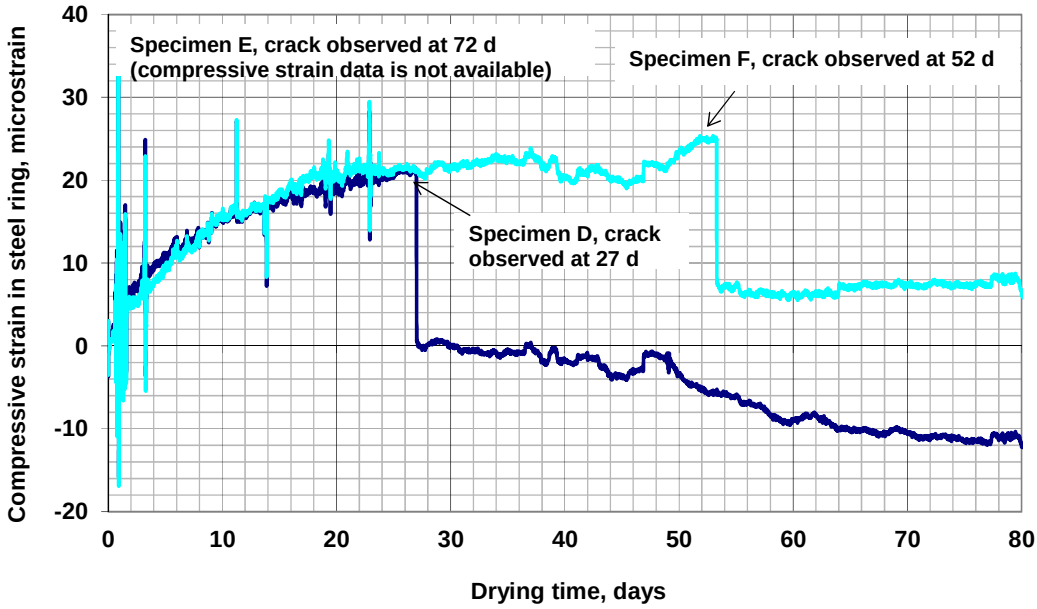

(a)

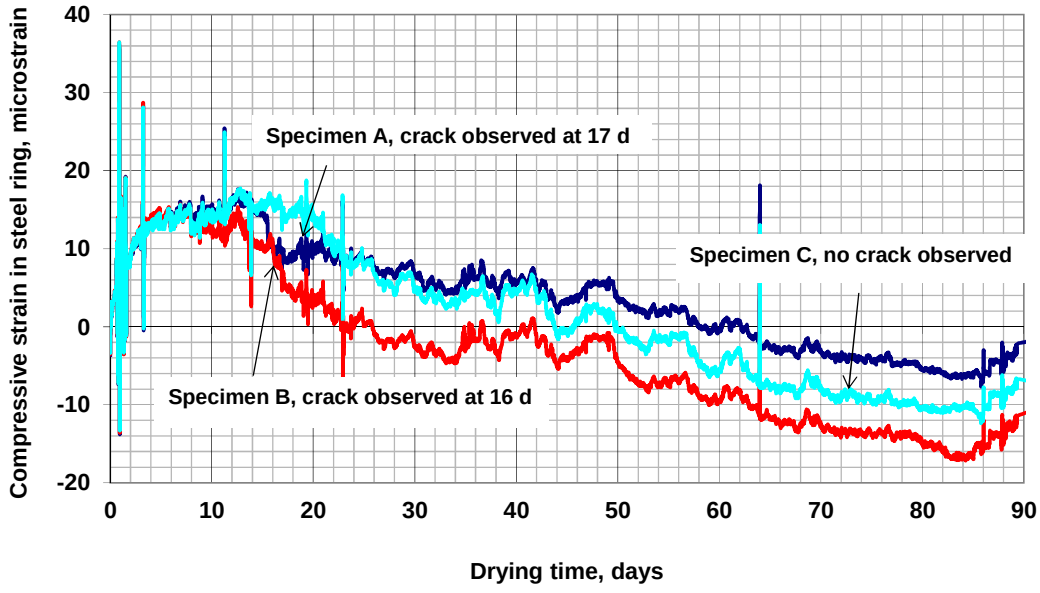

(b)

Figure D.7 Compressive strain in steel ring versus drying time: (a) Program II-0.45 *w/c* mix (batch 509) with 14-day curing, 2.5-in. (64-mm) concrete ring thickness (b) Program II-0.45 *w/c* mix (batch 509) with 14-day curing, 1.5-in. (38-mm) concrete ring thickness. Note: the channel of the data acquisition system for specimen C did not function properly.

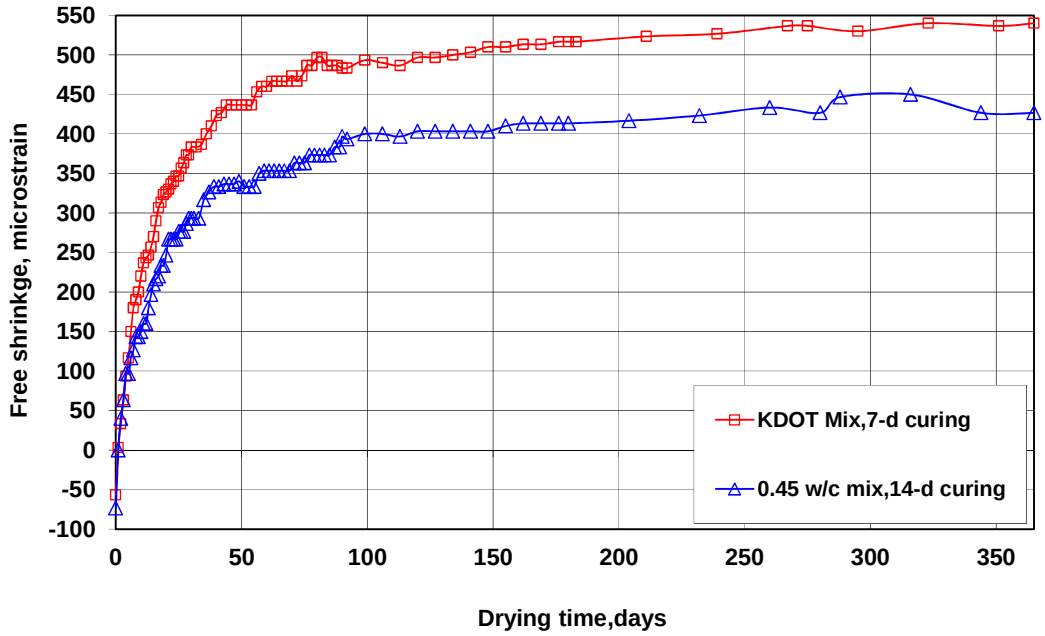

Figure D.8 Free shrinkage versus time through 365 days. Program II.

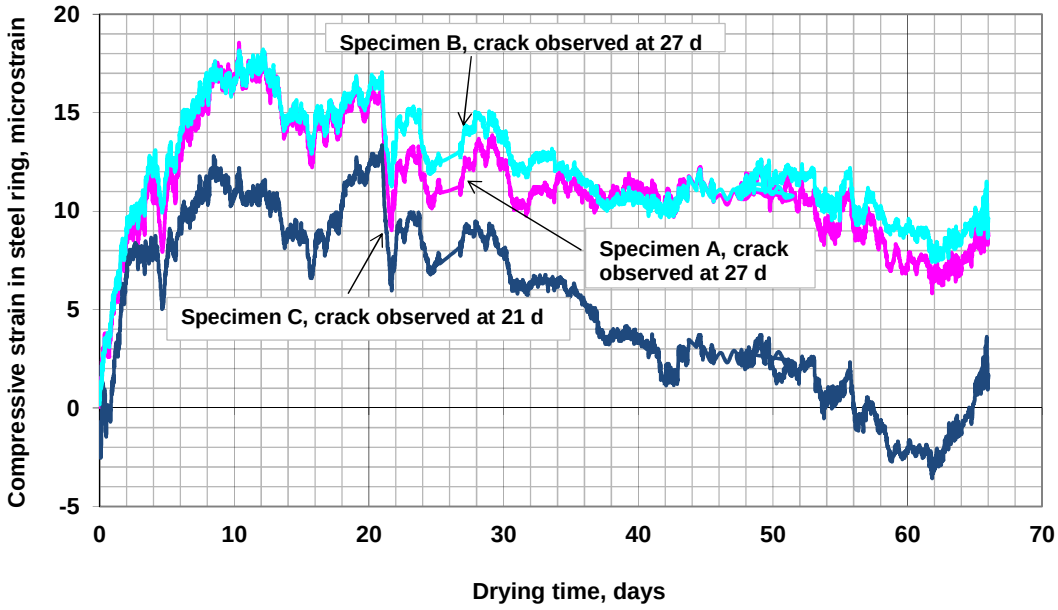

Figure D.9 Compressive strain in steel ring versus drying time: Program III-0.39 *w/c* mix (batch 532) with 14-day curing, 1.5-in. (38-mm) concrete ring thickness.

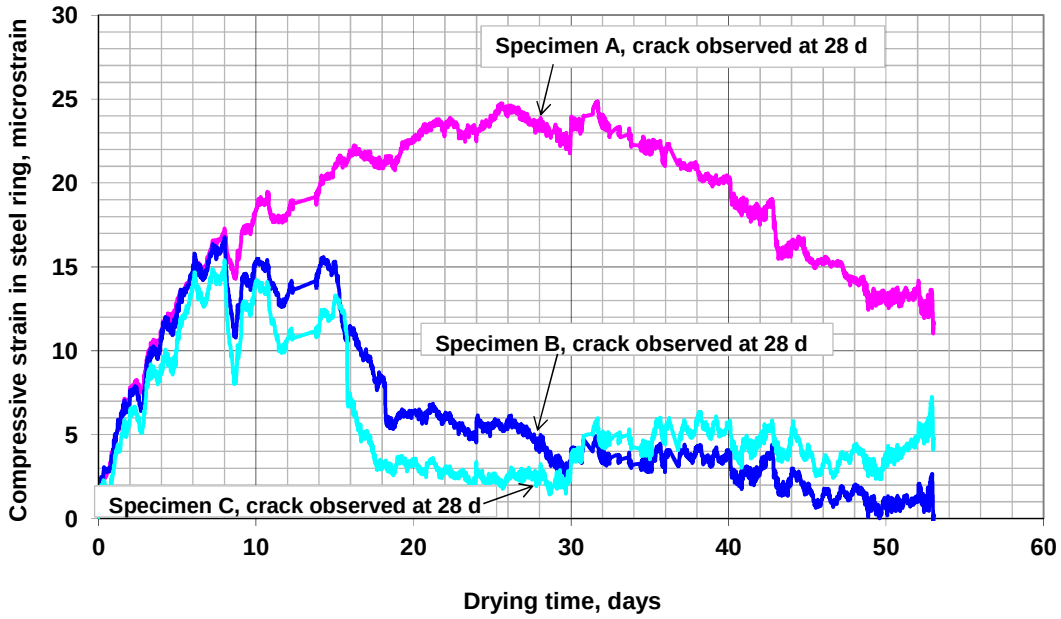

Figure D.10 Compressive strain in steel ring versus drying time: Program III-0.45 *w/c* mix (batch 537) with 14-day curing, 1.5-in. (38-mm) concrete ring thickness.

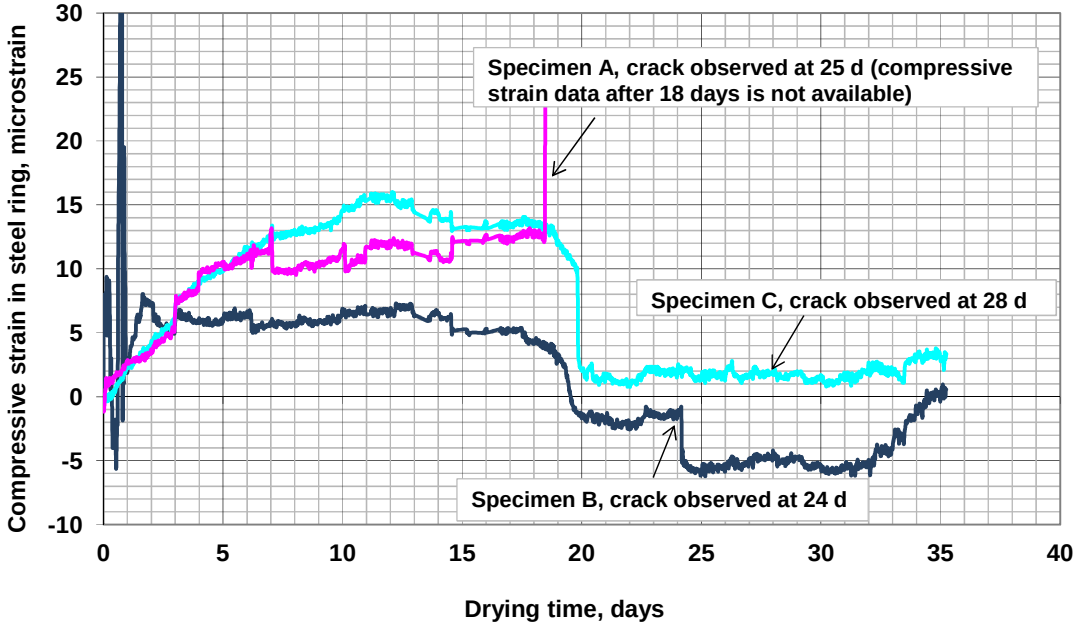

Figure D.11 Compressive strain in steel ring versus drying time: Program III-0.45 *w/c* mix (batch 539) with 14-day curing, 1.5-in. (38-mm) concrete ring thickness.

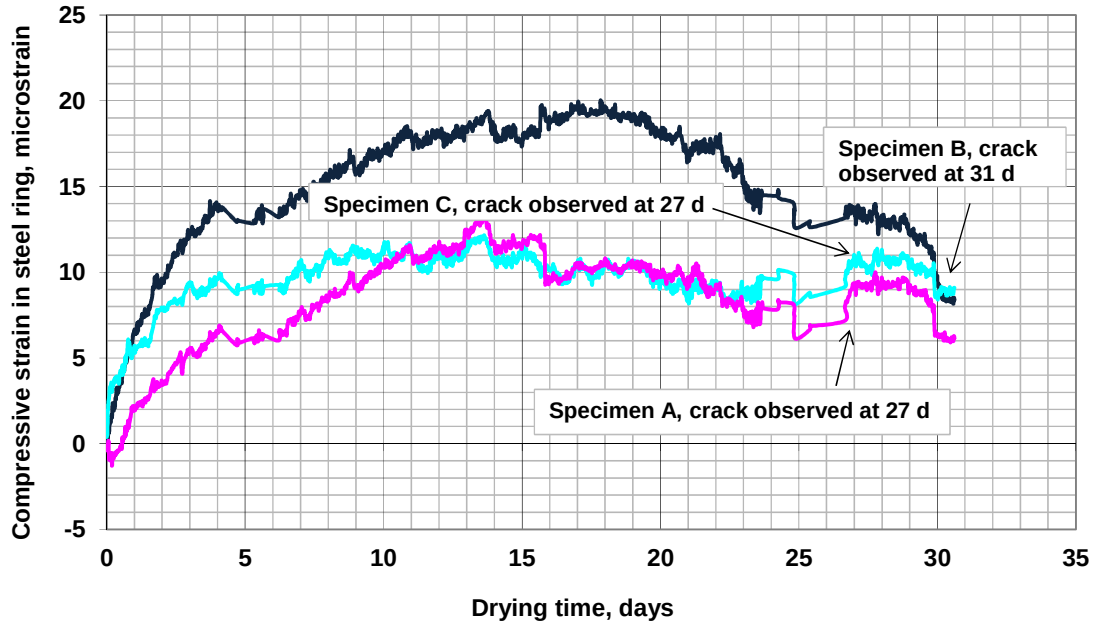

Figure D.12 Compressive strain in steel ring versus drying time: Program III-0.42 *w/c* mix (batch 544) with 14-day curing, 1.5-in. (38-mm) concrete ring thickness.

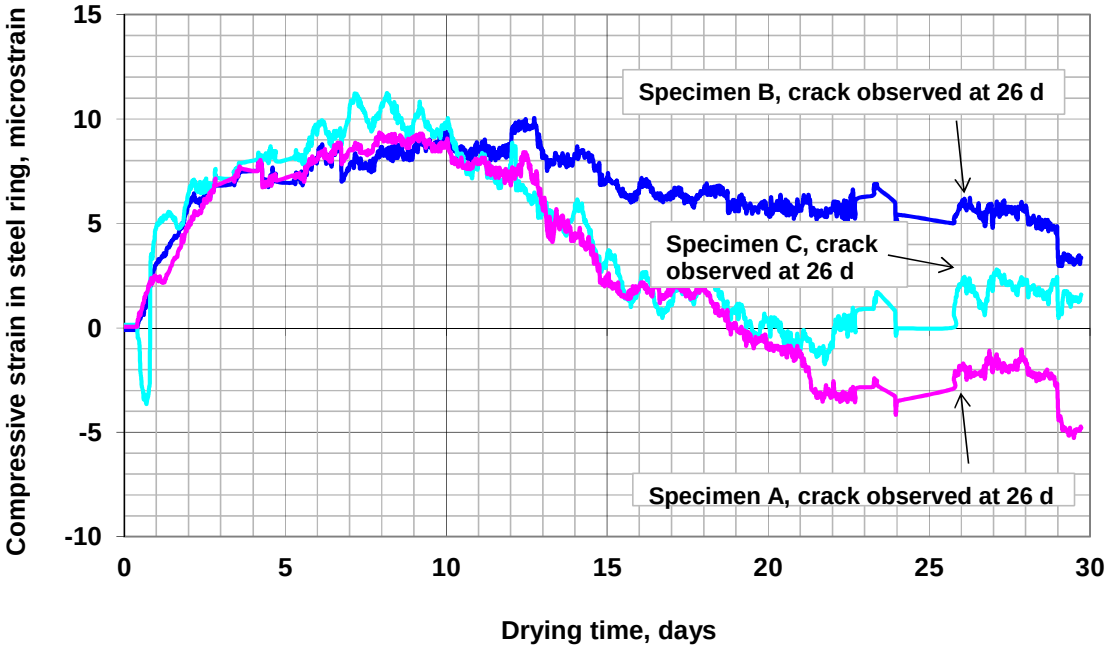

Figure D.13 Compressive strain in steel ring versus drying time: Program III - 40% FA, 0.45 *w/c* mix (batch 545) with 14-day curing, 1.5-in. (38-mm) concrete ring thickness.

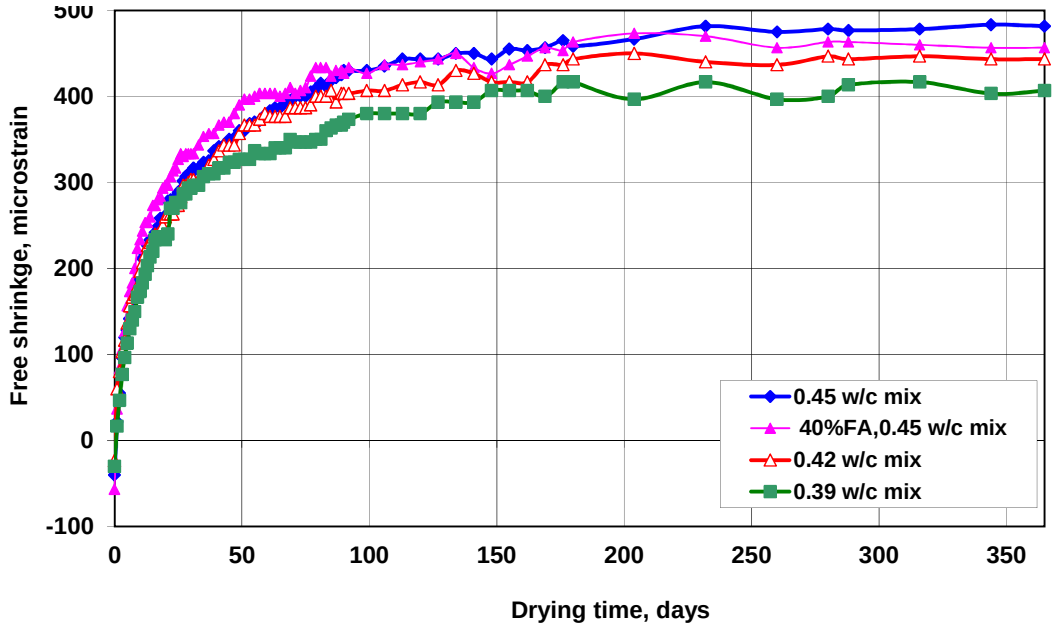

Figure D.14 Free shrinkage versus time through 365 days. Program III.

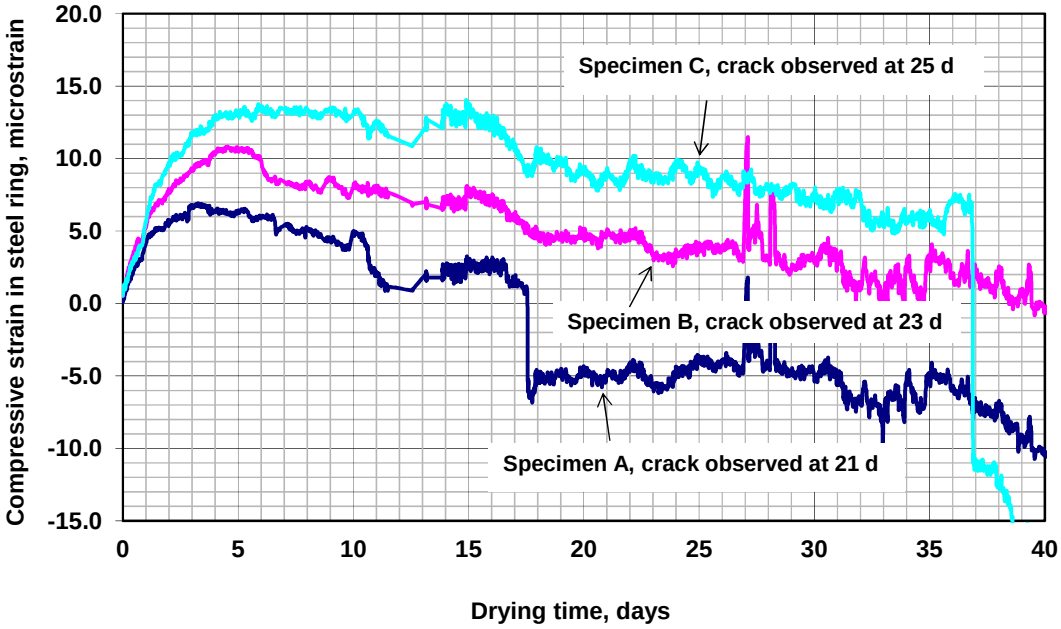

Figure D.15 Compressive strain in steel ring versus drying time: Program IV - 0.45 *w/c* mix (batch 563) with 14-day curing, 1.125-in. (29-mm) concrete ring thickness.

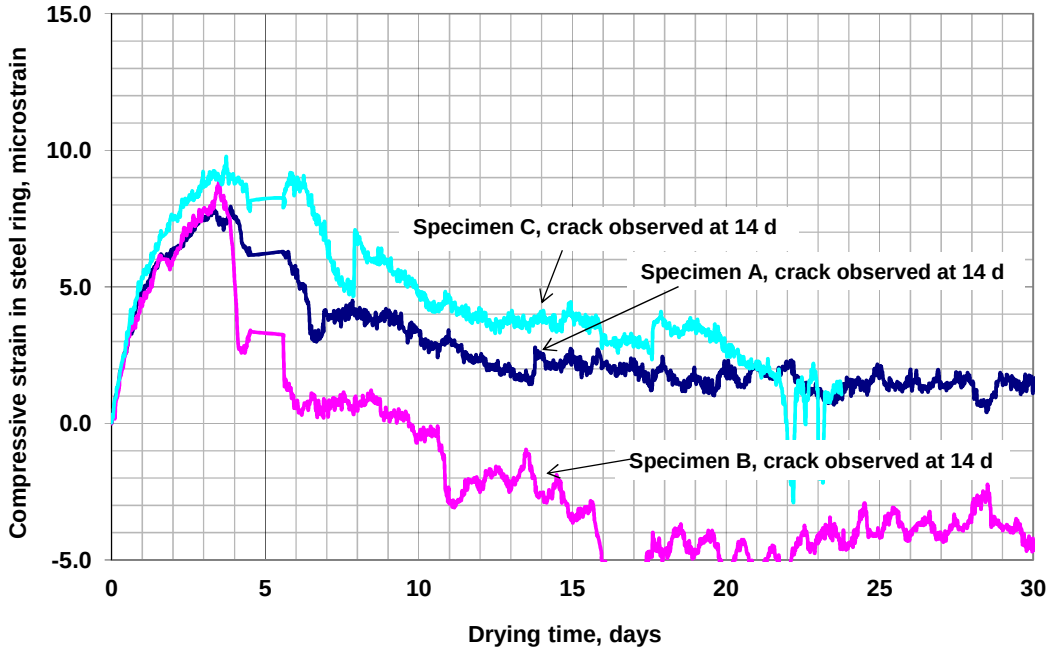

Figure D.16 Compressive strain in steel ring versus drying time: Program IV – 40% FA, 0.45 *w/c* mix (batch 566) with 14-day curing, 1.125-in. (29-mm) concrete ring thickness.

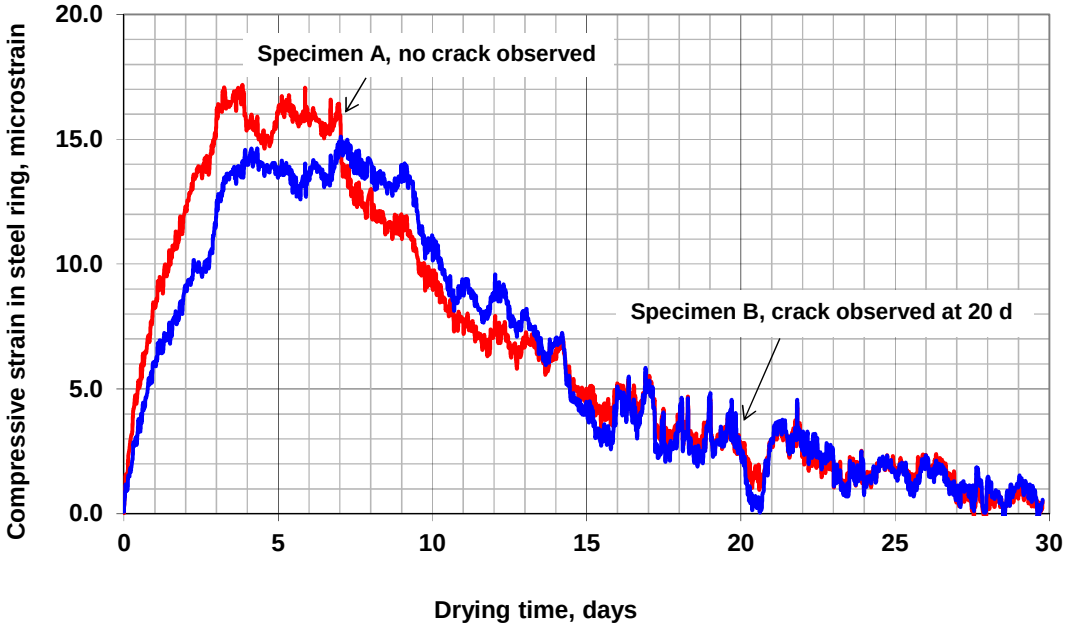

Figure D.17 Compressive strain in steel ring versus drying time: Program IV - 0.35 *w/c* mix (batch 568) with 14-day curing, 1.125-in. (29-mm) concrete ring thickness.

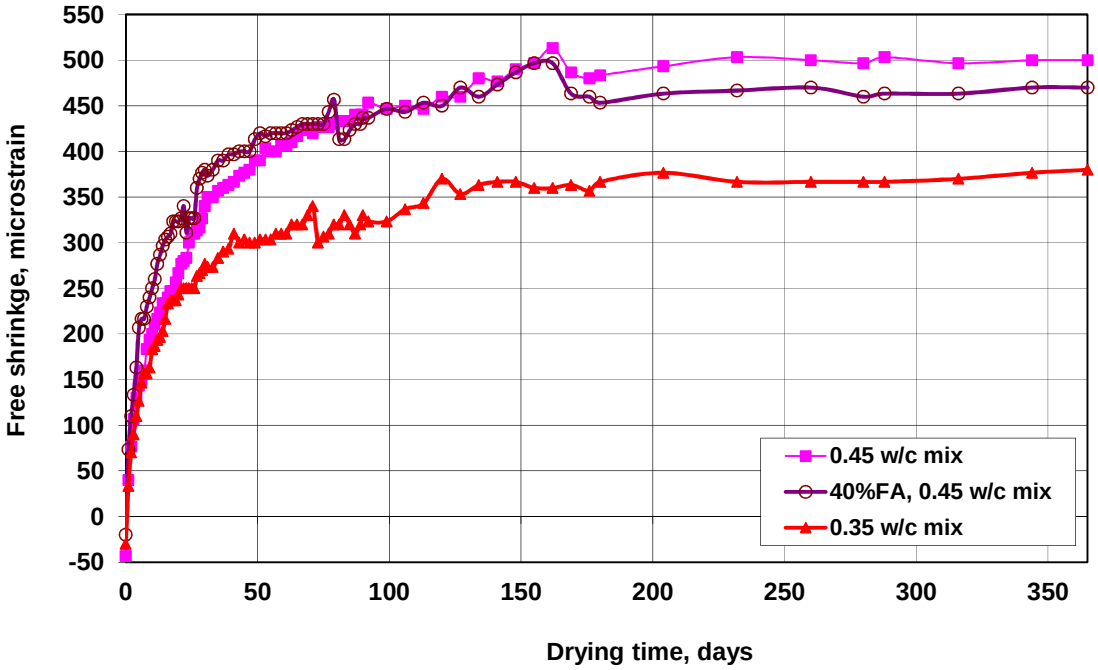

Figure D.18 Free shrinkage versus time through 365 days. Program IV.

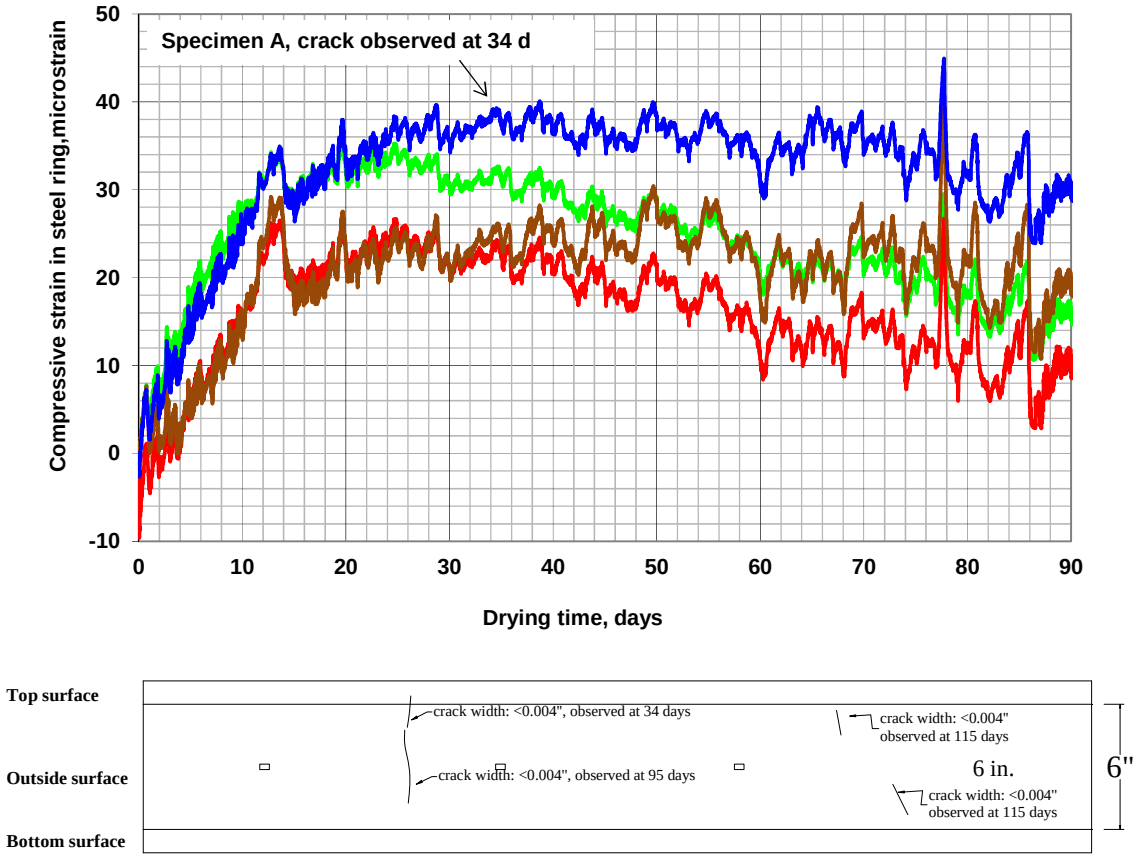

Figure D.19 Compressive strain in steel ring versus drying time: Program V Set 1– C 535 + 0.45 *w/c* mix (batch 597) with 14-day curing, Specimen A (quarter Wheatstone bridge), 2-in. (50-mm) concrete ring thickness. 1 in. = 25.4 mm.

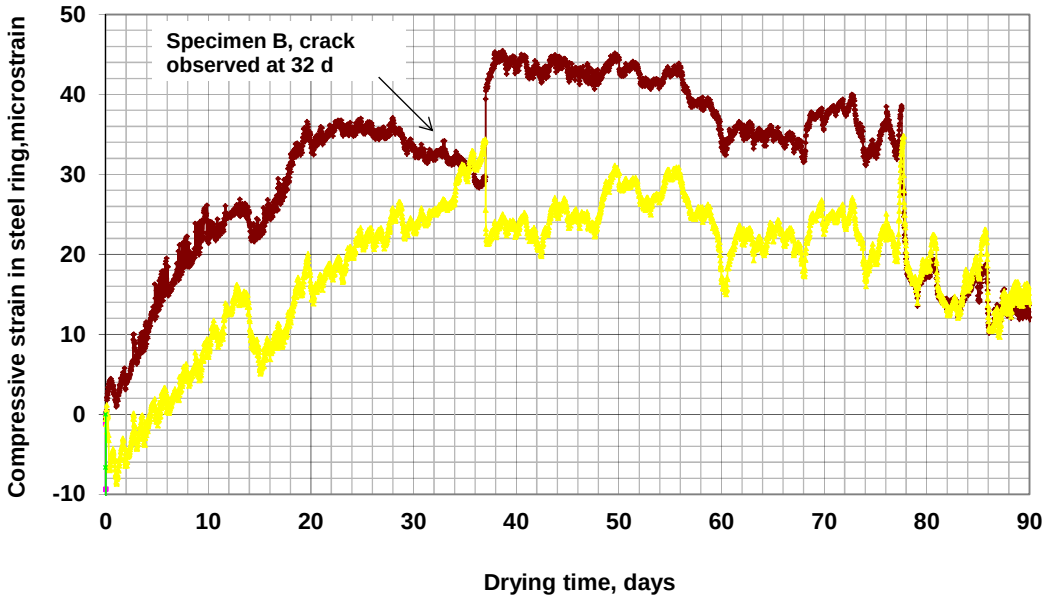

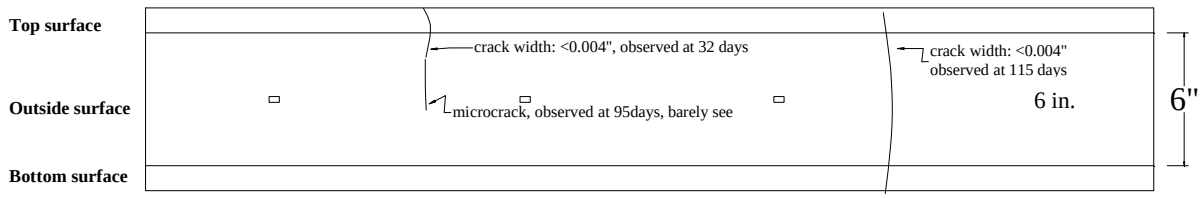

Figure D.20 Compressive strain in steel ring versus drying time: Program V Set 1– C 535 + 0.45 *w*/*c* mix (batch 597) with 14-day curing, Specimen B (quarter Wheatstone bridge), 2-in. (50-mm) concrete ring thickness. Note: Data from other two strain gage was not available. 1 in. = 25.4 mm.

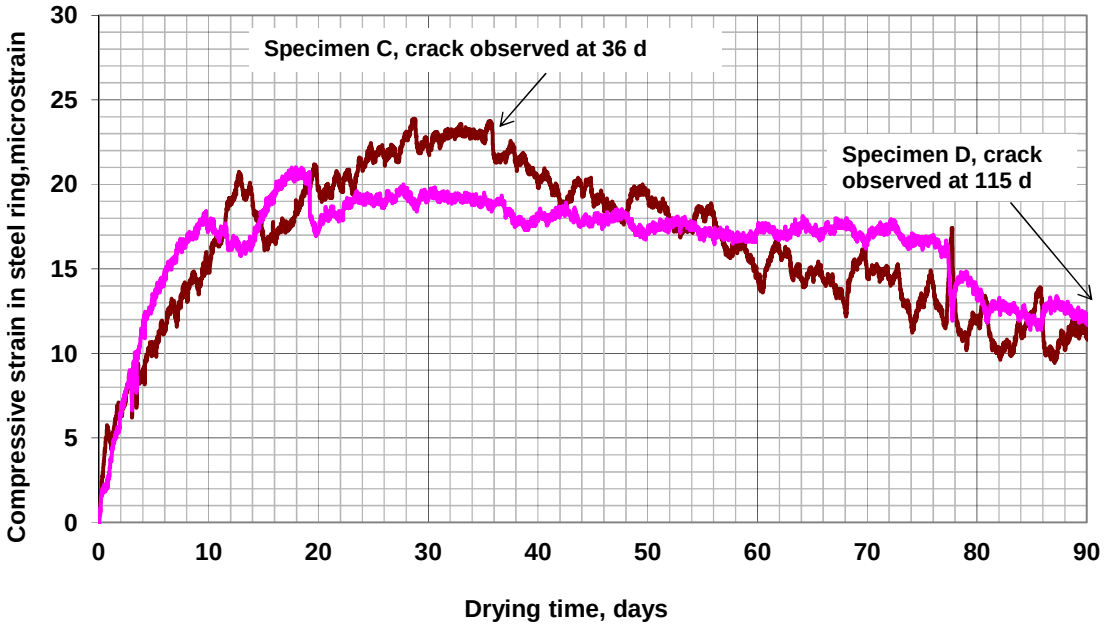

Specimen C

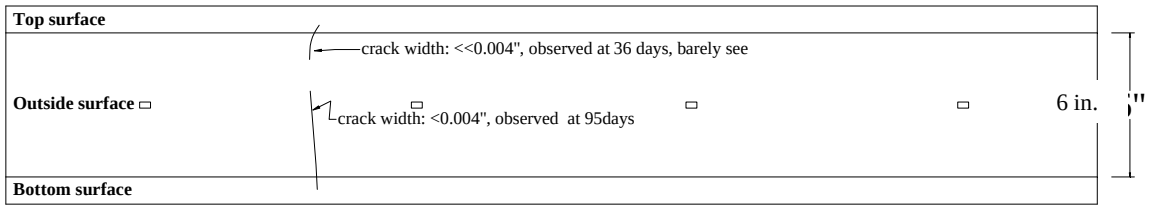

Specimen D

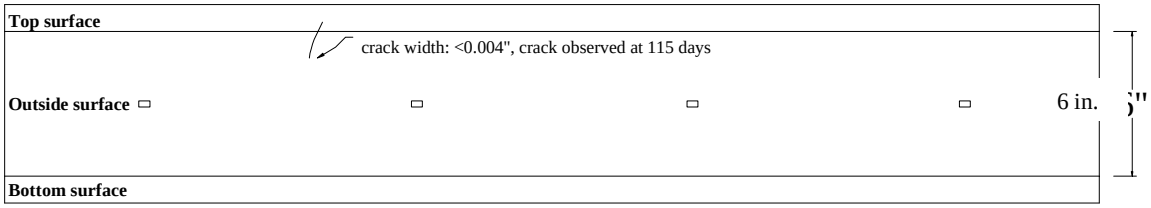

Figure D.21 Compressive strain in steel ring versus drying time: Program V Set 1– C 535 + 0.45 *w/c* mix (batch 597) with 14-day curing, Specimen C and D (Half Wheatstone bridge), 2-in. (50-mm) concrete ring thickness. 1 in. = 25.4 mm.

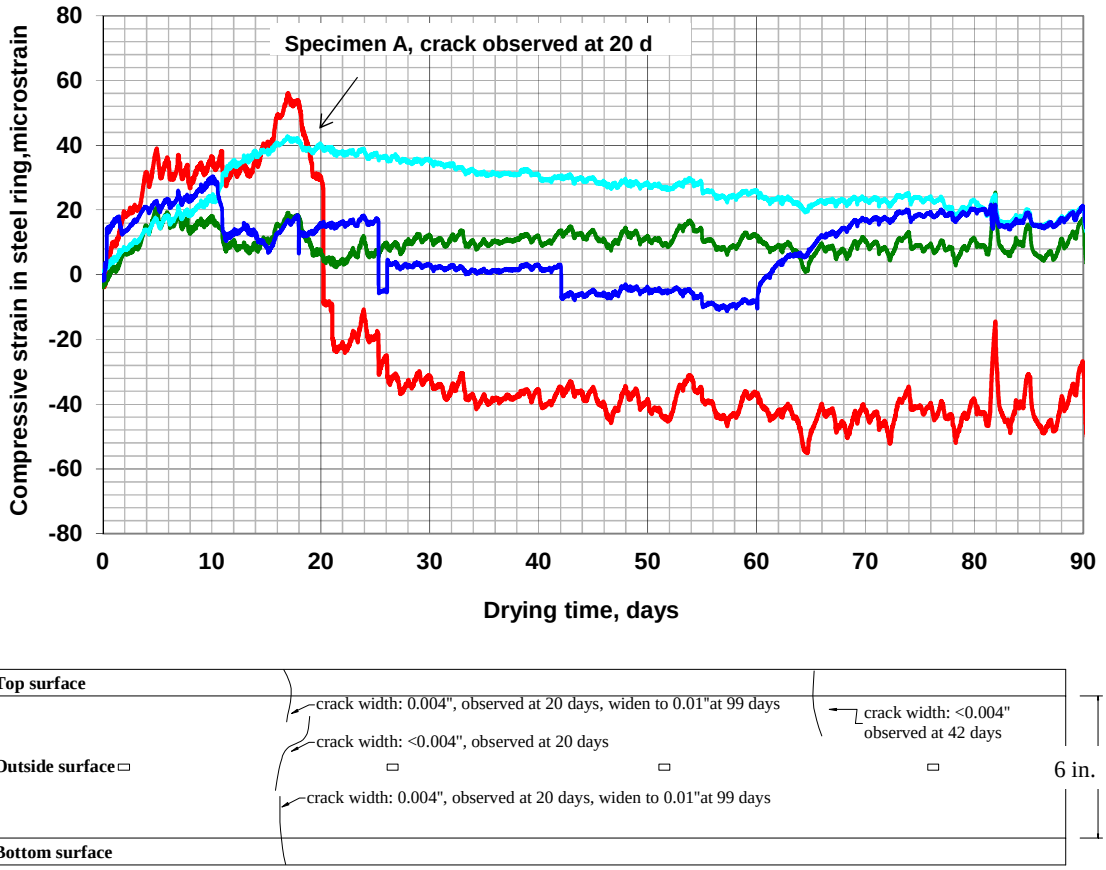

Figure D.22 Compressive strain in steel ring versus drying time: Program V Set 1 – C 729 + 0.45 *w/c* mix (batch 598) with 14-day curing, Specimen A (quarter Wheatstone bridge), 2-in. (50-mm) concrete ring thickness. 1 in. = 25.4 mm.

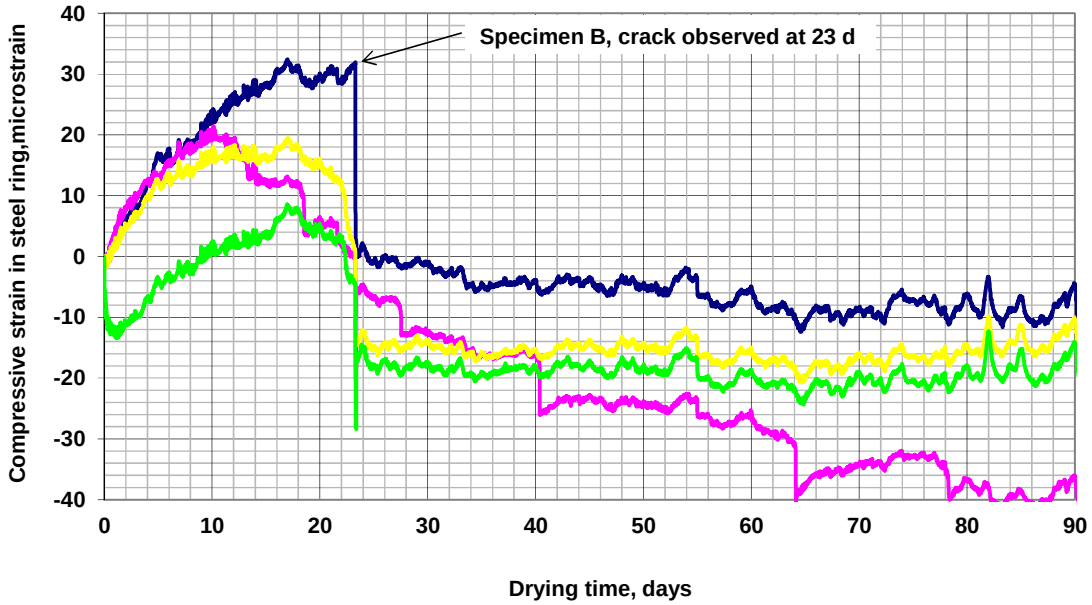

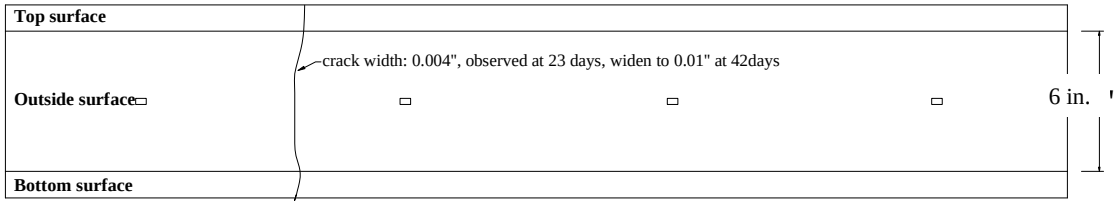

Figure D.23 Compressive strain in steel ring versus drying time: Program V Set 1– C 729 + 0.45 *w/c* mix (batch 598) with 14-day curing, Specimen B (quarter Wheatstone bridge), 2-in. (50-mm) concrete ring thickness. 1 in. = 25.4 mm.

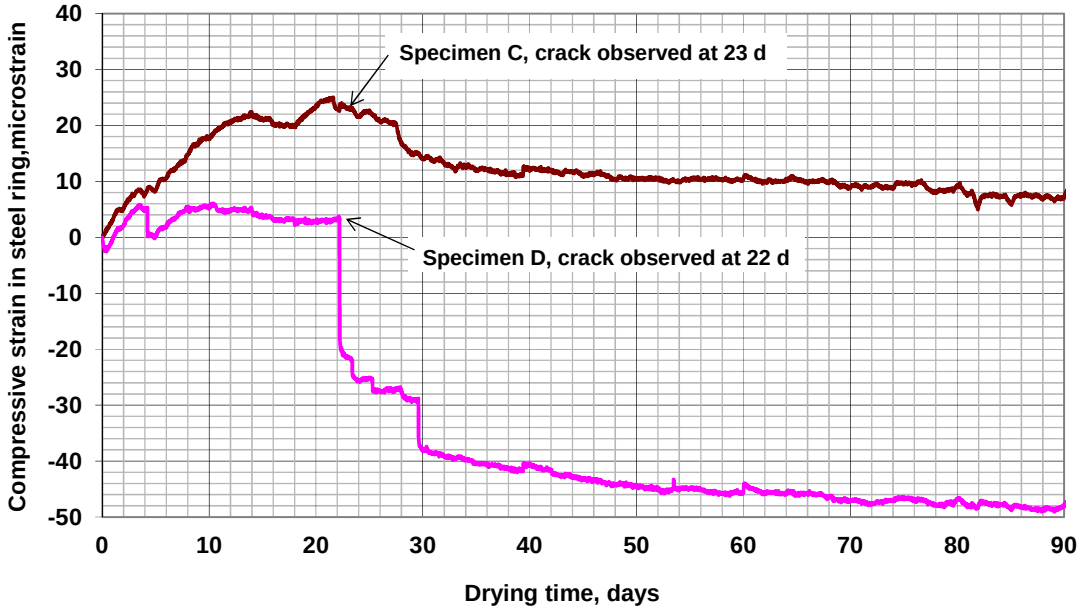

Specimen C

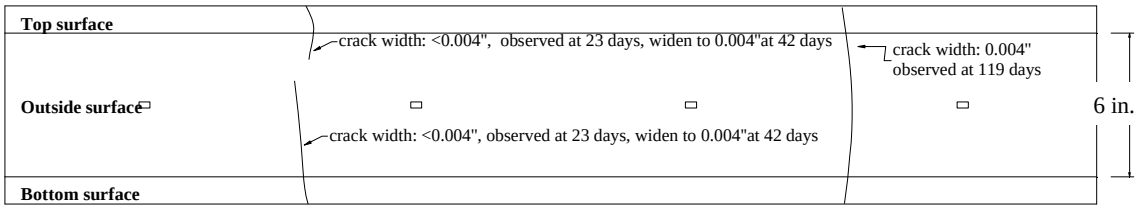

Specimen D

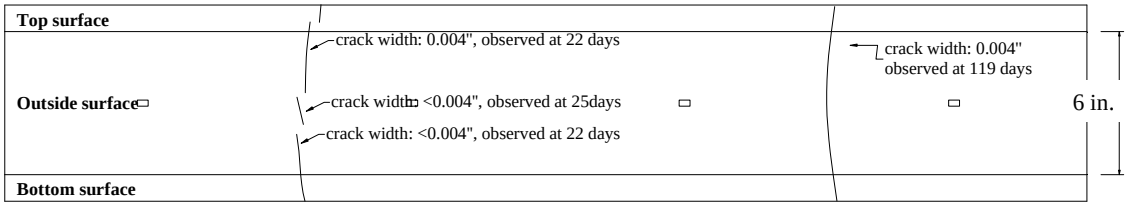

Figure D.24 Compressive strain in steel ring versus drying time: Program V Set 1 – C 729 + 0.45 *w/c* mix (batch 598) with 14-day curing, Specimen C and D (Half Wheatstone bridge), 2-in. (50-mm) concrete ring thickness. 1 in. = 25.4 mm.

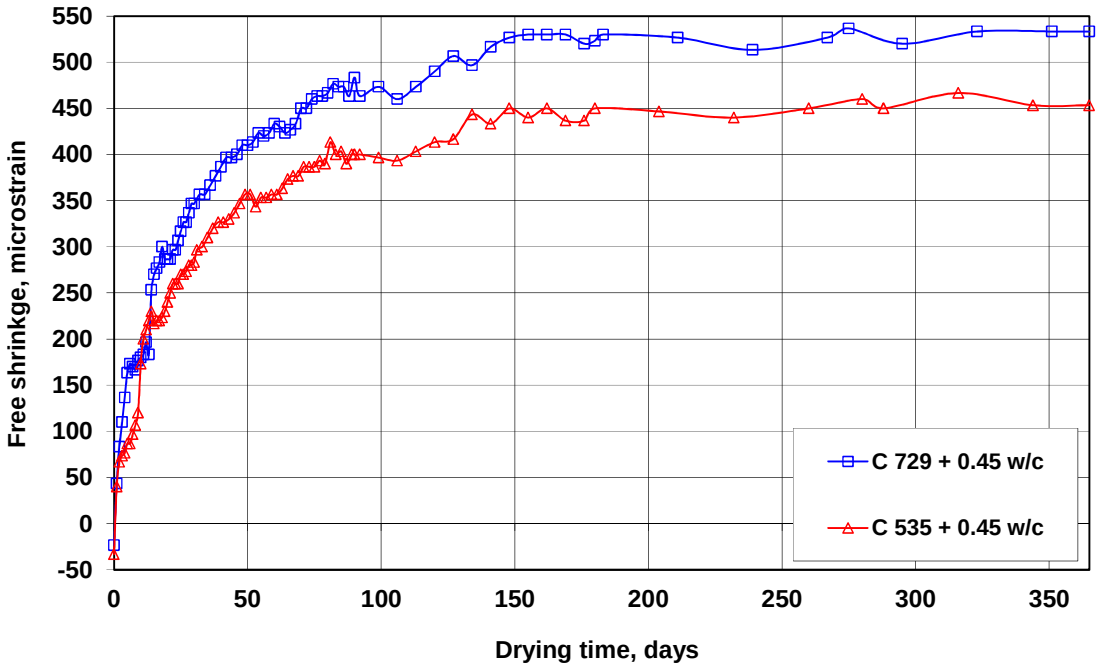

Figure D.25 Free shrinkage versus time through 365 days. Program V Set 1.

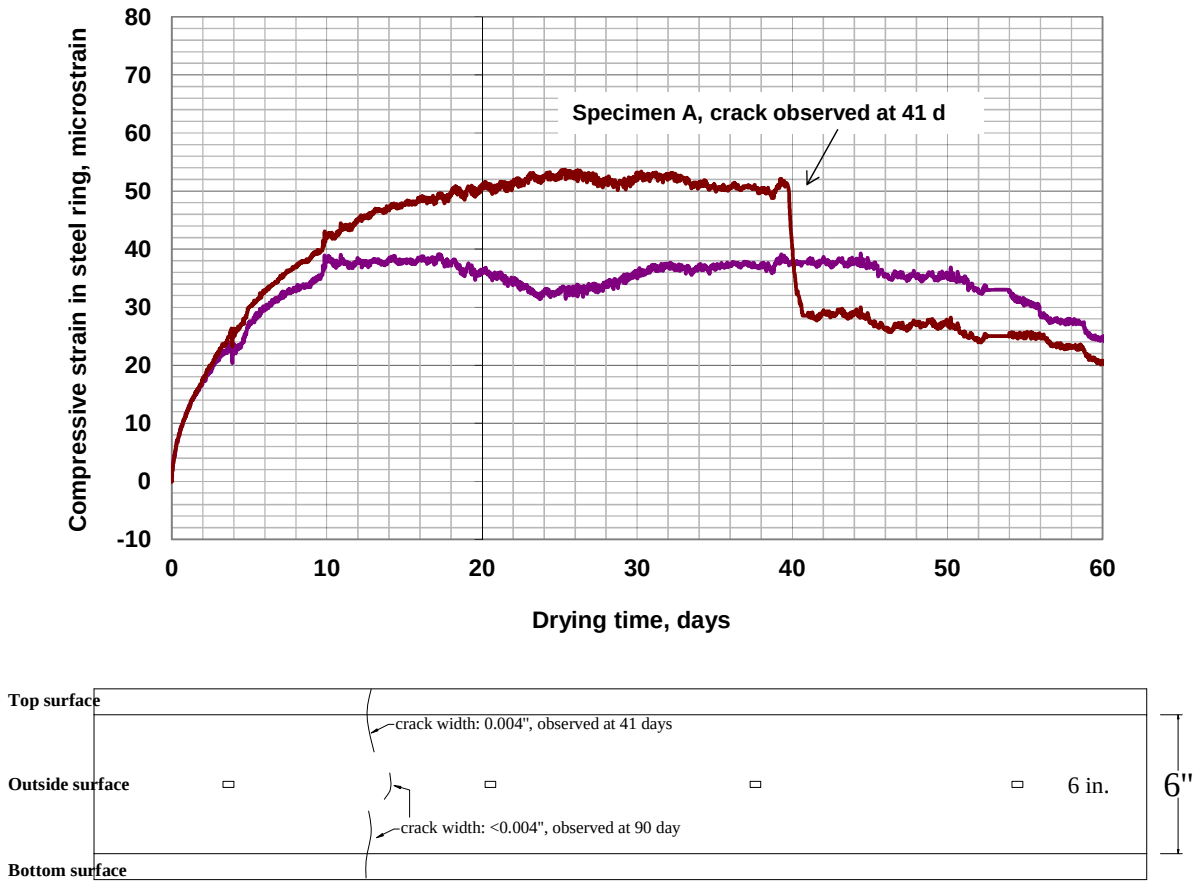

Figure D.26 Compressive strain in steel ring versus drying time: Program V Set 2– C 700 + 0.35 *w/c* mix (batch 649) with 14-day curing, Specimen A (Quarter Wheatstone bridge), 2-in. (50-mm) concrete ring thickness. . Note: Data from two strain gages was not available. 1 in. = 25.4 mm.

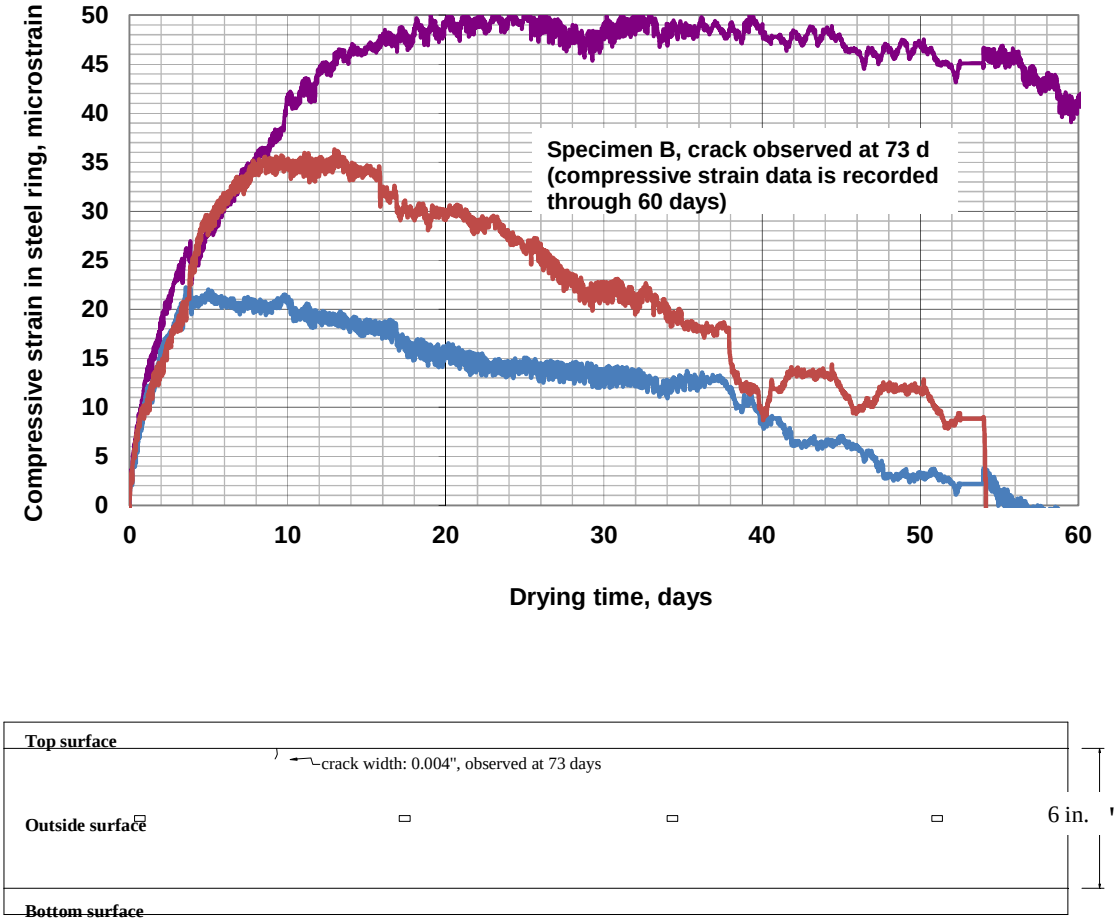

Figure D.27 Compressive strain in steel ring versus drying time: Program V Set 2– C 700 + 0.35 *w/c* mix (batch 649) with 14-day curing, Specimen B (Quarter Wheatstone bridge), 2-in. (50-mm) concrete ring thickness. Note: Data from one strain gage was disturbed. 1 in. = 25.4 mm.

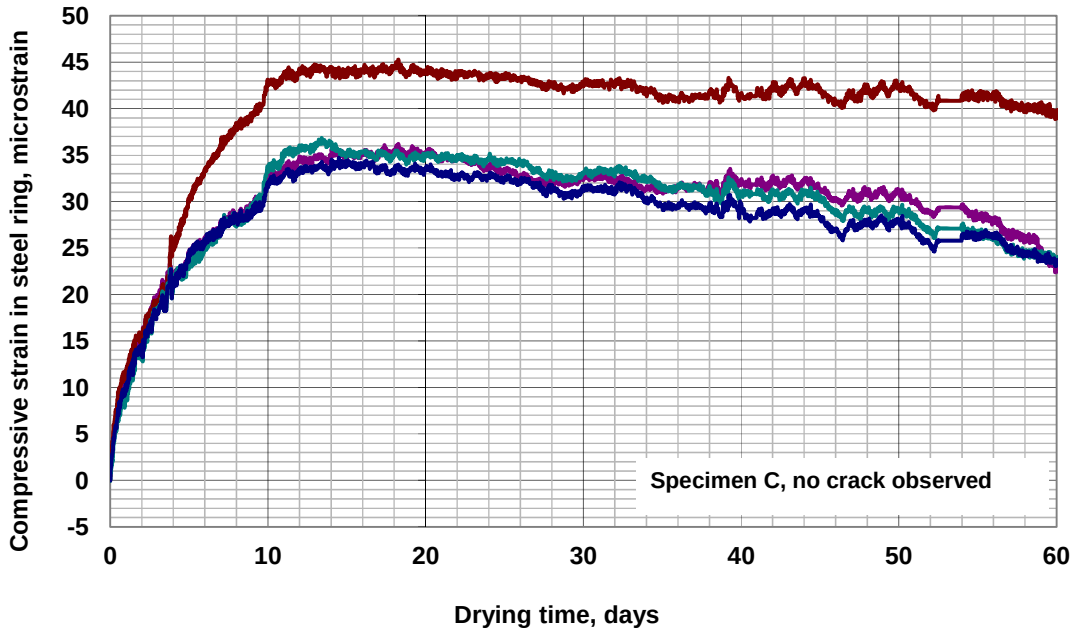

No crack observed in 90 days

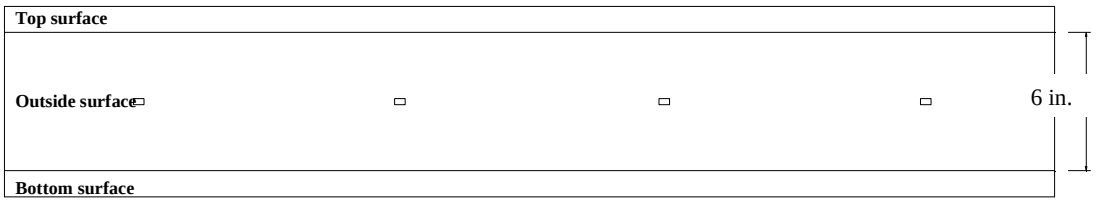

Figure D.28 Compressive strain in steel ring versus drying time: Program V Set 2– C 700 + 0.35 *w/c* mix (batch 649) with 14-day curing, Specimen C (Quarter Wheatstone bridge), 2-in. (50-mm) concrete ring thickness. 1 in. = 25.4 mm.

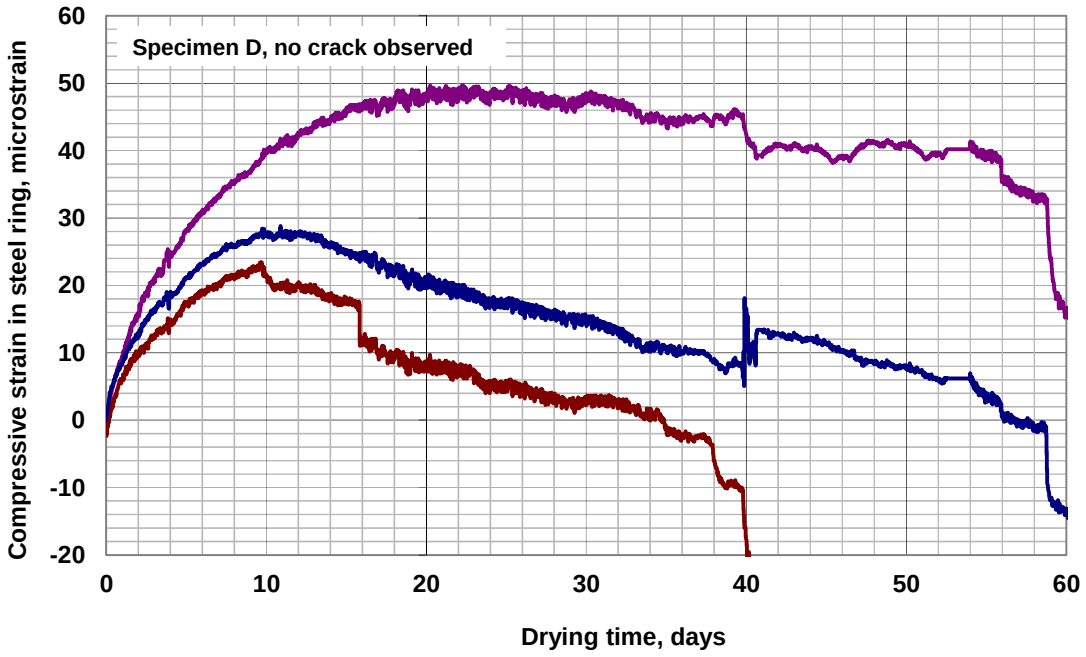

No crack observed in 90 days

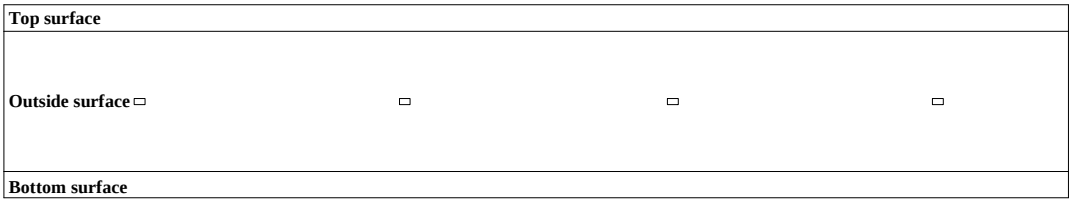

Figure D.29 Compressive strain in steel ring versus drying time: Program V Set 2– C 700 + 0.35 *w/c* mix (batch 649) with 14-day curing, Specimen D (Quarter Wheatstone bridge), 2-in. (50-mm) concrete ring thickness. Note: Data from other one strain gage was disturbed. 1 in. = 25.4 mm.

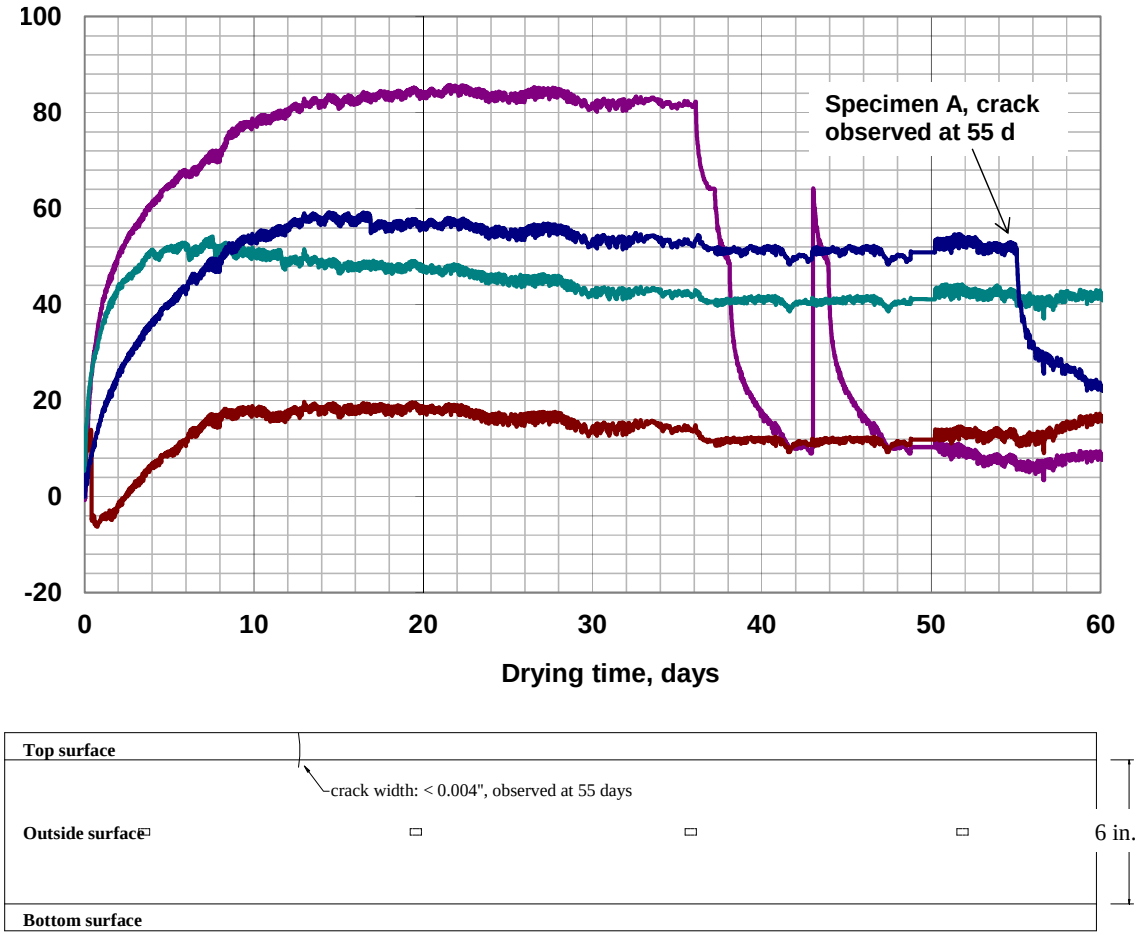

Figure D.30 Compressive strain in steel ring versus drying time: Program V Set 2– 40% FA + 0.35 *w/c* mix (batch 650) with 14-day curing, Specimen A (Quarter Wheatstone bridge), 2-in. (50-mm) concrete ring thickness. 1 in. = 25.4 mm.

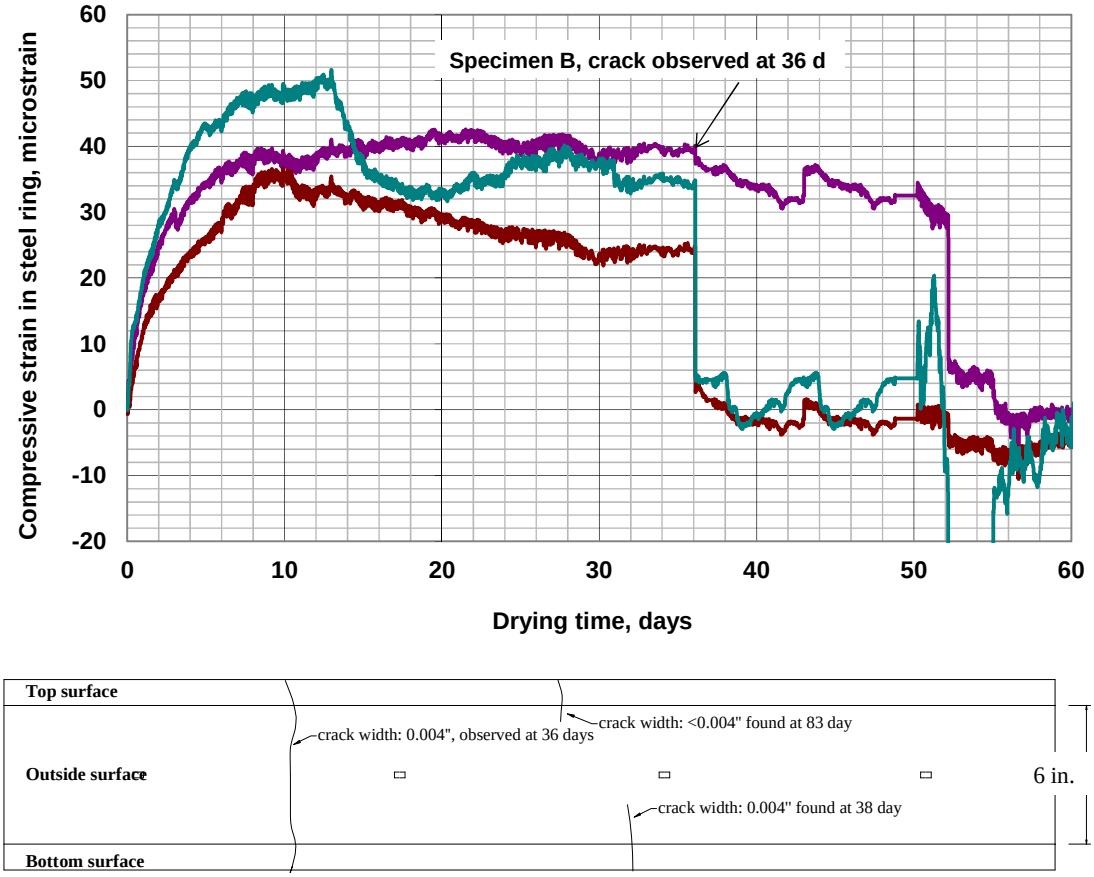

Figure D.31 Compressive strain in steel ring versus drying time: Program V Set 2– 40% FA + 0.35 *w/c* mix (batch 650) with 14-day curing, Specimen B (Quarter Wheatstone bridge), 2-in. (50-mm) concrete ring thickness. Note: Data from other one strain gage was disturbed. 1 in. = 25.4 mm.

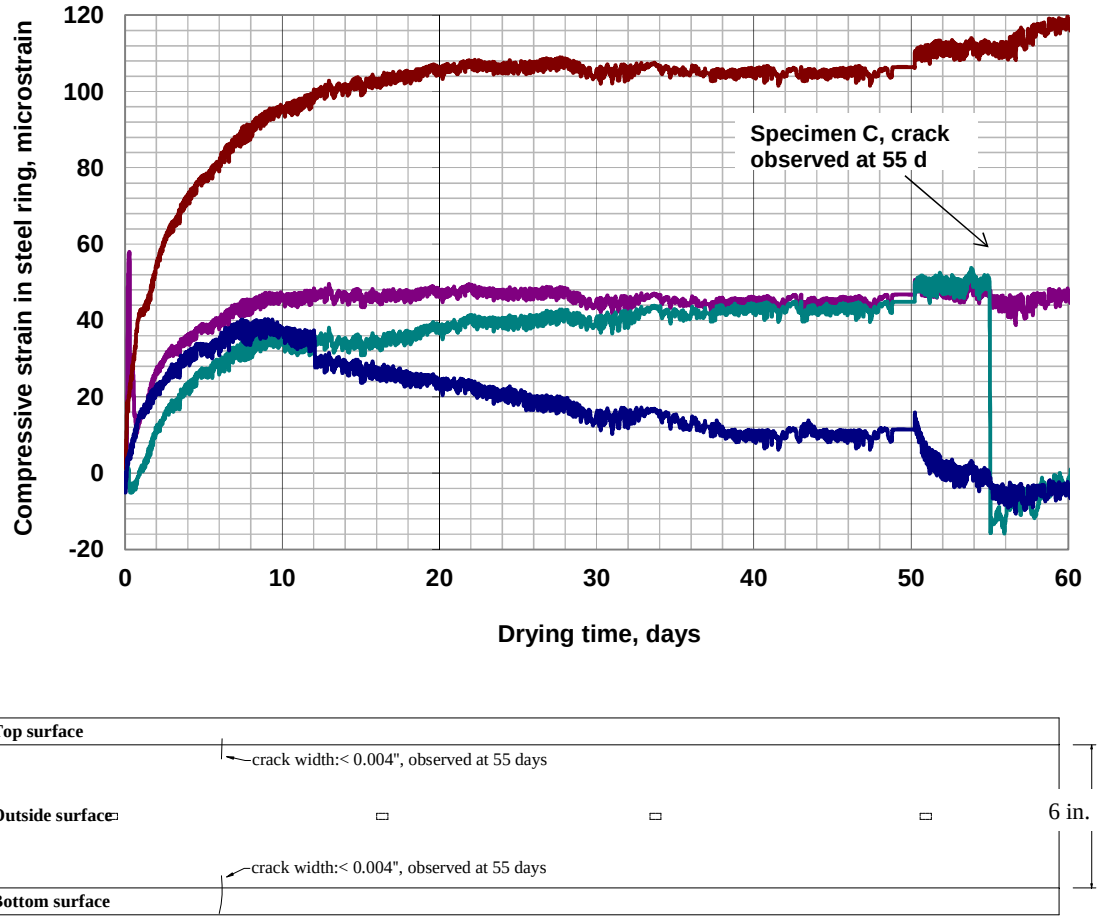

Figure D.32 Compressive strain in steel ring versus drying time: Program V Set 2– 40% FA + 0.35 *w/c* mix (batch 650) with 14-day curing, Specimen C (Quarter Wheatstone bridge), 2-in. (50-mm) concrete ring thickness. 1 in. = 25.4 mm.

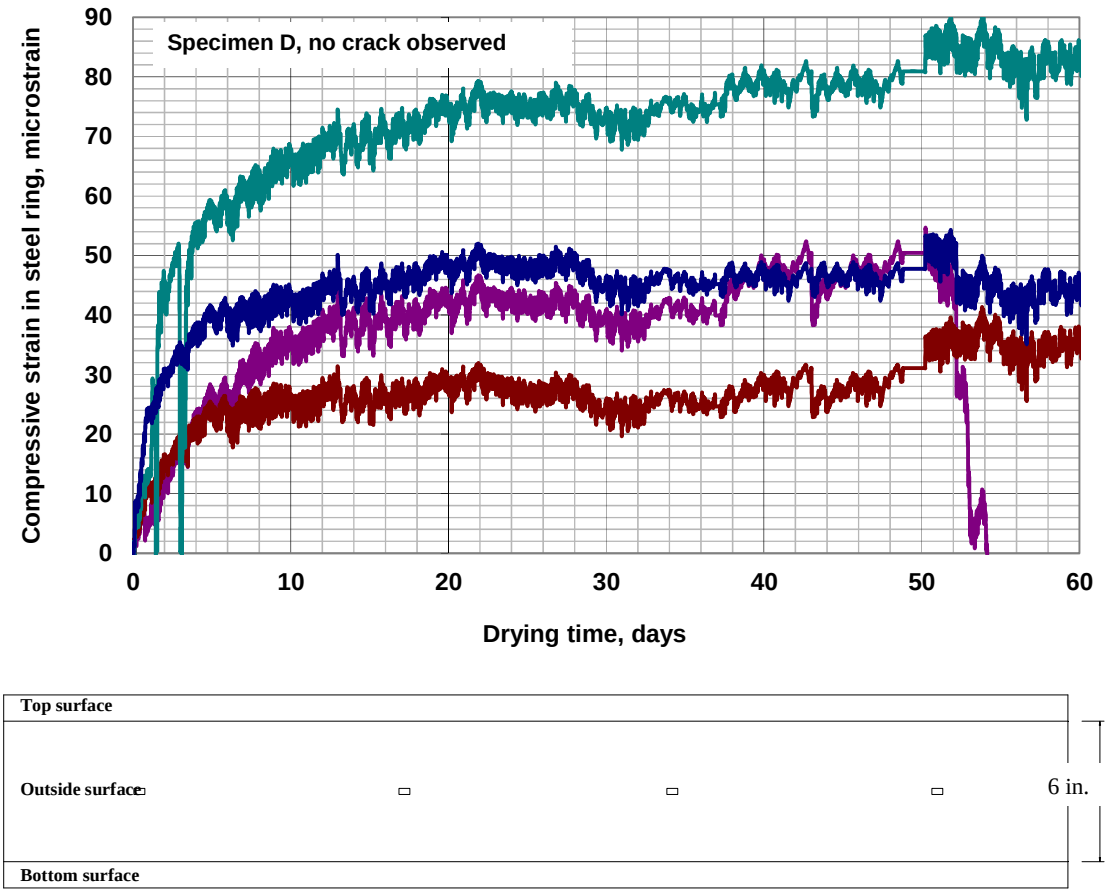

Figure D.33 Compressive strain in steel ring versus drying time: Program V Set 2– 40% FA + 0.35 *w/c* mix (batch 650) with 14-day curing, Specimen D (Quarter Wheatstone bridge), 2-in. (50-mm) concrete ring thickness. 1 in. = 25.4 mm.

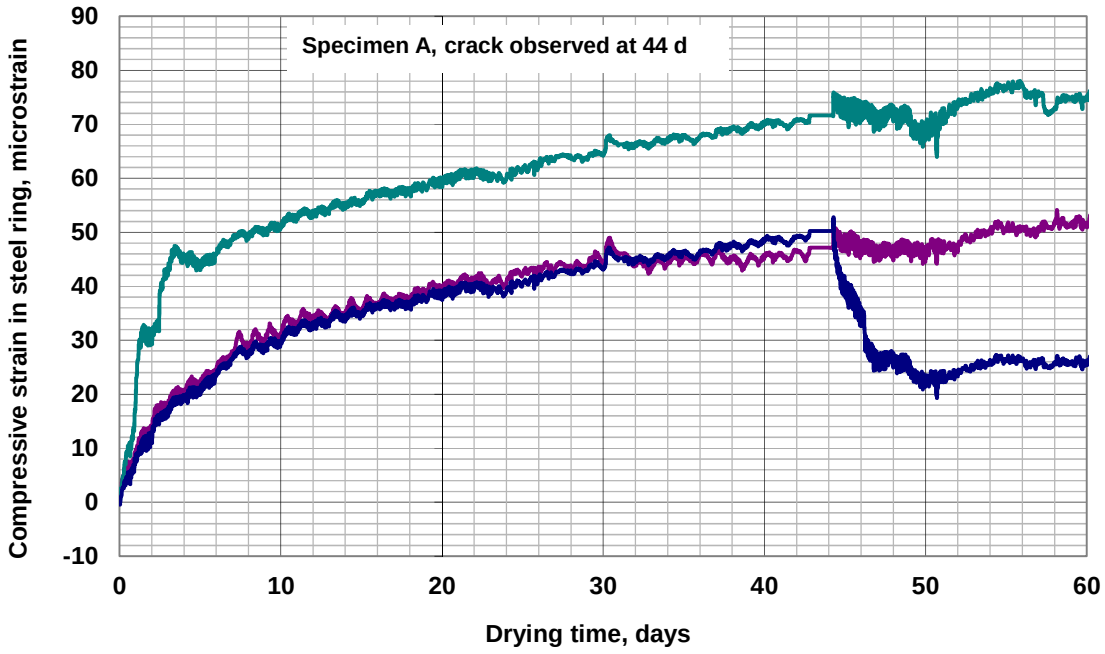

Specimen 651 A, observed between 44 and 49 days, all cracks width less than 0.004"

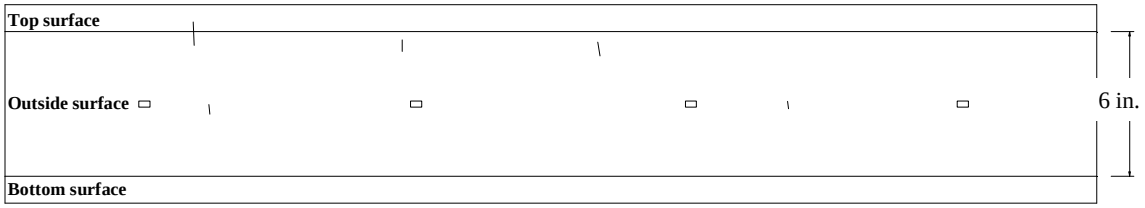

Figure D.34 Compressive strain in steel ring versus drying time: Program V Set 2– C700 + 0.44 *w/c* mix (batch 651) with 14-day curing, Specimen D (Quarter Wheatstone bridge), 2-in. (50-mm) concrete ring thickness. Note: Data from other one strain gage was disturbed. 1 in. = 25.4 mm.

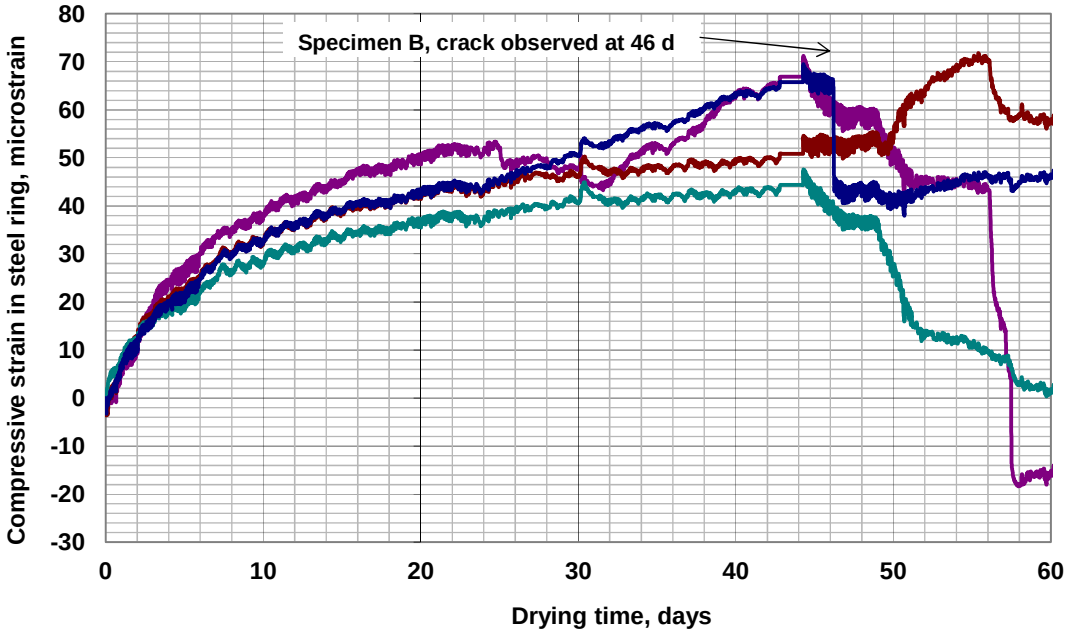

Specimen 651 B, observed between 46 and 49 days, all cracks width less than 0.004"

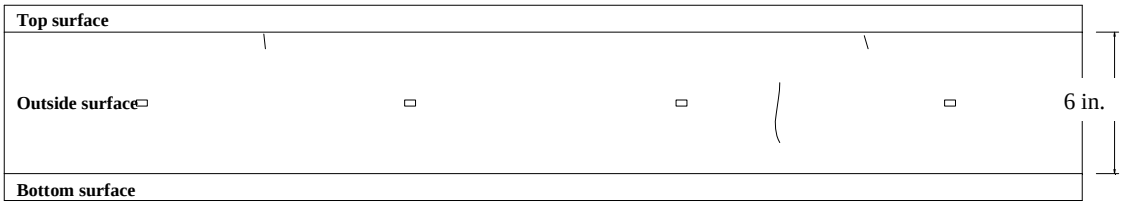

Figure D.35 Compressive strain in steel ring versus drying time: Program V Set 2– C700 + 0.44 *w/c* mix (batch 651) with 14-day curing, Specimen E (Quarter Wheatstone bridge), 2-in. (50-mm) concrete ring thickness. 1 in. = 25.4 mm.

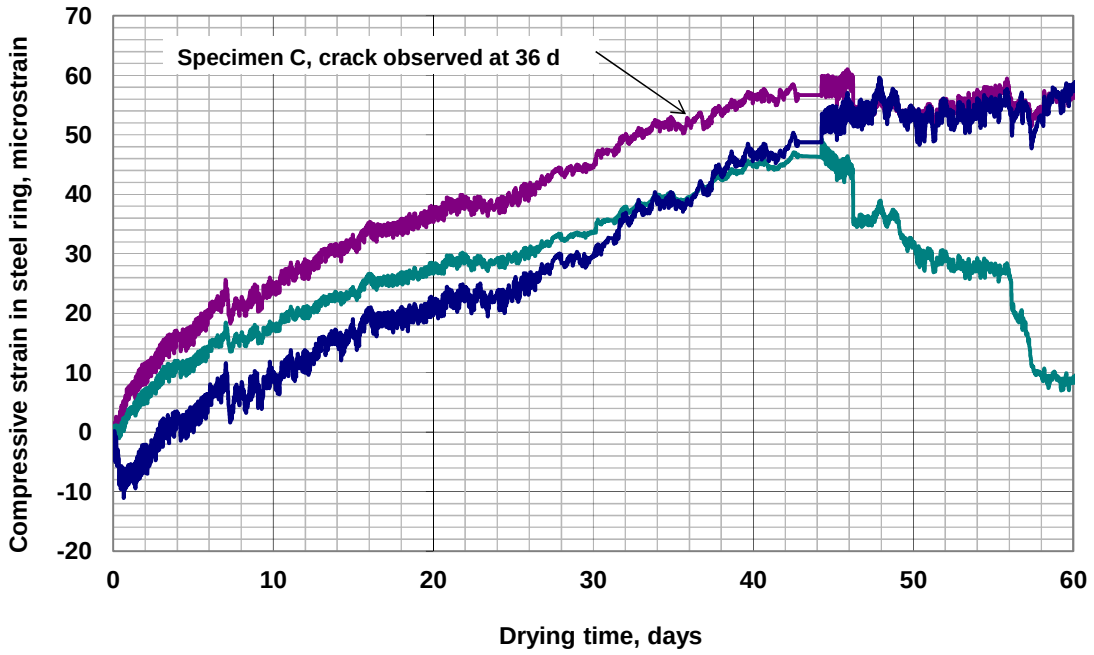

Specimen 651 C, the first micro crack was observed between 36 days

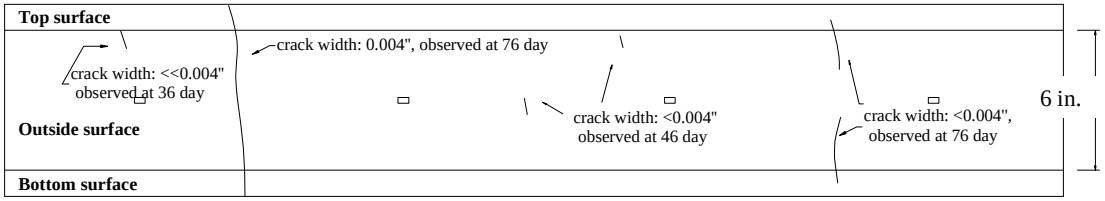

Figure D.36 Compressive strain in steel ring versus drying time: Program V Set 2– C700 + 0.44 *w/c* mix (batch 651) with 14-day curing, Specimen F (Quarter Wheatstone bridge), 2-in. (50-mm) concrete ring thickness. Note: Data from other one strain gage was not available. 1 in. = 25.4 mm.

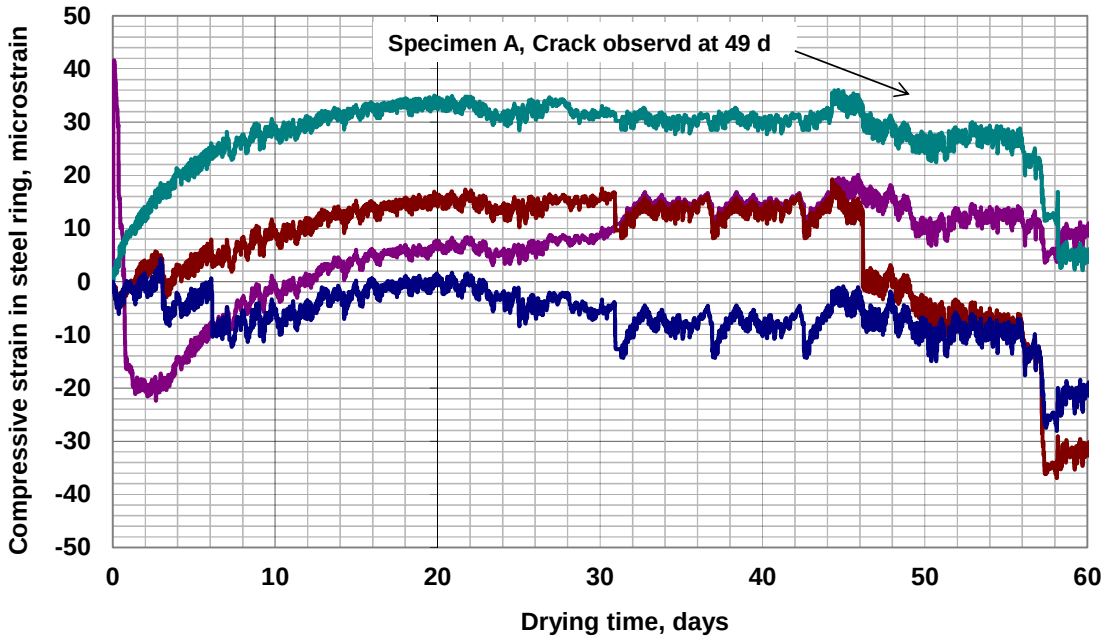

Specimen 652 A, observed between 49 days, all cracks width less than 0.004"

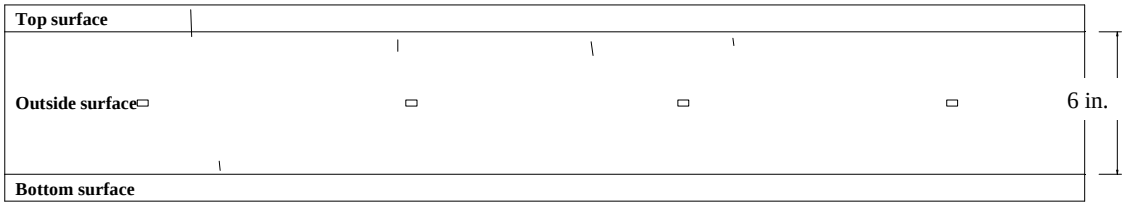

Figure D.37 Compressive strain in steel ring versus drying time: Program V Set 2– 40% FA + 0.44 *w/c* mix (batch 652) with 14-day curing, Specimen A (Quarter Wheatstone bridge), 2-in. (50-mm) concrete ring thickness. 1 in. = 25.4 mm.

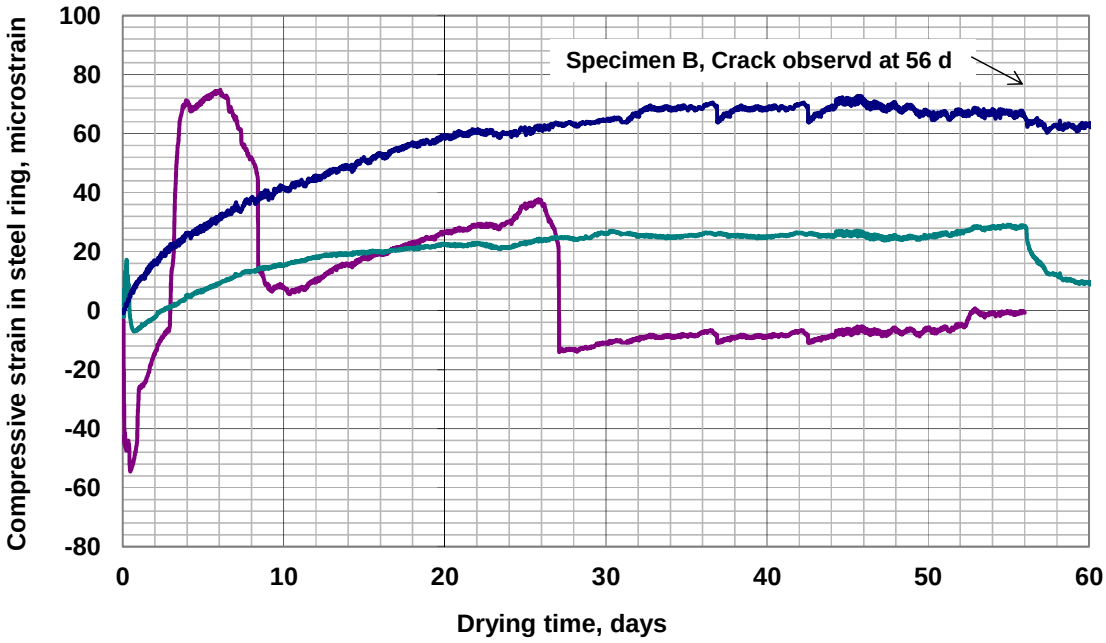

Specimen 652 B, observed between 56 days, all cracks width less than 0.004"

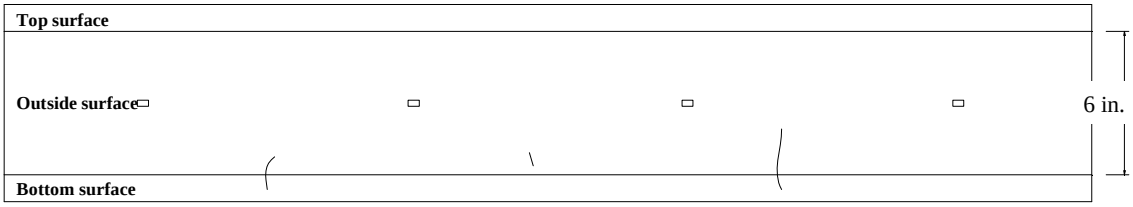

Figure D.38 Compressive strain in steel ring versus drying time: Program V Set 2– 40% FA + 0.44 *w/c* mix (batch 652) with 14-day curing, Specimen B (Quarter Wheatstone bridge), 2-in. (50-mm) concrete ring thickness. Note: Data from other one strain gage was disturbed. 1 in. = 25.4 mm.

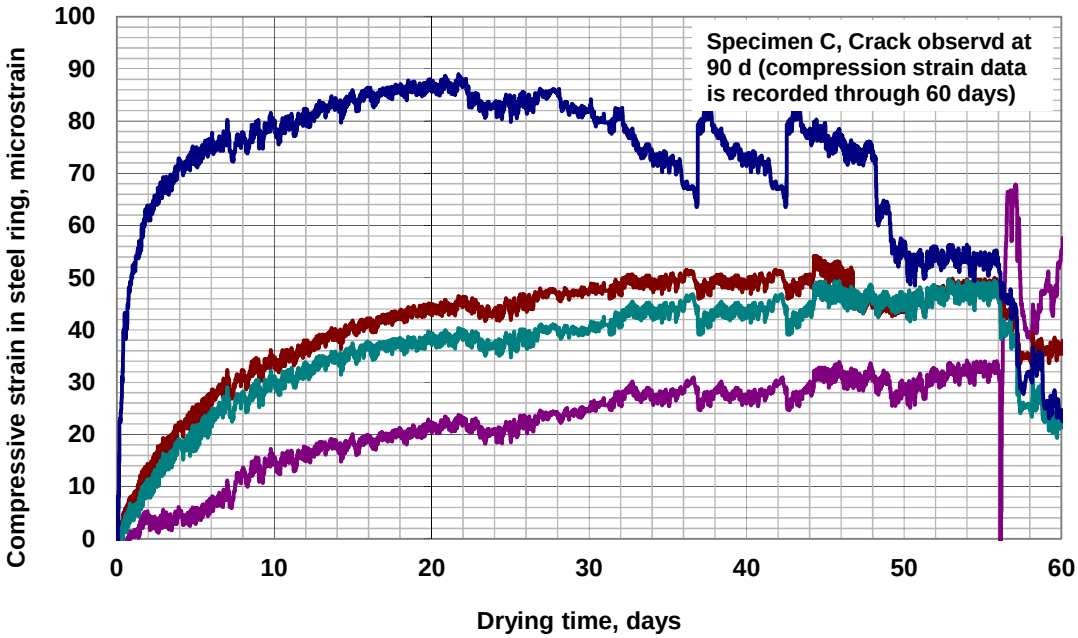

Specimen 652 C, observed between 90 days

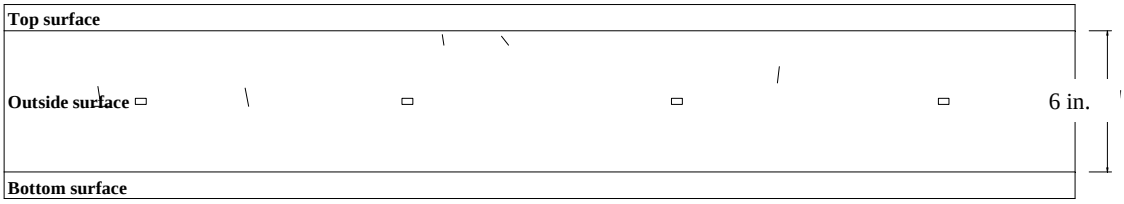

Figure D.39 Compressive strain in steel ring versus drying time: Program V Set 2– 40% FA + 0.44 *w/c* mix (batch 652) with 14-day curing, Specimen C (Quarter Wheatstone bridge), 2-in. (50-mm) concrete ring thickness. 1 in. = 25.4 mm.

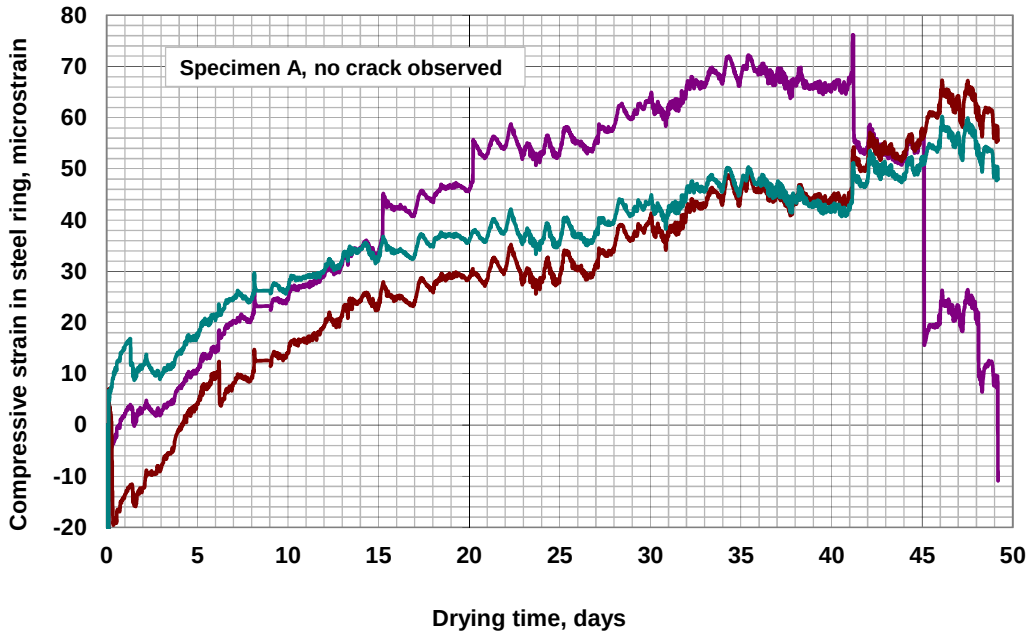

Figure D.40 Compressive strain in steel ring versus drying time: Program V Set 3– C540 + 0.44 *w/c* mix (batch 635) with 14-day curing, Specimen A (Quarter-Wheatstone bridge), 2 in. (50 mm) concrete ring thickness. 1 in. = 25.4 mm.

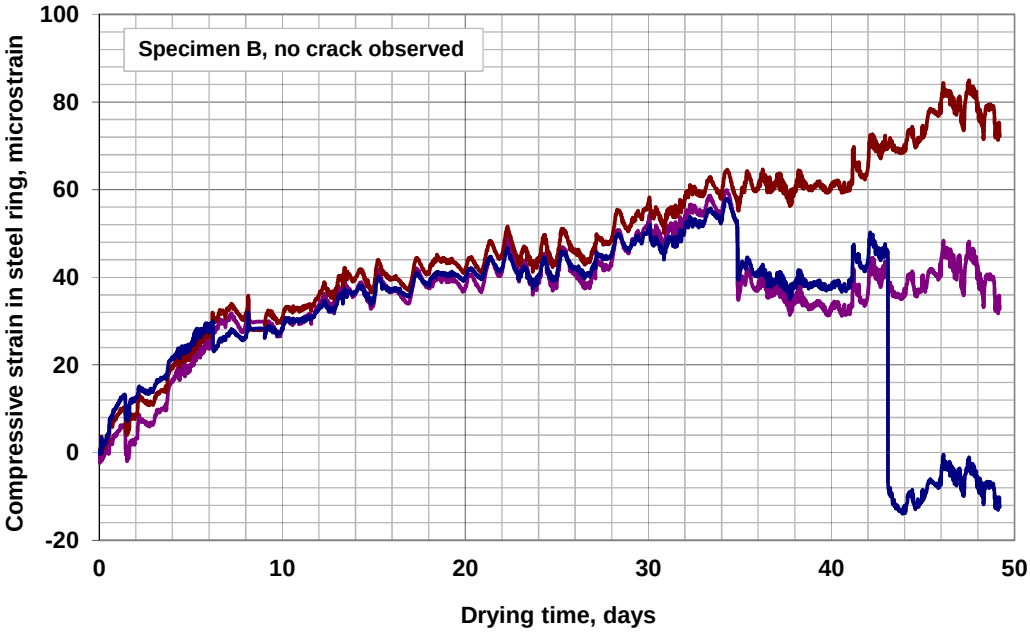

Figure D.41 Compressive strain in steel ring versus drying time: Program V Set 3– C540 + 0.44 *w/c* mix (batch 635) with 14-day curing, Specimen B (Quarter-Wheatstone bridge), 2 in. (50 mm) concrete ring thickness. 1 in. = 25.4 mm.

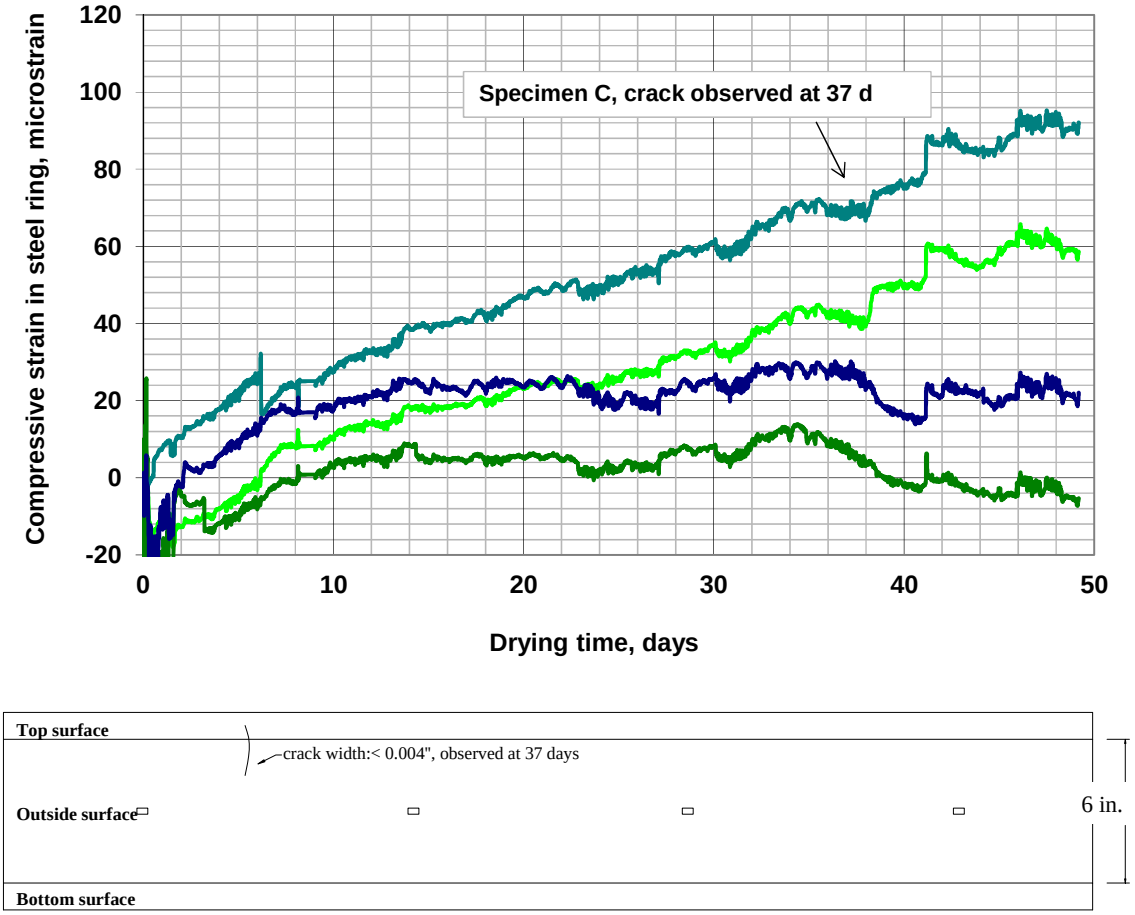

Figure D.42 Compressive strain in steel ring versus drying time: Program V Set 3– C540 + 0.44 *w/c* mix (batch 635) with 14-day curing, Specimen C (Quarter Wheatstone bridge), 2-in. (50-mm) concrete ring thickness. 1 in. = 25.4 mm.

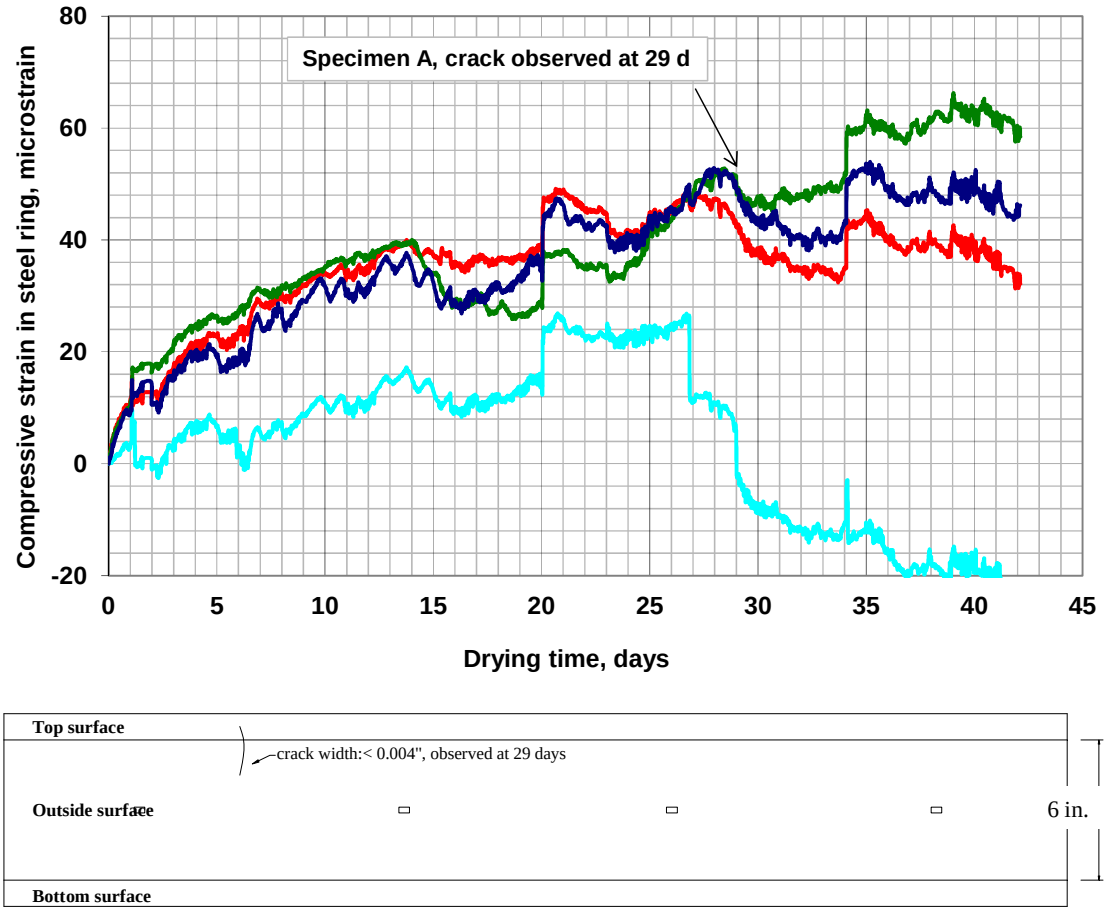

Figure D.43 Compressive strain in steel ring versus drying time: Program V Set 3– C535 + 0.45 *w/c* mix (batch 636) with 14-day curing, Specimen A (Quarter Wheatstone bridge), 2-in. (50-mm) concrete ring thickness. 1 in. = 25.4 mm.

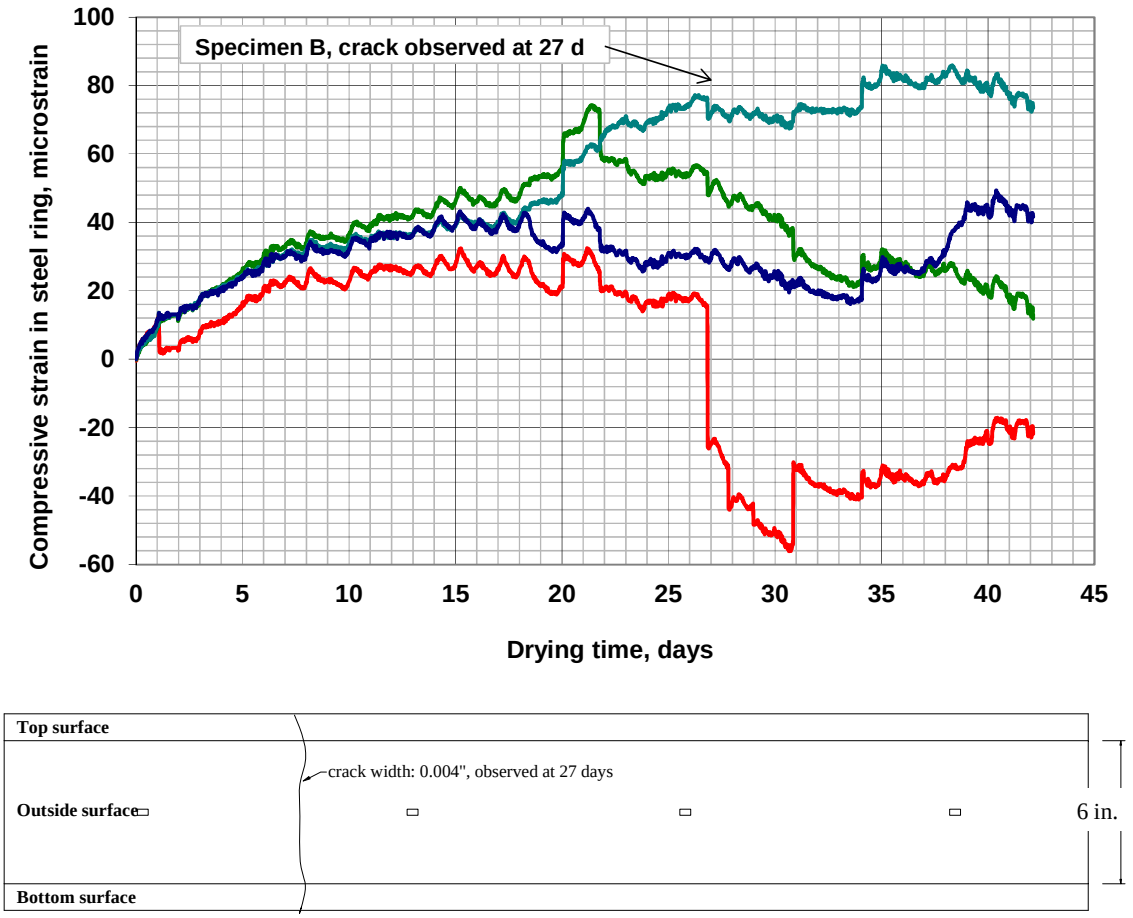

Figure D.44 Compressive strain in steel ring versus drying time: Program V Set 3– C535 + 0.45 *w/c* mix (batch 636) with 14-day curing, Specimen B (Quarter Wheatstone bridge), 2-in. (50-mm) concrete ring thickness. 1 in. = 25.4 mm.

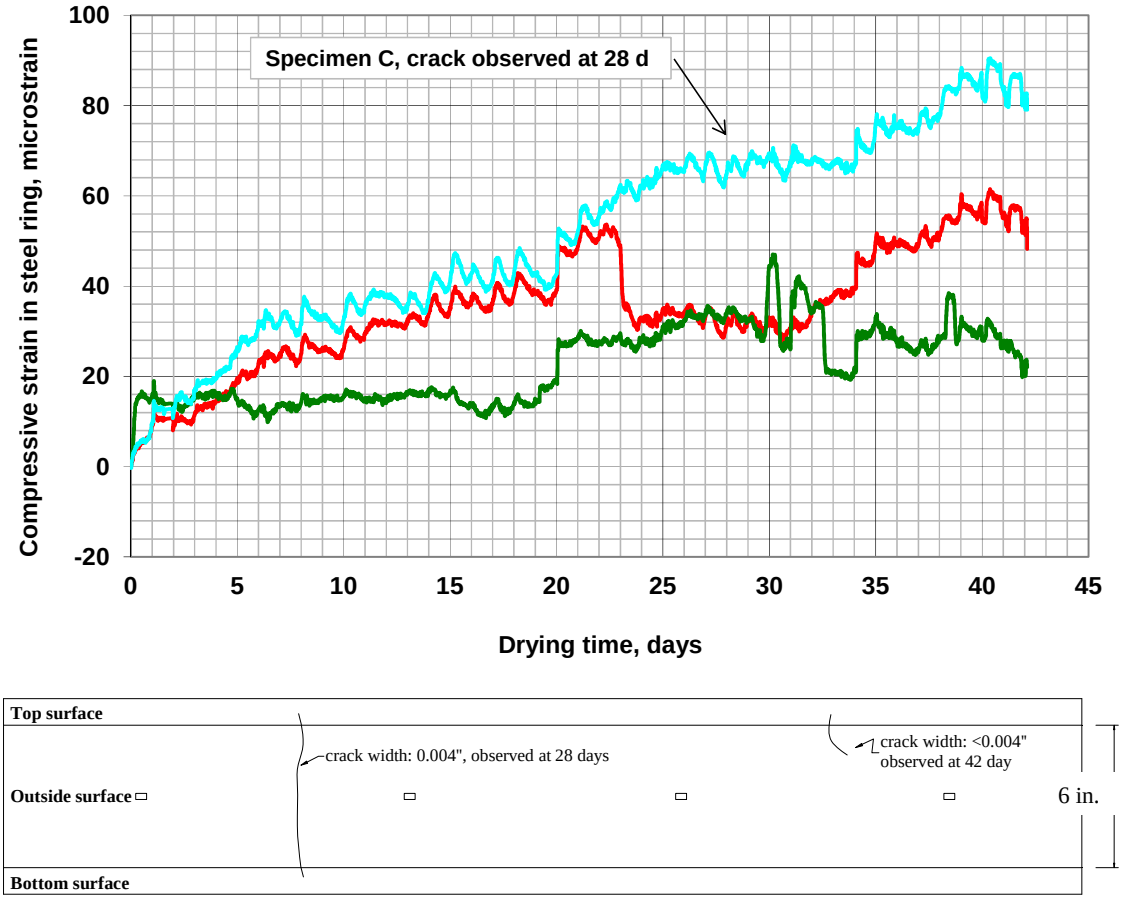

Figure D.45 Compressive strain in steel ring versus drying time: Program V Set 3– C535 + 0.45 *w/c* mix (batch 636) with 14-day curing, Specimen C (Quarter Wheatstone bridge), 2-in. (50-mm) concrete ring thickness. Note: Data from one strain gage was not available. 1 in. = 25.4 mm.

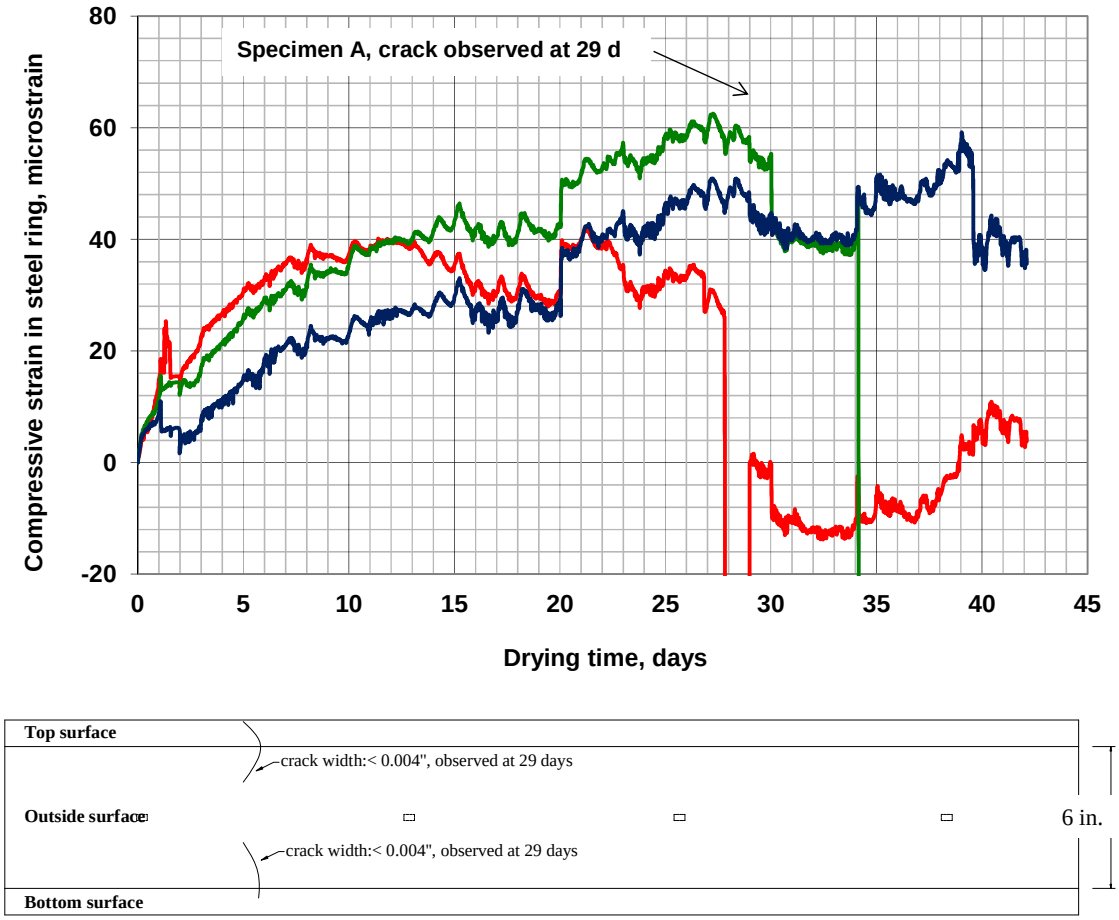

Figure D.46 Compressive strain in steel ring versus drying time: Program V Set 3– C535 + 0.35 *w/c* mix (batch 637) with 14-day curing, Specimen A (Quarter Wheatstone bridge), 2-in. (50-mm) concrete ring thickness. Note: Data from one strain gage was disturbed. 1 in. = 25.4 mm.

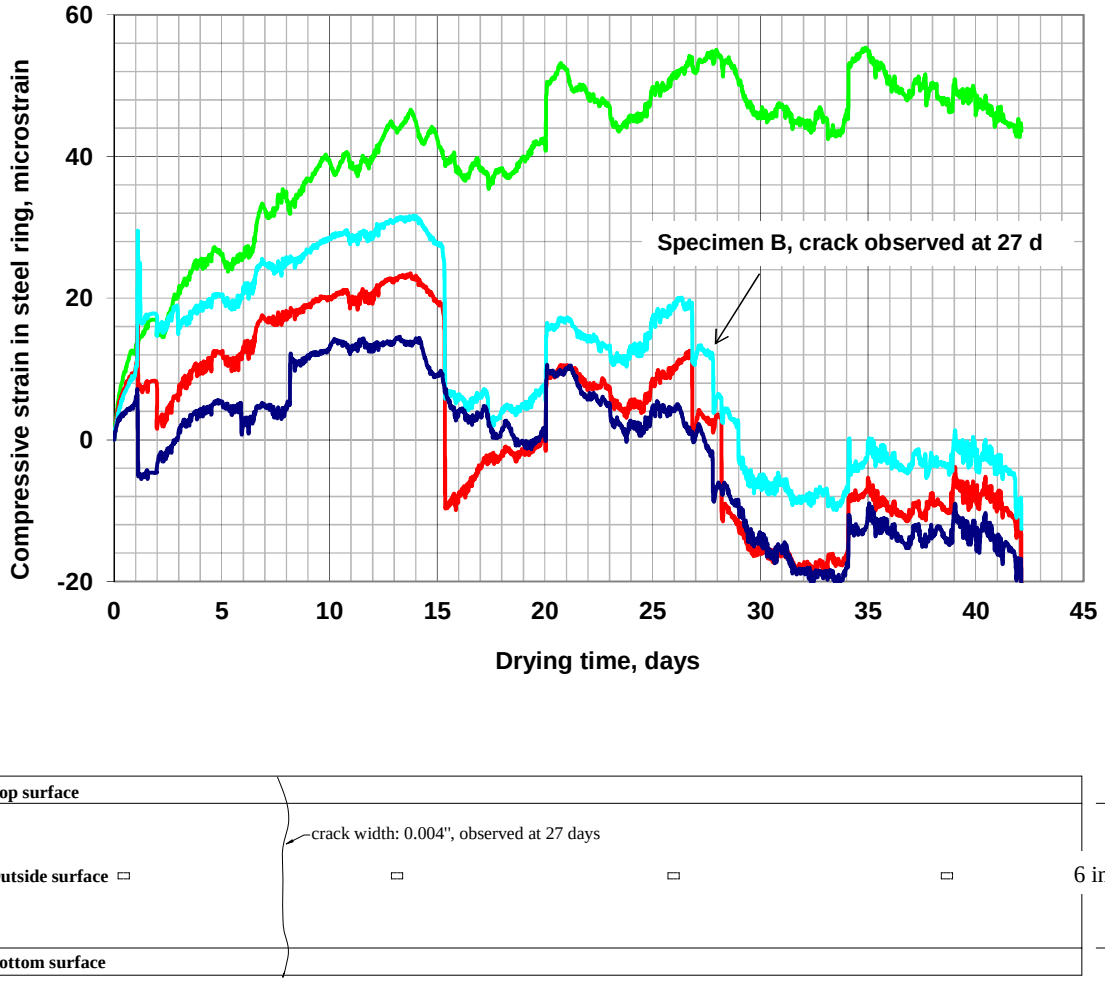

Figure D.47 Compressive strain in steel ring versus drying time: Program V Set 3– C535 + 0.35 *w/c* mix (batch 637) with 14-day curing, Specimen B (Quarter Wheatstone bridge), 2-in. (50-mm) concrete ring thickness. 1 in. = 25.4 mm.

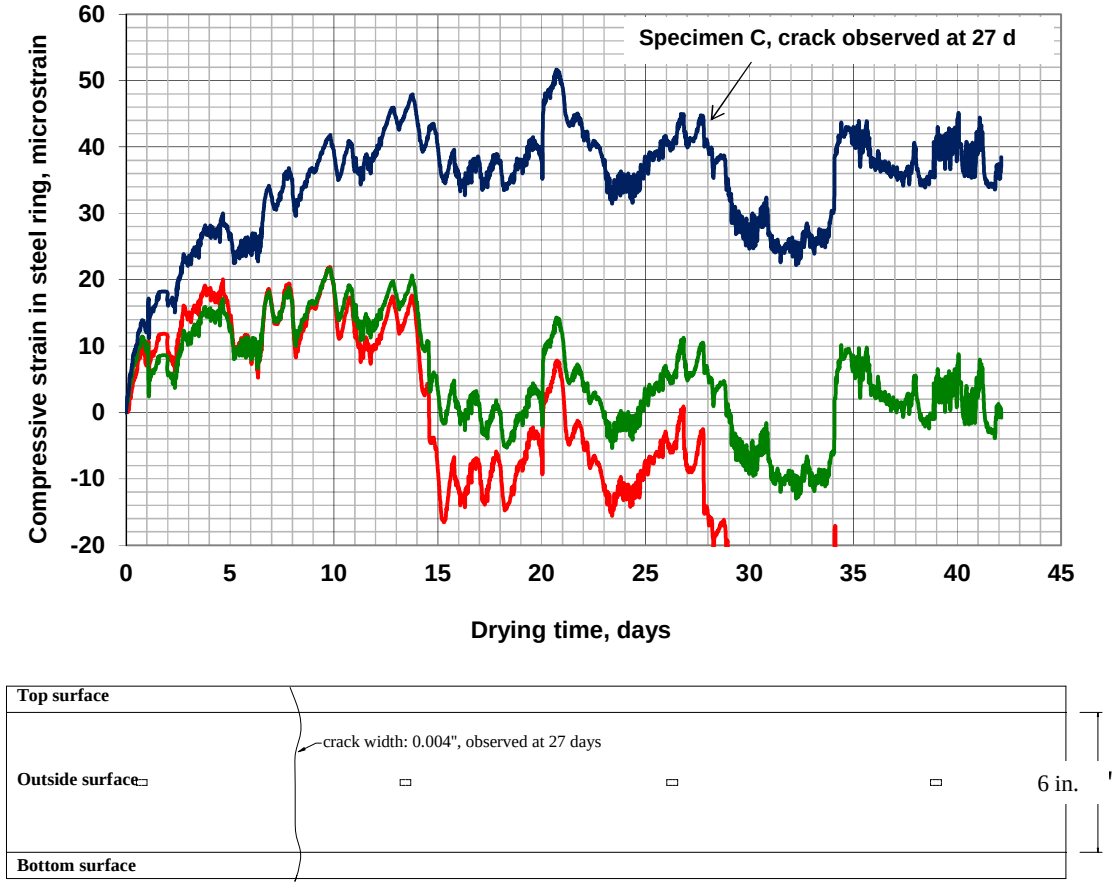

Figure D.48 Compressive strain in steel ring versus drying time: Program V Set 3– C535 + 0.35 *w/c* mix (batch 637) with 14-day curing, Specimen C (Quarter Wheatstone bridge), 2-in. (50-mm) concrete ring thickness. Note: Data from one strain gage was disturbed. 1 in. = 25.4 mm.

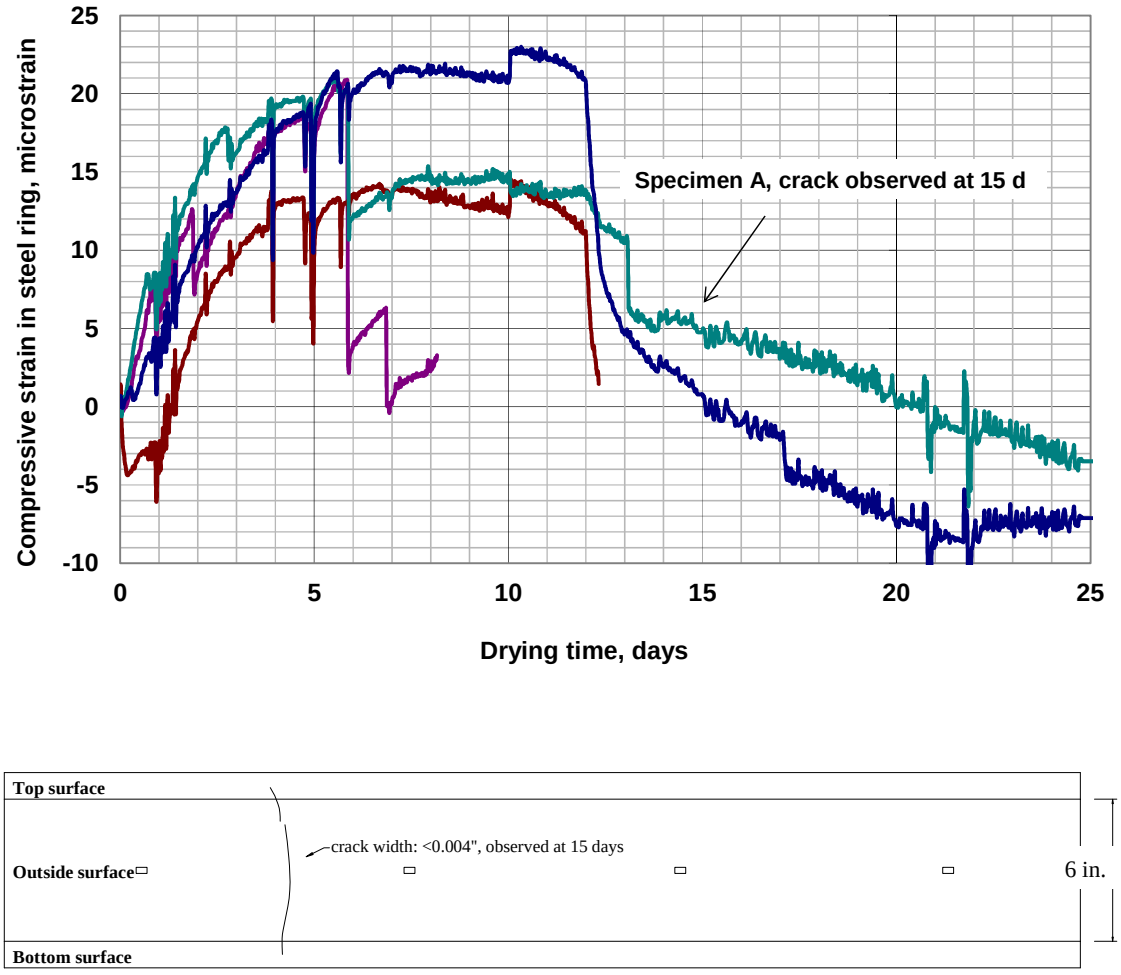

Figure D.49 Compressive strain in steel ring versus drying time: Program VI– C535 + 0.44*w*/*c* mix (batch 679) with 14-day curing, Specimen A (Quarter Wheatstone bridge), 2.5-in. (64-mm) concrete ring thickness. 1 in. = 25.4 mm.

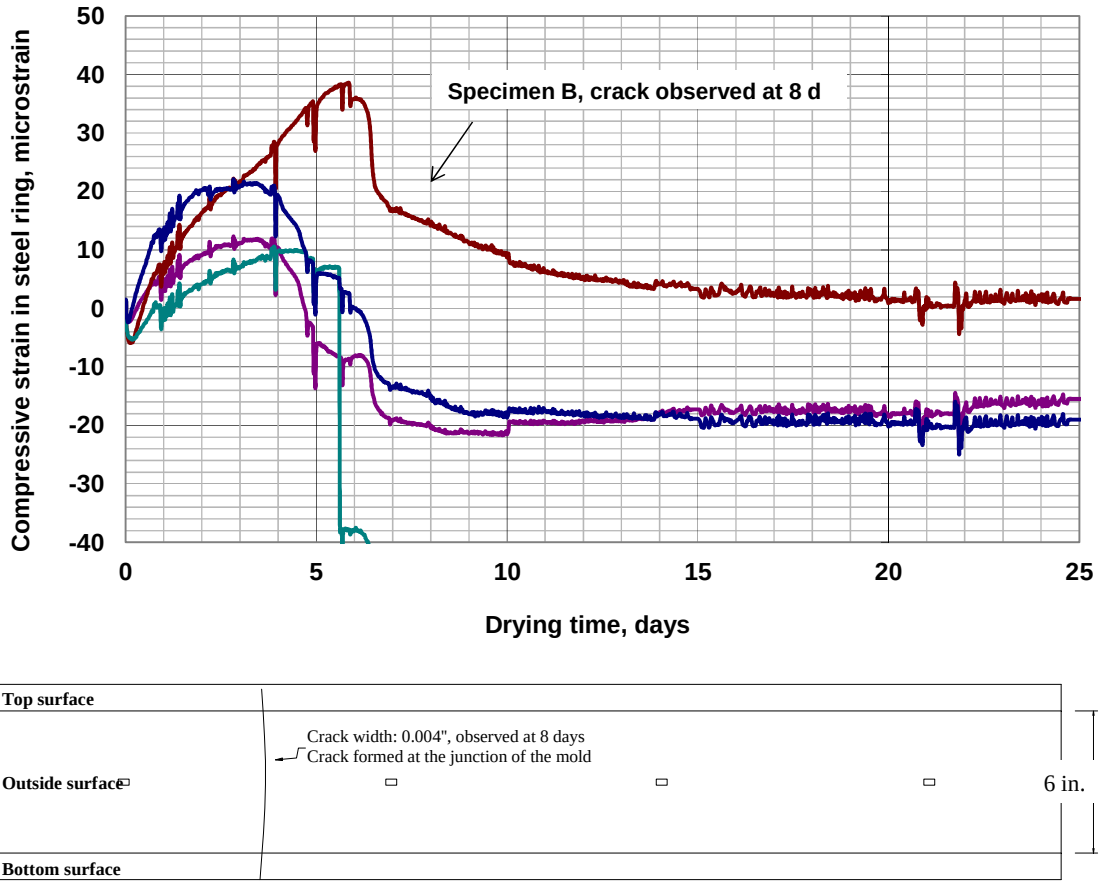

Figure D.50 Compressive strain in steel ring versus drying time: Program VI– C535 + 0.44*w*/*c* mix (batch 679) with 14-day curing, Specimen B (Quarter Wheatstone bridge), 2.5-in. (64-mm) concrete ring thickness. 1 in. = 25.4 mm.

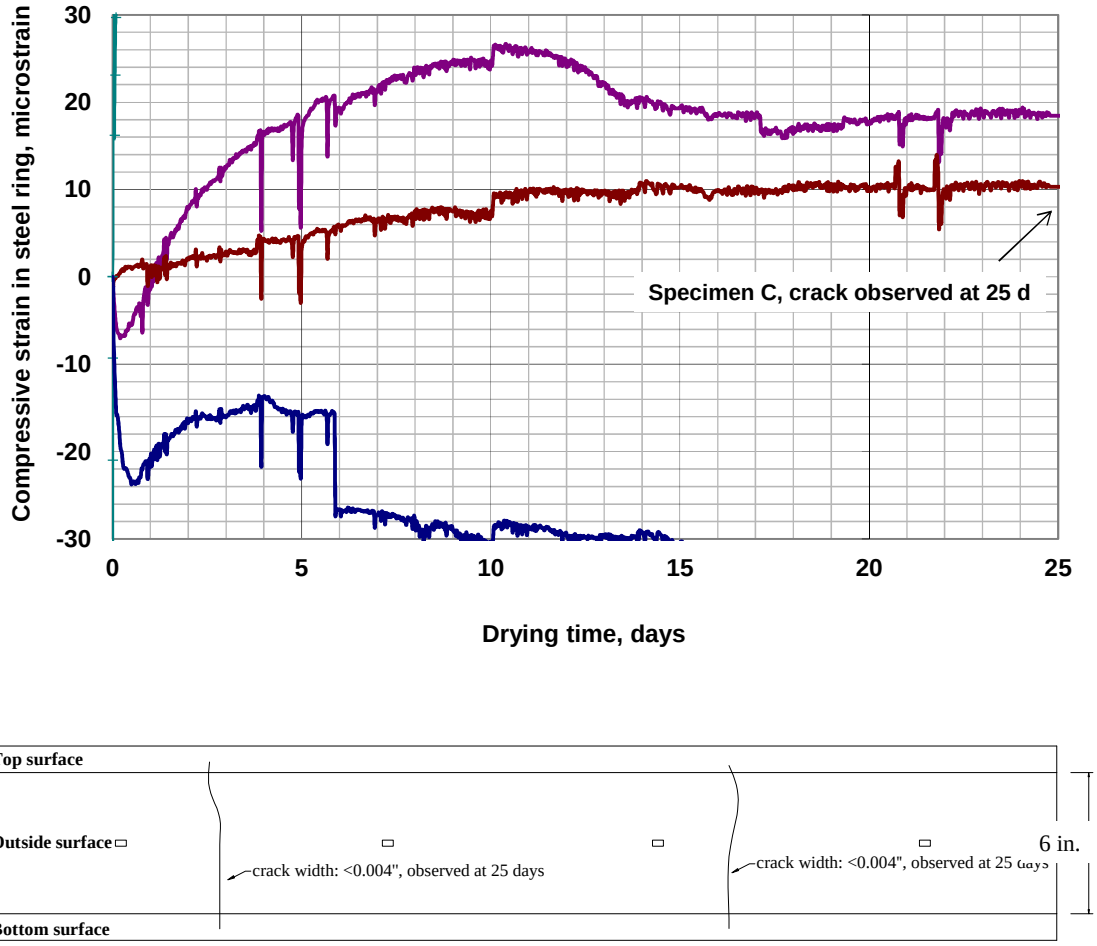

Figure D.51 Compressive strain in steel ring versus drying time: Program VI– C535 + 0.44*w*/*c* mix (batch 679) with 14-day curing, Specimen C (Quarter Wheatstone bridge), 2.5-in. (64-mm) concrete ring thickness. 1 in. = 25.4 mm.

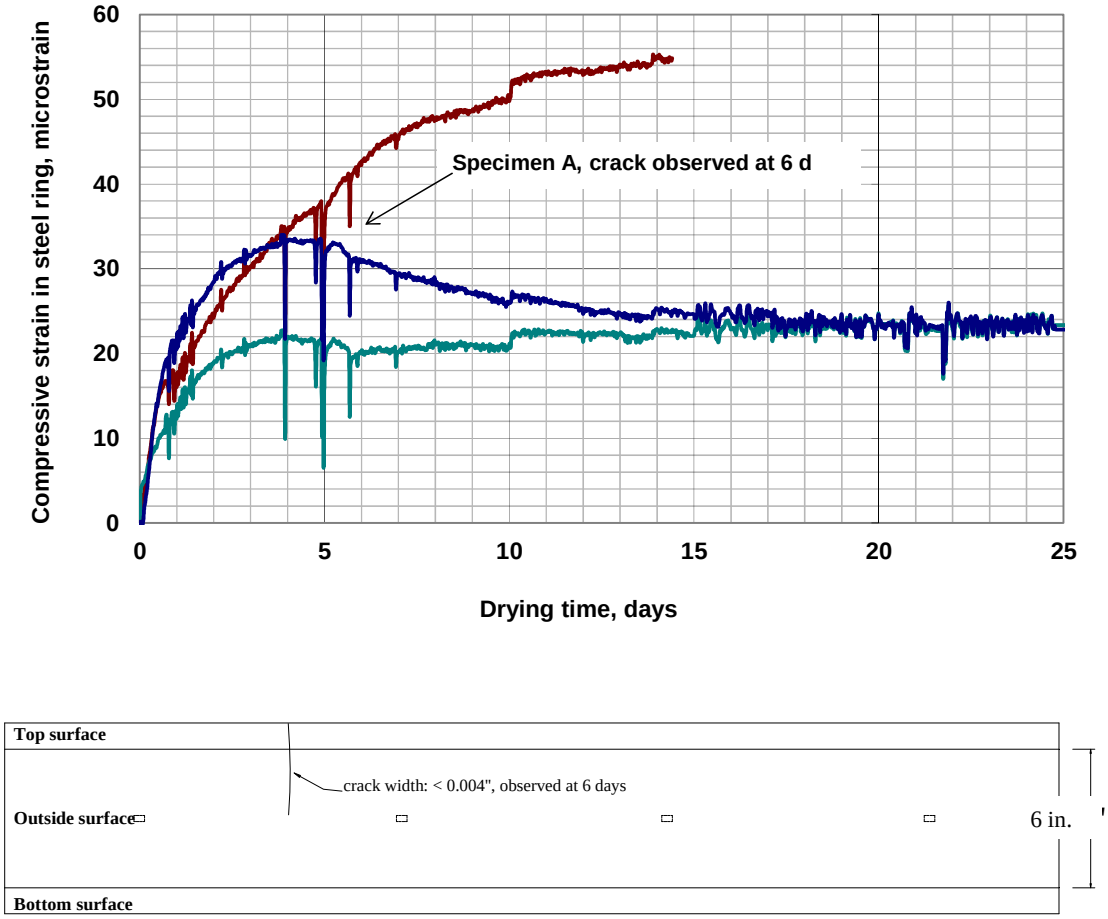

Figure D.52 Compressive strain in steel ring versus drying time: Program VI– 40% FA + 0.44*w*/*c* mix (batch 680) with 14-day curing, Specimen A (Quarter Wheatstone bridge), 2.5-in. (64-mm) concrete ring thickness. 1 in. = 25.4 mm.

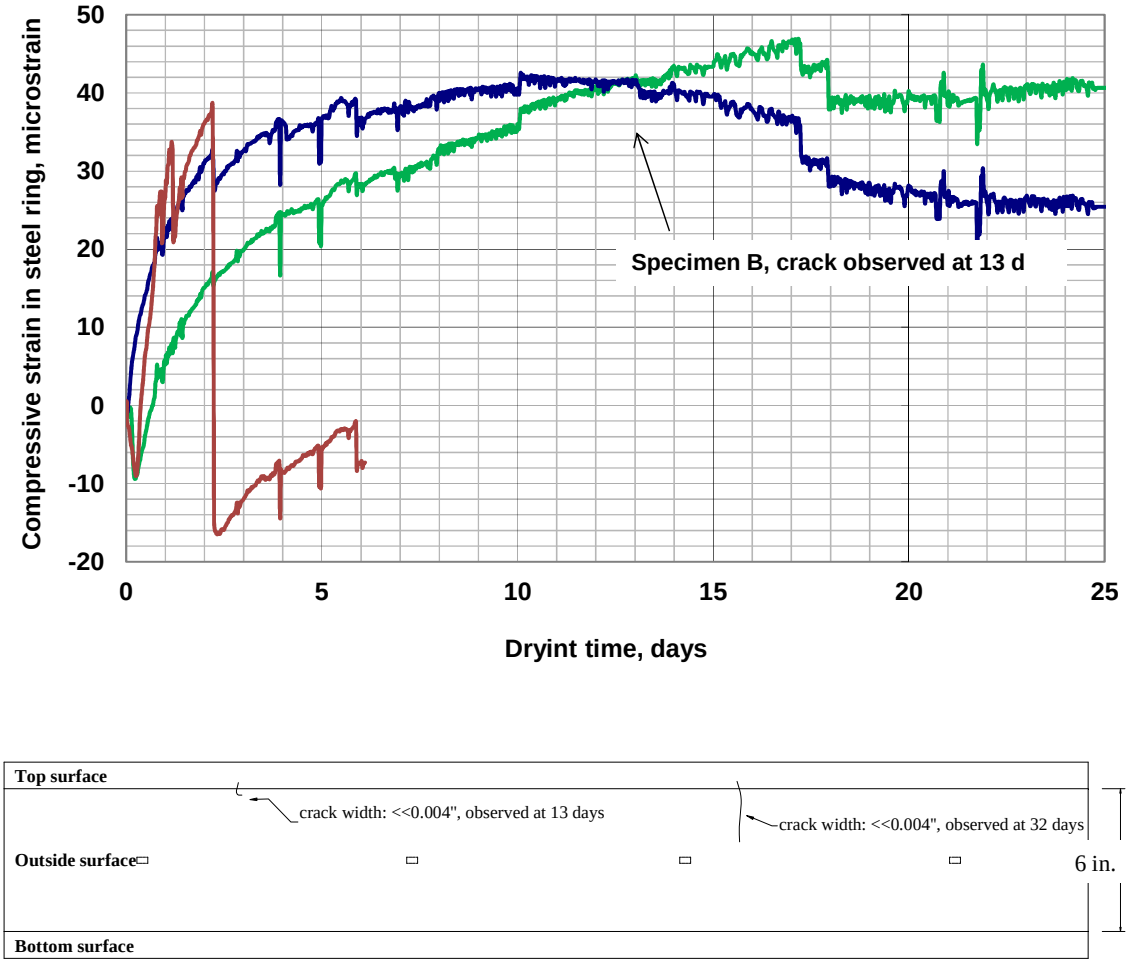

Figure D.53 Compressive strain in steel ring versus drying time: Program VI– 40% FA + 0.44*w*/*c* mix (batch 680) with 14-day curing, Specimen B (Quarter Wheatstone bridge), 2.5-in. (64-mm) concrete ring thickness. 1 in. = 25.4 mm.

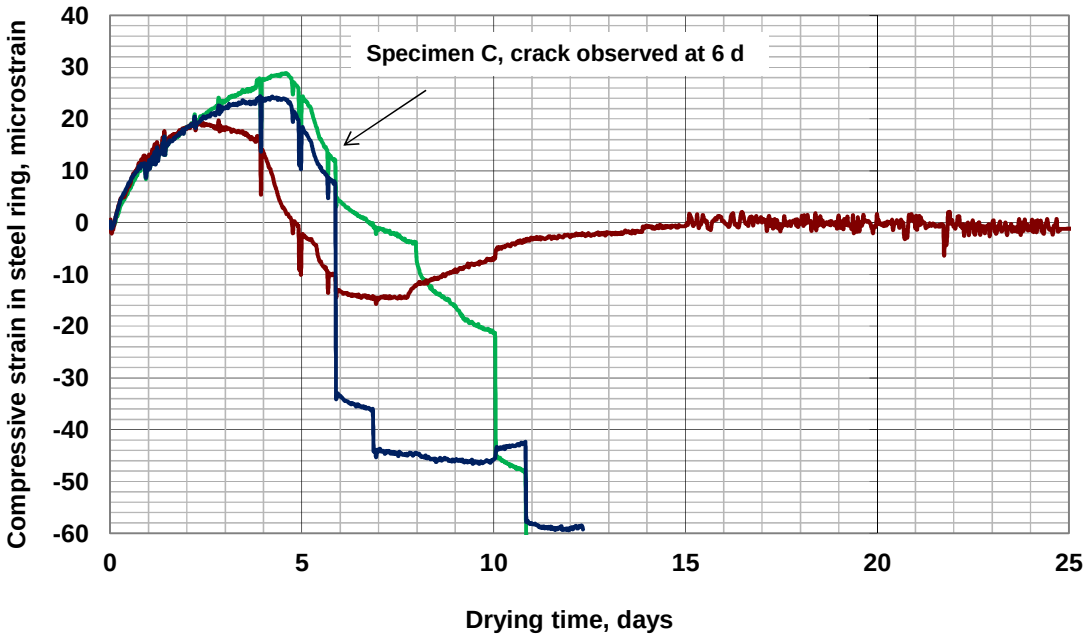

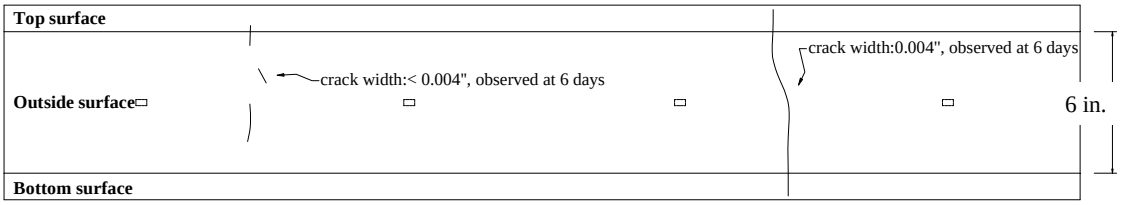

Figure D.54 Compressive strain in steel ring versus drying time: Program VI– 40% FA + 0.44*w*/*c* mix (batch 680) with 14-day curing, Specimen C (Quarter Wheatstone bridge), 2.5-in. (64-mm) concrete ring thickness. 1 in. = 25.4 mm.

APPENDIX E LOW-CRACKING HIGH-PERFORMANCE CONCRETE (LC-HPC) SPECIFICATIONS - AGGREGATES, CONCRETE, AND CONSTRUCTION

KANSAS DEPARTMENT OF TRANSPORTATION
SPECIAL PROVISION TO THE
STANDARD SPECIFICATIONS, 2007 EDITION

Add a new SECTION to DIVISION 1100:

LOW-CRACKING HIGH-PERFORMANCE CONCRETE – AGGREGATES

1.0 DESCRIPTION

This specification is for coarse aggregates, fine aggregates, and mixed aggregates (both coarse and fine material) for use in bridge deck construction.

2.0 REQUIREMENTS

a. Coarse Aggregates for Concrete.

(1) Composition. Provide coarse aggregate that is crushed or uncrushed gravel, chat, or crushed stone. (Consider calcite cemented sandstone, rhyolite, basalt and granite as crushed stone

(2) Quality. The quality requirements for coarse aggregate for bridge decks are in **TABLE 1-1**:

TABLE 1-1: QUALITY REQUIREMENTS FOR COARSE AGGREGATES FOR BRIDGE DECK

Concrete Classification	Soundness (min.)	Wear (max.)	Absorption (max.)	Acid Insol. (min.)
Grade 3.5 (AE) (LC-HPC) [1]	0.90	40	0.7	55

[1] Grade 3.5 (AE) (LC-HPC) – Bridge Deck concrete with select coarse aggregate for wear and acid insolubility.

(3) Product Control.

(a) Deleterious Substances. Maximum allowed deleterious substances by weight are:

- Material passing the No. 200 sieve (KT-2)..... 2.5%
- Shale or Shale-like material (KT-8)..... 0.5%
- Clay lumps and friable particles (KT-7)..... 1.0%
- Sticks (wet) (KT-35)..... 0.1%
- Coal (AASHTO T 113)..... 0.5%

(b) Uniformity of Supply. Designate or determine the fineness modulus (grading factor) according to the procedure listed in the Construction Manual Part V, Section 17 before delivery, or from the first 10 samples tested and accepted. Provide aggregate that is within ±0.20 of the average fineness modulus.

(4) Do not combine siliceous fine aggregate with siliceous coarse aggregate if neither meet the requirements of **subsection 2.0c.(2)(a)**. Consider such fine material, regardless of proportioning, as a Basic Aggregate that must conform to **subsection 2.0c**.

(5) Handling Coarse Aggregates.

(a) Segregation. Before acceptance testing, remix all aggregate segregated by transportation or stockpiling operations.

(b) Stockpiling.

- Stockpile accepted aggregates in layers 3 to 5 feet thick. Berm each layer so that aggregates do not "cone" down into lower layers.
- Keep aggregates from different sources, with different gradings, or with a significantly different specific gravity separated.
- Transport aggregate in a manner that insures uniform gradation.
- Do not use aggregates that have become mixed with earth or foreign material.

- Stockpile or bin all washed aggregate produced or handled by hydraulic methods for 12 hours (minimum) before batching. Rail shipment exceeding 12 hours is acceptable for binning provided the car bodies permit free drainage.
- Provide additional stockpiling or binning in cases of high or non-uniform moisture.

b. Fine Aggregates for Basic Aggregate in MA for Concrete.

(1) Composition.

(a) Type FA-A. Provide either singly or in combination natural occurring sand resulting from the disintegration of siliceous or calcareous rock, or manufactured sand produced by crushing predominately siliceous materials.

(b) Type FA-B. Provide fine granular particles resulting from the crushing of zinc and lead ores (Chat).

(2) Quality.

(a) Mortar strength and Organic Impurities. If the District Materials Engineer determines it is necessary, because of unknown characteristics of new sources or changes in existing sources, provide fine aggregates that comply with these requirements:

- Mortar Strength (Mortar Strength Test, KTMR-26). Compressive strength when combined with Type III (high early strength) cement:
  - At age 24 hours, minimum……..100%*
  - At age 72 hours, minimum……..100%*

  *Compared to strengths of specimens of the same proportions, consistency, cement and standard 20-30 Ottawa sand.
- Organic Impurities (Organic Impurities in Fine Aggregate for Concrete Test, AASHTO T 21). The color of the supernatant liquid is equal to or lighter than the reference standard solution.

(b) Hardening characteristics. Specimens made of a mixture of 3 parts FA-B and 1 part cement with sufficient water for molding will harden within 24 hours. There is no hardening requirement for FA-A.

(3) Product Control.

(a) Deleterious Substances.

- Type FA-A: Maximum allowed deleterious substances by weight are:
  - Material passing the No. 200 sieve (KT-2)……..……. 2.0%
  - Shale or Shale-like material (KT-8) ……. 0.5%
  - Clay lumps and friable particles (KT-7)……..……. 1.0%
  - Sticks (wet) (KT-35)……...…….…… 0.1%
- Type FA-B: Provide materials that are free of organic impurities, sulfates, carbonates, or alkali. Maximum allowed deleterious substances by weight are:
  - Material passing the No. 200 sieve (KT-2)…….…….…..... 2.0%
  - Clay lumps & friable particles (KT-7)……. 0.25%

(c) Uniformity of Supply. Designate or determine the fineness modulus (grading factor) according to the procedure listed in the Construction Manual Part V, Section 17 before delivery, or from the first 10 samples tested and accepted. Provide aggregate that is within ±0.20 of the average fineness modulus.

(4) Proportioning of Coarse and Fine Aggregate. Use a proven optimization method such as the Shilstone Method or the KU Mix Method.

Do not combine siliceous fine aggregate with siliceous coarse aggregate if neither meet the requirements of **subsection 2.0c.(2)(a)**. Consider such fine material, regardless of proportioning, as a Basic Aggregate and must conform to the requirements in **subsection 2.0c**.

(5) Handling and Stockpiling Fine Aggregates.

- Keep aggregates from different sources, with different gradings or with a significantly different specific gravity separated.
- Transport aggregate in a manner that insures uniform grading.
- Do not use aggregates that have become mixed with earth or foreign material.

- Stockpile or bin all washed aggregate produced or handled by hydraulic methods for 12 hours (minimum) before batching. Rail shipment exceeding 12 hours is acceptable for binning provided the car bodies permit free drainage.
- Provide additional stockpiling or binning in cases of high or non-uniform moisture.

c. Mixed Aggregates for Concrete.

(1) Composition.

(a) Total Mixed Aggregate (TMA). A natural occurring, predominately siliceous aggregate from a single source that meets the Wetting & Drying Test (KTMR-23) and grading requirements.

(b) Mixed Aggregate. A combination of basic and coarse aggregates that meet **TABLE 1-2**.

- Basic Aggregate (BA). Singly or in combination, a natural occurring, predominately siliceous aggregate that does not meet the grading requirements of Total Mixed Aggregate.

(c) Coarse Aggregate. Granite, crushed sandstone, chat, and gravel. Gravel that is not approved under **subsection 2.0c.(2)** may be used, but only with basic aggregate that meets the wetting and drying requirements of TMA.

(2) Quality.

(a) Total Mixed Aggregate.

- Soundness, minimum (KTMR-21) ……..……0.90
- Wear, maximum (KTMR-25) ……..……50%
- Wetting and Drying Test (KTMR-23) for Total Mixed Aggregate
  Concrete Modulus of Rupture:
  - At 60 days, minimum…….550 psi
  - At 365 days, minimum…..……..……550 psi

  Expansion:
  - At 180 days, maximum……..…….0.050%
  - At 365 days, maximum……..…….0.070%
  - Aggregates produced from the following general areas are exempt from the Wetting and Drying Test:
  - Blue River Drainage Area.
  - The Arkansas River from Sterling, west to the Colorado state line.
  - The Neosho River from Emporia to the Oklahoma state line.

(b) Basic Aggregate.

- Retain 10% or more of the BA on the No. 8 sieve before adding the Coarse Aggregate. Aggregate with less than 10% retained on the No. 8 sieve is to be considered a Fine Aggregate described in **subsection 2.0b**. Provide material with less than 5% calcareous material retained on the ⅜" sieve.
- Soundness, minimum (KTMR-21)…….0.90
- Wear, maximum (KTMR-25)……..……50%
- Mortar strength and Organic Impurities. If the District Materials Engineer determines it is necessary, because of unknown characteristics of new sources or changes in existing sources, provide mixed aggregates that comply with these requirements:
  - Mortar Strength (Mortar Strength Test, KTMR-26). Compressive strength when combined with Type III (high early strength) cement:
    - At age 24 hours, minimum……..100%*
    - At age 72 hours, minimum……..100%*

      *Compared to strengths of specimens of the same proportions, consistency, cement and standard 20-30 Ottawa sand.
  - Organic Impurities (Organic Impurities in Fine Aggregate for Concrete Test, AASHTO T 21). The color of the supernatant liquid is equal to or lighter than the reference standard solution.

(3) Product Control.

(a) Size Requirement. Provide mixed aggregates that comply with the grading requirements in **TABLE 1-2**.

TABLE 1-2: GRADING REQUIREMENTS FOR MIXED AGGREGATES FOR CONCRETE BRIDGE DECKS

Type	Usage	Percent Retained on Individual Sieves - Square Mesh Sieves										
		1½"	1"	3/4"	1/2"	3/8"	No. 4	No. 8	No. 16	No. 30	No. 50	No. 100
MA-4	Optimized for LC-HPC Bridge Decks*	0	2-6	5-18	8-18	8-18	8-18	8-18	8-18	8-15	5-15	0-10

*Use a proven optimization method, such as the Shilstone Method or the KU Mix Method.
Note: Manufactured sands used to obtain optimum gradations have caused difficulties in pumping, placing or finishing. Natural coarse sands and pea gravels used to obtain optimum gradations have worked well in concretes that were pumped.

(b) Deleterious Substances. Maximum allowed deleterious substances by weight are:

- Material passing the No. 200 sieve (KT-2)……..….. 2.5%
- Shale or Shale-like material (KT-8)……..……. 0.5%
- Clay lumps and friable particles (KT-7)…… 1.0%
- Sticks (wet) (KT-35)……...…… 0.1%
- Coal (AASHTO T 113)…..……..……. 0.5%

(c) Uniformity of Supply. Designate or determine the fineness modulus (grading factor) according to the procedure listed in the Construction Manual Part V, Section 17 before delivery, or from the first 10 samples tested and accepted. Provide aggregate that is within ±0.20 of the average fineness modulus.

(4) Handling Mixed Aggregates.

(a) Segregation. Before acceptance testing, remix all aggregate segregated by transit or stockpiling.

(b) Stockpiling.

- Keep aggregates from different sources, with different gradings or with a significantly different specific gravity separated.
- Transport aggregate in a manner that insures uniform grading.
- Do not use aggregates that have become mixed with earth or foreign material.
- Stockpile or bin all washed aggregate produced or handled by hydraulic methods for 12 hours (minimum) before batching. Rail shipment exceeding 12 hours is acceptable for binning provided the car bodies permit free drainage.
- Provide additional stockpiling or binning in cases of high or non-uniform moisture.

3.0 TEST METHODS

Test aggregates according to the applicable provisions of **SECTION 1117**.

4.0 PREQUALIFICATION

Aggregates for concrete must be prequalified according to **subsection 1101.2**.

5.0 BASIS OF ACCEPTANCE

The Engineer will accept aggregates for concrete base on the prequalification required by this specification, and **subsection 1101.4**.

KANSAS DEPARTMENT OF TRANSPORTATION
SPECIAL PROVISION TO THE
STANDARD SPECIFICATIONS 2007 EDITION

Add a new SECTION to DIVISION 400:

LOW-CRACKING HIGH-PERFORMANCE CONCRETE

1.0 DESCRIPTION

Provide the grades of low-cracking high-performance concrete (LC-HPC) specified in the Contract Documents.

2.0 MATERIALS

Coarse, Fine & Mixed Aggregate.....**07-PS0165, latest version**
Admixtures.....**DIVISION 1400**
Cement .....**DIVISION 2000**
Water .....**DIVISION 2400**

3.0 CONCRETE MIX DESIGN

a. General. Design the concrete mixes specified in the Contract Documents.

Provide aggregate gradations that comply with **07-PS0165, latest version** and Contract Documents.

If desired, contact the DME for available information to help determine approximate proportions to produce concrete having the required characteristics on the project.

Take full responsibility for the actual proportions of the concrete mix, even if the Engineer assists in the design of the concrete mix.

Submit all concrete mix designs to the Engineer for review and approval. Submit completed volumetric mix designs on KDOT Form No. 694 (or other forms approved by the DME).

Do not place any concrete on the project until the Engineer approves the concrete mix designs. Once the Engineer approves the concrete mix design, do not make changes without the Engineer's approval.

Design concrete mixes that comply with these requirements:

b. Air-Entrained Concrete for Bridge Decks. Design air-entrained concrete for structures according to **TABLE 1-1**.

TABLE 1-1: AIR ENTRAINED CONCRETE FOR BRIDGE DECKS

Grade of Concrete Type of Aggregate (SECTION 1100)	lb of Cementitious per cu yd of Concrete, min/max	lb of Water per lb of Cementitious*	Designated Air Content Percent by Volume**	Specified 28-day Compressive Strength Range, psi
Grade 3.5 (AE) (LC-HPC)				
MA-4	500 / 540	0.44 – 0.45	8.0 ± 1.0	3500 – 5500

*Limits of lb. of water per lb. of cementitious. Includes free water in aggregates, but excludes water of absorption of the aggregates. With approval of the Engineer, may be decreased to 0.43 on-site.

**Concrete with an air content less than 6.5% or greater than 9.5% shall be rejected. The Engineer will sample concrete for tests at the discharge end of the conveyor, bucket or if pumped, the piping.

c. Portland Cement. Select the type of portland cement specified in the Contract Documents. Mineral admixtures are prohibited for Grade 3.5 (AE) (LC-HPC) concrete.

d. Design Air Content. Use the middle of the specified air content range for the design of air-entrained concrete.

e. Admixtures for Air-Entrainment and Water Reduction. Verify that the admixtures used are compatible and will work as intended without detrimental effects. Use the dosages recommended by the admixture manufacturers to determine the quantity of each admixture for the concrete mix design. Incorporate and mix the admixtures into the concrete mixtures according to the manufacturer's recommendations.

Set retarding or accelerating admixtures are prohibited for use in Grade 3.5 (AE) (LC-HPC) concrete. These include Type B, C, D, E, and G chemical admixtures as defined by ASTM C 494/C 494M – 08. Do not use admixtures containing chloride ion (CL) in excess of 0.1 percent by mass of the admixture in Grade 3.5 (AE) (LC-HPC) concrete.

(1) Air-Entraining Admixture. If specified, use an air-entraining admixture in the concrete mixture. If another admixture is added to an air-entrained concrete mixture, determine if it is necessary to adjust the air-entraining admixture dosage to maintain the specified air content. Use only a vinsol resin or tall oil based air-entraining admixture.

(2) Water-Reducing Admixture. Use a Type A water reducer or a dual rated Type A water reducer – Type F high-range water reducer, when necessary to obtain compliance with the specified fresh and hardened concrete properties.

Include a batching sequence in the concrete mix design. Consider the location of the concrete plant in relation to the job site, and identify the approximate quantity, when and at what location the water-reducing admixture is added to the concrete mixture.

The manufacturer may recommend mixing revolutions beyond the limits specified in **subsection 5.0**. If necessary and with the approval of the Engineer, address the additional mixing revolutions (the Engineer will allow up to 60 additional revolutions) in the concrete mix design.

Slump control may be accomplished in the field only by redosing with a water-reducing admixture. If time and temperature limits are not exceeded, and if at least 30 mixing revolutions remain, the Engineer will allow redosing with up to 50% of the original dose.

(3) Adjust the mix designs during the course of the work when necessary to achieve compliance with the specified fresh and hardened concrete properties. Only permit such modifications after trial batches to demonstrate that the adjusted mix design will result in concrete that complies with the specified concrete properties.

The Engineer will allow adjustments to the dose rate of air entraining and water-reducing chemical admixtures to compensate for environmental changes during placement without a new concrete mix design or qualification batch.

f. Designated Slump. Designate a slump for each concrete mix design within the limits in **TABLE 1-2**.

TABLE 1-2: DESIGNATED SLUMP*

Type of Work	Designated Slump (inches)
Grade 3.5 (AE) (LC-HPC)	1 ½ - 3

* The Engineer will obtain sample concrete at the discharge end of the conveyor, bucket or if pumped, the piping.

If potential problems are apparent at the discharge of any truck, and the concrete is tested at the truck discharge (according to **subsection 6.0**), the Engineer will reject concrete with a slump greater than 3 ½ inches at the truck discharge, 3 inches if being placed by a bucket.

4.0 REQUIREMENTS FOR COMBINED MATERIALS

a. Measurements for Proportioning Materials.

(1) Cement. Measure cement as packed by the manufacturer. A sack of cement is considered as 0.04 cubic yards weighing 94 pounds net. Measure bulk cement by weight. In either case, the measurement must be accurate to within 0.5% throughout the range of use.

(2) Water. Measure the mixing water by weight or volume. In either case, the measurement must be accurate to within 1% throughout the range of use.

(3) Aggregates. Measure the aggregates by weight. The measurement must be accurate to within 0.5% throughout the range of use.

(4) Admixtures. Measure liquid admixtures by weight or volume. If liquid admixtures are used in small quantities in proportion to the cement as in the case of air-entraining agents, use readily adjustable mechanical dispensing equipment capable of being set to deliver the required quantity and to cut off the flow automatically when this quantity is discharged. The measurement must be accurate to within 3% of the quantity required.

b. Testing of Aggregates. Testing Aggregates at the Batch Site. Provide the Engineer with reasonable facilities at the batch site for obtaining samples of the aggregates. Provide adequate and safe laboratory facilities at the batch site allowing the Engineer to test the aggregates for compliance with the specified requirements.

KDOT will sample and test aggregates from each source to determine their compliance with specifications. Do not batch the concrete mixture until the Engineer has determined that the aggregates comply with the specifications. KDOT will conduct sampling at the batching site, and test samples according to the Sampling and Testing Frequency Chart in Part V. For QC/QA Contracts, establish testing intervals within the specified minimum frequency.

After initial testing is complete and the Engineer has determined that the aggregate process control is satisfactory, use the aggregates concurrently with sampling and testing as long as tests indicate compliance with specifications. When batching, sample the aggregates as near the point of batching as feasible. Sample from the stream as the storage bins or weigh hoppers are loaded. If samples can not be taken from the stream, take them from approved stockpiles, or use a template and sample from the conveyor belt. If test results indicate an aggregate does not comply with specifications, cease concrete production using that aggregate. Unless a tested and approved stockpile for that aggregate is available at the batch plant, do not use any additional aggregate from that source and specified grading until subsequent sampling and testing of that aggregate indicate compliance with specifications. When tests are completed and the Engineer is satisfied that process control is again adequate, production of concrete using aggregates tested concurrently with production may resume.

c. Handling of Materials.

(1) Aggregate Stockpiles. Approved stockpiles are permitted only at the batch plant and only for small concrete placements or for the purpose of maintaining concrete production. Mark the approved stockpile with an "Approved Materials" sign. Provide a suitable stockpile area at the batch plant so that aggregates are stored without detrimental segregation or contamination. At the plant, limit stockpiles of tested and approved coarse aggregate and fine aggregate to 250 tons each, unless approved for more by the Engineer. If mixed aggregate is used, limit the approved stockpile to 500 tons, the size of each being proportional to the amount of each aggregate to be used in the mix.

Load aggregates into the mixer so no material foreign to the concrete or material capable of changing the desired proportions is included. When 2 or more sizes or types of coarse or fine aggregates are used on the same project, only 1 size or type of each aggregate may be used for any one continuous concrete placement.

(2) Segregation. Do not use segregated aggregates. Previously segregated materials may be thoroughly re-mixed and used when representative samples taken anywhere in the stockpile indicated a uniform gradation exists.

(3) Cement. Protect cement in storage or stockpiled on the site from any damage by climatic conditions which would change the characteristics or usability of the material.

(4) Moisture. Provide aggregate with a moisture content of ± 0.5% from the average of that day. If the moisture content in the aggregate varies by more than the above tolerance, take whatever corrective measures are necessary to bring the moisture to a constant and uniform consistency before placing concrete. This may be accomplished by handling or manipulating the stockpiles to reduce the moisture content, or by adding moisture to the stockpiles in a manner producing uniform moisture content through all portions of the stockpile.

For plants equipped with an approved accurate moisture-determining device capable of determining the free moisture in the aggregates, and provisions made for batch to batch correction of the amount of water and the weight of aggregates added, the requirements relative to manipulating the stockpiles for moisture control will be waived. Any procedure used will not relieve the producer of the responsibility for delivery of concrete meeting the specified water-cement ratio and slump requirements.

Do not use aggregate in the form of frozen lumps in the manufacture of concrete.

07-PS0166

(5) Separation of Materials in Tested and Approved Stockpiles. Only use KDOT Approved Materials. Provide separate means for storing materials approved by KDOT. If the producer elects to use KDOT Approved Materials for non-KDOT work, during the progress of a project requiring KDOT Approved Materials, inform the Engineer and agree to pay all costs for additional materials testing.

Clean all conveyors, bins and hoppers of unapproved materials before beginning the manufacture of concrete for KDOT work.

5.0 MIXING, DELIVERY, AND PLACEMENT LIMITATIONS

a. Concrete Batching, Mixing, and Delivery. Batch and mix the concrete in a central-mix plant, in a truck mixer, or in a drum mixer at the work site. Provide plant capacity and delivery capacity sufficient to maintain continuous delivery at the rate required. The delivery rate of concrete during concreting operations must provide for the proper handling, placing and finishing of the concrete.

Seek the Engineer's approval of the concrete plant/batch site before any concrete is produced for the project. The Engineer will inspect the equipment, the method of storing and handling of materials, the production procedures, and the transportation and rate of delivery of concrete from the plant to the point of use. The Engineer will grant approval of the concrete plant/batch site based on compliance with the specified requirements. The Engineer may, at any time, rescind permission to use concrete from a previously approved concrete plant/batch site upon failure to comply with the specified requirements.

Clean the mixing drum before it is charged with the concrete mixture. Charge the batch into the mixing drum so that a portion of the water is in the drum before the aggregates and cementitious. Uniformly flow materials into the drum throughout the batching operation. Add all mixing water in the drum by the end of the first 15 seconds of the mixing cycle. Keep the throat of the drum free of accumulations that restrict the flow of materials into the drum.

Do not exceed the rated capacity (cubic yards shown on the manufacturer's plate on the mixer) of the mixer when batching the concrete. The Engineer will allow an overload of up to 10% above the rated capacity for central-mix plants and drum mixers at the work site, provided the concrete test data for strength, segregation and uniform consistency are satisfactory, and no concrete is spilled during the mixing cycle.

Operate the mixing drum at the speed specified by the mixer's manufacturer (shown on the manufacturer's plate on the mixer).

Mixing time is measured from the time all materials, except water, are in the drum. If it is necessary to increase the mixing time to obtain the specified percent of air in air-entrained concrete, the Engineer will determine the mixing time.

If the concrete is mixed in a central-mix plant or a drum mixer at the work site, mix the batch between 1 to 5 minutes at mixing speed. Do not exceed the maximum total 60 mixing revolutions. Mixing time begins after all materials, except water, are in the drum, and ends when the discharge chute opens. Transfer time in multiple drum mixers is included in mixing time. Mix time may be reduced for plants utilizing high performance mixing drums provided thoroughly mixed and uniform concrete is being produced with the proposed mix time. Performance of the plant must comply with Table A1.1, of ASTM C 94, Standard Specification for Ready Mixed Concrete. Five of the six tests listed in Table A1.1 must be within the limits of the specification to indicate that uniform concrete is being produced.

If the concrete is mixed in a truck mixer, mix the batch between 70 and 100 revolutions of the drum or blades at mixing speed. After the mixing is completed, set the truck mixer drum at agitating speed. Unless the mixing unit is equipped with an accurate device indicating and controlling the number of revolutions at mixing speed, perform the mixing at the batch plant and operate the mixing unit at agitating speed while traveling from the plant to the work site. Do not exceed 350 total revolutions (mixing and agitating).

If a truck mixer or truck agitator is used to transport concrete that was completely mixed in a stationary central mixer, agitate the concrete while transporting at the agitating speed specified by the manufacturer of the equipment (shown on the manufacturer's plate on the equipment). Do not exceed 250 total revolutions (additional re-mixing and agitating).

Provide a batch slip including batch weights of every constituent of the concrete and time for each batch of concrete delivered at the work site, issued at the batching plant that bears the time of charging of the mixer drum with cementitious and aggregates. Include quantities, type, product name and manufacturer of all admixtures on the batch ticket.

If non-agitating equipment is used for transportation of concrete, provide approved covers for protection against the weather when required by the Engineer.

07-PS0166

Place non-agitated concrete within 30 minutes of adding the cement to the water.

Do not use concrete that has developed its initial set. Regardless of the speed of delivery and placement, the Engineer will suspend the concreting operations until corrective measures are taken if there is evidence that the concrete can not be adequately consolidated.

Adding water to concrete after the initial mixing is prohibited. Add all water at the plant. If needed, adjust slump through the addition of a water reducer according to **subsection 3.0e.(2)**.

b. Placement Limitations.

(1) Concrete Temperature. Unless otherwise authorized by the Engineer, the temperature of the mixed concrete immediately before placement is a minimum of 55°F, and a maximum of 70°F. With approval by the Engineer, the temperature of the concrete may be adjusted 5°F above or below this range.

(2) Qualification Batch. For Grade 3.5 (AE) (LC-HPC) concrete, qualify a field batch (one truckload or at least 6 cubic yards) at least 35 days prior to commencement of placement of the bridge decks. Produce the qualification batch from the same plant that will supply the job concrete. Simulate haul time to the jobsite prior to discharge of the concrete for testing. Prior to placing concrete in the qualification slab and on the job, submit documentation to the Engineer verifying that the qualification batch concrete meets the requirements for air content, slump, temperature of plastic concrete, compressive strength, unit weight and other testing as required by the Engineer.

Before the concrete mixture with plasticizing admixture is used on the project, determine the air content of the qualification batch. Monitor the slump, air content, temperature and workability at initial batching and estimated time of concrete placement. If these properties are not adequate, repeat the qualification batch until it can be demonstrated that the mix is within acceptable limits as specified in this specification.

(3) Placing Concrete at Night. Do not mix, place or finish concrete without sufficient natural light, unless an adequate and artificial lighting system approved by the Engineer is provided.

(4) Placing Concrete in Cold Weather. Unless authorized otherwise by the Engineer, mixing and concreting operations shall not proceed once the descending ambient air temperature reaches 40°F, and may not be initiated until an ascending ambient air temperature reaches 40°F. The ascending ambient air temperature for initiating concreting operations shall increase to 45°F if the maximum ambient air temperature is expected to be between 55°F and 60°F during or within 24 hours of placement and to 50°F if the ambient air temperature is expected to equal or exceed 60°F during or within 24 hours of placement.

If the Engineer permits placing concrete during cold weather, aggregates may be heated by either steam or dry heat before placing them in the mixer. Use an apparatus that heats the weight uniformly and is so arranged as to preclude the possible occurrence of overheated areas which might injure the materials. Do not heat aggregates directly by gas or oil flame or on sheet metal over fire. Aggregates that are heated in bins, by steam-coil or water-coil heating, or by other methods not detrimental to the aggregates may be used. The use of live steam on or through binned aggregates is prohibited. Unless otherwise authorized, maintain the temperature of the mixed concrete between 55°F to 70°F at the time of placing it in the forms. With approval by the Engineer, the temperature of the concrete may be adjusted up to 5°F above or below this range. Do not place concrete when there is a probability of air temperatures being more than 25°F below the temperature of the concrete during the first 24 hours after placement unless insulation is provided for both the deck and the girders. Do not, under any circumstances, continue concrete operations if the ambient air temperature is less than 20°F.

If the ambient air temperature is 40°F or less at the time the concrete is placed, the Engineer may permit the water and the aggregates be heated to at least 70°F, but not more than 120°F.

Do not place concrete on frozen subgrade or use frozen aggregates in the concrete.

(5) Placing Concrete in Hot Weather. When the ambient temperature is above 90°F, cool the forms, reinforcing steel, steel beam flanges, and other surfaces which will come in contact with the mix to below 90°F by means of a water spray or other approved methods. For Grade 3.5 (AE) (LC-HPC) concrete, cool the concrete mixture to maintain the temperature immediately before placement between 55°F and 70°F. With approval by the Engineer, the temperature of the concrete may be up to 5°F below or above this range.

Maintain the temperature of the concrete at time of placement within the specified temperature range by any combination of the following:

- Shading the materials storage areas or the production equipment.
- Cooling the aggregates by sprinkling with potable water.
- Cooling the aggregates or water by refrigeration or replacing a portion or all of the mix water with ice that is flaked or crushed to the extent that the ice will completely melt during mixing of the concrete.
- Liquid nitrogen injection.

6.0 INSPECTION AND TESTING

The Engineer will test the first truckload of concrete by obtaining a sample of fresh concrete at truck discharge and by obtaining a sample of fresh concrete at the discharge end of the conveyor, bucket or if pumped, the piping. The Engineer will obtain subsequent sample concrete for tests at the discharge end of the conveyor, bucket

or if pumped, the discharge end of the piping. If potential problems are apparent at the discharge of any truck, the Engineer will test the concrete at truck discharge prior to deposit on the bridge deck.

The Engineer will cast, store, and test strength test specimens in sets of 5. See **TABLE 1-3**.

KDOT will conduct the sampling and test the samples according to **SECTION 2500** and **TABLE 1-3**. The Contractor may be directed by the Engineer to assist KDOT in obtaining the fresh concrete samples during the placement operation.

A plan will be finalized prior to the construction date as to how out-of-specification concrete will be handled.

TABLE 1-3: SAMPLING AND TESTING FREQUENCY CHART

Tests Required (Record to)	Test Method	CMS	Verification Samples and Tests	Acceptance Samples and Tests
Slump (0.25 inch)	KT-21	a	Each of first 3 truckloads for any individual placement, then 1 of every 3 truckloads	
Temperature (1°F)	KT-17	a	Every truckload, measured at the truck discharge, and from each sample made for slump determination.	
Mass (0.1 lb)	KT-20	a	One of every 6 truckloads	
Air Content (0.25%)	KT-18 or KT-19	a	Each of first 3 truckloads for any individual placement, then 1 of every 6 truckloads	
Cylinders (1 lbf; 0.1 in; 1 psi)	KT-22 and AASHTO T 22	VER	Make at least 2 groups of 5 cylinders per pour or major mix design change with concrete sampled from at least 2 different truckloads evenly spaced throughout the pour, with a minimum of 1 set for every 100 cu yd. Include in each group 3 test cylinders to be cured according to KT-22 and 2 test cylinders to be field-cured. Store the field-cured cylinders on or adjacent to the bridge. Protect all surfaces of the cylinders from the elements in as near as possible the same way as the deck concrete. Test the field-cured cylinders at the same age as the standard-cured cylinders.	
Density of Fresh Concrete (0.1 lb/cu ft or 0.1% of optimum density)	KT-36	ACI		b,c: 1 per 100 cu yd for thin overlays and bridge deck surfacing.

Note a: "Type Insp" must = "ACC" when the assignment of a pay quantity is being made. "ACI" when recording test values for additional acceptance information.

Note b: Normal operation. Minimum frequency for exceptional conditions may be reduced by the DME on a project basis, written justification shall be made to the Chief of the Bureau of Materials and Research and placed in the project documents. (Multi-Level Frequency Chart (see page 17, Appendix A of Construction Manual, Part V).

Note c: Applicable only when specifications contain those requirements.

The Engineer will reject concrete that does not comply with specified requirements.

The Engineer will permit occasional deviations below the specified cementitious content, if it is due to the air content of the concrete exceeding the designated air content, but only up to the maximum tolerance in the air content. Continuous operation below the specified cement content for any reason is prohibited.

As the work progresses, the Engineer reserves the right to require the Contractor to change the proportions if conditions warrant such changes to produce a satisfactory mix. Any such changes may be made within the limits of the Specifications at no additional compensation to the Contractor.

KANSAS DEPARTMENT OF TRANSPORTATION
SPECIAL PROVISION TO THE
STANDARD SPECIFICATIONS, 2007 EDITION

Add a new SECTION to DIVISION 700:

LOW-CRACKING HIGH-PERFORMANCE CONCRETE – CONSTRUCTION

1.0 DESCRIPTION

Construct the low-cracking high-performance concrete (LC-HPC) structures according to the Contract Documents and this specification.

BID ITEMS	**UNITS**
Qualification Slab	Cubic Yard
Concrete (*) (AE) (LC-HPC)	Cubic Yard
*Grade of Concrete	

2.0 MATERIALS

Provide materials that comply with the applicable requirements.

LC-HPC ..... **07-PS0166, latest version**
Concrete Curing Materials ..... **DIVISION 1400**

3.0 CONSTRUCTION REQUIREMENTS

a. Qualification Batch and Slab. For each LC-HPC bridge deck, produce a qualification batch of LC-HPC that is to be placed in the deck and complies with **07-PS0166, latest version**, and construct a qualification slab that complies with this specification to demonstrate the ability to handle, place, finish and cure the LC-HPC bridge deck.

After the qualification batch of LC-HPC complies with **07-PS0166, latest version**, construct a qualification slab 15 to 45 days prior to placing LC-HPC in the bridge deck. Construct the qualification slab to comply with the Contract Documents, using the same LC-HPC that is to be placed in the deck and that was approved in the qualification batch. Submit the location of the qualification slab for approval by the Engineer. Place, finish and cure the qualification slab according to the Contract Documents, using the same personnel, methods and equipment (including the concrete pump, if used) that will be used on the bridge deck.

A minimum of 1 day after construction of the qualification slab, core 4 full-depth 4 inch diameter cores, one from each quadrant of the qualification slab, and forward them to the Engineer for visual inspection of degree of consolidation.

Do not commence placement of LC-HPC in the deck until approval is given by the Engineer. Approval to place concrete on the deck will be based on satisfactory placement, consolidation, finishing and curing of the qualification slab and cores, and will be given or denied within 24 hours of receiving the cores from the Contractor. If an additional qualification slab is deemed necessary by the Engineer, it will be paid for at the contract unit price for Qualification Slab.

b. Falsework and Forms. Construct falsework and forms according to **SECTION 708**.

c. Handling and Placing LC-HPC.

(1) Quality Control Plan (QCP). At a project progress meeting prior to placing LC-HPC, discuss with the Engineer the method and equipment used for deck placement. Submit an acceptable QCP according to the Contractor's Concrete Structures Quality Control Plan, Part V. Detail the equipment (for both determining and controlling the evaporation rate and LC-HPC temperature), procedures used to minimize the evaporation rate, plans for maintaining a continuous rate of finishing the deck without delaying the application of curing materials within the time specified in **subsection 3.0f.**, including maintaining a continuous supply of LC-HPC throughout the placement with an

adequate quantity of LC-HPC to complete the deck and filling diaphragms and end walls in advance of deck placement, and plans for placing the curing materials within the time specified in **subsection 3.0f**. In the plan, also include input from the LC-HPC supplier as to how variations in the moisture content of the aggregate will be handled, should they occur during construction.

(2) Use a method and sequence of placing LC-HPC approved by the Engineer. Do not place LC-HPC until the forms and reinforcing steel have been checked and approved. Before placing LC-HPC, clean all forms of debris.

(3) Finishing Machine Setup. On bridges skewed greater than 10º, place LC-HPC on the deck forms across the deck on the same skew as the bridge, unless approved otherwise by State Bridge Office (SBO). Operate the bridge deck finishing machine on the same skew as the bridge, unless approved otherwise by the SBO. Before placing LP-HPC, position the finish machine throughout the proposed placement area to allow the Engineer to verify the reinforcing steel positioning.

(4) Environmental Conditions. Maintain environmental conditions on the entire bridge deck so the evaporation rate is less than 0.2 lb/sq ft/hr. The temperature of the mixed LC-HPC immediately before placement must be a minimum of 55°F and a maximum of 70°F. With approval by the Engineer, the temperature of the LC-HPC may be adjusted 5°F above or below this range. This may require placing the deck at night, in the early morning or on another day. The evaporation rate (as determined in the American Concrete Institute Manual of Concrete Practice 305R, Chapter 2) is a function of air temperature, LC-HPC temperature, wind speed and relative humidity. The effects of any fogging required by the Engineer will not be considered in the estimation of the evaporation rate (**subsection 3.0c.(5)**).

Just prior to and at least once per hour during placement of the LC-HPC, the Engineer will measure and record the air temperature, LC-HPC temperature, wind speed, and relative humidity on the bridge deck. The Engineer will take the air temperature, wind, and relative humidity measurements approximately 12 inches above the surface of the deck. With this information, the Engineer will determine the evaporation rate using KDOT software or **FIGURE 710-1**.

When the evaporation rate is equal to or above 0.2 $lb/ft^2/hr$, take actions (such as cooling the LC-HPC, installing wind breaks, sun screens etc.) to create and maintain an evaporation rate less than 0.2 $lb/ft^2/hr$ on the entire bridge deck.

(5) Fogging of Deck Placements. Fogging using hand-held equipment may be required by the Engineer during unanticipated delays in the placing, finishing or curing operations. If fogging is required by the Engineer, do not allow water to drip, flow or puddle on the concrete surface during fogging, placement of absorptive material, or at any time before the concrete has achieved final set.

(6) Placement and Equipment. Place LC-HPC by conveyor belt or concrete bucket. Pumping of LC-HPC will be allowed if the Contractor can show proficiency when placing the approved mix during construction of the qualification slab using the same pump as will be used on the job. Placement by pump will also be allowed with prior approval of the Engineer contingent upon successful placement by pump of the approved mix, using the same pump as will be used for the deck placement, at least 15 days prior to placing LC-HPC in the bridge deck. To limit the loss of air, the maximum drop from the end of a conveyor belt or from a concrete bucket is 5 feet and pumps must be fitted with an air cuff/bladder valve. Do not use chutes, troughs or pipes made of aluminum.

Place LC-HPC to avoid segregation of the materials and displacement of the reinforcement. Do not deposit LC-HPC in large quantities at any point in the forms, and then run or work the LC-HPC along the forms.

Fill each part of the form by depositing the LC-HPC as near to the final position as possible.

The Engineer will obtain sample LC-HPC for tests and cylinders at the discharge end of the conveyor, bucket, or if pumped, the piping.

(7) Consolidation.

- Accomplish consolidation of the LC-HPC on all span bridges that require finishing machines by means of a mechanical device on which internal (spud or tube type) concrete vibrators of the same type and size are mounted (**subsection 154.2**).
- Observe special requirements for vibrators in contact with epoxy coated reinforcing steel as specified in **subsection 154.2**.
- Provide stand-by vibrators for emergency use to avoid delays in case of failure.
- Operate the mechanical device so vibrator insertions are made on a maximum spacing of 12 inch centers over the entire deck surface.
- Provide a uniform time per insertion of all vibrators of 3 to 15 seconds, unless otherwise designated by the Engineer.

- Provide positive control of vibrators using a timed light, buzzer, automatic control or other approved method.
- Extract the vibrators from the LC-HPC at a rate to avoid leaving any large voids or holes in the LC-HPC.
- Do not drag the vibrators horizontally through the LC-HPC.
- Use hand held vibrators (**subsection 154.2**) in inaccessible and confined areas such as along bridge rail or curb.
- When required, supplement vibrating by hand spading with suitable tools to provide required consolidation.
- Reconsolidate any voids left by workers.

Continuously place LC-HPC in any floor slab until complete, unless shown otherwise in the Contract Documents.

d. Construction Joints, Expansion Joints and End of Wearing Surface (EWS) Treatment. Locate the construction joints as shown in the Contract Documents. If construction joints are not shown in the Contract Documents, submit proposed locations for approval by the Engineer.

If the work of placing LC-HPC is delayed and the LC-HPC has taken its initial set, stop the placement, saw the nearest construction joint approved by the Engineer, and remove all LC-HPC beyond the construction joint.

Construct keyed joints by embedding water-soaked beveled timbers of a size shown on the Contract Documents, into the soft LC-HPC. Remove the timber when the LC-HPC has set. When resuming work, thoroughly clean the surface of the LC-HPC previously placed, and when required by the Engineer, roughen the key with a steel tool. Before placing LC-HPC against the keyed construction joint, thoroughly wash the surface of the keyed joint with clean water.

e. Finishing. Strike off bridge decks with a vibrating screed or single-drum roller screed, either self-propelled or manually operated by winches and approved by the Engineer. Use a self-oscillating screed on the finish machine, and operate or finish from a position either on the skew or transverse to the bridge roadway centerline. See **subsection 3.0c.(3)**. Do not mount tamping devices or fixtures to drum roller screeds; augers are allowed.

Irregular sections may be finished by other methods approved by the Engineer and detailed in the required QCP. See **subsection 3.0c.(1)**.

Finish the surface by a burlap drag, metal pan or both, mounted to the finishing equipment. Use a float or other approved device behind the burlap drag or metal pan, as necessary, to remove any local irregularities. Do not add water to the surface of LC-HPC. Do not use a finishing aid.

Tining of plastic LC-HPC is prohibited. All LC-HPC surfaces must be reasonably true and even, free from stone pockets, excessive depressions or projections beyond the surface.

Finish all top surfaces, such as the top of retaining walls, curbs, abutments and rails, with a wooden float by tamping and floating, flushing the mortar to the surface and provide a uniform surface, free from pits or porous places. Trowel the surface producing a smooth surface, and brush lightly with a damp brush to remove the glazed surface.

f. Curing and Protection.

(1) General. Cure all newly placed LC-HPC immediately after finishing, and continue uninterrupted for a minimum of 14 days. Cure all pedestrian walkway surfaces in the same manner as the bridge deck. Curing compounds are prohibited during the 14 day curing period.

(2) Cover With Wet Burlap. Soak the burlap a minimum of 12 hours prior to placement on the deck. Rewet the burlap if it has dried more one hour before it is applied to the surface of bridge deck. Apply 1 layer of wet burlap within 10 minutes of LC-HPC strike-off from the screed, followed by a second layer of wet burlap within 5 minutes. Do not allow the surface to dry after the strike-off, or at any time during the cure period. In the required QCP, address the rate of LC-HPC placement and finishing methods that will affect the period between strike-off and burlap placement. See **subsection 3.0c.(1)**. During times of delay expected to exceed 10 minutes, cover all concrete that has been placed, but not finished, with wet burlap.

Maintain the wet burlap in a fully wet condition using misting hoses, self-propelled, machine-mounted fogging equipment with effective fogging area spanning the deck width moving continuously across the entire burlap-

covered surface, or other approved devices until the LC-HPC has set sufficiently to allow foot traffic. At that time, place soaker hoses on the burlap, and supply running water continuously to maintain continuous saturation of all burlap material to the entire LC-HPC surface. For bridge decks with superelevation, place a minimum of 1 soaker hose along the high edge of the deck to keep the entire deck wet during the curing period.

(3) Waterproof Cover. Place white polyethylene film on top of the soaker hoses, covering the entire LC-HPC surface after soaker hoses have been placed, a maximum of 12 hours after the placement of the LC-HPC. Use as wide of sheets as practicable, and overlap 2 feet on all edges to form a complete waterproof cover of the entire LC-HPC surface. Secure the polyethylene film so that wind will not displace it. Should any portion of the sheets be broken or damaged before expiration of the curing period, immediately repair the broken or damaged portions. Replace sections that have lost their waterproof qualities.

If burlap and/or polyethylene film is temporarily removed for any reason during the curing period, use soaker hoses to keep the entire exposed area continuously wet. Replace saturated burlap and polyethylene film, resuming the specified curing conditions, as soon as possible.

Inspect the LC-HPC surface once every 6 hours for the entirety of the 14 day curing period, so that all areas remain wet for the entire curing period and all curing requirements are satisfied.

(4) Documentation. Provide the Engineer with a daily inspection set that includes:

- documentation that identifies any deficiencies found (including location of deficiency);
- documentation of corrective measures taken;
- a statement of certification that the entire bridge deck is wet and all curing material is in place;
- documentation showing the time and date of all inspections and the inspector's signature.
- documentation of any temporary removal of curing materials including location, date and time, length of time curing was removed, and means taken to keep the exposed area continuously wet.

(5) Cold Weather Curing. When LC-HPC is being placed in cold weather, also adhere to **07-PS0166, latest version**.

When LC-HPC is being placed and the ambient air temperature may be expected to drop below 40ºF during the curing period or when the ambient air temperature is expected to drop more than 25°F below the temperature of the LC-HPC during the first 24 hours after placement, provide suitable measures such as straw, additional burlap, or other suitable blanketing materials, and/or housing and artificial heat to maintain the LC-HPC and girder temperatures between 40ºF and 75ºF as measured on the upper and lower surfaces of the LC-HPC. Enclose the area underneath the deck and heat so that the temperature of the surrounding air is as close as possible to the temperature of LC-HPC and between 40ºF and 75ºF. When artificial heating is used to maintain the LC-HPC and girder temperatures, provide adequate ventilation to limit exposure to carbon dioxide if necessary. Maintain wet burlap and polyethylene cover during the entire 14 day curing period. Heating may be stopped after the first 72 hours if the time of curing is lengthened to account for periods when the ambient air temperature is below 40ºF. For every day the ambient air temperature is below 40ºF, an additional day of curing with a minimum ambient air temperature of 50ºF will be required. After completion of the required curing period, remove the curing and protection so that the temperature of the LC-HPC during the first 24 hours does not fall more than 25°F.

(6) Curing Membrane. At the end of the 14-day curing period remove the wet burlap and polyethylene and within 30 minutes, apply 2 coats of an opaque curing membrane to the LC-HPC. Apply the curing membrane when no free water remains on the surface but while the surface is still wet. Apply each coat of curing membrane according to the manufacturer's instructions with a minimum spreading rate per coat of 1 gallon per 80 square yards of LC-HPC surface. If the LC-HPC is dry or becomes dry, thoroughly wet it with water applied as a fog spray by means of approved equipment. Spray the second coat immediately after and at right angles to the first application. Protect the curing membrane against marring for a minimum of 7 days. Give any marred or disturbed membrane an additional coating. Should the curing membrane be subjected to continuous injury, the Engineer may limit work on the deck until the 7-day period is complete. Because the purpose of the curing membrane is to allow for slow drying of the bridge deck, extension of the initial curing period beyond 14 days, while permitted, shall not be used to reduce the 7-day period during which the curing membrane is applied and protected.

(7) Construction Loads. Adhere to **TABLE 710-2**.

If the Contractor needs to drive on the bridge before the approach slabs can be placed and cured, construct a temporary bridge from the approach over the EWS capable of supporting the anticipated loads. Do not bend the reinforcing steel which will tie the approach slab to the EWS or damage the LC-HPC at the EWS. The method of bridging must be approved by the Engineer.

TABLE 710-2: CONCRETE LOAD LIMITATIONS ON BRIDGE DECKS		
Days after concrete is placed	**Element**	**Allowable Loads**
1*	Subdeck, one-course deck or concrete overlay	Foot traffic only.
3*	One-course deck or concrete overlay	Work to place reinforcing steel or forms for the bridge rail or barrier.
7*	Concrete overlays	Legal Loads; Heavy stationary loads with the Engineer's approval.***
10 (15)**	Subdeck, one-course deck or post-tensioned haunched slab bridges**	Light truck traffic (gross vehicle weight less than 5 tons).****
14 (21)**	Subdeck, one-course deck or post-tensioned haunched slab bridges**	Legal Loads; Heavy stationary loads with the Engineer's approval.***Overlays on new decks.
28	Bridge decks	Overloads, only with the State Bridge Engineer's approval.***

*Maintain a 7 day wet cure at all times (14-day wet cure for decks with LC-HPC).
** Conventional haunched slabs.
*** Submit the load information to the appropriate Engineer. Required information: the weight of the material and the footprint of the load, or the axle (or truck) spacing and the width, the size of each tire (or track length and width) and their weight.
****An overlay may be placed using pumps or conveyors until legal loads are allowed on the bridge.

g. Grinding and Grooving. Correct surface variations exceeding 1/8 inch in 10 feet by use of an approved profiling device, or other methods approved by the Engineer after the curing period. Perform grinding on hardened LC-HPC after the 7 day curing membrane period to achieve a plane surface and grooving of the final wearing surface as shown in the Contract Documents.

Use a self-propelled grinding machine with diamond blades mounted on a multi-blade arbor. Avoid using equipment that causes excessive ravels, aggregate fractures or spalls. Use vacuum equipment or other continuous methods to remove grinding slurry and residue.

After any required grinding is complete, give the surface a suitable texture by transverse grooving. Use diamond blades mounted on a self-propelled machine that is designed for texturing pavement. Transverse grooving of the finished surface may be done with equipment that is not self-propelled providing that the Contractor can show proficiency with the equipment. Use equipment that does not cause strain, excessive raveling, aggregate fracture, spalls, disturbance of the transverse or longitudinal joint, or damage to the existing LC-HPC surface. Make the grooving approximately 3/16 inch in width at 3/4 inch centers and the groove depth approximately 1/8 inch. For bridges with drains, terminate the transverse grooving approximately 2 feet in from the gutter line at the base of the curb. Continuously remove all slurry residues resulting from the texturing operation.

h. Post Construction Conference. At the completion of the deck placement, curing, grinding and grooving for a bridge using LC-HPC, a post-construction conference will be held with all parties that participated in the planning and construction present. The Engineer will record the discussion of all problems and successes for the project.

i. Removal of Forms and Falsework. Do not remove forms and falsework without the Engineer's approval. Remove deck forms approximately 2 weeks (a maximum of 4 weeks) after the end of the curing period (removal of burlap), unless approved by the Engineer. The purpose of 4 week maximum is to limit the moisture gradient between the bottom and the top of the deck.

For additional requirements regarding forms and falsework, see **SECTION 708**.

4.0 MEASUREMENT AND PAYMENT

The Engineer will measure the qualification slab and the various grades of (AE) (LC-HPC) concrete placed in the structure by the cubic yard. No deductions are made for reinforcing steel and pile heads extending into the LP-HPC. The Engineer will not separately measure reinforcing steel in the qualification slab.

Payment for the "Qualification Slab" and the various grades of "(AE) (LC-HPC) Concrete" at the contract unit prices is full compensation for the specified work.

FIGURE 710-1: STANDARD PRACTICE FOR CURING CONCRETE

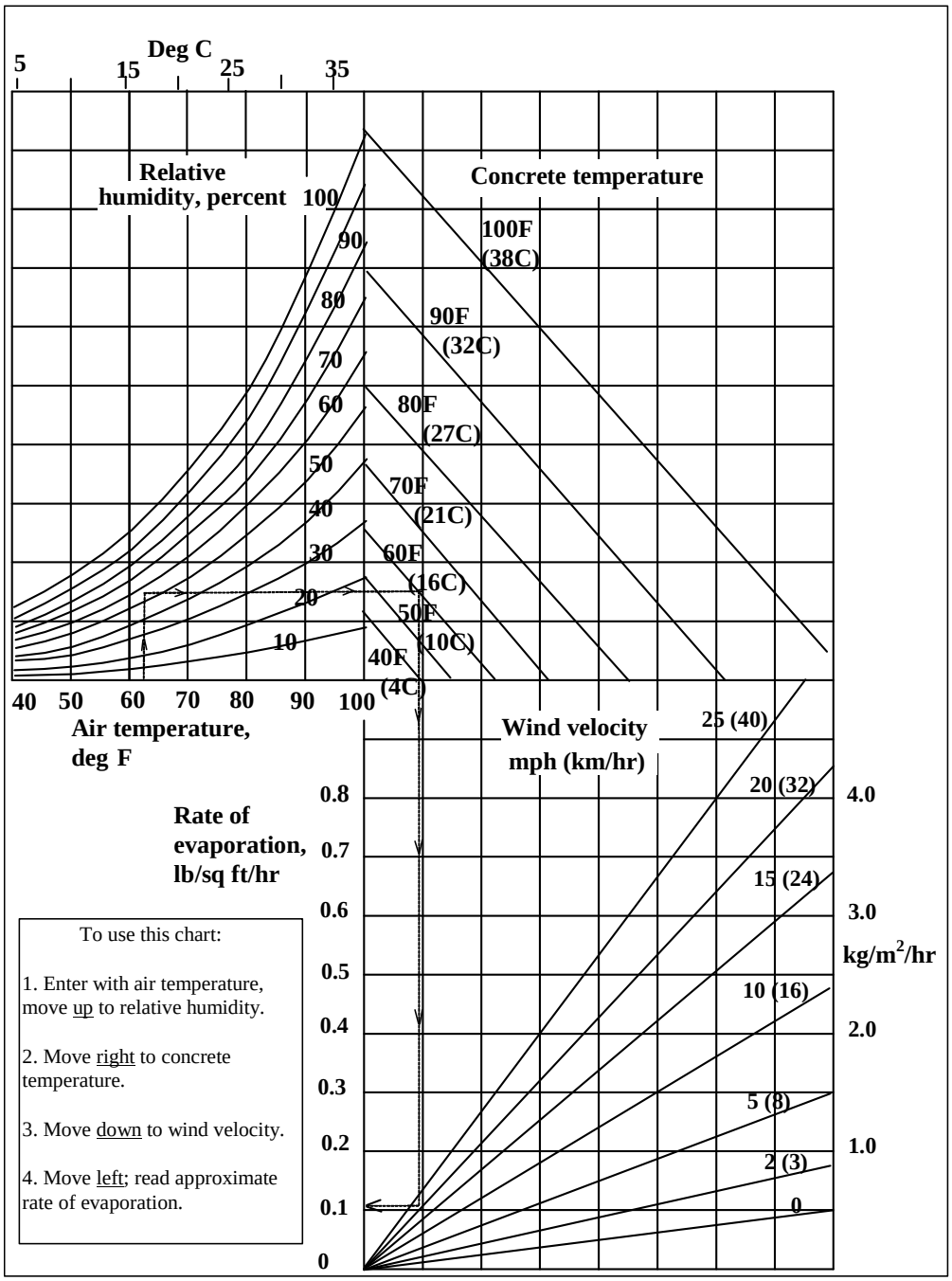

Effect of concrete and air temperatures, relative humidity, and wind velocity on the rate of evaporation of surface moisture from concrete. This chart provides a graphic method of estimating the loss of surface moisture for various weather conditions. To use the chart, follow the four steps outlined above. When the evaporation rate exceeds 0.2 lb/ft^2/hr (1.0 kg/ m^2/hr), measures shall be taken to prevent excessive moisture loss from the surface of unhardened concrete; when the rate is less than 0.2 lb/ft^2/hr (1.0 kg/m^2/hr) such measures may be needed. When excessive moisture loss is not prevented, plastic cracking is likely to occur.

APPENDIX F CRACK DENSITIES AT THE TIME OF SURVEY AND INTERPOLATED CRACK DENSITIES AT 36 MONTHS

Table F.1 Crack densities at the time of survey and interpolated crack densities at 36 months for LC-HPC decks and OP deck in this study

Bridge Number	Placements	Survey Age	Crack Density	Interpolated Crack Density at 36 months
		months	m/m^2	m/m^2
105-304	LC-HPC 1-p1	5.9	0.012	0.049
105-304	LC-HPC-1-p1	18.5	0.047	
105-304	LC-HPC-1-p1	32.1	0.044	
105-304	LC-HPC-1-p1	44.1	0.06	
105-304	LC-HPC-1-p1	55.6	0.032	
105-304	LC-HPC 1-p2	5.3	0.003	0.024
105-304	LC-HPC-1-p2	17.9	0.006	
105-304	LC-HPC-1-p2	31.5	0.024	
105-304	LC-HPC-1-p2	43.5	0.125	
105-304	LC-HPC-1-p2	55.0	0.023	
105-310	LC-HPC 2	7.2	0.013	0.048
105-310	LC-HPC 2	21.2	0.028	
105-310	LC-HPC 2	32.5	0.085	
105-310	LC-HPC-2	44.5	0.059	
46-338	LC-HPC 3	6.5	0.028	0.110
46-338	LC-HPC 3	19.2	0.11	
46-338	LC-HPC 3	31.5	0.108	
46-339	LC-HPC 4-p2	9.43	0.004	0.094
46-339	LC-HPC-4-p2	21.22	0.079	
46-339	LC-HPC-4-p2	32.72	0.094	
46-340 #1	LC-HPC 5	8.0	0.059	0.128
46-340 #1	LC-HPC-5	19.4	0.123	
46-340 #1	LC-HPC-5	31.1	0.128	
46-340 #2	LC-HPC 6	6.5	0.063	0.231
46-340 #2	LC-HPC-6	19.7	0.238	
46-340 #2	LC-HPC-6	31.4	0.231	
43-33	LC-HPC 7	11.4	0.003	0.012
43-33	LC-HPC 7	24.2	0.019	
43-33	LC-HPC 7	34.8	0.012	
43-33	LC-HPC 7	46.8	0.005	
78-119	LC-HPC-11	23.4	0.059	0.241
78-119	LC-HPC-11	36.2	0.241	
OP-p1	OP-p1	18.3	0.341	0.502
OP-p1	OP-p1	30.0	0.502	

Table F.2 Crack densities at the time of survey and interpolated crack densities at 36 months for control decks in this study

Bridge Number	Placements	Survey Age	Crack Density	Interpolated Crack Density at 36 months
		months	m/m^2	m/m^2
105-311	CONTROL 1/2-p1	6.1	0.00	0.117
105-311	CONTROL 1/2-p1	18.6	0.151	
105-311	CONTROL 1/2-p1	32.2	0.114	
105-311	CONTROL 1/2-p1	44.2	0.261	
105-311	CONTROL 1/2-p1	55.8	0.132	
105-311	CONTROL 1/2-p2	5.5	0	0.106
105-311	CONTROL 1/2-p2	18.0	0.044	
105-311	CONTROL 1/2-p2	31.6	0.0911	
105-311	CONTROL 1/2-p2	43.6	0.133	
105-311	CONTROL 1/2-p2	55.2	0.106	
46-337	CONTROL 3	10.4	0.037	0.232
46-337	CONTROL 3	22.6	0.216	
46-337	CONTROL 3	35.4	0.232	
46-347	CONTROL 4	6.8	0.050	0.473
46-347	CONTROL 4	19.7	0.366	
46-347	CONTROL 4	31.6	0.473	
46-334	CONTROL 7-p1	16.4	0.293	0.898
46-334	CONTROL 7-p1	27.1	0.476	
46-334	CONTROL 7-p1	38.2	1.003	
46-334	CONTROL 7-p1	51.1	1.037	
46-334	CONTROL 7-p2	10.8	0.03	0.298
46-334	CONTROL 7-p2	21.5	0.069	
46-334	CONTROL 7-p2	32.6	0.277	
46-334	CONTROL 7-p2	45.5	0.359	
56-155	CONTROL 11	16.5	0.351	0.665
56-155	CONTROL 11	27.1	0.665	
56-155	CONTROL 11	37.8	0.599	
56-155	CONTROL 11	50.2	0.636	

Table F.3 Crack densities at the time of survey and interpolated crack densities at 36 months for conventional monolithic decks in previous studies (Schmitt and Darwin 1995, Miller and Darwin 2000, Lindquist et al. 2005)

Bridge Number	Placement	Survey Age	Crack Density	Interpolated Crack Density at 36 months
		months	m/m^2	m/m^2
3-046	East Deck	210	0.53	0.353
3-046	East Deck	102	0.42	
3-046	West Deck	210	0.40	0.285
3-046	West Deck	102	0.33	
3-046	Ctr. Deck	210	0.34	0.033
3-046	Ctr. Deck	102	0.15	
75-044	Deck	155	0.28	0.180
75-044	Deck	48	0.19	
75-045	Deck	154	0.45	0.510
75-045	Deck	47	0.51	
89-204	Deck	132	1.05	0.754
89-204	Deck	82	0.84	
89-204	Deck	34	0.75	
3-045	West Deck	223	0.43	0.000
3-045	West Deck	112	0.12	
3-045	East Deck	223	0.39	0.088
3-045	East Deck	112	0.21	
3-045	W. Ctr. Deck	223	0.20	0.167
3-045	W. Ctr. Deck	112	0.18	
3-045	Ctr. Deck	220	0.28	0.195
3-045	Ctr. Deck	112	0.23	
3-045	E. Ctr. Deck	220	0.31	0.037
3-045	E. Ctr. Deck	112	0.15	
56-142	North End	188	0.04	0.000
56-142	North End	80	0.00	
56-142	N. + Moment	189	0.35	0.166
56-142	N. + Moment	80	0.22	
56-142	S. + Moment	189	0.19	0.037
56-142	S. + Moment	80	0.08	
56-142	N. Pier	188	0.07	0.000
56-142	N. Pier	80	0.02	
56-142	Ctr. Pier	188	0.36	0.133
56-142	Ctr. Pier	80	0.20	
56-142	S. Pier	188	0.07	0.041
56-142	S. Pier	80	0.05	
56-148	Deck	133	0.53	0.280
56-148	Deck	36	0.28	
56-148	Deck	85	0.31	

Table F.3 (con't) Crack densities at the time of survey and interpolated crack densities at 36 months for conventional monolithic decks in previous studies (Schmitt and Darwin 1995, Miller and Darwin 2000, Lindquist et al. 2005)

Bridge Number	Placement	Survey Age	Crack Density	Interpolated Crack Density at 36 months
		months	m/m^2	m/m^2
70-095	Deck	212	0.13	0.032
70-095	Deck	106	0.07	
70-103	Right	219	0.66	0.253
70-103	Right	102	0.40	
70-103	Left	219	0.84	0.416
70-103	Left	102	0.57	
70-104	Deck	212	0.10	0.085
70-104	Deck	106	0.09	
70-107	Deck	130	0.72	0.343
70-107	Deck	34	0.34	
70-107	Deck	82	0.42	
99-076	Placement 4	163	0.93	0.940
99-076	Placement 4	42	0.94	
99-076	Placement 5	163	0.74	0.900
99-076	Placement 5	42	0.90	
99-076	North (West Ln.)	161	0.57	0.770
99-076	North (West Ln.)	42	0.77	
99-076	North (East Ln.)	157	0.55	0.420
99-076	North (East Ln.)	42	0.42	
99-076	Placement 2	165	1.04	1.480
99-076	Placement 2	42	1.48	
99-076	Placement 3	164	0.81	0.950
99-076	Placement 3	42	0.95	
99-076	South End	--	0.48	0.460
99-076	South End	42	0.46	
89-208	Deck	73	0.11	0.030
89-208	Deck	36	0.03	
105-000	Deck	42	0.27	0.270
56-49	deck	12.0	0.077	0.246
56-49	deck	25.8	0.230	
56-49	deck	36.8	0.219	
56-49	deck	47.5	0.265	
56-49	deck	60.7	0.316	

Table F.4 Crack densities at the time of survey and interpolated crack densities at 36 months for conventional overlay (CO) decks in previous studies (Schmitt and Darwin 1995, Miller and Darwin 2000, Lindquist et al. 2005)

Bridge Number	Placement	Survey Age	Crack density	Interpolated Crack Density at 36 months
		months	m/m^2	m/m^2
81-49	BDWS 12' Rt of CL	133	1.060	0.625
81-49	BDWS 12' Rt of CL	76.0	0.803	
75-1	BDWS Rt of CL	139	0.581	0.234
75-1	BDWS Rt of CL	82.5	0.391	
46-295	Right	24	0.150	0.150
89-196	BDWS Lt. Side	124	0.431	0.383
89-196	BDWS Lt. Side	75.2	0.404	
81-49	BDWS Rt. 22'	134	0.686	0.500
81-49	BDWS Rt. 22'	76.2	0.577	
46-289	Outside 20'	118	0.653	0.622
46-289	Outside 20'	71.4	0.635	
89-186	Outside	130	0.695	0.415
89-186	Outside	94.3	0.755	
89-186	Outside	42	0.450	
89-183	BDWS Rt. Side	142	0.564	0.289
89-183	BDWS Rt. Side	94.0	0.439	
46-290	Inside 24'	118	0.748	0.586
46-290	Inside 24'	71.7	0.656	
46-301	BDWS Rt. CL 24' to 38'	95	0.780	0.336
46-301	BDWS Rt. CL 24' to 38'	48.8	0.432	
46-301	BDWS Lt. CL 24'	94	0.833	0.493
46-301	BDWS Lt. CL 24'	48.5	0.566	
89-186	Inside	130	0.790	0.545
89-186	Inside	94.4	0.688	
89-186	Inside	42	0.560	
89-200	Left	133	0.510	0.450
89-200	Left	83.5	0.437	
89-200	Left	33	0.450	

Table F.4 (con't) Crack densities at the time of survey and interpolated crack densities at 36 months for conventional overlay (CO) decks in previous studies (Schmitt and Darwin 1995, Miller and Darwin 2000, Lindquist et al. 2005)

Bridge Number	Placement	Survey Age	Crack density	Interpolated Crack Density at 36 months
		months	m/m^2	m/m^2
46-299	Rt. Of CL 22'	95	0.665	0.686
46-299	Rt. Of CL 22'	48.7	0.686	
89-183	BDWS Lt. Side	142	0.641	0.500
89-183	BDWS Lt. Side	93.9	0.577	
89-201	Right	133	0.688	0.593
89-201	Right	83.6	0.659	
89-201	Right	34	0.590	
89-185	Inside	145	0.631	0.950
89-185	Inside	97.1	0.568	
89-185	Inside	41	0.950	
46-289	Inside 24'	118	0.748	0.584
46-289	Inside 24'	71.7	0.655	
46-299	Lt. Of CL 18'	95	0.999	1.115
46-299	Lt. Of CL 18'	48.6	1.115	
89-196	BDWS Rt. Side	124	0.758	0.587
89-196	BDWS Rt. Side	75.3	0.664	
89-201	Left	133	0.729	0.770
89-201	Left	83.5	0.593	
89-201	Left	34	0.770	
75-1	BDWS Lt of CL	139	0.409	0.298
75-1	BDWS Lt of CL	82.5	0.348	
89-200	Right	133	0.771	0.576
89-200	Right	83.6	0.672	
89-200	Right	33	0.570	
89-185	Outside	145	0.955	0.582
89-185	Outside	97.2	0.806	
89-185	Outside	41	0.600	
46-301	BDWS Rt.CL 24'	95	0.719	0.975
46-301	BDWS Rt.CL 24'	48.6	0.976	
46-301	BDWS Lt.CL 24' to 38'	95	1.117	0.867
46-301	BDWS Lt.CL 24' to 38'	48.8	0.922	
89-198	Right	133	0.510	0.401
89-198	Right	83.3	0.412	
89-198	Left	133	0.445	0.700
89-198	Left	83.4	0.356	
89-198	Left	33	0.700	

Table F.4 (con't) Crack densities at the time of survey and interpolated crack densities at 36 months for conventional overlay (CO) decks in previous studies (Schmitt and Darwin 1995, Miller and Darwin 2000, Lindquist et al. 2005)

Bridge Number	Placement	Survey Age	Crack density	Interpolated Crack Density at 36 months
		months	m/m^2	m/m^2
89-199	Left	133	0.674	0.640
89-199	Left	83.4	0.750	
89-199	Left	35	0.640	
89-199	Right	133	0.729	0.710
89-199	Right	83.3	0.543	
89-199	Right	35	0.710	
46-300	BDWS 18' Rt. of CL	72	0.682	0.981
46-300	BDWS 18' Rt. of CL	36.1	0.981	
46-300	BDWS 22' Lt. of CL	72	0.629	0.491
46-300	BDWS 22' Lt. of CL	36.0	0.491	

Table F.5 Crack densities at the time of survey and interpolated crack densities at 36 months for 5% silica fume overlay (SFO) decks in previous studies (Schmitt and Darwin 1995, Miller and Darwin 2000, Lindquist et al. 2005)

Bridge Number	Placement	Survey Age	Crack density	Interpolated Crack Density at 36 months
		month	m/m^2	m/m^2
87-453	South 18'	15	0.32	0.590
87-453	South 18'	61	0.92	
46-317	SFO 12'	26	0.07	0.094
46-317	SFO 12'	73	0.19	
81-50	SFO Lt. Unit #2	32	0.70	0.747
81-50	SFO Lt. Unit #2	78	1.28	
46-302	Lt. 1/2 SFO	28	0.43	0.478
46-302	Lt. 1/2 SFO	75	0.71	
46-302	Rt. 1/2 SFO	28	0.56	0.606
46-302	Rt. 1/2 SFO	75	0.85	
87-454	Right of CL	24	0.82	0.849
87-454	Right of CL	70	0.93	
89-245	Lt. 1/2 Unit 1 SFO	9	0.03	0.231
89-245	Lt. 1/2 Unit 1 SFO	68	0.47	
89-234	SFO Center 12'	24	0.51	0.518
89-234	SFO Center 12'	87	0.57	
89-245	Lt. 1/2 Unit 2 SFO	9	0.03	0.267
89-245	Lt. 1/2 Unit 2 SFO	68	0.54	
89-244	SFO Lt.	8	0.00	0.075
89-244	SFO Lt.	67	0.15	
23-85	West 1/2 SFO	28	0.37	0.402
23-85	West 1/2 SFO	76	0.59	
46-317	SFO 16'	26	0.08	0.148
46-317	SFO 16'	72	0.39	
89-234	SFO North 18'	24	0.23	0.232
89-234	SFO North 18'	87	0.24	
89-240	Rt. 22' SFO	11	0.01	0.052
89-240	Rt. 22' SFO	68	0.10	
89-244	SFO Rt.	9	0.03	0.227
89-244	SFO Rt.	67	0.45	
89-245	Rt. 1/2 Unit 2 SFO	9	0.05	0.238
89-245	Rt. 1/2 Unit 2 SFO	68	0.45	
89-246	West 1/2 SFO	10	0.06	0.180
89-246	West 1/2 SFO	61	0.29	

Table F.5 (con't) Crack densities at the time of survey and interpolated crack densities at 36 months for 5% silica fume overlay (SFO) decks in previous studies (Schmitt and Darwin 1995, Miller and Darwin 2000, Lindquist et al. 2005)

Bridge Number	Placement	Survey Age	Crack density	Interpolated Crack Density at 36 months
		month	m/m^2	m/m^2
81-50	SFO Rt. Unit #2	33	0.67	0.688
81-50	SFO Rt. Unit #2	78	0.90	
89-247	Rt. 26' SFO	14	0.52	0.517
89-247	Rt. 26' SFO	72	0.51	
89-207	Right	27	0.39	0.397
89-207	Right	86	0.45	
89-234	SFO South 20'	25	0.17	0.175
89-234	SFO South 20'	88	0.18	
89-245	Rt. 1/2 Unit 1 SFO	9	0.09	0.208
89-245	Rt. 1/2 Unit 1 SFO	68	0.35	
87-454	Left of CL	25	0.66	0.695
87-454	Left of CL	71	0.80	
89-235	SFO Right 18'	14	0.38	0.323
89-235	SFO Right 18'	77	0.21	
89-240	Lt. 22' SFO	11	0.41	0.370
89-240	Lt. 22' SFO	68	0.32	
46-309	Lt. 1/2 SFO	33	0.38	0.391
46-309	Lt. 1/2 SFO	81	0.56	
87-453	North 22'	15	0.19	0.421
87-453	North 22'	61	0.71	
89-206	Left	33	0.27	0.284
89-206	Left	91	0.48	
89-210	Right	32	0.17	0.215
89-210	Right	70	0.62	
89-206	Right	33	0.58	0.569
89-206	Right	91	0.41	
89-246	East 1/2 SFO	10	0.08	0.229
89-246	East 1/2 SFO	61	0.37	

Table F.5 (con't) Crack densities at the time of survey and interpolated crack densities at 36 months for 5% silica fume overlay (SFO) decks in previous studies (Schmitt and Darwin 1995, Miller and Darwin 2000, Lindquist et al. 2005)

Bridge Number	Placement	Survey Age	Crack density	Interpolated Crack Density at 36 months
		month	m/m^2	m/m^2
89-248	Eastbound Lane	4	0.03	0.313
89-248	Eastbound Lane	62	0.55	
46-309	Rt. 1/2 SFO	34	0.32	0.326
46-309	Rt. 1/2 SFO	81	0.50	
89-247	Lt. 13' SFO	14	0.47	0.526
89-247	Lt. 13' SFO	72	0.62	
89-207	Left	33	0.33	0.335
89-207	Left	91	0.40	
89-248	Westbound Lane	4	0.02	0.270
89-248	Westbound Lane	62	0.48	
23-85	East 1/2 SFO	29	0.37	0.393
23-85	East 1/2 SFO	76	0.54	
89-210	Left	32	0.15	0.195
89-210	Left	70	0.55	
89-184	Inside	94	0.94	0.666
89-184	Outside	94	1.06	0.681
89-187	Inside	97	1.21	1.482
89-187	Outside	97	0.79	0.638